Author:
Cragg, Patricia Ann

Title:
Respiration and body weight in the reptilian genus Lacerta : a physiological, anatomical and morphometric study

RESPIRATION AND BODY WEIGHT IN THE REPTILIAN GENUS *LACERTA*: A PHYSIOLOGICAL, ANATOMICAL AND MORPHOMETRIC STUDY.

by

PATRICIA A. CRAGG

A dissertation submitted to the University of Bristol for the degree of Doctor of Philosophy (1975).

MEMORANDUM

The experiments described in this thesis were my own unaided work. They were performed in the Research Unit for Comparative Animal Respiration under the supervision of Professor G.M. Hughes during the period 1970-1973.

Patricia A. Cragg.

Patricia A. Cragg, B.Sc.

ACKNOWLEDGEMENTS

I wish to thank Professor G.M. Hughes for the supervision of this thesis and the facilities of the Research Unit for Comparative Animal Respiration (C.A.R.), Bristol University. I am very grateful to Professor E.R. Weibel and Dr. P.H. Burri for a two week training in the techniques of lung morphometry at Berne University and to Dr. P. Dejours (CNRS, Strasbourg) for allowing me to test for a week the suitability of his small mammal treadmill for exercising Lacerta.

I am much indebted to Miss Sally Rendell (C.A.R.) for some routine cutting of EM sections for morphometric analysis, to the photographers of the Physiology Department, Bristol University, for photographing and printing all line diagrams and to Mrs. Myra Cook for the excellent typing of this manuscript.

Much encouragement during my research was given by many members of the C.A.R., Zoology and Botany Departments. Special thanks are due to Dr. R.A. Avery for supplying many lizards and teaching me their ecology, to Dr. A.E. Dorey and Dr. A. Beckett for help with EM techniques and to Dr. C.R. Boyden for continuous encouragement and assistance in many ways. I am also most grateful to Dr. M.J. Purves, Physiology Department, for much freedom of time in the last few months which has enabled me to complete the presentation of this thesis.

Finally, I thank the Medical Research Council for their financial support during the period 1970-1973.

CONTENTS

Page

APPENDIX II - Anaesthetics

SUMMARY

CHAPTER 1 - The relationship between metabolism and body weight during rest and exercise.

(i) The generalised relationship between body weight and standard or maximum $\dot{V}o_2$, viz. $\dot{V}o_2 \propto W^{0.75}$, has been reviewed.

(ii) $\dot{V}o_2$ and $\dot{V}co_2$ were measured continuously in closed or open respirometry circuits for 24 hours in the following species: L. vivipara, L. sicula and L. viridis (size range 0.2 to 38g). Experiments were conducted at 28 $\pm$ 1°C under a 12 hour light/12 hour dark regime (light on between 06.00 and 18.00 hours) or total light or total dark. The animals were completely shielded from extraneous stimuli and were starved for 1 or 3 days.

(iii) Diurnal $\dot{V}o_2$ records showed that L. vivipara, under these experimental conditions, had an exogeneous rhythm which was totally dependent on the presence of light for activity. In contrast, L. sicula had a strongly endogeneous rhythm and were active between 07.00 and 18.00 hours with a reduction in activity around 12.00 hours. Total dark or total light for 24 hours did not alter this rhythm. L. viridis showed an endogeneous rhythm which could be inhibited by the dark only and was also dependent on social interactions. Spontaneous routine activity was greatest in L. sicula.

(iv) Using the diurnal $\dot{V}o_2$ data, it was found that different levels of activity (minimum, standard, routine or peak) all gave $\dot{V}o_2$ relationships to body weight of $W^{0.74}$ to $W^{0.8}$. After 1 day's starvation, standard $\dot{V}o_2$ = 0.328 (ml hr^{-1}) $W^{0.756}$(g) and after 3 day's starvation, standard $\dot{V}o_2$ = 0.216 $W^{0.77}$. Respiratory quotients were 0.85 $\pm$ 0.05 and 0.75 $\pm$ 0.04, respectively. The respiratory quotient for routine activity was 0.95 $\pm$ 0.05.

(v) Exercising $\dot{V}o_2$ was measured in 1 day starved lizards using open circuit respirometry and a treadmill. Lacerta were impossible to train

but would often spontaneously run well for 30 min on the treadmill.

The following facts were established:-

(a) Lacerta appeared to be able to reach exercising levels of $\dot{V}O_2$ within the first minute.

(b) The respiratory quotient, R, was always high and proportional to the speed indicating increasing dependence on anaerobic pathways. At the end of exercise, R never became low suggesting that the blood buffering system did not require the re-formation of bicarbonate.

(c) The relationship between $\dot{V}O_2$ and speed was curvilinear leading to a plateau but there was no sign of a change in gait. $\dot{V}O_2$ at zero speed was the same as the resting $\dot{V}O_2$. Rectilinear relationships and $\dot{V}O_2$ intercepts above resting levels are found in mammals and other lizards (Bakker, 1972, Taylor, 1973).

(d) Exercise $\dot{V}O_2 = 1.66\ W^{0.76}$.

(e) The minimum cost of running, $\dot{V}O_2 g^{-1}$ was proportional to $W^{-0.48}$ in Lacerta being similar in slope to the mammal and a little less in absolute cost.

(f) Speeds on the treadmill maintainable for 5 min were proportional to $W^{0.33}$ as was snout-vent length. Maximum speeds maintainable for a few seconds were proportional to $W^{0.53}$ as was limb length.

(vi) Maximum $\dot{V}O_2$ was measured on 1 day starved animals from their spontaneous activity using a head mask and open circuit respirometry: max $\dot{V}O_2 = 2.52\ W^{0.76}$ or $2.66\ W^{0.747}$ (latter included 1 week old (newborn) L. vivipara).

(vii) Max $\dot{V}O_2$/std $\dot{V}O_2$ ratio was 7.5 to 8 in both Lacerta and the mammal. Mammalian values for both maximum and standard $\dot{V}O_2$ were 10 times greater than in Lacerta.

CHAPTER 2 - Ventilation in Lacerta.

(i) Tidal volume, V_T, and breathing frequency, f, were measured with a pneumotachograph placed in a head mask or body chamber and $\dot{V}o_2$ and $\dot{V}co_2$ were measured simultaneously using a head mask and open circuit respirometry at a constant temperature of 28 $\pm$ 1°C. The level of spontaneous activity was the variable.

(ii) Tidal air flow was diphasic beginning with an active expiration followed immediately by an active inspiration and then a pause of variable duration. Thoracic movements were triphasic having a second expiratory phase which was small and passive and occurred immediately after inspiration. Closure of the glottis prevented this triphasic pattern from being reflected in the tidal air flow. In excited animals, the glottis can be delayed in closing and hence some triphasic air flow is seen. Anaesthesia by Nembutal paralyses the glottis first, then the expiratory and finally the inspiratory muscles. Pharyngeal or gular movements occur in sequence with the tidal air flow and are also in the order expiration:inspiration:pause. Their function is not understood. When, however, they occur in the respiratory pause they are olfactory. Buccal deglutition only occurs in diseased Lacerta.

(iii) The following ventilatory parameter relationships to body weight (in g) were found:- V_T minimum = 0.0026 (ml) $W^{1.088}$, V_T average = 0.008 $W^{0.985}$, V_T maximum = 0.03 $W^{1.12}$; the mean 'b' exponent was 1.036. Resting f (breaths min^{-1}) = 30 $W^{0.013}$ and resting ventilation volume, $\dot{V}_E$ = 0.078 (ml min^{-1}) $W^{1.1}$. Average air flow rate, $\dot{V}$, in ml min^{-1} = 5.85 $W^{0.85}$ and breath duration, in sec, t = 0.21 $W^{0.146}$.

(iv) Since $\dot{V}o_2 \propto W^{0.75}$ and $\dot{V}_E \propto$ approximately $W^{1.0}$, the ventilation requirement ratio $\dot{V}_E/\dot{V}o_2$ is proportional to $W^{0.25}$. Thus the larger the lizard the more of its ventilated volume is 'wasted'.

(v) The absolute value of f, V_T and $\dot{V}_E$ and their ranges have been compared in Lacerta and a mammal of the same body weight.

Resting f of a mammal is	5.8	times greater than Lacerta							
" V_T " "	"	"	2.0	"	"	"	"		
" $\dot{V}_E$ " "	"	"	10 to 12	"	"	"	"		
Max f/min f	of Lacerta is	10 ;	of a mammal is	2					
Max V_T/min V_T	"	"	"	14	"	"	"	"	5
Max $\dot{V}_E$/min $\dot{V}_E$	"	"	"	~20	"	"	"	"	8
Max $\dot{V}o_2$/min $\dot{V}o_2$	"	"	"	8	"	"	"	"	8

Although Lacerta has the capacity to increase f considerably, V_T increments are the major contribution to max $\dot{V}_E$. The ratio $\dot{V}_E/\dot{V}o_2$, the ventilation requirement, is constant irrespective of activity in the mammal but in Lacerta at high $\dot{V}o_2$ levels much of the $\dot{V}_E$ is 'wasted'.

(vi) Although there is a direct relationship between $\dot{V}_E$ and $\dot{V}o_2$, it has considerable data scatter. $\dot{V}_E/\dot{V}o_2$ increases from 11 to 210 (with a resting mean of 21) as activity increases. Expressed another way, the O_2 extraction coefficient (the reciprocal of the ventilation requirement) changes from 43.5 to 2.3% (with a resting mean of 24 to 27%). At resting $\dot{V}_E$ and $\dot{V}o_2$, the O_2 extraction can be much greater in Lacerta (43.5%) than in the mammal (15 to 18%). This is considered to be due to the fact that the lungs in Lacerta stay inflated during the pause and therefore allow a longer time for extraction. At low tidal volumes, a greater proportion of the air is in the alveoli as opposed to the central air space allowing better utilisation of $\dot{V}_E$; the reverse occurs at large tidal volumes.

(vii) The lack of a clear cut relationship between $\dot{V}_E$ and $\dot{V}o_2$ is discussed in relation to the small amount of evidence available concerning the imprecise responses of lizards to hypoxia and hypercapnia. During increasing activity f is kept virtually constant whilst V_T increases; this is interpreted in the light of chemoreceptor responses. The fact that metabolic demands may not be the principal adjustor of $\dot{V}_E$ is also considered.

CHAPTER 3 - Static pressure-volume curves of the respiratory system in Lacerta.

(i) Pressure-volume curves were determined for the total respiratory system and its components. For a 29.6g Lacerta, the following compliance values in ml cm H_2O^{-1} were obtained: the total respiratory system, 0.55; the ribs alone, 0.62; the liver and heart alone, 17.5; the ribs, liver and heart, 0.6; the exposed in situ lung with liver and heart intact, 5.0 and the exposed in situ lung, 7.0. The resting volume at zero pressure for each of the components is as follows: ribcage, 3.55 ml; ribs + liver + heart, 2.9 ml; total respiratory system, 2.6 ml; liver and heart, 1.4 ml and the lungs, 0.6 ml.

(ii) The expiratory reserve volume, ERV, is limited by the ribcage in mammals and Lacerta whereas the inspiratory capacity, IC, is limited by the lungs in mammals and by the ribcage, liver and heart in Lacerta.

(iii) The cross-over points of the total respiratory system and the in situ lung with the zero pressure axis and each other allow one to determine the sub-divisions of the lung. For a 31.0g L. viridis, minimal air = 0.6 ml, functional residual capacity, FRC = 2.6 ml, end-inspiratory volume = 2.925 ml giving a resting V_T of 0.3 ml which compares well with the 0.27 ml average V_T of Chapter 2. IC and ERV were in the ratio 2:1 so that the max V_T of Chapter 2 (1.5 ml) is estimated to cause an intrapulmonary pressure of + or - 0.7 to 0.9 cm H_2O. Maximum intrapulmonary pressure was measured as + or - 3.5 cm H_2O allowing an estimate of a possible V_T as great as 3.3 ml.

(iv) Volumes and compliances were greater in Lacerta than in the mammal. L/M ratios were as follows:- FRC, 5; compliance of total respiratory system, 18.5; its specific compliance, 4.0; the compliance of the lungs, 225 to 550; its specific compliance, 45; the ribcage compliance, 3.5 and its specific compliance, 0.67.

(v) Lung volumes at all pressures and all sub-divisions of the lung were proportional to $W^{1.0}$ approximately. Total respiratory system compliance

= 0.025 $W^{1.008}$ and its specific compliance = 0.35 $W^{-0.049}$. The latter is an indication that the pressures involved in ventilation are a constant for all body weights.

(vi) Evidence is presented to show that at the 20 cm H_2O air fixation pressure used on isolated amphibian and reptilian lungs by Tenney & Tenney (1970), Lacerta gave a volume 3 times the true total lung capacity, TLC. Intrapulmonary pressure data in the literature indicates that the large reptiles used in their study had higher pressures (because of their more complex lungs) than small reptiles. Hence use of the same fixation pressure for all sized reptiles would give an under-inflation of large lungs with respect to small lungs, i.e. TLC $\propto W^{0.75}$ instead of the $W^{1.0}$ found in Lacerta. Isolated air inflation also caused an abnormal over-inflation of posterior regions and a reduction in anterior lobe inflation in Lacerta, even at 5 cm H_2O.

(vii) All the components of the respiratory system showed hysteresis in their air P-V curves. Hysteresis of the lung was not found in saline P-V curves, indicating the presence of a surfactant. The isolated lung had a greater degree of hysteresis than the in situ lung because the former takes on a round shape in which the alveoli become small - this accentuates the effects of a surfactant. The large central air space of the Lacerta lung dampens the surfactant effect. Lung hysteresis in air can also be abolished by inflation to pressures greater than +10 cm H_2O or deflation to -10 cm H_2O or as a function of time. This contrasts with the mammal and is interpreted as a low surfactant reserve. The possible need for a surfactant in a primitive lung is considered.

CHAPTER 4 - The anatomy of the Lacerta respiratory system.

(i) The architecture, histology and ultrastructure of vertebrate lungs are reviewed and the development and evolution of capillaries and epithelial cells of the lung septa are considered.

(ii) The nasal cavity, thorax, pleural mesenteries and lung architecture of Lacerta are examined.

(iii) The Lacerta lung (fixed by airway instillation of glutaraldehyde) has a large central air space with peripheral alveoli formed by primary, secondary and tertiary septa and supported by a luminal trabecular network of smooth muscle. The septa have a fine core of smooth muscle which supports a predominantly double capillary network but with some capillaries exposed to air on both their surfaces (the latter is found in the mammal). The capillaries bulge into the air spaces such that only a small proportion of each capillary's surface fails to contribute to the air to blood pathway. Capillaries on the outer wall, trabecular network, nerves, walls of vein and on the septa of the peribronchium and arterial perivascular space form a single network but only one surface is exposed to the air.

(iv) Type I epithelial cells of Lacerta have thin and extensive cytoplasmic extensions which form the major part of the epithelial air to blood pathway. They are rich in micropinocytotic vesicles but poor in cellular organelles and the nuclei are usually in between capillaries. Endothelial cells are very similar to Type I but contain more micropinocytotic vesicles and rod-shaped bodies with a dense stain throughout or just at the periphery. The interstitium between Type I and endothelial cells is usually thin. Type II epithelial cells are semi-cuboidal and are found in niches between capillaries. They have no cytoplasmic extensions or micropinocytotic vesicles but instead possess many cellular organelles, many lamellated bodies in various stages of development and microvilli at the air surface. These three cells are virtually identical to those of the mammal. Type II are sometimes found in groups with many interdigitating cytoplasmic

processes (these have not been documented for mammals) which then desquamate to form the alveolar macrophage.

(v) A few cells intermediate between Type II and I were found in the adult Lacerta lung. These are believed to be Type II transforming into I for septal growth. Cuboidal non-ciliated cells of the trabecular epithelium have many similarities to Type II cells and are considered to be their stem cells. These patterns show evolutionary and developmental trends.

(vi) The newborn Lacerta lung has a very large central air space with a small amount of peripheral tissue forming small alveoli. Capillaries were still developing as in the mammalian canalicular stage. There were larger numbers of stem Type II cells and Type II transforming into I.

(vii) Lamellated bodies of Type II cells were formed from both small vesicles which develop lamellae and gradually grow and from large lipid droplets which amass osmiophilic material. These bodies expel the osmiophilic material into the air where it forms the surface lining surfactant which is seen after fixation as globular myelin figures, amorphous flocculent material and strongly osmiophilic lines. Tubular myelin figures were not found which may indicate a difference between Lacerta and mammalian surfactant.

(viii) The Lacerta lung architecture is considered primitive but the septa themselves are advanced and closely approximate to the mammal unlike any other vertebrate septa.

CHAPTER 5 - Lacerta lung morphometry.

(i) The mammalian and lower vertebrate data on lung morphometry is reviewed together with the methods of lung fixation. It was found that a fixation pressure of 20 cm H_2O used for instillation of glutaraldehyde into open chest mammals was equivalent to 10 cm H_2O for closed chest Lacerta. Closed chest conditions were necessary for Lacerta to keep natural lung contours. The morphometric methods of Weibel (e.g. 1969b, 1970/71) have been used and in some instances modified.

(ii) Nasal cavity volume (ml) = $0.0015\ W^{1.05}$, tracheal volume (ml) = $0.0022\ W^{0.94}$, tracheal length (cm) = $0.965\ W^{0.355}$ and tracheal diameter (cm) = $0.054\ W^{0.29}$. All tracheal parameters were larger in Lacerta than a mammal but the length/diameter ratio was the same. Tracheal resistance was 4 times greater in the mammal. Lacerta tracheal resistance is $\propto W^{-0.85}$ and since air flow rate $\dot{V}$ is $\propto W^{+0.85}$ (Chapter 2) and $\Delta P = \dot{V} \times R$, it can be said that the pressures involved in ventilation are a constant for all Lacerta body weights.

(iii) Total lung volume = $0.099\ W^{1.024}$ and is twice the volume of the mammalian lung. Lung weight = $0.0169\ W^{0.716}$ and is about 1.5 to 1.8 times less than in the mammal. This is further compared with the reptilian and amphibian data of Tenney & Tenney (1970).

(iv) 5 adult right lungs (3.0 to 29.3g body weight) were used for extensive morphometry at the light microscopic level. With a total lung volume = $0.0626\ W^{0.907}$ (lungs selected were not quite isometric), central air space, y, = $0.0339\ W^{0.97}$, alveolar air volume, x, = $0.0206\ W^{0.822}$ and lung tissue volume = $0.0098\ W^{0.711}$. This gives a y/x ratio $\propto W^{0.15}$ which is similar to the $\dot{V}_E/\dot{V}o_2$ ratio $\propto W^{0.25}$ found in Chapter 2 and indicates that the 'wasted' ventilation volume is necessary to inflate alveolar regions sufficiently.

(v) Alveolar mean size(μm)= $119\ W^{0.128}$, alveolar depth = $104.6\ W^{0.16}$, alveolar diameter = $124.8\ W^{0.127}$ and alveolar number = $5{,}356\ W^{0.454}$.

Thus growth of peripheral tissue is by expansion of existing alveoli and formation of new ones.

(vi) Respiratory surface area = $10.0\ W^{0.69}$ and is 3 times less than a mammal. 78% of the septa contain capillaries and 70% of the septal surface area is respiratory. Capillary 'bulging' causes an underestimation of surface area at x320 magnification by a factor of 1.45 in contrast to the 1.2 of the mammal in which there is less capillary 'bulging'.

(vii) One left lung of L. viridis (20g) was used for an EM morphometric study by a method of sub-sampling for capillarised regions of septa. Plasma volume in $cm^3 \times 10^{-3}$ = 16.1, capillary blood volume = 27.5 (hematocrit = 35%), the volume of respiratory epithelium = 5.0, respiratory interstitium = 9.08, respiratory endothelium = 4.5, non-respiratory interstitium = 3.57 and non-respiratory endothelium = 1.3. The arithmetic mean thickness $\bar{\tau}$ of the respiratory parts of the septa = 1.77 μm and the harmonic mean thickness of tissue = 0.527 μm and of plasma = 0.25 μm. A respiratory surface area of 98 cm^2 was estimated from this EM study which is close to the 85.5 cm^2 of the light microscopic study.

(viii) The proportionality of $W^{0.69}$ for respiratory surface area was assumed to be close to that for pulmonary diffusing capacity D_{Lo_2} since there was no thickening of the air to blood pathway with increasing body weight. Mammal/Lacerta ratios for the following were estimated:- respiratory surface area, 3.0, D_t = 5.1, D_p = 6.7, D_m = 5.5, D_e = 2.15 and D_{Lo_2} = 3 to 4. Although max $\dot{V}o_2$ of Lacerta was ten times less than a mammal, D_{Lo_2} was only 3 to 4 times less. Cardiovascular factors are considered to account for the remaining M/L differences.

(ix) In the newborn Lacerta, the lung volume is the value anticipated from adult data but its lung weight is 6 times less. Alveolar diameter and number fit adult regression coefficients but the depth is some 3 times smaller. Respiratory surface area is 4 times less than expected - it is not known what compensates for the fact that max $\dot{V}o_2$ is not similarly limited.

(x) The antero-posterior gradation in lung complexity has been quantified. In the newborn lung there is no gradation but in the adult (3.0g) there is a deeper rim of peripheral tissue in anterior regions which becomes more accentuated with increasing body weight. Lung growth in anterior regions is by expansion and division of alveoli but in posterior regions it is mainly by expansion.

(xi) The effect of inflation to 5, 10 and 15 cm H_2O fixation pressures was investigated in 3.0g lizards. Volumes within the physiological range for Lacerta (Chapter 3) were obtained. At 5 cm H_2O anterior regions were more expanded than posterior and since anterior regions contain more surface area this would use ventilated volumes more efficiently. At 10 cm H_2O posterior regions were more expanded but at 15 cm H_2O both regions were equally inflated. In the latter there was an excessive expansion of the central air space with some collapse of alveolar depth, folding of septa and a reduction in respiratory surface area. This correlates with the 'wasted' ventilation ($\dot{V}_E/\dot{V}o_2$) as $\dot{V}_E$ increases found in Chapter 2.

APPENDIX I

This describes the characteristics and errors of closed circuit respirometry and the derivations and errors of steady-state and dynamic equations used for analysing the open circuit respirometry data of Chapter 1 and 2.

APPENDIX II

This reviews anaesthetics used for reptiles. It describes the Lacerta dosage for intraperitoneal injection of Nembutal, the induction responses, the induction time, the period of surgical plane anaesthesia and the recovery period. L. viridis (20 to 30g) required 30-40 mg/kg and L. sicula (6 to 10g) required 20-30 mg/kg to reach a surgical plane. Such dosages for L. vivipara (2 to 4g) were not sufficient and higher dosages were lethal.

ABBREVIATIONS AND SYMBOLS

Symbol	Units	Definition
a	variable	Intercept of log. log. plots.
A-V difference	"	Arterial-venous differences in O_2 content or Po_2
b	"	Regression coefficient (i.e. slope) of log. log. plots.
BTPS	-	Body temperature and pressure and saturated with water vapour.
C	ml cm H_2O^{-1}	Compliance of total system.
C_L	"	Compliance of lung
C_w	"	Compliance of ribcage
CC or cc	-	Correlation coefficient
D	$cm^2 min^{-1}$	Diffusion coefficient
D_{Lo_2}	ml min^{-1} mm Hg^{-1}	Pulmonary O_2 diffusing capacity of the lung.
D_t	"	Pulmonary O_2 diffusing capacity of the tissue barrier.
D_p	"	Pulmonary O_2 diffusing capacity of the plasma layer.
D_m	"	Pulmonary O_2 diffusing capacity of the membrane.
D_e	"	Pulmonary O_2 diffusing capacity of the erythrocytes.
d	μm	Alveolar depth
di	"	Alveolar diameter
$\bar{d}i$	"	Mean corrected alveolar diameter
E_1 or E_2	-	Expiratory phases of ventilation
ERV	ml	Expiratory reserve volume
f	breaths min^{-1}	Frequency of breathing
f.s.d.	-	Full scale deflection
Fo_2	-	Fractional concentration of O_2
Fco_2	-	Fractional concentration of CO_2
ΔFo_2	-	Change in fractional concentration of O_2 in a stated period of time.
F_{Eo_2}	-	Fractional concentration of O_2 in outlet flow of the respirometer or head mask.
F_{Io_2}	-	Fractional concentration of O_2 in inlet flow of the respirometer or head mask.
ΔF_{Eo_2}	-	Change in F_{Eo_2} in a stated period of time.
FRC	ml	Functional residual capacity
I	-	Inspiratory phase of ventilation (Chapter 2)
		or Number of intersections with test line (Chapter 5).
IC	ml	Inspiratory capacity

Symbol	Units		Definition
IRV	ml		Inspiratory reserve volume
K	$cm^2\ min^{-1}\ mm\ Hg^{-1}$		Permeation coefficient
K_t	"		" " of tissue
K_p	"		" " of plasma
Kc	-		Velocity constant
l	cm		Length
L	"		Snout-vent length (Chapter 1)
	"	or	Test line length (Chapter 5)
L_T	"		Total test line length
LL	"		Lung length
L.vol	ml		Lung volume
LW	g		Lung weight
m	-		Number of fields
M_{run}	see text		Minimum cost of transport
n	-		Number of sections (Chapter 5)
	-	or	Number of alveoli (Chapter 5)
	-	or	Number of O_2 molecules per ml (Appendix I)
N	-		Number of experimental animals
NC.vol	ml		Nasal cavity volume
p	-		Number of points counted
P	cm H_2O or mm Hg		Pressure
ΔP	"		Change in pressure
P_{H_2O}	"		Water vapour pressure
P_B	"		Barometric pressure
Po_2	mm Hg		Partial pressure of O_2 in blood
P_{Ao_2}	"		" " " " " in alveoli
P_{Io_2}	"		" " " " " in inspired air or inlet of respirometer.
P_{Eo_2}	"		Partial pressure of O_2 in expired air or outlet of respirometer.
P_{50}	mm Hg		Po_2 at 50% O_2 saturation of blood
PBT	^oC		Preferred body temperature
P-V	-		Pressure-volume curve
r	cm		Radius
R	-		Respiratory quotient
	-	or	Gas constant (Appendix I)
	$cm\ H_2O\ ml^{-1}\ min^{-1}$	or	Resistance
RV	ml		Residual volume
$S_{1\ or\ 2\ or\ 3}$	-		Syringe
SC	$ml\ cm\ H_2O^{-1} FRC^{-1}$		Specific compliance
STP	-		Standard temperature and pressure
STPD	-		Standard temperature and pressure of dry gas.

Symbol	Units		Definition
S_a	cm^2		Surface area of alveolar surface
S_c	"		" " " capillaries
S_e	"		" " " erythrocytes
S_v	cm^2/cm^3		Surface density
t	sec or min		Time period
	^oC	or	Temperature
T	"		Standard temperature = t + 273^oC
TLC	ml		Total lung capacity
Tr.D	cm		Tracheal diameter
Tr.L	cm		Tracheal length
Tr.vol	ml		Tracheal volume
V	ml or L		Volume
Vc	ml		Capillary volume
V_L	"		Lung volume
V_S	"		Syringe volume
V_T	"		Tidal volume, minimum, average or maximum.
V_{Tu}	"		Tubing volume
V_v	cm^3/cm^3		Volume density
VC	ml		Vital capacity
$\Delta V/\Delta P$	ml cm H_2O^{-1}		Compliance
$\Delta V/\Delta P$. FRC	ml ml^{-1} cm H_2O^{-1}		Specific compliance
$\dot{V}$	ml min^{-1}		Flow rate
$\dot{V}_E$	"		Flow rate for outflow air
	"	or	Ventilation volume, $\dot{V}_E = f \times V_T$.
$\dot{V}_I$	"		Flow rate for inflow air
$\dot{V}o_2$	ml hr^{-1} or ml min^{-1}		Oxygen consumption; maximum, exercise, routine, minimum, resting or standard.
$\dot{V}co_2$	"		Carbon dioxide production
$\dot{V}o_2/\dot{V}_E$ x 100	ml min^{-1} STPD/ ml min^{-1} BTPS		O_2 extraction as a %
$\dot{V}_E/\dot{V}o_2$	ml min^{-1} BTPS/ ml min^{-1} STPD		Ventilation requirement
W	g		Body weight
Y	-		Correction factor for degree of capillarisation.
α	ml ml^{-1} mm Hg^{-1}		Bunsen's solubility coefficient
τ	sec or min		Time constant
τ_h	μm		Harmonic mean thickness
τ_{hp}	"		" " " of plasma
τ_{ht}	"		" " " of tissue
$\bar{\tau}$	"		Arithmetic mean thickness

Symbol	Units	Definition
α	$ml\ ml^{-1}\ min^{-1}\ mm\ Hg^{-1}$	Rate of association
μ	poises	Coefficient of air viscosity
12 hrL/12 hrD	-	12 hours of light/12 hours of dark
1 day S or 3 day S	-	1 or 3 days of starvation
x and y	-	Various definitions. Defined when locally used.

GENERAL INTRODUCTION

As is perhaps inevitable, the understanding of vertebrate aerial respiration is based predominantly on mammalian studies. Much research on lower vertebrates is now required to maintain a balance of knowledge. This will also allow factors that are essential and basic to the respiratory system to be distinguished from those that are specialisations either for an adaptation to a certain environment or for a greater metabolic capacity. By comparing the respiratory mechanisms of a lower vertebrate with those of the better understood mammal, a greater insight into the former system may be gained. Conversely, by examining a less complex respiratory system, greater insight into the mammalian system may be possible.

The choice of a completely aerial breather, other than a mammal, is restricted to the class Aves, Reptilia or Amphibia. Birds are homeotherms, like the mammal, but they have evolved very specialised lungs (Dunker, 1972) which are ventilated by a costal suction pump that creates a continuous air flow in contrast to the mammalian tidal air flow (Bretz & Schmidt-Nielsen, 1971, Brackenbury, 1971, Scheid & Piiper, 1972). Reptiles have lungs that are fairly easy to recognise as primitive counterparts of the mammalian lung (Marcus, 1937) and are ventilated by a costal suction pump producing tidal air flow (Boelaert, 1941). Even the limb pump of the Testudine creates a tidal air flow (Gans & Hughes, 1967, Gaunt & Gans, 1969). Reptiles are, however, poikilotherms although they can behaviourally (and to some extent, physiologically) thermoregulate often to temperatures close to the mammalian body temperature (Templeton, 1970). There is much species-dependent variability in this reptilian capacity for thermoregulation (Dawson, 1967, Templeton, 1970, Cloudsley-Thompson, 1971). Amphibians, whilst having similar primitive lungs to reptiles (Marcus, 1937), use a buccal force pump to create their tidal air flow (Gans, 1970). As well as a pulmonary

gas exchange surface, amphibians also make considerable use of bucco-pharyngeal and cutaneous surfaces (Whitford & Hutchison, 1963, Gans, 1970). At early stages of their life history, they are aquatic relying on gills, bucco-pharyngeal and cutaneous surfaces and in some species lungs never develop (Moore, 1964). Amphibians are poikilothermic but they have little of the reptilian capacity for thermoregulation (Brattstrom, 1970).

Thus the obvious choice for a respiratory system similar to the mammal but less complex resides in the class Reptilia. Within this class a further selection of a species has to be made from the orders Testudine, Crocodilia, Rhyn chocephalia and Squamata. The Testudine, by developing an outer shell to which the ribs have fused, have had to adopt a limb pump for ventilation. Many are capable of aquatic respiration using a highly vascularised buccal cavity and many can withstand a high degree of anaerobic metabolism (Belkin, 1968, Bellairs, 1969). Crocodilia, apart from caimans, are large and difficult animals unsuitable for most laboratory facilities. They are also considered to be similar to the reptilian stem from which birds evolved (Goodrich, 1958). The rarity of the Sphenodon (Rhyn chocephalia) eliminates itself as a selectable species. It is, however, very lizard-like.

Snakes and lizards (Squamata) are completely aerial breathers, have adopted a predominantly terrestrial mode of life and have many species which are adaptable to laboratory conditions. They are, however, capable of a greater degree of anaerobic metabolism than mammals (Bennett, 1972b, Bennett & Licht, 1972) and have recently been shown to make use of some cutaneous respiration (Schulteus & Crawford, 1969, Standaert & Johansen, 1974). During normal respiration only about 4% total CO_2 production and 2% total O_2 consumption were attributable to cutaneous pathways, in contrast to the 80% $\dot{V}co_2$ and 35-50% $\dot{V}o_2$ of amphibians (Whitford & Hutchison, 1963). Hence the Squamata were selected and lizards chosen as a closer mammalian counterpart than the limbless, long, cylindrical snake. The genus Lacerta

was further selected as a typical lizard without any obvious, exceptional specialisations.

In this respiratory study of Lacerta, the aim was to correlate physiological findings with anatomical and morphometric studies on the lung (such a dual investigation is rarely undertaken in any animal) and to compare each parameter with those of a mammal. Answers to the following questions were sought: how much O_2 is consumed by a lizard at rest, what is its maximum $\dot{V}o_2$, how frequently and with what tidal volume does it breathe at rest, what are the lizard's ranges of tidal volume, frequency and hence ventilation volume, does the lizard extract the same proportion of O_2 from the ventilated volume at all levels of activity and how do all these parameters compare with a mammal's? Such physiological limitations and/or advantages of the Lacerta versus the mammalian respiratory system are investigated in Chapters 1 and 2. Further questions were asked regarding the compliance of the respiratory system and its components, the pressures involved in its inflation, the volume of air left in the lungs after a normal or maximum expiration and the role of a lung surfactant in a primitive lung (Chapter 3).

The simplicity of the Lacerta lung was examined in terms of its histology and for the first time its ultrastructure (Chapter 4) .
To correlate anatomical and physiological facts, measurements were made of the amount of lung surface area, the capillary density in the lung tissue and hence its functional respiratory surface area, the size of the alveoli and the lung volume necessary to provide this surface area, the proportion of the lung volume that could be anatomically considered respiratory or wasted (dead space) and the diffusion distance between air and blood (Chapter 5). Using some of these measurements, it is possible to estimate the maximum pulmonary diffusing capacity for the lizard lung and compare it with mammalian values (Weibel, 1970/71) and with actual maximum $\dot{V}o_2$ values.

This can give some insight into any limitations the Lacerta respiratory system may have.

When making the Lacerta/mammalian comparisons, it is necessary to compare values from animals of the same body weight. One cannot assume that all parameters increase their value in direct proportion to body weight. A lot of work has been accomplished in determining the mammalian body size relationships of physiological, respiratory parameters (e.g. Stahl, 1967) and of lung parameters (e.g. Weibel, 1970/71, 1972) with attempts to correlate the two. It is fairly well established, for instance, that $\dot{V}o_2$ is proportional to body weight not directly as $W^{1.0}$ but as $W^{0.75}$. Tidal volume is, however, proportional to $W^{1.0}$ but the frequency proportionality of $W^{-0.25}$ adjusts the ventilation volume to $W^{0.75}$, thereby matching the $\dot{V}o_2$ relationship. Respiratory surface area in some studies is related to $W^{0.75}$ also (Tenney & Remmers, 1963) but in others it is related to $W^{1.0}$ (Weibel, 1972). Such studies of body weight relationships are of great interest. As Stahl (1967) has said, the integrated scaling of physiological and anatomical variables is a necessity for the correct functioning of the body over any substantial change in weight.

If the size range is adequate (10 to 100 times or more), allometry or log. log. plotting of variables against body weight can give clear regression relationships because individual variation is minimised. Values obtained for interspecific animals will give an overall generalised regression coefficient and then detailed intraspecific studies, or even individuals, can be compared with the predicted value for the body weight concerned. Any physiological specialisation may thus be demonstrated. Finally, by cancelling power law prediction formulas for various parameters, one can obtain theoretical power relationships for parameters not actually experimentally measured (Stahl, 1967). It was important, therefore, to examine Lacerta over a suitable size range not only to be sure of the correct

absolute values when making comparisons with mammals but also to gain valuable information about respiratory scaling.

It was impossible to get a sufficient size range within one Lacerta species, so an intrageneric study was undertaken using L. vivipara (adult 1.0 to 4.0g, newborn 0.2g), L. sicula (4.0 to 10.0g) and L. viridis (10.0 to 40.0g). Although Stahl (1967) has pointed out the value of intraspecific studies, they are rarely examined. It is difficult, however, to undertake an intraspecific study which does not involve the use of immature animals to provide lower weight values. This could easily give misleading information because of the differences between developmental and adult growth (see Burri, Dbaly & Weibel, 1974). An intrageneric study is an ideal situation in which only adults or juveniles, past developmental stages, are used and this to my knowledge has never before been undertaken. In the ensuing chapters, the term intraspecific has sometimes been used loosely to describe this intrageneric Lacerta study.

In analysing the body weight relationships of the various Lacerta respiratory parameters, logarithmic regressions were fitted by the method of least squares to obtain the regression coefficient (i.e. the slope of the log. log. plot), the intercept with the y axis and the correlation coefficient of the data. Lung morphometric data is treated in the same manner by Weibel (e.g. 1972). No attempt was made to assess confidence limits or standard deviations of the slope because the log. log. approximation to the regression equation itself has been shown to have errors (Glass, 1967, Zar, 1968, Jolicoeur & Heusner, 1971). This does not, however, detract from the usefulness and importance of logarithmic regression analysis, providing its limitations are remembered. Similarly, confidence limits and standard deviations of the slope are perhaps better than no test at all, especially if great importance is placed on small differences in slopes, e.g. $W^{0.85}$ and $W^{0.9}$. No such conclusions were attempted with

the Lacerta data. As a check, however, log. log. plots of Lacerta which had the most data scatter were found to have a standard deviation of no more than ± 0.05 for the regression coefficient. It must also be remembered that the correlation coefficient is a very uninformative index of data scatter, as will become apparent in the ensuing chapters.

CHAPTER 1

THE RELATIONSHIP BETWEEN METABOLISM AND BODY WEIGHT DURING REST AND EXERCISE

INTRODUCTION

Resting Metabolism

As Stahl (1967) has stated, an integrated scaling of physiological and anatomical variables is a necessity for the correct functioning of the body over any substantial change in body weight. Metabolic rate is probably the prime variable and was first studied by Rubner (1883) in dogs. He found a decrease in resting metabolic rate per unit body weight as size increased.

When oxygen consumption, $\dot{V}O_2$ ml hr^{-1}, is plotted on log. - log. co-ordinates against body weight, W,g, a linear relationship is obtained having a regression slope, b, and an intercept, a, in the equation,

$$\log \dot{V}O_2 = \log a + b \log W \quad \underline{OR} \quad \dot{V}O_2 = a\, W^b.$$

This equation can be converted to indicate weight-specific metabolic rate by dividing by W.

$$\frac{\dot{V}O_2}{W} = aW^{(b-1)}.$$

If metabolic rate per unit body weight is constant irrespective of size, then b equals +1.0, but if it increases or decreases with size, then b will equal > 1.0 or < 1.0, respectively.

Rubner found that b equalled 0.67 for dogs over one log. cycle of body weight. This is also the relationship by which body surface area is related to body weight and hence the metabolic 'surface law' was established together with the argument that temperature control was the prime reason for this b value. However, Kleiber (1947) reviewing further work and examining a much larger size range of placental mammals, obtained a slope of 0.756.

He stated that a size range of at least 9:1 (approximately one log. cycle) was necessary to distinguish between 0.67 and 0.75 and 3:1 to distinguish between 1.0 and 0.75. He did not mention the number or distribution of measurements necessary.

In 1953, Zeuthen reviewed data for a large number of organisms finding slopes of 0.7 for protozoa, 0.95 for metazoa, 0.8 for poikilotherms and 0.75 for homeotherms. Scatter in the data within a group was considered to be due to different states of growth, ageing, motility, digestive activity or body temperature. Bertalanffy (1951, 1957) has divided resting metabolic scaling into three types, those obeying $W^{0.66}$, i.e. fishes, mammals and lamellibranchs, $W^{1.0}$, i.e. insect larvae, and $W^{0.75}$, i.e. planorbids. However, in a later review, Hemmingsen (1960) has shown that if the 'short weight range' slopes of other authors are grouped together and standardised for a constant temperature, all groups give mean slopes of 0.75, though obviously with the intercept value increasing with increasing phylogenetic standing of the group. He suggested that deviations in short range lines from a common slope of 0.75 could be due to non-standardisation of the experimental conditions, e.g. variations in obtaining true resting states with no muscular effects, the fact that smaller animals are more quickly starved than larger ones, variations in season and temperature effects on animals within a single study.

A common slope of 0.75 for both homeotherms and poikilotherms would indicate that metabolic rate is not controlled by body surface area and that temperature regulation is not the main reason for metabolic scaling. Bartholomew (1972) discusses this in more detail. Hemmingsen (1960) has suggested that during evolution of sizes, there has been a tendency for energy metabolism to increase in proportion to size but it has been limited by surface area functions and thus a compromise slope of 0.75 has resulted.

More recent reviews for mammalian data (both placental and marsupial) continue to support the common 0.73 to 0.76 slope (Stahl, 1967,

Schmidt-Nielsen, 1970, Bartholomew, 1972). Slopes of 0.723 were obtained for birds (except the order Passeriformes) and 0.724 for Passeriformes with the combined data giving a slope of 0.668 (Lasiewski & Dawson, 1967), whilst a slope of 0.744 was found in an earlier study on birds (King & Farner, 1961). All data covered about 5 log. cycles of body weight.

Within the poikilotherms, Winberg (1956) has found an interspecific slope of 0.81 for resting fish metabolism, but for four species of fresh-water fish a slope of 0.7 was obtained (Kayser & Heusner, 1964). Fry (1957) and Brett (1965) reviewed further data finding intraspecific slopes between 0.7 and 1.0 which sometimes depended on the environmental temperature. For salmon, Brett (1965) determined a slope of 0.775 and states the need for determining metabolic slopes for each species over a range of temperatures. All fish data covered about 3 to 4 log. cycles of body weight within a single study.

A few amphibian slopes have been determined, being interspecifically 0.71 for anurans (Hutchison, Whitford & Kohl, 1968), 0.72 for lungless salamanders and 0.856 for lunged salamanders (Whitford & Hutchison, 1967) over 1 to 1.5 log. cycles of body weight. The size range within a species or genus is not great enough for meaningful interpretations to be given to the different slopes of 0.52 to 0.94.

Examination of the recent literature for reptiles shows considerable variation and deviation from the 0.75 value. Dawson & Bartholomew (1956) collected resting metabolic data at 30^{o}C interspecifically from lizards covering 3 log. cycles of body weight and derived the equation, $\dot{V}o_2 = 1.26\ W^{0.54}$. Values of 0.47 and 0.68 were found intraspecifically for Uta and Sceloporus, respectively, but they only covered a 0.5 log. cycle of body weight. Later, Bartholomew & Tucker (1964) replotted the inter-specific relationship using further data and obtained the equation, $\dot{V}o_2 = 0.82\ W^{0.62}$. The 95% confidence limits were rather wide but this was considered to be due

to the limited data (23 animals) and the different methods used by different workers. Templeton (1970) collected data for resting $\dot{V}O_2$ at 37°C in lizards over 3 log. cycles of body weight and found $\dot{V}O_2 = 1.33\ W^{0.65}$. In the latest review, not yet published, Bennett & Dawson (1973) give interspecific lizard slopes of 0.83 at 30°C and 0.82 at 37°C. This is also the value found within the varanid genus over 2 log. cycles of body weight (Bartholomew & Tucker, 1964).

Data for snakes is also very variable giving slopes of 1.09 for Boids and 0.98 for Colubridae, each over 2 log. cycles, but giving a slope of 0.86 together, over 3.5 log. cycles of body weight (Galvão, Tarasantchi & Guertzenstein, 1965). A slope of 1.12 (Benedict's data, 1932) and 0.66 (Vinegar, Hutchison & Dowling, 1970) has also been obtained for several species of Boids and a combination of these three sources of data yielded a slope of 0.85 over 2 log. cycles of body weight. Dmi'el & Borut, (1972) give a value of 0.62 for Spalerosophis over a 0.75 log. cycle.

Using only 0.5 log. cycle of body weight, Benedict (1932) and Hutton, Boyer, Williams & Campbell (1960) have stated that metabolic rate per unit body weight was more or less constant in tortoises, i.e. b = 1.0. Hughes, Gaymer, Moore & Woakes (1971), however, have shown intraspecifically in giant tortoises over 3 log. cycles of body weight, that resting metabolic rate is related to body weight by a regression slope of 0.82. Interspecific data over 3 log. cycles in Crocodilia has given a value of 0.926 (Huggins, Hoff & Valentinuzzi, 1971). Kayser (1951) combined his own results on amphibians and small reptiles with those obtained by Benedict (1932) on larger species and found a general proportionality of $W^{0.728}$.

Thus from the literature, one might expect that using very large size ranges and species numbers, interspecific metabolic variations, both real and experimental, would cancel out to give a common 0.75 slope. It has yet to be determined whether intraspecific studies (or within a genus or family) deviating from the 0.75 slope indicate physiological specialisation of that species or a lack of an adequate size range or whether rigorous

standardisation of the experimental conditions was ignored. Very often there is a great deal of imbalance between the numbers used at each specific body weight, especially at the top or bottom end of the range. This will obviously 'weight' the regression slope at either end of the size range causing slopes > 0.75 or < 0.75. Schmidt-Nielsen (1970) favours a lack of an adequate size range or standardisation explaining deviations from 0.75, whereas Bartholomew (1972) favours different slopes for different species which when pooled together obey the 0.75 relationship.

It is well known that within the reptiles (even amongst lizards) a range of species would vary very considerably in their lung structure complexity per unit body weight (see Chapter 4), in their preferred body temperature (Dawson, 1967) and their degree of spontaneous activity. Thus, there are two alternatives for studying lizard metabolic scaling, either (a) using extensive interspecific data with equal numbers at each body weight and a full representation of lizard types with each type represented evenly throughout the size range, or (b) employing rigorous standardisation within a species or genus providing at least 1 to 2 log. cycles of body weight are covered with equal numbers at each body weight. Alternative (b) can obviously be more easily achieved but an adequate method of standardisation has to be determined.

A stable minimal rate of energy metabolism, which represents an approximation of the rate of metabolism of a fasting adult animal at rest and under no thermal stress is defined as the mammalian basal metabolic rate. Since poikilotherms are temperature-dependent, the term standard metabolic rate is used for the minimum metabolism of fasting individuals at a given environmental temperature. As Bartholomew (1972) has pointed out, the environmental circumstances of minimum stress differ from species to species and the accuracy of the metabolic determination will depend largely on how well the investigator knows his experimental species.

In all reptiles so far investigated, standard $\dot{V}O_2$ has been taken as either the mean experimental minimum or as a resting average when the animal was quiet from periods of 15 minutes to a few hours. A few investigators (e.g. Roberts, 1968, Greenwald, 1971, Bennett & Licht, 1972) however, have left the animal for 18-24 hours in a respirometer until a minimum stable level was obtained and measured over an hour. In many instances, the animals were restrained and therefore probably not completely relaxed. Sometimes they were shielded from visual and auditory stimuli but were never subjected to their normal light/dark regimes. The degree of starvation, if any, was variable or never stated.

The study presented here was an attempt to rigorously standardise the determination of standard metabolic scaling within the genus, Lacerta, covering an adequate size range of 0.2 to 38g. The lizards were starved for 1 or 3 days before the experiment. $\dot{V}O_2$ was recorded continuously for a full 24 hours under the lizard's normal laboratory 12hrL/12hrD regime at a constant temperature of 28 $\pm$ 1^{o}C whilst the unrestrained lizard was shielded from visual and auditory stimuli. Constant dark or light conditions and restraining were also tested to see how much they influenced the lizards standard $\dot{V}O_2$. For the initial regression analysis, only lizards of at least 1 year of age were considered adult, since developmental changes in recently hatched 0.2g L. vivipara might obscure scaling relationships.

Active Metabolism

In many respects, active metabolic scaling is a far more informative parameter to measure since it is more likely to uncover interspecific variation. It is also experimentally much easier to measure the anatomical maximum gas exchanging surface area.

Hemmingsen (1960) reviewed maximum metabolic activity in mammals and found a common slope, again of 0.75. Pasquis, Lacaisse & Dejours (1970) have determined maximum $\dot{V}O_2$ sustainable for 1 to 2 min in small mammals under conditions of shivering through cold exposure and maximum muscular exercise

on a treadmill (with and without cold exposure). Maximum $\dot{V}O_2$ was related to body weight by a regression slope of 0.73 having an intercept 6 to 7 times greater than the standard $\dot{V}O_2$ (using 1.5 log. cycles of body weight). Wunder (1970) also found similar ratios of maximal to resting $\dot{V}O_2$ in small mammals. In reviewing data for larger mammals (dog, man and horse) Pasquis et al (1970) found a slope of 0.79 with a max.$\dot{V}O_2$/std.$\dot{V}O_2$ ratio varying from 11 to 22, i.e. max. $\dot{V}O_2$ had a larger intercept than that in small mammals. If max. $\dot{V}O_2$ data for small and large mammals were not separated, a slope of approximately 0.95 would be obtained.

Data available for bird flight would strongly suggest that the max. $\dot{V}O_2$ slope is approximately 0.75 with an intercept 10 times greater than at rest (Berger, Hart & Roy. 1970, Bartholomew, 1972). Much work has been published on swimming metabolism in fish and its scaling has been examined by Brett (1965, 1972). The slope of metabolism versus size increases regularly with increasing activity, starting at 0.775 for resting metabolism and finishing with 0.97 during maximal sustained swimming. Small salmon increase their metabolism 5 times whilst large salmon increase theirs 16 times.

Active metabolic data is very limited in the amphibians. Turney & Hutchison (1974) give the only account but they are not concerned with scaling. They discussed the importance of the time of day in determining metabolic scope. Max.$\dot{V}O_2$/min.$\dot{V}O_2$ gave a ratio of 30 times which was misleading since max.$\dot{V}O_2$/resting $\dot{V}O_2$ for a specific time of day is no higher than 1.5 times. Max.$\dot{V}O_2$ was caused by electrical stimulation. Active metabolic scaling has only been examined in one reptile, Testudo gigantea (Hughes, Gaymer, Moore & Woakes, 1971). A slope of 0.97 was obtained with increases above resting of 2-fold for small and 6-fold for large tortoises. Activity was stimulated only by periodic movement of the respirometer.

Metabolic scope is defined as the difference between maximal and minimal metabolic rates, max.$\dot{V}O_2$ - min.$\dot{V}O_2$, at a particular temperature and

it signifies the energy required for activity above that simply needed for body maintenance (Fry, 1947). Metabolic scope is very variable in reptiles and the temperature at which it is greatest varies from species to species. The temperature is often not the species' preferred body temperature (Templeton, 1970). Reptiles, with the exception of Varanus, however, depend extensively on anaerobic pathways to provide the major source of energy during short vigorous activity, which is in contrast to mammals (Moberly, 1968b, Bennett, 1972a, 1973b). Thus metabolic scope is only indicative of the aerobic capacity for activity.

Maximal $\dot{V}O_2$ rates have been obtained by using the data from spontaneous, violent struggles of the reptile against its restraining bonds or by subdermal electrical shocking. For some lizards, electrical shocking does not increase $\dot{V}O_2$ values above those found for spontaneous struggling (Bartholomew & Tucker, 1964). Anaerobic pathways are always operating during these maximal steady-state $\dot{V}O_2$ recordings, except in Varanus. In many respects, the ratio $\frac{\text{max.}\dot{V}O_2}{\text{std.}\dot{V}O_2}$ is easier to interpret than metabolic scope and hence the former is used here. The range of ratios for each species is a result of its variation with environmental temperature. Max.$\dot{V}O_2$/resting, min. or std. $\dot{V}O_2$ ratios have been recorded as 3.6 in Dipsosaurus (Dawson & Bartholomew, 1958) or 10 to 17 (Bennett & Dawson, 1972), 5 to 8 in Amphibolurus (Bartholomew & Tucker, 1963), 6.5 to 10 in Varanus (Bartholomew & Tucker, 1964), 5 in Tiliqua (Bartholomew, Tucker & Lee, 1965), 3 to 5 in Iguana (Moberly, 1968a), 6 to 7 in Cnemidophurus (Asplund, 1970), 7.5 to 20 in Varanus and 5 to 16 in Sauromalus (Bennett, 1972a). In snakes, ratios of 4 to 5 have been found by electrical shocking (Greenwald, 1971, Dmi'el & Borut, 1972) and a value of 9.3 for brooding pythons if the environmental temperature is decreased (Hutchison, Dowling & Vinegar, 1966).

Such variation in max.$\dot{V}O_2$ and the temperature at which the highest ratio occurs, indicates the futility of attempting to elucidate reptilian interspecific relationships between active metabolism and body weight, even

within lizards. Intraspecific (or within a genus) studies are obviously necessary.

Exercise

Lizards have only been exercised on a treadmill in two instances; once by Moberly (1968b) using 1 kg iguanas but only at low walking speeds, 2-6 m min^{-1}, and more recently by Bakker (1972) and Taylor (1973) using a number of different species (14g to 1.2 kg). Limbless terrestrial locomotion in 24g garter snakes has also been studied on a treadmill (Chodrow & Taylor, 1973) at speeds of 3 to 15 m min^{-1}.

Mammalian exercise on a treadmill has been well documented. Steady-state $\dot{V}O_2$ increases linearly with the running speed but the intercept is always above resting (Taylor, Schmidt-Nielsen & Raab, 1970, Yousef, Robertson, Dill & Johnson, 1970, 1973). Most mammals give this rectilinear relationship but a curvilinear one has been found in two species (Segrem & Hart, 1967, Wunder, 1970) with the line passing through resting $\dot{V}O_2$. In both cases, however, the data was not extensive. Moberly (1968b) found that Iguana also gave a curvilinear relationship between $\dot{V}O_2$ and speed, indicating that higher speeds were more efficient. Bakker (1972), Taylor (1973) and Chodrow & Taylor (1973) however, obtained rectilinear relationships for lizards and snakes but with the intercept only a little above resting $\dot{V}O_2$. Metabolism was always aerobic in all these studies. Walking in man gives an exponential relationship which becomes rectilinear when running occurs (Asmussen, 1964, Schmidt-Nielsen, 1972). $\dot{V}O_2$ of swimming in fish also increases exponentially as speed is increased (Brett, 1972), whilst $\dot{V}O_2$ was high at low and high flying speeds, but was low at medium flying speeds in birds (Tucker, 1968).

Attention has also been given to the scaling of the energetic cost of locomotion. Three terms are used for this cost:

(a) total cost of transport, determined for the maximum aerobic speeds = total $\dot{V}O_2$ g^{-1}/speed

(b) net cost of transport = exercise $\dot{V}O_2\ g^{-1}$ - resting $\dot{V}O_2\ g^{-1}$/speed, and

(c) minimum cost of transport = exercise $\dot{V}O_2\ g^{-1}$ - y intercept $\dot{V}O_2\ g^{-1}$/speed.

Weight specific costs are always greater in the smaller animal as with standard or maximum $\dot{V}O_2$. Cost of transport increases according to the mode of locomotion in the following order:- swimming, flying and running or walking. Poikilotherms (both invertebrate and vertebrate) and homeotherms have the same cost of transport for the same mode of locomotion (Tucker, 1970, Schmidt-Nielsen, 1972). Bipedal running is more expensive than quadrupedal running in larger animals, but the reverse is the case for small animals (Fedak, Pinshow & Schmidt-Nielsen, 1974).

Total metabolic cost of transport (weight-specific) when plotted against body weight on log. co-ordinates gives a straight line for both swimming and for flying, the slopes being -0.25 and -0.227, respectively (Schmidt-Nielsen, 1972). The relationship for quadrupedal walking/running, however, is not a straight line but is more complex, with the cost of transport becoming exponential in very small animals. If, on the other hand, the minimum cost of transport is plotted for these runners, a regression slope of $8.46\ W^{-0.4}$ is obtained. This method of presentation is necessary because the extent that the intercept is above the resting $\dot{V}O_2\ g^{-1}$ level in runners is inversely related to body weight on a slope of -0.37 (Tucker, 1970, Schmidt-Nielsen, 1972).

Bakker (1972) and Taylor (1973) calculated the minimum cost of transport for lizards finding that cost even in the wide-track sprawling gait of the lizard was the same or a little less than that of a mammal. Limbless, terrestrial, snake locomotion costs less than half that of a varanid lizard, indicating that like swimming, it requires less energy than moving with limbs (Chodrow & Taylor, 1973). None of the reports determined the scaling of metabolic cost, but for lizards values fell around the line for mammals (Taylor, 1973).

In the study presented here, another genus of lizards, Lacerta, has been subject to exercise on a treadmill to determine whether:

(a) the relationship of $\dot{V}O_2$ to speed is curvilinear or rectilinear,

(b) whether the regression line passes through the resting $\dot{V}O_2$ or not, and

(c) how minimum metabolic cost of transport is related to body weight.

Active metabolism was only recorded during the normal activity periods of Lacerta; a condition which has been suggested by Asplund (1970) and Turney & Hutchison (1974). Also the maximum sustainable $\dot{V}O_2$ over 1 to 2 minute periods has been measured to determine if active and standard metabolism are related in the same way to body weight and whether these relationships are similar to the common 0.75 slope.

$\dot{V}O_2$ and $\dot{V}CO_2$ Measurements

Reptilian $\dot{V}O_2$ and $\dot{V}CO_2$ measurements have been made in closed systems by Scholander analysis (e.g. Hughes, Gaymer, Moore & Woakes, 1971) or by absorption of CO_2 and manometric measurement of the O_2 consumed (e.g. Prieto & Whitford, 1971). Hughes, Gaymer, Moore & Woakes (1971) used a more sophisticated technique of circulating the air in a closed constant volume system to ensure adequate mixing, whilst monitoring continuously % O_2 and % CO_2. Using either whole animal respirometers (e.g. Dawson & Bartholomew, 1958; Boyer, 1963, 1967) or face masks (e.g. Tucker, 1966, Moberly, 1968a,b, Bennett, 1972a) open circuit systems have also been used in which the animal is never subjected to increasing levels of CO_2. In these open circuits, only % O_2 has been monitored (except Nielsen, 1961) and $\dot{V}O_2$ was only recorded during steady-state conditions.

During this study of Lacerta, both % O_2 and % CO_2 were monitored continuously in both closed and open circuit respirometer conditions. Diurnal rhythms and standard $\dot{V}O_2$ were determined by both methods, but exercising $\dot{V}O_2$ only by the latter. A re-appraisal of the equations and errors involved in estimating $\dot{V}O_2$ and $\dot{V}CO_2$ under closed circuit and steady-state open circuit conditions has also been undertaken. A dynamic method

of estimating $\dot{V}o_2$ and $\dot{V}co_2$ in open circuits has been devised to allow minute by minute calculations of gas exchange. This dynamic open circuit analysis has been extended for use with a face mask and is described in Chapter 2. Much of the description and testing of closed and open circuits together with the derivations of equations and errors have been placed in Appendix I.

METHODS

Animal Care

L. vivipara were collected locally in the Mendips between late March and August 1971-73. The viviparous young were born in captivity during July and August and were kept apart from the adults. *L. sicula* and *L. viridis* were obtained from various reptile importers between April and September and some were collected in France during the summer of 1971. The latter two species can be kept in captivity throughout the year and will remain healthy, but *L. vivipara* cannot live through the winter without hibernating. Under laboratory conditions, hibernation was not possible.

Each species was kept in separate 60 x 30 cm aquaria, the floor of which was covered with sand and hay. Rocky shelters and water dishes were provided, the terrain being kept moist around the latter. *L. viridis* were sometimes housed in a 240 x 60 cm cage with similar floor covering but including gravel. The plastic netting composing the sides and roof of this cage provided extensive climbing areas. Small pieces of this netting were also placed in the aquaria. Overhead lighting giving an incident temperature of 35°C was switched on by time clocks between 6.00 and 18.00 hours. Environmental temperatures were 28 ± 1°C for *L. sicula* and *L. viridis* and approximately 20°C for *L. vivipara*. At higher temperatures, a high death rate occurred after a few weeks or months in the latter species.

Tenebrio larvae and blowfly maggots formed the staple part of the lizard's diet in captivity, being supplemented occasionally with earthworms, cockroaches, spiders and other insects. Excess food was given three times a week. Avery (1971) has shown that during such *ad libitum* feeding, *L. vivipara* do not exceed the maximum feeding rates found in the wild. The recently hatched *L. vivipara* were continuously supplied with green and blackflies because if starved for more than 2 days they would not begin re-feeding. Liquid multivitamins were frequently given with either the food or water. Vogel (1963) proved a useful guide for reptilian care.

Mite epidemics of Ophionyssus sp. sometimes occurred with the arrival of a new batch of lizards from importers. These mites were found under the scales of axilla, inguinal and eye regions in L. sicula and L. viridis only and were best removed with swabs of liquid paraffin. 'Vapona' flystrips were then placed overnight in the cages (but out of the lizards' reach) to kill any remaining mites. The egg stage is very resistant and repetitive treatment was usually necessary. Providing the mites were removed within a few days, the lizards appeared unharmed. Inflammation of the eyes together with a general listlessness and wasting sometimes occurred and is thought to be due to vitamin deficiency (Reichenbach-Klinke & Elkan, 1965). Such diseased lizards never recovered. L. viridis occasionally suffered from dermal tumours, known as tree bark tumours, which are completely harmless. Their cause is not known (Reichenbach-Klinke & Elkan, 1965).

$\dot{V}O_2$ and $\dot{V}CO_2$ Measurements

% CO_2 was monitored using the micro-catheter sample cell in the pickup of the Beckman LB1 medical infra red CO_2 analyser. The sample pump of this analyser circulated the air through the closed circuit at 450 ml min^{-1} and through the open circuit at 100 ml min^{-1}, flow being measured accurately by a 0-500 ml min^{-1} rotameter. % O_2 was monitored with a Servomex industrial paramagnetic O_2 analyser by measuring the difference between a constant reference gas of 20.95% O_2 (i.e. fresh air taken from outside to avoid room fluctuations) and the varying sample gas of the respirometry circuit. This differential recording permitted 0.1% O_2 changes to be measured accurately without the necessity for backing off the zero. Analyser outputs were continuously displayed on a Rikadenki three channel pen recorder with a 0.5%, 1.0%, 2.0% or 5.0% full scale deflection at a paper speed of 5 mm min^{-1}. A full scale deflection (f.s.d.) of the Rikadenki pen covered 25 cm width of chart paper taking 0.33 secs. Both analysers were mechanically zeroed once a month and calibrated before and checked for drifts after each experiment. The CO_2 analyser was the more reliable. All calibration gases were made with an H. Wosthoff gas mixing pump giving $\pm$ 0.015% accuracy. Gas mixtures

were occasionally checked by Scholander analysis. (For further calibration details, see Appendix I).

Gases were dried in the sample circuit using calcium chloride because it had been shown in preliminary experiments that the recyclable silica gel absorbed CO_2 presumably by physical association and intermittently released it, whereas $CaCl_2$ did not. Cotton wool plugs served to retain the $CaCl_2$ particles which were replaced every 48 hours. Since the CO_2 level never changed in the reference circuit, drying with silica gel was adequate.

The third Rikadenki channel monitored temperature at a 500 mv gain using a thermistor probe in the respirometry tubing. Its output was linear over a 20-40^{o}C range and was used previously by Hughes, Gaymer, Moore & Woakes (1971). All experiments were conducted in a high temperature room cycling once every hour between 27 and 29^{o}C in extreme cases.

Closed Circuit

Fig. 1.1 illustrates the plumbing for the closed respirometry circuit with the lengths of interconnecting tubing being approximately to scale. 80% of the tubing was steel of i.d. 0.45 cm and a wall thickness of 0.2 cm, whilst 20% was transparent vinyl Portex tubing, i.d. 0.675 cm and 0.2 cm wall thickness, which gave pliability to an otherwise rigid system. Respirometers of 7, 225 and 510 ml were used according to animal size with the remaining closed circuit volume being 280 ml.

These respirometers were constructed of perspex cylinders (0.45 cm in wall thickness) sealed at one end by a 0.75 cm thick perspex sheet but containing an air outlet. The other end of the cylinder had a perspex sheet rim and could be sealed with 4 screws and high pressure silicone grease by apposition of another perspex sheet. The air inlet was placed in the wall of the cylinder at a point at right angles but as far away as possible from the outlet. Such an arrangement plus the cylindrical shape gave 95% mixing within 2 mins at 400 ml min^{-1} (for the largest respirometer) without the need for a mixing fan or secondary mixing circuit. (For measurements of volume

FIG. 1.1 Diagram of the continuous flow, constant pressure, closed circuit used to determine $\dot{V}o_2$ and $\dot{V}co_2$ in Lacerta. Note the direction of flow, the separate sample and reference circuits, the positions of calibration gas entry, the opening point, the position of the bleed and the point of injection of gases for determining mixing and circuit volume.

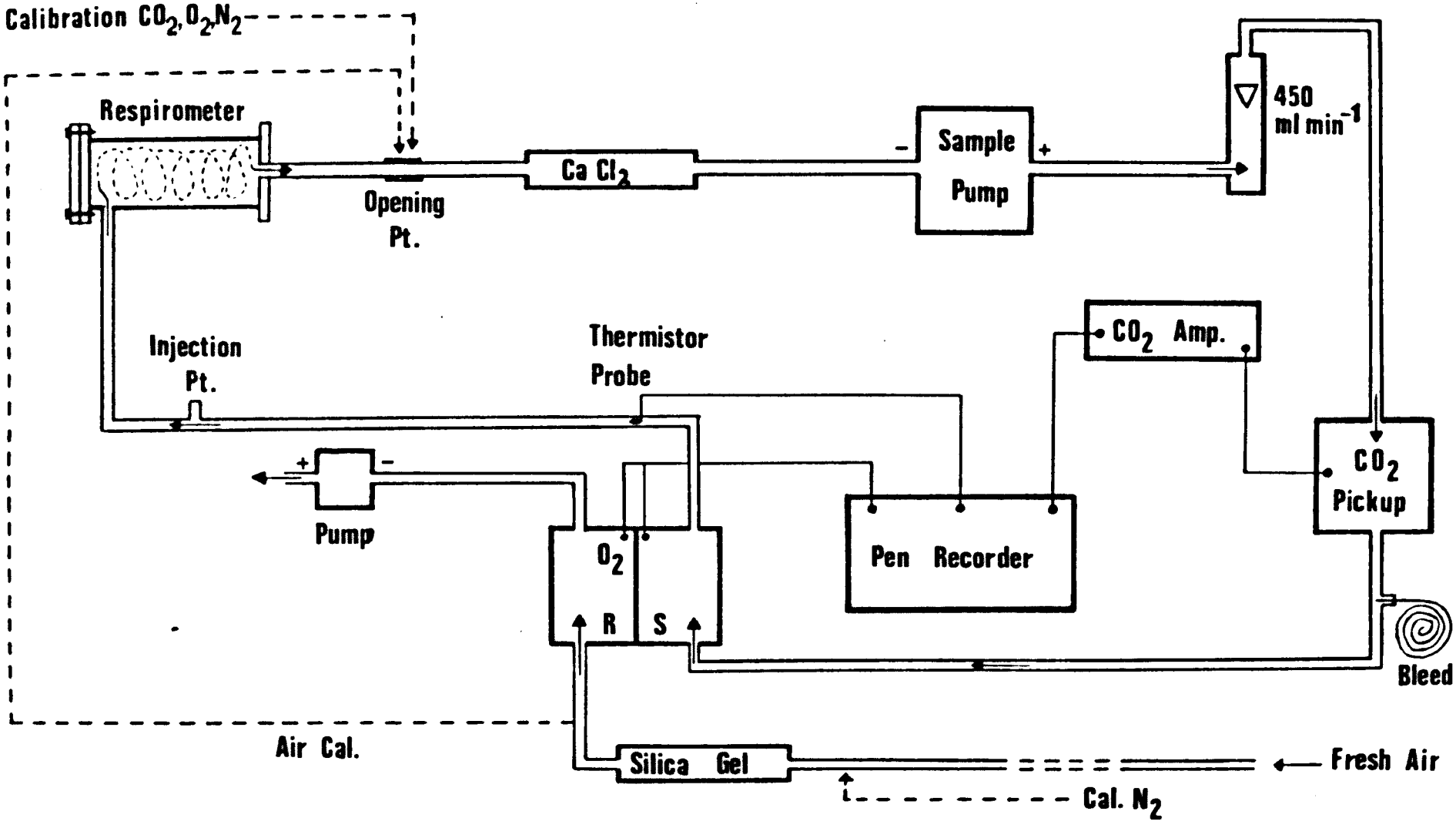
Calibration CO_2, O_2, N_2
Respirometer
Opening Pt.
Ca Cl_2
Sample Pump
450 ml min^{-1}
Injection Pt.
Thermistor Probe
CO_2 Amp.
CO_2 Pickup
Pump
O_2
R
S
Pen Recorder
Bleed
Air Cal.
Silica Gel
Fresh Air
Cal. N_2

FIG. 1.2 A typical closed circuit record of % O_2, % CO_2 and temperature over $1\frac{1}{2}$ hours. Note the pressure effect on the O_2 channel only, caused by closing and opening the circuit. % O_2 is at a sensitivity of 2% full scale deflection whilst % CO_2 is 1% f.s.d. Inactive $\dot{V}o_2$:active $\dot{V}o_2$ in this record is 1:4.

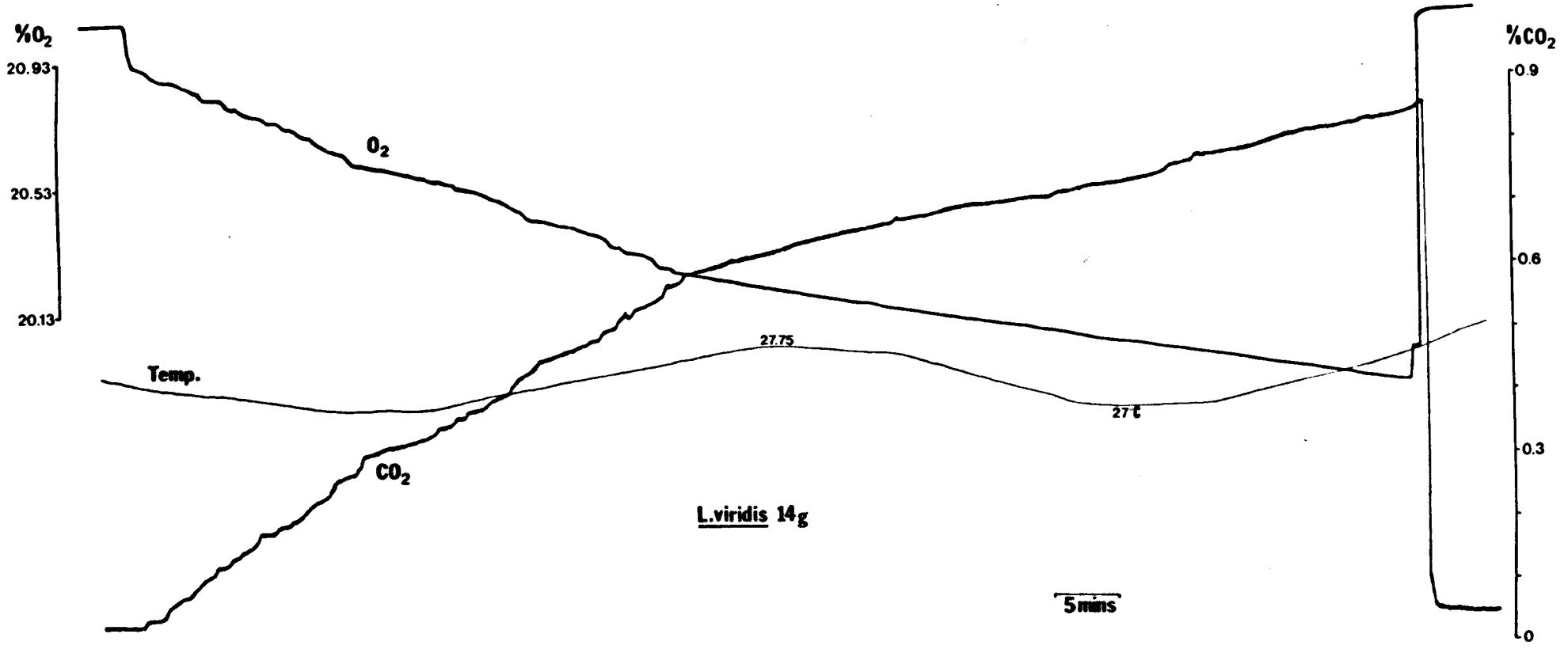
%O2
20.93
20.53
20.13
O2
Temp.
27.75
27°C
CO2
%CO2
0.9
0.6
0.3
0
L.viridis 14g
5mins

and mixing, see Appendix I).

Constant pressure conditions were obtained using an instantaneous bleed to compensate for temperature fluctuations and a mean respiratory quotient of less than unity. A fine hypodermic needle and a 60 cm length of capillary tubing, reducing diffusion leakages to a minimum, formed the bleed. The use of this bleed and the errors involved (maximum of 7%) are further discussed in Appendix I.

Fig. 1.2 illustrates a typical closed circuit % O_2, % CO_2 and temperature trace over $1\frac{1}{2}$ hours in which max.$\dot{V}o_2$/min.$\dot{V}o_2$ gave a ratio of 4. $\dot{V}o_2$ is calculated and corrected to STP in the following way:-

$$\dot{V}o_2 = \Delta Fo_2 \times V \times \frac{P_B}{760} \times \frac{273}{273 + t}$$

where ΔFo_2 is the charge in fractional concentration of O_2 in an hour in dry gas, V = volume of the system - volume of the animal in ml, P_B = barometric pressure, t = temperature ^oC and $\dot{V}o_2$ = ml hr^{-1}. $\dot{V}co_2$ is calculated in a similar manner from ΔFco_2.

Open Circuit

Fig. 1.3 illustrates the plumbing of the open respirometry circuit, inlet air in the sample circuit was identical to that of the reference air of the O_2 analyser. Since gas homogeneity in the circuit is essential for accurate steady-state and dynamic estimates of $\dot{V}o_2$ and $\dot{V}co_2$, a mixing circuit of 12 L min^{-1} was used. Homogeneity was tested by determining the time constant, τ, of the circuit. A constant calibration gas which elevated % CO_2 and decreased % O_2 was introduced into the system until a steady state was reached and maintained for 10 min. This gas was then replaced by the fresh air source. An experimental wash-out curve was obtained at the beginning and end of this operation (Fig. 1.4).

A time constant, τ, is the time in minutes taken to go from x% to $1/e$ its value and, with homogeneous mixing, τ is constant whatever the value of x. For the 510 ml respirometer, τ = 7.0 min and for the 225 ml

FIG. 1.3 Diagram of the open circuit used to determine $\dot{V}o_2$ and $\dot{V}co_2$ in Lacerta. Note the opening point, instrument calibration point, position of gas entry for determining the time constant, the fact that $\dot{V}_E$ is monitored and the mixing circuit.

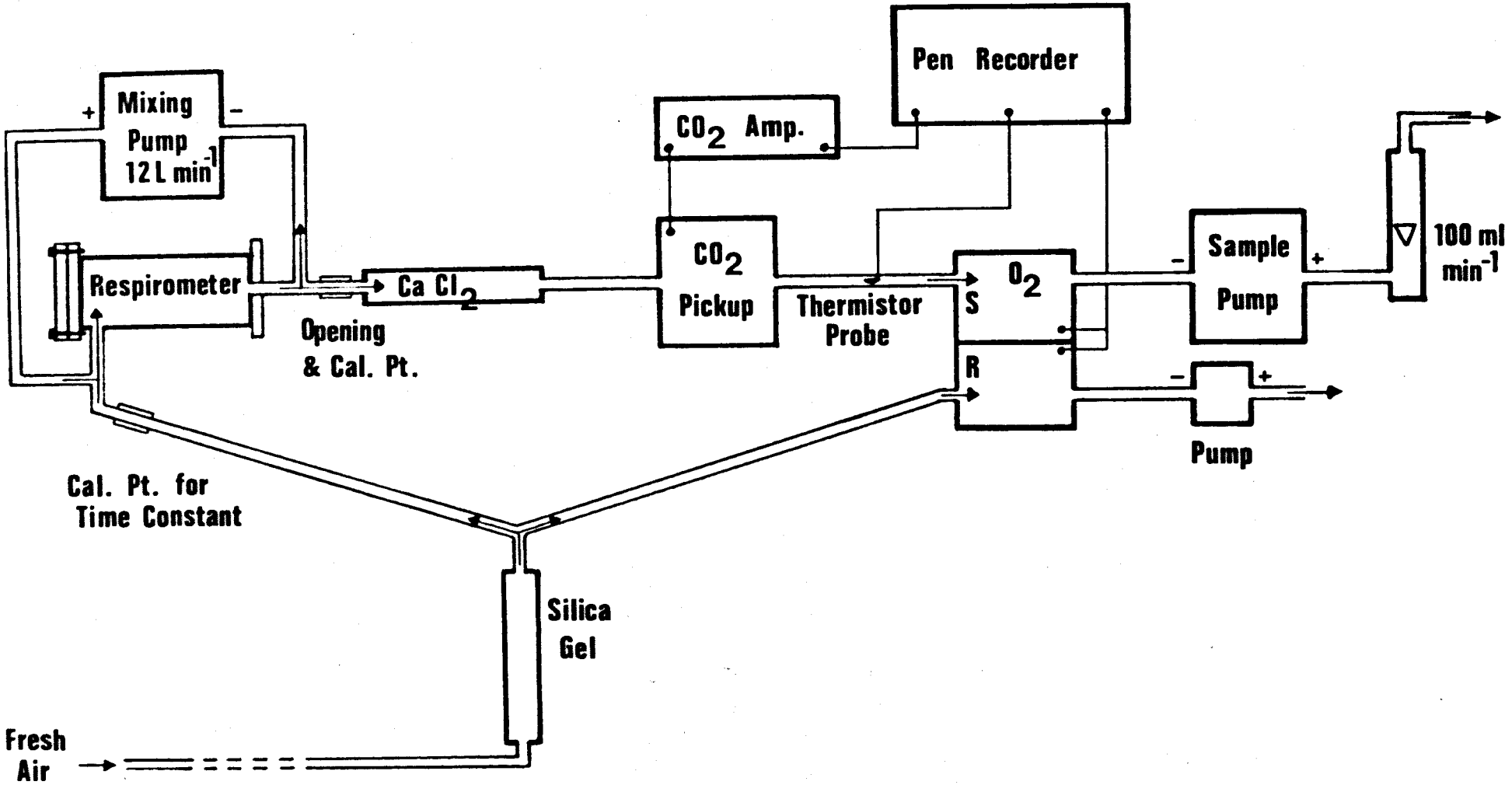
Pen Recorder
CO_2 Amp.
Mixing Pump 12 L min^{-1}
+
−
Respirometer
Ca Cl_2
Opening & Cal. Pt.
CO_2 Pickup
Thermistor Probe
S
O_2
R
Sample Pump
100 ml min^{-1}
Pump
Cal. Pt. for Time Constant
Silica Gel
Fresh Air

FIG. 1.4 Exponential wash-out curves for determining the time constant and homogeneity of mixing in the open circuit. Time constant, τ, = time between x% and $^{1}/_{e}$ x%. The inset illustrates how the dynamic equation is applied to a CO_2 trace.

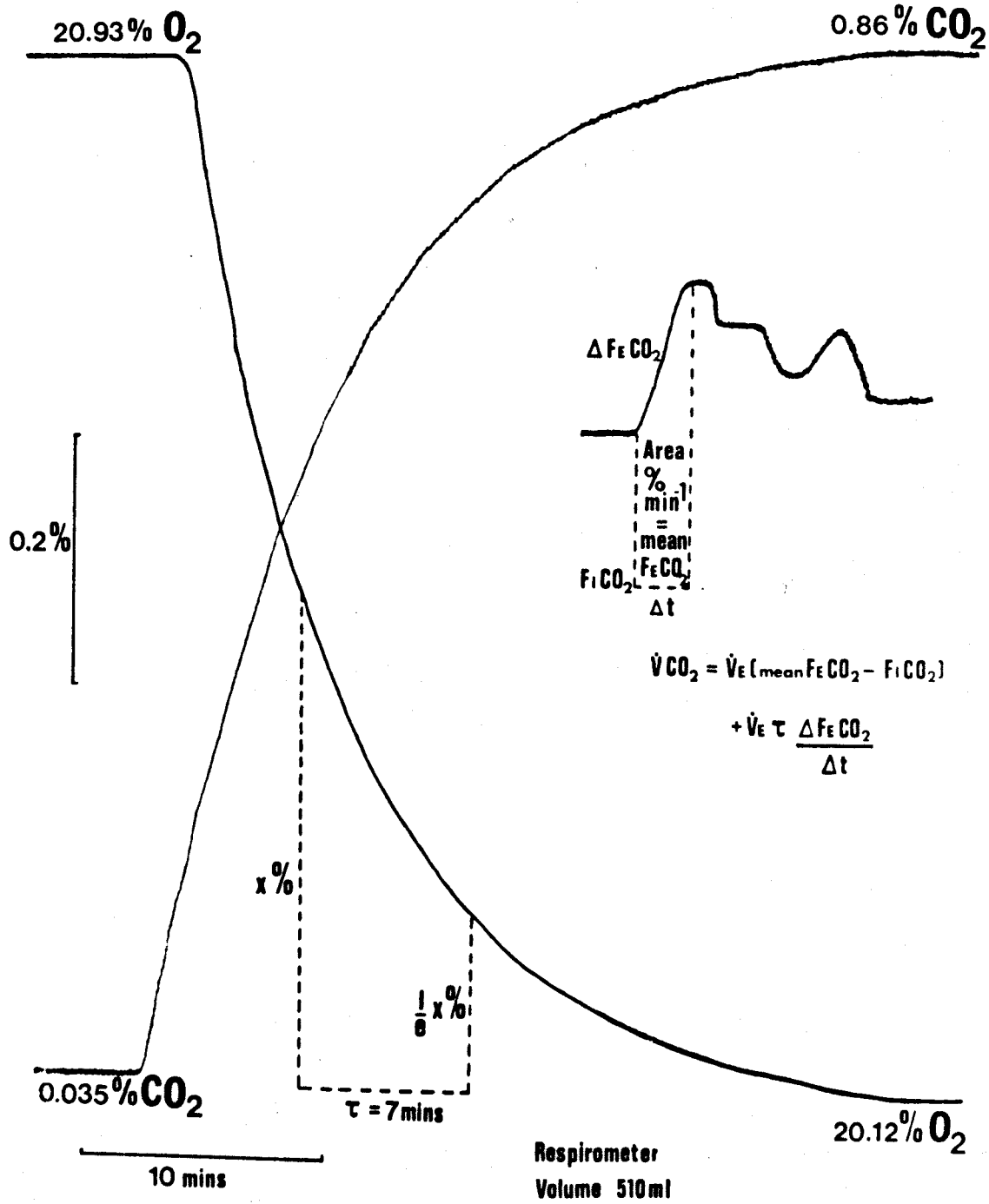
20.93% O_2
0.86% CO_2
$\Delta F_E CO_2$
Area % min^{-1} = mean $F_E CO_2$
$F_I CO_2$
Δt
0.2%
$\dot{V}CO_2 = \dot{V}_E (mean F_E CO_2 - F_I CO_2)$
$+ \dot{V}_E \tau \frac{\Delta F_E CO_2}{\Delta t}$
x %
$\frac{1}{e}$ x %
0.035% CO_2
τ = 7 mins
20.12% O_2
10 mins
Respirometer
Volume 510 ml

FIG. 1.5 A typical open circuit record of % O_2 and % CO_2 over $1\frac{1}{2}$ hours. Inactive $\dot{V}o_2$:active $\dot{V}o_2$ in this record is 1:4 and by comparison with Fig. 1.2 it is obvious that greater accuracy together with changes being easier to see, are present under open conditions. Sensitivity for % O_2 and % CO_2 is 1% f.s.d. It is not known whether the greater peaks in CO_2 are physiological or due to a slowness in response of the O_2 analyser to small fluctuating O_2 changes. Note that R, % CO_2/% O_2, is greater during active periods than inactive. The arrows mark the same instance of time.

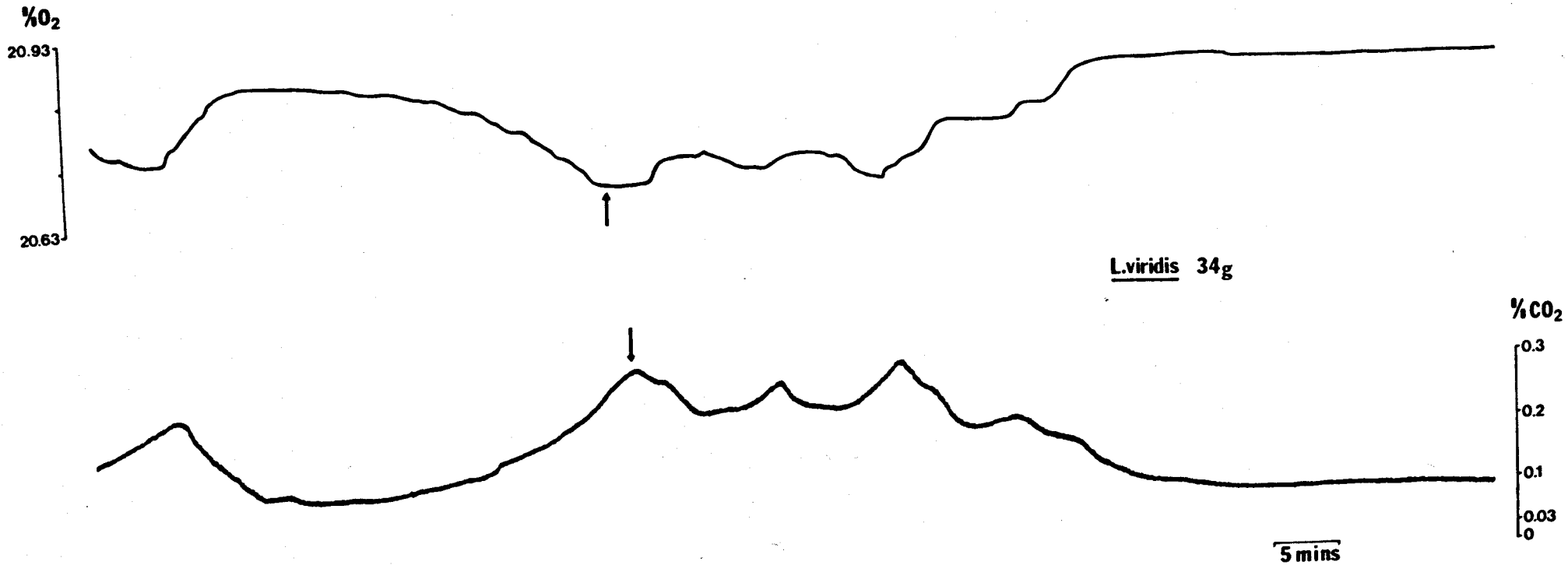
%O2
20.93
20.63
L.viridis 34g
%CO2
0.3
0.2
0.1
0.03
0
5 mins

respirometer, τ = 4.15 min for both O_2 and CO_2. Since mixing was complete, $V = \tau\dot{V}$ where V = volume ml of the system and $\dot{V}$ = flow rate, ml min^{-1}. Thus the effective volume of the open circuit was 700 and 415 ml respectively, indicating a volume of 190 ml for the mixing circuit. The volume between the respirometer and the analysers is not involved in mixing but is important because of its effect on time lag.

During steady state conditions whilst monitoring $\dot{V}_E$ (outlet flow rate ml min^{-1}),

$$\dot{V}co_2 \text{ ml min}^{-1} = \dot{V}_E (F_{Eco_2} - F_{Ico_2})$$

and

$$\dot{V}o_2 \text{ ml min}^{-1} = \frac{\dot{V}_E (F_{Io_2} - F_{Eo_2}) - \dot{V}co_2 F_{Io_2}}{1 - F_{Io_2}}$$

Use of the approximate form of the equation for $\dot{V}co_2$ is permissible because the accompanying error due to the respiratory quotient is negligible. These errors and the derivations of the equations are discussed in Appendix I in conjunction with those errors and equations published by Depocas and Hart (1957) and Hill (1972).

Under dynamic situations, the following equations have been derived,

$$\dot{V}co_2 = \dot{V}_E (\text{mean } F_{Eco_2} - F_{Ico_2}) \pm \dot{V}_E \tau \frac{\Delta F_{Eco_2}}{\Delta t}$$

and

$$\dot{V}o_2 = \frac{\dot{V}_E (F_{Io_2} - \text{Mean } F_{Eo_2}) - \dot{V}co_2 F_{Ico_2} \pm \dot{V}_E \tau \frac{\Delta F_{Eo_2}}{\Delta t}}{1 - F_{Io_2}}$$

Fig. 1.4 shows how these equations are applied to the Rikadenki trace. Deviations from a respiratory quotient R, of unity yields the same % errors as with steady-state equations. There is one other source of error applicable to dynamic measurements, which is due to the slow response of the O_2 analyser to small fluctuating O_2 changes as opposed to large step changes. This will cause an underestimation of $\dot{V}o_2$ but to an extent which is not measurable

since it is not known how different O_2 and CO_2 changes might be. All $\dot{V}o_2$ and $\dot{V}co_2$ values were converted to STP as in closed circuit equations.

Fig. 1.5 illustrates a typical open circuit trace for % O_2 and % CO_2 for approximately $1\frac{1}{2}$ hours showing inactive and active periods of 1:4. When comparing closed and open circuit traces, it is apparent that analysis of the latter is more accurate because smaller $\dot{V}o_2$ variations are recordable.

Diurnal Rhythm Procedure

Only lizards that were caught in the same year were used for diurnal rhythm studies and all were entrained to 12hrL/12hrD regimes for at least 1 month before studies commenced. Experiments were conducted during April to October only. Lizards were weighed before and after the diurnal recording to give a mean weight. Weight loss was approximately 5% (variation depending on whether defaecation and micturition had occurred during the 24 hour period) and was caused by dehydration and metabolic processes. This dehydration was a result of continual inhalation of dry air and when returned to its cage, the lizard immediately drank large quantities of water and completely replaced this 5% loss. The lizards were starved for 1 day (allowing minimum digestive processes only to be operating) and for 3 days or 2 days in the case of the viviparous young.

The diurnal recordings lasted for 24 hours plus 3 hours adjustment time, usually starting at 15.00 hours. The respirometer was shielded from all visual disturbances by placing it in a large black box which contained an overhead (i.e. 40 cm above) 12 cm strip light. This light gave no incident heat and was switched on by time clocks between 6.00 and 18.00 hours (i.e. identical to cages). Placing the respirometer on a 5 cm thick sponge base, shielded it from vibrations. It appeared that any external sounds were not transmitted to the lizard, presumably because of the already present internal 'noise' due to the circulating pump in conjunction with the narrow bore steel tubing. All experiments were conducted at a temperature of $28 \pm 1^{\circ}C$, usually on unrestrained animals.

All 12hrL/12hrD rhythms were recorded using closed circuit conditions for which a 1% f.s.d. (full scale deflection) was used during the day and a 5% f.s.d. at night (0.5% f.s.d. all the time for viviparous young). When at 1% f.s.d., the circuit was opened to fresh air at frequent but variable intervals (approximately once every 2 hours) to prevent the pens going off scale. The lizards were always totally unaware of this opening and closing. CO_2 accumulation only reached an average of 2% during the night but 4.5% occasionally did occur. Mixing in the closed circuit averaged out most active $\dot{V}o_2$ into approximately 20 minute periods - this was therefore chosen as the analysis period. Short bursts of activity lasting only 5 min, however, often occurred especially in L. sicula but were only readily apparent in open circuit traces.

All constant dark or light diurnal rhythms were recorded using open circuit conditions, a 20 min analysis period still being used. The greater fluctuations in the traces and histograms in comparison with closed circuits, are due only to a greater accuracy in determining $\dot{V}o_2$ by steady-state or dynamic open circuit methods.

Open Circuit for Exercise

The basic design of the exercise machine is illustrated in Fig. 1.6b,c. It was initially designed for closed circuit work with therefore careful attention being made to make all joints and fitments airtight. The outer box was made of 5-ply plywood covered with fibre-glass to prevent the wood warping under the high temperature and humidity of the experimental room and also to seal all joints. A series wound, brush-type mains motor (of the type used for electric food mixers) was geared down to drive the shaft of an aluminium pulley. This shaft entered the outer box through a gas-tight oil seal and rotated in nylon bearings at the two points of suspension in the sides of the box. A second aluminium pulley rotated on nylon bearings around a fixed shaft. The latter was fixed to a movable bracket thus allowing belt tension to be altered. The screw for positioning this bracket passed through an 'O'-ring seal in the wall of the outer box. Between the drive shaft pulley

FIG. 1.6 A. Design and dimensions of the exercise respirometers.

B & C. Top and side views of the exercise machine.

For description see text.

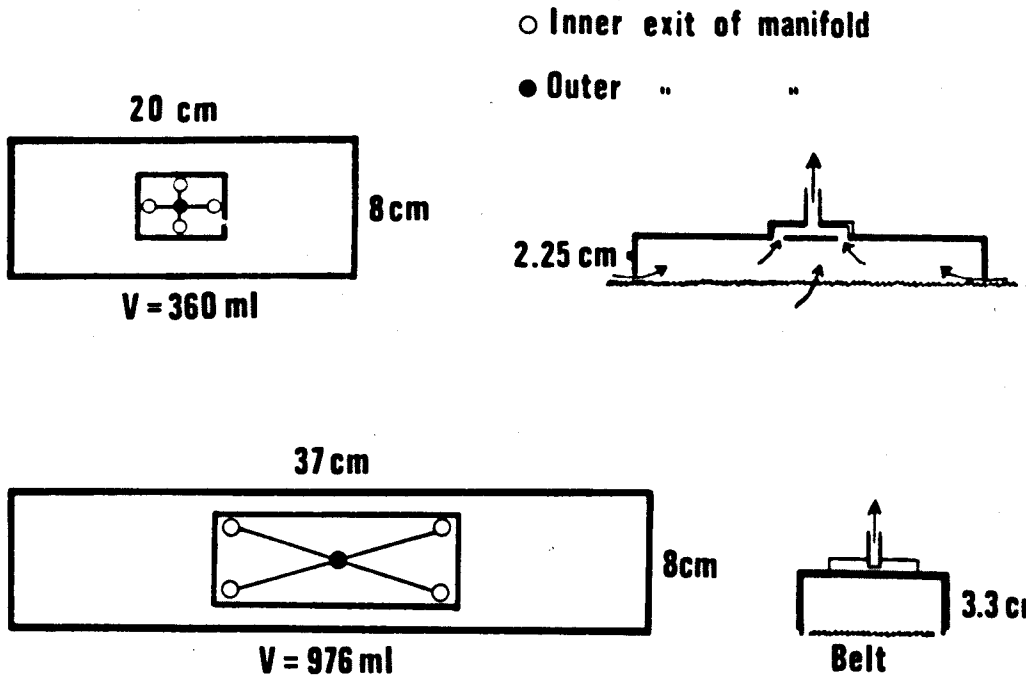
○ Inner exit of manifold
● Outer " "
20 cm
8 cm
V = 360 ml
2.25 cm
A
37 cm
8cm
V = 976 ml
3.3 cm
Belt

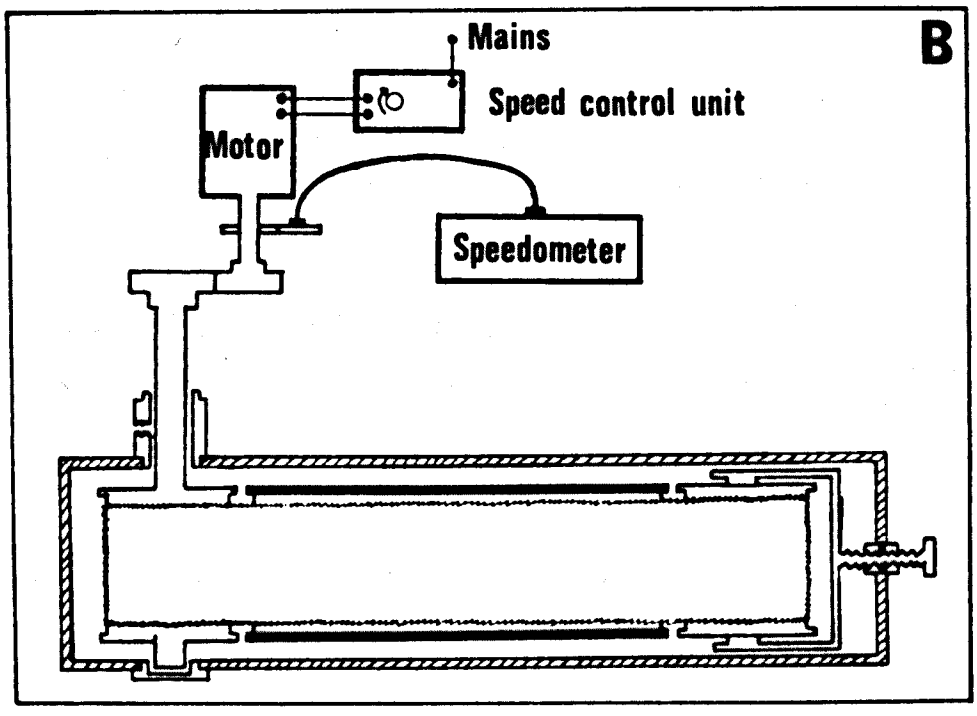
B
Mains
Speed control unit
Motor
Speedometer
Drive shaft assembly
Free pulley assembly with belt tensioner

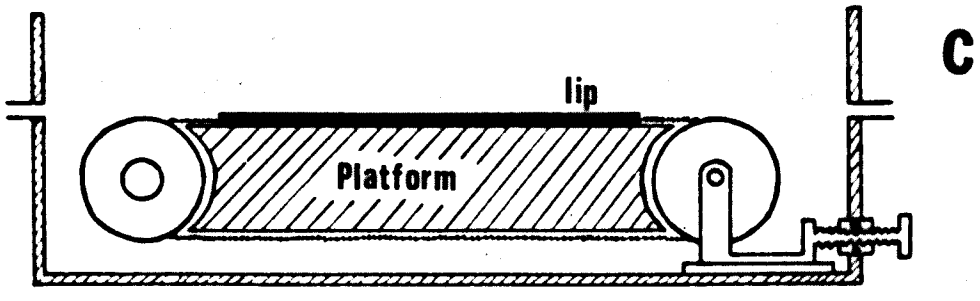
C
lip
Platform

and the free pulley, the belt was supported by a wooden platform (which also served to reduce dead space) covered with formica to reduce friction with the moving belt. To provide the necessary rough terrain for a lizard to run on, a linishing belt was used. A lip on the platform and pulleys prevented the belt from slipping laterally.

Pulley circumference was 23.4 cm so that at 1 rev sec^{-1} the speed of the belt was 14 m min^{-1}. The motor speed was determined by a variable speed control unit, the two being connected by extension leads. Belt speeds lower than 2 m min^{-1} were not possible. The maximum speed was 240 m min^{-1}. Rotation of the drive shaft was geared to the drive of a car speedometer to give a visual speed display. M.p.h. were re-calibrated for m min^{-1}.

This exercise machine was initially based on the design of Pasquis & Ganochaud (1964) which was used for 30g mice in closed circuits with an animal retaining chamber above the belt and an air-tight perspex lid. Because of construction difficulties, however, it was not possible to block out the unnecessary air spaces and hence the machine for lizards had an air volume twice that for the mammal. This, coupled to the fact that a 30g lizard consumed 10 times less O_2 than a mammal, caused low sensitivity in closed circuit conditions. Conversion to open circuit monitoring, although yielding high sensitivity under steady-state conditions, caused slow dynamic responses with a time constant, τ, of 48 min, since V (= 4,850 ml) = τ x $\dot{V}$ (= 100 ml min^{-1}). Increasing $\dot{V}$ would have certainly decreased τ but would also have reduced $F_{E_{O_2}}$ and hence the sensitivity.

Attempts were made to use open circuit face masks on exercising lizards as had been used by Moberly (1968b) on 1 kg iguanas. Because of the small size of Lacerta, however, the weight and bulk of the tubing from the face mask, whatever the system of suspension used, prevented the lizard from exercising freely. Reduction of tubing diameter, although reducing load, caused respiratory distress by creating negative pressures of -5 cm H_2O.

Details of the exercise methods used on small lizards by Bakker (1972) and Taylor (1973) were not available.

Since minute to minute dynamic analysis was considered important, it was finally decided to use small volume open circuit respirometers that seated tightly on the lip of the wooden platform. It was obviously impossible to obtain an airtight respirometer unit and to use mixing circuits because of the moving floor. Also during belt movement there was considerable dilution of the expired gases. These flaws were carefully tested.

Fig. 1.7 illustrates the plumbing for the exercise sample circuit which was identical to that of Fig. 1.3. Inlet air, again identical to the reference air of the O_2 analyser, was delivered at 3 L min^{-1} to the whole of the exercise box (4.85 L). The loose fitting, perspex lid with a central longitudinal slit covered by plastic flaps provided an escape route for the excess reference air and it also prevented the investigator's breath from contaminating the air. Reference air was sucked into the respirometer at 100 ml min^{-1} all round its periphery but mainly through the 2 mm belt clearance gap at either end. Two sizes of respirometer were used, a 360 ml one for L. vivipara and L. sicula and a 976 ml one for L. viridis. The width had been fixed to accommodate the gait of the largest L. viridis. To ensure mixing and sampling from all regions of the respirometer, the outlet was connected to a manifold of four further outlets (Fig. 1.6a).

Exponential washout curves were obtained by placing a length of fine tubing through a seal in the respirometer and injecting 100% CO_2 or O_2 at known constant flow rates. The time constant, τ, was 2.5 min for the small and 6.5 min for the large respirometer indicating 67% mixing or an 'effective' volume of 225 and 725 ml. By moving the tip of the injection tube systematically throughout the respirometer, no true 'dead' spaces were found and hence gases must reach well sampled sites by diffusion. Time constants were also determined for belt speeds between 2.5 and 15 m min^{-1}, being 1.4 and 1.2 min respectively, for the small respirometer, and 3.6 and

FIG. 1.7 Diagram of the open circuit system used during exercise. Note the identical sample circuit to Fig. 1.3 and the manner of reference air flow through the exercise machine. The system is opened by removal of the respirometer from the lip of the wooden platform.

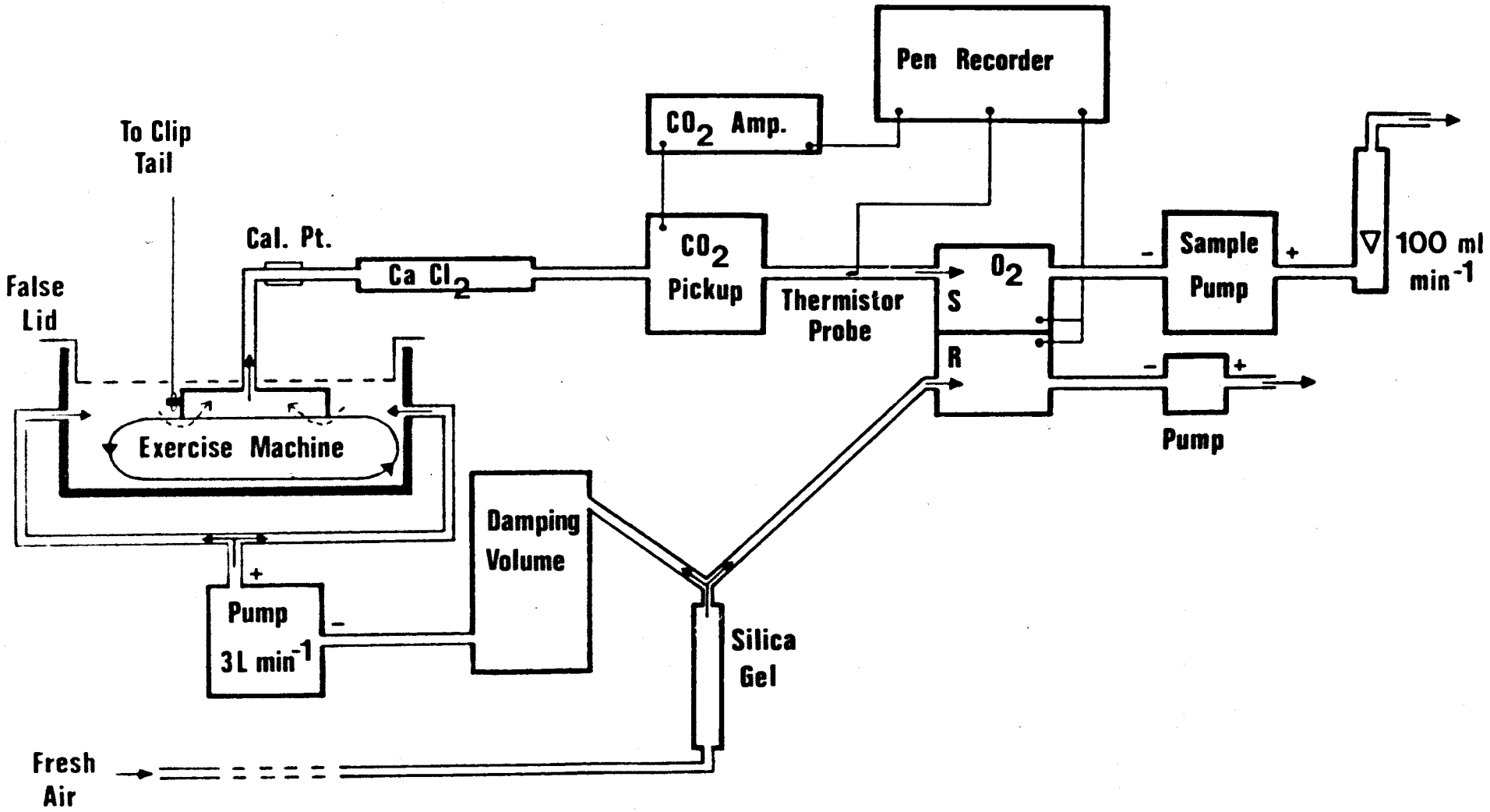
Pen Recorder
CO_2 Amp.
To Clip Tail
Cal. Pt.
False Lid
$Ca\ Cl_2$
CO_2 Pickup
Thermistor Probe
O_2
S
R
Sample Pump
100 ml min^{-1}
Pump
Exercise Machine
Damping Volume
Pump 3L min^{-1}
Silica Gel
Fresh Air

FIG. 1.8 Correction graphs for % O_2 and % CO_2 dilution at belt speeds between 2.5 and 15 m min^{-1}. O_2 on right, CO_2 on left.

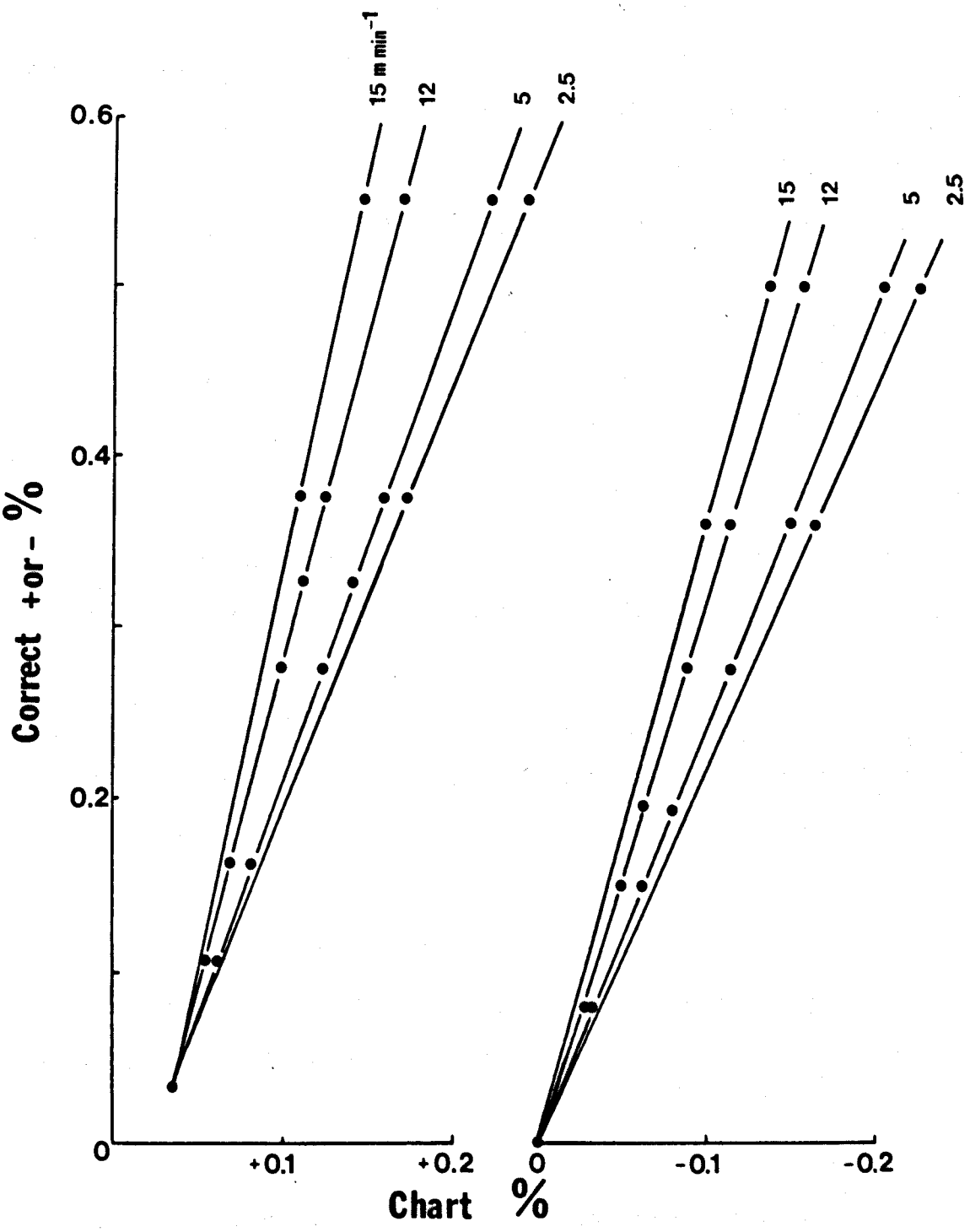
15 m min⁻¹
12
5
2.5
15
12
5
2.5
0.6
0.4
0.2
0
Correct +or- %
+0.1
+0.2
0
-0.1
-0.2
Chart %

3.1 min for the large. Thus the 'effective' volume decreased with belt movement. 'Dead' spaces were found for running belt speeds in the posterior part of the respirometer and at a height of 0.2 cm above the belt in all regions. The small amount of lateral and vertical belt movement acting as a pulsatile pump caused injected gases to be sucked out before mixing could occur. However, during running the lizard always maintained its head in the well sampled region. How the presence of the lizard affects mixing is not known but it has to be assumed to be negligible.

The pulsatile action of the belt not only caused a reduction in 'effective' volume but also diluted the expired gases by removing these gases before mixing was complete and replacing it with reference air. Correction graphs for different levels of O_2 and CO_2 at different belt speeds were constructed (Fig. 1.8). Since mixing was the same in both respirometer sizes, so also were their correction graphs. There was a slightly greater dilution of CO_2 than of O_2 presumably due to the slightly greater diffusion coefficient of O_2 which allowed more O_2 mixing to occur before dilution. (Do_2 = 12.6, Dco_2 = 11.1 ml/min/cm²/cm length conc. gradient cm² time^{-1} from Altman & Dittmer, 1971). Diffusion coefficient differences were only effective because the time constants of the system were within the same time scale.

Calculation of exercise $\dot{V}o_2$ and $\dot{V}co_2$

(i) With no belt movement before exercise. Steady-state and dynamic equations derived for diurnal rhythm open circuits were used but with the time constant 2.5 or 6.5 min determined for the 'effective' volume.

(ii) With belt movement during exercise. Under steady-state conditions the % O_2 and % CO_2 level recorded were converted to their undiluted values F_{Eo_2} or F_{Eco_2} using the correction graph for the speed concerned. These corrected values were then used in the steady-state equation. For dynamic changes which occur at the beginning of and sometimes during exercise, mean F_{Eo_2} or mean F_{Eco_2} (by the area method previously described)

were converted to their undiluted values. If the corrected value was y times greater than the uncorrected value, then the dynamic part of the equation was $\pm \dot{V}_E \tau_c \frac{\Delta F_{Eo_2}}{\Delta t} y$ where ΔF_{Eo_2} is the uncorrected change in O_2 and τ_c is the appropriate time constant for the speed concerned.

(iii) With no belt movement at the end of exercise. The O_2 and CO_2 trace invariably overshot the exercising level although $\dot{V}o_2$ and $\dot{V}co_2$ usually declined immediately. This trace overshot (Fig. 1.17) was a result of diluted gas levels returning to undiluted values because the belt had stopped. Dynamic and steady-state conditions were analysed as in (i).

Exercise Procedure

Lizards, that had been starved for one day only, were allowed to settle down for at least an hour in the exercise respirometer, but always in sight of the investigator. Some became quiet quickly, others continued to explore the respirometer for possible exits and some were aggressive to or disturbed by the investigator's surveillance. The same lizard never reacted consistently, but a constant low $\dot{V}o_2$ was eventually reached, if only for 10 min before another burst of activity. During exercise training periods of 5 to 30 min between 9.00 and 17.00 hours, the lizards showed no sign of learning. If a lizard ran well the first time, it might refuse to exercise satisfactorily a few hours later by either running in spurts, alternately fast and slow, attacking the front or rear of the respirometer or curling up at the rear oblivious to any pain caused by the moving belt. Low voltage electrical stimulation of the tail or hindlegs gave localised twitches but did not encourage exercise; higher voltages caused running in spurts or aggressive behaviour. It was found more satisfactory to mechanically stimulate the lizard to run, when necessary, by slightly raising the rear of the respirometer and clipping the tail, but this was not always effective. The lizards were continually observed during exercise and the belt stopped immediately the lizard became permanently trapped at the rear of the respirometer or showed signs of exhaustion or distress.

Because of the lack of learning, it was decided to proceed with the exercise experiments whilst noting extensively how the lizard behaved before, during and after exercise. Exercise was maintained for 30 min wherever possible, but at maximum speeds the lizard would not exercise for more than 3 to 7 min. $\dot{V}o_2$ and $\dot{V}co_2$ were determined for 5 average weights (between 3.5g and 34g) from 5 to 10 exercises at each speed, from 2 to 5 individuals for each average weight. Exercise was not commenced until resting $\dot{V}o_2$ was reached and monitoring continued after exercise until this level was again reached. Each experiment was analysed at 1 min intervals for $\dot{V}o_2$, $\dot{V}co_2$ and R having rejected all data from lizards that were considered to be exercising unsatisfactorily. Any increases in body temperature during exercise were not recorded. Respirometer temperature did not change.

RESULTS

DIURNAL RHYTHMS

L. vivipara

Behavioural activity studies on both adult and recently hatched L. vivipara (in their laboratory cages at room temperature - 20°C with the light on between 06.00 and 18.00 hours giving an incident temperature of 35°C) showed that activity occurred throughout the light period. The lizards would emerge from their rocky shelters either as soon as the light came on or up to two hours later. During the 'day', their time was spent basking, sheltering and foraging (defined here as an active exploratory phase which is not connected necessarily with feeding). Periods of activity appeared to be spread throughout the 'day' although some lizards were rather inactive in the 'afternoon'. Basking periods would often last for 20 min or more, whereas foraging periods were much shorter at a maximum of 5 min. There was no obvious social interaction or dominance and they were not easily disturbed by observers. Some lizards were often basking when the lights went out but within a few minutes they took shelter and remained there.

In the experimental situation (which was even more unnatural since there was neither shelter nor undergrowth to forage through, not a heat-giving light, the temperature being constant at 28 ± 1°C) spontaneous unrestrained activity was recorded in terms of $\dot{V}o_2$. Fig. 1.9 and Fig. 1.10 illustrate the diurnal rhythm of 20 min $\dot{V}o_2$ periods in adults and recently hatched young under a 12hrL/12hrD regime. $\dot{V}o_2$ was never completely constant during the dark hours but fluctuated about a mean with the rare occurence of small peaks. During these 12 hours of dark the lizards lay curled up with their eyes closed and if disturbed by handling were slow to respond.

The beginning of the light period was immediately marked by an increase of $\dot{V}o_2$ but there was no consistent pattern of peak activities during the light period. Sloughing appeared to increase activity considerably as

FIG. 1.9 Diurnal $\dot{V}o_2$ histograms under 12hrL/12hrD in adult L. vivipara determined by closed circuit respirometry. 4.0g lizard was sloughing. In all histograms the hatched bar denotes the dark period.

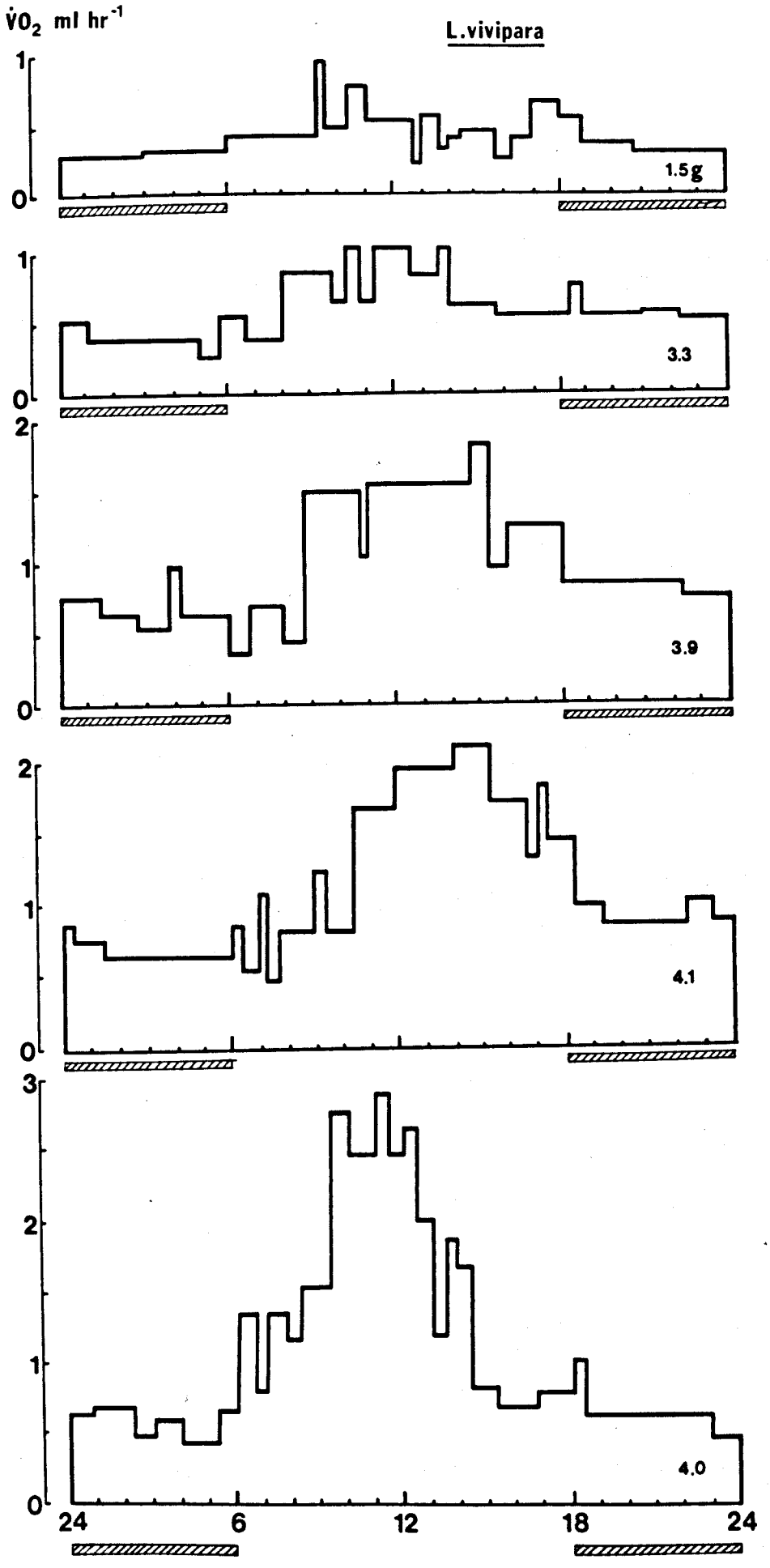
$\dot{V}O_2$ ml hr^{-1}
L.vivipara
1
0
1.5g
1
0
3.3
2
1
0
3.9
2
1
0
4.1
3
2
1
0
4.0
24
6
12
18
24
Time of Day — Hrs.

FIG. 1.10 Diurnal $\dot{V}o_2$ histograms under 12hrL/12hrD in recently hatched *L. vivipara* determined by closed circuit respirometry.

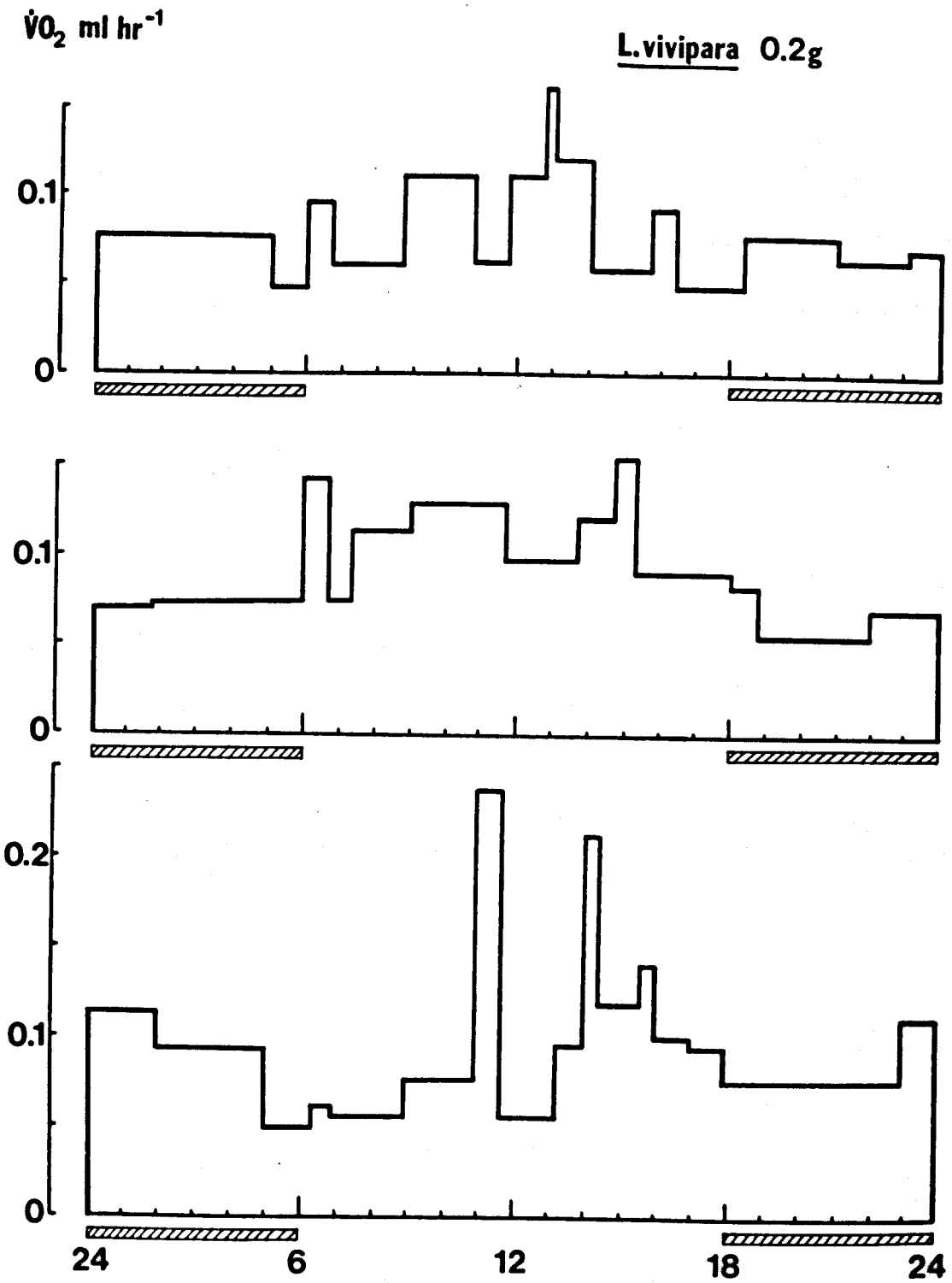
$\dot{V}O_2$ ml hr^{-1}
L.vivipara 0.2g
0.1
0
0.1
0
0.2
0.1
0
24
6
12
18
24
Time of Day — Hrs.

FIG. 1.11 Effect of constant dark and constant light on diurnal $\dot{V}o_2$ in L. vivipara determined by open circuit respirometry.

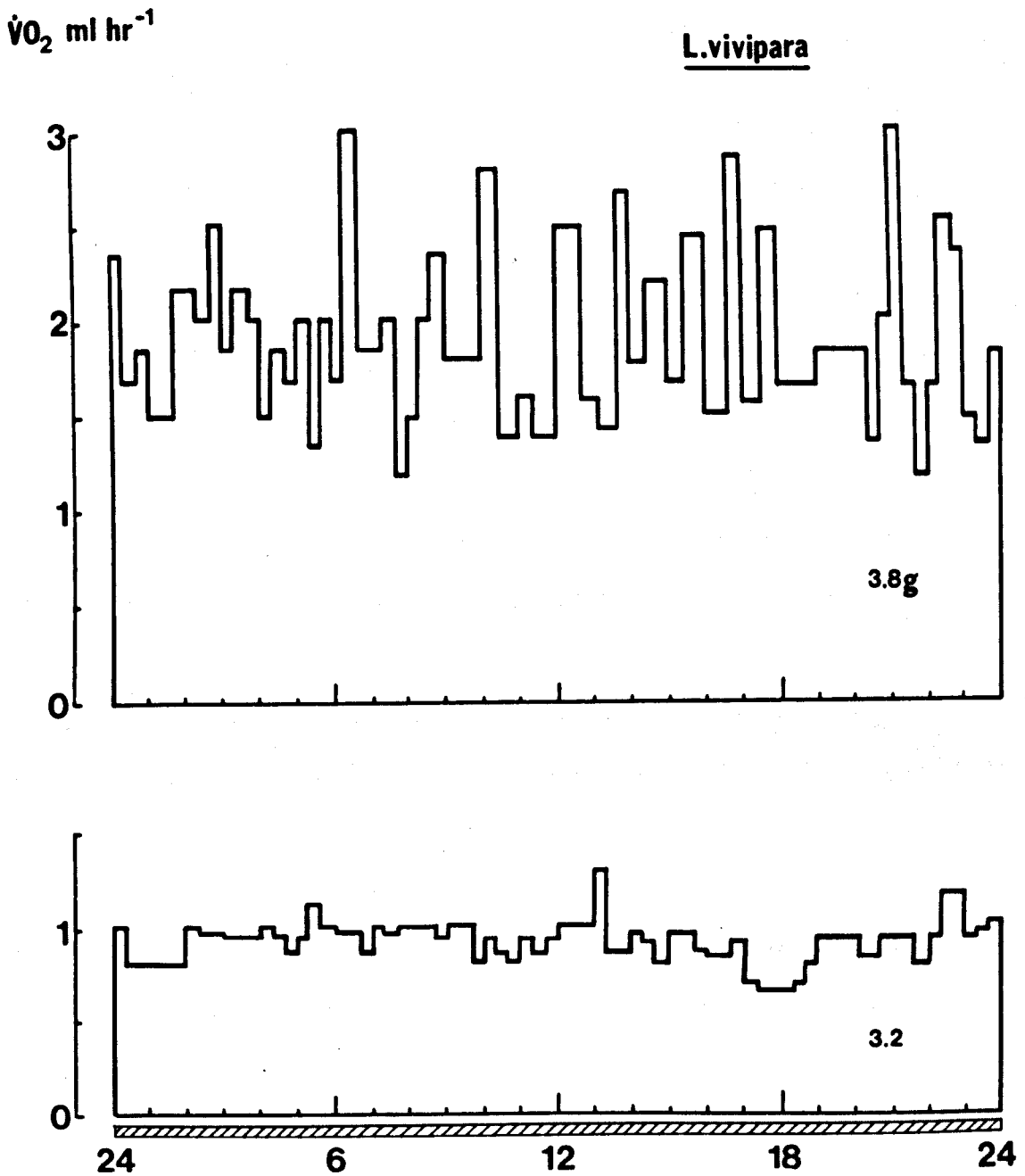
$\dot{V}O_2$ ml hr^{-1}
L.vivipara
3
2
1
0
3.8g
1
0
3.2
24
6
12
18
24
Time of Day — Hrs.

the animal presumably tried to assist the removal of dead skin. The beginning of the dark period at 18.00 hours was marked by an immediate lowering of $\dot{V}O_2$ or by a small increase. It is thought that these small on and off peaks are probably due to an artificial response to the abrupt transition into complete light or dark. In the laboratory cage conditions of all three species, the background room lighting changed gradually. There would appear to be no obvious difference in the diurnal rhythm of adults and recently hatched L. vivipara.

Under conditions of total dark, Fig. 1.11, for 24 hours, L. vivipara showed no diurnal rhythm and remained inactive throughout the 'day', maintaining the 'night' mean $\dot{V}O_2$. 24 hour light also caused no diurnal rhythm (Fig. 1.11) but stimulated constant elevated activity with a mean $\dot{V}O_2$ twice that of a normal 'night'. The normal mean day $\dot{V}O_2$/mean night $\dot{V}O_2$ ratio is only 1.6 times (see Table 1.1). In short experiments in which the light was switched on and off each hour, L. vivipara responded immediately by becoming active in light and quiet during dark periods. Similar constant light and light on/off tests in cages where shelter and a lower environmental temperature were present, still showed activity in the light period only but interspersed with bouts of sheltering. In experimental situations, L. vivipara were greatly disturbed by constant light with one, apparently healthy, individual even dying. Such frenzied activity was not apparent when shelter was available, whatever the temperature.

L. sicula

Behavioural activity studies in the laboratory cage (at a constant, $28 \pm 1^{\circ}C$, temperature with the light on between 06.00 and 18.00 hours giving an incident heat of $35^{\circ}C$), showed that L. sicula were active between 07.00 and 18.00 hours but tended to be less active around 12.00 when they were mainly sheltering. Although the light came on at 06.00, the lizards did not emerge until approximately 07.00. On the other hand, when the light went out, the lizards, if they had not already anticipated it, quickly retired.

L. sicula were very active, restless creatures only basking for much shorter periods (5 min maximum) than L. vivipara and spending much more time foraging (maximum 10 min period) and less sheltering. They were very easily disturbed by observers, being inquisitive, and interacted socially within a group, the largest lizard always being dominant and occasionally fighting. The non-dominant lizards always spent more time sheltering and were not often allowed to bask directly under the light. No difference could be seen behaviourally between L. sicula sicula and L. sicula campestris except that the latter were often the larger and hence dominant.

Fig. 1.12 illustrates the diurnal rhythm of L. sicula in the experimental situation. During the dark hours $\dot{V}o_2$ was again never completely constant but fluctuated about a mean. These lizards were quicker in responding to handling at night than were the L. vivipara. In the light period, L. sicula showed exactly the same rhythm of activity as had been noted in the laboratory cages with peak activities between 07.00 and 11.00 and between 13.00 and 15.00. The secondary peak had an average $\dot{V}o_2$ greater than the first peak but with the amplitude of maximum 20 min $\dot{V}o_2$ periods usually less. The mid-day level, i.e. 11.00 to 13.00, maintained a mean level higher than dark mean $\dot{V}o_2$. Although individual variation is obvious, a strong diurnal rhythm of two activity peaks was present. As might be expected from the behavioural studies, there were far more short bursts of high $\dot{V}o_2$ in L. sicula than in L. vivipara.

Constant dark for one day in no way altered the strong diurnal rhythm and pattern of peaks, nor the mean 'day' and mean 'night' rates except in one case where activity began at 06.00 hours instead of 07.00 hours and ceased at 19.00 instead of 18.00 (Fig. 1.13). Under conditions of constant light for one day, activity still began at 07.00 and finished at 18.00 with identical peaks to normal. Switching the light on and off each hour did not cause stimulation or inhibition of activity, respectively.

FIG. 1.12 Diurnal $\dot{V}o_2$ histograms under 12hrL/12hrD in *L. sicula* determined by closed circuit respirometry.

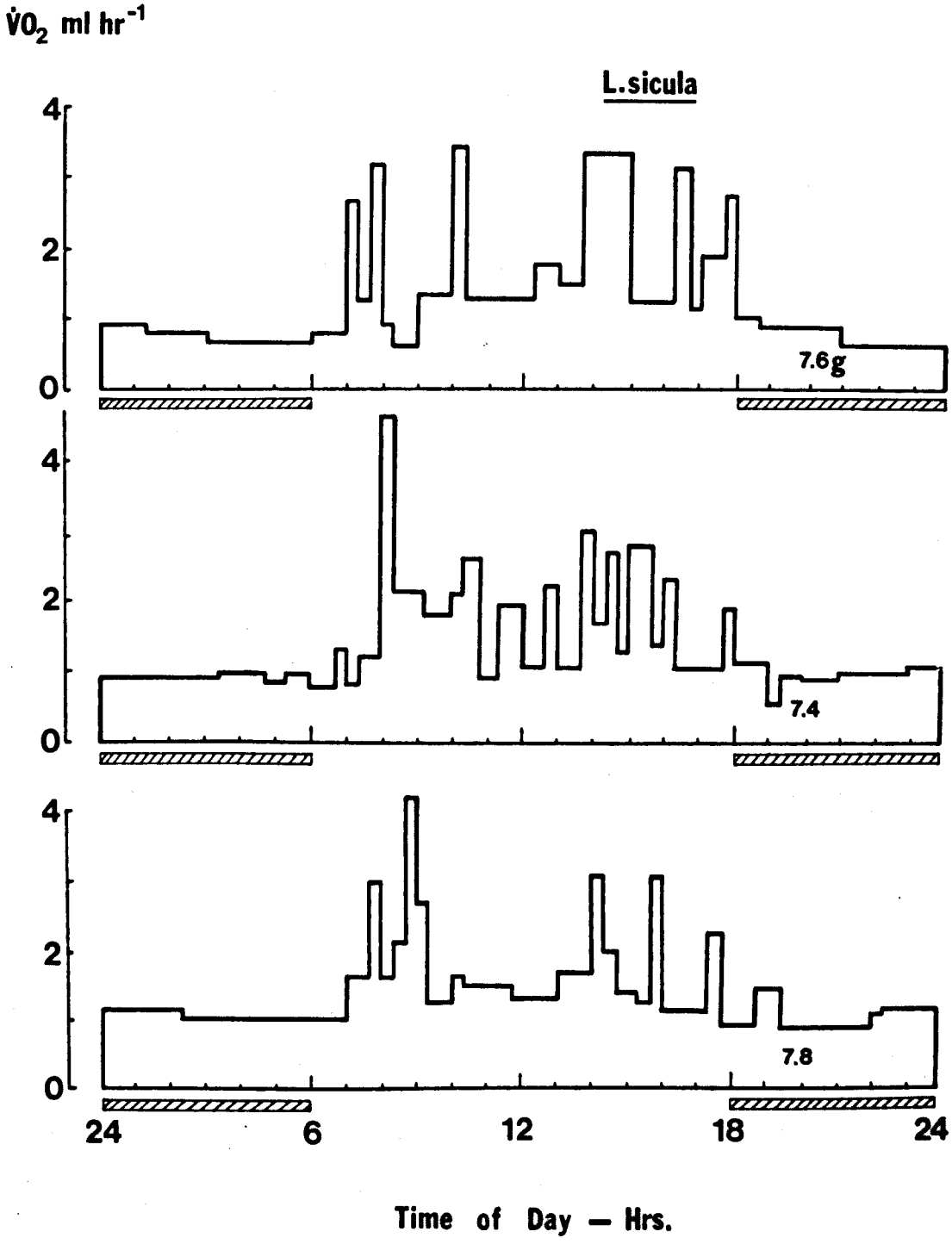
$\dot{V}O_2$ ml hr^{-1}
L.sicula
4
2
0
7.6g
4
2
0
7.4
4
2
0
7.8
24
6
12
18
24
Time of Day — Hrs.

FIG. 1.13 Effect of constant dark and constant light on diurnal $\dot{V}o_2$ in *L. sicula* determined by open circuit respirometry.

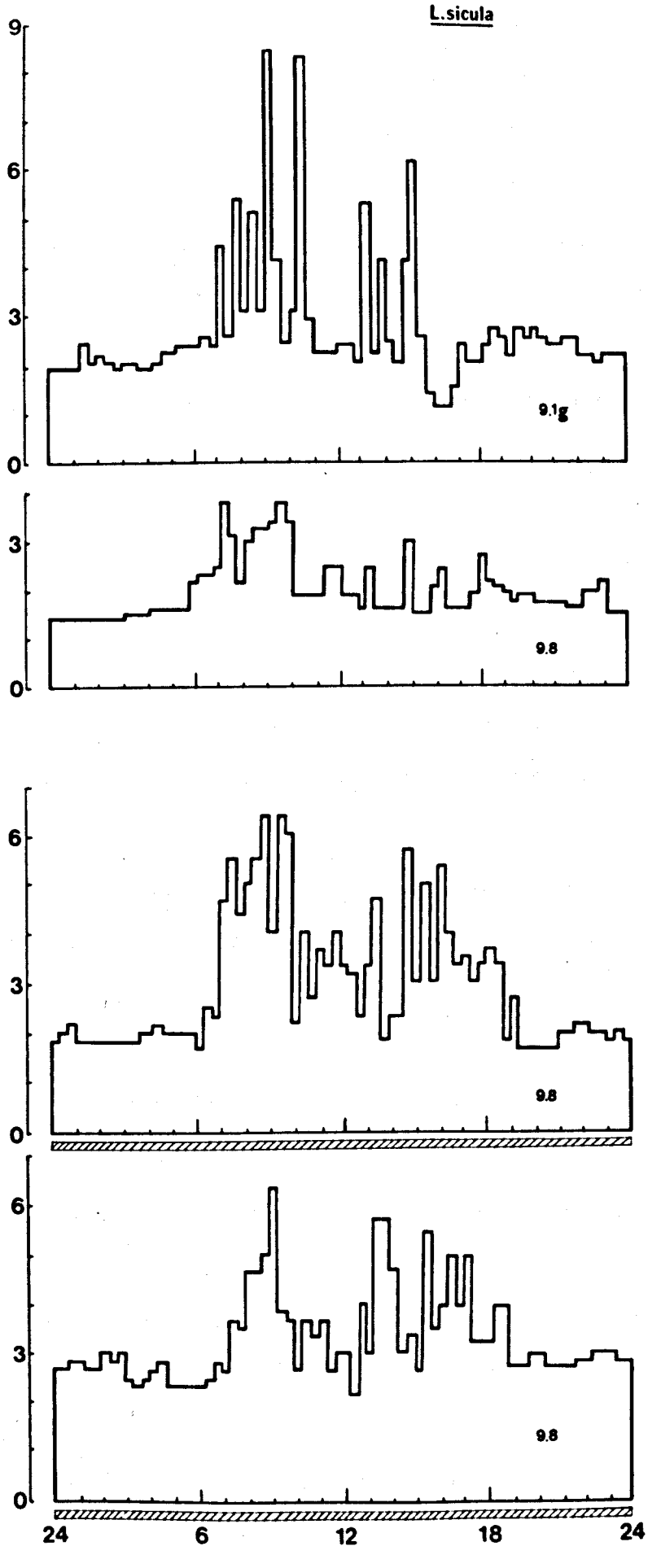
L.sicula
9
6
3
0
9.1g
3
0
9.8
6
3
0
9.8
6
3
0
9.8
24
6
12
18
24
Time of Day — Hrs.

L. viridis

Behavioural activity in the laboratory cage (under the same conditions as L. sicula) showed that L. viridis were active between 06.00 and 18.00 hours but there was considerable individual variation in how early they emerged or retired or when they were most active. Periods of basking could be as long as 45 minutes and they would forage for long periods (30 min or more) without basking or sheltering. L. viridis were very socially interacting animals and would spend much time guarding their own territory, often fighting especially over food. (Overcrowding can lead to mutilation of the weaker, smaller lizards). The largest lizard was always the more dominant and would often show threatening behaviour both to other lizards and to observers intent on handling. If L. viridis are placed alone in 24" x 12" cages with no large rocks or wire netting to climb and investigate, they will spend most of the time stationary, interspersed with some basking and some sheltering periods.

In the experimental situation, L. viridis showed a diurnal rhythm but with very variable activity patterns during the light (Fig. 1.14). As with the other two species, $\dot{V}o_2$ fluctuated slightly about a mean during the 12 hours of dark but, in contrast, this mean dark value often occurred during some part of the light period. The response to handling at night was variable between docile and aggressive. Activity during the light period was very variable - sometimes activity began when the light came on, or it peaked at anytime or was evenly distributed throughout the 06.00 to 18.00 hours or sometimes there was hardly any activity at all.

During constant dark, L. viridis showed no activity at all exactly as with L. vivipara, the mean night $\dot{V}o_2$ being kept all the time (Fig. 1.15). Under conditions of total light, the 'night' rate in one case was normal but in three were elevated by 1.5 times (not as much as the double increment in L. vivipara). However, in contrast to L. vivipara, there were no periods of peak activity during the 'night'. Presumably, sleep was not possible in 3 out of 4 cases causing the elevated $\dot{V}o_2$. Under constant light, activity

FIG. 1.14 Diurnal $\dot{V}o_2$ histograms under 12hrL/12hrD in L. viridis determined by closed circuit respirometry.

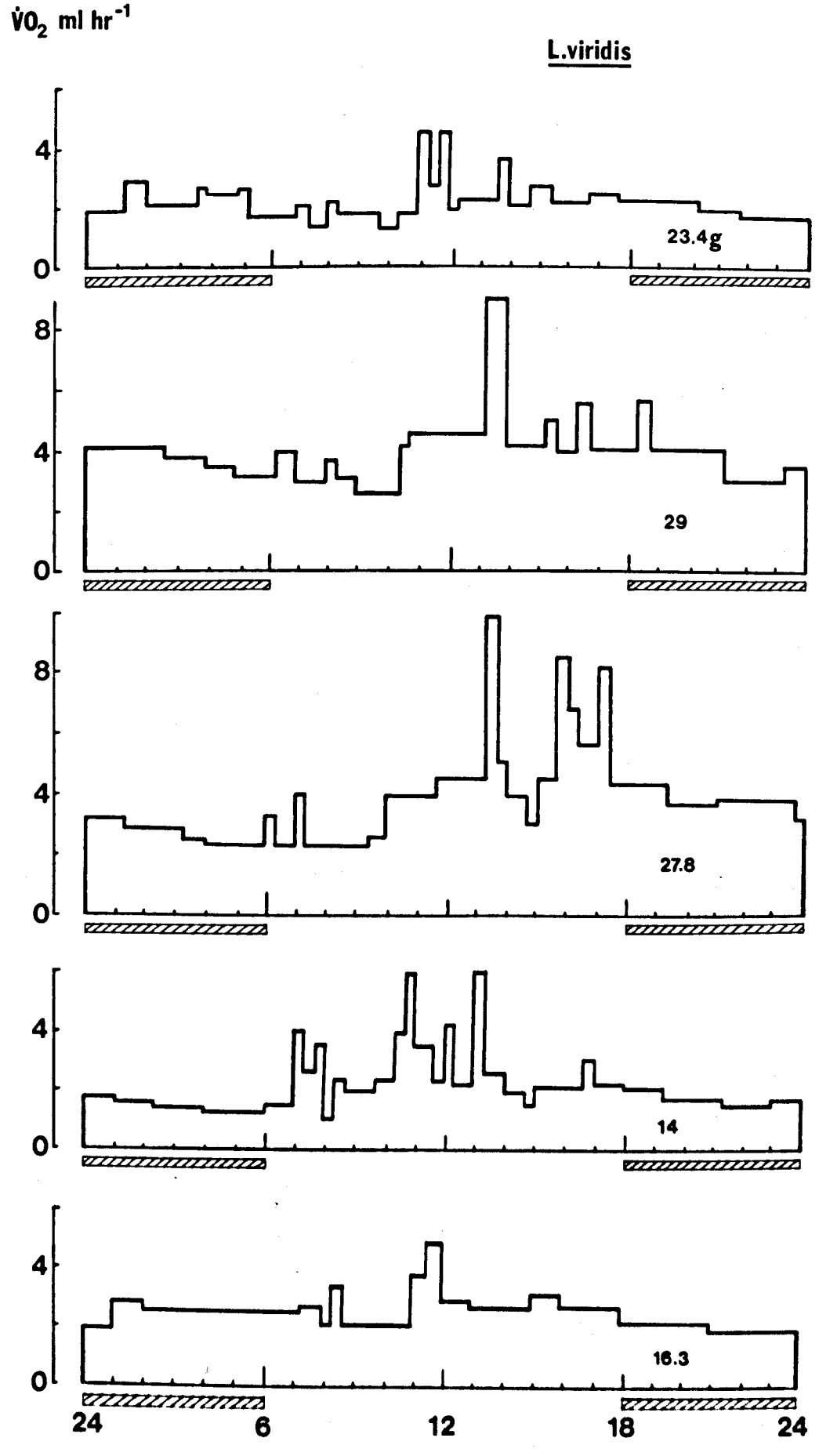
$\dot{V}O_2$ ml hr^{-1}
L.viridis
4
0
23.4g
8
4
0
29
8
4
0
27.8
4
0
14
4
0
16.3
24
6
12
18
24
Time of Day — Hrs.

FIG. 1.15 Effect of constant dark and constant light on diurnal $\dot{V}o_2$ in *L. viridis* determined by open circuit respirometry.

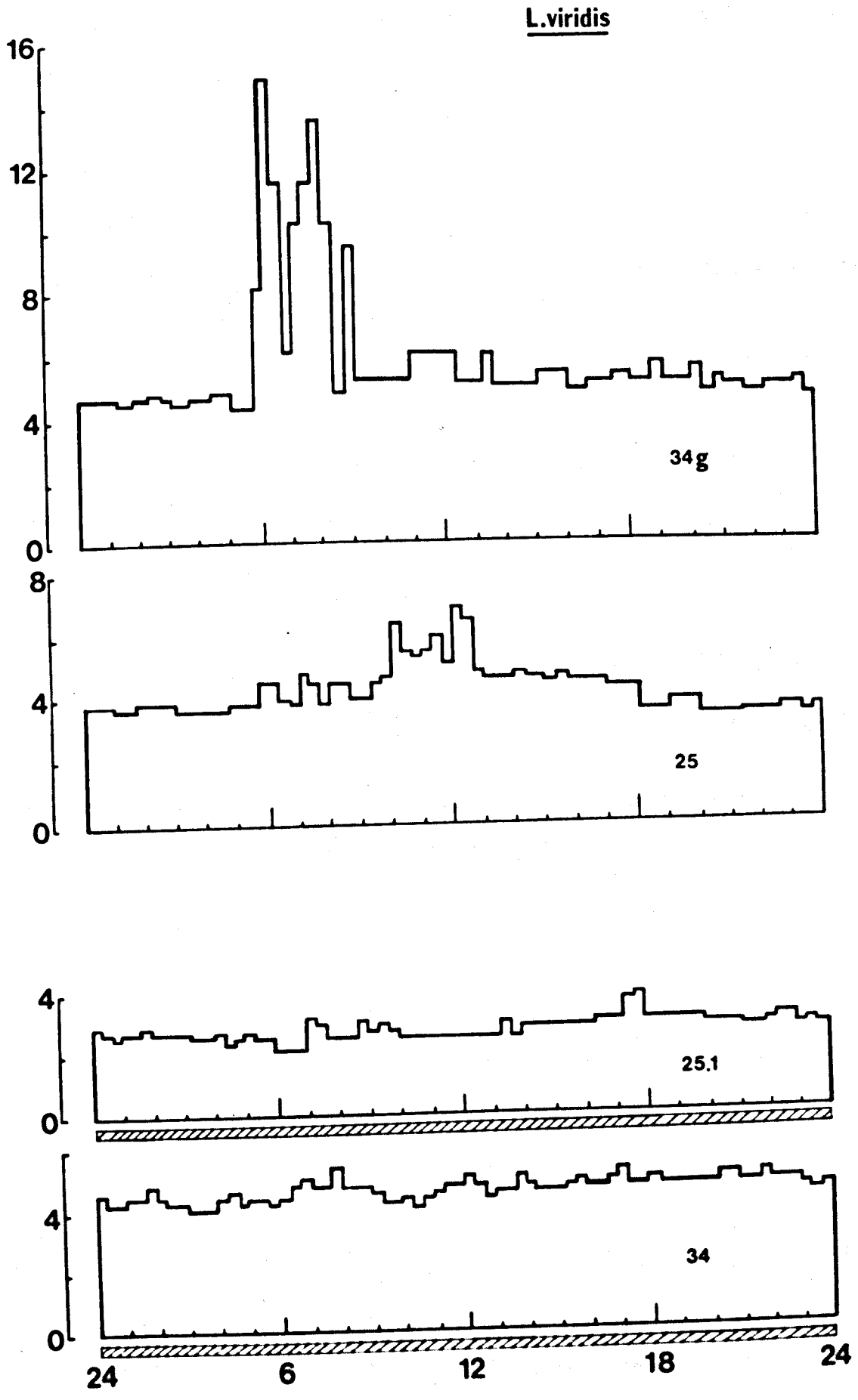
L.viridis
16
12
8
4
0
34 g
8
4
0
25
4
0
25.1
4
0
34
24
6
12
18
24
Time of Day — Hrs.

peaks occurred within the hours 06.00 to 18.00 (i.e. normal 'day') but they were as variable in pattern as had been found in 12hrL/12hrD regimes.

Table 1.1 compares the ratios of mean light $\dot{V}O_2$/mean dark $\dot{V}O_2$ and max.20 min $\dot{V}O_2$/min.20 min $\dot{V}O_2$ for all three species to indicate differences in unrestrained behaviour under 12hrL/12hrD regimes. It is obvious that 0.2g L. vivipara and L. viridis were less active in the experimental situation than were adult L. vivipara and L. sicula, the latter being the most active. There was no difference either in these ratios or in the pattern of peak activities during the light period when the animals were starved for 1 or 3 days. However, the respiratory quotient, R, did vary, being a mean of 0.85 ± 0.05 for 1 day's starvation and 0.75 ± 0.04 for 3 days' starvation (dark rates). A mean of 0.95 ± 0.05 was obtained for all 'light' rates. For mean values there was no difference between closed or open circuit estimations.

TABLE 1.1

A comparison of spontaneous, unrestrained activity in Lacerta under 12hrL/12hrD.

Animal	Mean Light $\dot{V}O_2$/mean Dark $\dot{V}O_2$	Max.20 min $\dot{V}O_2$/min.20 min $\dot{V}O_2$
L. vivipara 0.2g	1.35 ± 0.22	3.77 ± 0.8
L. vivipara adult	1.6 ± 0.15	4.44 ± 0.35
L. sicula	1.83 ± 0.38	5.25 ± 2.02
L. viridis	1.24 ± 0.2	3.6 ± 0.84

METABOLIC SCALING: STANDARD AND ROUTINE

From the data obtained in the 12hrL/12hrD $\dot{V}O_2$ recordings, 8 categories of $\dot{V}O_2$ were considered - mean dark, mean light, maximum 20 minute period and minimum 20 minute period $\dot{V}O_2$ under 1 and 3 days of starvation. Maximum $\dot{V}O_2$ only occurred during the light hours but minimum

FIG. 1.16 Logarithmic plot of standard $\dot{V}o_2$ versus body weight determined by a mean 'dark/night' rate after 3 days of starvation. See Table 1.2 for further details.

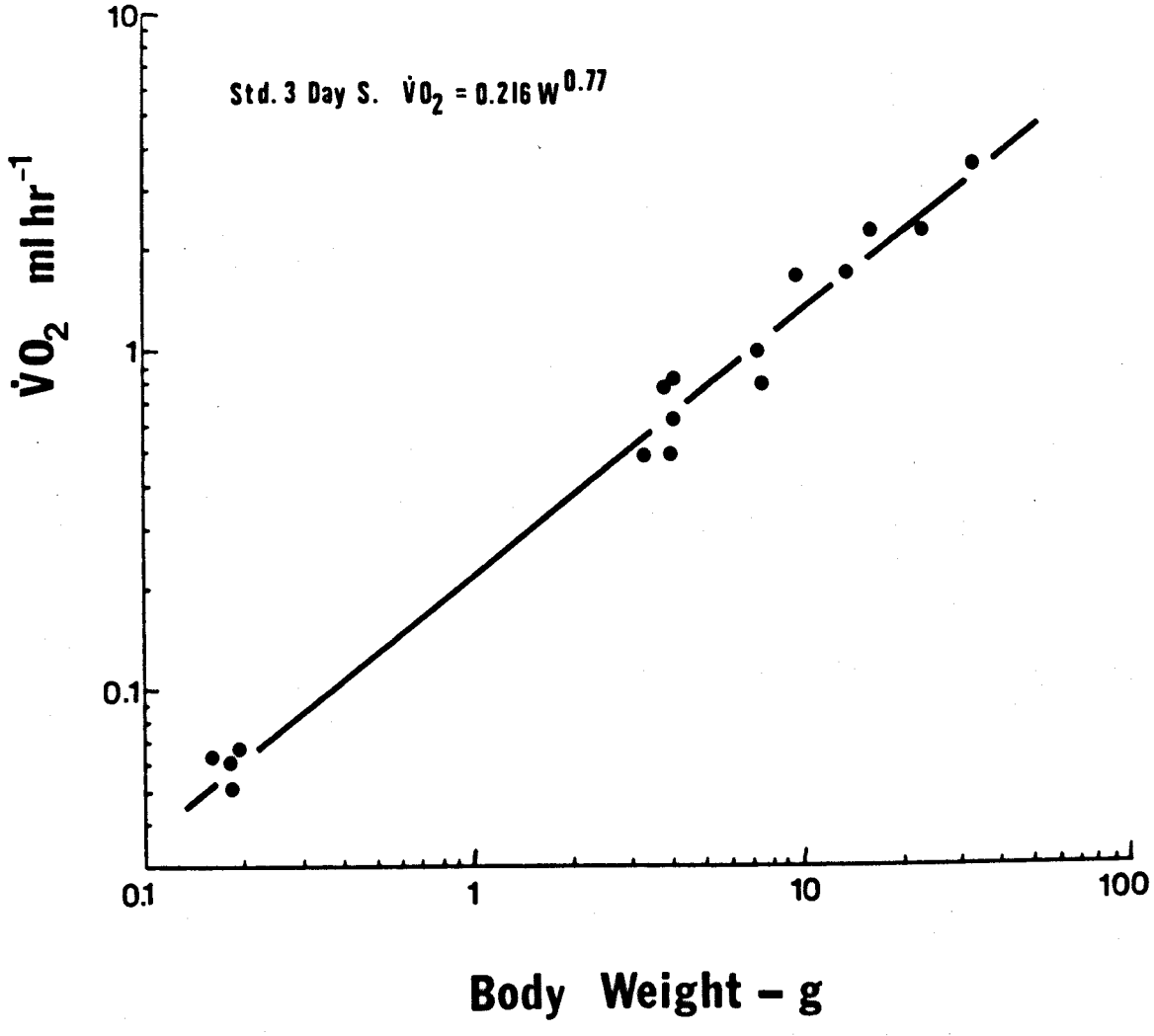
Std. 3 Day S. $\dot{V}O_2 = 0.216\,W^{0.77}$
$\dot{V}O_2$ ml hr^{-1}
10
1
0.1
0.1
1
10
100
Body Weight – g

TABLE 1.2

The relationship of $\dot{V}o_2$ to body weight under different conditions

$\dot{V}o_2 = aW^b$; N = number of animals; CC = correlation coefficient.

Condition		(Adult)b	(Adult)CC	N	(Total)a	(Total)b	(Total)CC
Dark $\dot{V}o_2$ (Night)	1 day starved	0.736	0.95	16	0.328	0.756	0.98
	3 " "	0.806	0.96	16	0.216	0.77	0.99
Min.$\dot{V}o_2$	1 " "	0.784	0.93	15	0.208	0.83	0.97
	3 " "	0.94	0.93	15	0.147	0.77	0.97
Light $\dot{V}o_2$ (Day)	1 " "	0.567	0.8	13	0.547	0.77	0.92
	3 " "	0.627	0.89	12	0.355	0.76	0.98
Diurnal Max.$\dot{V}o_2$	1 " "	0.74	0.9	16	0.975	0.8	0.957
	3 " "	0.692	0.89	14	0.608	0.78	0.98
MEAN		0.737 ± 0.1				0.779 ± 0.022	

$\dot{V}O_2$ occurred in both light and dark, but usually the latter. Logarithmic plots of $\dot{V}O_2$ against body weight are shown in Fig. 1.16 and Table 1.2.

It is apparent that regression slopes for 3 days' starvation have the least scatter of data. Inclusion of the 0.2g L. vivipara data gives better regression analysis for two reasons: (a) because the size range is increased from 1 to 2 log. cycles and (b) because the L. viridis and 0.2g L. vivipara data, occupying the two extremes of body weight, gave the lower $\dot{V}O_2$ ratios (Table 1.1) and are therefore required to balance each other. Since the average b value of 0.735, without 0.2g L. vivipara, is similar to the b of 0.78, with these young lizards, there seems to be no developmental reason for not including them with the adult data.

The best regression line of 0.77 (i.e. with the correlation coefficient of 0.99) was obtained for the mean dark $\dot{V}O_2$ under 3 days of starvation which one might expect to provide the best method of interspecific standardisation. However, it is considered that any slope between 0.735 and 0.78 would be an acceptable value for standard and routine metabolic scaling.

EXERCISE

Fig. 1.17 illustrates the change in % O_2 and % CO_2 occurring during exercise in open circuit conditions. In this example, the lizard consistently ran well throughout the 30 min adequately matching its running speed to that of the belt. Fig. 1.18 depicts the actual $\dot{V}O_2$ and $\dot{V}CO_2$ calculated from the raw data of Fig. 1.17 using the steady state and dynamic equations derived in the methods section whilst correcting for gas dilution caused by the moving belt. It is to be noted that the gradual decrease in % O_2 from a steady level taking approximately 8 minutes from the onset of exercise and the immediate further decrease at the end of the exercise, followed by an exponential return to the pre-exercise % O_2 level (Fig. 1.17) are artifactual properties of a dynamic open circuit system with dilution problems due to belt movement. The dynamic equations allow minute to minute monitoring of $\dot{V}O_2$ without the necessity of waiting for steady state conditions, the latter being capable

FIG. 1.17 Open circuit trace of % O_2 and % CO_2 during exercise at a sensitivity of 0.5% f.s.d. The arrows mark the beginning and end of exercise.

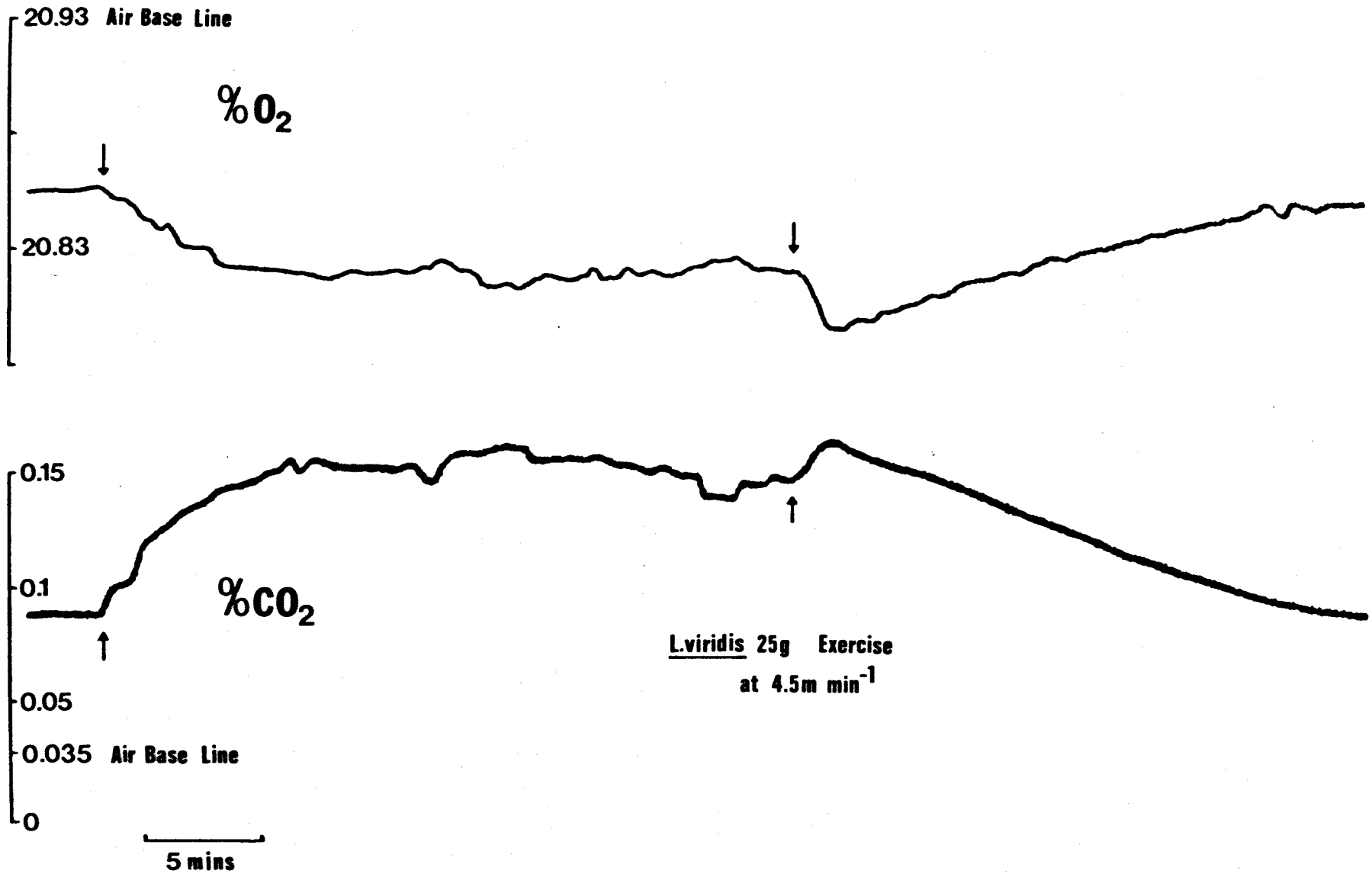
20.93 Air Base Line
%O2
20.83
0.15
0.1
%CO2
0.05
0.035 Air Base Line
0
5 mins
L.viridis 25g Exercise
at 4.5m min-1

FIG. 1.18 $\dot{V}o_2$ and $\dot{V}co_2$ analysed by steady-state and dynamic equations (whilst correcting for gas dilution) from the trace of Fig. 1.17.

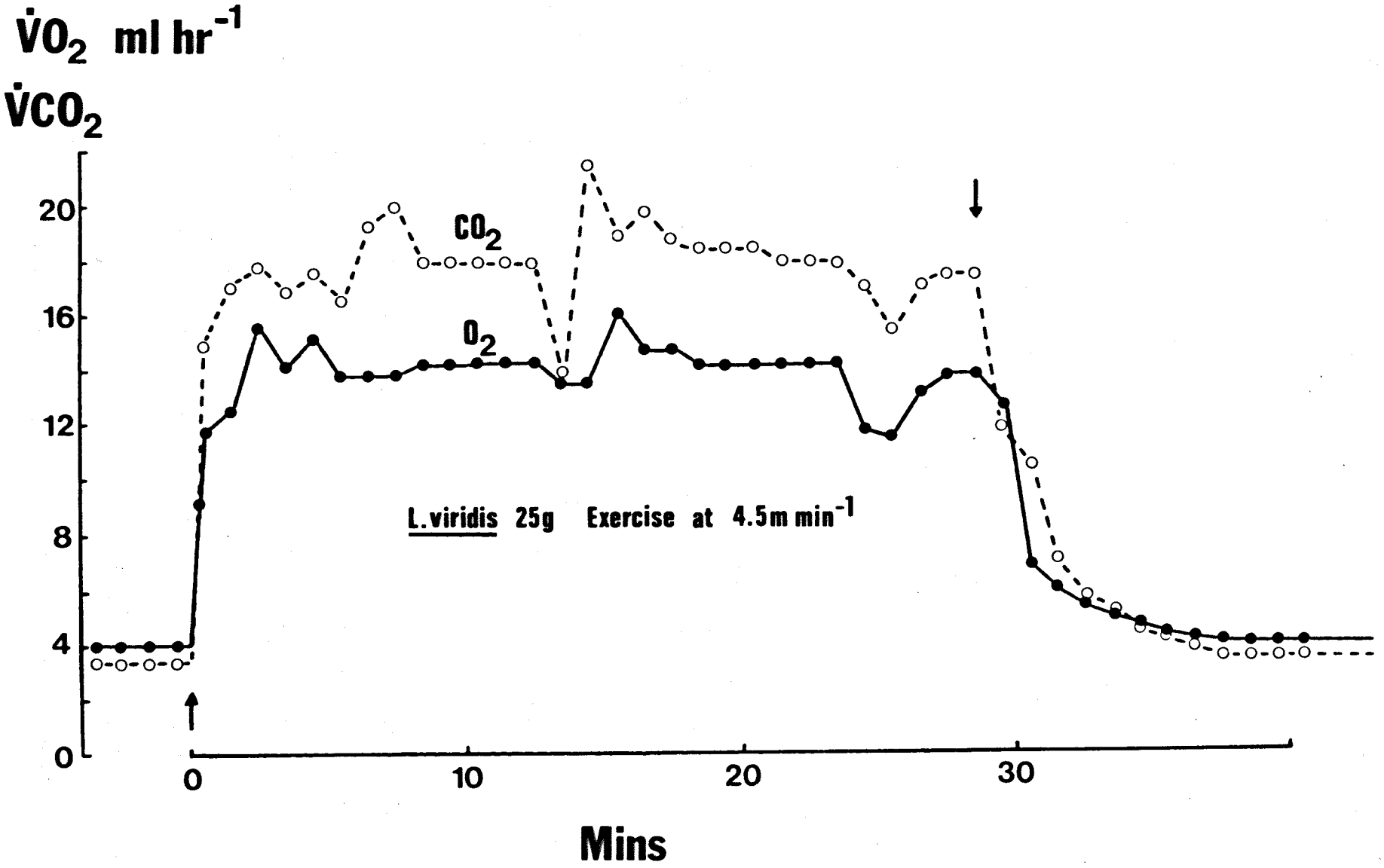
$\dot{V}O_2$ ml hr^{-1}
$\dot{V}CO_2$
20
16
12
8
4
0
CO_2
O_2
L. viridis 25g Exercise at 4.5m min^{-1}
0
10
20
30
Mins

only of estimating average $\dot{V}O_2$ values.

Thus, by dynamic monitoring, the exercise shown in Fig. 1.18 caused an immediate increase in $\dot{V}O_2$ which rose in $3\frac{1}{2}$ min to a high plateau level but then overshot for a further $3\frac{1}{2}$ min before returning to the plateau level. During the 30 min of constant exercise, there was one instance of a $\dot{V}O_2$ increase when the lizard tried to run faster than the belt and an instance of $\dot{V}O_2$ decrease when the lizard began to keep travelling to the back of the exercise machine and required clipping encouragement. At the end of the exercise, $\dot{V}O_2$ had returned to low levels within 2 min but took a further 7 min to finally return to a true pre-exercise $\dot{V}O_2$ level.

$\dot{V}CO_2$ more or less followed the pattern of $\dot{V}O_2$. It is not known whether the few differences reflect a true dissimilarity due to hypo- or hyperventilation or whether they are an artifact caused by the greater sensitivity of the CO_2 analyser to small changes in %. During 4.5 m min^{-1} exercise, the pre-exercise respiratory quotient, R, of 0.84 immediately rose to a mean of 1.28. After exercise, R declined gradually in 9 min back to 0.84, but it never undershot.

At the beginning and during moderate exercise in Lacerta, there were 4 alternative patterns which were independent of speed (Fig. 1.19). $\dot{V}CO_2$ followed these patterns but at a higher ml hr^{-1}:

(a) $\dot{V}O_2$ immediately (i.e. within the first minute) reached a plateau level which was maintained throughout exercise.

(b) The $\dot{V}O_2$ plateau was sometimes higher in the first 8-10 min before falling to a new level.

(c) $\dot{V}O_2$ overshot immediately for 3 to 10 min before stabilising at a lower level.

(d) $\dot{V}O_2$ was sometimes delayed for 2-3 min before reaching a plateau or before overshooting prior to stabilising. This delay rarely occurred in L. sicula, though when present was directly attributable to a

FIG. 1.19 Different patterns of response to exercise in Lacerta. See text. Arrows indicate the beginning and end of exercise.

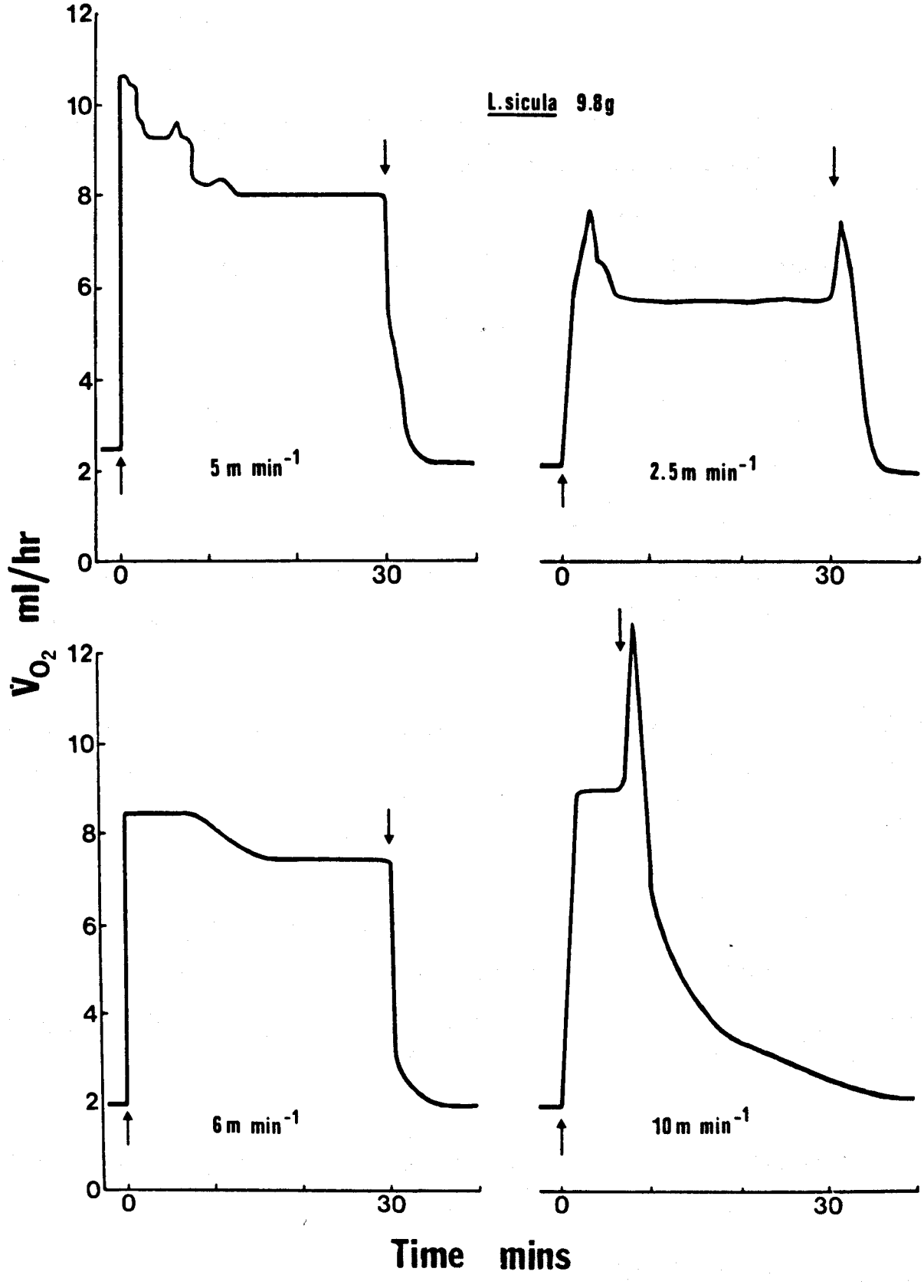
L. sicula 9.8g
5 m min-1
2.5 m min-1
6 m min-1
10 m min-1
V̇O2 ml/hr
Time mins
0
2
4
6
8
10
12
30

reluctance to begin exercise. L. sicula usually sprang into action as soon as the belt started, in contrast to L. viridis and L. vivipara in which delays were more frequent.

At the end of moderate exercise, $\dot{V}O_2$ either declined immediately almost reaching the base line within a few minutes as in Fig. 1.18 or it momentarily overshot before rapidly declining (Fig. 1.19). In either case the base line was not always reached because the lizard became spontaneously active, often in a futile attempt to get out of the exercise enclosure. This was more obvious in L. sicula and L. viridis than in both the more placid and least aggressive L. vivipara. Table 1.3 compares the time taken to reach resting levels and the extra $\dot{V}O_2$ above resting, the O_2 deficit, during this period. A relationship between the O_2 deficit and speed of moderate exercise could not be discerned because of the frequent occurrence of spontaneous activity. It is thought that the apparently higher O_2 deficit in L. viridis may be due to its more aggressive nature.

TABLE 1.3

A comparison of O_2 deficit and O_2 debt repayment time in Lacerta

Animal	Moderate Exercise (30 min)		Severe Exercise (3-5 min)
	O_2 Deficit	Repayment Time	Repayment Time
L. vivipara	0.057 ml $hr^{-1}g^{-1}$	5-8 min	15-20 min
L. sicula	0.04	4-8 min	15-25 min
L. viridis	0.147	10-20 min	20-35 min

Under severe exercise (e.g. 10 m min^{-1} in Fig. 1.19) $\dot{V}O_2$ rose immediately to a high level which could be maintained for 3 to 5 min in the best performing lizards. At the termination of exercise, $\dot{V}O_2$ overshot momentarily before declining slowly to the base line. The response was

often not as clear cut as this; sometimes there was a delay in reaching the $\dot{V}O_2$ plateau if the lizard did not immediately spring into action, sometimes the $\dot{V}O_2$ plateau fluctuated if the lizard required too much clipping encouragement and sometimes the overshoot at the end of the exercise was not present. However, the slow decline to base line was always present indicating the utilisation of anaerobic pathways during exercise and this extra $\dot{V}O_2$ above that of resting is termed the O_2 debt. The O_2 debt incurred and to some extent the repayment time appeared proportional to the severity of the exercise (Table 1.3 and see O_2 requirement in Fig. 1.20). At these severe speeds, the lizard always refused to run before it became completely exhausted since some spontaneous activity or slight aggressive behaviour (the latter in L. viridis) could occur during the repayment of the O_2 debt.

From the data available, the relationship between $\dot{V}O_2$ and speed in Lacerta would appear to be linear (line fitted by eye) intersecting the y axis at resting $\dot{V}O_2$ for a zero speed (Fig. 1.20). Values to the left of the linear part were from lizards running moderately well but always with a jerky, darting action and therefore alternating between being faster and then slower than the belt. At higher speeds the relationship became curvilinear and finally plateaued at a constant mean $\dot{V}O_2$ over several increments of speed. Once the curvilinear phase was reached, the lizards refused to exercise properly during the latter part of the 30 minutes. Thus in the transition from curvilinear to a plateau relationship, the lizards were only being exercised for 30, 20, 10 and finally 5 minutes. During the severest exercise (5 min) the actual O_2 requirement for a particular speed could be calculated by including the O_2 debt paid back at the end of exercise. The slope of O_2 requirement versus speed, again fitted by eye, would appear to be the same or slightly greater than the linear phase of moderate exercise (Fig. 1.20).

During the exercise experiments, the average resting $\dot{V}O_2$ recorded was identical to (L. viridis) or up to 30% more (L. vivipara and L. sicula)

FIG. 1.20 Relationship between $\dot{V}o_2$ and speed (solid line and symbols). Open symbols and dashed line for O_2 requirement = $\dot{V}o_2$ + O_2 debt paid back later. Lines are fitted by eye. Vertical bars indicate the range of $\dot{V}o_2$ obtained

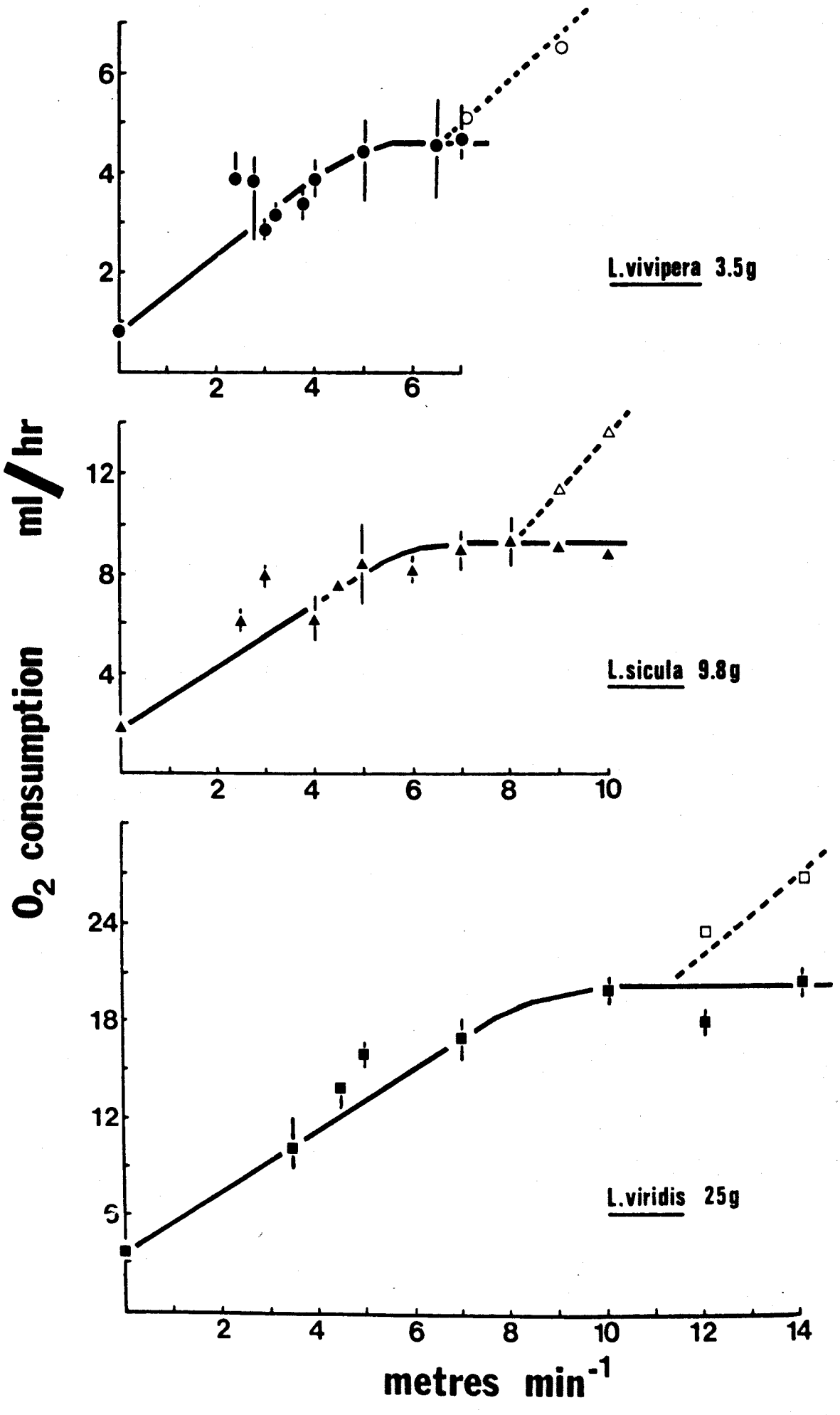
O2 consumption ml/hr
L.vivipera 3.5g
L.sicula 9.8g
L.viridis 25g
metres min-1

FIG. 1.21 Relationship between respiratory quotient, R, and speed.

The open symbol denotes resting R. Regression analysis for solid symbols gives

L. vivipara	$\dot{V}o_2 = 1.18 + 0.014\ m\ min^{-1}$ Correlation coefficient = 0.113
L. sicula	$\dot{V}o_2 = 1.079 + 0.0306\ m\ min^{-1}$ Correlation coefficient = 0.36
L. viridis	$\dot{V}o_2 = 1.09 + 0.0384\ m\ min^{-1}$ Correlation coefficient = 0.645

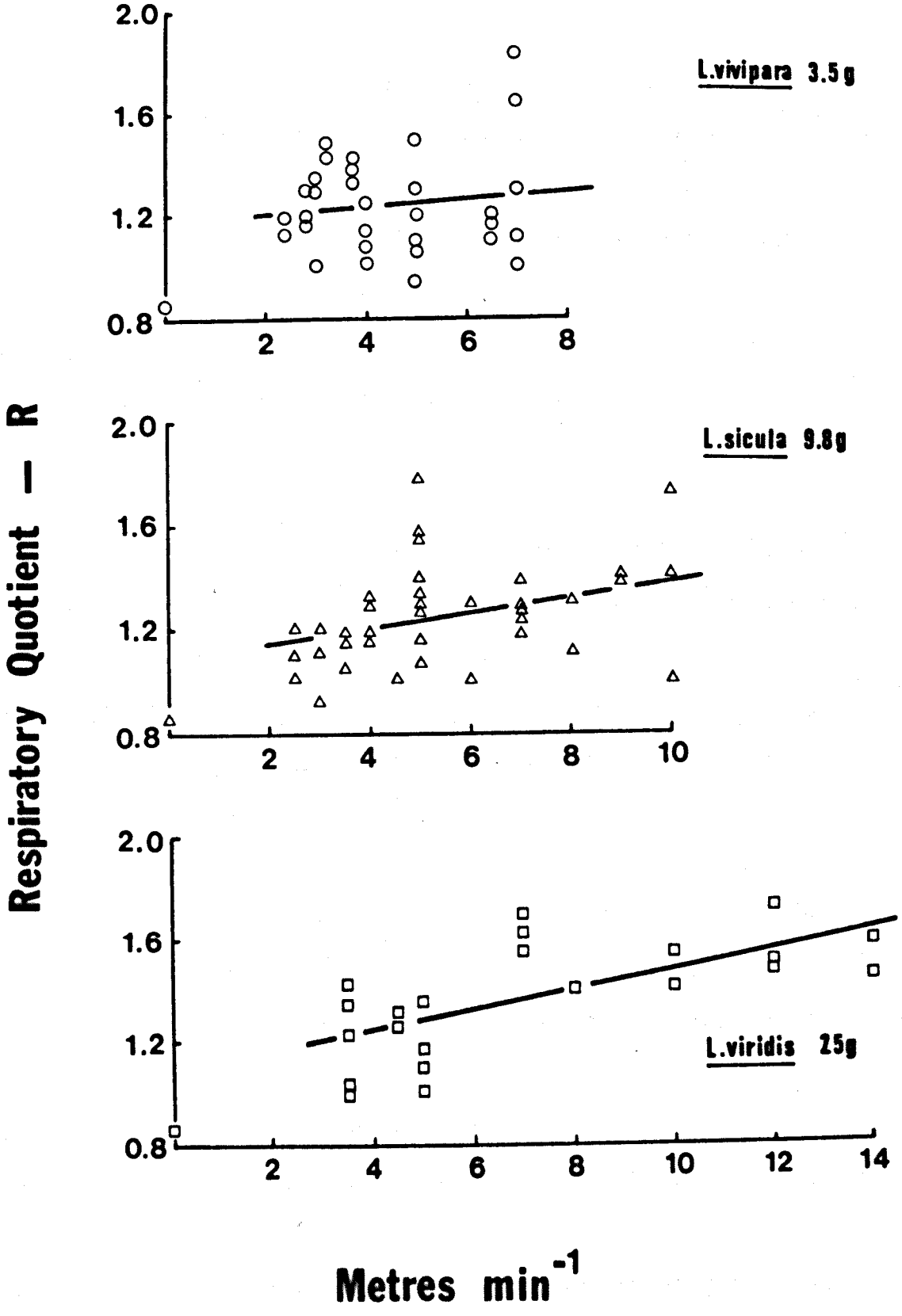
Respiratory Quotient — R
2.0
1.6
1.2
0.8
2
4
6
8
L.vivipara 3.5g
10
L.sicula 9.8g
12
14
L.viridis 25g
Metres min-1

than the mean dark $\dot{V}O_2$ recorded for 1 day of starvation. Since locomotor activity was not always absent before exercise in the latter two species, the mean dark $\dot{V}O_2$ was considered the more accurate measurement to use in the relationship between $\dot{V}O_2$ and speed.

R, the respiratory quotient, was not related in a curvilinear manner to speed in contrast to $\dot{V}O_2$, but was linearly proportional (albeit with much scatter of data) having a y intercept of 1.18, 1.08 and 1.09 in the three Lacerta species (Fig. 1.21). These values were much higher than the resting value of 0.85. Thus any level of exercise caused a substantial increment in R, indicating that a background of anaerobic pathways may operate even at low levels of activity. The dependence on anaerobic pathways increased with speed. Alternatively, there may be considerable hyperventilation. At the end of exercise, the return of R to a resting level was dependent on the repayment time for O_2 deficit and debt and followed the course of the decline in $\dot{V}O_2$ (Fig. 1.18). R never decreased to values below 0.85 $\pm$ 0.04 during the repayment period.

SCALING OF EXERCISE PARAMETERS

The mean $\dot{V}O_2$ sustainable for 3-5 min during the severest exercise, i.e. plateau $\dot{V}O_2$, was related to body weight by a 0.76 regression line with an intercept 5 times that of the resting values (Fig. 1.22). The metabolic minimum cost of exercise, expressed here as exercise $\dot{V}O_2$-intercept $\dot{V}O_2$/km hr^{-1} in accordance with that of Taylor, Schmidt-Nielsen & Raab (1970), was determined for the linear part of the $\dot{V}O_2$:speed relationship, cost therefore being its slope in ml km^{-1}. Intercept $\dot{V}O_2$ and resting $\dot{V}O_2$ in Lacerta were synonomous. Minimum cost was related to body weight by a regression of 0.53, or in weight-specific terms, by -0.48 (Fig. 1.22 and 1.26).

It is obvious that to run a km in a small lizard requires many more strides than in a large lizard and hence metabolic cost is greater at -0.48 instead of the -0.25 expected from $\dot{V}O_2$ relationships. The scaling of Lacerta speeds might be expected to be governed by their body length and/or

FIG. 1.22 Logarithmic plots of exercise parameters and body weight. All slopes had correlation coefficients of 0.99 or 0.98.

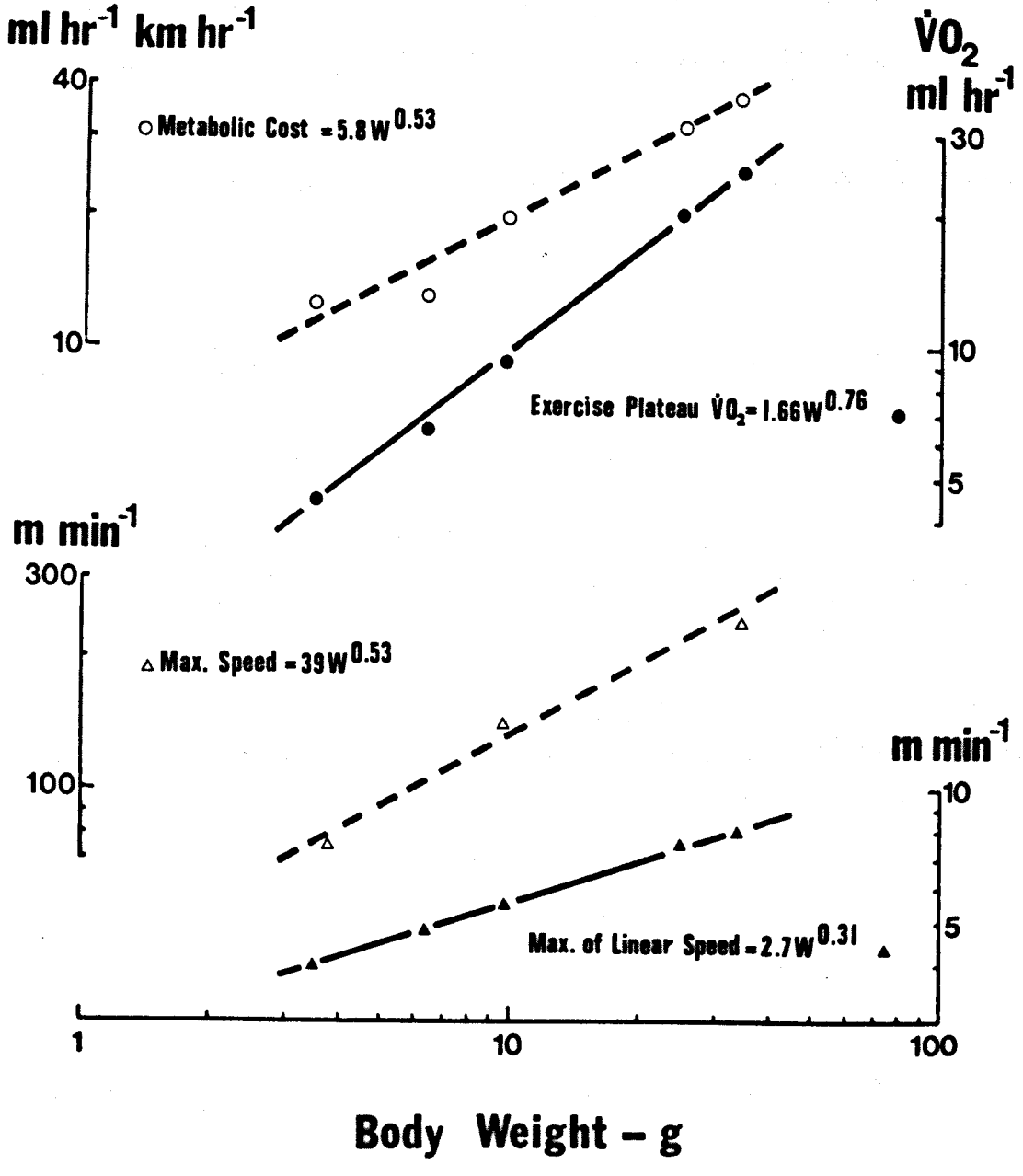
ml hr-1 km hr-1
40
10
○ Metabolic Cost = 5.8 W 0.53
V̇O2
ml hr-1
30
10
5
Exercise Plateau V̇O2 = 1.66W 0.76
m min-1
300
100
△ Max. Speed = 39W 0.53
m min-1
10
5
Max. of Linear Speed = 2.7W 0.31
1
10
100
Body Weight – g

limb length. It was found that the maximum speed of the linear $\dot{V}o_2$ relationship was proportional to $W^{0.31}$ but the maximum speeds that the lizards could run spontaneously when released into narrow channels was proportional to $W^{0.53}$ (Fig. 1.22). These speeds were some 10 to 20 times greater than on the treadmill but were maintained for only 0.2 to 0.6 sec. They are however more typical of the lizard's natural running activity.

Snout-vent length was proportional to $W^{0.33}$ in all three species (Fig. 1.23). The size range was not sufficient to give accurate regression analysis for L. viridis alone and thus L. sicula and L. viridis data have been combined. This also applied to L. vivipara adult and juveniles. Table 1.4 gives the regression analysis for the individual species.

TABLE 1.4

Relationship between snout-vent length, L, and body weight, W, where a is the intercept, b the regression coefficient and CC the correlation coefficient in the power series $L = aW^b$. The number of individuals examined is in parenthesis. L = cm, W = g.

Animal	a	b	CC
L. sicula (43)	3.55	0.331	0.956
L. viridis & L. sicula (88)	3.58	0.329	0.985
L. vivipara total (50)	3.56	0.329	0.98
All lizards (181)	3.56	0.331	0.99
L. vivipara ♂ + newly hatched (34)	3.46	0.312	0.994
L. vivipara ♀ + " " (24)	3.712	0.357	0.991
L. vivipara ♂ + ♀ juveniles (20)	3.436	0.305	0.995

Only in L. vivipara was there any sex difference in snout-vent length for a particular body weight. Female adult L. vivipara always had a longer body length than the male. A relationship of $L = aW^{0.33}$ is

FIG. 1.23 Logarithmic relationship of snout-vent length and body weight. Correlation coefficients were all 0.99. See also Table 1.4.

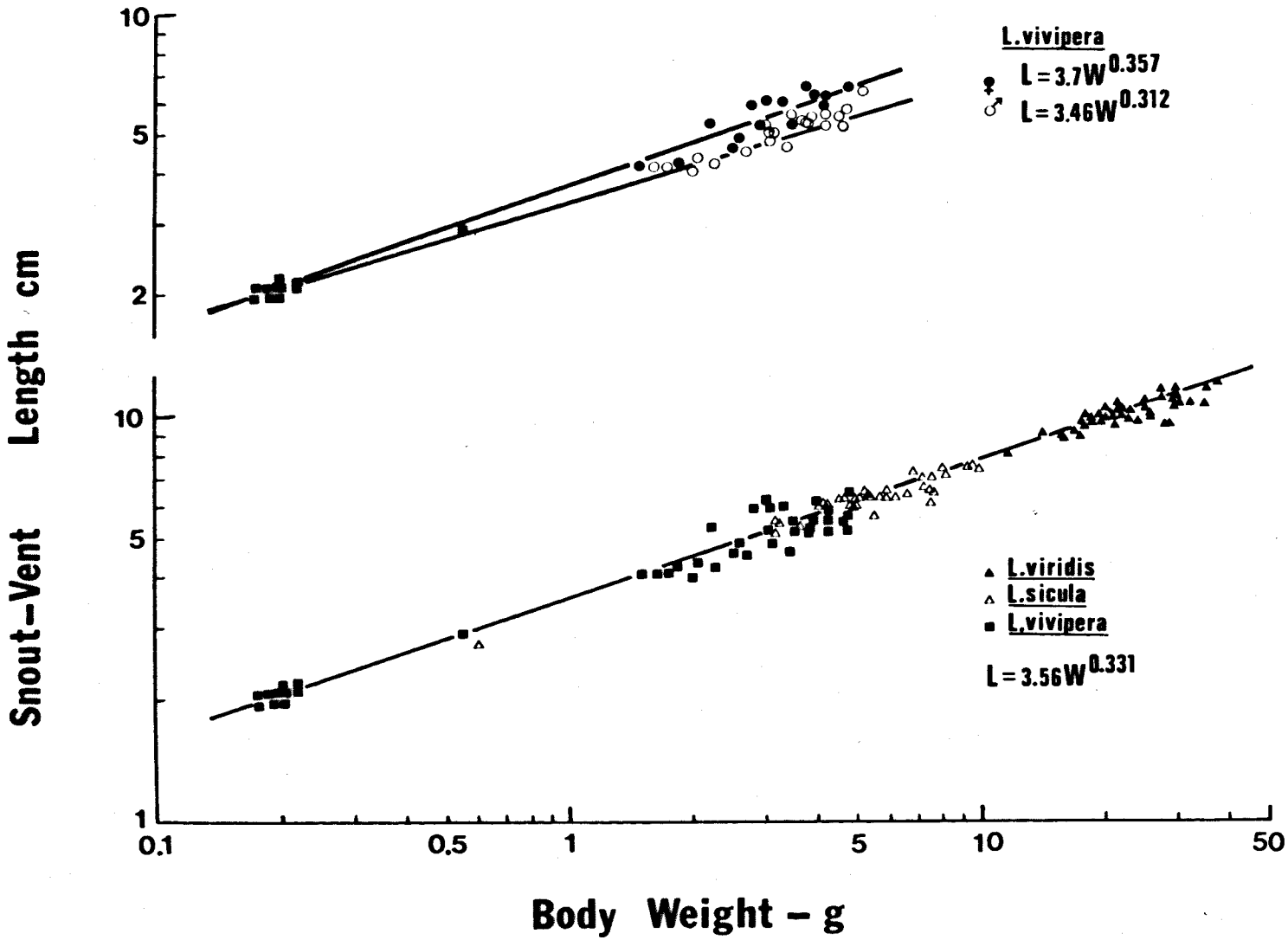
Snout-Vent Length cm
10
5
2
10
5
1
0.1
0.5
1
5
10
50
Body Weight – g
L.vivipera
♀ L = 3.7W^0.357
♂ L = 3.46W^0.312
▲ L.viridis
△ L.sicula
■ L.vivipera
L = 3.56W^0.331

FIG. 1.24 Logarithmic relationship of limb length and snout-vent length. Correlation coefficients of 0.98 and 0.99. N = 43 *L. sicula*, 45 *L. viridis*, 50 *L. vivipara*.

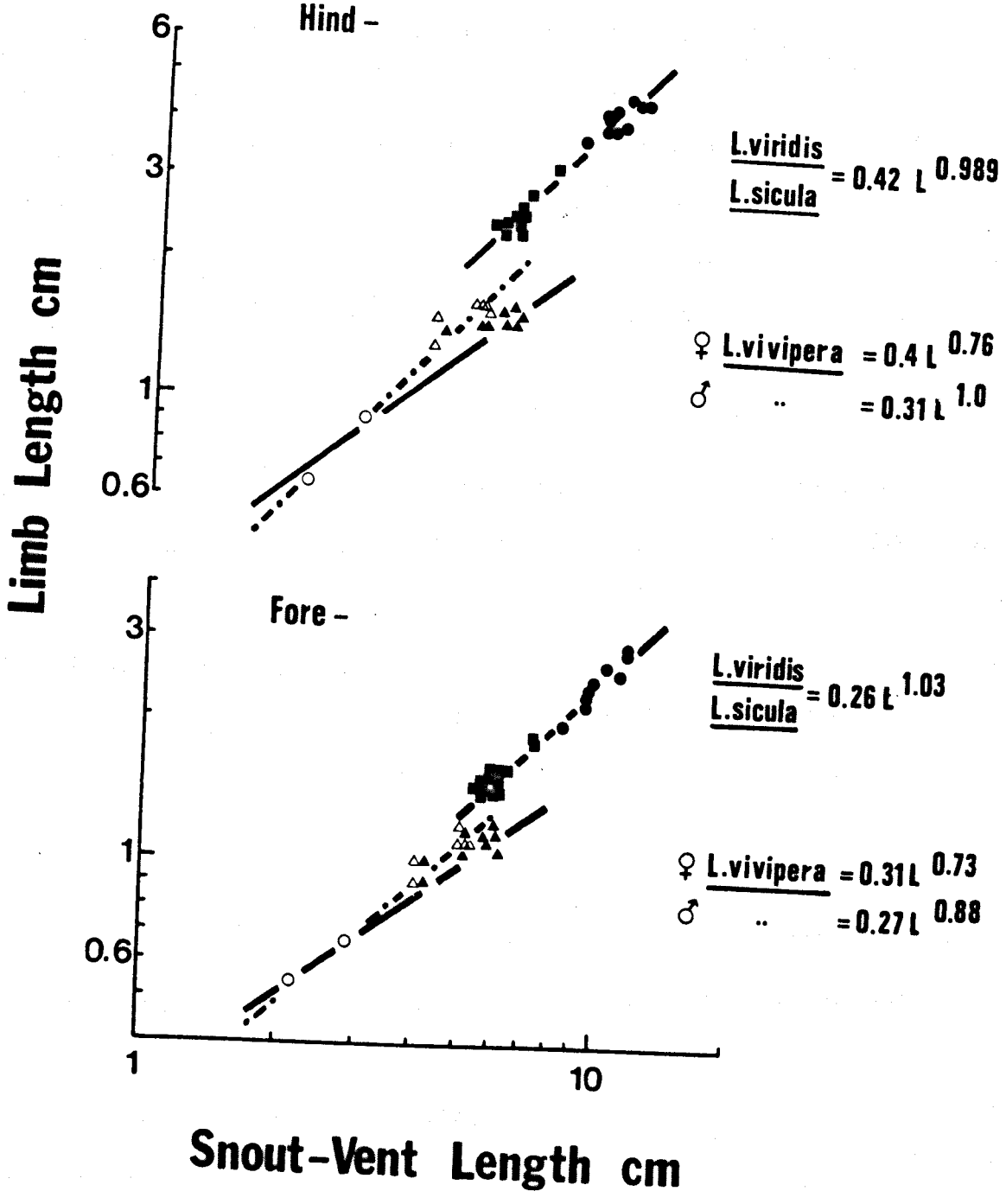
Hind –
6
3
1
0.6
L.viridis / L.sicula = 0.42 L 0.989
♀ L.vivipera = 0.4 L 0.76
♂ .. = 0.31 L 1.0
Fore –
3
1
0.6
1
10
L.viridis / L.sicula = 0.26 L 1.03
♀ L.vivipera = 0.31 L 0.73
♂ .. = 0.27 L 0.88
Limb Length cm
Snout-Vent Length cm

synonomous with that of $W = aL^{3.0}$ and considering L. vivipara data only, female weight varied rather less than the cube of snout-vent length $W = aL^{2.773}$ whereas male weight varied somewhat more $W = aL^{3.17}$. Juvenile L. vivipara were related as $W = aL^{3.239}$.

Limb lengths in L. sicula and L. viridis were virtually isometric with body length and hence were also related to body weight as $W^{0.33}$ (Fig. 1.24). The hind-legs were 1.6 times longer than that of the forelegs and were undoubtedly the power source for exercise. However, L. vivipara had much shorter limb lengths, especially the hind-limbs, for the same snout-vent length and body weight as L. sicula. The increase in snout-vent length in the female L. vivipara is not accompanied by elongation of the limbs and hence in females the limb length was related to $L^{0.73}$ or $L^{0.76}$ whereas the males were still virtually isometric $L^{1.0}$ and $L^{0.88}$ (the latter value is possibly an underestimate). A regression analysis for the hind-limb length versus snout-vent length using all three species, gave a slope of $L^{1.7}$ or in terms of hind-limb length and body weight, $W^{0.5}$.

METABOLIC SCALING: MAXIMUM

Data of short term maximum $\dot{V}o_2$ has been taken from three sources -

(a) 1 minute periods during severest exercise and repayment of O_2 debt.

(b) 1 - 3 minute periods of frantic activity when lizards were first introduced into the respirometer for diurnal $\dot{V}o_2$ studies, and

(c) 30 sec periods of maximum spontaneous struggling when tied to a jig and breathing through a mask in open circuit. This latter data is taken from Chapter 2.

Adult data was from (a), (b) and (c) but recently hatched L. vivipara data was only possible from (b).

It was found that maximum $\dot{V}o_2$ was related to body weight by a 0.76 regression line with an intercept 8 to 12 times that of resting values (1 or 3 days starved) (Fig. 1.25). This was true for both adult data, $\max.\dot{V}o_2 = 2.57\ W^{0.76}$ (correlation coefficient 0.95) and with the inclusion of 0.2g L. vivipara, $\max.\dot{V}o_2 = 2.66\ W^{0.747}$ (correlation coefficient 0.975).

FIG. 1.25 Logarithmic relationship between max.$\dot{V}o_2$ and body weight. Dashed line is for std.$\dot{V}o_2$ (1 day S) with an intercept 8.1 fold less.

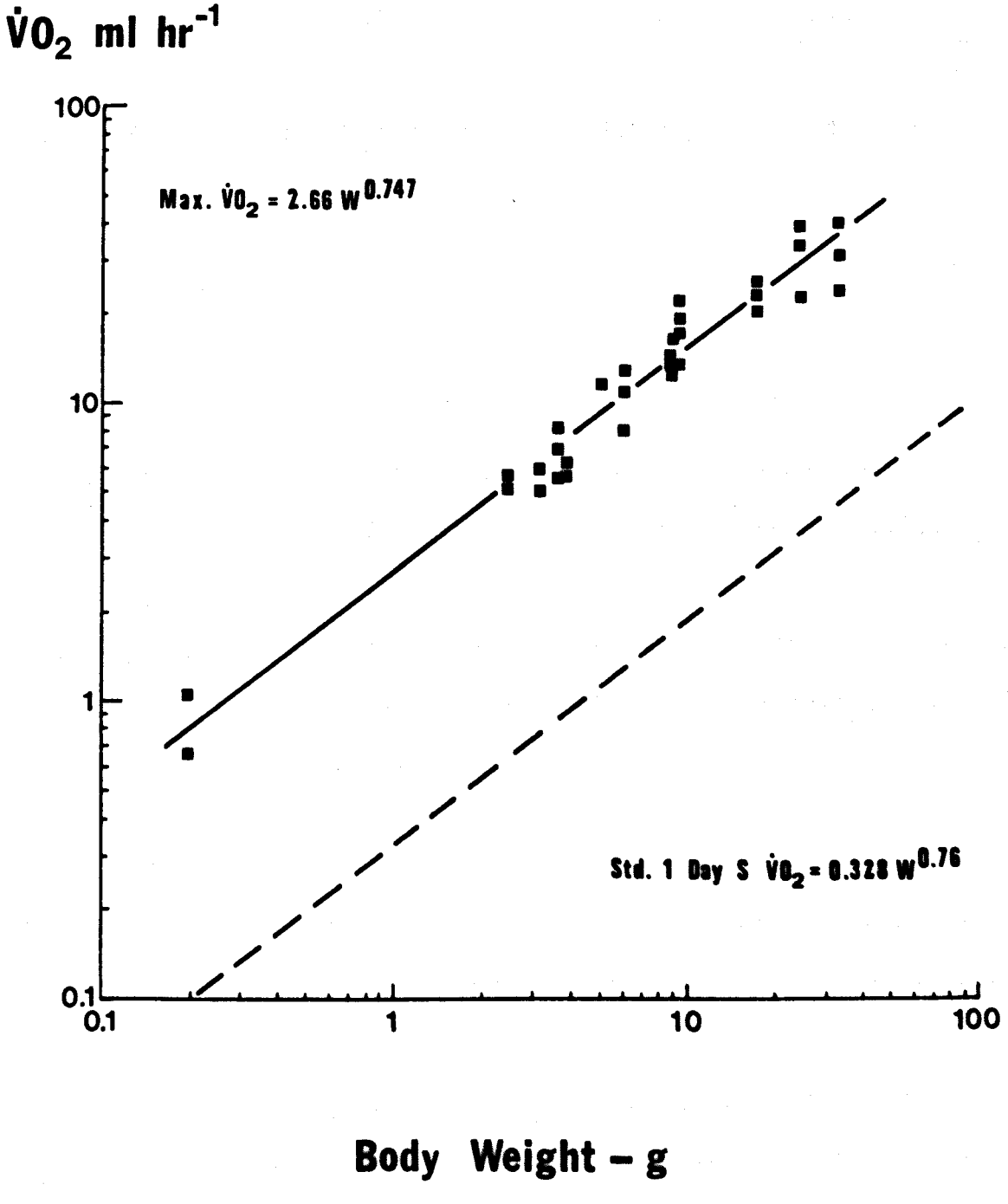
$\dot{V}O_2$ ml hr^{-1}
100
10
1
0.1
0.1
1
10
100
Max. $\dot{V}O_2 = 2.66\ W^{0.747}$
Std. 1 Day S $\dot{V}O_2 = 0.328\ W^{0.76}$
Body Weight – g

DISCUSSION

Diurnal Rhythms

Although this work was not designed to study diurnal rhythms, it does, however, contribute further information for Lacerta. Cloudsley-Thompson (1971) has recently reviewed such rhythms in reptiles studied either in their natural habitat or in experimental aktographs under natural or artificial light. Some reptiles are diurnal, some nocturnal; all have a periodicity of approximately 24 hours with either one or two periods of activity. Under constant light or darkness the activity pattern remains, as does the 24 hour periodicity for many days, indicating an endogeneous rhythm. However, in these reptiles the rhythm can be adjusted by alternating light and darkness of a different periodicity and by regular temperature fluctuations. Temperature is often the more dominant of the two (Evans, 1966). The endogeneous rhythm of Cnemidophorus (Barden, 1942) is shifted as the day lengthens or shortens by another mechanism - in constant light the periodicity remains but the active period occurs half an hour earlier each day, while the initiation of activity is similarly delayed by constant darkness. Reversal of the light/dark phase causes constant activity. In reptiles having an endogeneous rhythm, entrainment to reversed lighting takes many days.

In contrast some reptiles, e.g. Agamids (Toye, 1972, Subba & Rajabai, 1973) become arrhythmic in constant conditions, especially under constant light, and will entrain immediately, or by the second day, to reversed lighting. These rhythms are thus exogeneously controlled by the environment. There is considerable variation in the mechanisms controlling diurnal rhythms in reptiles and a clear distinction between endogeneous and exogeneous rhythms is not always made but nor is it always possible.

Only three groups have studied the diurnal rhythm of Lacerta. Kayser & Marx (1951) found an active period between 10.00 and 16.00 hours

at 19°C and between 07.15 and 18.00 hours at 29°C under conditions of constant light in L. muralis and L. agilis. Their rhythm synchronised immediately to reversed light/dark becoming completely entrained by the third day. No other light/dark patterns were tested. Hoffman (1955, 1960) has shown that L. sicula under constant light over a few days shorten the cycle from 23.5 to 22 hours although the active period lengthens (i.e. the latter is similar to Barden, 1942), whilst constant dark increased the cycle from 24 to 24.5 hours and reduced the active period. This lizard species can also be entrained in constant light by cycles of fluctuating temperature to be active during the higher temperature (Hoffman, 1969). He has not studied entrainment to different light/dark cycles at a constant temperature nor to reversed lighting. Fischer (e.g. 1961) has shown that L. sicula, L. muralis and L. viridis are able to use orientation of the sun to judge the time of day.

Oxygen consumption has not been used before in reptiles to study diurnal rhythms, possibly because it demands too many unnatural conditions. However, this method was still able to show convincingly consistent diurnal patterns of activity in L. sicula which remained in both constant light and dark. The one hour delay before activity began in the normal 'day' is in agreement with that found by Kayser & Marx (1951) at the same temperature for a very similar species L. muralis (L. sicula and L. muralis are often considered to be the same species). The fact that L. sicula had been entrained for some weeks or months to a light period beginning at 06.00 hours but failed to become active before 07.00 hours suggests a strong endogeneous rhythm. This is further supported by the consistent decrease in activity around mid-day (which has not been documented before) which may be due to an environmental, high, mid-day temperature in the wild. However, the rapid entrainment to reversed lighting (Kayser & Marx, 1951) must indicate an over-riding exogeneous control. Unfortunately, reversed lighting has not been tested by any other workers. Avery (personal communication) has found that L. sicula can be conditioned to be active only during a light period

lasting from 10.00 to 16.00 hours. Activity began at the onset of light, though not before, and finished at the onset of dark. However, the environmental temperature was only $\sim 20^{\circ}C$ (c.f. similar active period at this temperature, Kayser & Marx, 1951). At the lower temperature, reduced activity was found in the latter hours of the light period (Avery) in contrast to the increased activity at the higher temperature of this study.

L. vivipara, on the other hand, showed no endogeneous rhythm, activity only being possible in the light. There was no distinct pattern of activity during the 12 hour light period, although there may be some consistent tendency to be less active in the first two hours. No difference could be discerned between the activity at $20^{\circ}C$ (in cage) and at $29^{\circ}C$ ($\dot{V}o_2$ measurements). Avery & McArdle (1973) have found that the emergence of L. vivipara is governed by the amount of incident solar radiation and in laboratory conditions (personal communication) is sometimes delayed for an hour after the onset of light at $20^{\circ}C$. In the wild, temperature is a stronger exogeneous stimulus than light as might be expected for a poikilothermic animal. Constant light greatly disturbed L. vivipara causing a higher mean $\dot{V}o_2$ than even the normal 'day'. One apparently healthy individual even died under constant light at $29^{\circ}C$. Shelter reduced the disturbance but did not alter the stimulation effect of light. Without light, whatever the temperature, activity could not occur. L. vivipara is the first reptile shown to have a diurnal rhythm completely controlled by exogeneous stimuli.

L. viridis showed a diurnal rhythm which was similar in some respects to both L. vivipara and L. sicula. Activity was not possible in the dark even during the 'day' but in constant light, a normal diurnal rhythm persisted. This may indicate an endogeneous rhythm which is completely inhibited by the dark. The situation during normal 12 hour light/12 hour dark is complicated by the fact that L. viridis are often inactive when there is nothing to investigate. Aktograph experiments pertaining more closely

to the natural environment, i.e. with shelter, water, food, etc., are obviously necessary for diurnal studies in this species of Lacerta. Hoffman (1959) has used L. viridis for some diurnal studies and has documented no difference between L. sicula and L. viridis.

Much further work is clearly required for the understanding of mechanisms controlling both endogeneous and exogeneous rhythms in Lacerta and other reptiles.

Metabolic Scaling

By means of the diurnal rhythm studies, it was possible to determine the experimental conditions needed for minimum stress in the three Lacerta species. Whatever the time of day, constant dark together with shielding from all extraneous stimuli, caused minimum stress to L. vivipara and L. viridis. In L. sicula, this minimum stress period was found only during 18.00 to 06.00 hours irrespective of the presence of light or dark. Roberts (1968) also found that dark during the 'day' would not yield standard $\dot{V}o_2$ in Uta. It is important to note that all three species took two to three hours to settle down in the respirometer; this adjustment time being shorter if it occurred in the lizard's minimum stress period. Although the effects of tying a lizard to a jig within the respirometer were not extensively studied, it was found that L. viridis would 'accept' the restriction and be inactive during the 'day', whilst L. sicula would have bursts of struggling activity even during the 'night'. L. vivipara when restrained would only struggle if it was light.

Standard $\dot{V}o_2$ determined in the minimum stress period was found to be proportional to $W^{0.74 \text{ to } 0.8}$ (Table 1.2). Measurements that depended on the spontaneous actions of the lizard gave a much greater range of values for the b exponent; 0.77 to 0.94 for minimum $\dot{V}o_2$, 0.57 to 0.77 for routine day $\dot{V}o_2$ and 0.69 to 0.8 for diurnal maximum $\dot{V}o_2$. It is only perhaps by chance that these latter $\dot{V}o_2$ parameters came near to the 0.75 relationship since L. viridis and 0.2g L. vivipara had lower routine, etc. $\dot{V}o_2$ but occupied

the two extremes of body weight. When the lizards were exercised during their normal activity periods, this controlled activity yielded a plateau $\dot{V}O_2 = 1.66\ W^{0.76}$ and maximum $\dot{V}O_2 = 2.57\ W^{0.76}$ or $2.66\ W^{0.747}$. Thus within the genus Lacerta the 0.75 metabolic:body weight relationship is obeyed for both resting and active metabolism providing these determinations are rigorously standardised. This agrees with the 0.7 to 0.79 exponent found for food consumption versus body weight in L. vivipara 0.5 to 4g (Avery, 1971). Data from Kramer (1934) for L. viridis, L. serpa and L. major (1.7 to 71g) gives a slope of 0.794 by regression analysis (a = 0.086, cc = 0.995). Roberts (1968) in determining true standard $\dot{V}O_2$ found an average slope of 1.03 for Uta with a 0.89 or 1.17 slope depending on the season. This data, however, only covered 0.5 log. cycle.

Three days of starvation caused a 1.5 fold decrease in the $\dot{V}O_2$ recorded after one day's starvation for all diurnal $\dot{V}O_2$ categories. It also decreased the respiratory quotient, as would be expected. Gist (1972) found that it took two days to clear one Tenebrio larvae from the stomach of Anolis and that a few days' starvation reduced blood sugar level but not liver or muscle glycogen stores. This is probably true for Lacerta. For Uta, standard $\dot{V}O_2$ decreased during the two days after feeding but then remained constant for the next two weeks (Roberts, 1968).

Table 1.5 lists the resting $\dot{V}O_2$ values found by previous investigators. Even accounting for the lower temperature of Kramer's study (1934), his values for $\dot{V}O_2$ are considerably lower than in any of the other studies (underestimated by a factor of 10?). Krehl & Soetbeer (1899) give a $\dot{V}O_2$ similar to that determined for routine day activity after one day of starvation. All other investigators give much higher $\dot{V}O_2$ estimations than in the study presented here which may be due to the less accurate method of manometric analysis, lack of complete visual and auditory isolation and less than 24 hours of unrestrained recording. This may also partly explain the higher intercept values for the interspecific data of Bartholomew & Tucker (1964). More

TABLE 1.5

Resting $\dot{V}o_2$ in Lacerta as determined by different investigators. Note that the larger the animal the lower is its weight specific $\dot{V}o_2$.

Animal	$\dot{V}o_2$ ml hr^{-1} g^{-1}	Temperature °C	Reference
Lacerta spp (110g)	0.22	30	Krehl & Soetbeer (1899)
L. viridis (1.7g) L. serpa L. major (71g)	0.0675 to 0.028	20	Kramer (1934)
L. muralis (5g)	0.408	30	Gelineo & Gelineo (1955)
L. sicula (5.5g)	0.323		
L. melisellensis (6.8g)	0.436		
L. viridis (19.2g)	0.425		
L. sicula	0.4 to 0.9 mean 0.6	30	Nielsen (1961)
L. vivipara (4.0g)	0.75 mean	30	Avery (1971)
L. vivipara (3.0g)	0.187 to 0.25	28 ± 1°C	This study 3 and 1 days starved. 'Night'.
L. sicula (9.0g)	0.14 to 0.22		
L. viridis (30.0g)	0.1 to 0.15		
L. vivipara (3.0g)	0.266 to 0.435	28 ± 1°C	This study 3 and 1 days starved. 'Day'.
L. sicula (9.0g)	0.206 to 0.334		
L. viridis (30.0g)	0.153 to 0.254		
Lacerta (1.0g)	0.547	28 ± 1°C	This study 1 day starved. 'Day'.
Lizards (1.0g)	0.82	30	Bartholomew & Tucker (1964)
Lizards (1.0g)	0.42	37	Bennett & Dawson (1973)

recently Roberts (1968) and Bennett & Licht (1972) have determined true standard metabolism finding values three times less (Uta) and two times less (Dipsosaurus) than had previously been reported.

Templeton (1970) has compared resting $\dot{V}o_2$ in lizards and mammals, finding that at 37°C metabolism is three times greater in mammals, $\dot{V}o_2 = 1.33\ W^{0.65}$ and $3.9\ W^{0.75}$, respectively. For many of the lizards studied, however, 37°C is higher than their preferred body temperature (PBT). The PBT for L. vivipara is 30.2 ± 2.5°C and 33.7°C for L. sicula (Avery, 1971, Licht, Hoyer & Oordt, 1969). Lacerta are one of the few lizard species that show perfect thermal acclimation, i.e. if acclimated to 13 or 24°C for a few weeks identical $\dot{V}o_2$ measurements are found for both temperatures (Gelineo & Gelineo, 1955, Templeton, 1970). Since Lacerta were thermally acclimated to 28 ± 1°C for several weeks, a variation in PBT between the three species becomes unimportant and $\dot{V}o_2$ should be the same as at 37°C (assuming that this temperature would not distress the lizard).

Table 1.6 compares resting and maximum $\dot{V}o_2$ parameters in Lacerta and mammals. For both $\dot{V}o_2$ parameters, metabolism is ten times greater in the mammal, not three (or six times as in Dipsosaurus). The majority of lizards in Templeton's study (1970) had far more complex lungs than in Lacerta and hence may be expected to have a greater metabolism.

TABLE 1.6

A comparison of Lacerta and mammalian $\dot{V}o_2$

Parameter	Lacerta 30°C	Mammal 37°C	M/L ratio	Reference
Std.$\dot{V}o_2$ 1 day S	$0.328\ W^{0.756}$	$3.42\ W^{0.75}$	10.65	Pasquis, Lacaisse & Dejours (1970)
		$3.5\ W^{0.75}$		Stahl (1967)
Max.$\dot{V}o_2$ 1 day S	$2.66\ W^{0.747}$	$26.16\ W^{0.73}$	10	Pasquis, Lacaisse & Dejours (1970)
	$2.57\ W^{0.76}$			
$\frac{\text{Max.}\dot{V}o_2}{\text{Std.}\dot{V}o_2}$	8.0	7.5	0	

Response to Exercise

In large mammals, breath by breath analysis is used to measure the respiratory response to exercise. At moderate speeds, $\dot{V}o_2$ rises gradually to reach a steady level approximately two minutes after the onset of exercise and during the recovery period $\dot{V}o_2$ declines as a logarithmic function of time (Asmussen, 1965, Dejours, 1964). In the first two minutes, an O_2 deficit occurs which is paid back during the recovery period. This initial lag in $\dot{V}o_2$ is believed to be due to the delay in blood O_2 transport. Pulmonary ventilation, at any stage of exercise, is not limiting. Thus, anaerobic pathways are utilised initially, but not to any degree that would alter the respiratory quotient, R. Recovery time is related to the intensity of mammalian exercise.

In severe mammalian exercise, the same $\dot{V}o_2$ lag occurs but after the first two minutes, lactic acid builds up and is buffered by bicarbonate thereby liberating large amounts of CO_2 without any equivalent utilisation of O_2. Thus the extent that R exceeds 1.0 is some index of the severity of exercise. The recovery time and O_2 debt are related to the degree of exhaustion and therefore to the intensity of work and the length of time for which this work was conducted. At the end of exercise, R becomes very low, e.g. 0.5, because CO_2 is being retained in the blood to reform bicarbonate.

In contrast, Lacerta appear to have no time lag for the $\dot{V}o_2$ increase at the beginning of the exercise. It cannot, however, be ruled out that the method of dynamic calculation, which uses a mean change in F_{Eo_2} for an exponential function, would initially overestimate $\dot{V}o_2$ and then underestimate it. Only Moberly (1968b) has published the $\dot{V}o_2$ changes (but not $\dot{V}co_2$ and hence R) during lizard exercise. His graph for Iguana suggests that there was a time lag in reaching steady-state $\dot{V}o_2$ but since his method of $\dot{V}o_2$ analysis did not use dynamic calculations, the absence

of a time lag may have been obscured. Iguana sometimes showed similar overshoots in $\dot{V}o_2$ at the beginning and end of exercise as was found in Lacerta. Recovery times in Iguana were also similar to L. viridis taking 10 to 40 minutes after exercise with only a small background level of anaerobic metabolism. This time was greater than in a mammal (Asmussen, 1965) but considerably less than the three to four hours found in fishes (Brett, 1972). In Lacerta recovery time was shorter in the smaller animals in contrast to the data of Bennett & Licht (1972). Their data was, however, for maximum activity at high levels of anaerobic metabolism.

R always exceeded 1.0 whatever the level of activity in Lacerta and it increased as speed increased. Since the lizards refused to undergo very severe exercise on a treadmill, it is not known whether R would rise very rapidly at high speeds. The presence of a high R and a small recovery time even in moderate exercise in Lacerta would indicate that there is always a background level of anaerobic activity, which increases as speed increases. Since the recovery time is, however, quite quick it is possible that some of the increment in R may be due to progressively increasing hyperventilation as speed of exercise increases. Lactate levels need to be recorded at different levels of activity in Lacerta. Moberly's data (1966) for exercising Iguana covered speeds in which there was virtually no anaerobic metabolism determined by lactate measurements. Only a tenth to a thirtieth of the maximum possible Lacerta speed can be supported by aerobic metabolism. For strenuous activity the lizard becomes very reliant on anaerobic pathways. Normal daytime activity in the diurnal rhythm studies also showed a background of anaerobic activity (or hyperventilation) with R = 0.95 during the day compared with R = 0.85 during rest at night.

If the immediate increase in $\dot{V}o_2$ in Lacerta is genuine, it is of interest to consider why and how this may occur. In non-varanid lizards, lactate levels are high during electrically stimulated maximum struggling (Bennett & Licht, 1972, Bennett, 1973b). These workers have shown that

the blood of these lizards does not buffer this acid very efficiently so that the decreased pH and increased temperature of activity markedly shifts the oxyhaemoglobin dissociation curve to the right, decreasing O_2 affinity and maximum saturation but facilitating the unloading of O_2 in the muscle. This Bohr shift during exercise progressively increases the dependence on anaerobic pathways. If there is always some anaerobic metabolism even at low activity levels, this Bohr shift by favouring unloading of O_2 may partly explain the absence of a time lag in $\dot{V}o_2$ at the onset of moderate exercise in Lacerta.

Other factors may be that the P_{50} of lizards is approximately twice that of mammals of the same size (Bennett, 1973b), again favouring unloading and also that in both lizards and mammals, the smaller animals have a higher P_{50} (Schmidt-Nielsen & Larimer, 1958, Bennett, 1973b). $\dot{V}o_2$ lag times have only been studied in large mammals so that it is quite likely that a much shorter lag may be found in small mammals similar in size to the Lacerta. In smaller mammals, cardiac output is scaled as $W^{0.8}$ (Stahl, 1967) and hence transport times are quicker.

In reptiles, the cardiac output versus $\dot{V}o_2$ ratio is 40 in contrast to the mammalian 15 (Tucker, 1966, Dejours, Garey & Rahn, 1970) so that the excess cardiac output of the reptile may also favour quicker O_2 unloading. Tucker (1966) has shown that during Iguana activity, venous O_2 content is lowered whilst arterial O_2 content remains much the same, thereby increasing the A-V difference. These lizards can tolerate very low venous O_2 levels in contrast to a mammal. By extracting more O_2 from the blood already available to the muscle, the $\dot{V}o_2$ time lag could be reduced. It is, however, known that the rate of glucose metabolism is lower in reptiles than in mammals (Beloff-Chain & Rookledge, 1970, Bennett, 1972b) which may not favour short $\dot{V}o_2$ time lags at the onset of exercise.

Lack of a low R during the recovery period in Lacerta after severe exercise must indicate a lack of bicarbonate depletion as might be

expected with an inefficient H^+ buffering capacity in the blood. Considering the high anaerobic levels reached, it is surprising that recovery times were still fairly short. This is possibly because lizards easily tolerate lactic acid and its effects without the necessity for a complete repayment of the O_2 debt before undergoing further activity.

$\dot{V}o_2$: speed relationship

In Lacerta, the relationship between $\dot{V}o_2$ and aerobic speed is rectilinear with a plateau in $\dot{V}o_2$ at high speeds. This would appear to be intermediate between Moberly's curvilinear data (1966) and Bakker (1972) and Taylor's (1973) rectilinear data. The greater efficiency in terms of $\dot{V}o_2$ of faster speeds in Lacerta may be in keeping with their normal spontaneous running activity. The intercept of the linear phase in Lacerta is considered to be the same as resting $\dot{V}o_2$. However, as (a) the relationship was only fitted by eye, (b) Lacerta preferred to run faster than the slowest treadmill speeds, and (c) these lizards were difficult to train, it is possible that with further data intercepts above resting $\dot{V}o_2$ and even a rectilinear response may be found. Lacerta may not be a suitable lizard for studying reptilian metabolic costs during exercise. Certainly Bakker could only find five species out of a large number which would run well on a treadmill.

Scaling of exercise parameters

Minimum cost of running in Lacerta and mammals are similarly scaled (Fig. 1.26) being $W^{-0.48}$ and $W^{-0.4}$, respectively. The difference between these b exponents is not considered significant; especially as the shorter limbs of L. vivipara may increase the metabolic cost. Varanid data (Bakker, 1972, Taylor, 1973) for cost of running easily fits that of the mammal but lizards with less complex lungs (Lacerta and other lizards of Bakker, 1972 and Taylor, 1973) have a cost approximately 1.5 times less. For a 1 kg Iguana, Moberly (1968b) found that the net cost of running was 1.0 to 1.9 ml $g^{-1}km^{-1}$, i.e. higher than a 1 kg mammal. If, however, the

FIG. 1.26 Logarithmic relationship between minimum metabolic cost and body weight. *Lacerta* data this study. Mammalian data from Taylor, Schmidt-Nielsen & Raab (1970). Lizards and *Varanus* data from Taylor (1973) and Bakker (1972).

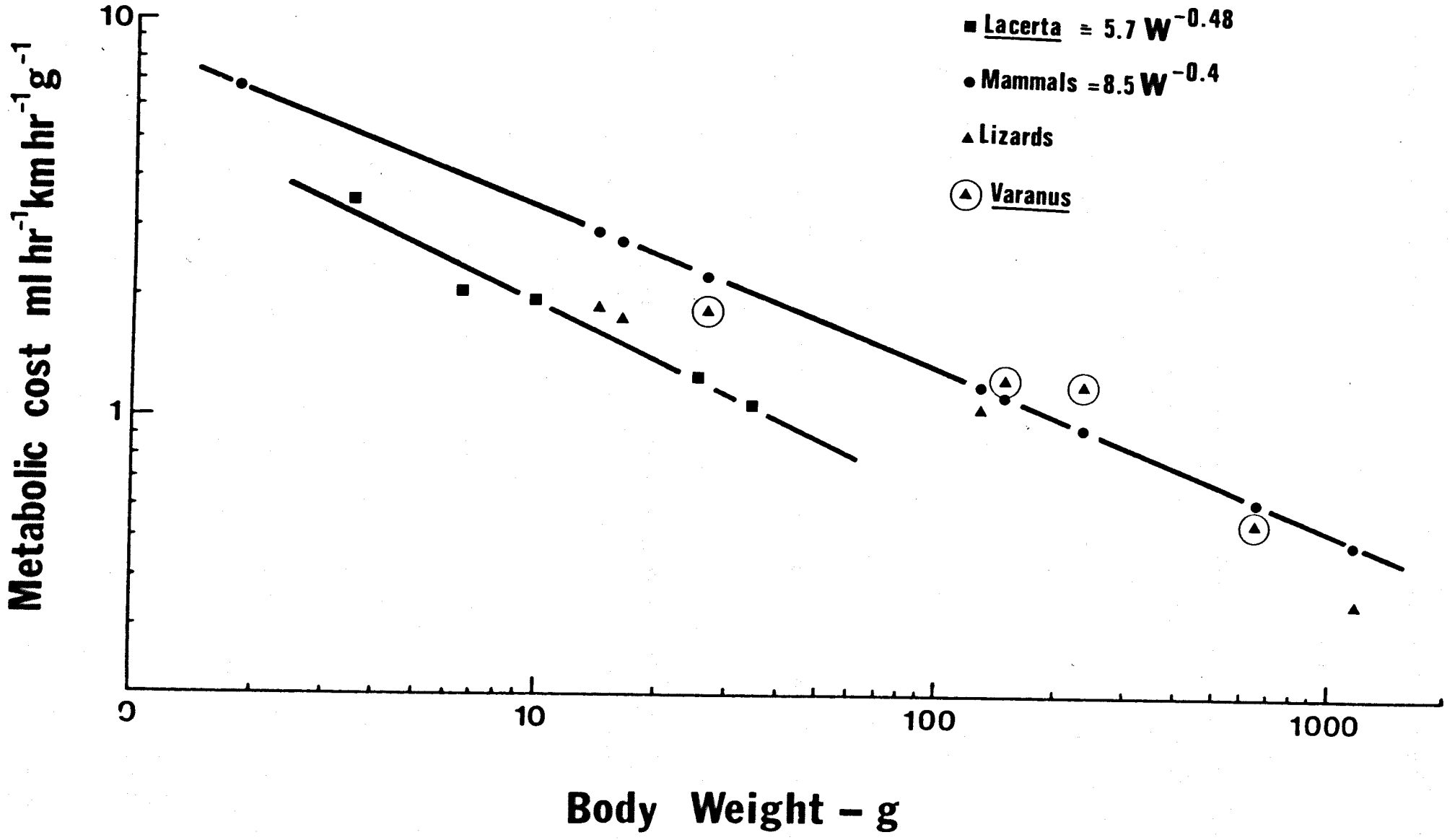
Metabolic cost ml hr^{-1}km hr^{-1}g^{-1}
10
1
0
10
100
1000
Body Weight – g
■ Lacerta = 5.7 W$^{-0.48}$
● Mammals = 8.5 W$^{-0.4}$
▲ Lizards
Ⓐ Varanus

small speed range of curvilinear data is treated as linear, the intercept becomes 0.2 to 0.18 ml $hr^{-1}g^{-1}$ above resting and M_{run} is approximately 0.4 to 0.6 ml $g^{-1}km^{-1}$, i.e. similar to the data of Bakker (1972) and Taylor (1973). In the snake, the cost of limbless, terrestrial locomotion is 2.5 times less than a mammal (Chodrow & Taylor, 1973).

Lizards have a sprawling wide-track gait which might be expected to require extra energy during running to maintain the lizard's body off the ground. Such extra energy would not be required by a mammal because of its erect gait (Taylor, 1973). Surprisingly, quadrapedal reptilian locomotion is only as costly (Varanus)or less costly (Lacerta) than a mammal when considering M_{run}, i.e. the slope of $\dot{V}o_2$ versus speed. Since, however, the difference between the y intercept and resting metabolism was either zero (Lacerta) or up to half the mammalian difference, it becomes apparent that all lizards expend much less energy than a mammal of the same size during running at the same velocity.

The speed that a lizard can attain is governed by its body length and/or limb lengths. Snout-vent length of all Lacerta varied as the cube root of body weight. Male L. vivipara, however, had a body weight related to body length by a 'b' value of 2.773 and 3.239, respectively. Avery (1973) found b to equal 3.09 in the male, 2.55 in the female and 2.81 in the juvenile. Although having different regression coefficients, the results of both this study and Avery's show that female L. vivipara have a longer snout-vent length for a given body weight than the male. Accommodation for the viviparous egg-clutch during the summer months must be the reason for this extra length. No such sex difference was found in the non-viviparous L. sicula and L. viridis thus supporting the above conclusion. Since old L. vivipara males are usually relatively heavier (Smith, 1964), it is not known why the juveniles of this study had the greatest b exponent.

The maximum speed attained in the linear phase of the $\dot{V}o_2$:speed relationship was scaled as $W^{0.33}$. This speed would appear, therefore, to be

governed by body length. Maximum running speed recorded when the lizards were released, however, was scaled as $W^{0.53}$. This is very similar to the relationship between hind-limb length and body weight, $W^{0.5}$, suggesting that maximum running speed is governed by hind-limb length and not by snout-vent length. During exercise, both on the treadmill and in the narrow channels, it was observed that L. vivipara used more sinusoidal (snake-like) movements of the body than were used by the other two species. Such movements could compensate for the shorter limbs, especially in the female, and allow greater speeds than might be expected giving a speed scaling of $W^{0.33}$. At extreme speeds such snake-like movements can, perhaps, not compensate and speed becomes governed by the hind-limb length causing a speed scaling of $W^{0.53}$. Another possibility is that the weight relationships of slow and fast speeds indicate a different gait. No attempt was made to examine this possibility. Since the hind-limb length of L. viridis and L. sicula was related to body weight in the same manner as snout-vent length, i.e. $W^{0.33}$, more extensive data for maximum running speeds for these two species may yield the scaling of $W^{0.33}$ or some value near $W^{0.5}$. The former would indicate the importance of hind-limb length, the latter would indicate a change in gait between slow and fast speeds.

Scaling of maximum running speeds has not been undertaken for mammals, but swimming speeds in fishes are scaled as $L^{0.5}$, even though the relative proportion of muscle increases in larger fishes (Brett, 1965). Expressed this way, Lacerta slow speeds are scaled as $L^{1.0}$ and fast speeds as $L^{1.7}$. As Belkin (1961) has pointed out, true maximum speeds are rarely reached after releasing lizards even in the wild. One cannot dismiss the fact that the three Lacerta species may react differently when released giving spurious results, but the similarity of this maximum speed scaling to that predicted from hind-limb length may be genuine.

CHAPTER 2

VENTILATION IN LACERTA

INTRODUCTION

Ventilation and Body Weight

Since it has been shown that $\dot{V}o_2$ is related to $W^{0.75}$ for both resting and active conditions in Lacerta (Chapter 1), it is important to determine whether pulmonary ventilation volume (often called minute volume), $\dot{V}_E$, is also related to $W^{0.75}$. Likewise, the relationships of tidal volume, V_T, and respiratory frequency, f, to body weight must also be examined as $\dot{V}_E = fV_T$.

In birds and mammals, in which $\dot{V}o_2$ is proportional to $W^{0.72}$ and $W^{0.76}$, respectively, it is found that $\dot{V}_E$ is also similarly related, $W^{0.77}$ and $W^{0.8}$. V_T, being a volume but not necessarily a metabolic parameter, is directly proportional to body weight, $W^{1.08}$ and $W^{1.04}$, whilst f is inversely proportional, $W^{-0.31}$ and $W^{-0.26}$, thereby adjusting ventilation to match metabolic rate, $\dot{V}_E$ and $W^{0.77}$ and $W^{0.8}$ (Stahl, 1967, Lasiewski & Calder, 1971). For fishes, $\dot{V}_E$ is again related to $W^{0.73}$ thus matching many of the documented $\dot{V}o_2$ relationships (Hills & Hughes, 1970). The individual scaling of f and ventilation volume in fishes is not known.

With such evidence, it might be anticipated that lizards and other reptiles would give similar relationships. At the commencement of this study on Lacerta, no data existed for reptilian ventilation scaling apart from a suggestion that f was inversely correlated with body weight (1 log. cycle) interspecifically in the four reptilian orders. No slope values were given and the size range 34 to 70g was insufficient to show any correlation for lizards alone (Boyer, 1966).

During the course of this Lacerta study, however, Bennett (1973) has published interspecific lizard data of his own and from the literature to the effect that f is not significantly related to body weight, even over 2.75 log. cycles. There was, however, considerable variation in this resting f, 6 to 38 min^{-1}. From the same sources, Bennett (1973a) also found that V_T was proportional to $W^{0.85}$ which exactly matched lizard interspecific data for $\dot{V}O_2$ being related to $W^{0.83}$ (Bennett & Dawson, 1973). Thus, in complete contrast to mammals and birds, V_T appears to be the principal adjustor of ventilatory factors to weight-dependent changes in metabolism. Lacerta data, which provides conflicting evidence and interpretations, will be examined and discussed in this chapter. Absolute values for ventilatory parameters of Lacerta, other reptiles, birds and mammals will also be compared under both resting and active conditions.

Ventilation and $\dot{V}O_2$

Another important aspect of lizard ventilation is the degree to which its increments are controlled by increasing oxygen demands. For instance, can $\dot{V}O_2$ increase by keeping $\dot{V}_E$ constant but using an increase in pulmonary blood perfusion or does $\dot{V}_E$ increase as $\dot{V}O_2$ increases? How finely matched are $\dot{V}_E$ and $\dot{V}O_2$ increments and what is the range of variation? Is $\dot{V}_E$ increased by f or V_T increments or both or does one parameter dominate? Is O_2 extracted from the ventilation volume with equal efficiency at all levels of $\dot{V}O_2$ and $\dot{V}_E$? Is maximum $\dot{V}O_2$ limited by a physical inability to raise $\dot{V}_E$ further?

Such information is well documented for mammals in which $\dot{V}O_2$ increments demand finely matched $\dot{V}_E$ increases that have only a small amount of experimental scatter (Dejours, 1964). The ventilation requirement, $\dot{V}_E/\dot{V}O_2$, is a constant for rest and increasing activity levels until near maximum $\dot{V}O_2$ when $\dot{V}_E$ increases disproportionately. Ventilation requirement is the term used in this study but it is the same as the respiratory requirement of Bennett (1973a) or ventilation quotient of Nielsen (1961), or air-convection requirement of Dejours, Garey & Rahn (1970).

Maximum $\dot{V}o_2$ is therefore limited by perfusion, not by ventilation volumes. $\dot{V}_E$ increments are mainly dependent on V_T until a point of discontinuity is reached when a greater V_T is physically impossible (Hey, Lloyd, Cunningham, Jukes & Bolton, 1966). f increases quickly at low $\dot{V}o_2$ levels, then changes only slowly but when further V_T increments are impossible, it rapidly increases. Except in thermal panting mammals, f does not increase by more than 20%, whilst V_T increases by 80%. This problem has yet to be studied in birds.

The balance between ventilatory parameters and $\dot{V}o_2$ in reptiles has received little attention. The problem is also made more complicated because, being poikilothermic, $\dot{V}o_2$ increases with temperature as well as with activity. If $\dot{V}o_2$ increments for these two conditions are attained by different ventilatory changes, when both conditions occur together ventilation must be a combined result of two causes.

Nielsen (1961) was the first to study the relationship between $\dot{V}_E$ and $\dot{V}o_2$ in reptiles and, using Lacerta, she found that at different temperatures under resting conditions, $\dot{V}_E$ was proportional to $\dot{V}o_2$. There was, however, considerable variation in $\dot{V}_E$ for a specific $\dot{V}o_2$. The ventilation requirement, therefore, also varied a great deal but was the greater at lower temperatures. In other words, O_2 extraction was better at higher temperatures. Ventilation requirements between 65 and 97 were given for Lacerta showing great inefficiency when compared with man, 20 to 24, and were considered due to the rather primitive structure of the lizard lungs. Increased $\dot{V}_E$ was entirely due to increments in f, 8 to 65 min^{-1}, V_T remaining completely constant.

This constancy of V_T during temperature increases is shown by all lizard species later investigated, except for two. In contrast, only a few species showed such a strong thermal dependence of f. Resting $\dot{V}o_2$ increments at different temperatures, are due to an increment in f, if it occurs, or to the occasional V_T increments or usually to a greater extraction

of O_2 from the ventilated air (see Bennett, 1973a, for extensive references). $\dot{V}O_2$ and $\dot{V}_E$, in many species, are therefore often unrelated implying functions other than respiratory for $\dot{V}_E$ changes.

The relationship between $\dot{V}_E$ and $\dot{V}O_2$ at different temperatures but under maximum activity (by electrical stimulation under restrained conditions) has been investigated in only a few instances, but not in Lacerta (Wilson, 1971, Dmi'el, 1972, Bennett, 1973a). $\dot{V}_E$ and $\dot{V}O_2$ were directly related but with considerable experimental scatter. Increments in $\dot{V}_E$ were met by both f and V_T but the latter was the more dominant. In some instances, high $\dot{V}_E$ increments were disproportionate to high $\dot{V}O_2$ levels. The relationships between $\dot{V}O_2$ and $\dot{V}_E$ have only been directly plotted by Nielsen (1961). In the other publications, $\dot{V}O_2$, $\dot{V}_E$, f and V_T are separately plotted against temperature and their relationships to each other have to be deduced.

If values are taken for rest and maximal activity at the preferred body temperature, PBT, from the data of Wilson (1971), Dmi'el (1972) and Bennett (1973a), it is found that the increment in $\dot{V}O_2$ is accompanied by a large increment in $\dot{V}_E$ but with either greater or constant or reduced O_2 extraction depending on the species. The increment in $\dot{V}_E$ is caused almost exclusively by V_T with f remaining constant or increasing by a factor of only 0.5.

The efficiency of the reptilian respiratory system can be examined in terms of how much O_2 is extracted from the O_2 ventilated, i.e. the O_2 extraction coefficient as a %, and the value compared to that of a mammal. Values between 8.6 and 30% have been found for resting lizards and are reviewed by Bennett (1973a) and compared to the mammalian 17.6% and bird 23% (Stahl, 1967, Lasiewski & Calder, 1971). Thus it would appear that some lizards are more efficient and some less efficient (the Lacerta value being the lowest) than the homeotherms. An explanation for reptilian O_2 extractions greater than a mammal has not been given, although it has been suggested that a low respiratory frequency, which increases the total time

in which the reptilian lung is inflated, allows higher O_2 extractions (Bennett, 1973a). As Bennett (1973a) has said, the intriguing question is how efficient is O_2 extraction at maximum ventilation rates which would be equivalent to those of a resting mammal. Under these conditions, O_2 extraction was lower, 8.3 to 15.4%, but for some of these lizards, notably those with more advanced lungs, the value was not dissimilar to the 17.6% of the mammal.

For the Lacerta study presented here, it was decided to re-examine O_2 extraction at rest and see if the values were really as low as Nielsen (1961) recorded. By measuring f, V_T and $\dot{V}O_2$ simultaneously, at different levels of activity, but at the same PBT, it would be possible to examine their inter-relationships from a different aspect, i.e. an aspect free from temperature effects. Since activity in the wild normally occurs at the PBT, this study may pertain more closely to natural conditions. Attempts at measuring $\dot{V}_E$ and $\dot{V}O_2$ simultaneously, whilst exercising at different speeds wearing a head mask, failed for reasons described in Chapter 1. Instead, $\dot{V}_E$ and $\dot{V}O_2$ were recorded simultaneously during spontaneous activity of restrained and unrestrained lizards (this could be considered even more natural). This method may have the disadvantage that unnecessary hyperventilation may occur more frequently if activity levels are not controlled. From visual inspection, however, f and V_T levels were not dissimilar from exercising lizards.

Methods of Ventilation Measurement

It was considered that many of the methods used previously for reptiles were awkward, inaccurate or could cause the animal extra respiratory effort. Often they did not allow simultaneous measurement of $\dot{V}O_2$. Respiratory frequency has been more frequently measured than tidal volume by visual counting (e.g. Dawson & Bartholomew, 1958, Bennett, 1973a), by lever systems touching the thorax (e.g. Boelaert, 1941), by a strain gauge attached to the thoracic cage (e.g. Dawson, 1960, Templeton & Dawson, 1963)

and by impedance pneumography (e.g. Boyer, 1966, Huggins, Hoff & Pena, 1969). An indication of tidal volume changes can be recorded by all but the first of these methods but they are difficult to calibrate accurately. Huggins, Valentinuzzi & Hoff (1971) have, however, injected known volumes into alive animals to calibrate their impedance pneumograph.

Tidal volumes and respiratory frequency have been measured in a body plethysmograph (with the head outside) recording pressure changes with a spirometer (e.g. Nielsen, 1961) or with a pressure transducer (e.g. Naifeh, Huggins, Hoff, Hugg & Norton, 1970) and later calibrating the system by injecting known volumes into the chamber. Body plethysmographs are obviously limited to resting animals since any activity will introduce considerable artifacts. In lizards wearing head masks for open circuit $\dot{V}O_2$ measurements, the system has been closed intermittently to allow V_T only to be recorded with a pressure transducer. This causes respiratory disturbances (e.g. Templeton & Dawson, 1963). Both head and body plethysmographs cause a back pressure of 1 to 3 cm H_2O (calculated when sufficient information has been published) requiring extra respiratory effort for the lizard. This back pressure was considered too great, especially for Lacerta and evidence for this will be presented in Chapter 3.

Using open circuits through a head mask, the small fluctuations in pressure occurring with each respiratory cycle can be recorded by a side-arm water manometer and the displacement of water visually monitored (Bennett, 1973a) or by a micromanometer/pressure transducer (Dmi'el, 1972). The former has to be calibrated by injecting known volumes at speeds and time courses mimicking a normal breath and is the less accurate. The latter was calibrated by a fast slug injection and the area under a resultant breath curve measured to give V_T. Both these methods gave a baseline pressure of less than 1 mm H_2O.

For Lacerta, a pneumotachograph sensitive to low air flows was made and incorporated into a head mask or a body chamber. It was very

accurately calibrated and gave baseline pressures of less than 3 mm H_2O. To allow simultaneous, accurate measurements of small $\dot{V}O_2$ changes, which occur with the more easily measured changes in $\dot{V}_E$, the dynamic methods of calculating $\dot{V}O_2$ described in Chapter 1 were extended for use with the head mask. Here the volume of the open system is considerably reduced and hence the time constant is in seconds rather than minutes. Analysis of 30 second periods were easily and accurately accomplished.

Ventilatory Patterns

The ventilation cycle in mammals begins with an inspiration which is immediately followed by an expiration. There may sometimes be a short pause before the next inspiration. Reptiles, however, begin with an expiration followed immediately by an inspiration and then a respiratory pause of variable length. The terms diphasic and triphasic have been coined for reptilian respiration to describe tidal volume changes and ribcage movements, respectively (Boelaert, 1941). After inspiration, the ribcage has a small, second expiratory phase before the pause commences. Closure of the glottis at the end of inspiration, however, prevents this triphasic pattern being reflected in tidal volume changes. Lacerta were frequently the experimental animals used for those studies (Boelaert, 1941, Willem & Bertrand, 1936). Triphasic tidal volumes have been recorded sometimes, however, by Willem & Bertrand (1936) and by Saalfield (1934), but in reviewing the evidence, Serfaty & Peyraud (1960) supported Boelaert's diphasic pattern for all tidal volumes.

More recently, Templeton & Dawson (1963) extensively examined ventilation in Crotaphytus finding that the tidal volume was usually triphasic; 5 to 25% of the air being lost before the glottis closed. Data for alligators and caimans, indicate that tidal volume is diphasic in quiet but triphasic in excited animals (Naifeh, Huggins, Hoff, Hugg & Norton, 1970, Naifeh, Huggins & Hoff, 1970).

Bucco-pharyngeal (gular) oscillations are very obvious in reptiles and there is some controversy as to whether they are respiratory or olfactory (Drummond, 1946, Serfaty & Peyraud, 1960). Recent evidence for caimans and alligators indicate that gular movements have only an olfactory role (Huggins, Parsons & Pena, 1968, Naifeh, Huggins, Hoff, Hugg & Norton, 1970). The problem has not been recently examined in lizards.

The development of body and head mask pneumotachographs allow an easy re-examination of tidal air flow in Lacerta and can answer the question as to whether triphasic tidal flow can occur in this species. Air flow from gular movements was also recorded. This examination of ventilatory patterns is by no means extensive, since it is basically a by-product from the study of ventilatory scaling and O_2 extraction efficiency. It does, however, contribute records of ventilatory patterns in relatively unrestricted unanaesthetised lizards at minimum and maximum levels of ventilation.

METHODS

Tidal Volume and Respiratory Rate

Nose masks were made from the ends of 1 and 2 ml polystyrene syringes. After removing the Luer male fitting and increasing its tapered bore to a constant 2.0 mm internal diameter, it was sealed into a secondary hole made in the curved wall of the syringe. The existing 1.5 mm Luer hole was retained for the small mask but enlarged to 4 mm for the larger mask and its inner surface was beveled to minimise turbulent flow. This hole was covered by a single sheet of plankton net containing 4,900 perforations/cm^2 which was sealed in position with a polystyrene ring of matching hole diameter but with beveling on its outer surface (Fig. 2.1).

A latex rubber collar, sealed with neoprene glue to the lizard's skin, covered the caudal margin of the lower jaw and an area just behind the nostrils. This also firmly sealed the lizard's mouth but in no way hindered gular movements. After sealing the collar to the open end of the mask, the resulting nost mask was completely airtight. To remove the mask, the neoprene glue was peeled off but this did not cause damage to the skin. The masks used for L. vivipara and L. sicula weighed 0.4g with a volume of 0.1 ml which, with the lizard's nose inside, was reduced to 0.05 ml. For L. viridis, the mask weighed 1.0g and had a 0.63 ml volume reduced to 0.3 ml.

Body chambers, of 28 or 170 ml total volume, were similarly constructed from larger syringes with the same size, 1.5 or 4 mm, resistive, plankton covered hole. The latex collar was this time sealed around the pectoral girdle, such that it neither hampered gular nor thoracic movements. After taping the lizard to a small rod, the collar was sealed to a larger polystyrene collar which fitted, and was sealed, over the open end of the body chamber (Fig. 2.1).

FIG. 2.1 Nose mask and body chamber pneumotachographs for Lacerta.

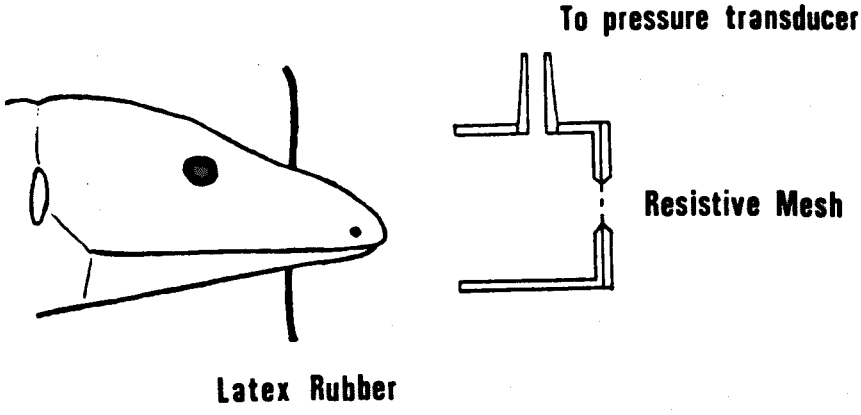
To pressure transducer
Resistive Mesh
Latex Rubber

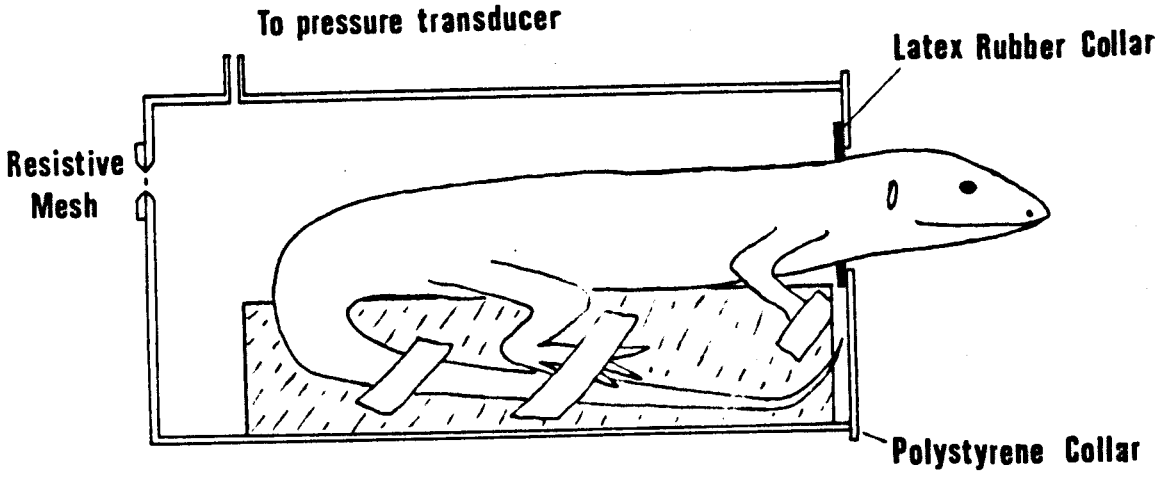
To pressure transducer
Latex Rubber Collar
Resistive Mesh
Polystyrene Collar

FIG. 2.2 Calibration graphs for pneumotachographs. Solid line for + and - flow in the body chamber and for - inspiratory flow in the nose mask. Dashed line for + expiratory flow in the nose mask. R.M. = resistive mesh.

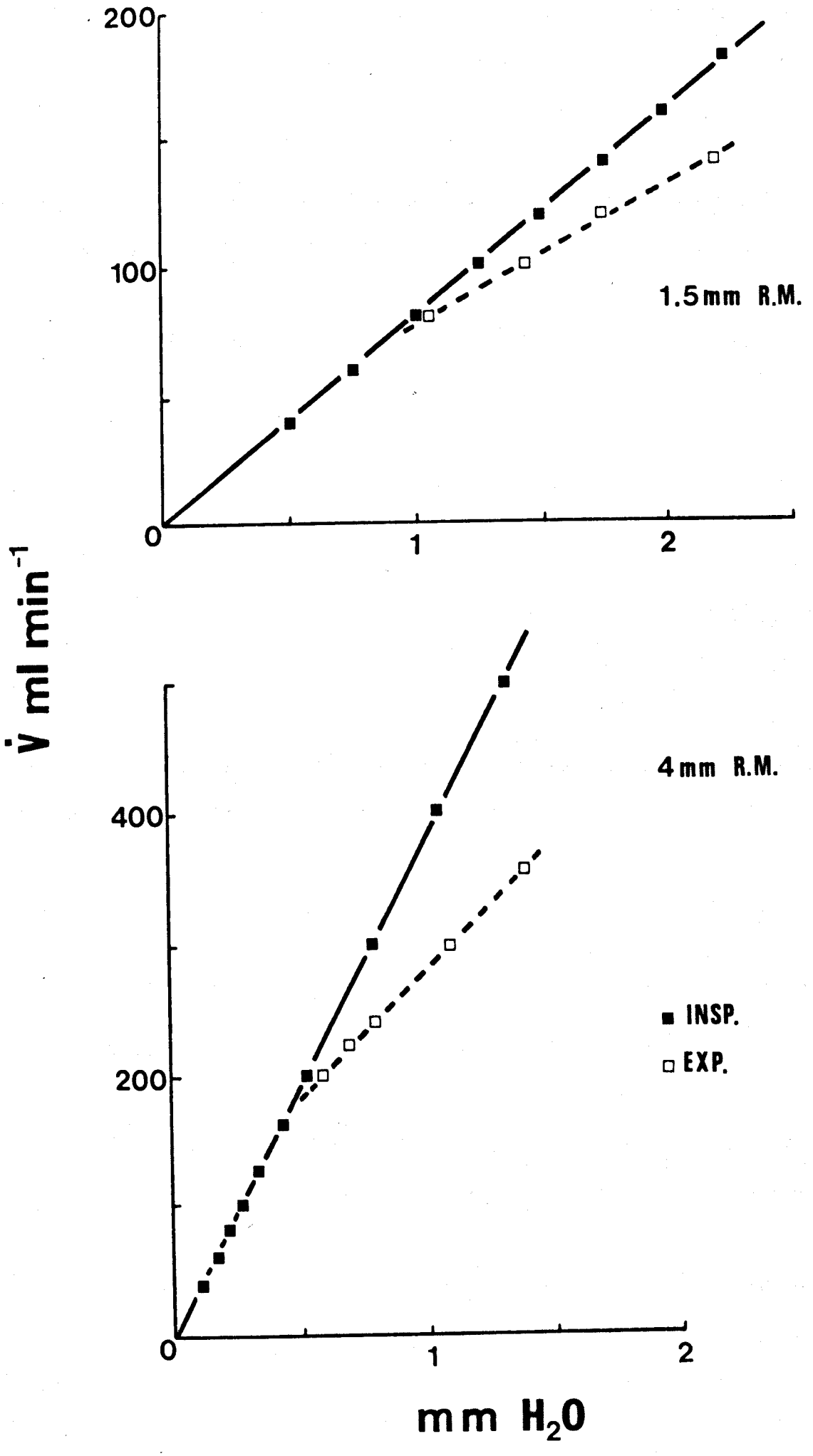
200
100
0
1
2
1.5mm R.M.
$\dot{V}$ ml min^{-1}
400
200
0
1
2
4mm R.M.
INSP.
EXP.
mm H_2O

Pressure changes in the mask or body chamber were recorded, differentially against atmospheric, via the Luer fitting with a 270 Sanborn pressure transducer (maximum sensitivity of 400 mm H_2O) whose output was amplified by a Sanborn pre-amplifier and recorded with a Devices and DC5 power drive amplifier (response of 100 cps). Sensitivities between 0.1 and 1.0 mm H_2O/cm, depending on the depth of ventilation, were used with a full scale deflection of 5 cm. Since an individual breath took approximately 0.6 sec, the paper speed was at 10 mm/sec. With the nose mask, negative pressures were recorded during inspiration and positive pressures during expiration. The reverse was the case for the body chamber. Zero pressure occurred during respiratory pauses. The area under the resultant pressure curves was measured and the tidal volume calculated from calibration graphs in which 0.01 mm H_2O equalled 0.8 or 3.78 ml min^{-1} (Fig. 2.2).

Calibration curves were constructed by sealing the mask or body chamber (without a lizard present) and inserting through the seal, constant negative and positive flow rates between 40 and 500 ml min^{-1} (measured with a Rotameter 1100). Linearity of the resultant pressure was obtained between $\pm$ 40 and $\pm$ 180 ml min^{-1} (for the 1.5 mm resistive element) and $\pm$ 40 and 500 ml min^{-1} (4 mm resistive element) which extrapolated to the origin (Fig. 2.2). Mock lizard bodies or noses in no way altered the calibration which was constant for a resistive element and unaffected by the volume difference between mask and chamber. A plasticene lizard nose with air delivery through two holes mimicking the nostrils in size and position, however, caused non-linearity in the mask to begin at + 80 or + 180 ml min^{-1} for expiratory flows only (Fig. 2.2). This was presumably a result of air turbulence in such small mask volumes, caused by the jet-like action of the nostrils.

Although maximum flow rates were recorded which were just outside the linearity range, their occurrence was rare. Thus these pneumotachographs were ideally suited for measuring Lacerta ventilation. In using the nose

mask, two sources of error were possible: (a) an overestimation of V_T during expiration because of turbulence from the nostrils if flow rates became greater than + 80 or + 180 ml min^{-1}, and (b) the effect of dead space in the mask which was approximately equal to the average resting V_T. When this type of nose mask was in use, non-linear expiratory flow rates were not encountered because the lizard was restrained, thereby giving low enough ventilation volumes. Dead space errors did not appear to affect the lizard's respiration - checked by body chamber and through-flow mask data (see later). The error involved in the body chamber was one due to rarefraction and compression of air within the thoracic cage which would tend to overestimate inspiratory and underestimate expiratory volumes. However, as V_T equalled the mean of these two volumes, the errors would cancel out.

These nose masks and body chambers were used initially to investigate the pattern of respiration and to estimate routine values for f and V_T. In all cases, the lizards were taped to a piece of wood but were not always shielded from visual and auditory stimuli.

Pulmonary Ventilation, $\dot{V}o_2$ and $\dot{V}co_2$

Nose masks were again constructed from syringes but the existing Luer fitting was kept intact and a secondary one sealed into the curved wall. Both internal bores were enlarged to 2 mm. These masks were of the same weight and volume as described previously. The Luer fittings formed the inlet and outlet for an open circuit respiratory system with air circulating at 100 ml min^{-1} (Fig. 2.3). This system was basically the same as that used in the diurnal open circuit respirometer but without the mixing circuit. Whatever the size of the mask or inlet/outlet bore diameter, the plumbing caused - 3.0 mm H_2O at 100 ml min^{-1}.

The volume from the mask to the CO_2 analyser was 20 ml (estimated from a 12 sec delay at 100 ml min^{-1}) and from the mask to the O_2 analyser, it was 104 ml of which approximately 50 ml was inherent in its internal plumbing. Time constants for mixing were determined as described in

FIG. 2.3 Diagram of open circuit $\dot{V}o_2$ and $\dot{V}co_2$ system used with the nose mask (compare similarity with Fig. 1.3).
Animal taped to a jig in body chamber pneumotachograph.

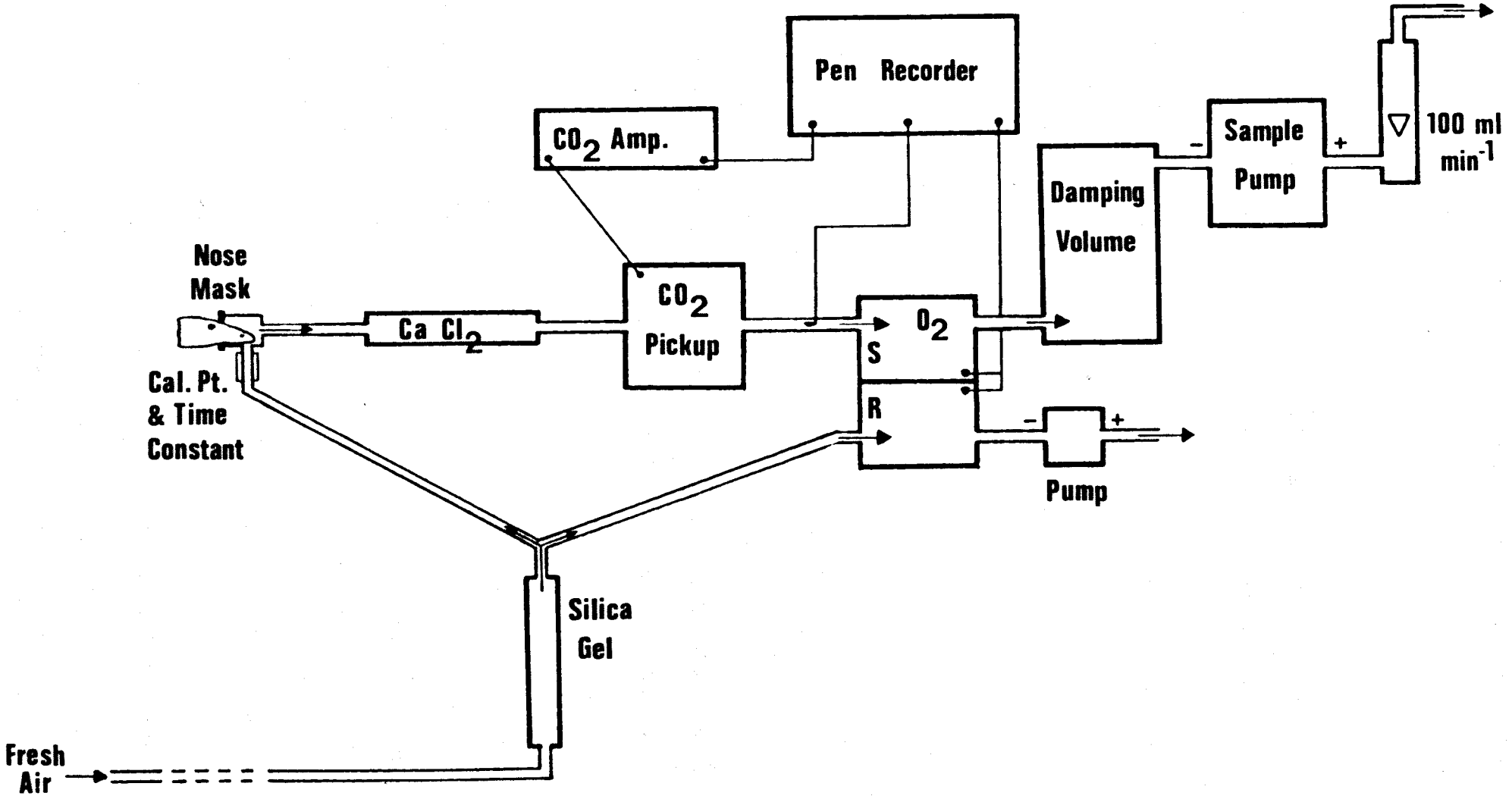
Pen Recorder
CO_2 Amp.
Sample Pump
100 ml min^{-1}
Damping Volume
Nose Mask
CO_2 Pickup
O_2
Ca Cl_2
S
R
Cal. Pt. & Time Constant
Pump
Silica Gel
Fresh Air

Chapter 1. A true exponential washout curve was not obtained but the time constant only increased during the final 0.03% change. The time constant for CO_2 was 4.8 sec and for O_2, 8.4 sec. Mixing was obviously very incomplete with the effective volume, V = flow rate x τ, being 8 ml for CO_2, i.e. 40% mixing and 14 ml for O_2, i.e. 13.4% mixing. This discrepancy between the two gases was due to the major proportion of the mixing occurring in the $CaCl_2$ drying tube whilst the extra volume, but of a narrow bore, between CO_2 and O_2 analysers allowed only slight, further mixing. Hence O_2 had a greater time constant but a lower degree of mixing.

By splitting the outlet air to enter O_2 and CO_2 analysers simultaneously, with a volume lag of 70 ml between analysers and mask, it would, in theory, be possible to obtain the same time constants for O_2 and CO_2. The difference in resistance to flow in the two analysers, however, caused unequal flow rates, i.e. not 50 ml min^{-1} each, when using a single pump. Time lags and time constants were, therefore, still different. It was considered easier to keep to the original plumbing.

To obtain complete mixing with nose mask circuits, would involve the introduction of large volumes thereby elevating the time constant to a minimum of 60 sec, as well as averaging out considerably the changes in O_2 and CO_2. Since ventilation above resting levels was found to be constant for an average period of only 30 sec, it was necessary to be able to analyse small, fast changes in $\dot{V}o_2$ and $\dot{V}co_2$. This was only possible if incomplete mixing circuits were used. Whether this produces large errors in $\dot{V}o_2$ and $\dot{V}co_2$ measurements is difficult to ascertain but it is thought unlikely.

Pulmonary ventilation was measured using the body pneumotachograph whilst simultaneously measuring $\dot{V}o_2$ and $\dot{V}co_2$ with the open circuit nose mask. Fig. 2.4 illustrates the O_2 and CO_2 trace obtained. Using a paper speed of 20 mm/min, 30 sec intervals were analysed to determine $\dot{V}o_2$ and $\dot{V}co_2$ by the dynamic and static equations derived in Chapter 1 and Appendix I.

FIG. 2.4 Typical open circuit nose mask record of fast changes in % O_2 and % CO_2. Note the greater CO_2 fluctuations due to its faster time constant. Sensitivity for O_2 and CO_2 is 1% f.s.d.

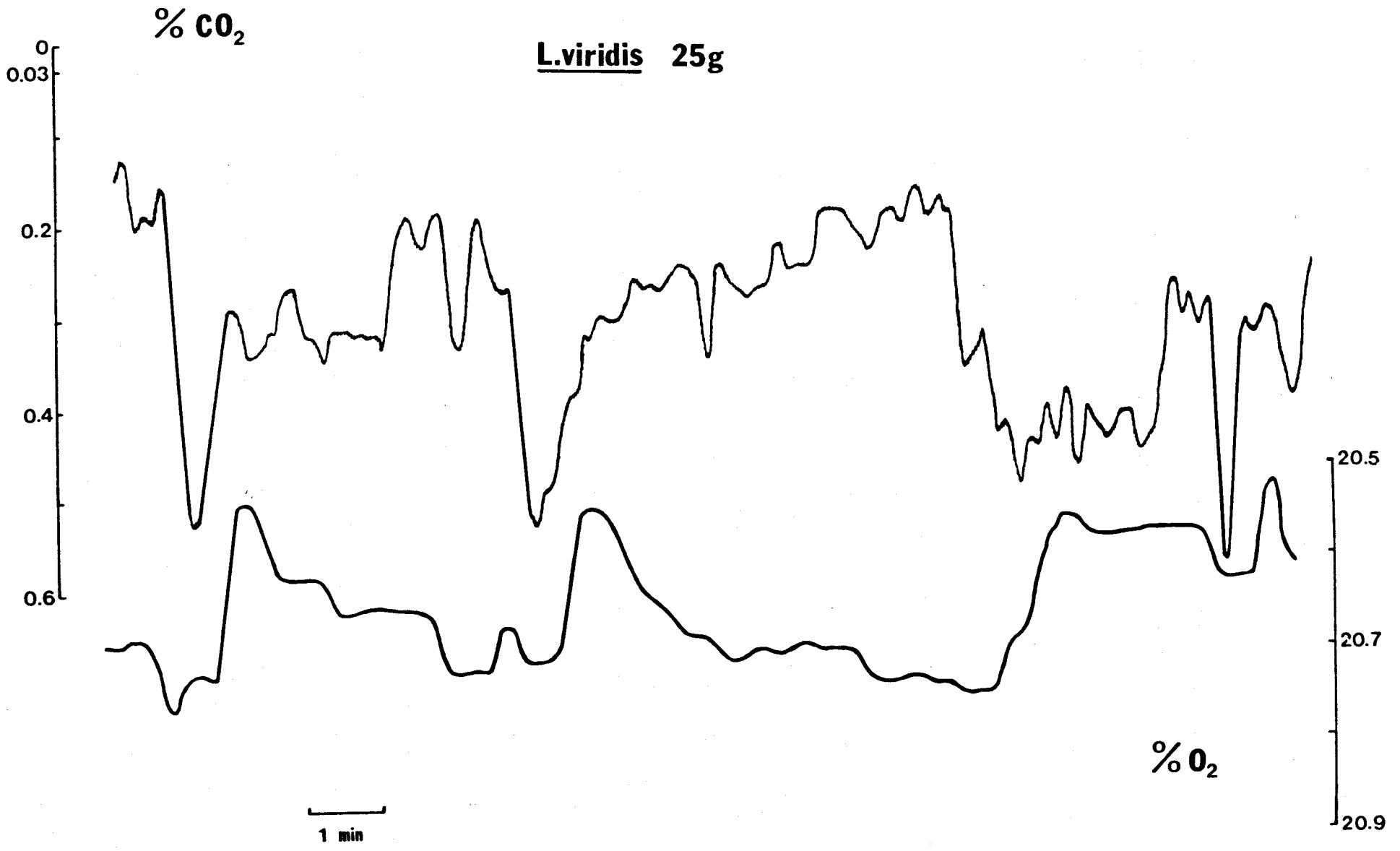
% CO_2
L.viridis 25g
0
0.03
0.2
0.4
0.6
20.5
20.7
20.9
% O_2
1 min

FIG. 2.5 Diagram of combined nose mask pneumotachograph and open circuit system for $\dot{V}o_2$ and $\dot{V}co_2$ determination (compare similarity with Fig. 1.7). Animal's body free to move.

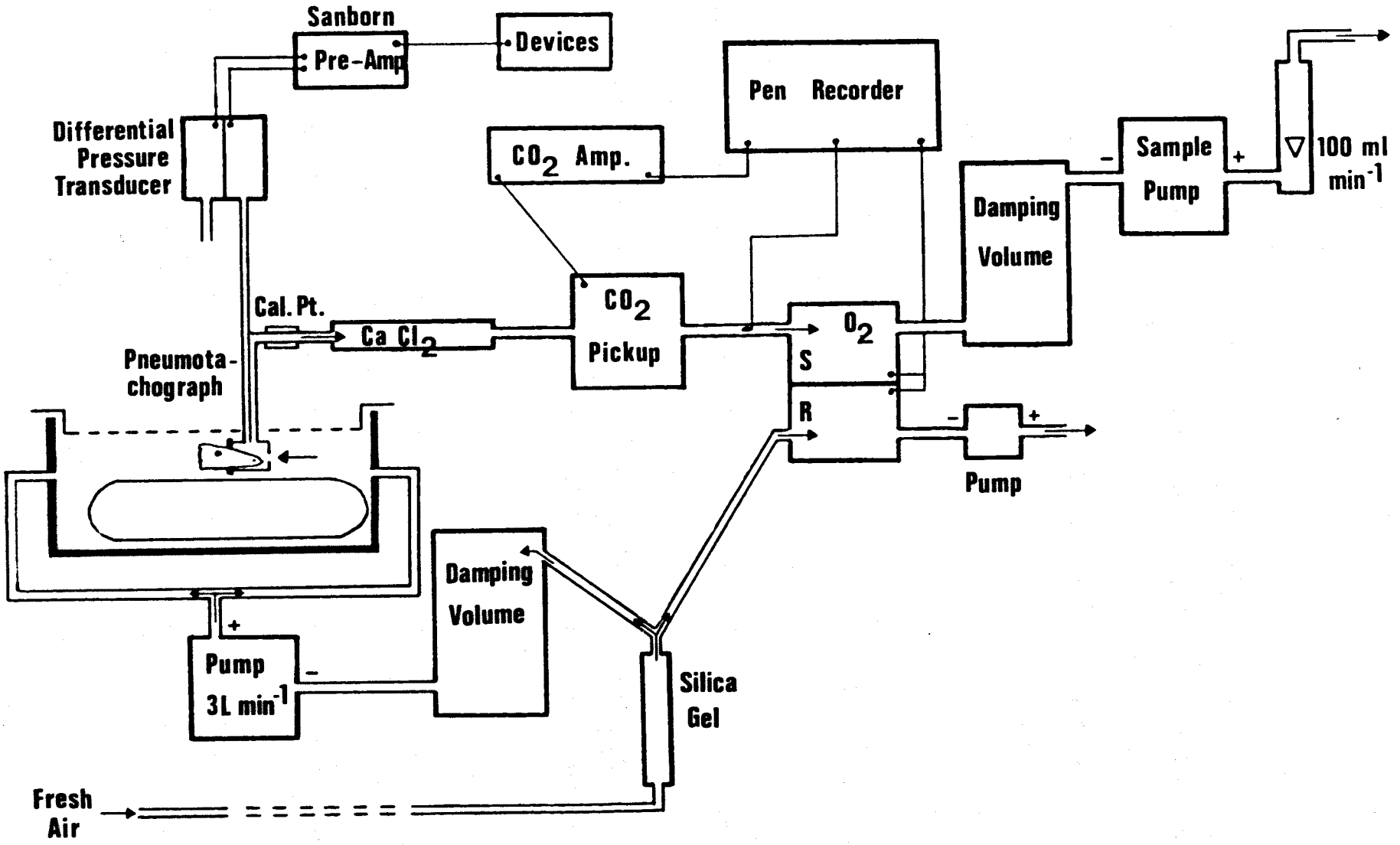
Sanborn
Pre-Amp
Devices
Pen Recorder
Differential Pressure Transducer
CO_2 Amp.
Sample Pump
100 ml min^{-1}
Damping Volume
Cal. Pt.
Ca Cl_2
CO_2 Pickup
O_2
S
R
Pneumota-chograph
Pump
Damping Volume
Pump 3L min^{-1}
Silica Gel
Fresh Air

These intervals exactly coincided with 30 second records of pulmonary ventilation in which V_T and f were constant throughout that period. Occasionally, the lizard would hold its breath for 30 sec and analysis of the gas traces yielded zero $\dot{V}o_2$, which is indicative of the accuracy of the method.

It was also possible to record $\dot{V}o_2$, $\dot{V}co_2$ and pulmonary ventilation using only the pneumotachograph mask and thereby leaving the body of the lizard free to move. In this manner, very active respiration could be recorded. The plumbing is basically that of the exercise respirometer circuit and is illustrated in Fig. 2.5. Inlet air was taken from a large source of fresh uncontaminated air and entered the mask through the resistive element. Outlet air passed through the Luer fitting through which pressure changes were also monitored. Because of the removal of inlet tubing and its resistance, a flow rate of 100 ml min^{-1} only caused a baseline pressure of - 0.26 mm H_2O in the L. viridis mask (see calibration graph). The juxtaposition of the outlet and pressure transducer tubing, however, caused a further - 0.2 mm H_2O. In the L. vivipara and L. sicula masks, 100 ml min^{-1} caused - 1.25 mm H_2O (calibration curve) plus a further - 0.2 mm H_2O. By offsetting the zero, these background negative pressures, due to the plumbing, were used as the new baseline zero for the pneumotachographs. Since the extra - 0.2 mm H_2O pressure did not affect the linearity range of the resistive element, the new calibration graphs for the masks were linear between - 80 and + 180 ml min^{-1} or between - 400 and + 280 ml min^{-1}. Maximum flow rates outside this range were rare and, since they occurred for such a short duration, their contribution to total V_T was negligible. Open circuit nose masks obviously removed the error of re-breathing expired air.

Lizards covering seven body weights between 2.6 and 34.5g were taken and at least five recording sessions for each weight were made. Each recording session lasted approximately 3 hours during which $\dot{V}o_2$ and $\dot{V}co_2$ were recorded continuously, whilst pulmonary ventilation was registered for

30 seconds at random intervals. In this way, all three parameters were measured from minimum to maximum values in restrained and unrestrained spontaneously active lizards (starved for 1 day only). V_T was expressed as ml (BTPS)/breath, f as breaths min^{-1} and $\dot{V}o_2$ and $\dot{V}co_2$ as ml hr^{-1} (STPD).

RESULTS

Pattern of Ventilation

The respiratory cycle, recorded by flow rates through the nostril mask, began with expiration and was immediately followed by inspiration and then a pause of variable length (Fig. 2.6a). Pause length was dependent on the frequency of breathing but was usually within the range, 0.5 to 3.0 sec. It could sometimes be totally absent (Fig. 2.6c & d) or could extend for periods up to 60 sec. The latter case was rare, only being found in highly disturbed lizards not conditioned to the experiments. Pause length variability persisted even under light anaesthesia or during sleep. Inspiratory and expiratory duration varied from 0.15 to 0.8 sec but was usually in the range 0.25 to 0.4 sec. During a breath, inspiration and expiration could take the same length of time or one could be longer than the other (Fig. 2.6). Very often inspiration took 0.1 sec longer than expiration.

Air flow profiles of the respiratory cycle had many patterns and within a breath, inspiration and expiration profiles were rarely identical. There are three alternatives for increasing V_T, either (i) increasing air flow rate but maintaining the same breath duration, (ii) increasing both flow rate and breath duration, or (iii) increasing breath duration only. Alternatives (i) and (ii) were usually shown by Lacerta but (iii) was not uncommon in disturbed individuals (Fig. 2.6e, 2.8b). A quick expiratory and slow inspiratory duration, or vice-versa, within the same breath was never found. In contrast, either phase of the cycle could show the greater flow rate. Over a 30 sec period of regular ventilation, the total expired volume always equalled the total inspired volume indicating a constant retained lung volume during the pause. During irregular ventilation, this retained volume could be increased or decreased over a 30 sec period but during the return to regular ventilation inspiratory and expiratory volume

FIG. 2.6 Air flow profiles in Lacerta. Expiration is downward, inspiration upward. a,b,c,d, L. sicula (9.8g) e, L. viridis (34.5g). Variations in frequency, depth and time course of breathing.

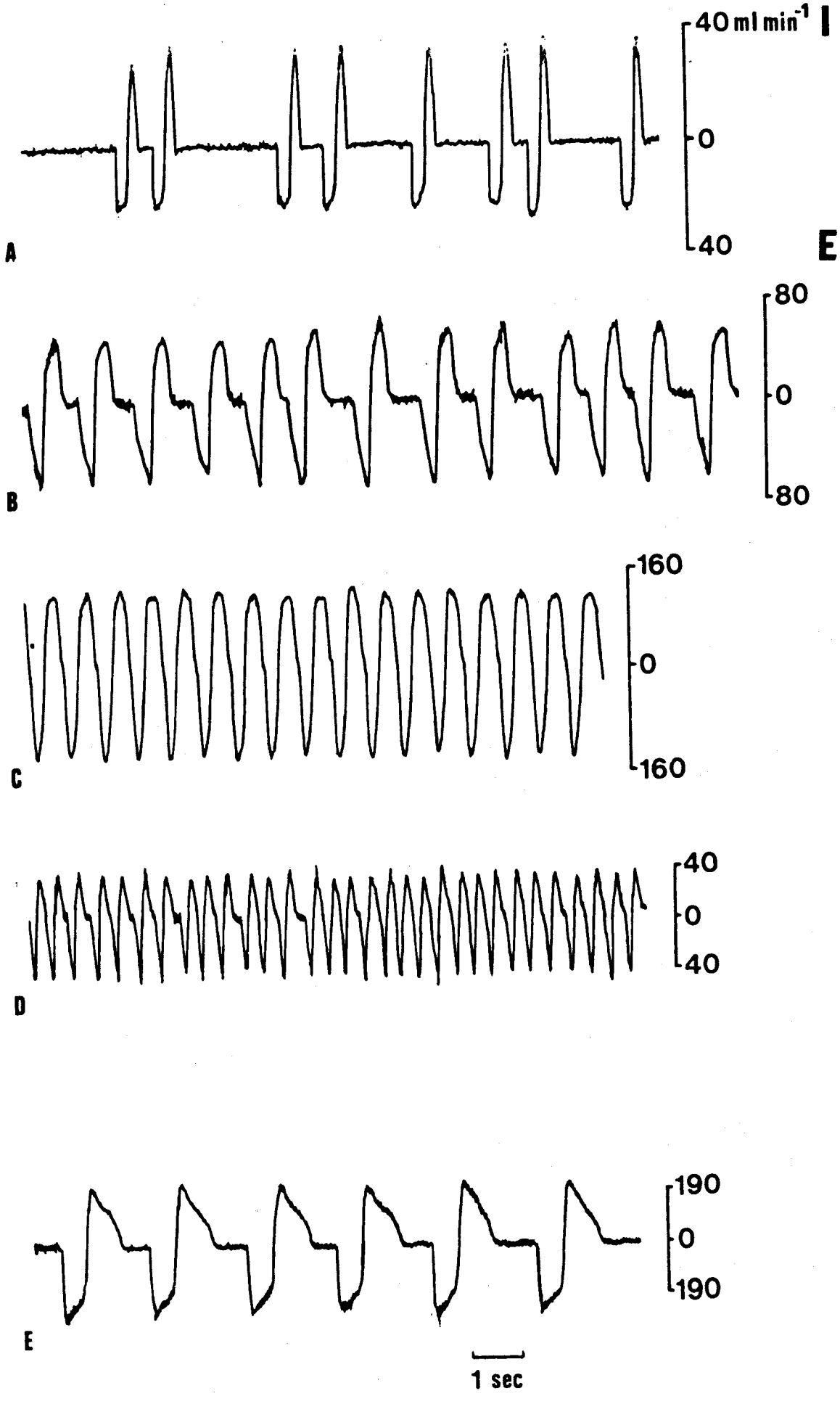
40 ml min-1
0
40
A
E
80
0
80
B
160
0
160
C
40
0
40
D
190
0
190
E
1 sec

FIG. 2.7 Air flow profiles in Lacerta. Expiration downward, inspiration upward in a,b,c,d, reverse in e,f. L. sicula (9.8g) a,b,c,d. a, normal diphasic tidal volumes; b,c,d, triphasic tidal volumes - note how the E_2 phase is variable in amplitude; e, L. viridis (24.5g) under deep (20 mg/kg) anaesthesia - note long time course, low flow rates and presence of E_2 phase; f, under deeper anaesthesia (35 mg/kg) - note increased respiratory rate, low amplitudes, presence of a small active expiration E_2 in middle of slow passive expiration and no respiratory pauses.

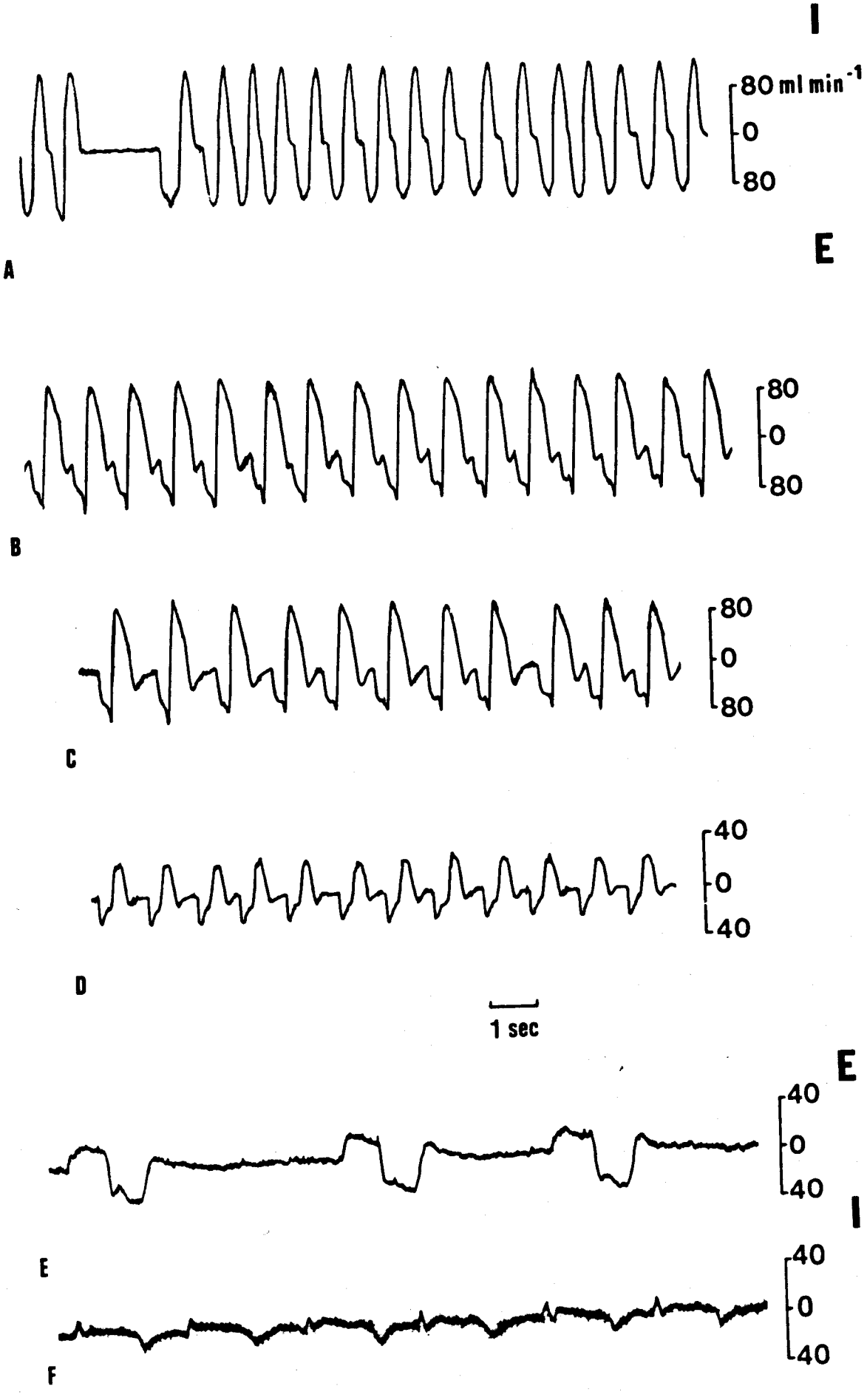
I
80 ml min⁻¹
0
80
A
E
80
0
80
B
80
0
80
C
40
0
40
D
1 sec
E
40
0
40
I
E
40
0
40
F

FIG. 2.8 Air flow profiles in Lacerta. Expiration upward, inspiration downward. a,c, L. sicula (7.6g); b,d,e, L. viridis (28g). Low amplitude E_2 phase in a. Long deep breaths and long respiratory pauses in b. Gular air flow superimposed on tidal flow in c. Isolated gular movements in d,e.

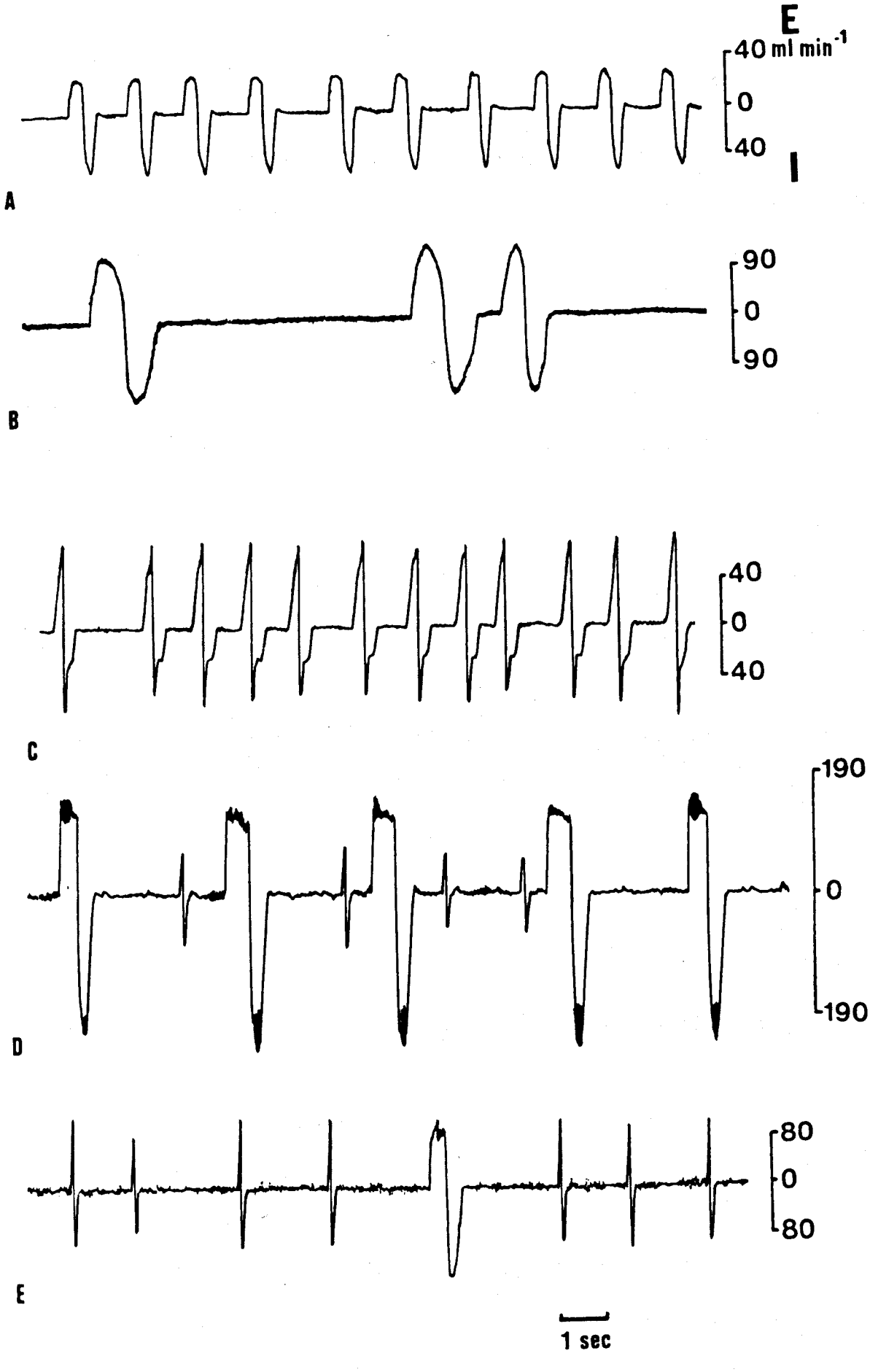
E
40 ml min-1
0
40
A
90
0
90
B
40
0
40
C
190
0
190
D
80
0
80
E
1 sec

differences also caused the return to a 'normal' retained volume. From visual inspection and a few long term plethysmograph recordings, it would appear that this retained volume (equivalent to the functional residual capacity, FRC, see Chapter 3) was normally maintained at a constant level whatever the frequency or tidal volume of respiration. Normally, when respiratory frequency increased so also did V_T but large breaths at low frequencies and small breaths at high frequencies could also be recorded (Fig. 2.6d & e).

Visual examination of the thoracic cage movements did not, however, show the diphasic tidal volume pattern recorded with a nose mask. Thoracic movements were triphasic:- pause, expiration, inspiration and then a second expiration, E_2, of smaller amplitude but similar duration and followed by a pause. The E_2 amplitude increased as V_T increased. If the respiratory pause was absent or very short, E_2 could not be discerned. Examination of the glottis showed that it opened at the beginning of the first expiration and closed at the end of inspiration before E_2 had occurred. Hence glottal closure prevented the triphasic thoracic pattern being reflected in nostril and ventilation air flow. When the respiratory pause was absent, the glottis remained open all the time.

Triphasic movements were not, however, recorded when a body chamber was used, whether it acted as a plethysmograph or as a pneumotachograph. Respiratory movements were diphasic and identical in profiles to those recorded by the nose mask, except that inspiration caused positive and expiration negative pressure. During the E_2 thoracic phase, it was noted that a small, hardly discernible expansion of the abdomen occurred. This compensatory movement of the abdomen must explain the registering of a diphasic rather than a triphasic ventilation when using the body chamber.

An excited or disturbed lizard sometimes showed triphasic respiratory cycles both in mask and body chamber recordings (Fig. 2.7b,c,d).

At such times, thoracic E_2 movement occurred completely or partly before the glottis closed and hence air was expelled from the lung. The volume expelled in this manner was never more than 10% of the total V_T. During this 'excited' breathing, the E_2 air flow and volume recorded was very variable and was not dependent on the absolute value of V_T, indicating the effect of mis-timing the moment of glottal closure rather than a true reflection of E_2 amplitude.

During anaesthesia of a sufficient depth to prevent the righting reflex (see Appendix II) not only was V_T considerably reduced with a long breath duration and low flow rate but the triphasic pattern was also very marked (Fig. 2.7e). Examination of the glottis showed that it was failing to close completely at the end of inspiration and under deeper anaesthesia, the glottis remained permanently open. The volume of E_1 and E_2 always equalled inspiratory volume and there was no indication from thoracic circumference measurements that FRC was decreasing because of anaesthesia. Arousal of a lightly anaesthetised lizard by tail pinching caused glottal closure timing to convert a triphasic into a diphasic cycle for a few breaths. Diphasic V_T patterns were continually present in very lightly anaesthetised lizards in which glottal closure occurred at the correct time. Under very deep anaesthesia (Fig. 2.7f) the amplitude of expiration was considerably reduced in comparison with inspiration. Both amplitudes were very low. Expiration appears to consist of a small active phase in the middle of a long slow passive expiration. A respiratory pause is no longer present and f is increased.

Thoracic respiratory movements were also accompanied by pharyngeal ones. During expiration the throat contracted slightly and during inspiration it expanded. These movements can be seen superimposed on the lung flow rates recorded by the mask but not by the body chamber (Fig. 2.8c). They were always complementary and coincident with inspiratory and expiratory thoracic movements occurring at the end of expiration and beginning of

inspiration. Often, however, the pharyngeal flow was lost in the tidal flow pattern. In disturbed lizards, especially L. viridis in which the respiratory pause was longer, isolated pharyngeal flow profiles could be recorded (Fig. 2.8d & e) which were identical to those coincident with respiration. Pharyngeal flow rates ranged from 22 to 130 ml min^{-1} taking only 0.1 sec and were of a volume of 0.02 to 0.09 ml (L. viridis). Flow rates were 33 to 50% and volume 10% of the values found for thoracic movements. Inspiratory and expiratory pharyngeal profiles were identical in profile and very fast indicating the active nature of both. Pharyngeal movements coincident with thoracic movements also occurred in anaesthetised animals. Isolated pharyngeal movements never occurred in lightly anaesthetised lizards unless the lizard was firmly touched.

Buccal deglutition has been noted in very disturbed or ill Lacerta individuals and in lightly anaesthetised lizards when the nares were blocked by mucus. Air was taken in through the nares or an open mouth and with a visibly expanded pharynx, the mouth closed. The pharynx then contracted causing the thorax to expand. Presumably the nares must be sealed by placing the forked tongue into the internal choanae (anatomically this is possible) whilst the buccal/pharyngeal force pump forces air into the lungs through an open glottis. The lungs can remain so inflated for several minutes but since the mouth often opened during this time, the glottis must have (and can be seen to be) closed after the deglutition. Part of the threatening behaviour of L. viridis involved the maintained expansion of the pharynx and thorax. It is highly probable that air was retained in the pharynx by the tongue sealing the internal nares rather than by a continued muscle action. There are no valves to the nares which would assist this buccal/pharyngeal expansion.

Ventilation and Body Weight

$\dot{V}O_2$ recorded from restrained lizards tied to a jig varied from that of the mean day rate, recorded in 1 day starved diurnal rhythm

experiments, to a struggling value approximately half that of the exercise plateau $\dot{V}O_2$. Normally, $\dot{V}O_2$ was about twice that of the mean day rate. In lizards free to move their limbs and body and being restrained only by the lead from the mask and the confines of the exercise respirometer, struggling $\dot{V}O_2$ values were often greater than that of the exercise plateau. All these $\dot{V}O_2$ values were from 30 sec periods.

Tidal volume, V_T, and respiratory frequency, f, recorded at the same time as the above $\dot{V}O_2$ measurements were grouped into minimum V_T and f (corresponding to 1 day starved, mean day $\dot{V}O_2$), average V_T and f (corresponding to 2 x the above $\dot{V}O_2$) and maximum V_T and f (corresponding to maximum $\dot{V}O_2$). It was found that V_T min. = $0.0026\ W^{1.088}$, V_T average = $0.008\ W^{0.985}$ and V_T max. = $0.03\ W^{1.12}$, where V_T is in ml, W in g (Fig. 2.9). Considering that V_T max. was dependent on the spontaneous struggling of each lizard and was not controllable, it is perhaps not surprising that its slope is higher than for V_T min. and V_T average. It would appear that V_T is directly proportional to body weight (mean b = 1.036). For the three groupings considered, $\dot{V}O_2$ was in the proportions of 1:2:8 which contrasts with the V_T proportions of 1:3:11.5 (values for 1.0g lizards).

Respiratory frequency, f, varied between 20 and 100 min^{-1} for all sized lizards and for all three $\dot{V}O_2$ classes. The average minimum f is plotted against body weight in Fig. 2.10 and is constant about a mean of 30 min^{-1}. As a check for this minimal stress frequency, f in lightly anaesthetised animals (eyes closed but no loss of righting reflex) was counted for all body weights between 3.0 and 38g and f = 30 $\pm$ 5 min^{-1}. Similar values were also found for the 0.2g L. vivipara. Thus with f independent of body weight, ventilation volume, ml min^{-1}, is directly proportional to body weight (Fig. 2.9).

The average flow rate, $\dot{V}$, for each breath (corresponding to a $\dot{V}O_2$ of 2 x mean day $\dot{V}O_2$, 1 day starved) is related to body weight by a regression slope of 0.85 (Fig. 2.10). It might be expected that flow rate

FIG. 2.9 Logarithmic relationship between tidal volume and body weight. Correlation coefficients 0.9795 (V_T min), 0.9663 (V_T aver.) and 0.99 (V_T max). Logarithmic relationship between minimum ventilation volume, $\dot{V}_E$, and body weight, correlation coefficient 0.97.

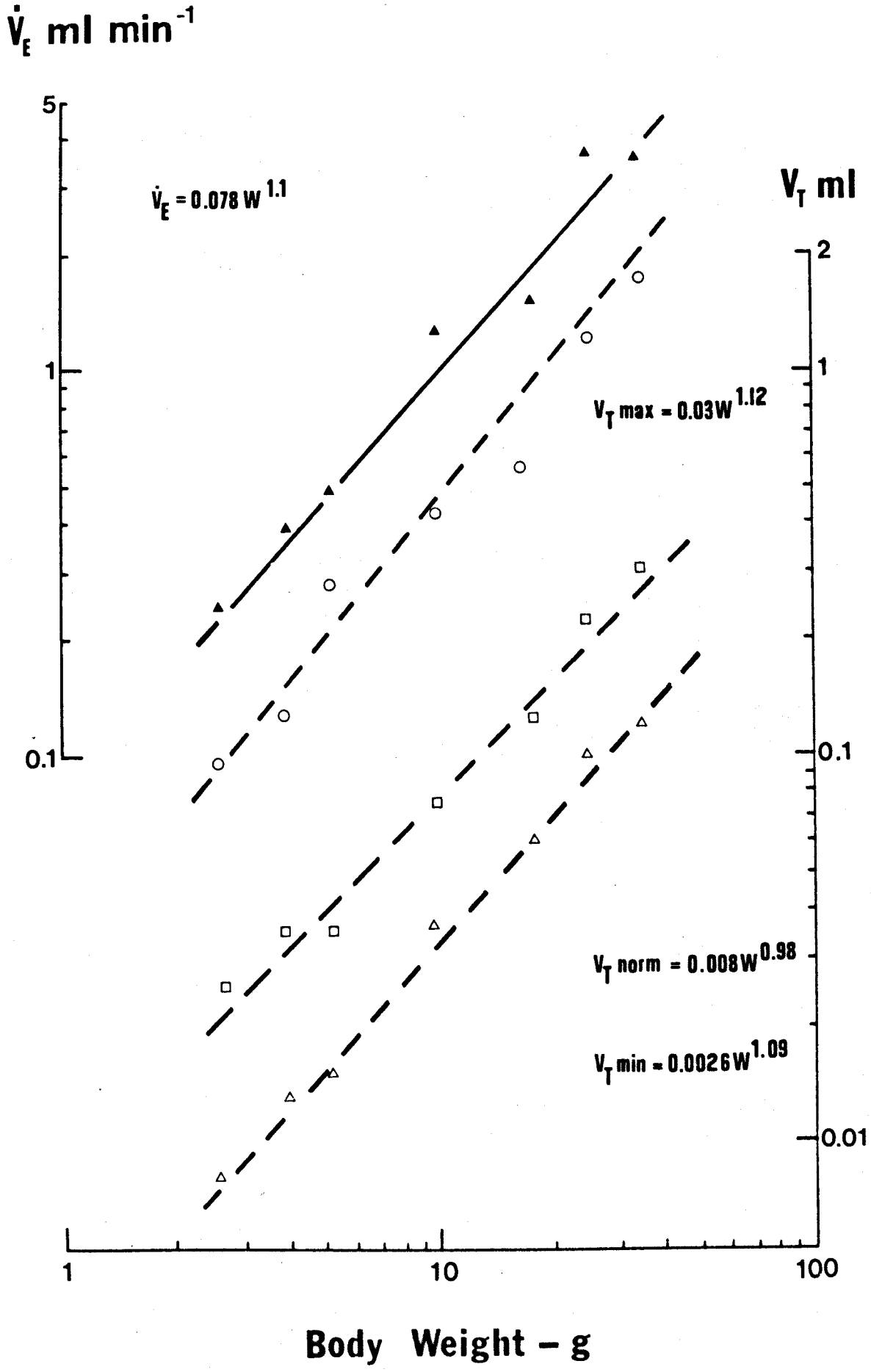
$\dot{V}_E$ ml min^{-1}
5
1
0.1
$\dot{V}_E = 0.078\,W^{1.1}$
V_T ml
2
1
0.1
0.01
V_T max = $0.03W^{1.12}$
V_T norm = $0.008W^{0.98}$
V_T min = $0.0026W^{1.09}$
1
10
100
Body Weight – g

FIG. 2.10 Logarithmic relationship of respiratory frequency, air flow rate and breath duration against body weight. Correlation coefficients 0.095 (f), 0.96 ($\dot{V}$) and 0.99 (t).

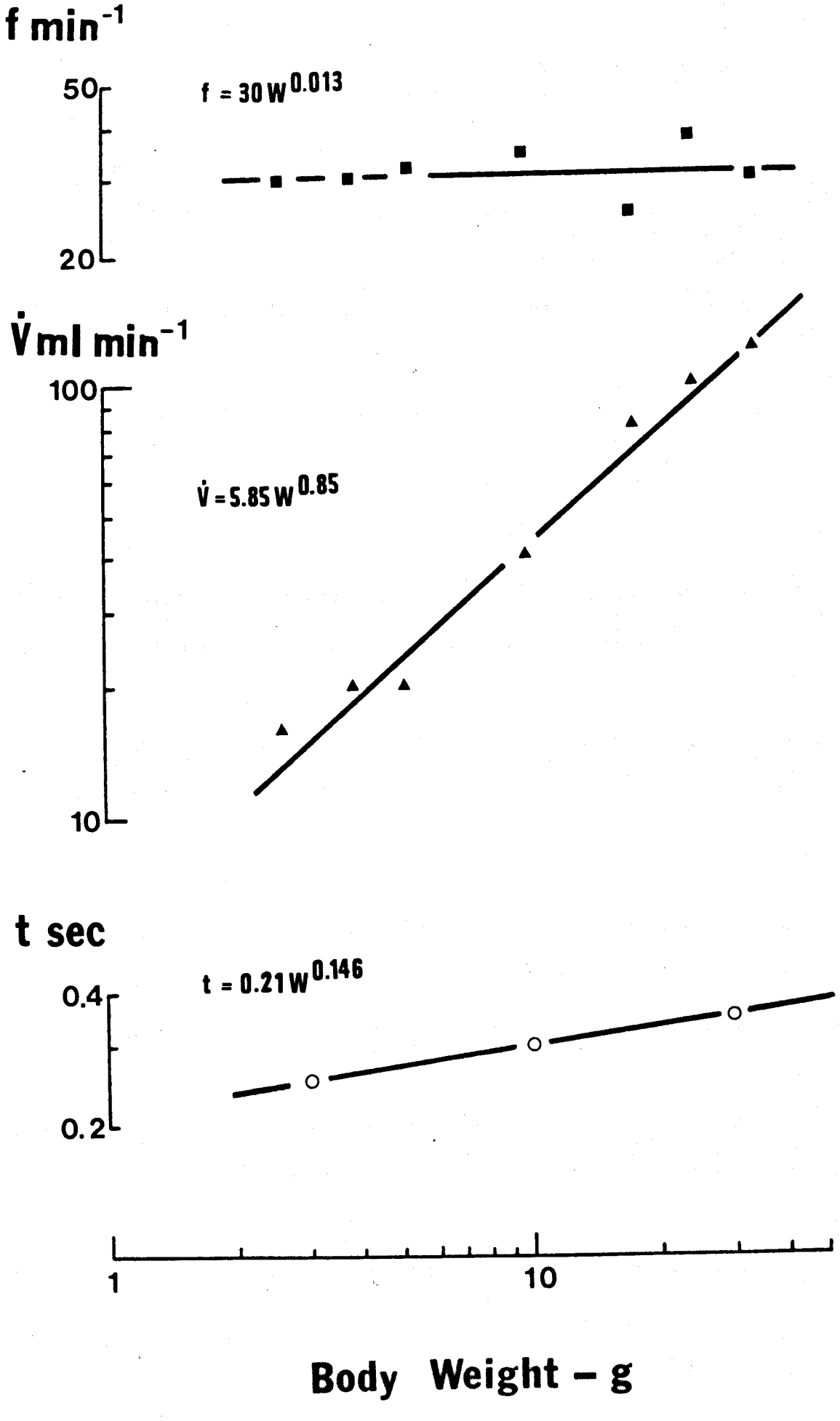
f min^{-1}
50
20
$f = 30 W^{0.013}$
$\dot{V}$ ml min^{-1}
100
10
$\dot{V} = 5.85 W^{0.85}$
t sec
0.4
0.2
$t = 0.21 W^{0.146}$
1
10
Body Weight – g

would be dependent on V_T and the duration of each breath, t, in the equation $\dot{V} \propto \frac{V_T}{\frac{1}{2}t}$. Although f is a constant, average breath duration becomes longer with increasing body weight, $t = 0.21\ W^{0.146}$ where t is in sec (Fig. 2.10). Thus, a V_T and t proportionality of 1.0 and 0.146, respectively, would cause a flow rate relationship of $W^{0.85}$. A maximum flow rate relationship with body weight has not been plotted since it is rather an arbitrary value depending not only on the spontaneous activity of the lizard, but also on its particular air flow profile. Maximum flow rates of 3.5 to 4 times the average flow rate were recorded.

Minute Volume and $\dot{V}o_2$ Relationships during rest and increasing activity

These parameters, from resting to various levels of spontaneous activity, have been graphed for all 7 groups of lizard weights. There was much similarity between these groups and graphs for the 25g L. viridis have been selected for illustration (Fig. 2.11 to 2.16). Increments in $\dot{V}o_2$ were dependent on $\dot{V}_E$ increases with the latter becoming disproportionately greater at higher $\dot{V}o_2$ levels. For a particular $\dot{V}o_2$ level, however, $\dot{V}_E$ could double, or even quadruple, its required minimum thereby 'wasting' much of the ventilation volume (Fig. 2.11).

Minute volume can be altered by changes in f, V_T or both. It was found that $\dot{V}_E$ was directly proportional to V_T with a small amount of scatter in the data. In contrast, f varied between 35 and 85 min^{-1} and was only proportional to $\dot{V}_E$ at low frequencies but with considerable data variation (Fig. 2.12). For 4 out of the 7 body weight groups, there was no proportionality even at low frequencies. It would appear that $\dot{V}_E$ is controlled mainly by V_T increments and not by changes in frequency. Thus $\dot{V}o_2$ is related to V_T in a manner mimicking its relationship with $\dot{V}_E$. In the example illustrated here, $\dot{V}o_2$ and f show a direct proportionality but with considerable scatter. Often there is no relationship between f and $\dot{V}o_2$ (Fig. 2.13).

Ventilation requirement is a measure of the amount of air that has to ventilate the lungs in order to supply a unit volume of O_2 to the

FIG. 2.11 Relationship between minute volume, $\dot{V}_E$, and oxygen consumption, $\dot{V}o_2$. Fig. 2.11 to 2.16 are data for one L. viridis (25g) individual.

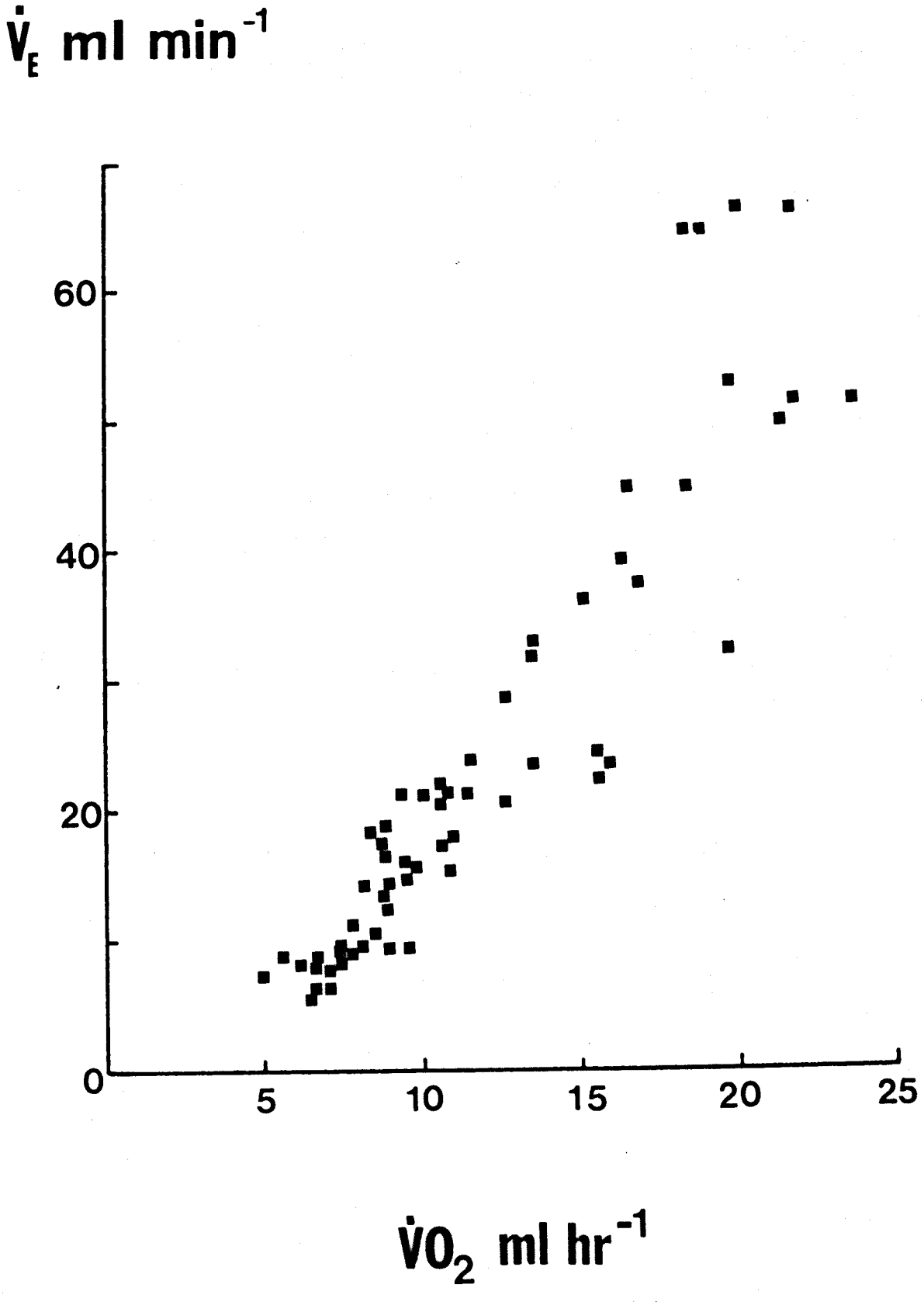
$\dot{V}_E$ ml min^{-1}
60
40
20
0
5
10
15
20
25
$\dot{V}O_2$ ml hr^{-1}

FIG. 2.12 Relationship of tidal volume, V_T, and respiratory frequency, f, to minute volume, $\dot{V}_E$.

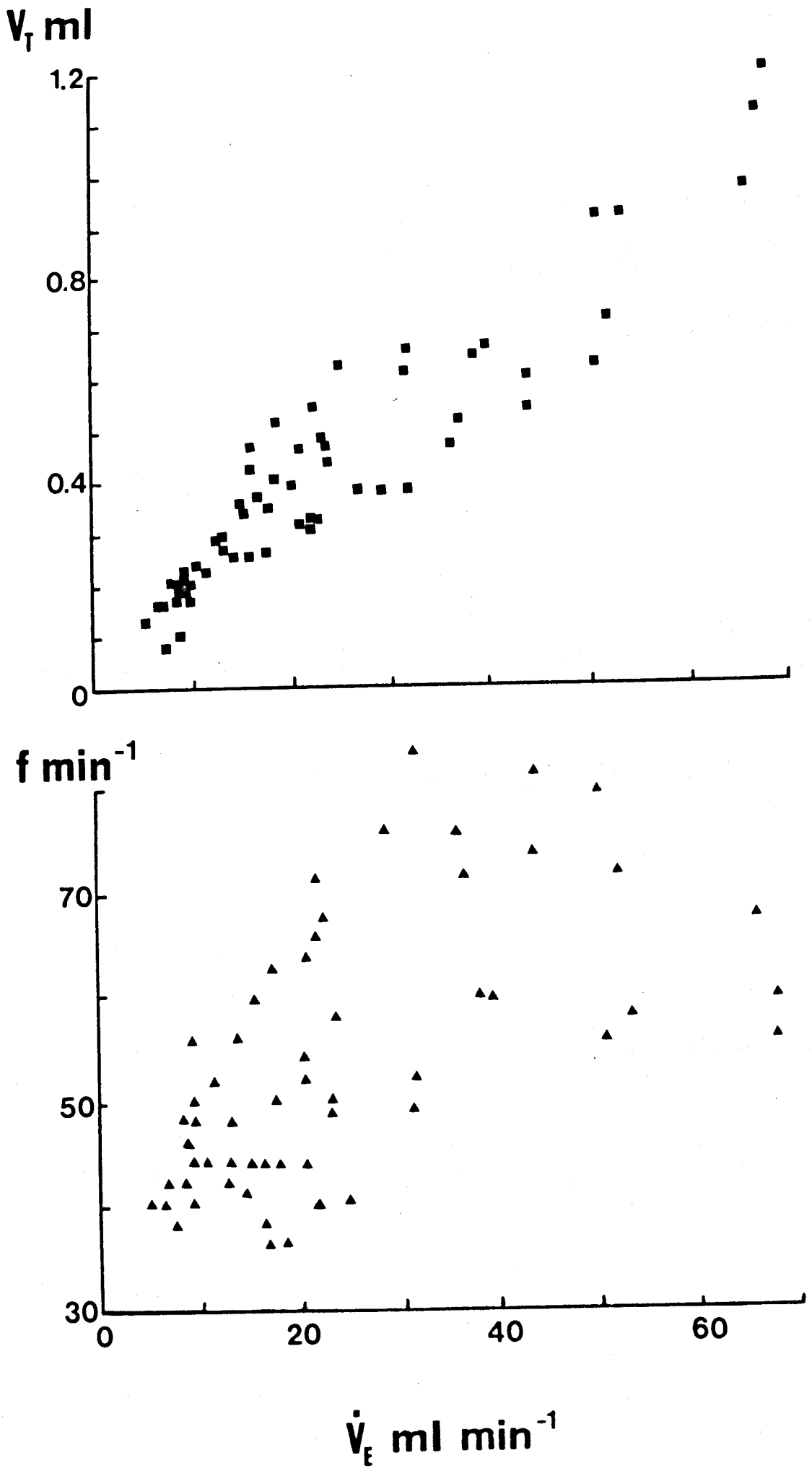
V_T ml
1.2
0.8
0.4
0
f min^{-1}
70
50
30
0
20
40
60
$\dot{V}_E$ ml min^{-1}

FIG. 2.13 Relationship of tidal volume, V_T, and respiratory frequency, f, to $\dot{V}o_2$.

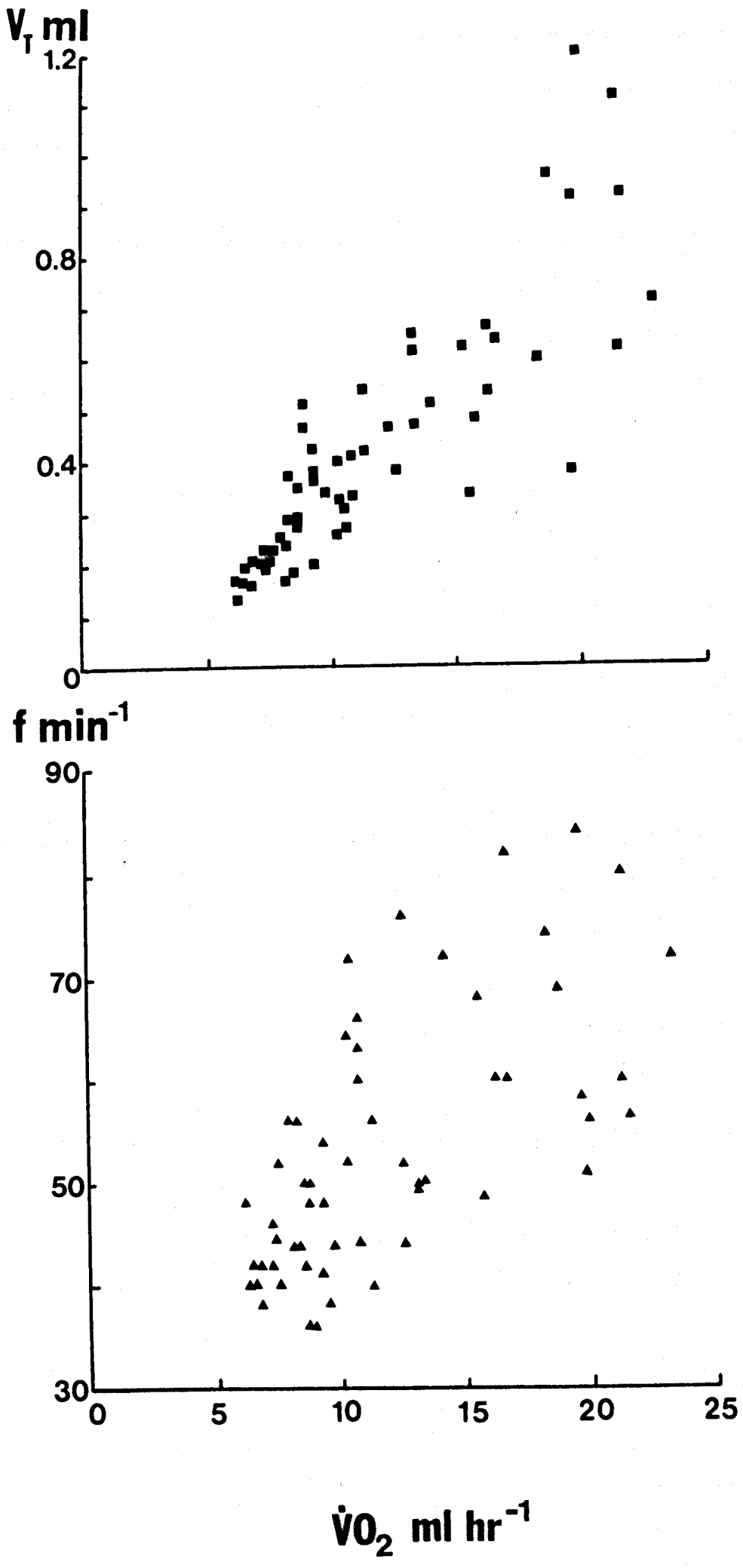
V_T ml
1.2
0.8
0.4
0
f min^{-1}
90
70
50
30
0
5
10
15
20
25
$\dot{V}O_2$ ml hr^{-1}

tissues. It is therefore the ratio $\dot{V}_E/\dot{V}o_2$ expressed as ml min^{-1} (BTPS)/ ml min^{-1} (STPD). For L. viridis (25g), this ventilation requirement varied from 50 to 210 increasing as $\dot{V}_E$ and $\dot{V}o_2$ increased (Fig. 2.14). Since $\dot{V}_E$ is the larger volume (50 to 210 times) there would obviously be less scatter in its relationship to ventilation requirement than in the $\dot{V}o_2$ relationship with ventilation requirement.

'Wasted' ventilation increases as V_T increases but bears no relationship to f. If a full range of f for the same V_T are plotted against respiratory requirement, there is still no obvious relationship between f and respiratory requirement (Fig. 2.15). Thus f changes may not be controlled by metabolic demands. However, in animals that respired at very low frequencies, i.e. 10 to 30 min^{-1} and low tidal volumes, i.e. minimum V_T, the ventilation requirement was very low being between 12 and 30. If a high V_T near the maximum level was combined with a low f, then the respiratory requirement was not as great as expected from normal V_T ventilation requirement relationships. When high frequency breathing occurred, i.e. 100 to 200 min^{-1} this was always combined with low tidal volumes near the minimum level. Such respiration was very inefficient, having ventilation requirements of 150 to 200. Obviously, the longer the lungs can stay in the inflated state of a respiratory pause after inspiration, the more O_2 is extracted per unit of ventilated volume. This extraction is also greater at low levels of lung inflation.

It is apparent that in order to attain high $\dot{V}o_2$ levels, excessive 'extra' ventilation has to occur. The question arises as to whether this is an unnecessary hyperventilation of disturbed animals subjected to stress or whether the hyperventilation is compulsory to meet the high O_2 demands. The respiratory quotient, $R = \dot{V}co_2/\dot{V}o_2$, is an indicator of both the extent of hyperventilation and the degree of anaerobic metabolism. Both conditions cause an R value greater than unity and the two cannot be distinguished without blood lactate analysis. R was, however, more closely related in a

FIG. 2.14 Relationship of ventilation requirement, $\dot{V}_E/\dot{V}o_2$, to minute volume, $\dot{V}_E$, and to $\dot{V}o_2$

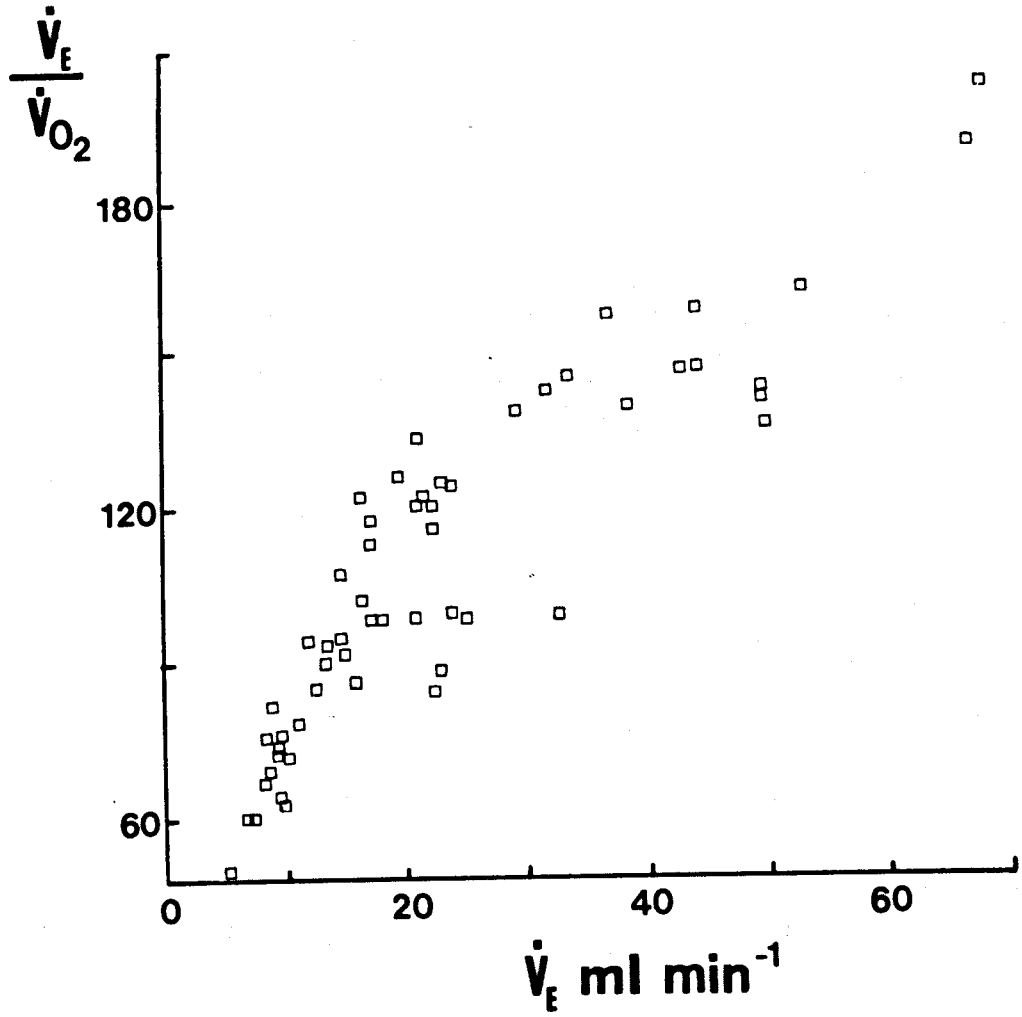
$\frac{\dot{V}_E}{\dot{V}_{O_2}}$
180
120
60
0
20
40
60
$\dot{V}_E$ ml min^{-1}

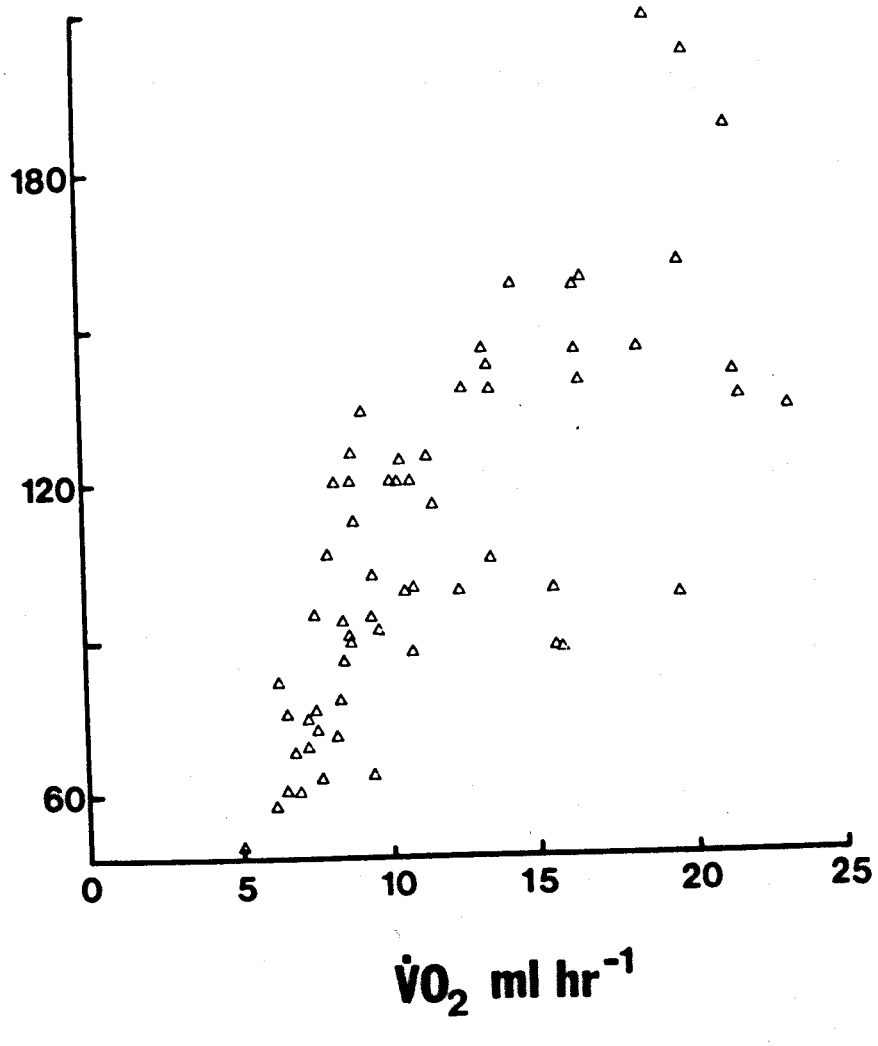
180
120
60
0
5
10
15
20
25
$\dot{V}O_2$ ml hr^{-1}

FIG. 2.15 Relationship of ventilation requirement, $\dot{V}_E/\dot{V}o_2$, to V_T and f.

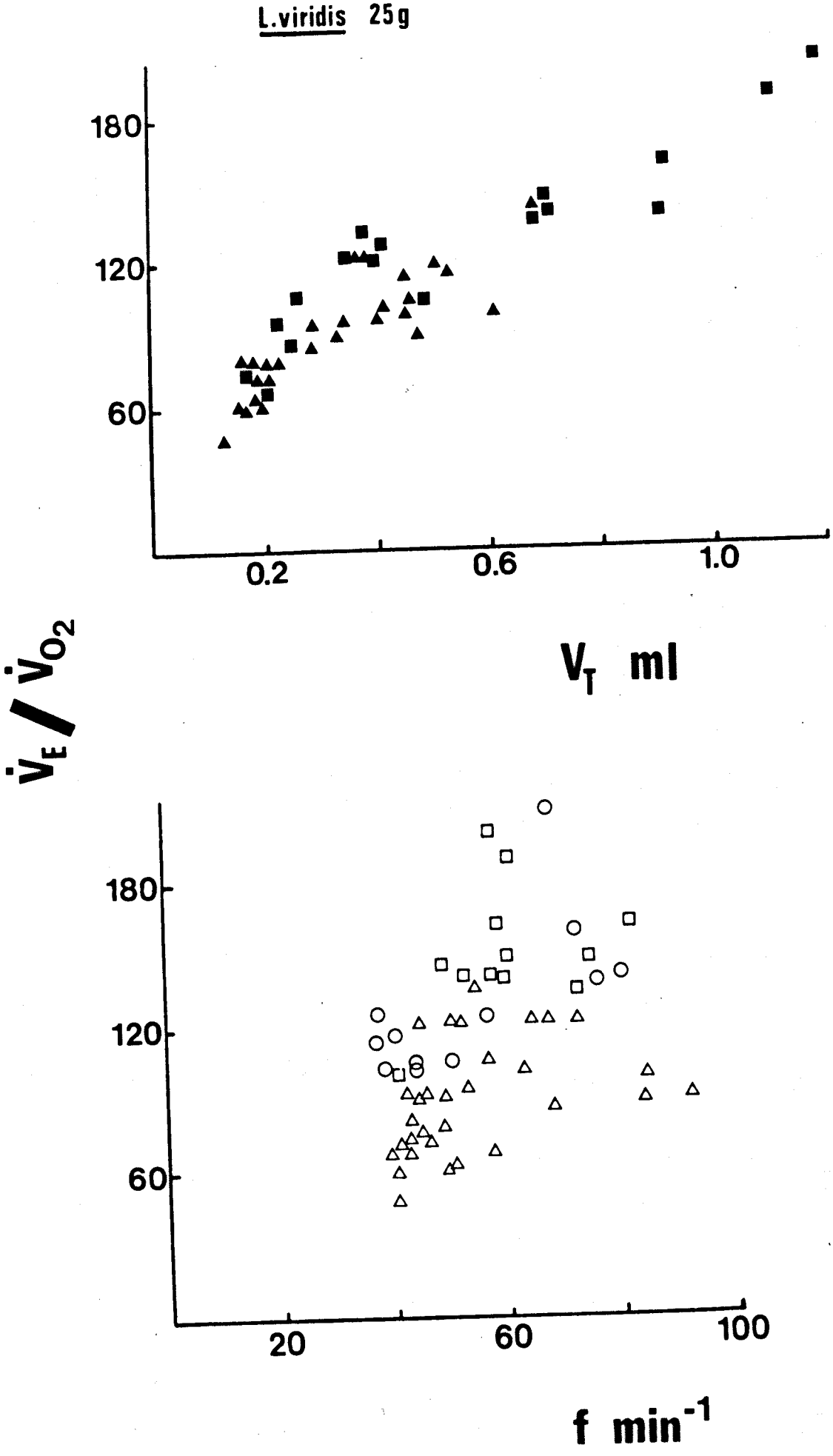
L.viridis 25g
180
120
60
0.2
0.6
1.0
$\dot{V}_E / \dot{V}_{O_2}$
V_T ml
180
120
60
20
60
100
f min^{-1}

FIG. 2.16 Relationship of respiratory quotient, R, to $\dot{V}o_2$ and minute volume, $\dot{V}_E$.

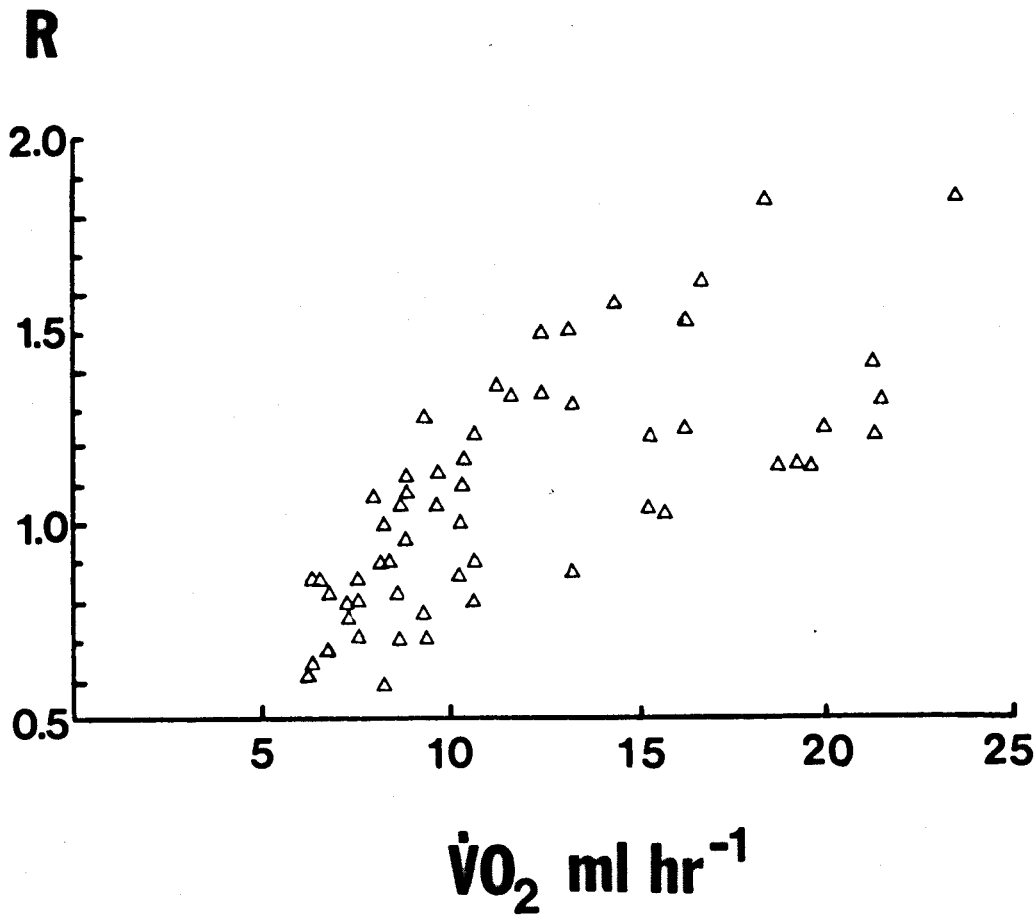
R
2.0
1.5
1.0
0.5
5
10
15
20
25
$\dot{V}O_2$ ml hr^{-1}

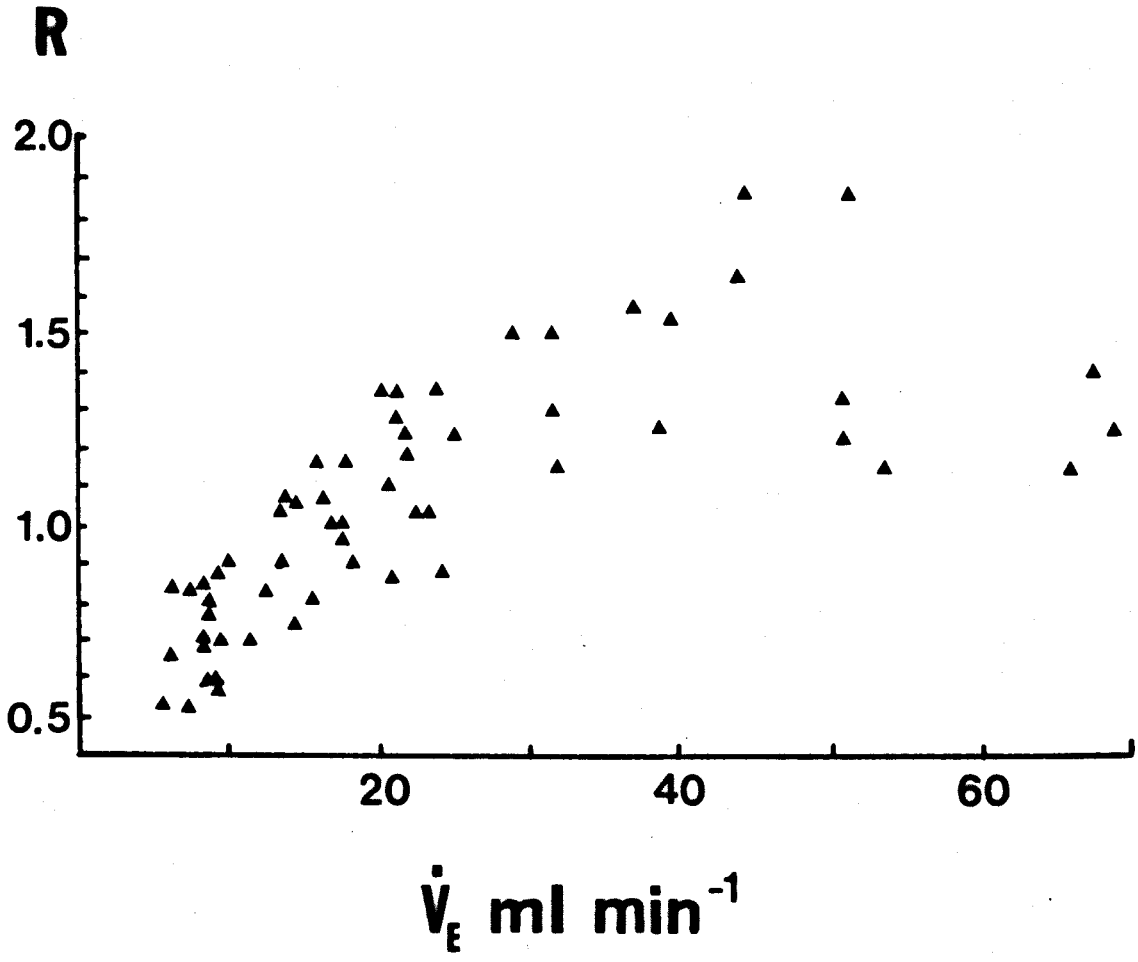
R
2.0
1.5
1.0
0.5
20
40
60
$\dot{V}_E$ ml min^{-1}

FIG. 2.17 Logarithmic relationship between ventilation requirement and body weight. Correlation coefficient for maximum requirement = 0.76 and for minimum requirement = 0.47. Inverted right hand scale gives the values in terms of O_2 extraction coefficients (per cent). Average relationship is $\dot{V}_E/\dot{V}o_2 \propto W^{0.24}$.

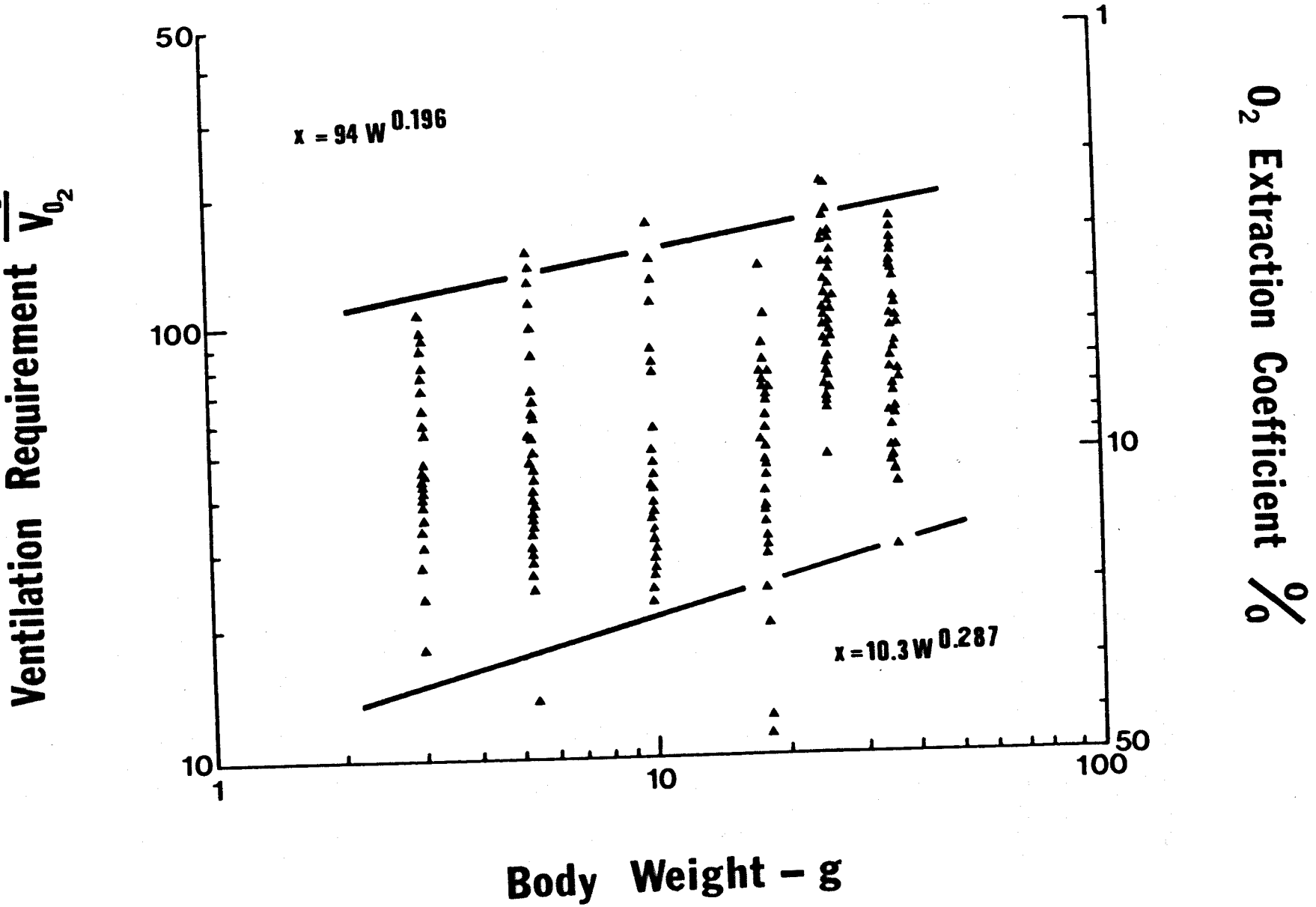
$\frac{\dot{V}_E}{V_{O_2}}$ Ventilation Requirement
50
100
10
1
10
100
1
10
50
O_2 Extraction Coefficient %
x = 94 W 0.196
x = 10.3 W 0.287
Body Weight – g

linear manner to $\dot{V}o_2$ than it was to $\dot{V}_E$. At high $\dot{V}_E$, R gave a plateau relationship (Fig. 2.16). This is considered indicative of a compulsory rather than a disturbed hyperventilation.

Since $\dot{V}o_2$ was proportional to $W^{0.75}$ and $\dot{V}_E \propto W^{1.0}$, it follows that the ventilation requirement must be related to $W^{0.25}$. Fig. 2.17 shows the full range of ventilation requirements measured in lizards of six different weights and the average ventilation requirements gave a slope of 0.24. The overall requirements ranged from 11 to 210 which is equivalent to an O_2 extraction coefficient (the ratio of amount of O_2 extracted to the amount of O_2 ventilated) of 43.5 to 2.3%. A high ventilation requirement represents a low capacity for O_2 extraction.

DISCUSSION

Ventilatory Patterns

Diphasic tidal volumes but with triphasic thoracic movements were recorded in Lacerta which is in agreement with the work of Boelaert (1941). The thoracic E_2 phase is not recorded with the nose mask because the glottis closes at the end of inspiration. Neither is it recorded by a whole body chamber because it is counteracted by an expansion of the abdomen. The pleuro-peritoneal cavities are not anatomically separated by a diaphragm in lizards, so that compression of the lungs by the thoracic cage, against a closed glottis, need not necessarily elevate intra-pulmonary pressure but may cause caudal expansion of the lungs into the abdomen. Caudal regions are the most compliant region of the lizard lung (see Chapters 3 and 5). Boelaert (1941), recording with levers touching the body, has shown similar inverse passive movements of the abdomen during E_2, as well as during E_1 and I phases. Abdominal movements related to E_1 and I were not necessarily inverse but were certainly passive.

Boelaert (1941) was, however, unable to record any instances of triphasic tidal volumes, whilst the evidence from Willem & Bertrand (1936) and the study presented here, shows that this can occur in highly excited Lacerta, in which closure of the glottis is delayed. Similar conclusions were reached for alligators and caimans (Naifeh, Huggins & Hoff, 1971a,b,c). Sauromalus may be an easily excitable lizard since its tidal volumes were usually triphasic (Templeton & Dawson, 1963).

Anaesthesia by Nembutal paralysed the glottal closing musculature or its nervous control long before the intercostals were markedly affected. The fact that this can occur and that the glottis can be delayed in closing (excited animal) or correctly timed (arousal of an anaesthetised animal by tail pinching), must indicate that it is separately controlled by the medulla. Hence its timing with respect to thoracic movements is not always precisely

matched. This agrees with the work of Naifeh, Huggins & Hoff (1971b,c) in which by brain stem sectioning or anaesthesia, they were able to demonstrate three separate respiratory centres:- inspiratory, expiratory and glottal. During anaesthesia, the glottal, then the expiratory and finally the inspiratory centre was paralysed in caimans and alligators. A similar situation is found in Lacerta, except that under deep anaesthesia, Naifeh et al (1971b) found that the active phase in E_1 (EMG recordings) was abolished, whilst in Lacerta a small active phase still persisted (judging from air flow measurements). A continuous ventilation with virtually no pause and a prolongation of the expiratory phase was also recorded sometimes in caimans and alligators and always in very deeply anaesthetised Lacerta. Respiratory frequency and tidal volume decrease with increasing depth of anaesthesia but paradoxically under very deep anaesthesia, f appeared to increase, although still below the resting minimum (resting f = 30 min^{-1}, anaesthetised f = 12 min^{-1}, very deeply anaesthetised f = 24 min^{-1}).

All records in the literature concerning the phases of specific muscular activity during the respiratory cycle, are in agreement that E_1 and I are active, but that E_2 is passive (Boelaert, 1941, Templeton & Dawson, 1963, Naifeh, Huggins, Hoff, Hugg & Norton, 1970). This contrasts with the mammal in which I is active but E is passive (there being no E_2 phase), only becoming active when the expiratory reserve volume is being expelled. Lizards are, therefore, like mammals in that elastic recoil favours expiration rather than inspiration, but like birds (in which E is active and I is passive) in that they retain an inspired volume with minimal muscular effort.

During mammalian inspiration, the glottis and trachea enlarge whereas they narrow during expiration (Bartlett, Remmers & Gautier, 1973). If an apneic pause then ensues, the glottis may close. Although expiration/inspiration/pause is the pattern in crocodiles, the glottis (and perhaps the trachea) follow the mammalian narrowing during expiration and widening

during inspiration but then the glottis closes for the pause (Naifeh, Huggins & Hoff, 1970). This pause requires little muscular effort and cannot therefore be equated with mammalian apneusis (Naifeh, Huggins & Hoff, 1971a). The reptilian persistence in completely closing the glottis at the end of the respiratory cycle is partly an evolutionary remnant of glottal closure in the amphibians which use a buccal force pump and not a costal suction pump (Gans, 1970) and partly a necessity for retaining inspired air during the respiratory pause.

A buccal force pump can, however, occur in some reptiles, but it is termed buccal deglutition and is part of a threatening display, e.g. in Sauromalus (Salt, 1943, Templeton, 1964). It is of interest to note that it has only been recorded in diseased or heat distressed individuals of Uromastix (Saalfield, 1934) and in diseased Lacerta (this study). Gular activity in reptiles may also reflect the primitive buccal force pump of the Amphibia.

Gular movement may ventilate the buccopharyngeal cavity, which, if vascular enough, could provide an extrapulmonary gas exchanging area (Drummond, 1946). Conversely, it may serve to circulate and mix air within the lungs if the nostrils are closed but the glottis open (Lumsden, 1924). The latter suggestion is not possible in Lacerta because when isolated gular movements were noted, there was never any corresponding air flow into the lungs (recorded with the body pneumotachograph). Such gular movements were against a closed glottis, as has been found in crocodiles (Naifeh, Huggins & Hoff, 1970). Also, Lacerta nostrils do not have valves and can never be completely closed (Chapter 4 and Appendix II).

In crocodiles, gular activity always occurred in phase with thoracic movements but it was of an inspiratory nature (expansion) during expiration and an expiratory nature during inspiration. It was considered to represent mainly a passive reflection of thoracic movements, but it was, however, accompanied by some gular muscular activity, especially during thoracic expiration. The amplitude of this synchoronous gular movement was

minimal in quiet animals (Huggins, Parsons & Pena, 1968, Naifeh, Huggins, Hoff, Hugg & Norton, 1970). In Lacerta gular movements were also minimal in quiet animals but, in contrast, were expiratory during expiration and inspiratory during inspiration. They were also quicker than thoracic movements and air flow profiles would indicate that both gular expiration and inspiration involved muscle activity and were unlikely to be attributable to passive phenomena. During the respiratory pause, isolated gular activity, when it occurred, was in the sequence I and E in crocodiles but, again in Lacerta, it was the reverse.

The absence of isolated gular activity from many long ventilatory pauses, its occurrence in only excited animals (spontaneously excited or induced by attempted exercise) and its absence from lightly anaesthetised Lacerta, would suggest that it has no respiratory significance. The fact that synchronous gular activity (i.e. with thoracic respiration) is only marked in excited animals would also support this conclusion. It is considered that gular movements are solely olfactory. Huggins, Parsons & Pena (1968) found that all gular movements in caimans were coincident with EEG activity in the olfactory bulbs. Thus ventilation of the buccopharyngeal cavity has no respiratory role and its lack of vascularity is considered in Chapter 4.

Many, as yet, unanswered questions are raised by the occurrence of synchronous gular activity. Why should it be necessary when pulmonary tidal flow would serve the same purpose of ventilating olfactory regions in the nasal cavities? Gular flow usually augments the tidal volume by only 1 to 2% and never by more than 10% (rare). Although, in Lacerta, gular expiration might assist thoracic expiration by reducing the volume of the buccopharyngeal cavity, gular inspiration would only be increasing the dead space. Why should gular air flow be in the same direction as thoracic air flow, i.e. E - I, in Lacerta whilst, in crocodiles, the former is reversed for both synchronous and isolated activity?

Respiratory Frequency

Data for respiratory frequency in the Lacerta genus is in complete agreement with the interspecific data of Bennett (1973a) in stating that f is independent of body weight. At 29°C the mean minimum f was 30 min^{-1} which compares well with the other Lacerta value from Nielsen (1961), in which conditions of minimal stress may not have been reached; L. viridis and L. sicula (20g mean) had an f of 38 min^{-1} at 30°C. Lacerta respiratory frequencies are much higher than the average lizard value of 13 (full range being 6 to 38 for resting, f, Table 2.1). Reference must be made here to the interspecific table for f collected by Bennett (1973a).

Nielsen (1961, 1962) found frequencies between 5 and 75 min^{-1} in Lacerta caused during warming or cooling the resting lizard or by administration of low O_2 and/or high CO_2. A frequency range of 10 to 100 min^{-1} was obtained in resting or spontaneously active animals at or near their preferred body temperature (Lacerta of this study). Hyperventilating 'flutter' breathing frequencies of up to 200 min^{-1} were also recorded but only in disturbed/ excited individuals. Frequency ranges in other lizards are given in Table 2.1. Some lizards had a greater ability to increase f than others, but this may be a reflection of the few studies on active animals. Lack of data for abnormally high frequencies from excited animals may be due to a lack of documentation.

Lizard respiratory frequencies are much higher than the resting 1 to 5 min^{-1} reported for snakes (active, as well), turtles and crocodiles (Boyer, 1966, Jackson, 1971, Huggins, Valentinuzzi & Hoff, 1971, Dmi'el, 1972).

Table 2.2 compares the respiratory frequencies of lizards, birds and mammals of a 10g body weight. Birds had frequencies 2.5 times greater and mammals 5.8 times greater than Lacerta. In contrast, however, lizards are capable of a 10-fold change in f whilst in mammals only a 2-fold change is possible (Hey, et al, 1966), although values nearer those of a lizard are reached in panting mammals. It is not known what range of frequency is possible in birds.

TABLE 2.1

Respiratory Frequencies in Lizards.

Species	Weight (g)	Standard f min^{-1} 30°C	Range of f	Panting/ Excited f	Reference
Lacerta	3.0 to 38	30	10 - 100*	200	This study.
Lacerta	~ 20	38	5 - 75	-	Nielsen, 1961, '62.
Crotaphytus	25 to 40	17	10 - 100	-	Templeton & Dawson, 1963.
Dipsosaurus	~ 70	18	9 - 90	-	Dawson & Bartholomew, 1958.
Eurneces	~ 30	17	9.5 - 50	-	Dawson, 1960.
Gerrhontus	~ 30	7	0.5 - 50	-	Dawson & Templeton, 1963.
Lygosoma	1.0	38	10 - 70	-	Hudson & Bertram, 1966.
Sauromalus	574	14	2 - 25*	-	Bennett, 1973a.
Sauromalus	140	8.3	5 - 67	-	Crawford & Kampe, 1971.
Sceloporus	12.8	35	28 - 45	-	Francis & Brooks, 1970.
Uma	30	18	10 - 20	-	Pough, 1969.
Uta	~ 14	19	2 - 75	-	Murrish & Vance, 1968.
Varanus	674	8	0.5 - 30*	150	Bennett, 1973a.
Xantusia	1.1	6	4 - 15	-	Snyder, 1971.
Eurneces	253	22			≠Wilson, 1971.
Physignathus	585	26			≠Wilson, 1971.
Tiliqua	477	7.2			≠Wilson, 1971.

* Resting and Active

≠ from Bennett, 1973a.

TABLE 2.2

Respiratory Frequency in a 10g Lizard, Bird and Mammal.

	Standard f	Range of f	Reference
Lacerta	30	10 - 100	This study.
Lizard	13	0.5 - 100	Bennett, 1973a and Table 2.1.
Bird	73	?	Lasiewski & Calder, 1971.
Mammal	175	150 - 300*	Stahl, 1967.

* estimated from Hey et al (1966).

In lizards, this high frequency range can occur without affecting tidal volumes, because of their low resting frequencies and the fact that extra breaths can, therefore, occur in place of a respiratory pause. Mammals have no such pause and thus to increase f, the time course of each breath has to decrease thereby reducing V_T. To maintain or increase V_T, whilst f also increases, requires very large increments in tidal flow rates.

Tidal Volume, Ventilation Volume and Body Weight

Tidal volume in Lacerta is directly proportional to body weight ($W^{1.036}$) which is in agreement with mammalian and bird data (Stahl, 1967, Lasiewski & Calder, 1971), but not with the interspecific data collected for lizards where $V_T \propto W^{0.85}$ (Bennett, 1973a). Both lizard studies, however, found f to be independent of body weight, whereas in mammals $f \propto W^{-0.25}$ and in birds, $f \propto W^{-0.31}$. Thus pulmonary ventilation, $\dot{V}_E$, is matched to the $\dot{V}o_2$ relationship with body weight in mammals, birds and interspecific lizards:- mammal $\dot{V}_E \propto W^{0.8}$ and $\dot{V}o_2 \propto W^{0.76}$, bird $\dot{V}_E \propto W^{0.77}$ and $\dot{V}o_2 \propto W^{0.72}$, interspecific lizards $\dot{V}_E \propto W^{0.85}$ and $\dot{V}o_2 \propto W^{0.83}$. However, in Lacerta, $\dot{V}_E$ is proportional to $W^{1.0}$ whilst $\dot{V}o_2$ is proportional to $W^{0.75}$, so that as the lizard becomes larger, more of the ventilation volume is wasted. This inefficiency will be considered later. Firstly, the discrepancy between a study of the Lacerta genus and an interspecific study of lizards must be examined.

Table 2.3 compares the minimum V_T measurements obtained at 30°C for a variety of lizards. In Lacerta (of this study) the minimum V_T for a 10g individual gave a $\dot{V}o_2$ of 5.4 ml hr^{-1} which corresponded to a 1 day starved, routine day oxygen consumption. Examination of the methods used by other authors indicates that a similar level of activity was probably present in their studies. This is not true for Nielsen's work (1961) in which corresponding $\dot{V}o_2$ measurements were as high as 12 ml hr^{-1}. Her V_T measurements were approximately 3 times greater than those of this study. It is possible that in Nielsen's study, the restrictions imposed on the

FIG. 2.18 Logarithmic relationship of $\dot{V}_E$ and $\dot{V}_T$ to body weight. ■ ▲ Data from Bennett (1973a), ★ Lacerta, Nielsen (1961), ✪ Lacerta, this study.

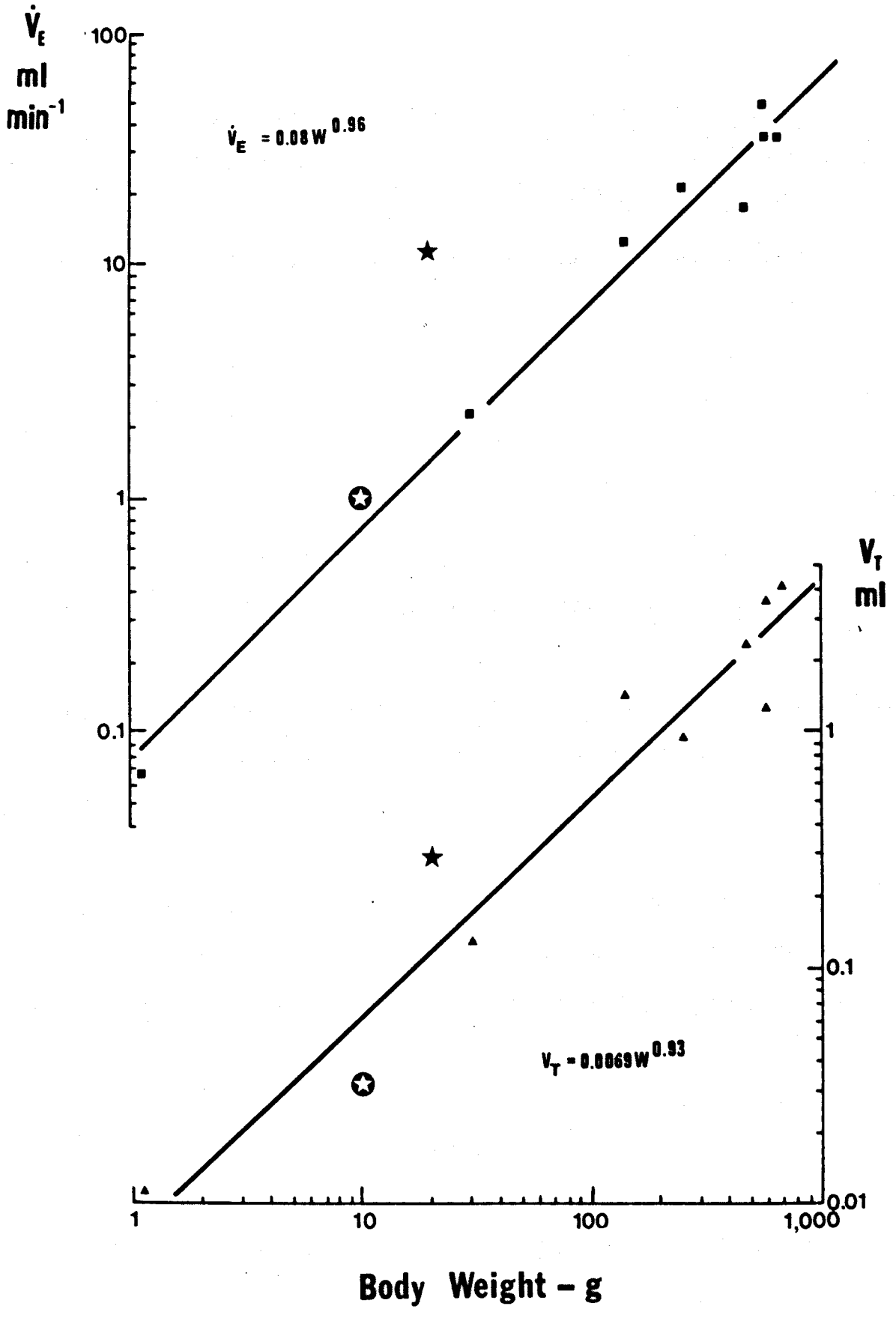
$\dot{V}_E$
ml
min^{-1}
100
10
1
0.1
$\dot{V}_E = 0.08W^{0.96}$
V_T
ml
1
0.1
0.01
$V_T = 0.0069W^{0.93}$
1
10
100
1,000
Body Weight – g

lizards by using a head mask and a spirometer connected to the body chamber could cause considerable back pressures. Certainly, back pressures caused abnormally high V_T and wasted ventilation when used in my investigations.

Fig. 2.18 plots the V_T data collected by Bennett (1973a) (Table 2.3) and shows that Nielsen's values could be responsible for a V_T proportionality of $W^{0.85}$. Without Nielsen's data, $V_T = 0.009\ W^{0.88}$ and with, instead, inclusion of my Lacerta data, $V_T = 0.007\ W^{0.93}$ (both correlation coefficients = 0.974). The discrepancy caused by Nielsen's data is even more apparent when $\dot{V}_E$ is considered (Table 2.4 and Fig. 2.18). Without Nielsen's data, $\dot{V}_E = 0.07\ W^{0.98}$ and with, instead, inclusion of my Lacerta data, $\dot{V}_E = 0.08\ W^{0.96}$ (both CC = 0.99). Considering that f is high in some lizards but low in others (Table 2.1), V_T might be expected to be the reverse, such that, together, they would cause $\dot{V}_E$ to fit a common slope more closely. This, indeed, was the case (Fig. 2.18).

It is, therefore, possible that $\dot{V}_E$ in all lizards, whether examined interspecifically or within a genus, is directly proportional to body weight. To check this an interspecific re-examination of $\dot{V}_E$ scaling is required in which conditions of stress and, therefore, the level of $\dot{V}O_2$ are carefully controlled for all lizards studied. It is perhaps possible that a similar re-examination of interspecific standard $\dot{V}O_2$ scaling might yield a body weight relationship to the 0.75 power rather than the 0.85 power of Bennett & Dawson (1973). In Lacerta, definitely, and possibly in all lizards, 'wasted' ventilation increases as body weight increases since $\dot{V}_E/\dot{V}O_2 \propto W^{0.25}$.

Tidal Volumes

Minimum V_T measurements obtained at 30°C, together with the minimum to maximum range obtained during rest and activity or with temperature, low O_2 or high CO_2 effects, have been tabulated for a variety of lizards in Table 2.3. The true capacity for altering V_T has not been measured in many of the lizards investigated. Even temperature increments at rest will

TABLE 2.3

Tidal Volumes in Lizards.

Species	Weight (g)	V_T min. 30°C (ml)	Range of V_T	Reference
Lacerta	10	0.032	0.032 - 0.45*	This study
Lacerta	~ 10	0.125	0.06 - 0.3/	Nielsen, 1961, 1962.
			0.15 - 0.55⁷	Nielsen, 1961, 1962.
	~ 30	0.375	0.375 - 0.5/	Nielsen, 1961, 1962.
Crotaphytus	~ 30	0.13	0.055 - 0.55⁷	Templeton & Dawson, 1963.
Sauromalus	574	3.5	1.0 - 40*/	Bennett, 1973a.
Sauromalus	140	1.45	1.0 - 1.46/	Crawford & Kampe, 1971.
Varanus	674	4.17	1.0 - 35*/	Bennett, 1973a.
Xantusia	1.1	0.011	0.015 - 0.018	Snyder, 1971.
Eumeces	253	0.94		ø Wilson, 1971.
Physignathus	585	1.26		Wilson, 1971.
Tiliqua	477	2.37		Wilson, 1971.

* Rest to Activity / Temperature ⁷ High CO_2 or low O_2

ø from Bennett, 1973a.

TABLE 2.4

Resting minute volume ml min^{-1}, $\dot{V}_E$, at 30°C from f x min. V_T

Species	Weight (g)	$\dot{V}_E$	Reference
Lacerta	10	0.96	This study.
Lacerta	~10	4.75	Nielsen, 1961.
	~ 30	14.25	Nielsen, 1961.
	~ 20	11.0	Value used by Bennett, 1973a.
Crotaphytus	~ 30	2.2	Templeton & Dawson, 1963.
Sauromalus	574	49.0	Bennett, 1973a.
Sauromalus	140	12.0	Crawford & Kampe, 1971.
Varanus	674	33.0	Bennett, 1973a.
Xantusia	1.1	0.066	Snyder, 1971.
Eumeces	253	20.6	* Wilson, 1971.
Physignathus	585	33.0	Wilson, 1971.
Tiliqua	477	17.0	Wilson, 1971.

* from Bennett, 1973a.

not necessarily increase V_T (or f) in all lizards (see Introduction). Activity and temperature independently affect respiration.

Resting tidal volumes in snakes, turtles and crocodiles are approximately 0.1 ml for a 10g body weight (assuming direct proportionality), being 2 to 3 times greater than the values found for lizards (Atland & Parker, 1955, Huggins, Valentinuzzi & Hoff, 1971, Jackson, 1971, Dmi'el, 1972). In snakes V_T can increase by 6-fold during temperature and activity variation. This increase is considerably less than the 14 to 40-fold found in lizards (Table 2.3). No data are available for either temperature or activity effects on V_T in crocodiles. In turtles V_T changed by a factor of 2 (Jackson, 1971).

Table 2.5 compares the tidal volumes of lizards, birds and mammals of a 10g body weight. Birds had a V_T 3 times greater than Lacerta, whilst mammalian volumes were twice as great as Lacerta. At a 1 kg body weight, Bennett (1973a) found that lizard tidal volumes were 1.5 times less than a mammal but 2.75 times less than a bird. This is very similar to values at 10g body weights, using Lacerta data. If, however, lizards in general are considered (data in Fig. 2.18), their tidal volumes are closer to the mammal's. Bennett's $V \propto W^{0.85}$ data (1973a) causes tidal volumes at 10g body weight to be closer to the bird's. Remembering the earlier criticism of a V_T proportionality to $W^{0.85}$, it is probably correct to state that minimum tidal volumes for resting animals are least in lizards and greatest in birds.

TABLE 2.5

Tidal volumes in a 10g lizard, bird and mammal.

	Temp. °C	Min. V_T(ml)	Range of V_T	Reference
Lacerta	30	0.032	0.032 - 0.45	This study.
Lizards	30	0.056	-	This study Fig. 2.18.
Lizards	30	0.086	0.022 - 0.83	Bennett, 1973a.
Birds	37	0.094	?	Lasiewski & Calder, 1971.
Mammals	37	0.062	0.05 - 0.25*	Stahl, 1967.

*estimated from Hey et al, 1966.

Tidal volume in mammals can be increased by a factor of 5 from rest to maximum activity (Hey et al, 1966), whilst Lacerta are capable of 14-fold increments. The 40-fold increment of Bennett's data (1973a) is due to the augmenting effect of a 10 to 40°C temperature range. The range of tidal volume possible in birds has not been documented. The enormous increments in V_T found in lizards raises an interesting question concerning the pressures required for inflation. How much intrapulmonary pressure is required to reach such high lizard tidal volumes? After taking into consideration the greater compliance of this primitive lung, are there relatively greater pressures involved in lizard inflation than in the mammal? This is examined in detail in Chapter 3. In order to increase V_T so considerably, the lizard must either increase breath duration for the same flow rate (i.e. reduce the length of the respiratory pause) or markedly increase respiratory air flow for each breath to rates possibly greater than the mammal. A combination of both alternatives could also occur.

Inspiratory/Expiratory Flow Rates and Breath Duration

These parameters in Lacerta and mammals are compared in Table 2.6. Breath duration can be calculated for mammals from the respiratory frequency and the fact that there is no respiratory pause. Hence for a resting mammalian f of 175 min^{-1}, breath duration equals 60/175 or 0.34 sec. If tidal air flow was in the form of a square wave, $\dot{V}$ would equal $\frac{V_T}{\frac{1}{2}t}$ where $\frac{1}{2}t$ = the time for inspiration or expiration, i.e. $\frac{1}{2}$ breath duration. This gives a value of 23 ml min^{-1} for resting mammals but a factor of 2 is necessary to convert it to the true value of 46 ml min^{-1} for a peak flow wave. This factor was established by calculations from V_T, t and measured $\dot{V}$ data of King (1966) and Diamond & Lipscomb (1970). The same factor also applies to Lacerta data which indicates the similarity of peak flow shape between the two.

TABLE 2.6

Comparison of minimum and maximum respiratory flow rates in Lacerta and mammals of a 10g body weight.

Parameter	Lacerta	Mammal	M/L ratio
Min. breath duration (sec)	0.6	0.34	0.56
Min. V_T (ml)	0.032	0.065	2.0
Min. peak flow rate $\dot{V}$ (ml min^{-1})	13	46	3.5
Max. breath duration (sec)	0.6	0.172	0.3
Max. V_T (ml)	0.45	0.25	0.55
Max. peak flow rate $\dot{V}$ (ml min^{-1})	180	346	1.9

It can be seen from Table 2.6 that Lacerta breaths are of longer duration than the mammal and do not become shorter at high respiratory frequencies. Extra breaths occur in place of the respiratory pause in Lacerta. Thus, because of the longer breaths, peak flow rates are still some 2.0 times less than the mammal, even at max. V_T. Respiratory flow rates in Lacerta were proportional to $W^{0.85}$ whereas in the mammal $\dot{V}$ is related to $W^{0.75}$ (V_T being proportional to $W^{1.0}$ and breath duration proportional to $W^{0.25}$, Guyton, 1947).

Ventilation Requirement and O_2 Extraction

Values for reptilian ventilation requirements and O_2 extraction efficiency have been collected from the literature (Table 2.7). It is very evident that the Lacerta of Nielsen's study (1961) wasted a large proportion of their ventilation volume in comparison with other lizards. This was probably due to the experimental technique, as already stated, and provides further evidence to substantiate that the V_T measurements of Nielsen's study are abnormally high. There is a great deal of variation in the maximum O_2 extraction coefficient, 13.7 to 30%, giving a mean of 18.3% if Nielsen's 7.2% is included (Bennett, 1973a). The Lacerta of this study gave even better extractions of 45% under minimum stress conditions, although the mean routine minimum was 24%. The maximum O_2 extraction coefficients for

TABLE 2.7

Reptilian ventilation requirements and O_2 extraction coefficients.

Species	Min. $\frac{\dot{V}_E}{\dot{V}O_2}$	Range of $\frac{\dot{V}_E}{\dot{V}O_2}$	Max. O_2 Extraction	Range of O_2 Extraction	Reference
Lacerta*	11	11 - 210	45	2.4 - 45	This study
	21 mean		24 mean		
Lacerta*	65	65 - 97	7.2	5.0 - 7.2	Nielsen, 1961.
Crotaphytus	29	29 - 37.5	17.9	13.5 - 17.7	Dawson & Templeton, 1963; Templeton & Dawson, 1963.
Sauromalus	36	36 - 120	14.0	4.1 - 14.0	Bennett, 1973a.
Sauromalus	16.5	16.5- 37	29.9	13.5 - 29.9	Crawford & Kampe, 1971.
Varanus	25	25 - 110	19.7	4.5 - 19.7	Bennett, 1973a.
Xantusia	24	24 - 51	20.8	9.8 - 20.8	Snyder, 1971.
Eumeces	36		13.7		≠ Wilson, 1971.
Physignathus	33		15.0		Wilson, 1971.
Tiliqua	19.5		25.4		Wilson, 1971.
Snakes*	31	31 - 100	16	5 - 16	Dmi'el, 1972.
Turtles*	10.8	10.8 - 76.2	46	6.3 - 46	Jackson, 1971.
Caiman	17	17 - 180	30	2.8 - 30	Huggins, Valentinuzzi & Hoff, 1971.
	51 mean		9.7 mean		

* When calculating ratios, $\dot{V}_E$ was expressed in BTPS not STPD. A conversion factor of x 1.2 for O_2 extraction can be used and $\frac{\cdot}{\cdot}$ 1.2 for respiratory requirement.

≠ from Bennett, 1973a.

snakes, turtles and caimans are within the range for saurian values.

Resting extraction coefficients for birds were 23.3 to 29% (Lasiewski & Calder, 1971) and for mammals 14.7 to 17.6% (Stahl, 1967) which compares well with the 27% for Lacerta (Table 2.8). When considered at a 1 kg body weight, instead of 10g, the extraction coefficient is 23% for birds, 17.6% for mammals and 15 to 18% for lizards (Bennett, 1973a). The higher extractions in Lacerta when compared with interspecific lizards are considered to be a result of minimum stress conditions in this experiment. In such conditions hyperventilation due to excitement will not occur.

TABLE 2.8

Resting respiratory parameters in a 10g Lacerta, bird and mammal.

	Lacerta (30°C)	Bird (37°C)	Mammal (37°C)
f (min^{-1})	30	73	175
Min.V_T (ml)	0.032	0.094	0.062
Min.$\dot{V}_E$ BTPS (ml min^{-1})	0.96	6.75* or 8.4′	11.4* or 9.5′
Std.$\dot{V}o_2$ STPD (ml min^{-1}) (1 day S mean day)	0.054	0.41	0.35
$\dot{V}_E/\dot{V}o_2$	17.8	16.5* or 20.5′	32.5* or 27.2′
O_2 extraction, %	27	29* or 23.3′	14.7* or 17.6′

* Value if calculate from f x V_T.

′ Value if calculate from logarithmic plots of Lasiewski & Calder (1971) and Stahl (1967)

From Table 2.8 it is apparent, therefore, that the lower resting $\dot{V}o_2$ of lizards is matched by a lower $\dot{V}_E$ such that the O_2 extraction % is approximately equal in these three groups. The higher ventilation rate of birds is produced by doubling the frequency and tripling the tidal volume of a lizard, whilst for a mammal the lizard f is increased by 6-fold with only a doubling of V_T.

The important question to ask now is whether lizards are capable of such good extractions during activity and at $\dot{V}O_2$ levels comparable to resting $\dot{V}O_2$ in a mammal. From rest to near maximum activity in a mammal, f increases by 2.5 times and V_T by 5 times but together only causing an 8-fold increase in $\dot{V}_E$. This exactly matches the 8-fold increase in $\dot{V}O_2$ (Hey et al, 1966) so that O_2 extraction ratio, $\dot{V}O_2/\dot{V}_E$, remains constant whatever the level of activity. At even greater $\dot{V}O_2$ levels, however, $\dot{V}_E$ increases disproportionately using f increments since V_T has reached its physical limits. In contrast, from routine activity to maximum activity in Lacerta, $\dot{V}_E$ increased by approximately 20 times (13 to 27) for a $\dot{V}O_2$ increment of only 5.5 times (4 to 7). Thus there is a 4-fold decrease (maximum of 9-fold) in O_2 extraction efficiency. High O_2 extractions were never found in Lacerta during activity. Examination of the range of extractions in Table 2.7 would indicate that this is also the case for other lizards, snakes and caimans. Bennett (1973a), however, states that since O_2 extractions at ventilation rates equivalent to those of a resting mammal are within the range for resting lizards at 35°C, then a lizard lung can still be as efficient as a resting mammal. He also states that the increasing complexity of bird and mammal lungs is mainly in response to the demands of activity above these resting levels. The following O_2 extractions were found for $\dot{V}_E$ rates comparable to those of a mammal: 8.3% Eumeces, 12.6% Physignathus and 9.0% Sauromalus (Bennett, 1973a). These are not considered to be anywhere near the efficiency of a mammal and, although $\dot{V}_E$ rates were comparable to those of a mammal, the actual $\dot{V}O_2$ values were considerably lower. Thus the simple lung structure of lizards is not sufficient to meet even the resting demands of a mammal. The more complex lung structure of the Varanid lizards would appear to be nearly as efficient as a mammal even during activity; 13 to 20% extraction (Bennett, 1973a). Active data for the complex lungs of crocodiles is not available.

Importance of V_T and f increments

Increasing temperature during rest and activity generally increases the ventilation requirement and therefore decreases the O_2 extraction according to Bennett (1973a). He considers that this is partially due to the effect of increased temperature causing a shift to the right, thereby reducing the O_2 affinity of the haemoglobin (Bennett, 1973b). However, Nielsen (1961) found that increased temperature during rest increased the O_2 extraction. A similar situation was found in desert snakes but in non-desert snakes, O_2 extraction decreased with increasing temperature (Dmi'el, 1972). During rest in turtles, increasing temperature also caused increasing O_2 extraction (Jackson, 1971). An explanation other than Bennett's must be sought.

In turtles, f remained constant but V_T decreased by a factor of 1.5 to 2 during increasing temperature such that O_2 extraction increased from 2.8 to 30%. In Lacerta (Nielsen's study), f increased whilst V_T remained constant allowing O_2 extraction to increase from 5.0 to 7.2%. In desert snakes, if the V_T increases were accompanied by f increases, the O_2 extraction could increase slightly. Finally, in the non-desert snakes, f decreased whilst V_T increased and O_2 extraction decreased. A common interpretation for all this data could be that increases in f increase O_2 extraction, whilst V_T increments decrease it. Considering the simple lung anatomy of these reptiles, viz. peripheral alveolar tissue surrounding a large central air reservoir, it is perhaps not surprising that V_T increments could cause a disproportionate ventilation of an effective dead space. Increases in f, on the other hand, for low tidal volumes would serve to replenish the relatively small volume of the central air space which by virtue of its anatomy is in unrestricted communication with the alveoli. In contrast, f increments in mammals at low V_T increases dead space ventilation, whilst V_T increments reduce its relative proportion.

Temperature effects on the lizard cardiac output, however, cannot be ignored since this will strongly influence lung perfusion and the degree of O_2 extraction. Cardiovascular changes must be responsible for the increase in O_2 extraction in resting Sauromalus and the decrease in Varanus at high body temperatures (Bennett, 1973a). Simultaneous cardiac output, ventilation volume and $\dot{V}o_2$ measurements are necessary to elucidate this problem.

From rest to activity, O_2 extraction decreases in all lizards and snakes so far studied including Lacerta (of this study) except in Varanus. Bennett (1973a) has interpreted this in terms of the large Bohr shift to the right, induced by the release of lactic acid into the blood during the anaerobic metabolism which always accompanies reptilian activity. Blood buffering abilities of reptilian blood are poor and thus O_2 affinity is greatly reduced by an acidic shift in blood pH (Bennett, 1973b). Varanus, on the other hand, undergoes very little anaerobic metabolism and has a very good blood buffering capacity. Bennett's explanation seems entirely reasonable but it is suggested here that O_2 extraction is further decreased by the exceptionally large increments in V_T (20 times in Lacerta in contrast to the 5 times in mammals) which disproportionately increase the volume of the central air space as opposed to the alveolar area of the lung. Again, a possible relative decrease in cardiac output and lung perfusion during activity cannot be ignored.

During rest to activity, especially at the PBT, f increased very little, pulmonary ventilation being increased solely by V_T increments (Sauromalus and Varanus, Bennett, 1973a). This is also true for Lacerta in which $\dot{V}_E$ increased by 20-fold owing to a 14-fold increase in V_T but only a 1.4-fold increase in f. Although lizards have a great capacity for altering their respiratory frequency, there appears to be no relationship to metabolic scaling (Fig. 2.10) and very little to oxygen consumption (Fig. 2.13). Why should this be so? Unlike the mammal or bird, the lizard

lung is inflated during the respiratory pause of the breathing cycle. An increment in frequency would, therefore, decrease the total time for which the lung was inflated. This was first pointed out by Templeton & Dawson (1963). At low frequencies, e.g. 40 to 55 min^{-1} (Fig. 2.13) increments in f may augment metabolism without greatly reducing inflation time.

Inflation during a respiratory pause has a considerable advantage for a primitive lung because it allows the peripheral alveoli to be exposed by diffusion to the large reservoir of air in the central air space. This can give a better O_2 extraction. Indeed, at very low V_T and f, O_2 extractions as great as 45% have been measured in Lacerta which is considerably greater than that for a mammal or bird (Table 2.7 and 2.8).

Metabolism is increased mainly by V_T increments but why does a lizard require a 20-fold V_T increase? Is this an attempt to compensate for insufficient alveolar surface area and pulmonary diffusing capacity, D_LO_2, by maintaining a large reservoir of air which will keep P_{Ao_2} high and therefore possibly elevate the A-V difference of the blood? ($\dot{V}o_2 = D_LO_2$ x A-V difference)? Or could it be that in order to inflate the peripheral alveoli by equal volume increments, disproportionately greater increases have to occur in the volume of the central air space? This and the extent of alveolar surface area as a function of total lung volume are investigated in Chapter 5.

Control of V_T and f.

In reptiles, it is evident that ventilation and metabolism are not finely matched (Fig. 2.11 and 2.14). This conclusion was also reached by Huggins, Valentinuzzi & Hoff (1971) and Bennett (1973a) who suggest that respiratory parameters are controlled by factors other than metabolic demands and are themselves serving functions other than metabolism. This may also be the case in Lacerta. It may be important, however, that V_T is fairly

well correlated with $\dot{V}o_2$ (Fig. 2.13) and that lack of a clear cut $\dot{V}_E$ to $\dot{V}o_2$ correlation is due to very variable respiratory frequencies.

The possible chemical stimuli controlling respiration must be examined - few workers have studied this. Hypoxia below 10% causes a decrease in f but an increase in V_T in Lacerta (Nielsen, 1962) but an increase in both occurs in Crotaphytus (Templeton & Dawson, 1963). Hypercapnia at 1 to 2% concentrations causes an immediate increase in f and V_T (Templeton & Dawson, 1963) but after 5 or more minutes, V_T increases further but f then decreases considerably (Nielsen, 1961, Pough, 1969). Higher CO_2 concentrations cause an immediate and greater depression of f and elevation of V_T.

Two sets of chemoreceptors have been postulated to explain the different CO_2 effects. Blood Pco_2 receptors, presumably both peripheral chemoreceptors in the carotid epitheloid tissue which resemble to some extent the mammalian carotid body (Sidky, 1967, Rogers, 1967) and central chemoreceptors in the medulla, respond to the small CO_2 changes produced by metabolism (and mimicked by 1 to 2% CO_2 inhalation). These cause f and V_T to increase. Higher inhaled CO_2 concentrations continue to augment both V_T and f in the mammal but in the lizard it is thought that this causes stimulation of receptors in the lung or the caudal part of the trachea which relay via the vagus to the medulla and cause f to diminish whilst still augmenting V_T. Thus $\dot{V}_E$ and $\dot{V}o_2$ both decrease at high CO_2 levels because of an anaesthetic effect (Saalfield, 1934, Boelaert, 1941, Nielsen, 1961, Templeton & Dawson, 1963).

With respect to the Lacerta data of this study, it is suggested that during low levels of activity when anaerobic metabolism is low, the slightly increased Pco_2 or H^+ of the blood causes f and V_T increments. When activity becomes greater and anaerobic metabolism is high (Bennett, 1973b), the elevated Pco_2 and high respiratory quotient will increase alveolar P_{Aco_2}. It is possible that the second set of receptors, i.e. in

the lung are then stimulated and a balance has to be reached between the chemoreceptive inputs causing further increments in V_T but no further changes in f.

Considerable work has yet to be done on the chemical control of respiration in reptiles including even the elementary effect of hypoxia on V_T and f to discern if there is a consistent response for all species. Since CO_2 overrides the effects of hypoxia, the combined stimulus causes a decrease in f but an increase in V_T, the latter to much greater degrees. The question arises as to why lizards decrease f when the reverse is found in mammals. This decrease must, presumably, be advantageous. It may relate to the benefits of a longer retention of inspired air during the respiratory pause. The larger tidal volumes, although necessary to maximally expose the alveolar surface area, cause high respiratory requirements and low O_2 extraction efficiency (Nielsen, 1961).

Responses to hypoxia and hypercapnia do, however, give considerable data scatter and this may explain the lack of precise correlation between ventilatory parameters and metabolism. This fact and the high degree of tolerance to anaerobic metabolism may allow the large O_2 extractions of up to 45% found in Lacerta, since the resultant high $P_{A_{CO_2}}$ and low $P_{A_{O_2}}$ can be tolerated. Mammals are far more responsive to hypoxia and hypercapnia than reptiles.

CHAPTER 3

STATIC PRESSURE-VOLUME CURVES OF THE RESPIRATORY SYSTEM IN LACERTA

The lung and chest act like two opposing springs within the thorax, their visceral and parietal pleura, respectively, being in intimate contact via a thin film of liquid. Sliding of one across the other is easy but separation is difficult. Movements of the thorax are transmitted all the time to the lungs through this thin liquid film. Without the pull of the thoracic cage, the lungs collapse to minimal air and without the pull of the lungs, the thoracic cage enlarges. During breathing, enlargement of the thoracic cage creates a negative pressure within the lung which causes air to be inspired. During compression of the thoracic cage, the positive pressure created in the lungs forces the air to be expired. These movements are also enhanced by the diaphragm.

The above description pertains to the mammalian respiratory system but is equally applicable to that of Lacerta, except for the lack of a diaphragm. There are also anatomical differences (but not functional) in the arrangement of the pleura but this is examined in Chapter 4. Since both Lacerta and the mammal use a costal suction pump for inspiration, it is of interest to compare the mechanics of the two systems.

Total System

Static pressure-volume (P-V) curves of the mammalian lung, thoracic cage and total respiratory system are well documented (Agostoni & Mead, 1964). These curves are simply the measurement of volume and retractive pressure during stepwise inflation and deflation of the respiratory system allowing a few seconds for equilibrium at each step. By recording mouth or intra-tracheal pressure at each volume step, the pressure of the total respiratory system is measured and by recording simultaneously the intrapleural pressure

(using an oesophageal balloon), the difference between intratracheal and intrapleural pressure is a measure of the pressure exerted by the lung. Subtraction of lung pressure from that of the total respiratory system at a particular volume yields the retractive pressure of the ribcage at that volume.

There are two alternative methods for determining a static P-V curve.

(i) Each lung volume is initiated from resting volume and the subsequent pressure measured with relaxed respiratory muscles (relaxed by human subject, or manoeuvre performed in anaesthetised, paralysed humans or animals). This gives a relaxation P-V curve for inspired and expired volumes (Rahn, Otis, Chadwick & Fenn, 1946, Agostoni, Thimm & Fenn, 1959).

(ii) Step-wise volume changes are performed at 5 sec intervals and the pressures recorded after equilibrium. The full inflation/deflation cycle takes only about a minute and is performed under anaesthetised, paralysed conditions (Butler, 1957).

In both methods, it is found that the relationship between pressure and volume for the total respiratory system gives a sigmoid shape, greater pressures being required for small volume changes at the extremes of inspiration and expiration. When both inflation and deflation P-V curves are measured, it is found that inflation requires greater pressures than deflation thus causing a hysteresis loop. P-V curves for the ribcage and lungs also show hysteresis. This is greater in the latter (Agostoni & Mead, 1964). P-V curves for the ribcage and lung are not sigmoid but the ribcage has a curvilinear phase during expired volumes and the lung a curvilinear phase during the extremes of inspired volumes. During resting tidal volumes there is little hysteresis. Most of the published data has, however, been concerned with relaxation P-V curves of the total respiratory system and its components rather than their hysteresis. The mean curve of a hysteresis loop is approximately that of a relaxation curve.

From relaxation P-V curves of the lung and total system, it is possible to sub-divide lung volume into total lung capacity, TLC, residual volume, RV, vital capacity, VC, functional residual capacity, FRC, inspiratory capacity, IC, inspiratory reserve volume, IRV, expiratory reserve volume, ERV, resting tidal volume, V_T, and minimal air (Agostoni & Mead, 1964, Briscoe, 1965). The volume of the total system at zero pressure equals that of the FRC. It is also the volume of end-expiration during a resting tidal volume. The cross-over point of the lung and total system curves gives the volume at the end-inspiration of a normal breath for a pressure of 4 to 6 cm H_2O. At zero pressure of the lung relaxation curve, the volume left in the lung is that of minimal air. It is the volume to which the lungs would collapse if the ribcage was removed and is usually determined by extrapolation to in vivo data.

It is also possible to determine the volumes for IC, IRV and ERV and hence also VC, TLC and RV. As Agostoni & Mead (1964) have pointed out, however, this part is limited to humans since voluntary manoeuvres are required. Pressures as high as -40 and + 40 cm H_2O can be recorded at the two extremes of the static P-V curve of the total system.

The ratio of the lung volume increment produced by a change in retractive pressure, $\Delta V/ \Delta P$, measures pulmonary compliance; the reciprocal relationship being a measure of pulmonary elastance. Compliance is usually calculated from the linear part of the relaxation P-V curve for volumes near FRC and is expressed in ml cm H_2O^{-1}. The compliance of the total system, C, lungs, C_L, and ribcage, C_w, are related by the equation,

$$\frac{1}{C} = \frac{1}{C_L} + \frac{1}{C_w}$$

In small mammals, the ribcage is more compliant than the lungs but in larger mammals (3 to 70 kg) both are about equally compliant (Crosfill & Widdicombe, 1961). The larger the animal the more compliant its lungs, etc. appear when

measured in terms of ml cm H_2O^{-1}. If, however, a measurement which relates compliance to lung volume, e.g. that of FRC, is used then an approximately constant value irrespective of body weight is found. This is called the specific compliance $\frac{\Delta V}{\Delta P.FRC}$. The relationships between the compliance of the components of the respiratory system and body weight have been examined in mammals by Agostoni, Thimm & Fenn (1959), Crosfill & Widdicombe (1961), Stahl (1967) and Spells (1969/70). They have also studied lung volume, e.g. FRC, TLC, VC, etc., and body weight relationships. This data is given in Table 3.4 and 3.5 and considered in the discussion.

Compliance can also be measured under dynamic conditions, i.e. air flowing during a respiratory cycle. In this measurement, volume and pressure are determined for the two points of zero flow at end-inspiration and end-expiration. There is close agreement between dynamic and static compliance values (Spells, 1969/70).

As far as is known, static P-V curves have not been determined in any lower vertebrate. A dynamic compliance measurement from maximum tidal volumes has recently been given for the turtle Chelonia (Tenney, Bartlett, Farber & Remmers, 1974). It was decided to examine static P-V curves in Lacerta for four reasons:-

(a) to determine the extent of hysteresis in the ribcage, lungs and total system,

(b) to see if the cross-over point of the curves of the lung and total system gave V_T values that bore any resemblance to those determined for resting conditions in Chapter 2 and to attempt estimations of other lung volume sub-divisions.

(c) to examine the relationship between body weight and lung volume (at different pressure levels) to determine whether the tidal volume proportionality of $W^{1.0}$ found in Chapter 2 was also shown by other lung volume sub-divisions.

(d) to measure the compliance of the lungs, ribcage and total system for (i) a comparison with mammalian data, (ii) to determine body weight

relationships, and (iii) to help in predicting a fixation pressure for the *in situ*, chest closed *Lacerta* lung which is comparable in terms of TLC to the 20 cm H_2O used for open chest mammals by Weibel (1970/71) and co-workers (Chapter 5).

For technical reasons, it was not possible to use an oesophageal balloon for recording intrapleural pressures in *Lacerta*. Instead, P-V curves for the total system and for the *in situ* lung (but with ribcage removed) were measured separately. For reasons given in the discussion, this is not considered to cause any serious errors. In mammalian work, the volume is usually measured by plethysmography and P-V curves plotted instantly on an X-Y plotter. With *Lacerta* a less sophisticated method was used of calculating volume from the amount injected by correction for compression or rarefraction and later plotting P-V curves from tabulated data of the equilibrium pressure and volume values.

Isolated lung P-V curves

Isolated mammalian lung hysteresis has and is being extensively studied. Since the literature is considerable, only earlier review articles and some recent publications are cited in this chapter. The extent of lung hysteresis is dependent on the time course of each volume step. For example, under static conditions, a rubber balloon may appear almost ideally elastic but under dynamic conditions there is considerable visco-elastic hysteresis (Hildebrandt, 1969). Otis, McKerrow, Bartlett, Mead, McIlroy, Selverstone & Radford (1956) have shown that an interruption of 0.05 sec is sufficient to equilibrate gas pressures within the lung of the cat or human. The rapid phase of equilibration occurs in this 0.05 sec period to give quasi-static conditions and it is followed by a delayed slow response taking up to 60 sec and called stress relaxation (during inflation) or stress recovery (during deflation) (Marshall & Widdicombe, 1961). A P-V curve allowing for this delayed equilibrium shows less hysteresis.

Providing the isolated lung is not allowed to collapse beyond volumes normally present in the intact chest, it produces P-V curves for

inflation and deflation which are very similar to those of the in situ lung (chest open or closed) (Radford, 1957, 1964, Mead, 1961). If the lung is allowed to collapse to its minimal volume, the next P-V loop has considerable hysteresis caused by an increase in inflation pressures. The inflation pressures have to reach +10 to +18 cm H_2O (depending on the species) before there is any marked change in the volume. This opening pressure required by the collapsed alveolar units is followed by a very compliant phase. The deflation curve remains the same. The opening pressure is dependent on the radius of the alveoli, the pressure being greater the smaller the mammal (Radford, 1964).

Within a P-V loop, it is possible to do two types of manoeuvres. One can inflate between zero pressure and successively increasing end-inflation pressures returning to zero pressure between each inflation or one can inflate to TLC and successively lower the end-deflation pressure. In the former case, the inflation curve is more or less common to each loop and whatever the end-inflation, the hysteresis is much the same. In the latter case, the deflation curve is more or less common to each loop and the lower the end-deflation pressure, the greater is the hysteresis between inflation and deflation curves (Glaister, Schroter, Sudlow & Milic-Emili, 1973). If inflation to successively increasing end-inflation pressures is performed returning only to volumes above minimal air, e.g. in the in situ lung, the inflation curve is again still common to each loop, but the lower the end-inflation, the lower the hysteresis (Radford, 1964).

The hysteresis and pressures involved in air-filled lungs could be due to (a) visco-elastic properties of the elastic, collagen, reticulum matrix and smooth muscle of the alveoli and airways, (b) surface tension forces at the gas-liquid interface, (c) differences in closing and opening pressures of alveolar units, (d) effects of blood volume changes during a P-V cycle together with resultant changes in extracellular fluid volume and alveolar transudation, and (e) elastic behaviour of the bronchial mucus

(Radford, 1957, 1964, Mead, 1961). During dynamic P-V cycles when there are no equilibrium periods, further sources of hysteresis are from resistance in the airways to gas flow from lung tissue and bronchial mucus resistance and from inertia of gas and lung tissue (Radford, 1957, Mead, 1961).

Surface tension forces due to the air-liquid interface of the alveoli can be abolished by extracting all the air under vacuum and investigating P-V curves of fluid-filled lungs. This was first undertaken by von Neergaard (1929) who found a complete lack of hysteresis and also a large reduction in the pressures necessary to inflate and deflate the lungs. Radford (1957) found that the initial saline P-V curves did have some hysteresis due to a large amount of bronchial mucus which could only be removed during the course of a few deflations. Once removed, there was no hysteresis. The conclusion from such studies was that all the hysteresis found in the air-filled lung was due to surface tension at the air-liquid interface. This surface tension was high during inflation and low during deflation. The lung tissue, itself, caused no hysteresis and gave little resistance to inflation and deflation when compared with the surface component, except at the extremes of inflation when elastic limits were being reached.

These original studies allowed equilibrium periods of 3 to 5 min for saline P-V curves because of the high viscosity of saline when compared with air (ratio of 60). Air equilibrium periods were usually 5 sec. It has recently been pointed out that since an air equilibrium of 0.05 sec is sufficient, 3 sec for saline equilibrium is all that is necessary. Because of the greater compliance of the fluid-filled lung, 5 sec is, however, actually used (Bachofen, Hildebrandt & Bachofen, 1970, Fisher, Wilson & Weber, 1970). With such equilibration, saline P-V curves do give some hysteresis even over resting tidal volume cycles, but the large reduction in inflation and deflation pressures is still found. Thus, tissue visco-elastic properties do contribute to some of the air-filled lung hysteresis, but the

major part is due to the air-liquid interface. Hills (1971) considers that all the hysteresis in the isolated lung is due to tissue visco-elastic properties and to de-recruitment of alveolar units during deflation not retracing inflation recruitment. The latter is called geometric irreversibility and can be abolished by saline filling. It is thought to occur more in the isolated lung than *in vivo* because the former will have many more degrees of freedom for geometric changes.

Surface tension and surfactant

A surface tension exists at any air-liquid interface. When this surface is a sphere as in the mammalian alveolus, the force required to open the alveoli of a terminal unit is determined by the surface tension of the interface and by the mean radius, r, of the terminal units. This is the Laplace relationship in which

$$P = \frac{2 \times \text{surface tension}}{r}$$

If the surface tension is a constant, the smaller the alveolus, the greater is the pressure required to keep it open. Thus, all small alveoli would collapse into the large ones. The fluid at an interface can contain a surfactant, e.g. of a soap bubble, which considerably reduces the surface tension and hence the pressure needed to maintain the bubble. A surfactant molecule is typically a polar/non-polar molecule orientated so that the non-polar groups project into the air and the polar groups into the liquid (Clements & Tierney, 1965, Scarpelli, 1968). If the non-polar part of the molecule is not too bulky, the molecule can readily pass in and out of the surface film of liquid when the interfacial area changes. Under these circumstances, the amount of surfactant per unit area is practically constant. If, however, the non-polar part is bulky, the surfactant molecule cannot enter the liquid (often called the hypophase) and is confined to the surface film. Thus, the concentration of surfactant in the surface film varies inversely with the surface area of the film. This causes low surface tensions at small

surface areas and high surface tensions for large surface areas. Such a surfactant molecule is found in the mammalian lung and is responsible for much of the hysteresis of the air-filled lung. It also prevents small alveoli from collapsing into larger alveoli. The lung surfactant is a phospholipid containing a high proportion of lecithin and its properties have been extensively reviewed by Scarpelli (1968).

By air and saline P-V curves of the lung, it is possible to demonstrate the presence and effect of surfactant in the lungs. From such data one can also calculate the surface tension at any volume on the deflation and inflation curve and construct area-tension loops (Bachofen, Hildebrandt & Bachofen, 1970, Fisher, Wilson & Weber, 1970). The surface tension of the surfactant and hypophase can also be measured from lung extracts and washings on a Langmuir-Wilhelmy surface balance in which a film of the extract is alternately compressed and expanded. There are, however, important differences between in vivo and extract area-surface tension loops (Bachofen, Hildebrandt & Bachofen, 1970). It is also possible to make a direct measurement of the pressure in different sized bubbles blown in a pulmonary extract (reviewed by Scarpelli, 1968).

Surface tension estimates can also be made on the material that lines the bubbles of pulmonary edema foam. These bubbles are examined microscopically in air-saturated saline hanging from a slide. The initial surface area and the area 20 min later are measured to give a stability ratio. A ratio between 0.6 and 0.87 (mean 0.71) is indicative of normal mammalian surfactants (Pattle, 1958, 1965, 1966). Similar measurements on bird, slow-worm (reptile), frog or toad and lungfish foam extracts give identical stability ratios to those of mammals (Pattle & Hopkinson, 1963, Hughes, 1967, Pattle, 1969). In contrast, the newt lung contains unstable bubbles (Pattle, 1969). Mammalian pulmonary bubbles when placed in de-aerated water, first flatten as the air dissolves and then suddenly resume a spherical shape. This repeats itself rhythmically as the bubble dissolves and is known

as 'clicking'. Bird lung bubbles behave in a similar way, whilst those of the slow-worm and lungfish 'clicked' less frequently and those of the toad lung just slowly contracted without 'clicking'.

Pattle & Hopkinson (1963) also found that when these lungs were collapsed to the air-free state and then re-inflated with air, saline washings gave stable bubbles in both the mammal and bird, but in the reptile and toad few stable bubbles occurred. A similar result was found from washings from fresh uncollapsed lungs which had been freed of any existing bubbles and then frothed by bubbling air in through a syringe needle. The conclusions from these studies were that all these vertebrates (except the newt) contained a lung surfactant but in the reptile and lungfish there was only a small reserve of surfactant in the lining film. This reserve was even smaller in the frog or toad.

Frog, turtle, snakes, crocodiles and chicken lung extracts have also been examined on the surface balance (Miller & Bondurant, 1961, Clements, 1962, Klaus, Reiss, Tooley, Piel & Clem ents, 1962, Avery & Said, 1965). In contrast to the bubble stability method, it was found that all five vertebrates had extracts giving higher minimum surface tensions. This has been explained for the reptile and amphibian by Pattle & Hopkinson (1963) to be due to the lack of surfactant reserve which would seriously affect the surface tension of lung washing extracts. The difference in the findings between the two studies on avian lungs are difficult to reconcile; an explanation is attempted by Scarpelli (1968). Biochemical assays indicate no significant differences in the fatty acid residues of the surfactant phospholipids from any of these vertebrates (Scarpelli, 1968).

The advantages of having a surfactant in the fluid lining of the alveoli have been summarised for mammals. It gives (a) alveolar stability, (b) a low surface tension at small lung volumes thus reducing the pressure and hence the energy required for resting tidal volumes, and (c) a reduction in the tendency for transudation of fluid from the pulmonary capillaries into

the alveoli; the greater the curvation, the greater would be the transudation if a low surface tension was not present (Fisher, Wilson & Weber, 1970). The site of surfactant synthesis is examined in Chapter 4.

Isolated lung P-V curves have never been determined in lower vertebrates except for one study on inflation of a frog lung (Klein, 1896) in which the sigmoid curve was likened to the stress-strain curve of rubber which also does not obey Hooke's law at the two extremes of volumes. It was decided to examine inflation/deflation curves of the isolated Lacerta lung to determine (a) the extent of any hysteresis in air, (b) whether hysteresis could be abolished in saline-filled lungs (for technical reasons, see methods, it was not possible to perform saline P-V curves using short equilibrium periods), and (c) to consider a role for a surfactant in a primitive lung like Lacerta.

No attempt was made to study Lacerta surfactant by bubble or surface balance methods. As Pattle (1965) has emphasised the reliability of conclusions regarding actual lung functioning of the lining complex decreases as one progresses away from direct P-V studies to bubbles, extracts or washings.

METHODS

All lizards were anaesthetised with pentobarbitone (Nembutal) by intraperitoneal injection to a level at which respiration ceased. The doses necessary for this are described in Appendix II. A tracheotomy was then performed using a cannula whose cranial end was sealed to a female Luer fitting. The trachea was exposed some distance caudally so that a micro-clip could be applied to the trachea, caudal to the end of the cannula.

Volume-pressure curves for air.

With the animal supine and raised to the level of the horizontal tubing of the air inflation/deflation apparatus (Fig. 3.1), the Luer fitting was connected to its three-way tap. Syringe 2 was used to inflate or deflate the lungs and thoracic cage in steps of 0.1 ml (for a 3.0g lizard) or 0.5 ml (30g lizard). Each step caused an inequality in the levels of the two arms of the liquid manometer. Syringe 1 was used to adjust the pressure in the system to bring the difference in water levels back to zero after each step. By this method, the volume connected to the right of the liquid manometer was maintained constant (apart from pressure effects on the non-rigid part, i.e. thorax) whilst the pressure was recorded by a pressure transducer (Mercury micro-manometer, range -30 to +30, -10 to +10 and -3 to +3 cm H_2O) connected to the left.

The quickest speed at which air could be accurately injected and the liquid manometer adjusted back to zero level difference was 5 sec. When tested at 5 sec intervals of injection using a mock 'lung' of rubber of similar volume to that of the large lizards, it was found that there was no hysteresis between the inflation and deflation P-V curves. Thus, there was no hysteresis inherent in the apparatus. If the lumen of the entrance to the rubber 'lung' was the same size as the three-way tap, there was no overshoot of pressure during inflation or undershoot during deflation. When this lumen was of a size mimicking tracheal diameters, a 1 to 2 sec

FIG. 3.1 Inflation/deflation apparatus for air and saline.

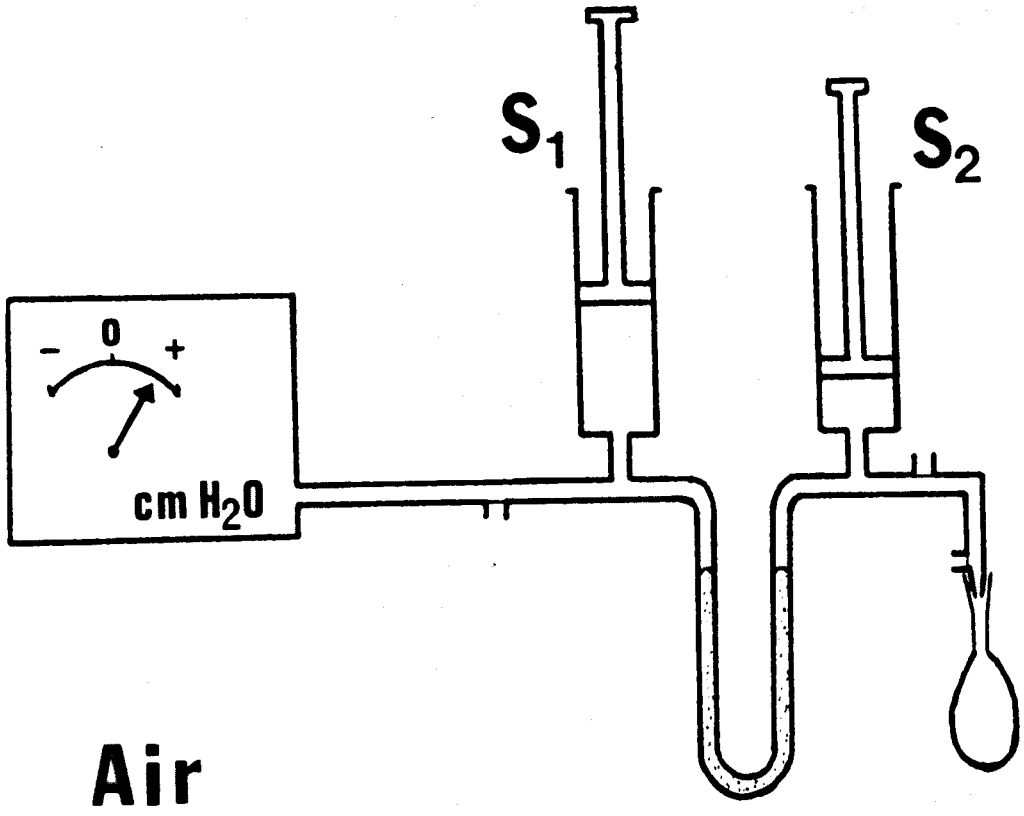

Air

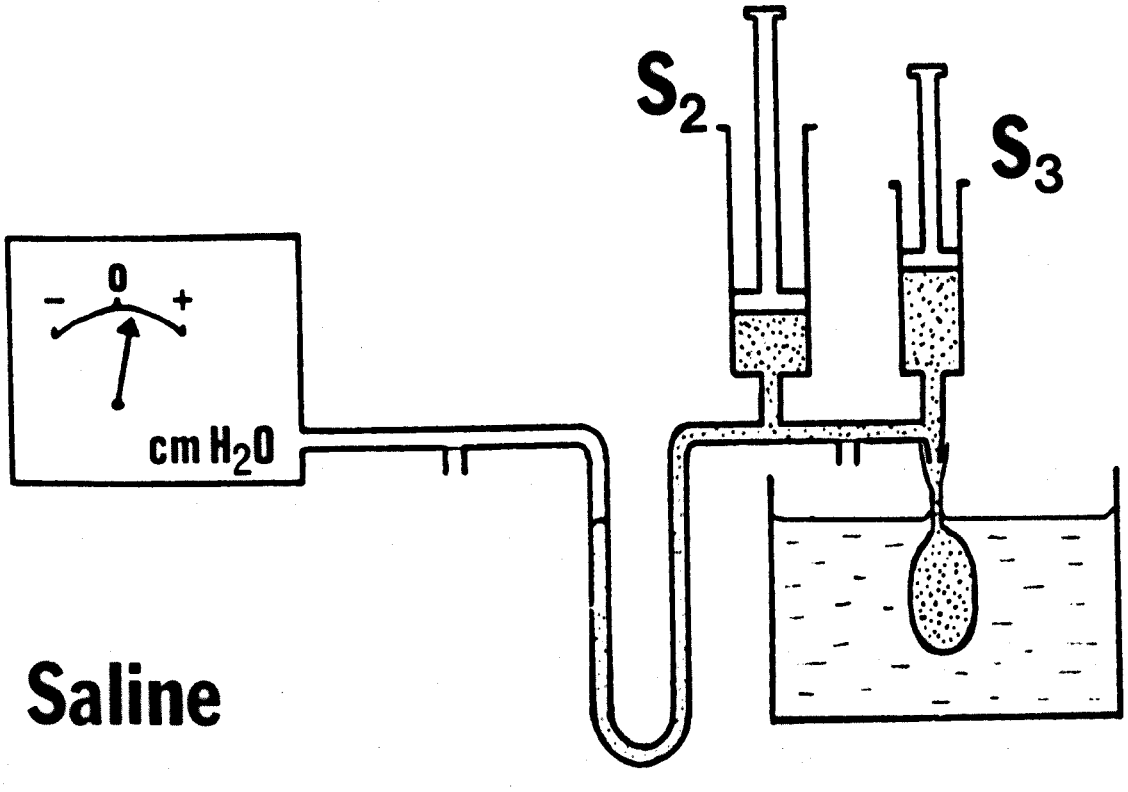

Saline

duration over- and under-shoot were present, increasing with decreasing size of the lumen.

During inflation of the lizard thorax, greater overshoots occurred. Air was, therefore, injected over a 5 sec period and during the 10 sec further allowed for equilibration, syrings 1 was slowly adjusted during the last 5 sec. A total inflation/deflation P-V cycle took approximately 6 to 8 min for pressures between -5 and +15 cm H_2O at 15 sec intervals of injection.

This method and apparatus is very similar to that used by Young, Tierney & Clements (1970) for 200-250g rats. They did not, however, correct for water vapour, temperature or compression of the air. In the lizard experiments, volume-pressure curves were determined at 20 or 28°C, the temperature being kept constant to $\pm$ 1°C. By making the initial volumes to the right and left of the liquid manometer equal (i.e. S_1 + tubing to left = S_2 + tubing to right), the effects of temperature fluctuations and thereby also vapour pressure would affect both sides equally and therefore cancel out. It is to be remembered that the temperature effect on vapour pressure is only instantaneous during a temperature rise.

Compression or rarefraction of the air was corrected by using the following equation:-

$$P_B + P_1 - P_{H_2O} (V_{L1} + V_{S1} + V_{Tu}) = P_B + P_2 - P_{H_2O} (V_{L2} + V_{S2} + V_{Tu})$$

$$\frac{P_B + P_1 - P_{H_2O}}{P_B + P_2 - P_{H_2O}} (V_{L1} + V_{S1} + V_{Tu}) - V_{S2} - V_{Tu} = V_{L2}$$

in which P_B = barometric pressure, mm Hg, P_{H_2O} = water vapour pressure at the relevant temperature, P_1 = pressure for the minimum lung volume, measured in cm H_2O, differential to atmospheric and converted to mm Hg, P_2 = pressure for any volume step, V_{L1} = minimum lung volume, ml, V_{L2} = lung volume of any step, V_{S1} = volume in syringe 2 for the minimum lung volume, V_{S2} = volume in

syringe 2 for any volume step and V_{Tu} = volume in tubing between lung and right side of liquid manometer. 2 ml, 5 ml and 10 ml syringes were used depending on lizard size.

The usual experimental procedure for air pressure-volume curves in the intact situation was to inflate from the initial volume retained in the deeply anaesthetised lizard in suitable volume steps at 15 sec intervals. At each step, the volume in syringe 2 and the equilibrated pressure were recorded. Pressures as high as +25 cm H_2O (usually +15 cm H_2O) and as low as -20 cm H_2O (usually -5 cm H_2O) were reached. After sufficient manoeuvres with an intact ribcage had been performed, the cycle was stopped at the volume present at zero pressure during inflation and the trachea clamped. The ribcage was then carefully dissected away and cut back to the dorso-lateral margins. Care was taken not to puncture the lungs or to displace the liver lobes which lie ventrally over the lungs (Chapter 4).

The retractive force (pressure) of the exposed <u>in situ</u> lungs was not measured. After re-connecting the tracheal cannula to the inflation/deflation apparatus which was at zero pressure, the tracheal clamp was removed. The lung immediately shrank slightly causing approximately a 0.1 cm H_2O change in pressure in the case of the 3.0g lizard which was equivalent to approximately 0.08 ml. This must be taken into account when calculating volumes at zero pressure for the total respiratory system and the exposed <u>in situ</u> lungs. The lungs were then inflated to + 5 or + 10 cm H_2O (sometimes higher) and deflated to zero pressure for several cycles. Sometimes deflation pressures as low as -2 to -5 cm H_2O were tried. After clamping the trachea at zero pressure of the inflation cycle, the liver and heart, which both overlie the ventral surface of the lungs, were removed. On re-connection to the apparatus, a pressure and hence volume change of approximately 0.04 ml for 3.0g lizard occurred. Further inflation/deflation cycles were then measured, it being noted that at volumes above +5 cm H_2O, posterior regions of the lung expanded abnormally.

Finally, after clamping the trachea, the lungs were cut away from the mesenteries binding them to the vertebral column and the lateral remains of the thorax (see Chapter 4 and Fig. 4.7). The isolated lungs took on a round shape in contrast to the oval one found *in situ*. The retractive force was again not measured but on re-connection to the inflation/deflation apparatus at zero pressure, no change in pressure could be recorded. Further inflation/deflation cycles were then measured and finally on the last deflation a pressure of -20 cm H_2O was reached. The volume at this pressure was the minimum attainable by suction and is V_{L1} of the compression/rarefraction equation. By volume displacement of the deflated lung and tissue weight measurements (see Chapter 5), a trapped air volume of approximately 0.005 ml (3.0g) and 0.05 ml (30g) can be roughly estimated. Hence V_{L1} is taken as zero ml.

Volume-pressure curves for saline

A recipe for a reptilian Ringer solution has not been documented except for that of Proske & Vaughan (1968) for use with isolated muscle fibres of the skink, *Tiliqua nigrolutea*. They used per litre, 130 mM NaCl, 20 mM $NaHCO_3$, 2.0 mM $CaCl_2$, 1.0 mM $MgCl_2$, 3.0 mM KCl and 11 mM glucose. Such a composition gave an osmolarity of 300 mOsm/litre.

This recipe has been slightly modified here to satisfy the blood composition of *Iguana* which is not dissimilar to *Lacerta* and for which there is more data (Dessauer, 1970). *Iguana* blood has 157 mM Na^+, 3.5 mM K^+, 2.7 mM Ca^{2+}, 0.9 mM Mg^{2+}, 118 mM Cl^-, 24 mM HCO_3^- and 2.0 mM PO_4^- per litre at a pH of 7.48. The glucose concentration is 155 mg % giving a final blood osmolarity of 300 to 380 mOsm/litre (range for all lizards).

Table 3.1 documents the constituents of the reptilian saline used for *Lacerta*. The salts were dissolved in 1 litre of boiled distilled water in the order tabulated and the pH was adjusted to pH 7.4 before addition of Na_2HPO_4. Glucose was added just before use. The osmolarity was 338 mOsm/litre.

TABLE 3.1

Constituents of the reptilian saline used for Lacerta.

Salt	mM/litre	gms/litre
NaCl	156.0	9.0
KCl	3.0	0.2235
$CaCl_2.6\ H_2O$	2.0	0.44
$MgCl_2.6\ H_2O$	1.0	0.095
$NaHCO_3$	15.0	1.26
Na_2HPO_4	2.0	0.284
Glucose	8.6	1.55

The saline inflation/deflation apparatus (Fig. 3.1) was first tested using the rubber 'lung'. After an air deflation to -20 cm H_2O on the air apparatus, the entrance region was clamped and the rubber 'lung' removed from the three-way tap. It was connected to the saline filled apparatus after replacing the air in the cannula with saline and removing all air locks. The rubber lung was then submerged up to its cannula in a dish of saline. With the air side of the saline manometer open to the atmosphere, its level was adjusted using syringe 3 to correspond with the level of saline in the dish. This gave the zero pressure of the system and with a large enough volume in the dish, the saline level did not measurably change during 'lung' inflation. With the whole system closed to the atmosphere, syringe 3 was used to give a pressure of -20 cm H_2O. This caused only a 0.5 cm H_2O change in the manometer saline level but the volume change was important for later calculations of volume injected into the rubber 'lung'. The clamp was then removed from the entrance region and there was no pressure change.

Saline was injected using syringe 2 in similar volume steps to those of the air inflation. The first step invariably caused changes in the saline manometer returning the pressure to about -4 cm H_2O and replacing the volume

in the manometer as opposed to the rubber 'lung'. It was found that each subsequent step overshot in pressure and required about 2 min to reach equilibrium. Similarly, during deflation, the pressure undershot returning in 2 min to equilibrium. To avoid unnecessarily high (or low) initial pressures, it was decided to inject the volume step slowly over 30 sec allowing a further $1\frac{1}{2}$ min for equilibrium. Much of this overshooting was due to the narrow lumen of the cannula. With only the cannula dipped in the saline bath, a constant pressure of +0.6 cm H_2O was required during injection and -0.6 cm H_2O during removal of liquid, to overcome the resistance of the cannula. Thus the true pressure for inflation equalled P_I - 0.6 cm H_2O and for deflation, P_E + 0.6 cm H_2O. Different cannula used for the lizard lungs required different corrections.

At each inflation step, the saline manometer level increased slightly so that the volume that entered the 'lung' had to be calculated by subtracting this displaced volume from the volume registered as injected by syringe 2.

During the first inflation curve, air bubbles that had not been previously removed by -20 cm H_2O air deflation, collected near the cannula and were entrapped at the right-angled bend during the first steps of deflation. After clamping the rubber 'lung', these bubbles could be removed and replaced by saline using syringe 3, taking care to return the saline manometer to the same level and pressure before unclamping the 'lung'. It was often necessary to repeat the bubble removing procedure and up to 3 inflation/deflation curves were sometimes required before all the air bubbles had dissolved or been removed. Once this stage had been reached, there was no hysteresis in a saline P-V curve of a rubber 'lung' and it exactly matched an air P-V curve.

Identical procedures were thus adopted for the lizard lung. It was impossible to remove all the air under vacuum from a lizard's lung without perforating the delicate tissue, so the -20 cm H_2O air deflation was

accepted. It was found easier for subsequent manoeuvres to remove the cannula from the clamped trachea and fill it with saline before replacing it in the trachea.

23 lizards were used *in toto*. Some were subjected to all the manoeuvres, some to saline or air only and some to total respiratory system, air P-V curves or to isolated air curves only.

RESULTS

Air P-V curves of the total respiratory system

Typical P-V curves for air inflation and deflation of the total respiratory system are depicted in Fig. 3.2. Both curves are sigmoid and there is a marked degree of hysteresis between them, being greatest at the extreme of inflation. This hysteresis causes considerable entrapping of air at zero pressure of deflation but this is reduced by allowing a longer time for equilibrium at each injection step - compare the 5 sec and 2 min P-V loops in Fig. 3.2. All subsequent P-V loops were allowed 15 sec for equilibrium since this was technically easier.

The greater the hysteresis, the greater is the negative pressure required to remove the entrapped air (Fig. 3.2 and Fig. 3.3A). It was found that if P-V loops were determined with successively increasing end-inflation pressures, a family of loops was obtained having a common inflation curve and the lower the end-inflation pressure, the smaller was the hysteresis and the smaller the negative pressure required for end-deflation (Fig. 3.3A). P-V loops determined with successively decreasing end-deflation pressures caused a family of loops having a common deflation curve. The lower the end-deflation pressure, the greater was the hysteresis (Fig. 3.3B). These families of loops must not be confused with those determined for the isolated mammalian lung.

Since an X-Y plotter was not used for these experiments, it was often difficult to judge the correct turning point at the extreme of negative deflation pressures, such that the subsequent inflation curve would follow the path of the initial one and therefore repeat an identical P-V loop. If the respiratory system was deflated beyond this turning point, the subsequent inflation curve would be less compliant and shifted towards the pressure axis, although it may coincide with the initial inflation curve when high inflation volumes and pressures are reached. If the respiratory system is inflated beyond the normal turning point, the subsequent deflation

FIG. 3.2 Typical air inflation and deflation P-V curves of the total respiratory system of Lacerta (30.0g) and the effect of 5 sec or 2 min equilibrium periods. Circles denote each volume step and are omitted in subsequent figures.

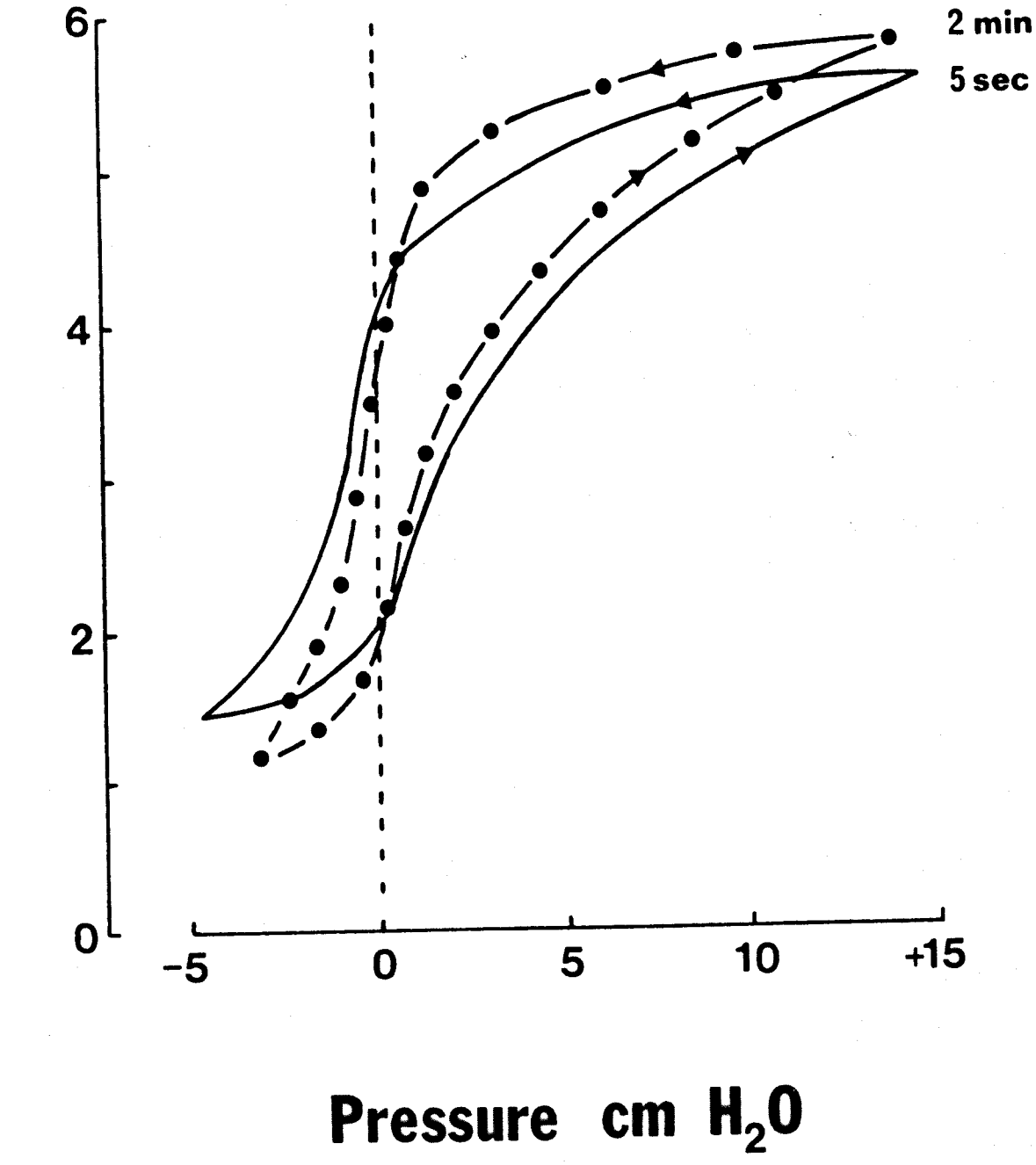
V ml
6
4
2
0
2 min
5 sec
-5
0
5
10
+15
Pressure cm H_2O

FIG. 3.3 A. P-V loops determined with successively increasing end-inflation pressures. B. P-V loops with successively decreasing end-deflation pressures in Lacerta (28.0g).

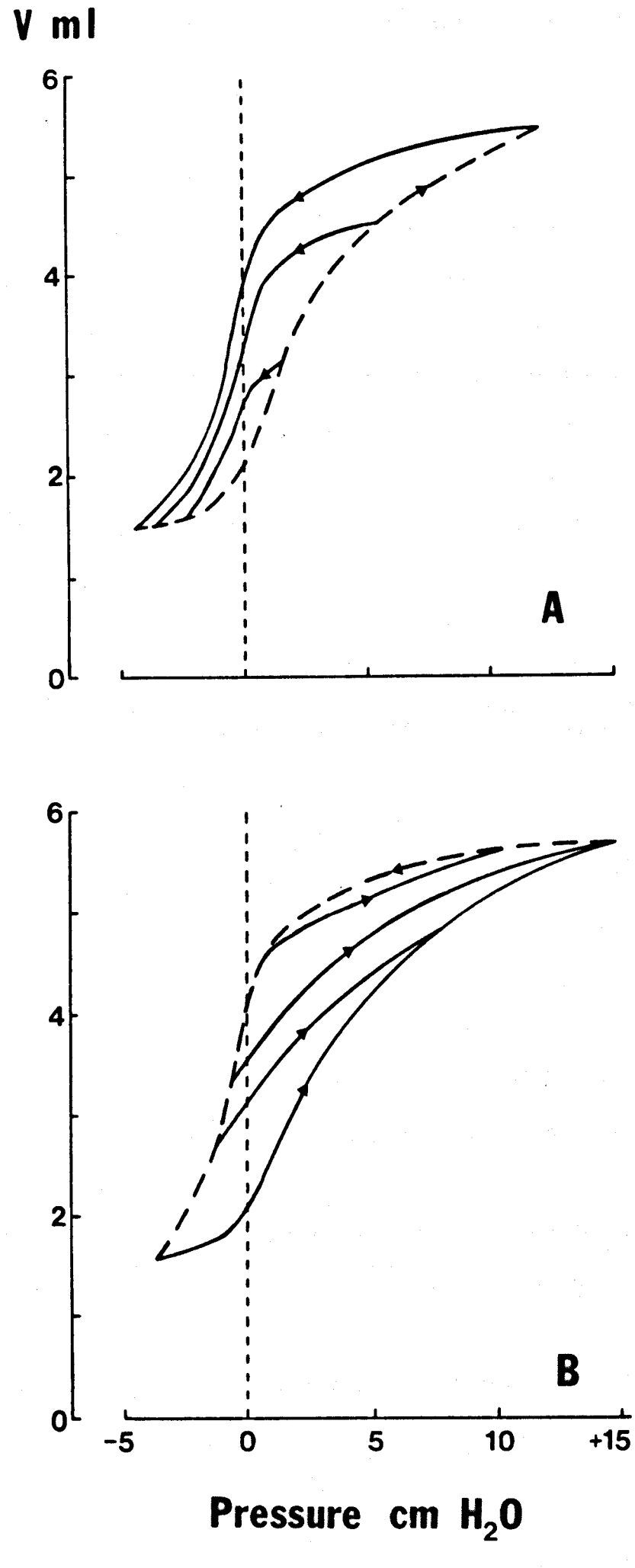
V ml
6
4
2
0
A
6
4
2
0
B
-5
0
5
10
+15
Pressure cm H_2O

curve may be less compliant and shifted away from the pressure axis. Under-deflation and under-inflation causes loops as depicted in Fig. 3.3B and 3.3A, respectively.

The very first inflation of the lizard's respiratory system often showed a P-V loop of reduced compliance but by the second or third loop a constant degree of compliance was reached. The fact that some lizards did not show this initial resistance probably indicates an initial muscle tonicity in the ribcage due to different levels of anaesthesia. Overstretching the respiratory system, e.g. to +25 cm H_2O (Fig. 3.4) did not appear to reach the limits of elasticity since hysteresis around zero pressure was not markedly different and only slightly greater negative pressures were needed for the turning point of deflation.

During the positive pressure phase of the inflation curve and the negative pressure phase of the deflation curve, stress relaxation and recovery, respectively, occurred. Equilibration was, however, immediate during the negative pressure phase of inflation and the positive pressure phase of deflation.

A. P-V curves of the exposed *in situ* lung

The volume at zero pressure is much smaller in the *in situ* lung than in the total respiratory system (Fig. 3.4). It is even smaller when the liver and heart are removed from the ventral surface of the *in situ* lung. There are pleural mesenteries attaching the lungs to these structures (Chapter 4) and these would still keep the lungs expanded to some degree even when the ribcage is removed.

The lungs are very much more compliant than the total respiratory system but this compliance is reduced by the ventral presence of the liver and pericardium, to an extent perhaps not expected. Hysteresis is greatest in the total respiratory system and least in the *in situ* lung with the liver and pericardium removed. When the liver and pericardium are present, the

FIG. 3.4 P-V loops for the total respiratory system (a), the *in situ* lung with liver and heart intact (b), and the *in situ* lung alone (c) in *Lacerta* (29.6g).

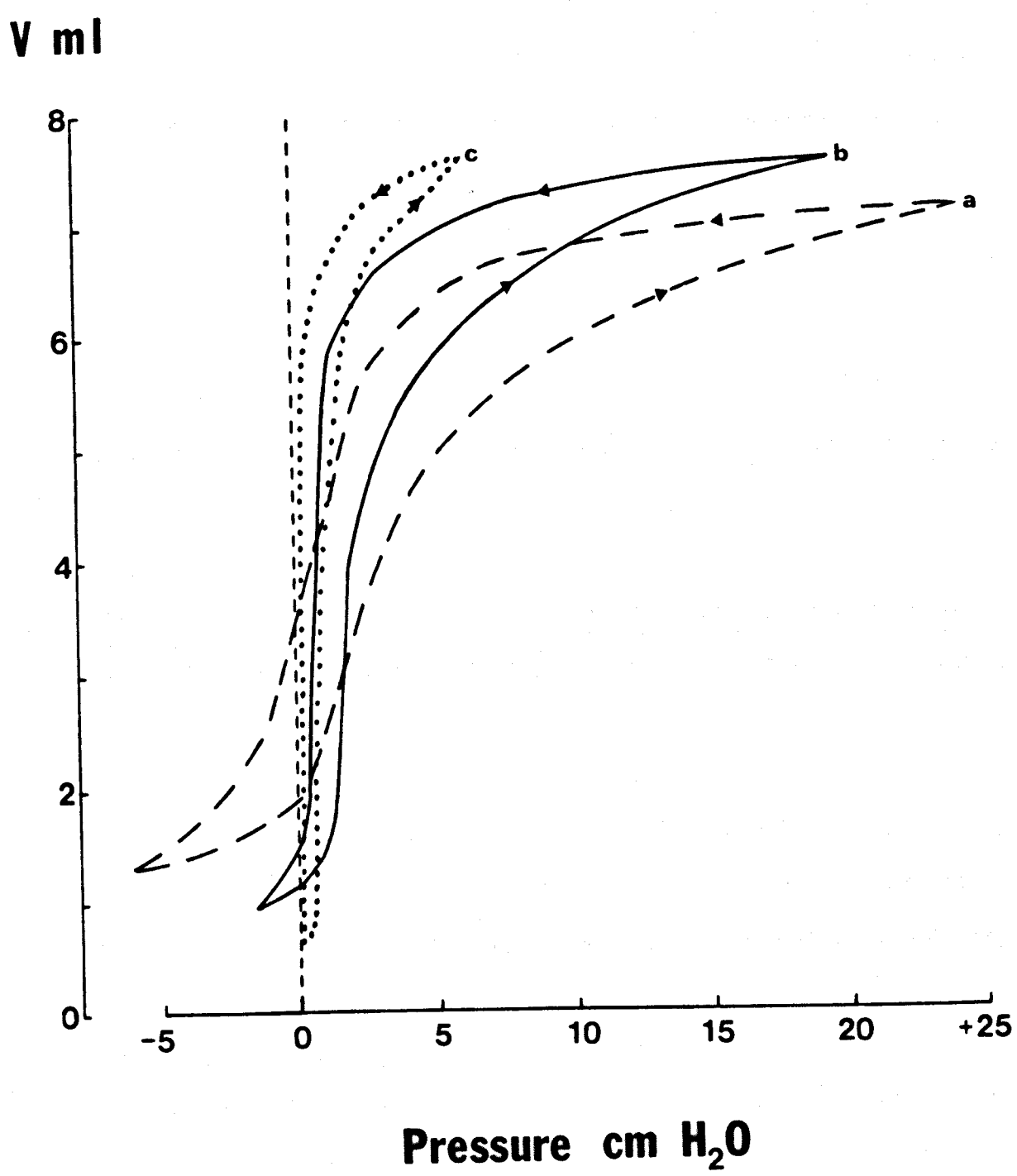
V ml
8
6
4
2
0
c
b
a
-5
0
5
10
15
20
+25
Pressure cm H_2O

in situ lung has the widening of the hysteresis loop noted at high inflation volumes and pressures for the total respiratory system. It also requires about -2 cm H_2O pressure to reach the deflation to inflation turning point. The in situ lung without these structures has its turning point at zero pressure. Equilibrium periods were required during both inflation and deflation of the in situ lung but they were shorter during deflation.

For the 29.6g Lacerta depicted in Fig. 3.4, the compliance of the total respiratory system in the region around zero pressure is 0.55 ml cm H_2O^{-1} (calculated from the mean of the inflation and deflation curves, i.e. the relaxation P-V curve). The compliance of the in situ lung with liver and heart intact is 5 ml cm H_2O^{-1} and for the in situ lung alone is 7 ml cm H_2O^{-1}. Since the lung volume at zero pressure of the total respiratory system's relaxation P-V curve is 2.7 ml (i.e. the FRC), the specific compliances are 0.204, 1.8 and 2.6 ml cm H_2O^{-1} ml^{-1}, respectively. Compliance proportions are 1 : 8.8 : 12.75.

Air P-V curves of the components of the respiratory system

By subtracting the pressure for the in situ lung (liver and heart intact) from the pressure of the total respiratory system at each lung volume step, the pressures due to the ribcage alone can be determined. Similarly, subtraction of the pressure of the in situ lung alone from that with liver and heart intact, gives the hysteresis due to the heart and liver. Fig. 3.5 illustrates the P-V loops of the respiratory system when separated into its components. (N.B. The end-inflation pressure is +16 cm H_2O in Fig. 3.5 not the +25 cm H_2O of Fig. 3.4).

It is apparent from Fig. 3.5 that the ribcage has a nearly symmetrical shape about the zero pressure axis and that there is a widening of its hysteresis loop at about +2.5 and -2.5 cm H_2O. Much of the hysteresis in the positive pressure range of high inflations appears to be due mainly to the presence of the liver and heart. The lungs also have increased hysteresis at the extremes of inflation but it never reaches the magnitude of

FIG. 3.5 P-V loops of the components of the respiratory system in Lacerta (29.6g). The arrows indicate the resting volume of the component.

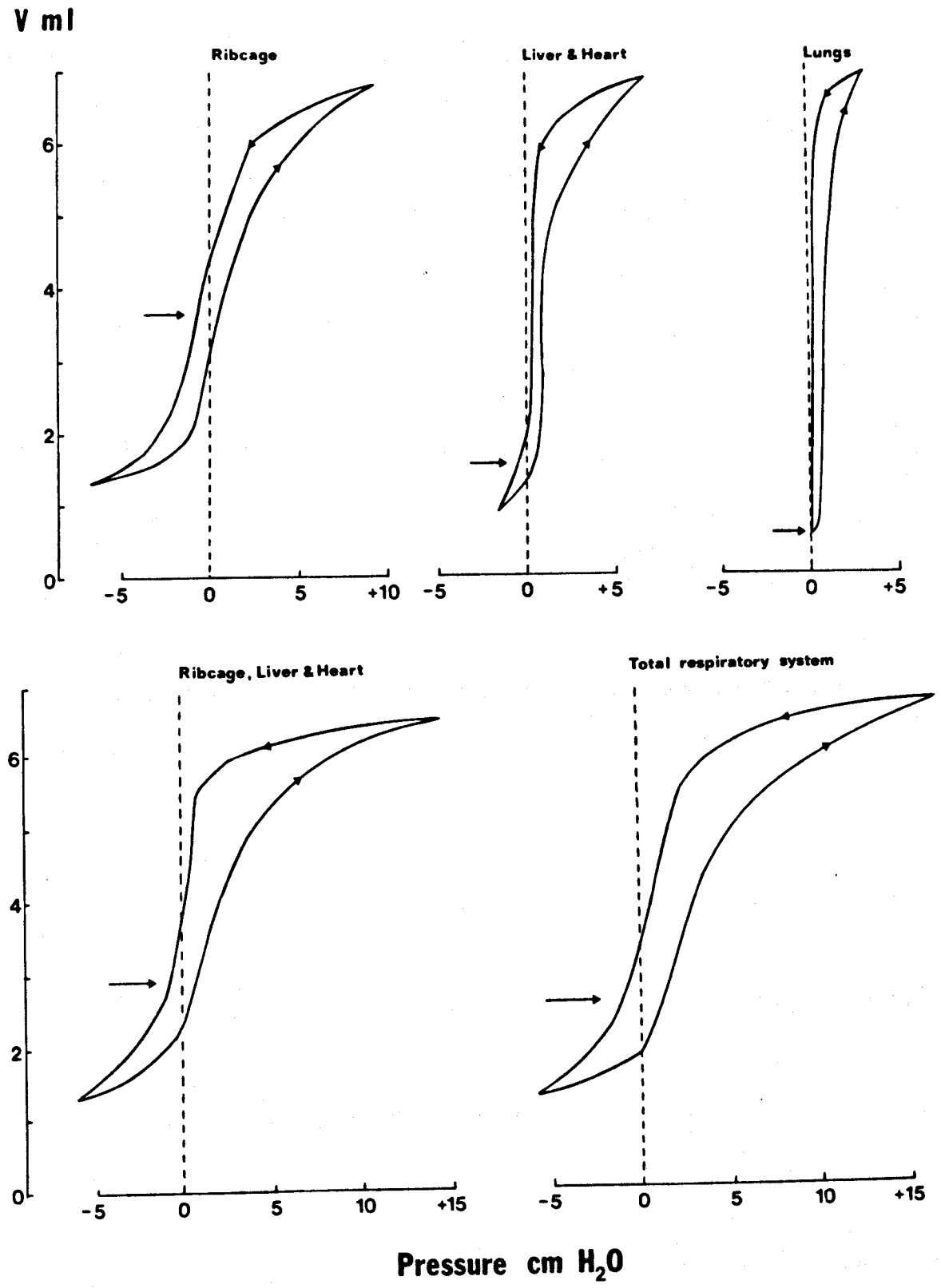
V ml
Ribcage
Liver & Heart
Lungs
Ribcage, Liver & Heart
Total respiratory system
0
2
4
6
-5
0
5
+10
+5
10
+15
Pressure cm H_2O

the other components.

The compliance of the ribs, liver and heart is 0.6 ml cm H_2O^{-1}, that of the ribs alone is 0.62 ml cm H_2O^{-1} and that of the liver and heart is 17.5 ml cm H_2O^{-1}. The resting volume of each of the components are as follows:- ribcage, 3.55 ml, ribcage + liver + heart, 2.9 ml, total respiratory system, 2.6 ml, liver + heart, 1.4 ml and the lungs, 0.6 ml.

Relaxation P-V curves of the in situ lung and total respiratory system

The volume at which the relaxation curve of the total respiratory system crosses the zero pressure axis has been interpreted in mammals as the FRC. A similar interpretation in Lacerta gives FRC values of 2.6 ml for the 31.0g lizard and 0.33 ml for the 4.9g lizard (Fig. 3.6). The volume at which the in situ lung curve crosses the total respiratory system curve is considered to be the mammalian end-inspiratory volume for a resting tidal volume. End-expiratory volume is that present at FRC. In Lacerta, the end-inspiratory volume was 2.925 ml or 0.37 ml (31.0 and 4.9g lizards, respectively) such that a resting tidal volume of 0.3 or 0.04 ml could be estimated. This compares favourably with the 0.27 ml and 0.039 ml recorded in Chapter 2 (Fig. 2.9) for routinely active tidal volumes. It is, however, greater than the minimum tidal volumes recorded.

Maximum tidal volumes recorded for these two lizard weights in Chapter 2 were 1.5 ml and 0.26 ml. It is difficult to know whether these maximum volumes are placed symmetrically around the FRC volume or whether IC is greater than the ERV. From preliminary experiments in which lightly anaesthetised lizards with a tracheotomy were subjected to small P-V cycles, it was found that inspiratory and expiratory efforts ceased at approximately +3.5 and -3.5 cm H_2O. Such pressures had, however, caused a proportion of 2 : 1 in the volume changes that could be injected or removed. This is considered to be indicative of the volume proportions of IC : ERV. When maximum tidal volumes were placed in this proportion around the FRC volume

FIG. 3.6 Relaxation P-V curves of the total respiratory system and the *in situ* lung. Sub-divisions of lung volume on the right as predicted by these curves and data from Chapter 2. (a) to (d) max.V_T, (b) to (c) average V_T. Zero volume to (d) = FRC, zero volume to (e) = minimal air. Star denotes volume at + and - 3.5 cm H_2O and is thought to represent VC. 30.0g and 4.9g *Lacerta* compared.

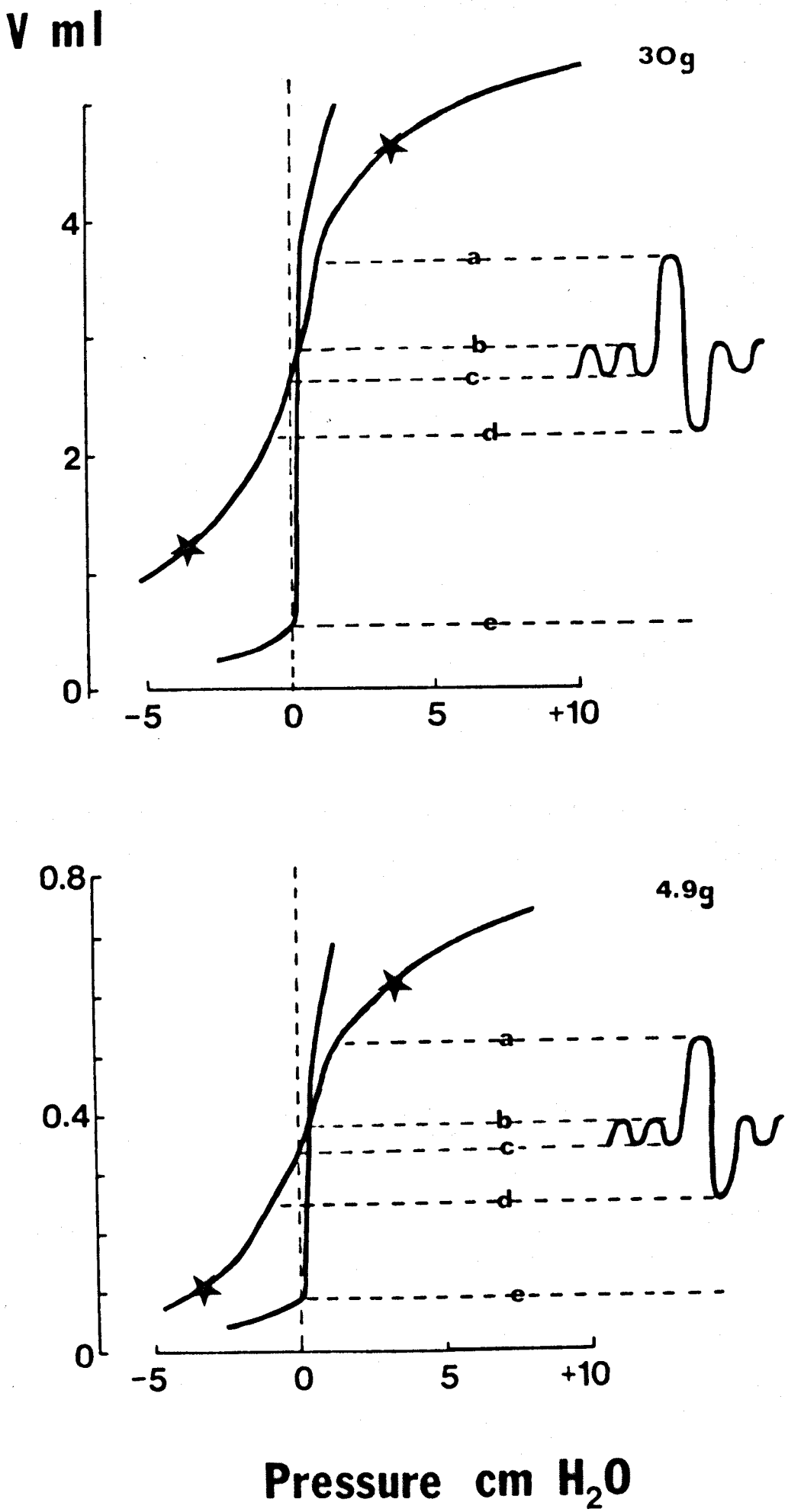
V ml
30g
4
2
0
a
b
c
d
e
-5
0
5
+10
0.8
0.4
0
4.9g
a
b
c
d
e
-5
0
5
+10
Pressure cm H_2O

level, inspiratory and expiratory end-tidal pressures were both 0.7 to 0.9 cm H_2O, (Fig. 3.6). If respiratory efforts to 3.5 cm H_2O are possible in lightly anaesthetised lizards, such levels (if not greater) must also be possible in the active lizard. Predicted tidal volumes for this end-tidal pressure are 3.3 ml and 0.54 ml for the lizards of Fig. 3.6.

The volume at which the in situ lung crosses the zero pressure axis is that of minimal air being 0.6 and 0.08 ml in the lizards of Fig. 3.6. Of the 23 animals used for the P-V studies, only 9 produced enough data to plot both total respiratory system and in situ lung relaxation curves. Results similar to Fig. 3.6 were found in all of them.

Volume and compliance relationships to body weight

The volumes of the total respiratory system measured at any one pressure were virtually directly proportional to body weight (Table 3.2). This proportionality between volume and body weight was also found for FRC, end-inspiratory level and minimal air (Table 3.3). Other lung sub-divisions were not examined for their body weight relationships. The compliance of the respiratory system was also proportional to body weight with, therefore, specific compliance being a constant of 0.35 (range 0.44 to 0.24) ml cm H_2O^{-1} FRC^{-1}. The body weight relationship for the compliance of other components of the respiratory system were not examined.

TABLE 3.2

The relationship between volume (total respiratory system) and body weight for different inflation curve pressures.

$V = aW^b$ in which V is in ml, W in g.

Pressure (cm H_2O)	a	b	CC	n
0	0.048	1.047	0.983	15
2.5	0.098	1.044	0.991	15
5.0	0.128	1.028	0.987	12
10.0	0.148	1.045	0.986	9
15.0	0.16	1.051	0.989	8
20.0	0.165	1.11	0.985	7

TABLE 3.3

The relationship between volume or compliance and body weight, $X = aW^b$. Volume in ml, compliance of the total respiratory system in ml cm H_2O^{-1}, specific compliance in ml cm H_2O^{-1} FRC^{-1}.

Parameter	a	b	CC	n
FRC	0.064	1.079	0.989	16
End-inspiratory level	0.085	1.021	0.971	9
Minimal air	0.016	1.012	0.965	14
Compliance	0.025	1.008	0.944	22
Specific compliance	0.35	-0.049	-0.257	16

Air P-V curves of the isolated lung

When the lung was cut away from its mesenteric connections to the thorax, its shape completely altered from an oval to a round one. On reconnection to the air inflation/deflation apparatus, there appeared to be no change in pressure and hence in calculated volume, but after a few P-V cycles it became apparent that the volume at zero pressure was lower than in the *in situ* lung (Fig. 3.7). Any change in pressure caused by isolation of the lung is too small to be registered in the dead space of the apparatus.

The *in situ* lung gave P-V loops of a shape illustrated in Fig. 3.4, 3.5 and 3.7a irrespective of the previous history of P-V manoeuvres. In contrast, the isolated lung gave two types of hysteresis loops. The first type (Fig. 3.7b) had more hysteresis and required greater positive inflation and deflation pressures than the *in situ* lung. This P-V pattern was obtained in the isolated lungs from lizards which had either been subjected to several P-V cycles of the total respiratory system to extreme levels of inflation or had been deflated in the total system or *in situ* lung to negative pressures of -15 to -20 cm H_2O. If the lung had not had this treatment and had only cycled between -3.5 and +3.5 cm H_2O in the total respiratory system, then the second type of P-V loop was found (Fig. 3.7c).

FIG. 3.7 Lung P-V loops from *Lacerta* (4.2 to 5.8g lizards) (a) air *in situ*, (b) air, isolated, type 1, (c) air, isolated type 2 showing 1st and 2nd loops, (d) air, isolated loops for successively increasing end-inflation pressures, (e) air, isolated loops for successively decreasing end-deflation pressures and (f) isolated air and saline P-V curves.

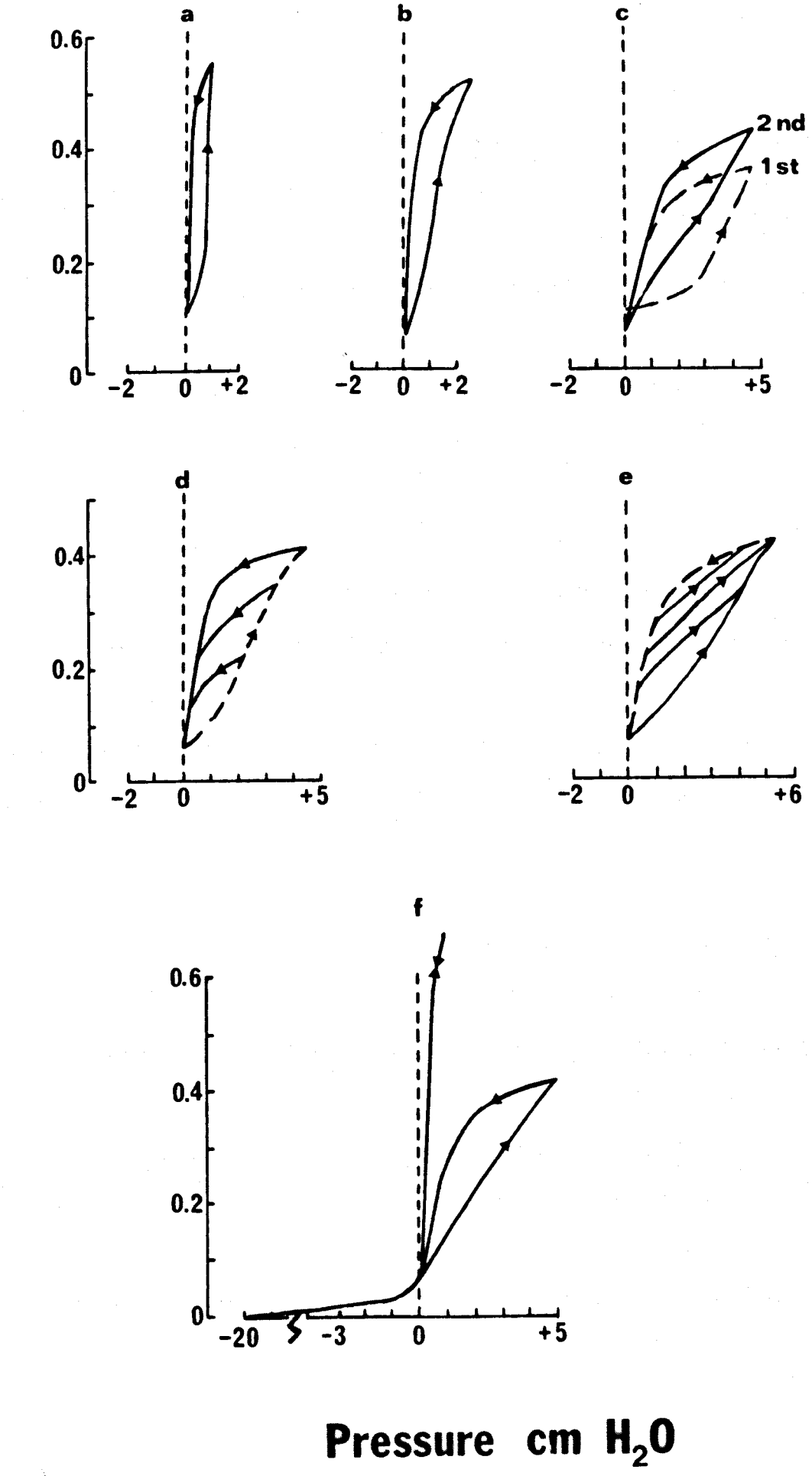
V ml
a
b
c
d
e
f
0.6
0.4
0.2
0
-2
0
+2
+5
+6
-20
-3
2nd
1st
Pressure cm H_2O

This loop had even greater hysteresis and required even higher positive pressures during inflation and deflation.

If the lungs giving this second isolated loop pattern were subjected to inflations of +10 cm H_2O or more or were deflated to -10 or -20 cm H_2O, the next hysteresis loop took the shape of the first pattern (Fig. 3.7b). A reduction in the hysteresis of the isolated lung could also be produced as a function of time. After 3 or 4 hours, with or without intermittent P-V cycles, there was a progressive reduction in hysteresis. After 6 hours or so, there was even less hysteresis than that of the in situ lung. (The outer surface of the lung was kept moist with saline all the time).

With this second type of P-V loop in the isolated lung (Fig. 3.7c), it was often found that the first P-V loop had a reduced compliance and a suggestion of a mammalian opening pressure phenomenon, but by the second P-V loop it traversed a constant cycle. After negative pressures, the pattern of Fig. 3.7b may also show an 'opening pressure' but this was due to internal moist surfaces sticking and inflation would suddenly occur with a concomitant drop in the positive pressure.

Fig. 3.7d and e show the families of curves obtained by successively increasing the end-inflation pressure or successively decreasing the end-deflation pressure. The latter is very similar to that of the total respiratory system (Fig. 3.3B) and suffers from the same problem of the correct judging of the inflation to deflation turning point such that a common deflation curve is obtained. In the former this judging problem does not arise because the correct turning point is always at zero pressure. There is a common inflation curve when successively increasing the end-inflation pressure but, in contrast to that of the total respiratory system, the deflation curves coincide as they approach zero pressure. Thus hysteresis at the lower volumes remains much the same when the lungs are collapsed to minimal air.

It was noted in all isolated lungs that the posterior area expanded before anterior regions - the reverse occurred in the *in situ* lung although it was not markedly reversed. Even at +10 cm H_2O or higher, the anterior region of the isolated lung was never completely expanded.

Saline P-V curves of the isolated lung

After deflation of the isolated lung to -20 cm H_2O air pressure (Fig. 3.7f), the lung was filled with saline. As described in the methods, several P-V cycles were required to remove all the trapped air bubbles. This removal was more difficult than in the rubber 'lung' because (i) the alveoli entrapped many bubbles, and (ii) the air bubbles formed were very stable.

Once all air bubbles and loose pulmonary foam had been removed, the saline P-V curve had a common inflation and deflation curve, that is to say there was no hysteresis (Fig. 3.7f). The volume at zero pressure was similar to the minimal air of the isolated lung. The saline P-V curve had a compliance and pressure level similar to that of the deflation curve of the isolated lung in which hysteresis was reduced (Fig. 3.7b). Many of the lungs contracted spasmodically when filled with saline.

DISCUSSION

In situ respiratory system

One of the striking differences between mammalian and Lacerta P-V curves is the latter's much greater compliance. This increase in compliance for the total respiratory system is by a factor of 18.5 which is due to a 3.5 fold increase in ribcage compliance accompanied by a 225 to 550 fold increase in lung compliance (Table 3.4). The anatomy of the Lacerta ribcage would also suggest less rigidity (Chapter 4). Lacerta lungs are very primitive having a large central air space with alveolar tissue only around the periphery (Chapter 4). Such a structure would be very compliant.

A 100 kg Chelonia has a lung compliance of 0.7 to 0.85 L cm H_2O^{-1} (Tenney, Bartlett, Farber & Remmers, 1974) which is about 3 to 4 times more compliant than that of a 100 kg mammal. The Chelonia lung does not have the large central air space found in Lacerta but its alveoli are larger than in a mammal (Chapter 4).

The absolute pressures, as opposed to the compliance, for the components of the respiratory system can be compared between Lacerta and mammal by examining their relaxation P-V curves (Fig. 3.5 and 3.8). For volumes below FRC, the ribcage requires greater negative pressures than the total system since the former is counteracted by the small positive pressures required by the lungs. This is true for both Lacerta and mammal showing that ERV is limited by the ribcage. For volumes above FRC (near TLC) in the mammal, the ribcage requires least, the lungs greater and the total system the greatest positive pressures. In Lacerta, this order becomes lungs, ribcage and total system (Fig. 3.5). Thus IC is limited by the lungs in the mammal but by the ribcage in Lacerta.

In Fig. 3.8, the volumes between -3.5 and +3.5 cm H_2O only (i.e. for the estimated VC) have been used for Lacerta. Thus, much of

FIG. 3.8 Relaxation P-V curves for a 70 kg man , 200g rat and 3 to 30g Lacerta. Volume expressed as % vital capacity, VC. Solid line for total respiratory system, dashed line for ribcage and dotted line for lungs. Total system only shown for Lacerta, refer to Fig. 3.5 for other components. Proportions of RV and FRC compared.

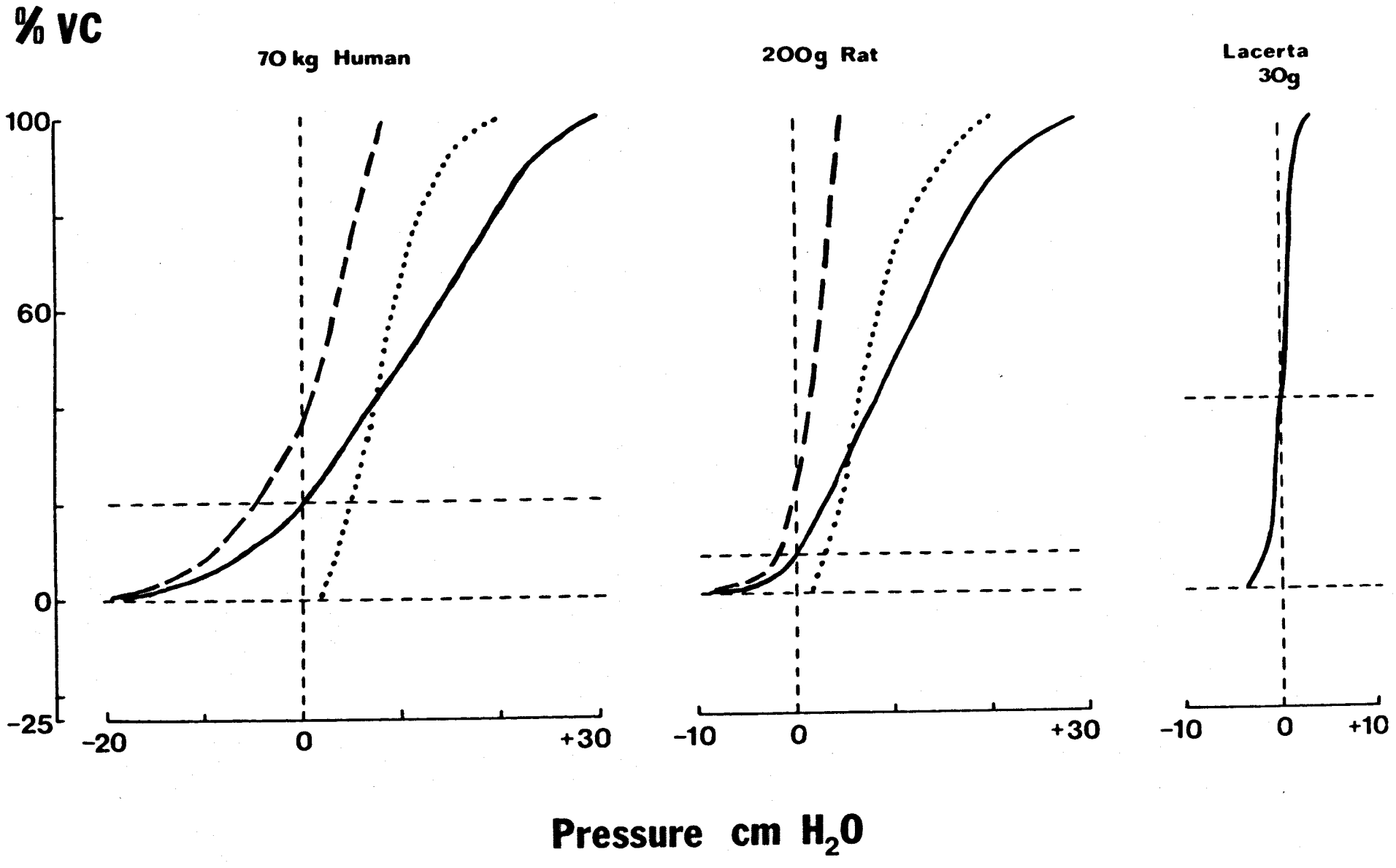
% VC
70 kg Human
200g Rat
Lacerta
30g
100
60
0
-25
-20
0
+30
-10
0
+30
-10
0
+10
Pressure cm H_2O

the curvilinear phase in the positive pressure range found in Fig. 3.2 to 3.5 has not been reached by +3.5 cm H_2O. In fact at this pressure, the ribcage has only just started to become curvilinear whereas the liver and heart are already curvilinear. Thus IC in Lacerta is also limited by the liver and heart.

When considering the extent of hysteresis in Lacerta, the degree shown at high inflations above +3.5 cm H_2O is not encountered during physiological vital capacities. At VC, the extensive hysteresis due to the liver and heart has just begun. In Lacerta, ribcage hysteresis is about twice that of the lung and causes about a 1 cm H_2O pressure width in the P-V loop. In the human, ribcage hysteresis was about half that of the lung and caused about 2 cm H_2O width (Agostoni & Mead, 1964). Presumably, the greater compliance of the Lacerta ribcage causes a lower hysteresis. There is, however, very little mammalian ribcage data available for comparison.

During the comparison of mammalian and Lacerta relaxation P-V curves, it is necessary to use supine, anaesthetised data from mammals. This is because in the upright human, FRC and ERV are greater (Agostoni & Mead, 1964) as is the compliance, but the specific compliance remains the same (Lim & Luft, 1959). Also, anaesthesia reduces the compliance of all components of the respiratory system (Butler & Smith, 1957). It is also necessary to compare Lacerta with small mammals because the smaller the body weight, the smaller is FRC and ERV relative to TLC and the smaller the maximum negative pressure of the ERV (Agostoni, Thimm & Fenn, 1959, Crosfill & Widdicombe, 1961).

Fig. 3.8 illustrates these differences between large and small mammals and contrasts them with that of Lacerta. It is apparent that the ERV of Lacerta is greater even than a large mammal in its proportion relative to VC or TLC. Thus at the 10g body weight level, the FRC of Lacerta is about 5 times that of a mammal (Table 3.4). Such a large FRC

TABLE 3.4

Comparison of total respiratory compliance, C, lung compliance, C_L, and ribcage compliance, C_w, in various mammals and Lacerta over a large size range. Body weight, W in g. C in ml cm H_2O^{-1}. Specific compliance, SC, in ml cm H_2O^{-1} FRC^{-1}. Function residual capacity, FRC, in ml. Supine, anaesthetised data.

Animal	W	FRC	C	SC	C_L	SC_L	C_w	SC_w	Source
Man	70,000	3,070* 2,000	102*	0.033*	200	0.065	208	0.068	Crosfill & Widdicombe (1961)
Dog	12,600	334* 252	17.8*	0.054*	40	0.12	32	0.098	Crosfill & Widdicombe (1961)
Cat	3,700	84* 66	6.7*	0.08*	13.4	0.16	13.4	0.16	Crosfill & Widdicombe (1961)
Monkey	2,450	106* 87.5	4.65*	0.044*	12.3	0.12	7.3	0.069	Crosfill & Widdicombe (1961)
Rabbit	2,400	20.7* 11.3	3.68*	0.18*	6.0	0.28	9.4	0.47	Crosfill & Widdicombe (1961)
Guinea Pig	690	8.3* 4.75	0.935*	0.113*	1.26	0.15	3.66	0.46	Crosfill & Widdicombe (1961)
Rat	250	3.14* 1.55	0.31*	0.0985*	0.39	0.12	1.47	0.55	Crosfill & Widdicombe (1961)
Mouse	32	0.46* 0.29	0.0425*	0.093*	0.049	0.11	0.33	0.68	Crosfill & Widdicombe (1961)
Mammal	10	0.13	0.013	0.1*	0.0142	0.11*	0.084	0.65*	Stahl, 1967
Mammal	10	-	0.014	-	0.00575	-	0.074	-	Spells 1969/70
Lacerta	10	0.64	0.25	0.39	3.2	5.0	0.28	0.435	This study
L/M ratio		5.0	18.5	4.0	225 to 550	45	3.5	0.67	

* Calculated from data of reference

causes specific compliance values to give a much lower Lacerta/mammal ratio than was obtained for compliance. Specific compliance ratios are 4.0, 45 and 0.67 for the total system, lungs and ribcage, respectively (Table 3.4).

The cross-over points of zero pressure axis, total system and lungs in the relaxation P-V curves of Lacerta, produced reasonable estimates of resting tidal volumes and the pressures involved (the latter compared with Sauromalus data (Templeton, 1964). Since, however, the P-V curve for lung was in situ and not in vivo, there may be some inaccuracies in applying this technique to Lacerta. In the in situ lung, the posterior region expands more than the anterior but this does not occur in vivo. It is likely, therefore, that an in vivo lung P-V curve would give lower volumes for a certain pressure when compared with the in situ lung because of the greater resistance of the more complex anterior regions. This might cause an estimation of minimum V_T rather than average V_T.

A comparison of Lacerta and mammalian lung sub-divisions has been made in Fig. 3.9 for a body weight of 10g in order to correlate the findings of this chapter with those of Chapter 2 and to relate them to the volumes obtained at different fixation pressures in Chapter 5. An instillation fixation pressure of 10 cm H_2O caused a lung volume found at maximum V_T and equal to $\frac{3}{4}$ TLC. Fixation pressures of 15 cm H_2O caused a volume a little greater than TLC and 5 cm H_2O gave volumes found near the maximum measured expiration.

It is difficult to be accurate in the sub-divisions for the mammal because all data has to be obtained from extrapolation of various body weight relationships (Table 3.5). According to Stahl (1967), VC is 8 times resting tidal volume, but according to Schmidt-Nielsen (1970) it is 10 times and according to data from Agostoni, Thimm & Fenn (1959) and Crosfill & Widdicombe (1961), it is 5 to 12.5 (mean 7.5) times. Although TLC is greater than VC, in Stahl's collected data (1967), TLC is only 6.5 times V_T. In Chapter 2, mammalian resting V_T was considered to be only one fifth VC.

FIG. 3.9 Comparison of lung sub-divisions in 10g mammal (right) and 10g *Lacerta* (left). Zero volume to (c) = FRC, (b) to (c) = min V_T, (a) to (e) = *Lacerta* max V_T. Solid stars = estimated VC in *Lacerta*. Open stars = VC in mammal - different VC volumes are possible (see text). Numbers 5, 10, 15 and 20 = fixation pressures (instillation) in cm H_2O.

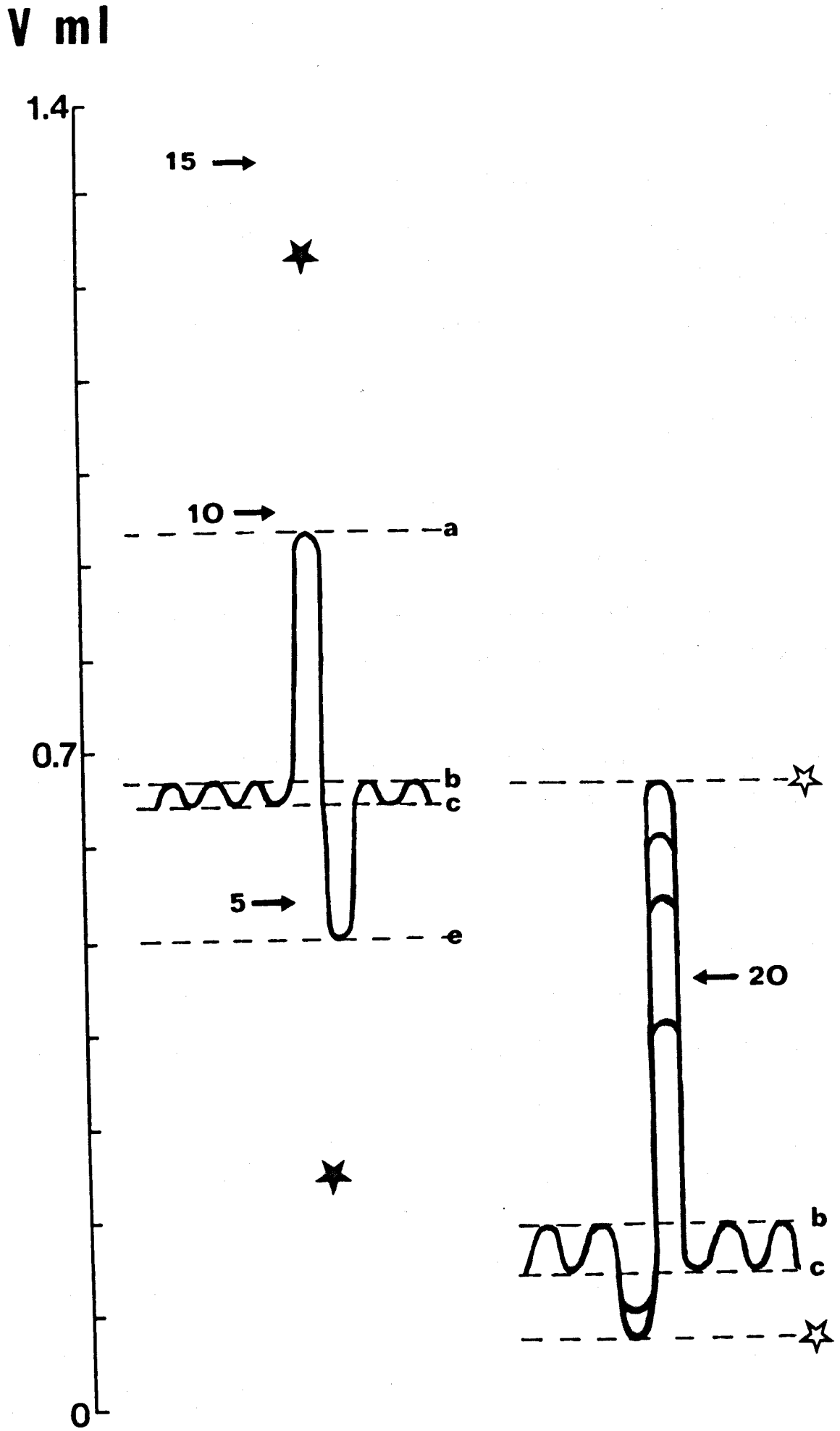
V ml
1.4
0.7
0
15
10
5
20
a
b
c
e
b
c

This ratio was obtained during active metabolism from human data since maximum V_T, as far as is known, is never recorded in small mammals. It is most likely, however, that under conditions in which maximum V_T is specifically being studied, i.e. for relaxation P-V curves, higher maximum V_T values will be obtained than from active metabolism data. The fixed lung volume used for mammals by Weibel and co-workers (Chapter 5) was considered by them to give $^3/_4$ TLC and this value is half the $^3/_4$ TLC of Lacerta. The mammalian instillation pressure was 20 cm H_2O for open chest. The discrepancy between the 2-fold difference between Lacerta and mammalian fixation pressures and the 18.5 fold difference in total respiratory compliance will be discussed in Chapter 5.

Volume and compliance relationships to body weight

An indication of the absolute values for mammals is given in Table 3.4 and the body weight scaling compared in Table 3.5. From the mammalian data, it is said that all lung volumes except FRC are isometric with body weight. The relatively greater FRC in large mammals is considered a necessity to allow dampening of the large oscillations of alveolar gas tension caused by their lower breathing frequency (Agostoni, Thimm & Fenn, 1959, Bartels, 1964). Also, although total compliance in the mammal is isometric with body weight, the lungs are relatively more compliant and the ribcage less in larger mammals.

TABLE 3.5

Volume and compliance relationships to body weight in Lacerta and mammal. Absolute values for 10g animals compared. Source is for mammalian data.

Parameter	Lacerta 10g	Lacerta b	Mammal 10g	Mammal b	Source
Total compliance ml cm H_2O^{-1}	0.25	1.008	0.013 0.014	1.04 1.005	Stahl, 1967 Spells 1969/70
Lung compliance	-	-	0.0142 0.00575	1.08 1.2	Stahl, 1967 Spells, 1969/70
Ribcage compliance	-	-	0.084 0.074	0.86 0.898	Stahl, 1967 Spells, 1969/70
FRC ml	0.64	1.079	0.13	1.13	Stahl, 1967
TLC	1.2	$\sim$1.0	0.41	1.06	Stahl, 1967
VC	0.98	$\sim$1.0	0.5	1.03	Stahl, 1967
Min V_T	0.026	1.088	0.056	1.04	Stahl, 1967

It is impossible from the size range of Lacerta used here to state anything other than isometric relationships for compliance and lung volumes. Any functional role for an increased FRC in larger Lacerta cannot be envisaged since alveolar gas tensions are already more damped than in a mammal (Chapter 2). Because Lacerta lungs are so compliant, there is virtually no difference between ribcage and total compliance or their body weight relationship. It was impossible to be very accurate in measuring the high compliance of the lung, but to anticipate a result from Chapter 5 where it was found that lung weight was proportional to $W^{0.7}$, one might perhaps expect a b exponent greater than 1.0 for lung compliance and body weight.

Specific total respiratory system compliance is virtually a constant in both Lacerta and mammals being related to $W^{-0.049}$ and $W^{-0.09}$, respectively. This means that a constant change in pressure is required during breathing irrespective of body weight. In the mammal this pressure is about 4 to 6 cm H_2O for resting V_T and it is estimated to be

about 0.6 to 0.8 cm H_2O in Lacerta. Examination of the literature revealed that the only lizard in which any measurement of end-tidal tracheal pressures had been made was Sauromalus (Templeton, 1964). Similar pressures to Lacerta were recorded and for maximum V_T a pressure of +1.5 cm H_2O was reached. Pressures as high as +15 to +25 cm H_2O were also recorded in Sauromalus during buccal deglutition so that, although Lacerta do not behaviourally do this (Chapter 2), the high inflation pressures used in the P-V data may give physiological information.

End-tidal tracheal or pulmonary pressures show changes during resting tidal volumes of 1 cm H_2O in Testudo (Gans & Hughes, 1967) 2 cm H_2O in Chelydra (Gaunt & Gans, 1969) and 5.5 cm H_2O in crocodiles (Naifeh, Huggins & Hoff, 1970). This information is relevant to the $W^{0.75}$ scaling of the isolated lung TLC found for reptiles by Tenney & Tenney (1970) in contrast to the $W^{1.0}$ for the isolated lung TLC in their amphibians and the in situ lung of the Lacerta of this study. The amphibians all had similar lung complexity but in the reptiles, in general, the larger ones were testudines or crocodilia with more complex lungs than the smaller ones (lizards). Thus the same fixation pressure for all the isolated reptilian lungs would over-inflate the small lungs and cause a proportionality of $W^{0.75}$ instead of $W^{1.0}$. Tenney & Tenney (1970) used 20 cm H_2O for air drying fixation, but at pressures of this magnitude in Lacerta volumes 3 times TLC were obtained with grossly abnormal over-inflated posterior regions. The lungs frequently leaked at this pressure and even 'burst'.

Equilibrium periods

Equilibrium periods of the total respiratory system in Lacerta were longer than in a mammal presumably because the more compliant the structure the longer it takes for equilibrium (Bachofen, Hildebrandt & Bachofen, 1970). In the mammal, equilibrium periods were required for both inflation and deflation (Butler, 1957) but when the lung was isolated the inflation equilibrium became longer due to the gradual opening of alveolar units (Radford, 1957). In contrast, equilibrium for the total

system in Lacerta was immediate if zero pressure was being approached but required a finite time if inflation or deflation was occurring away from zero pressure. This would be expected for an elastic system like the ribcage and is not seen in the mammal because of the over-riding influence of the lungs. Lacerta lungs in situ or isolated require an equilibrium period for both inflation and deflation and it is longer during inflation especially in those isolated lungs giving a high degree of hysteresis. This is due to the effect of surfactant.

Anderson & Madsen (1972) have recently shown that much of the stress relaxation seen in very small mammalian lungs (mouse) was due to transpleural loss of gases. Such an error could be present in Lacerta.

P-V curves of the lung

Since saline abolished all lung hysteresis and lowered the pressures required for inflation, this is considered indicative of the presence of surfactant in Lacerta lungs. The results for air inflation under different conditions will be explained on the basis of this.

Hysteresis in the in situ Lacerta lung is not extensive because the mesenteries holding the lung within the thorax maintain its oval shape and keep the peripheral tissue in an uncollapsed state. When isolated, however, the lung becomes spherical due to smooth muscle contraction (Chapter 4) and many of the alveoli in the periphery collapse or become very small and more spherical instead of cylindrical. Under such conditions the action of the surfactant becomes important and causes greater hysteresis than when in situ. There was never a true mammalian type of opening pressure during inflation from minimal air. This is because the alveoli are much larger than in the mammal and the central air space will expand to some extent even with collapsed peripheral alveoli. Even if the peripheral alveoli had an adequate amount of surfactant (i.e. equivalent to mammal), the large central air space will reduce much of the hysteresis and the pressures involved. The reduction in minimal air between in situ and

isolated lungs found in Lacerta is also present in mammals (D'Angelo & Agostoni, 1975). It is due to the removal of the limitations of the ribcage (and diaphragm).

Lacerta isolated lung hysteresis was considerably reduced by (a) deflation under negative pressures, (b) inflation to volumes greater than TLC, and (c) as a function of time. In mammals, hysteresis is enhanced by (a) and only slightly modified by (c) when it causes air trapping (Bachofen, Hildebrandt & Bachofen, 1970). (b) has not been examined in mammals. The Lacerta evidence can be interpreted in the light of Pattle & Hopkinson's data (1963) and Pattle's (1969) from bubble estimations of reptilian surfactant. They found that since there was little reserve of surfactant, negative deflations squeezed out all the surfactant into the pulmonary edema leaving little to line the alveoli. In Lacerta, stable bubbles were also found in the pulmonary edema and the subsequent P-V loop had very reduced hysteresis. Loss of surfactant within a few hours was also found by Pattle (1969). Another way of losing the surfactant, which was not tested by Pattle & Hopkinson's experiments, is by over-inflation. It is thought that this may mechanically overstretch the surface lining leading to utilisation of all the reserve and may, in some way, cause the lining to become discontinuous and unable to reform during the subsequent deflation.

It could be considered that much of the hysteresis present in the lungs of Lacerta was due to the 'sticking' of moist surfaces of the alveolar septa both to each other or to their own foldings (Chapter 4) rather than to a surfactant effect. But since 'sticking' and hysteresis were not greater after negative pressures, this is not the case.

The Lacerta alveolar configuration does not require an extensive surfactant to increase its alveolar stability or to reduce transudation of fluid into the air spaces. It is probable that the reserve of surfactant is adjusted to the needs of the alveoli in the in situ configuration.

P-V estimations need to be done on many other reptiles and for that matter amphibians. It is predicted that the newt lung, which does not have stable bubbles, will give no hysteresis at all for air P-V curves. A more complex reptilian lung, e.g. crocodile or testudine, will have a lower compliance than Lacerta accompanied by greater hysteresis and it may be more difficult to abolish this hysteresis.

CHAPTER 4

THE ANATOMY OF THE LACERTA RESPIRATORY SYSTEM

INTRODUCTION

The preceding chapters have examined the Lacerta respiratory system from a physiological point of view. In this chapter and the ensuing one, the anatomy and morphometry of this system have been studied to find if there are anatomical bases for some of the physiological limitations. The Lacerta respiratory system has never been extensively studied anatomically and no work has been published on electron microscopic findings nor even on histology. Much of the gross anatomy (with some histology) of the reptilian lung was investigated in the early 1900s and was presented in German papers (Milani, 1894, 1897, Marcus, 1927, 1937, Wolf, 1933). The recent French review by Guibé (1970) does not contribute any further information. In this chapter another reptilian lung review is attempted whilst paying more attention to recent histological and electron microscopic evidence. Much can be gained in terms of understanding lung evolution and function by comparing and contrasting the Lacerta lung with lungs of other vertebrates, in particular the mammal, in both adult and newborn(or foetal) states.

Gross anatomy

Inspired air reaches the lungs by travelling through a series of passages; the paired nasal cavities, part of the buccal cavity, the larynx, the trachea and the paired bronchi. Reptilian nasal cavity morphology has been extensively reviewed by Parsons (1970) and previously by Barge (1937). The positioning of the reptilian external nares is determined by habitat demands and the elongation and complication of the nasal vestibulum is governed by the need to trap sand grains or water to prevent deeper entry

into the cavum nasi proprium. This is assisted by the mucus secreting, external nasal gland and the whole trapped mass can be expelled by a sudden strong expiration (Pratt, 1948, Stebbins, 1948, Bellairs, 1969). This gland lies within the nasal concha which is a projection of the lateral wall of the cavum nasi proprium and divides the latter into a dorsal olfactory region and a ventral respiratory choanal tube. The choanal tubes open via the internal nares, choanae, into the roof of the buccal cavity.

The cavernous erectile tissue and radial smooth muscle fibres which surround the vestibulum can fill with blood to completely or partially occlude the vestibular lumen, thus acting as a valve (Bruner, 1907, Stebbins, 1948). Dilator and constrictor muscles further control narial size in Crocodilia (Bellairs, 1969). The vestibulum and its blood supply prepare the inspired air for contact with the delicate lung tissue by moistening, warming and cleansing it and the narrowness of the vestibulum and narial aperture reduces evaporation losses (Stebbins, 1948).

The choanae lead anteriorly to the Jacobson's organ (olfactory) which is situated ventral to the vestibulum, and posteriorly through the orbitonasal troughs to the larynx. If a secondary palate is partially or completely present a long nasopharyngeal tube is formed instead of the troughs (Goodrich, 1958, Bellairs, 1969, Parsons, 1970). Further details must be left to these reviews. The entrance to the larynx is a ventral, dorso-ventral slit called the glottis whose aperture is controlled by dilator and constrictor muscles attached to the cartilaginous framework of the larynx (Göppert, 1937). In some Squamata and in mammals, an epiglottis projects forward from the ventral surface of the larynx to act as a flap-like valve preventing food from entering the trachea. Geckos and anurans have folds of tissue stretched across the internal lumen of the larynx which resemble the vocal cords of birds and mammals. In snakes and some lizards, hissing is produced by the forcible expulsion of air through the glottis which impinges on the epiglottis. The pitch is controlled by the glottal

aperture (Bellairs, 1969). The vertebrate trachea may or may not bifurcate into extrapulmonary bronchi but their combined length is dependent mainly on neck length and the need to keep the lungs at the centre of buoyancy. Goodrich (1958) has described the evolution of the diaphragm and pleural mesenteries attaching the lung to the ribcage.

Gross lung architecture

The most primitive, but possibly degenerate, lung is found in the aquatic, urodelous amphibians Proteus and Necturus which have persistent gills throughout their life history (Fig. 4.1). The lung is a simple sac having no projections from the wall into the lumen (Marcus, 1937). Septa are also absent from the lungs of the semi-aquatic newt, Triturus (Okada et al, 1962a). The more terrestrial salamanders, however, have a few short, thick, anterior wall foldings thereby increasing the respiratory surface area (Marcus, 1937). The more active terrestrial anurans, Rana and Bufo, have many thinner radial septa (primary) which may give secondary septa that are tangential to the outer wall. These in their turn may give rise to further radial septa (tertiary) which have no direct connection with the outer lung wall (Fig. 4.1). The part of the primary septa and any secondary septa near the lumen are always thickened by extra smooth muscle bundles into a supporting trabecular network continuous with the smooth muscle of the trachea (Marcus, 1937, Okada et al, 1962a). When viewed from the inner surface, the lung is seen to be covered with a honeycomb of primitive polygonal alveoli, which are smaller in diameter, but deeper, anteriorly. Bufo has a thicker skin than Rana and compensates for the reduced cutaneous respiration by increasing the lung's respiratory surface area. The apodan, Hypogeophis, has a long tubular right and a reduced left lung which have only primary septa, the alveoli becoming larger and shallower towards the posterior, and a trabecular network. Cartilage from the trachea also infiltrates anterior septa (Marcus, 1937, George & Shah, 1965, Gaymer, 1971). This is also found to a small degree in the anuran, Pipa.

FIG. 4.1 Diagram to show increasing complexity of vertebrate lungs.

M, medial, L, lateral, V, ventral, D, dorsal surface.

(a) Simple sac of Proteus, Necturus, and Triturus (amphibians).

(b) Short, thick, primary septa of Siren and Hypogeophis (amphibian) and Polypterus and Calamoichthys (Polypteridae fish).

(c) Thick, primary, secondary and tertiary septa of Rana and Bufo (amphibians), Amia and Lepisosteus (fish air bladders) and Neoceratodus, Protopterus and Lepidosiren (lungfishes).

(d) Thin primary septa of Sphenodon (reptile).

(e) Thin, primary, secondary and tertiary septa of tegus, skinks, worm-lizards, geckos and zonures. Also typical of snakes.

(f) Thin, primary, secondary and tertiary septa together with partitioning in the dorsal ridge, Lacertidae and Agamidae.

(g) Diagrammatic sketch of primary, secondary and tertiary septa, the outer wall, w, and smooth muscle thickening of luminal secondary septa to form trabecular network (trab)

(h) Greater partitioning by primary septa and the presence of an intrapulmonary bronchus in Iguanidae.

(i) Long intrapulmonary bronchus and extensive alveolation in Varanus.

(j) Long intrapulmonary bronchus, secondary bronchi, bronchioles and extensive alveolation in marine turtles.

(k) Long intrapulmonary bronchus, extensive sub-division of airways and groups of alveoli at the final airway termination of the mammal. These alveolar groups are discrete units.

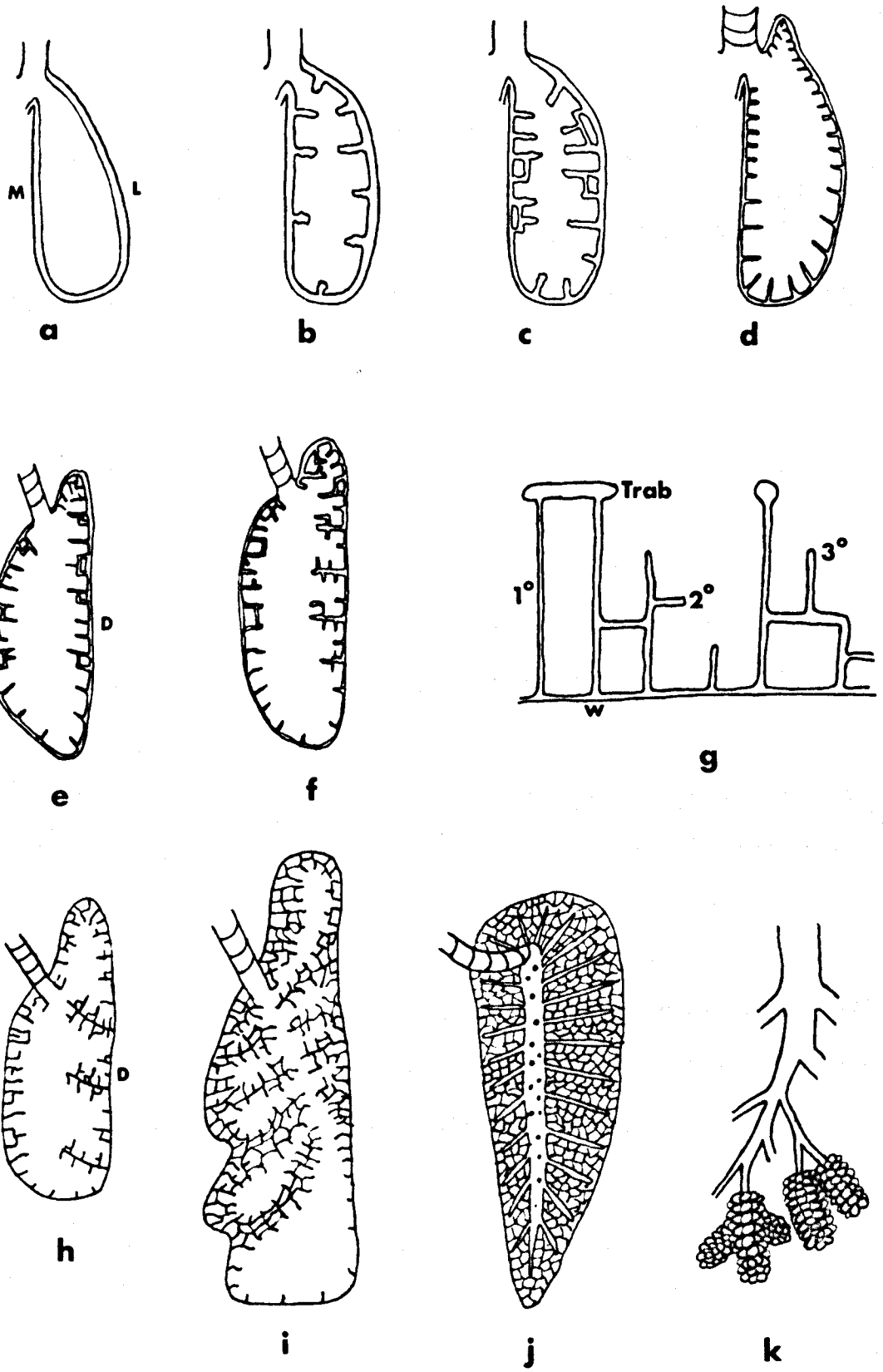
M
L
a
b
c
d
V
D
e
f
Trab
1°
2°
3°
w
g
V
D
h
i
j
k

Some fish air bladders even have primary, secondary and tertiary septa to give peripheral alveolation around a narrow central lumen (Amia and Lepisosteus, Rahn et al, 1971). True lungs, i.e. originating from the ventral surface of the oesophagus and thus differing from the dorsally originating gas bladders, are found in the Actinopterygian Polypteridae (Polypterus, Calamoichthys) and in the Dipnoi (Neoceratodus, Protopterus and Lepidosiren). The internal lung architecture of Polypterus resembles that of terrestrial salamanders whilst Neoceratodus resembles Rana in complexity and Protopterus and Lepidosiren resemble Bufo (Marcus, 1937, Grigg, 1965, Bertin, 1970, Johansen, 1970, Hughes & Weibel, 1976). Details of relative sizes of right and left lungs, their innervation and blood supply can be found in Marcus (1937) and Bertin (1970).

Sphenodon has the most primitive reptilian lung having only primary septa supported internally by the trabecular network. The alveoli are smaller in diameter anteriorly but deeper posteriorly (Fig. 4.1). The tracheal entrance is not at the lung apex as in fish or amphibia but is displaced caudally to the medial surface, thus forming a small pointed anterior lobe which is a constant feature of reptilian (and mammal) lungs (Milani, 1894). Amongst the lizards, the tegus, skinks, worm-lizards, geckos and zonures have the simplest lungs with primary, secondary and tertiary septa forming alveoli that decrease in depth and diameter posteriorly. In some cases there may be no septa posteriorly (Milani, 1894, Marcus, 1937). Greater complexity is found in the Lacertidae and Agamidae where primary septa extend from one side of the lung to the other. This occurs at intervals along a dorsal ridge and the deep pockets thus formed are lined on all sides by secondary and tertiary septa. Partitioning of the lung is more extensive in the Iguanidae where a complete primary septa partition separates the lung into a small anterior and a large posterior chamber. The anterior chamber is more extensively divided into alveoli and the bronchus enters it for some distance as an intrapulmonary bronchus (Marcus, 1937). Chameleons

possess two incomplete, longitudinal, primary septa partitions as well as an incomplete transverse one. Certain chameleons also have many long finger-like extensions of posterior lung regions which are air sacs completely lacking alveoli and are inserted into the viscera. These sacs enable the lizard to inflate its body when attacked thus intimidating an enemy (Milani, 1894).

The greatest degree of saurian lung development is found in the Varanidae and Helodermatidae families (Miller, 1893, Milani, 1894). The bronchial entrance is displaced caudally to a position a quarter of the way along the lung length thus forming a large anterior lobe. The intrapulmonary bronchus bifurcates into a short branch to this anterior lobe and a principal branch which communicates along its length with numerous posterior chambers (Fig. 4.1). These chambers with their central lumen have the three orders of septa near the bronchus but only the primary septa are present near the outer wall. This arrangement can be likened to a series of skink-like lungs grouped together in which the adjacent outer walls have fused (although allowing inter-alveolar communications) and a common bronchus has formed. Some of these chambers project into the forelimbs and the base of the neck and may serve to inflate the body during threatening behaviour (George & Shah, 1965). Recently, Kirschfield (1970) has extensively studied alveolar configuration and their blood supply in many species of Varanus.

Variations in lung architecture are also found in the Ophidia (snakes) but they are basically skink-like having no partitions. Snake lungs show the typical antero-posterior gradation of alveolar size and often the posterior region is devoid of all but the trabecular network and constitutes a simple air sac (often called a mechanical or reservoir region) which sometimes receives its blood supply from the gut (Marcus, 1937, Bellairs, 1969, Guibé, 1970). Some snakes, e.g. Naja replace a narrow strip of ventral alveolar tissue with a membranous connective tissue pad (George & Shah, 1956). Certain snakes, e.g. Vipera possess a tracheal lung which is alveolar tissue that has developed on the dorsal surface of the trachea (above the level of the heart) to replace the smooth muscle that usually

exists between the ends of the C-shaped cartilaginous rings. Often the tracheal lung becomes so large that it has its own central cavity which can be continuous with that of the main lung. In Sibon, only the tracheal lung has alveoli (Underwood, 1967). Beddard (1906) has described in the king cobra a series of tracheal lungs along the tracheal length which were completely unconnected except via the trachea. The left lung of all snakes is shorter than the right or is reduced to a rudiment or even completely absent. This left lung reduction can occur in snake-like lizards except in amphisbaenids in which the right is reduced. A lizard lung is oval whereas a snake lung is tubular.

Chelonia lungs are triangular in cross-section and show two main types of architecture. The first is basically akin to the Varanid lung having an intrapulmonary bronchus opening along its length into a variable number (species dependent) of chambers formed by primary septa partitions passing between the outer wall and the bronchus (Milani, 1897, Gräper, 1931, Marcus, 1937, Perry, 1972). In Testudinidae and Trionychidae, there is no antero-posterior gradation in alveolar complexity but within each chamber lateral surfaces are least complex. In Chelydridae and Emydidae, there is a posterior decrease in alveolar complexity being most apparent in the large posterior chambers. This is accompanied by the bronchus to outer wall alveolar gradation found in varanids. Small groups of alveoli discrete from the main chambers have independent openings into the intrapulmonary bronchus in Chelydridae. The second type of chelonian lung is found in the marine turtles (Cheloniidae) in which the intrapulmonary bronchus gives rise to radially diverging secondary bronchi which further subdivide (but always contain cartilage) and extend right up to the outer lung wall. The alveoli are extensive between bronchi and there are no central lumens (Fig. 4.1). Alveoli of one bronchus communicate with those of another. The lung tissue is thinnest and least complex at the lung periphery (Milani, 1897, Gräper, 1931, Marcus, 1937).

Compact lungs also occur in the Crocodilia and are very similar to the marine turtles, although not all the large air cavities are eliminated. Subdividing passages whose supporting muscular trabeculae are reinforced with cartilage, however, connect the intrapulmonary bronchus with the periphery. They are not considered true bronchi (Milani, 1897, Marcus, 1937).

Further compact, lung complexity is reached in mammals in which the bronchi divide into many generations of irregular dichotomous branches called secondary bronchi, bronchioles, respiratory bronchioles, alveolar ducts and finally end in numerous alveoli, clustered together in an alveolar sac (Krahl, 1964). Alveolar communication with the airways begins at the level of the respiratory bronchiole and from this point to the alveolar sac, the unit is a discrete one although lying intertwined with neighbouring units (Fig. 4.1). No such discrete unit structure exists in reptiles, not even in the marine turtles or crocodiles, because the alveoli of their adjacent airways freely communicate with each other. Microscopic pores in the alveolar walls of neighbouring units, however, do occur in terrestrial mammals and are called pores of Kohn. In marine mammals a connective tissue sheath around each unit prevents these small communications (Krahl, 1964). No cartilate and very little smooth muscle are present in the respiratory bronchioles of the terrestrial mammal whereas the opposite is the case in marine mammals (Engel, 1962, Denison & Kooyman, 1973). It is said that this airway strengthening limits nitrogen absorption during deep dives and aids in rapid ventilation at the surface between dives. Whether this could be true for marine turtles is speculative.

Lung evolution has taken an entirely different course in the bird lung being composed of bronchi and air capillaries. Architectural details are not relevant to this chapter and reference must be made to such papers as Marcus (1937) and Duncker (1972).

Various authors have made different classifications of lung types together with possible patterns of lung evolution. Milani (1894, 1897) stated that there were four designs based on the number of septal orders and presence of partitions and chambers:-

(i) primary septa only, e.g. Salamanders, Sphenodon,

(ii) all three orders of septa, e.g. frogs, lungfish, snakes, many lizards,

(iii) three septal orders plus complete or incomplete partitions, e.g. Iguana, Chamaeleo, and

(iv) partitions extensive enough to form separate chambers, e.g. Varanus, chelonians and crocodiles, which when they eliminate large air spaces form compact lungs, e.g. marine turtles, birds and mammals.

Marcus (1937) considered there was too much variation in Milani's classification and described two types (i) cartilaginous, and (ii) muscular dependent on the structure of the trabecular network, but this gives no indication of evolutionary trends.

Wolf (1933) dealing solely with amphibian and reptilian lungs distinguished seven types of increasing, evolutionary, architectural complexity designed to give better air circulation. Three basic patterns are shown during gradation through these seven types. Firstly, a division into a respiratory and mechanical region, the latter being present posteriorly and sometimes in the anterior lobe. Snakes are the most extreme example of this and various theories as to the function of the air sac have been postulated (George & Shah, 1957, 1965, McDonald, 1959, Bellairs, 1969). Secondly, the development of an intrapulmonary bronchus opening into various chambers. And thirdly, the development of communications which were independent of the bronchus, between chambers and between these and air sacs. It is doubtful whether this scheme has any importance for vertebrate lung evolution as a whole. Gans (1970) proposes a complex pattern of lung evolution which involves multiple disappearances and reappearances of single or paired air utilising organs evolving from a generalised single septate lung of Placoderm Devonian ancestors which lacked internal cartilaginous support.

Histology and ultrastructure

There is a wealth of histological and ultrastructural detail for the mammalian lung but the study of lower vertebrate lungs lags far behind. A review, but by no means an extensive one of the recent mammalian literature, is presented here so that any important similarities and differences between mammalian and more primitive lungs can be examined.

The trachea is composed of incomplete rings of hyaline cartilage ensheathed in a collagenous and elastic membrane with smooth muscle in the dorsal ring gap (Rhodin, 1963, 1974, Patt & Patt, 1969). Such a structure prevents airway collapse but allows lumen dimension changes. In chelonians and crocodiles and the cranial regions of snake and certain lizard tracheas, there is no dorsal gap (Bellairs, 1969, Guibé, 1970). The pseudostratified columnar epithelium of the mammalian trachea is composed of ciliated cells with microvilli, basal cells, intermediate cells, mucus secreting goblet cells and airway brush cells with villi that also have cytoplasmic filaments (Krahl, 1964, Meyrick & Reid, 1968). The submucosa contains an extensive lymphatic network which drains the lymphatic channels of the lung.

As the mammalian airway becomes narrower, so the histology progressively alters. The cartilage is replaced completely or partially by smooth muscle depending on whether the mammal is terrestrial or marine. The epithelium becomes simple columnar and then cuboidal still containing ciliated and non-ciliated cells but with the goblet cells replaced by Clara cells. Some workers believe that the Clara cells secrete the components of the lung surfactant (Niden, 1967, Etherton & Conning, 1971) but many believe they do not (e.g. Petrick & Collet, 1970). Clara cells have also been found on the alveolar septa of Rana (Kilburn, 1969). Another type of epithelial cell has also been found in the mammalian airways (often at the bifurcation of bronchioles) which has a very small, microvillied, part exposed to the air with sometimes a single cilium. The base of these cells is always associated with non-myelinated nerves and the cells are believed to be sensory receptors,

possibly chemoreceptors (Hung, Hertweck, Hardy & Loosli, 1973, Hung & Loosli, 1974).

At the entrance to a mammalian alveolus, the non-ciliated cuboidal epithelium and Clara cells abruptly give way to squamous epithelium (Type I cell) and a different kind of almost cuboidal cell (Type II). This abrupt transition in the epithelium also occurs whenever the occasional capillary is met in the respiratory bronchioles or alveolar ducts (Krahl, 1964). The alveolar septum is very thin containing a minimum of supporting collagen, elastin and smooth muscle and an extensive single capillary network (Fig. 4.2). The Type I cell of the alveolar septum has a central nucleated portion (usually lying in between capillaries) which sends out many long, thin, non-nucleated cytoplasmic extensions to overlie the capillaries (Weibel, 1971, 1973). These extensions were referred to by earlier workers as 'non-nucleated plates' of epithelium (Bertalanffy, 1964a). The rest of the air-blood barrier is also very thin except where the endothelial nucleus of the capillary intervenes. The basement membranes of endothelium and Type I sometimes fuse so that the interstitium is virtually absent. Numerous micro-pinocytotic vesicles are present in both endothelium and epithelium Type I cells, especially in the former. These and the inter-cellular junctions are thought to represent a small pore system of transport (Bruns & Palade, 1968, Weibel, 1969a).

Type II epithelial cells are found in the niches between capillaries and are characterised by a lack of cytoplasmic extensions, an abundance of cellular organelles, numerous short microvilli projecting into the air space, no pinocytotic vesicles and many large dense osmiophilic bodies usually having an internal lamellated structure (Weibel, 1969a) (Fig. 4.2). The osmiophilic material is frequently discharged onto the air surface leaving empty vacuoles (Macklin, 1954, Kikkawa, Motoyama & Gluck, 1968). Type II cells appear as non-vacuolated and vacuolated cells under the light microscope (Bertalanffy, 1964a,b, 1968). These cells desquamate into the

FIG. 4.2 A. Thick septa of amphibian. Note smooth muscle core (sm) terminal part thickened to form trabecular network (tb) and covered with ciliated columnar epithelium, blood vessels (bv) in septa and the double capillary network (cap). EM sketch shows endothelial cells (endo), interstitium (int) and Type II cells having microvilli, cytoplasmic extensions and lamellated bodies (LB). (From Okada et al, 1962a).

B. Thin septa of snake. Note some smooth muscle in septa, trabecular network with ciliated columnar epithelium, double capillary network. EM sketch shows endothelial cells, Type I cells with extensive cytoplasmic extensions and Type II cells with microvilli and lamellated bodies but no cytoplasmic extensions. Note the narrowing of the interstitial gap between Type I and endothelial cells. (From Okada et al, 1962b).

C. Very thin septa of mammal. Note single capillary network with virtually no smooth muscle, smooth muscle and non-ciliated cuboidal epithelium of alveolar duct (al.d.) (equivalent to trabecular network) and alveolus (al). EM sketch shows endothelial cells, Type I and II cells the same as in B. Note both sides of a single capillary are exposed to air and virtually no interstitium between Type I and endothelial cells.

N.B. Scale incorrect: capillaries and their distance apart largest in A, smallest in C.

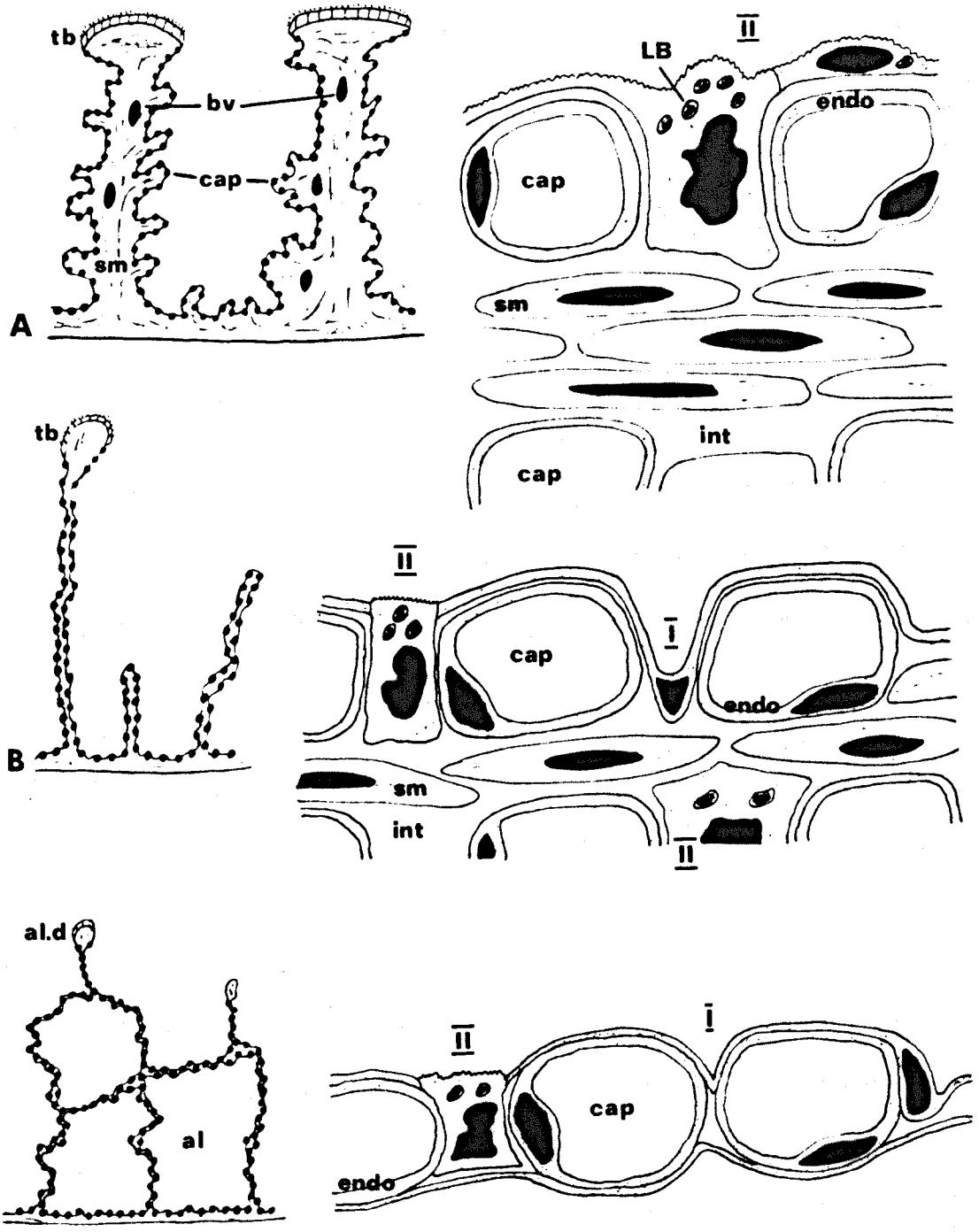
tb
bv
cap
sm
A
II
LB
endo
cap
sm
int
cap
tb
B
II
cap
I
endo
sm
int
II
al.d
al
C
II
I
cap
endo

air spaces and are then called alveolar macrophages. There is a third type of epithelial cell, the alveolar brush cell, which resembles closely the airway brush cell but has only been documented once (Meyrick & Reid, 1968).

The osmiophilic material discharged by the Type II cells is believed to be the source of lung surfactant which is continually renewed. In lungs fixed by airway instillation, remnants of this surface lining layer are found taking the form of globular myelin figures of osmiophilic phospholipid which resemble very closely the lamellated bodies of Type II cells. A further form, tubular myelin figures, is sometimes found which has a periodic structure of densely packed tubules (Weibel, Kistler & Tondury, 1966). A continuous surface lining layer smoothing out the irregularities and depressions of the alveolar surface can be demonstrated by vascular fixative perfusion (Weibel & Gil, 1968, Gil & Weibel 1969/70), by freeze-drying (Chase, 1959), by fixation from the pleural side of the lung (Finley, Pratt, Laoman, Breweer & McKay, 1968), by freeze-etching (Untersee, Gil & Weibel, 1971) or by critical-point drying using the scanning electron microscope (Kuhn & Finke, 1972). Further electron microscopic evidence for surfactant production and lamellated body origination from the golgi complex can be found in Sorokin (1966) Dermer (1969, 1970b), Gil & Reiss (1973), Meyrick, Reid (1973), Schock, Pattle & Creasey (1973) and Pattle, Schock, Dirnhuber & Creasey (1974).

Various pathways for the removal of surfactant have been suggested. Alveolar macrophages phagocytose the myelin figures and other cell remnants and are removed from the lung as sputum (Gil & Weibel 1969/70). Dermer (1970a) using a tricomplex fixation method for saturated phospholipids, says that surfactant breakdown products are removed by the pinocytosis of Type I cells into the interstitium and thence mainly to the lymphatic system but with a small amount to the capillary system. Gil (1972) has, however, produced evidence for the non-specificity of this tricomplex fixation method. Supporters of Niden's (1967) Clara cell source of surfactant state that the

Type II cells are removing the surfactant. Weibel (1969a) has discussed lymphatic and airway routes for the removal of excess fluid leaked from the capillaries.

The mammalian lung receives its blood supply from the pulmonary artery whose branches follow the course of the airways. Venous drainage, in contrast, takes a superficial path from the alveolar septum to the surface of the lung or travels in the connective tissue between lung lobules (Krahl, 1964). Pulmonary arteries and bronchioles are invested by a connective tissue sleeve which is rich in lymphatics, so that blood pressure and airway diameter can alter without affecting lung alveolar size and vice versa. Compression of the lymph vessels by these two structures aids lymphatic return. The pulmonary veins lack lymphatics and thus their diameters and venous return are dependent on lung volume and respiratory movements.

Histology and ultrastructure, non-mammalian

Available evidence shows that the alveolar septum of lower vertebrates is much thicker than in the mammal and supports a double capillary network (Marcus, 1937). The septa are thickened by the incorporation of smooth muscle into the interstitium between capillaries and the embedding of the capillaries in this and the juxtaposition of capillaries opposite those of the other side of the septum, considerably reduce the available capillary surface area for gas exchange (Fig. 4.2). Septal thickening is marked in lungfishes (Hughes, 1973, Hughes & Weibel, 1976), in amphibians (Okada et al, 1962a) and in terrapins (Perry, 1972) but is reduced in snakes and lizards (Okada et al, 1962b, Burnstock & Wood, 1967). There is very little difference in septal thickness between the mammalian and bird lungs and the latter also has a single capillary network and Type I and II cells (Okada et al, 1964, King & Molony, 1971).

Only Type II cells are found in lungfishes (Klicka & Lelek, 1967) and amphibians (Weibel, 1972) but they have cytoplasmic extensions. Both Type I and II are found in terrapins, snakes and lizards (Perry, 1972,

Okada et al, 1962b) (Fig. 4.2). The Type II cells of the terrapin, however, sometimes showed cytoplasmic extensions which is a Type I characteristic. Okada et al (1962a) were able to distinguish some Type II cells in their amphibians which had similarities to Type I cells. The evolution of these epithelial cells will be considered in the discussion.

Although all the non-mammalian Type II cells contain osmiophillic lamellated bodies, these bodies and surfactant ultrastructure have only been examined in lungfish and amphibians (Hughes, 1967, 1970a, Hughes, Ryan & Ryan, 1973, Pattle, 1973). The lamellated bodies were very similar to those of the mammal (which often have species differences, Scarpelli, 1968) but only globular myelin figures could be found in the air at the surface (Hughes, Ryan & Ryan, 1973).

Lung development, histology and ultrastructure, in the mammal

Lungs develop as a ventral diverticulum of the oesophagus and have a glandular appearance due to repeated ramifications of blindly-ending epithelial (cuboidal) tubes which after a certain period (16 weeks in the human) represent in miniature all the airways of the adult (Reid, 1967, Boyden, 1974). When vascularisation of tissue in between the tubes occurs this is known as the canalicular stage. Further vascularisation and evagination of the terminal airways into large primitive alveoli occur in a period known as the alveolar stage. At birth the septa between these large alveoli are thick and contain a double capillary network covered by typically adult Type I and II cells (Loosli & Baker, 1962, Weibel, 1967a, Reid, 1967, Kikkawa, Motoyama & Gluck, 1968, Burri, 1974). Postnatal development continues the alveolar stage by further capillarisation of new septa which divide the primitive alveoli into typically adult alveoli and by remodelling the double into a single capillary network (Burri, 1974).

Towards the end of the glandular stage, the cuboidal cells contain a few dense osmiophilic bodies but during the canalicular stage, some cuboidal cells lose these bodies and begin to become squamous whilst some remain

cuboidal and gain lamellae in the osmiophilic bodies (Kikkawa, Kotoyama & Gluck, 1968). At this point, the presence of surfactant can be measured physiologically (Reid, 1967). Balis & Conen (1964) consider that in the canalicular stage, cuboidal stem Type II cells progress to Type II or become transformed into Type I. During postnatal development, Klauffman, Burri & Weibel (1974) using H-thymidine labelling have shown that Type II cells are labelled but Type I are not, indicating that only Type II divide. It was thought, therefore, that Type II cells were the stem cells for Type I, agreeing with Balis & Conen (1964). Further evidence to support this idea comes from the fact that after O_2 poisoning or during ordinary epithelial repair, Type II cells become cuboidal and may even transform into Type I cells to replace damaged Type I cells (Kapanci, Weibel, Kaplan & Robinson, 1969, Bachofen & Weibel, 1974).

METHODS

Dissection

Nasal, buccal and pharyngeal cavities, the larynx and trachea were examined in freshly killed Lacerta or in specimens that had died from natural causes or disease and had been stored in the deep freeze. The mesenteric connections of the lungs within the thorax were studied in both inflated and deflated states.

Silicon rubber casting

ICI 'Silcoset' 105, white rubber was used to make casts of the nasal cavities. 'Silcoset' 105 is the least viscous paste (120 poises) of the ICI range and when used with a 0.5% volume of curing agent A has a tack-free time of 2 to 4 hours and a cure time of 24 hours. Its specific gravity is 1.18 and it has a linear shrinkage of 0.5% (ICI, 1972).

0.01 ml of curing agent A was thoroughly mixed with 2 ml of 'Silcoset' 105 paste in a short plastic test tube. The upper jaw was cut away along a line caudal to the eyes in freshly killed Lacerta and placed in the liquid rubber. (The upper jaw was never allowed to dry out since this caused nasal mucosa destruction and hence an artificially enlarged nasal cast). By means of a syringe, 3-way tap and rubber bung, the pressure in the air space above the liquid rubber was alternately reduced and increased over a period of 15 minutes. These changes in air pressure ensured adequate cast filling.

After 24 hours, the excess solid rubber surrounding the upper jaw was carefully cut away but leaving intact the rubber filling the naso-pharyngeal canal up to the known position of the larynx. The bone was softened by leaving it overnight in 12.5% EDTA, a decalcifying solution. The nasal cast was exposed by carefully clipping away bone. Occasionally small air pockets were present in the cast, but the cast was not rejected unless these were extensive.

Lung structure, gross anatomy

This was examined in lungs fixed by glutaraldehyde instillation under various pressures. The details of this technique are described in Chapter 5. Macroscopic lung structure was photographed using a Prinzflex 500 camera with extension tubes or a Russian binocular with one of the eyepiece barrels fitted with a Leitz camera plus viewing 'T'-tube.

Histology, paraffin sections

After washing in cacodylate buffer for 2 hours, strips or rings of glutaraldehyde-fixed lungs were dehydrated, cleared and embedded in paraffin wax. 7 μm sections were cut in various planes on a Cambridge rotary, rocking microtome and stained with one of the following stains:- Haematoxylin & eosin, Masson's trichrome, Weigert's elastin & Van Gieson's stain and Mallory's triple stain. A variety of clearing agents and waxes of different melting points were used, but all caused shrinkage, distortion and collapse of the central air lumen. Photographs were taken with a Zeis photomicroscope, often using an orange filter.

Epon sections, light and electron microscopy

A stock solution of 25% glutaraldehyde was diluted to 2% in 0.1M cacodylate buffer to give an osmolarity of 340 mOsm/L and pH of 7.4. These values were similar to those of blood in terrestrial lizards (Dessauer, 1970). The lungs were fixed in this solution for 2 hours and then washed for an hour in two changes of 0.1M cacodylate buffer (osmolarity adjusted to 340 mOsm/L by addition of sucrose). During this washing the lung tissue was diced into 1-2 mm squares.

If circumstances made it necessary to store the lungs before epon embedding, this was done in 2% glutaraldehyde in cacodylate buffer at $4^{o}C$ for a maximum period of a week. Storage in cacodylate buffer alone was found to leech out stainable material.

After washing, the tissue squares were post-fixed for 2 hours in 1% osmium tetroxide made up in 0.1M cacodylate buffer (osmolarity adjusted to 340 mOsm as before, pH adjusted to 7.4). This was followed by two washes

in 0.1M cacodylate buffer for 20 min and then a gradual dehydration in 10% through to 70% ethanol (10 min for each 10% ethanol step). En bloc staining in 2% uranyl acetate made up in 70% ethanol was then performed in the dark for 2 hours. This was followed by 10 min stages in 90%, 2 x 100% ethanol and in 2 x propylene oxide.

A 'not-very-hard' epon recipe was used, the constituents of which were thoroughly mixed so that no stratification of densities could be seen. The constituents were:-

Epon 812	10 ml
DDSA	17.5
Nadic methyl anhydride	2.0
BDMA	0.2

The same volume of propylene oxide, P.O., was added and thoroughly mixed with the above to give a 1:1 ratio. This was added to the propylene oxide already surrounding the tissue pieces to give a 3 P.O.:1 epon mix. After 30 min, the 3:1 mix was removed and the 1:1 mix poured over the tissue pieces and left overnight with the containers sealed.

The next day the 1:1 mix was replaced by a 1 P.O.:3 epon mix for 5 hours. The tissue pieces were then carefully picked up on a needle, blotted free of excess 1:3 and put in clean containers holding 100% epon. After being placed under vacuum for 10 min, the unsealed containers and tissue were left for at least 5 hours. Again the tissue pieces were blotted free of excess epon and placed in freshly made 100% epon in the final embedding dishes. They were then subjected to vacuum for 10 min in a 45^{o}C oven and finally left overnight at this temperature. Polymerisation of the resin was then allowed to occur in a 60^{o}C oven and a suitable cutting hardness was obtained after 48 hours.

Sections were cut with a LKB III ultratome using glass knives. 1 μm thick sections were routinely made and stained with methylene blue (1% methylene blue in 1% borax in distilled H_2O was placed on the section and the slide heated in a naked flame for a few seconds and then rinsed

under tap water). Photographs were taken as for paraffin sections; the thinner section allowing higher magnifications and better resolution. Epon blocking gave no shrinkage or distortion.

Ultra-thin sections were cut at 70 nm to 90 nm, i.e. pale yellow to grey interference colour, and picked up on uncoated 200 mesh copper grids previously dipped in 0.1% NaOH to reduce surface tension. When dry, the grids and sections were stained in the dark for 10 min with 2% uranyl acetate in 70% ethanol followed by 15 min in lead citrate in NaOH in an atmosphere free from carbon dioxide (Reynolds, 1963, Frasca & Parks, 1965). The grids were quickly washed in 0.1M NaOH to remove any lead carbonate, washed in distilled water and the excess liquid blotted away.

Examination of the sections was accomplished using an AEI 6G electron microscope at an accelerating voltage of 60 Kv. Electron micrographs were taken using the 70 mm camera attachment on Kodak sheet film or Ilford glass plates.

RESULTS

Gross Anatomy

In Lacerta, the external nares open laterally but are directed dorso-posteriorly (Fig. 4.3L). They lead internally into a narrow tubular vestibulum which runs in an anteromedial direction for a very short distance before turning posteriorly towards the cavum nasi proprium (Fig. 4.4). The opening from the vestibulum to the cavum is encircled by a deep post-vestibular ridge in front of which opens (onto the dorso-lateral surface) the duct from the external nasal gland. The vestibulum is short and uncomplicated because the Lacerta habitat is neither aquatic nor very sandy. The vestibular bend should, however, assist in trapping foreign particles.

Lacerta has a relatively simple form of nasal concha which is attached ventro-laterally to the lateral wall of the nasal capsule and projects dorso-medially and posteriorly into the cavum. The depression in the nasal cast formed by the concha can be seen in Fig. 4.4. Within the concha lies the external nasal gland. The region anterior and ventral to the concha is the choanal tube connecting the vestibulum with the internal nares (choanae). There is no nasopharyngeal tube in Lacerta. The region of the cavum medial to the concha is the ductus olfactorius and the region lying caudally dorsal and dorso-lateral is the extraconchal space. The region posterior to the concha is the antorbital space (Fig. 4.4). Air from the external nares need only take the direct route through the choanal tube to the choanae.

The choanae open into the dorsal part of the buccal cavity (Fig. 4.3D). Their medial margin is formed by the vomerine cushion and their lateral margin by the maxilla and its more ventral, medial extension the choanal fold. The posterior margin is formed by the palatine bone and the anterior margin by the fused vomerine cushion and maxilla. The choanal fold continues anteriorly to the opening of the duct of Jacobson's organ,

FIG. 4.3 L. Lateral view of Lacerta upper jaw showing external nares (EN).

V. Lower jaw, ventral floor of buccal cavity.
CBl and 2, ceratobranchial 1 and 2. CS, ceratostyal.
HP, hypophyal - all part of the hyoid cartilage.
Ep, epiglottis. G, glottis. L, larynx. T, trachea.
Te, teeth. To, tongue.

D. Upper jaw, dorsal roof of buccal cavity.
Basi, basisphenoid covered by muscle. Ch, choanae.
ChF, choanal fold of the maxilla. ChG, choanal groove connecting Ch with JO, duct to Jacobson's organ.
Eust, Eustachian tube opening. M, muscle covering lower and upper jaw bone. Pal, palatine. Ptery, pterygoid.
PC, parasphenoid canal. Ty, position of tympanum.
V, vomer forming primitive secondary palate.

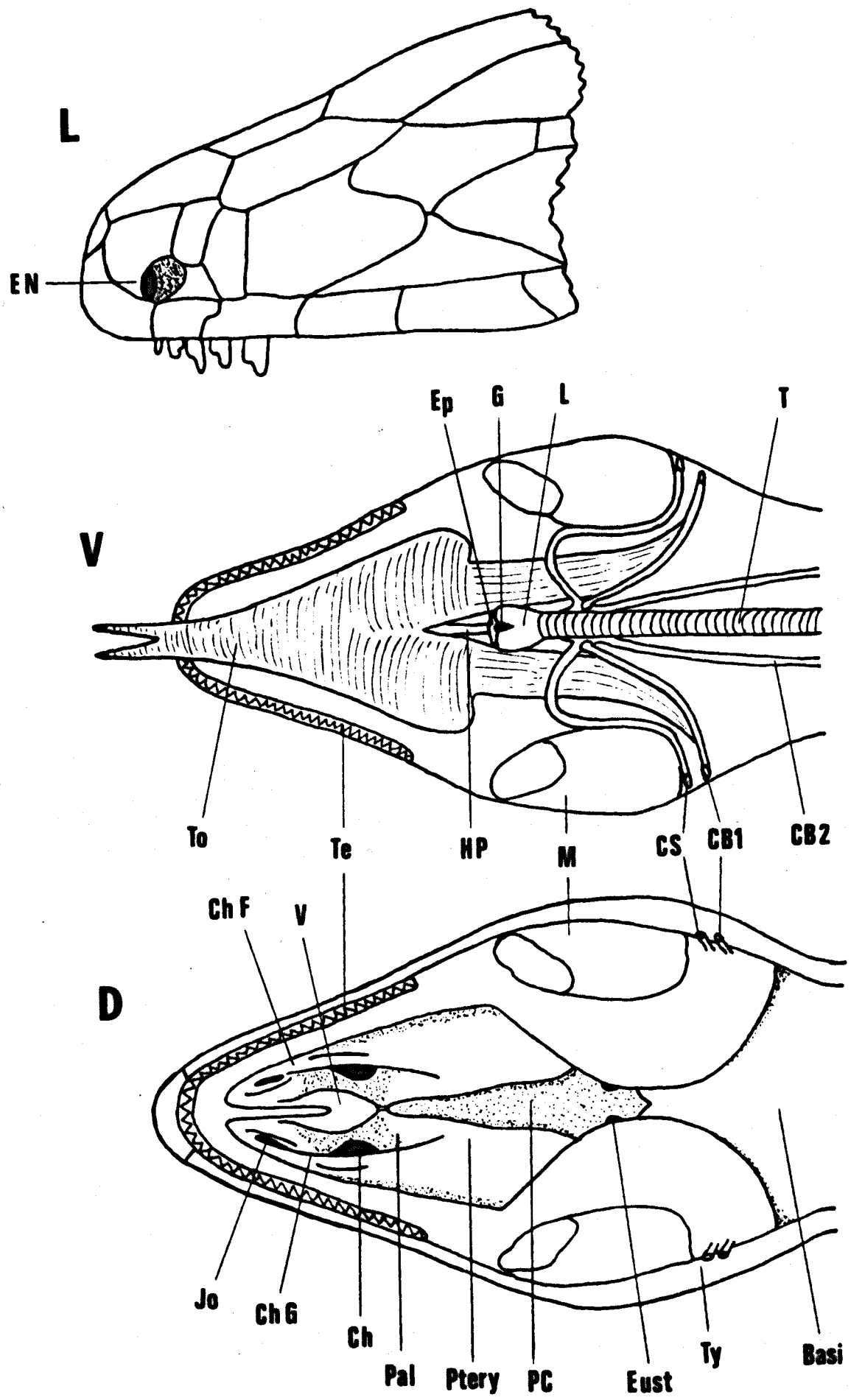
L
EN
V
Ep
G
L
T
To
Te
HP
M
CS
CB1
CB2
D
Ch F
V
Jo
Ch G
Ch
Pal
Ptery
PC
Eust
Ty
Basi

FIG. 4.4 Silicone rubber cast of nasal air cavities of L. sicula.

Dorsal, medial and lateral views.

AS, antorbital space. CNP, cavum nasi proprium.

CT, choanal tube. DO, ductus olfactorius.

EN, external nares. ES, extrachonchal space.

NC, depression of nasal concha. OT, orbitonasal trough.

PVR, postvestibular ridge. V, vestibulum.

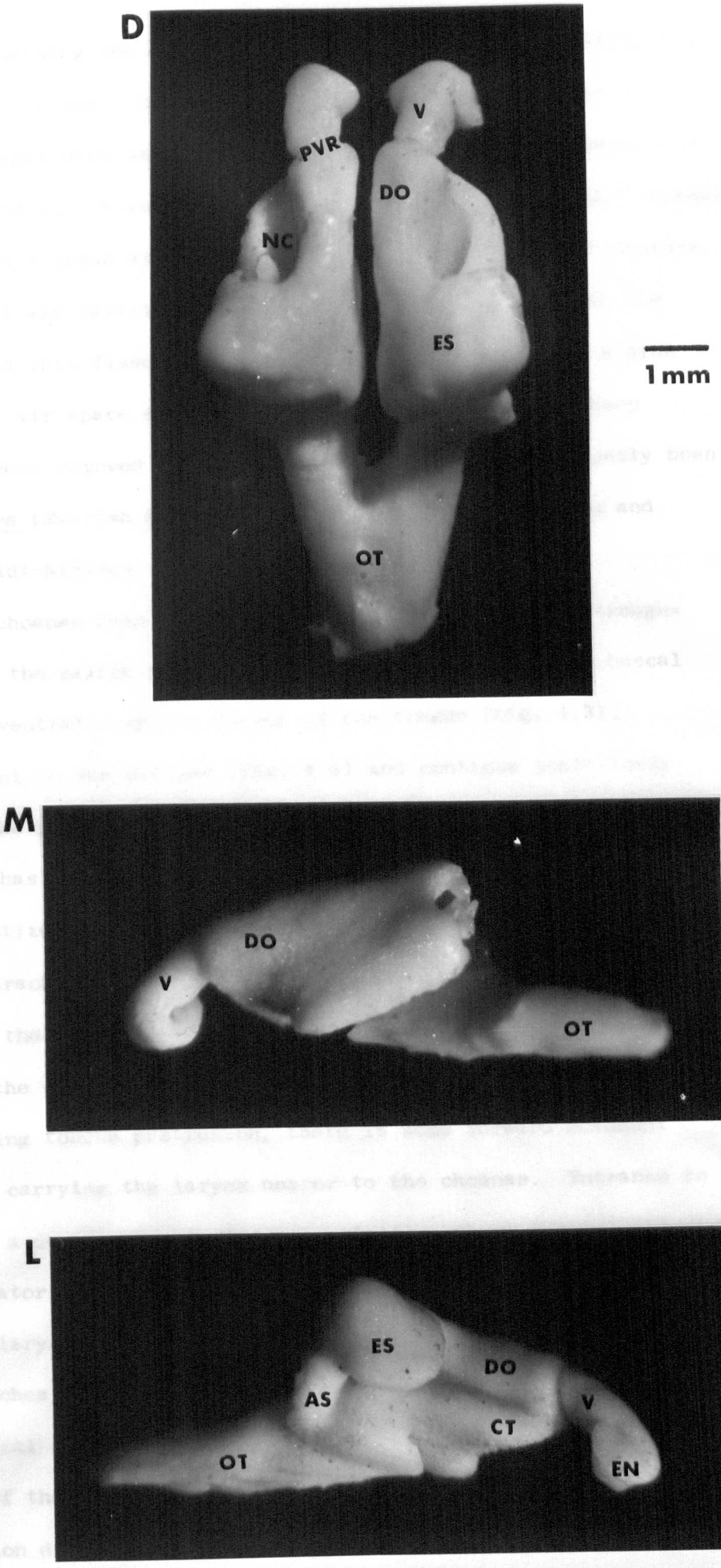
D
V
PVR
DO
NC
ES
1mm
OT
M
DO
V
OT
L
ES
DO
AS
V
CT
OT
EN

its choanal groove marking the deeper fusion and connecting externally the choana and Jacobson's organ. Bellairs & Boyd (1950) have described the course of the lachrymal duct which lies along the ventro-lateral margin of the posterior part of the choanal tube and follows the course of the choanal fold to the Jacobson's organ whilst making its own lateral choanal fissure. In casting the nasal air cavities, the rubber solution entered both the Jacobson's organ and this fissure but since they do not represent a true nasal (respiratory) air space and were delicate and difficult to keep intact, they have been removed in Fig. 4.4. Nasal casts have recently been made for Dipsosaurus (Murrish & Schmidt-Nielsen, 1970) and in bird and Kangaroo rat (Schmidt-Nielsen, Hainsworth & Murrish, 1970).

The two choanae lead posteriorly into two orbito-nasal troughs formed dorsally by the paired palatine and pterygoid bones of the buccal cavity and closed ventrally by the dorsum of the tongue (Fig. 4.3). The two troughs meet in the midline (Fig. 4.4) and continue posteriorly until they reach the parasphenoid canal in which lies the larynx (Fig. 4.3). The buccal cavity has no exceptional degree of vascularity and is not considered to constitute a possible respiratory surface. The larynx and beginning of the trachea are supported ventrally by the hyoid cartilage to which is attached the posterior margin of the tongue muscles and the three muscle layers of the pharyngeal floor (as in Ctenosaura, Oelrich, 1956) (Fig. 4.3V). During tongue protrusion, there is some forward movement of the hyoid thus carrying the larynx nearer to the choanae. Entrance to the larynx is via a dorso-ventral slit, the glottis, whose aperture is controlled by dilator and constrictor muscles supported by the cartilaginous framework of the larynx. There is a primitive epiglottis.

The trachea, with its rings of incomplete cartilage and smooth muscle in the dorsal gap, traverses the neck lying ventral to the oesophagus until the level of the collar fold. Here the trachea turns dorsally into the thoracic region dorsal to the heart and at about the level of the

posterior margin of the forelimb, the trachea divides into two short bronchi. The bronchal combined diameter is greater than that of the trachea. Bronchal entrance into the right lung is at a slightly more anterior position than into the left lung. Above this entrance is a small anterior lung lobe, the tip of which is slightly more anterior in the right lung. The left lung, however, extends further posteriorly. Since the peritoneal lining of the thorax and abdomen is cream and black, respectively, and the transition from one to another abrupt, the posterior limit of the lungs and the extra length of the left are clearly shown. Burnstock & Wood (1967) similarly found a longer (but also larger) left lung in Trachysaurus.

The two lungs lie on either side of the oesophagus and stomach and if the latter contains food, the posterior regions of the lung are restricted to some degree during inflation. An indentation occurs in the posterior, medial part of the right lung because of the stomach's deflection to the left. The posterior two thirds of the lung are covered by ventral and dorsal liver lobes, whilst the anterior third and part of the trachea are covered ventrally by the heart and its blood vessels ensheathed in the pericardium (Fig. 4.5).

Flanking the sides of the trachea are the two pulmonary arteries which enter their respective lung with, and anterior to, the bronchus. The artery immediately divides into a branch to the ventral surface of the lung and a branch which curves round the dorsal surface of the intrapulmonary bronchus supplying deep branches to the anterior lobe before turning medially to lie in the medio-dorsal lung ridge (Fig. 4.5, 4.6, 4.8). Both arteries maintain a superficial position in the external lung surface. Deep and superficial transverse branches of the dorsal and ventral pulmonary artery ramify across the lung interdigatating with transverse branches of the medial and lateral pulmonary veins (Fig. 4.8). The lateral pulmonary vein of the right lung courses onto the ventral surface and crosses the base of the anterior lobe, which it also drains. After crossing the right

FIG. 4.5 Arteries, veins and nerves of the neck, heart, lungs and liver. The heart has been removed. Note early branching of external carotid artery from carotid arch. Internal carotid artery arises by several roots from the carotid arch, (see Adams, 1939, 1953).

Ant lobe, anterior lung lobe. Aor arch, aortic arch. Br Pt, position of bronchus. Car arch, carotid arch. CBl ceratobranchial hyoid cartilage 1. Cer Symp T, cervical sympathetic trunk. Dor X, dorsal branch of vagus nerve. Duct car, ductus caroticus. Ext car A, external carotid artery. Inf Lar N, inferior laryngeal nerve. Inf v c, inferior vena cava. Int car A, internal carotid artery. Jug V, jugular vein. Lat Pul V, lateral pulmonary vein. Liv, liver. Lt L, left lung. Lt Lar Tr A, left laryngeal, tracheal artery. Med Pul V, medial pulmonary vain. Mus cerv A, cervical muscle artery. N to Aor arch, nerve to aortic arch. N to Hrt, nerve to heart. N to Int car, nerve to internal carotid. N to oes, nerve to oesophagus. N to Pul A, nerve to pulmonary artery. Nod gang, nodose ganglion. Parathy, parathyroid. Pul A, pulmonary artery. Pul V, pulmonary vein. Rt Azy V, right azygos vein. Rt L, right lung. Rt Tr V, right tracheal vein. Sin Ven, sinus venosus. Sub V, subclavian vein. Sup Lar N, superior laryngeal nerve. Syst A, systemic aorta. Th II and III, thymus II and III. Thy G, thyroid gland. Tr, trachea. Ult b, ultimo-branchial body. Vent Pul A, ventral pulmonary artery. X to Stom, vagus nerve to stomach. IX, glossopharyngeal nerve. XII, hypoglossal nerve.

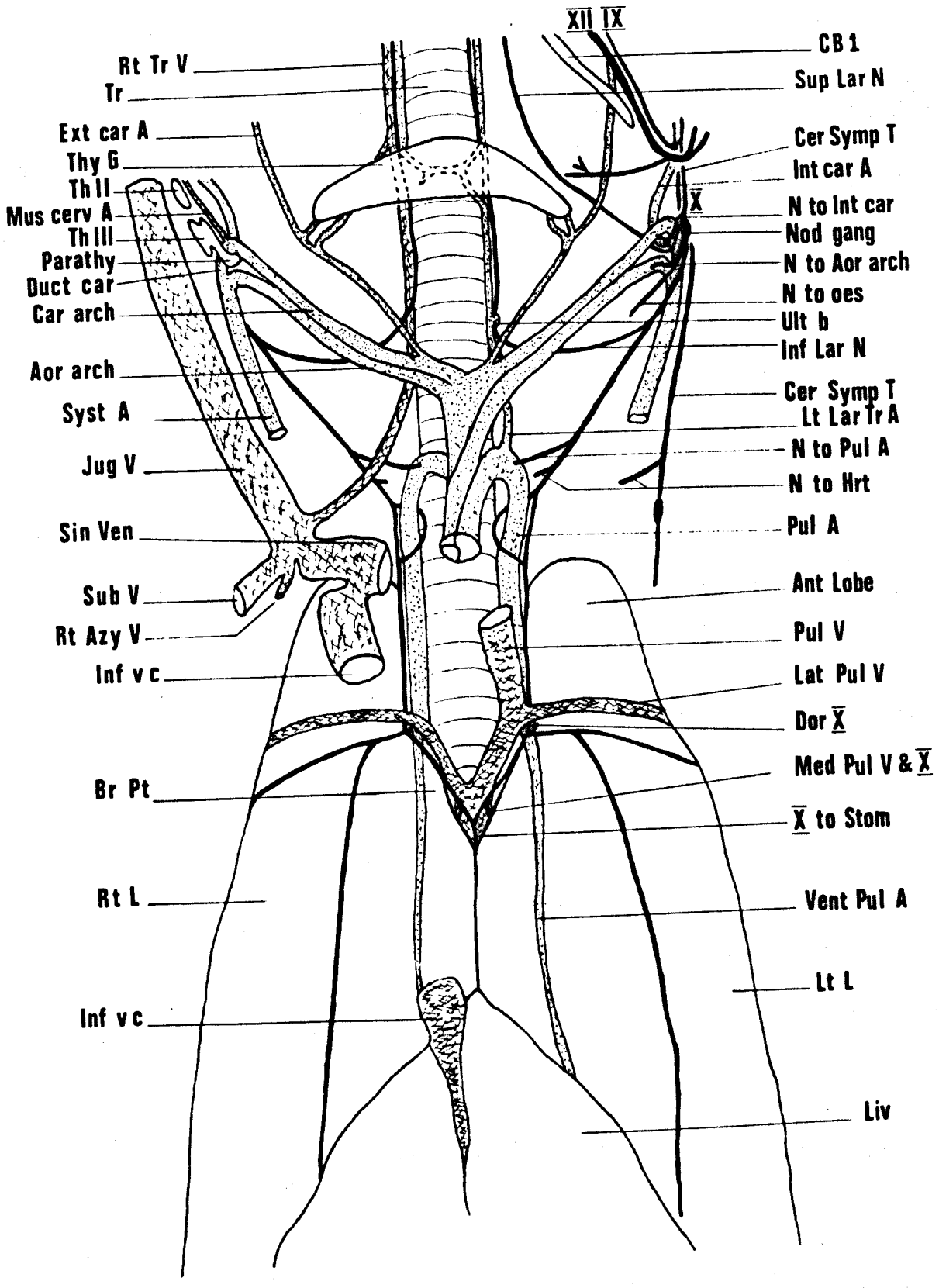
XII IX
CB 1
Sup Lar N
Rt Tr V
Tr
Ext car A
Thy G
Th II
Mus cerv A
Th III
Parathy
Duct car
Car arch
Aor arch
Syst A
Jug V
Sin Ven
Sub V
Rt Azy V
Inf v c
Br Pt
Rt L
Inf v c
Cer Symp T
Int car A
X
N to Int car
Nod gang
N to Aor arch
N to oes
Ult b
Inf Lar N
Cer Symp T
Lt Lar Tr A
N to Pul A
N to Hrt
Pul A
Ant Lobe
Pul V
Lat Pul V
Dor X
Med Pul V & X
X to Stom
Vent Pul A
Lt L
Liv

FIG. 4.6 Paired lungs and trachea showing anterior lobe, ventral pulmonary artery, vpa, and medial (right lung) and ventral (left lung) mesenteric connections, m.

Ventral, medial, dorsal and lateral aspects of the left lung showing trachea, bronchi, anterior lobe, mesenteric attachment lines and the ventral pulmonary artery, vpa, medial pulmonary vein, mpv, dorsal pulmonary artery, dpa, and lateral pulmonary vein, lpv.

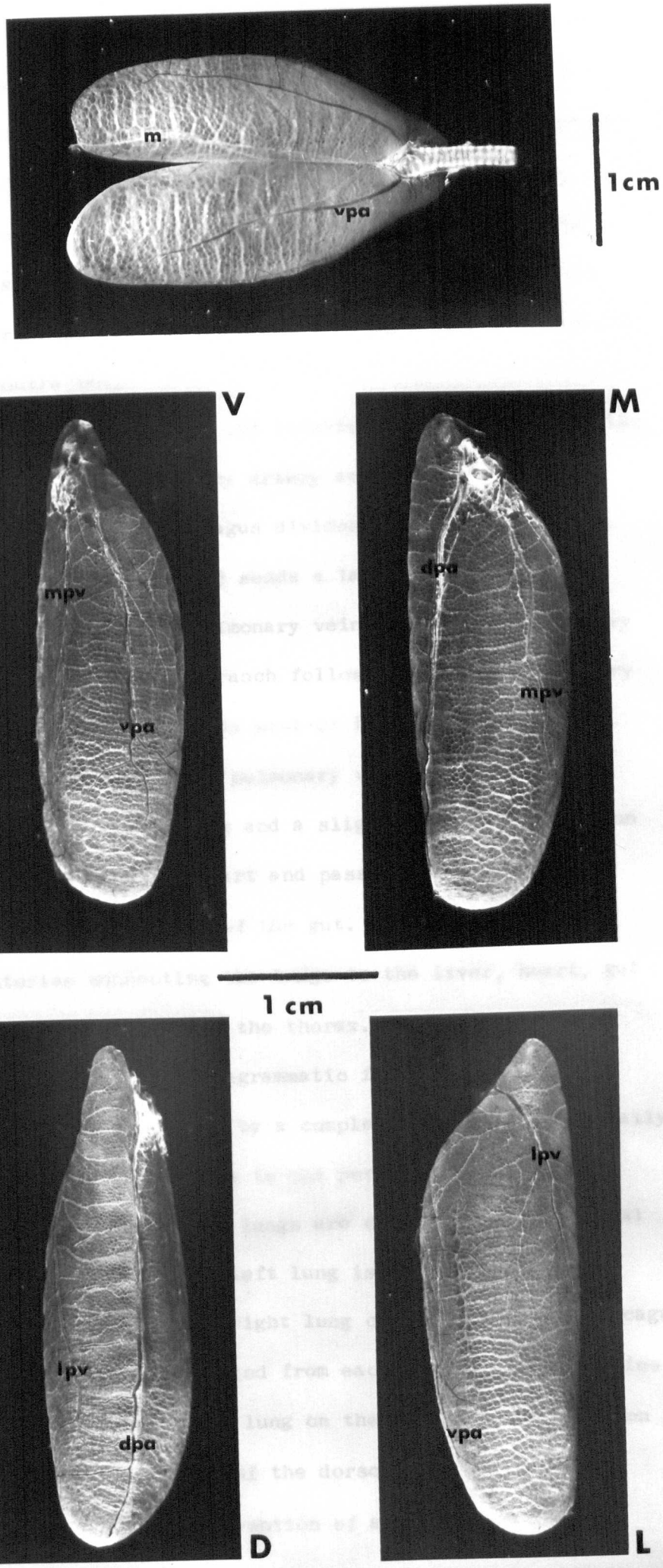
m
vpa
1cm
V
mpv
vpa
M
dpa
mpv
1 cm
lpv
dpa
D
lpv
vpa
L

pulmonary artery it joins with right and left medial pulmonary veins to continue its course across the trachea and then deflects anteriorly towards the heart (Fig. 4.5). After receiving the left lateral pulmonary vein, the four united vessels constitute the left pulmonary vein. There is no right one. Although these veins and arteries are superficial in the lung surface, only the main arteries are raised from the surface (in a convoluted path) when the lung is contracted.

Each vagus nerve, after sending off inferior laryngeal and cardiac branches, follows the path of the pulmonary artery around which it loops (Fig. 4.5). On reaching the lung, each vagus divides into three branches. One follows the lateral pulmonary vein and sends a large branch to innervate the area between the lateral pulmonary vein and ventral pulmonary artery (Fig. 4.5). Another thick vagal branch follows the dorsal pulmonary artery but half way along the lung it sends most of its fibres to the gut. The third vagal branch follows the medial pulmonary vein (which has a slightly dorsal situation in the left lung and a slightly ventral situation in the right) until it meets its counterpart and passes as a single nerve bundle right round to the ventral aspect of the gut.

Pleural mesenteries connecting the lungs to the liver, heart, gut and thoracic cage support the lung within the thorax. The arrangement of these mesenteries is best explained in diagrammatic form (Fig. 4.7). Only the anterior lung lobes are invested by a complete pleura both ventrally and dorsally which has fibrous connections to the pericardium and lateral ribcage (Fig. 4.7a). Both left and right lungs are connected to the dorsal aorta and vertebral column, but only the left lung is directly connected to the lateral wall of the ribcage. The right lung connects with the ribcage only via the liver. The lungs are separated from each other in the mid-line by a mesentery, but movement of the right lung on the gut, of both lungs on most of the liver and both lungs on much of the dorso-ventral surface of the ribcage is intimate without the intervention of a mesentery. Because

FIG. 4.7 Series of anterior to posterior (a to f) transverse sections through the thorax and abdomen (g) to show the mesenteric support (thick line) of the lung. RL, right lung. LL, left lung. T, trachea. G, gut. Li, liver. H, heart. vpa, ventral pulmonary artery. dpa, dorsal pulmonary artery. da, dorsal aorta on vertebral column. The gaps between organs are over-exaggerated for clarity - they are only wide enough to permit a fluid seal.

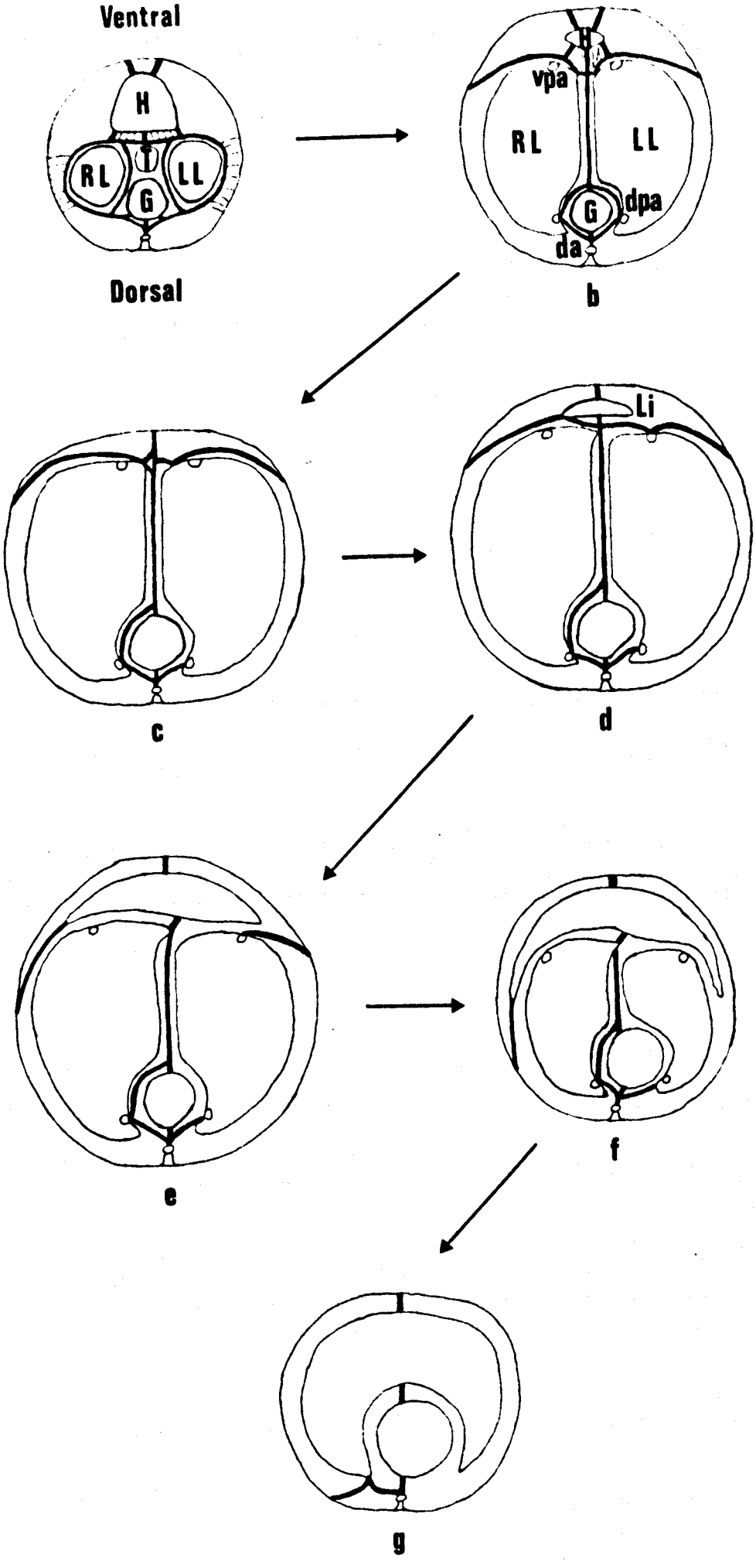
Ventral
H
RL
LL
G
Dorsal
vpa
RL
LL
dpa
G
da
b
Li
c
d
e
f
g

of the non-lobular structure of the Lacerta lung compared with the mammal, its external surface is smooth enough not to require a pulmonary pleura. The mesenteries described here are parietal pleura and are essential for maintaining the fluid seal between lungs and ribcage. In mammals, the only structural connection between parietal and pulmonary pleura is at the anterior tip of the lung (Krahl, 1964). Ribcage anatomy for Lacerta has been adequately described by Nierstrasz & Hirsch (in Storer, Usinger, Stebbins & Nybakken, 1972). There is no diaphragm.

Gross lung architecture

From the external surface of the inflated lung (Fig. 4.6), the tissue can be seen to be divided into small polygonal alveoli. The tissue is dense anteriorly but thin posteriorly and an internal, muscular, trabecular network is easily apparent surrounding a large central air space. When the lung is pinned out to show the internal surface of the peripheral tissue (Fig. 4.8a), this trabecular network is immediately obvious supporting the delicate septa extending to it from the outer wall. This network is continuous with the smooth muscle of the short intrapulmonary bronchus. Fig. 4.8a also shows the marked dorso-medial ridge of tissue extending from the end of the intrapulmonary bronchus to the posterior lung margin. This ridge is composed of alternating partitions of alveolated tissue and of shallow pockets lined by only a few alveoli. There are approximately 14 to 15 pockets. In between the trabecular network are the free endings of septa which terminate at different levels before reaching the network and divide the peripheral tissue into polygonal alveoli which are smaller anteriorly and occupy more layers than in posterior regions (Fig. 4.9).

Transverse wedges of the whole lung clearly show the large central air space with tissue only around the periphery (Fig. 4.10). Paraffin sections show the many configurations of the alveoli in T.S. (tall or short cylinders and polygons) together with the thin primary, secondary and tertiary septa which if they reach the luminal surface thicken with smooth muscle to

FIG. 4.8 (a) Internal surface of the lung showing intrapulmonary bronchus, b, anterior lobe, ant, dorsal ridge, dr, trabecular network, tb, and alveoli.

(b) Internal surface of the lung showing the two main veins, mpv and lpv, and the two main arteries, vpa and dpa. Also enlarged region of the ventral pulmonary artery branching between trabecular network and outer wall.

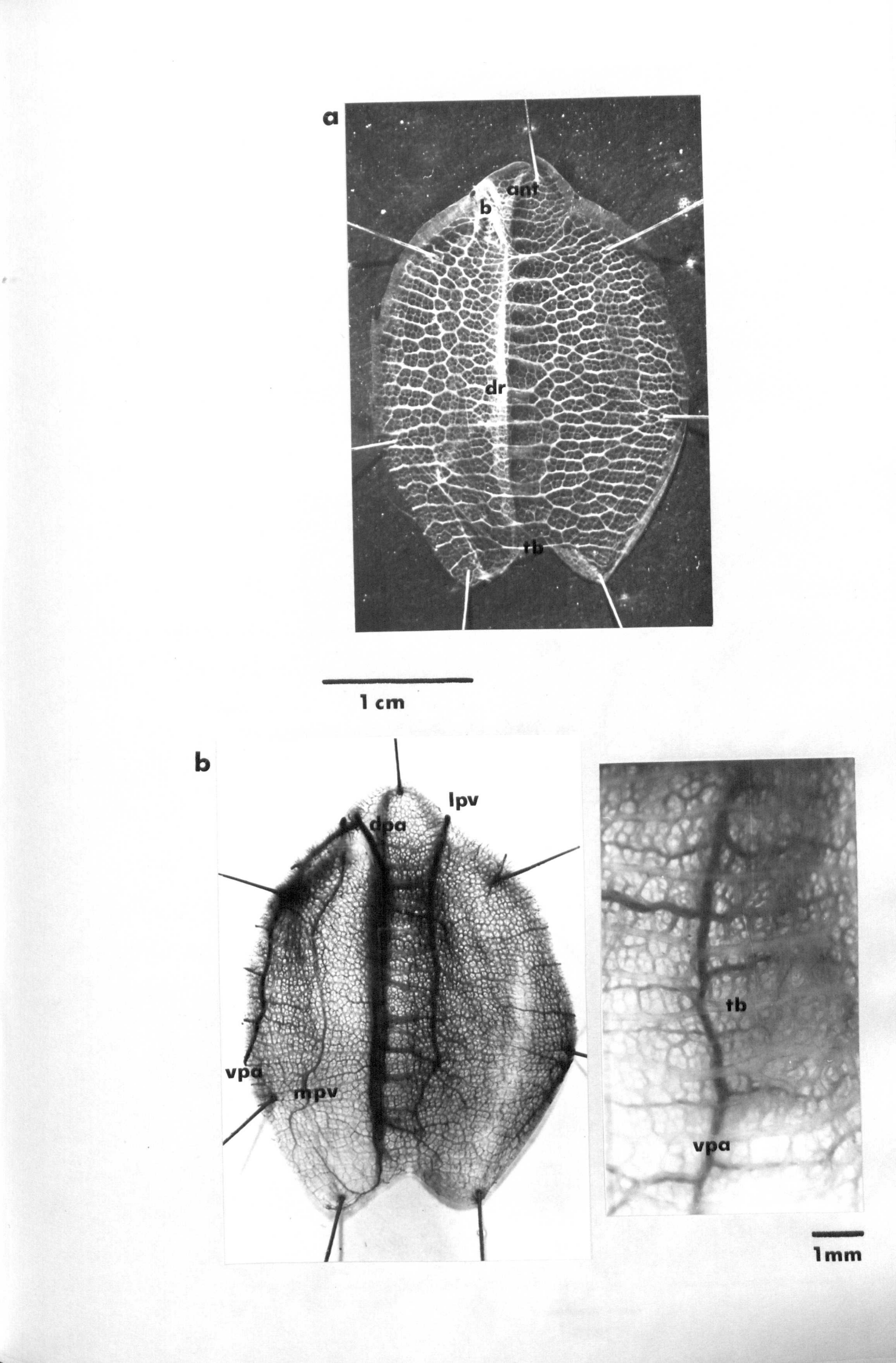
a
ant
b
dr
tb
1 cm
b
lpv
dpa
vpa
mpv
tb
vpa
1mm

FIG. 4.9 Greater detail of anterior, A, posterior, P, and dorsal ridge, DR, regions to show different complexities of alveoli. tb, trabecular network. bv, blood vessel.

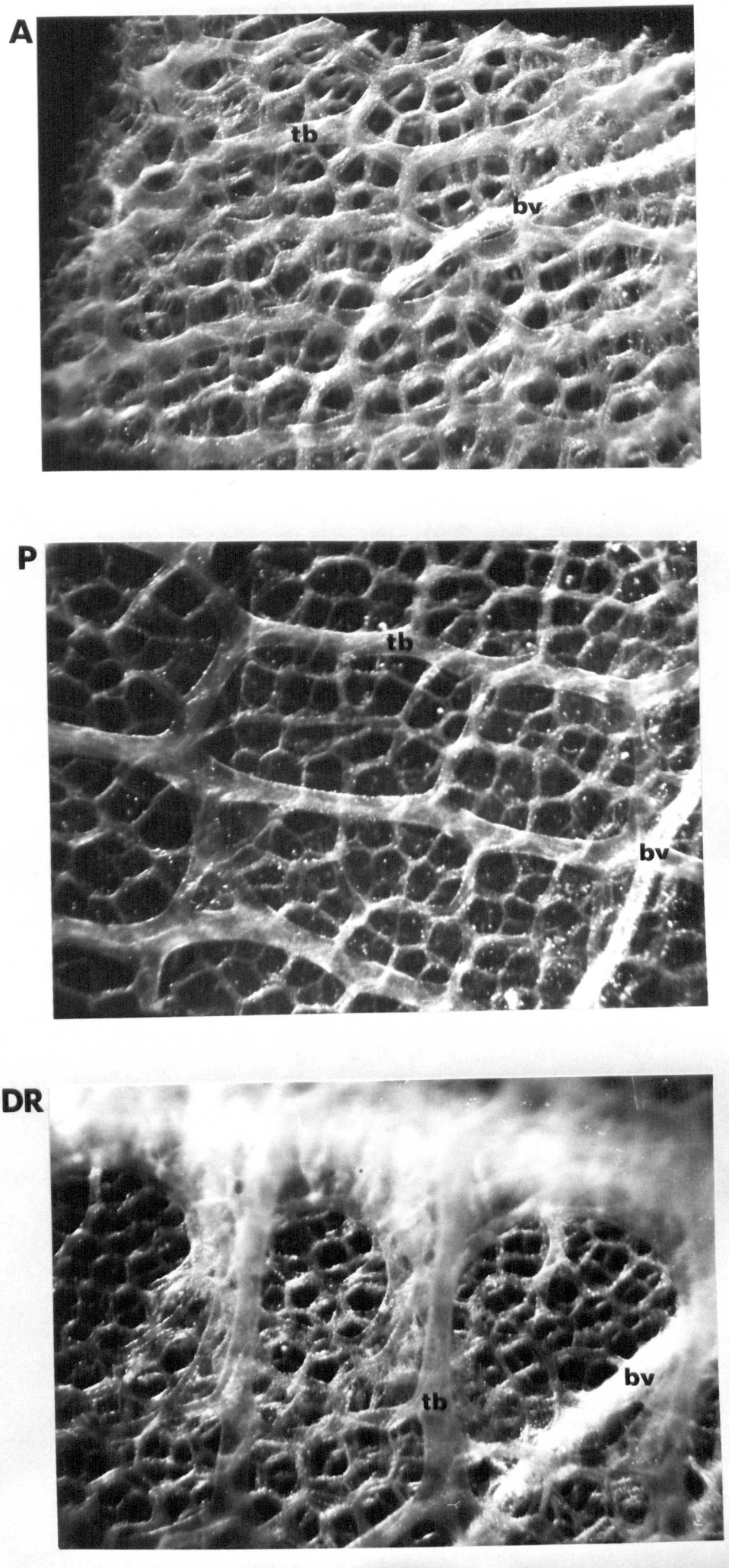
A
tb
bv
P
tb
bv
DR
tb
bv
1 mm

FIG. 4.10 (a) Transverse section of whole lung showing central air space, peripheral alveolar tissue and the dorsal ridge, dr.

(b) Paraffin section (Mallory's triple stain) through pocket of dorsal ridge, and

(c) through partition of dorsal ridge. s, septa. tb, trabecular network of smooth muscle. w, outer wall. dpa, dorsal pulmonary artery. n, vagus nerve. m, mesenteric connection of parietal pleura.

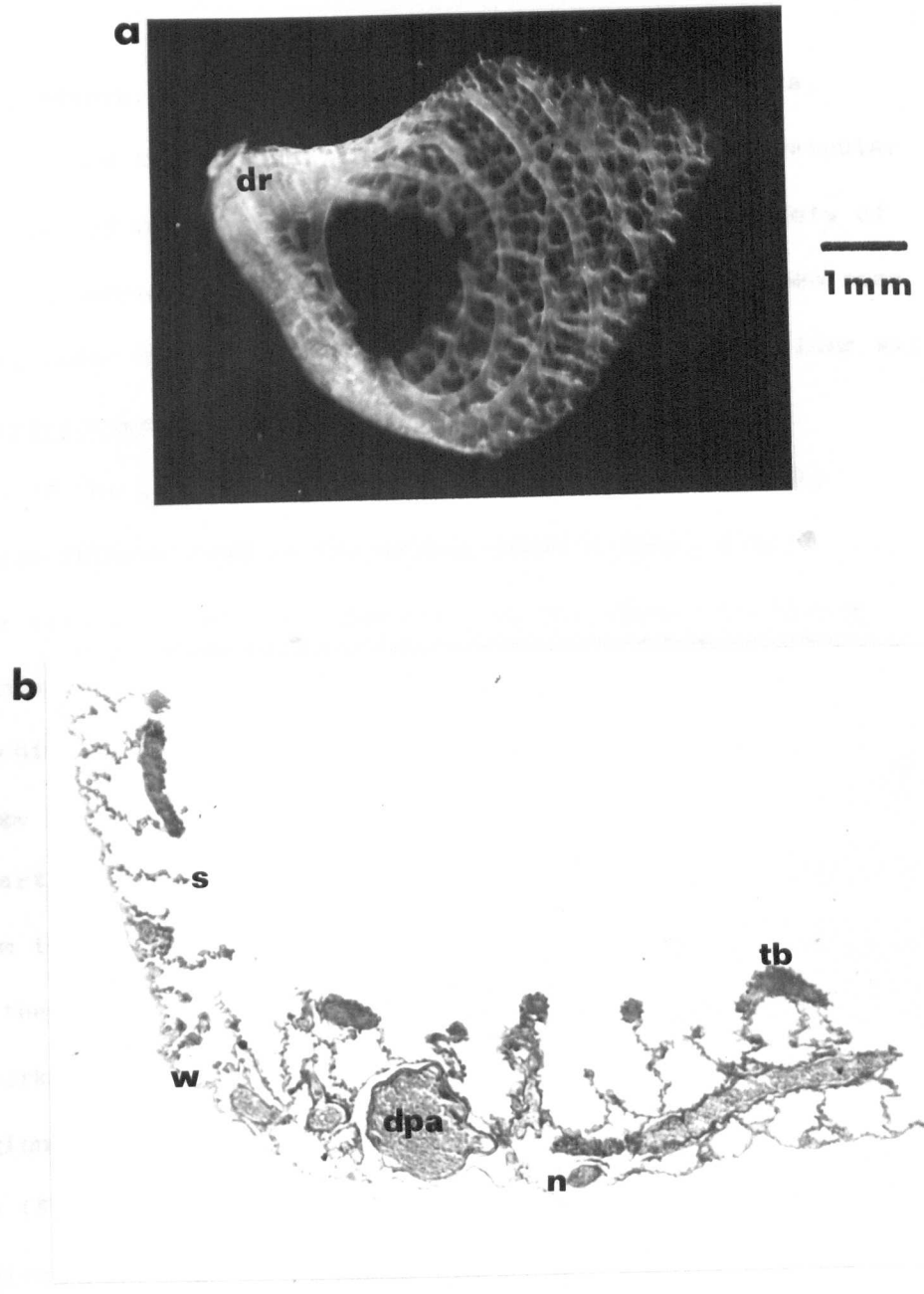
a
dr
1mm
b
s
tb
w
dpa
n
100 µm
c
tb
s
dpa
n
m
w

form the trabecular network. There are many very short primary septa. Fig. 4.10b and c also show the dorsal pulmonary artery and its perivascular space in various stages of branching through the partitions and pockets of the dorsal ridge. The vagus nerve following this artery can also been seen together with a mesenteric connection of the parietal pleura to the lung wall.

Histology and ultrastructure

The walls of the Lacerta trachea, bronchi and intrapulmonary bronchi are very much thinner than in the mammal (Patt & Patt, 1969) because they have a reduced amount of submucosa and perichondrial tissue and lack mucus glands. The loose connective tissue sleeve of the intrapulmonary peribronchium is continuous with that of the pulmonary artery as are also their large peribronchial and perivascular lymphatic spaces (Fig. 4.11b). These conducting cartilaginous airways are lined by ciliated columnar and cuboidal epithelium interspersed with goblet cells (Fig. 4.11c). By the time the walls of the intrapulmonary bronchus has merged with the trabecular smooth muscle network, the epithelium of both luminal and alveolar surfaces is composed of regions of ciliated and non-ciliated cuboidal epithelium and lacks goblet cells (Fig. 4.12A, 4.13a, 4.19b, 4.20). Interspersed between these cuboidal regions are areas containing respiratory capillaries and Type I and II epithelial cells. In the terrapin, goblet cells have been found, however, on the trabecular network (Perry, Albright & Patt, 1970, Perry, 1971).

At the light microscope level, the alveolar septa of Lacerta can be seen supporting a double protruding capillary network (Fig. 4.11a). Capillaries (10 to 15 μm in diameter) on either side of a septum may appose each other or may lie partially or completely unapposed with varying degrees of interstitial and epithelial thicknesses on one surface. Sometimes a capillary will have very thin walls on both sides. Thus although a double capillary network predominates, a single network, similar to the mammal, is in places present. Because of the extensive capillary bulging and the fact that only a small part of each capillary is embedded in interstitium away

FIG. 4.11 1 μm epon sections stained with methylene blue showing (a) double and single capillary networks, cap, large vein without a perivascular space, V, alveolar air spaces, al, outer wall, w, and nerve bundle, n, containing myelinated and non-myelinated fibres,

(b) intrapulmonary bronchal lumen, br, bronchal cartilage, cart, connective tissue of peribronchium, ct, perivascular and peribronchial lymphatic space, ls, pulmonary artery, A, and smooth muscle of trabecula, tb, which is closely associated in this photograph with an arteriole, and

(c) ciliated columnar epithelium, cil, of bronchus, goblet cells, gb, and lymphatic vessels, lv, of connective tissue of peribronchium, ct.

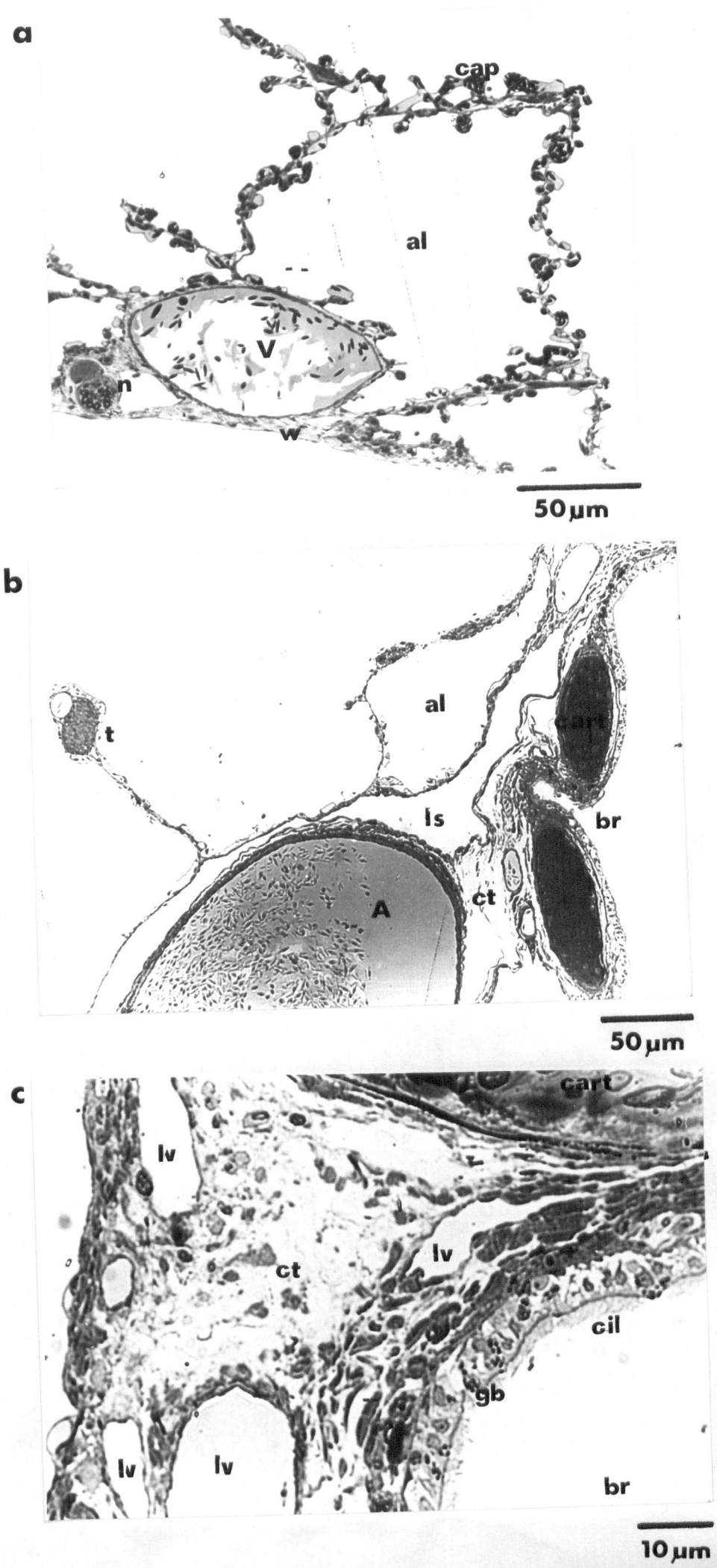
a
cap
al
V
n
w
50 µm
b
t
al
cart
ls
br
A
ct
50 µm
c
cart
lv
lv
ct
cil
gb
lv
lv
br
10 µm

FIG. 4.12 1 μm epon sections stained with methylene blue showing

A. high capillary density on septa in anterior lung regions, regions of respiratory capillaries and ciliated cuboidal epithelium lining the trabecular network and large nerve bundle, and

P. low capillary density on septa in posterior lung regions and large blood vessel, bv, branch lying within trabecular network.

Symbols as in previous figures.

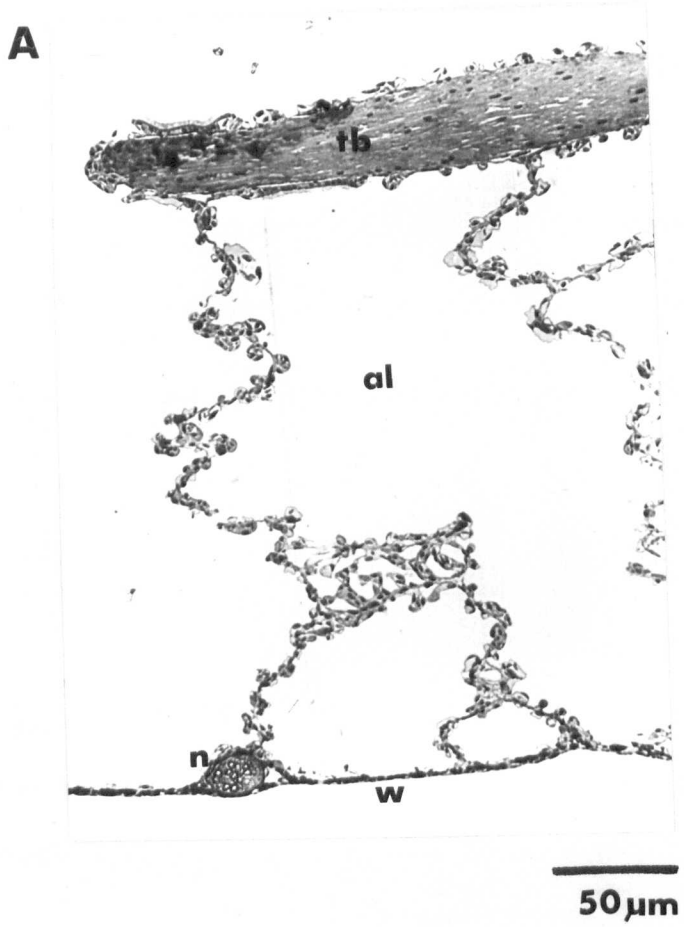
A
tb
al
n
w
50 µm

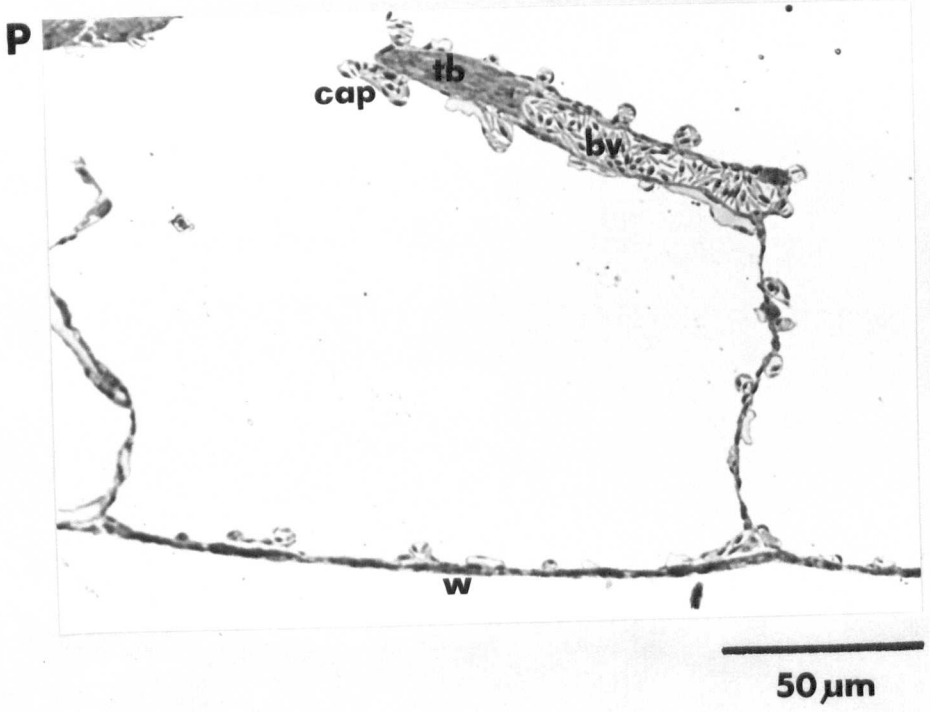
P
cap
tb
bv
w
50 µm

FIG. 4.13 1 μm epon sections stained with methylene blue showing

(a) smooth muscle of trabecula, its respiratory capillaries and a region of non-ciliated cuboidal epithelium, cub. Note also arteriole, Art, nucleated erythrocytes, ery, very thin capillary wall and Type II epithelial cells, and

(b) septa folded in a zig-zag manner and perivascular space, ls, of a main artery. Very little sign of single capillary network in folded septa.

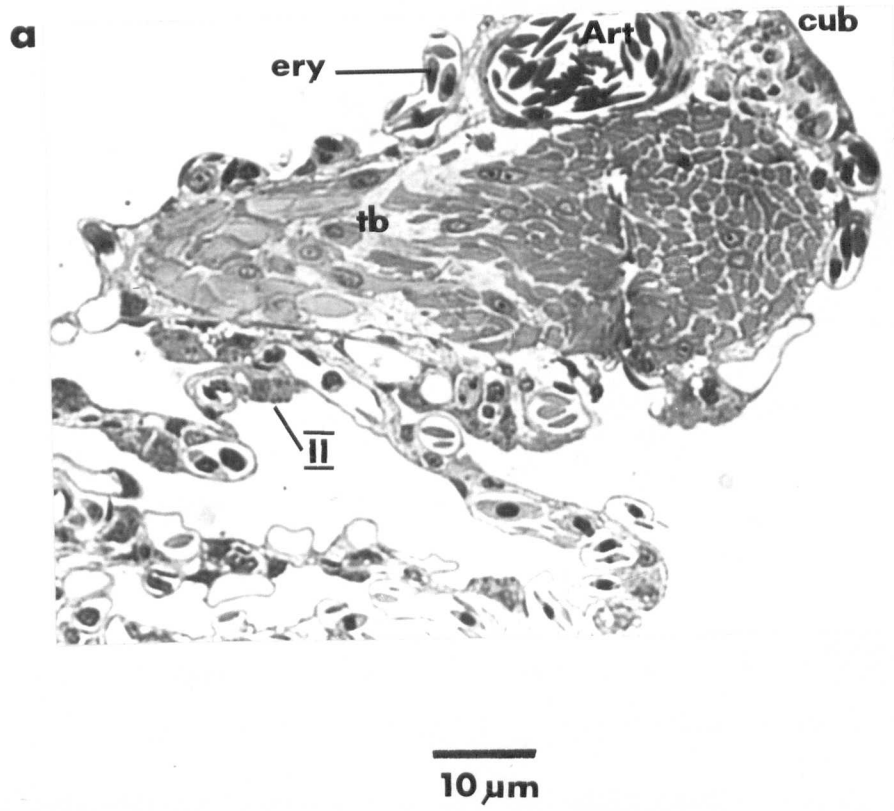
a
ery
Art
cub
tb
II
10 µm

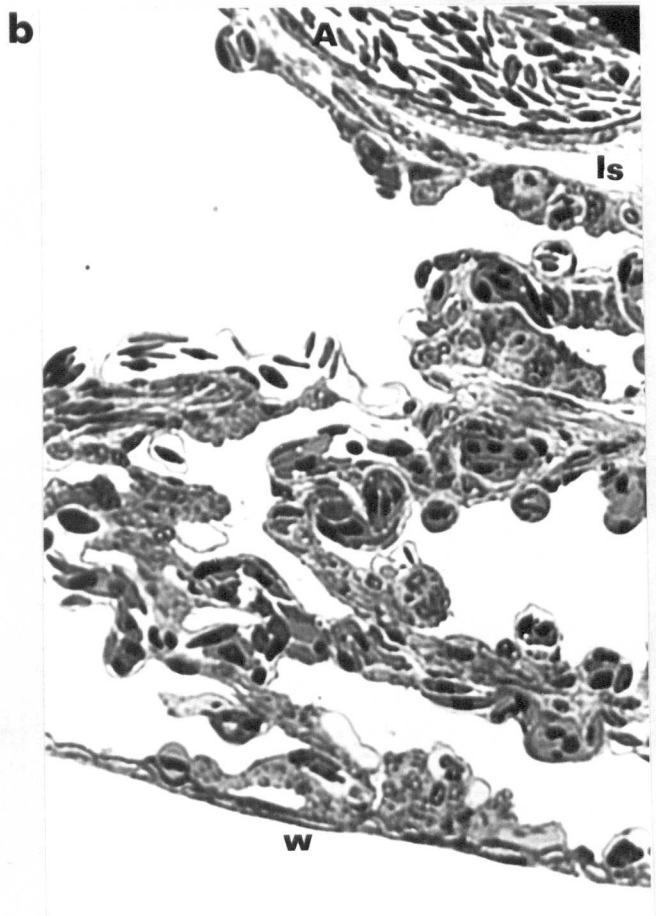
b
A
ls
w

FIG. 4.14 1 μm epon sections stained with methylene blue showing

(a) shallow foldings and mesothelial wrinkles of outer wall, single and double capillary networks, arteriole and Type II cells, and

(b) the above plus smooth muscle core, sm, in septum and at its trabecular tip.

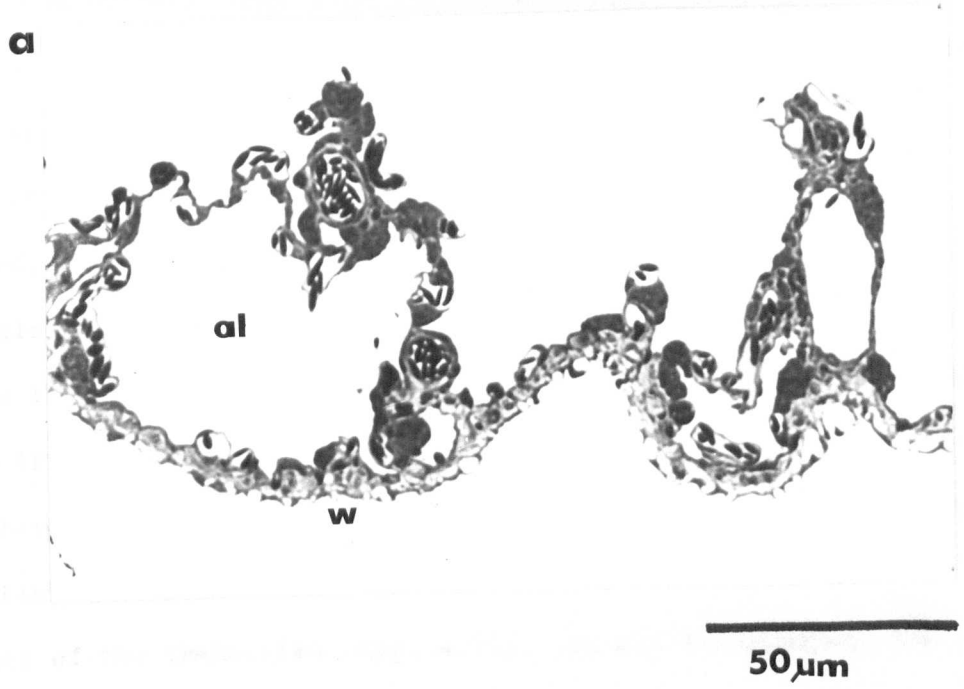
a
al
w
50µm


b
tb
II
Art
sm
w
10µm

from an air to blood pathway, only 16% of the surface area is wasted in terms of gas exchange (Chapter 5). There is a greater density of capillaries on the septa of the anterior and middle lung regions when compared with posterior areas (Fig. 4.12). The septa in between capillaries is usually thinly attenuated.

A single capillary network is found on the outer wall (Fig. 4.12, 4.13b, 4.14), on the septa forming the peribronchial and arterial perivascular lymphatic space (Fig. 4.11b), on the septa attached directly to the walls of veins which have no perivascular space (Fig. 4.11a), on septa attached to nerve bundles (Fig. 4.11a, 4.12A) and on the septa lining luminal and alveolar surfaces of the trabeculae (Fig. 4.12). In all these cases, the capillary is only exposed to air on one side and this network is not, therefore, comparable with the mammalian single capillary network of the septa. It is, however, identical to the single network found on the mammalian outer walls, peribronchial septa, etc.

In fully inflated lungs, the septa are fairly straight (Fig. 4.12) whereas in the partially inflated lung they take on a zig-zag appearance (Fig. 4.13). When fully inflated the external surface of the outer wall is smooth curving outwards slightly in between septa (Fig. 4.12P), but when partially inflated it is thrown into shallow folds and the mesothelium becomes wrinkled (Fig. 4.14). At the points of pleural mesenteric attachment to the outer wall, the mesothelium and interstitium of the latter become continuous with the pleura. Smooth muscle was never found in the interstitium of the pleura, whereas it is frequently present in the outer wall, especially near the roots of a septum. Fig. 4.14b shows the smooth muscle in the core of the septum forming a continuous supporting network between the trabecula and the outer wall. This is in contrast to the work of Burnstock & Wood (1967) in the lizard Trachysaurus in which they found no smooth muscle in the septa or outer wall. Their investigation was, however, only at low magnifications at which it was difficult in Lacerta to identify smooth muscle

other than in the trabecular network.

Large nerve bundles enter the lung to travel near the outer wall (Fig. 4.11a and 4.12A) and not with the trabecular network. The latter, therefore, receives its innervation via the pathways through the septa. This was also found by fluorescent microscopy in Trachysaurus (Burnstock & Wood, 1967). There are myelinated (sensory) and non-myelinated (motor to smooth muscle) fibres (Krahl, 1964).

Greater detail of the structure of the alveolar septum can be seen in the 1 μm epon sections of Fig. 4.13 and 4.14. The capillaries have very thin tissue separating them from the alveolar air and contain spindle-shaped nucleated erythrocytes. In between some capillaries are large, 7 μm, epithelial cells containing vacuoles and/or dark staining granules. These are the Type II epithelial cells. With electron microscopy the finer details of the alveolar septum become clear (Fig. 4.15). The air to capillary barrier is composed of thin squamous Type I epithelial cells separated by the minimum of interstitium from thin endothelial cells. The basement membranes of these cells often fuse (Fig. 4.16a andb).

The nucleus of the Type I cell rarely lies over the capillaries but either protrudes in between capillaries into the interstitium or into the alveolar air space. The perinuclear cytoplasm may contain mitochondria, a golgi complex, a small amount of rough endoplasmic reticulum and free ribosomes. Ribosomes and mitochondria are the only organelles found in the thin cytoplasmic extensions. Numerous micropinocytotic vesicles are present in the cytoplasm opening into the air or interstitium (Fig. 4.16a). Because of the extensive cytoplasmic extensions, non-nucleated portions of Type I cells are frequently found. The endothelium of the capillary is very similar to the Type I cell having organelles concentrated in the perinuclear cytoplasm, thin cytoplasmic walls and larger numbers of micropinocytotic vesicles opening into the blood and into the interstitium (Fig. 4.16a). Endothelial cells also have rod-shaped darkly staining

FIG. 4.15 Electron micrograph of the alveolar septum.

al, alveolar air space. I, type I cell squamous extensions. nI, nucleus of Type I cell. endo, endothelial cell. cap, capillary lumen. ery, erythrocyte. leuc, leucocyte. II, Type II cell with microvilli and lamellated bodies. int, interstitium. sep, septal cells. sm, smooth muscle cells. n, nerve fibres.

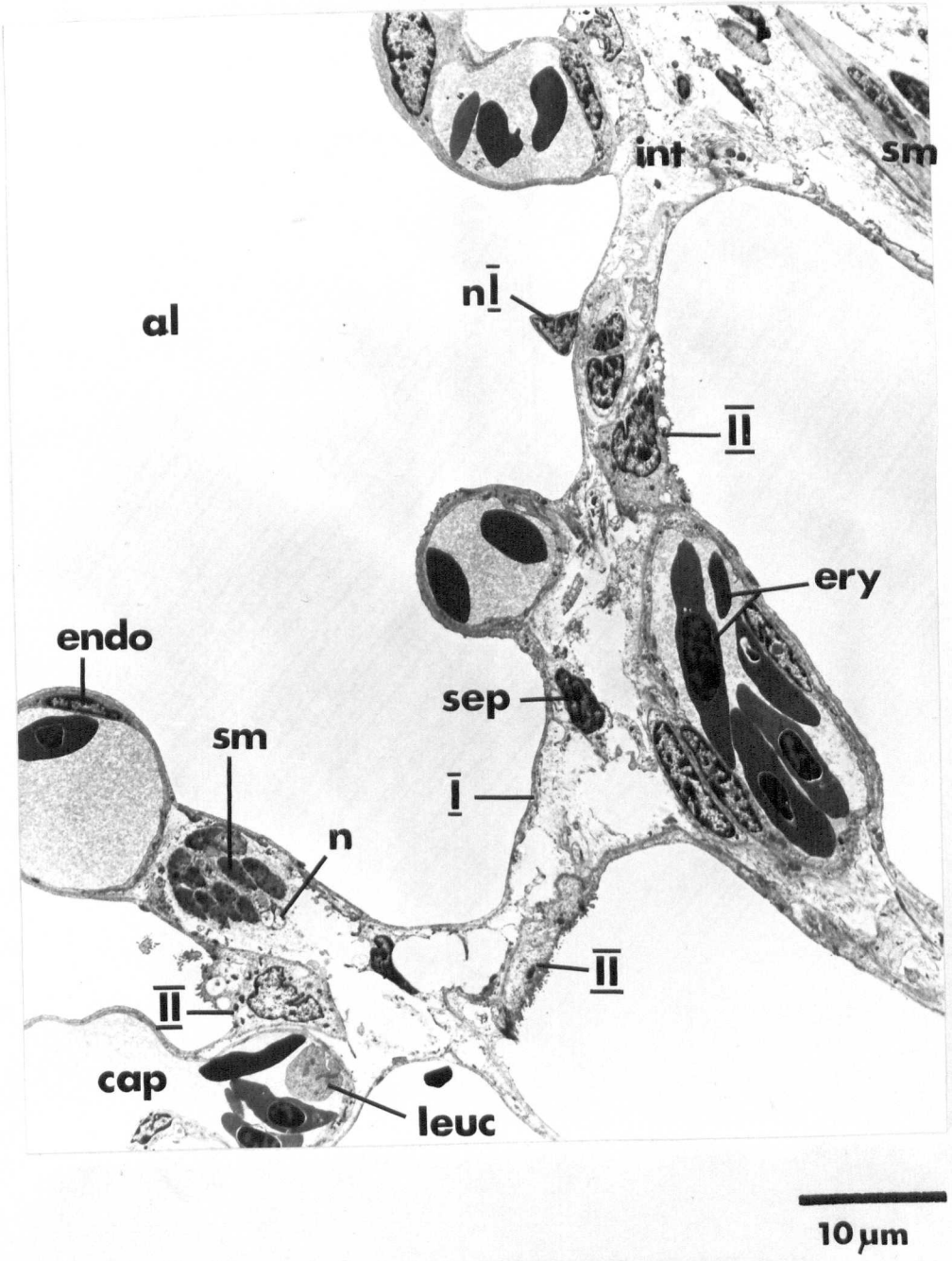
int
sm
nI
al
II
ery
endo
sep
sm
I
n
II
II
cap
leuc
10 µm

FIG. 4.16 (a) Electron micrograph of parts of endothelial cell, Type I cytoplasmic extensions and Type II cell. al, alveolar air space. bm, basement membranes, peri, pericyte. int, interstitium. lip, lipid droplet. mit, mitochondria.

(b) Electron micrograph of Type I cytoplasmic extension, junction of two endothelial cells, endo, with collagen, col, in the interstitium

(c) Electron micrograph of endothelial cell showing rod-shaped darkly staining organelles, R, and similar bodies with stain only around the rim, B.

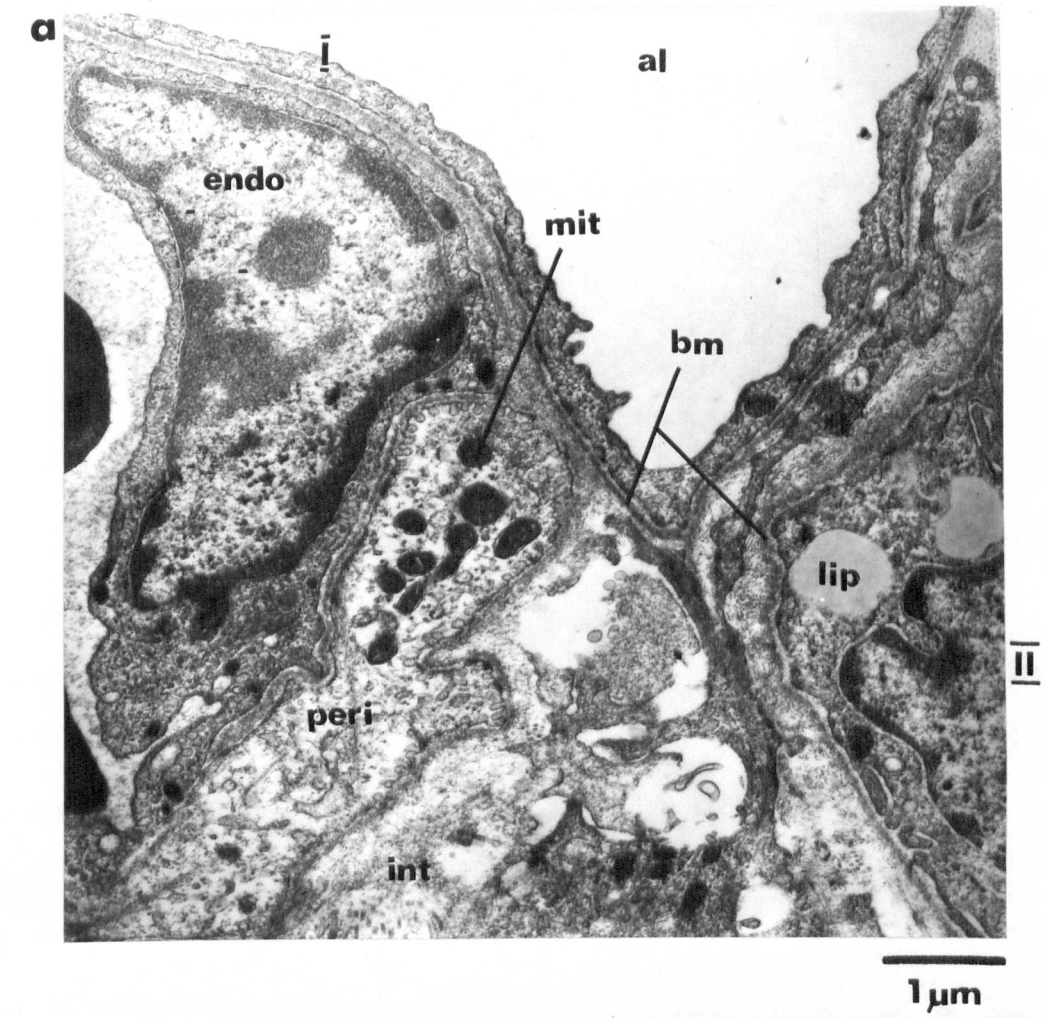
a
I
al
endo
mit
bm
lip
II
peri
int
1 µm
b
al
endo
cap
mit
I
col
bm
0.5 µm
c
B
R

FIG. 4.17 (a) Electron micrograph of Type II cell showing microvilli, mv, with extracellular fuzz, lamellated bodies, LB, mitochondria, mit, multilobed nucleus, nu, golgi complex, go, small osmiophilic vesicles, v, and interdigitating cytoplasmic processes, cp. Also note part of Type I cell and the alveolar air space, al.

(b) Electron micrograph of 3 Type II cells. lip, lipid droplets amassing osmiophilic lamellated material. sLB, small lamellated bodies. gmf, globular myelin figures. fl, amorphous flocculent material of surfactant. col, collagen. w, mesothelium of outer lung wall.

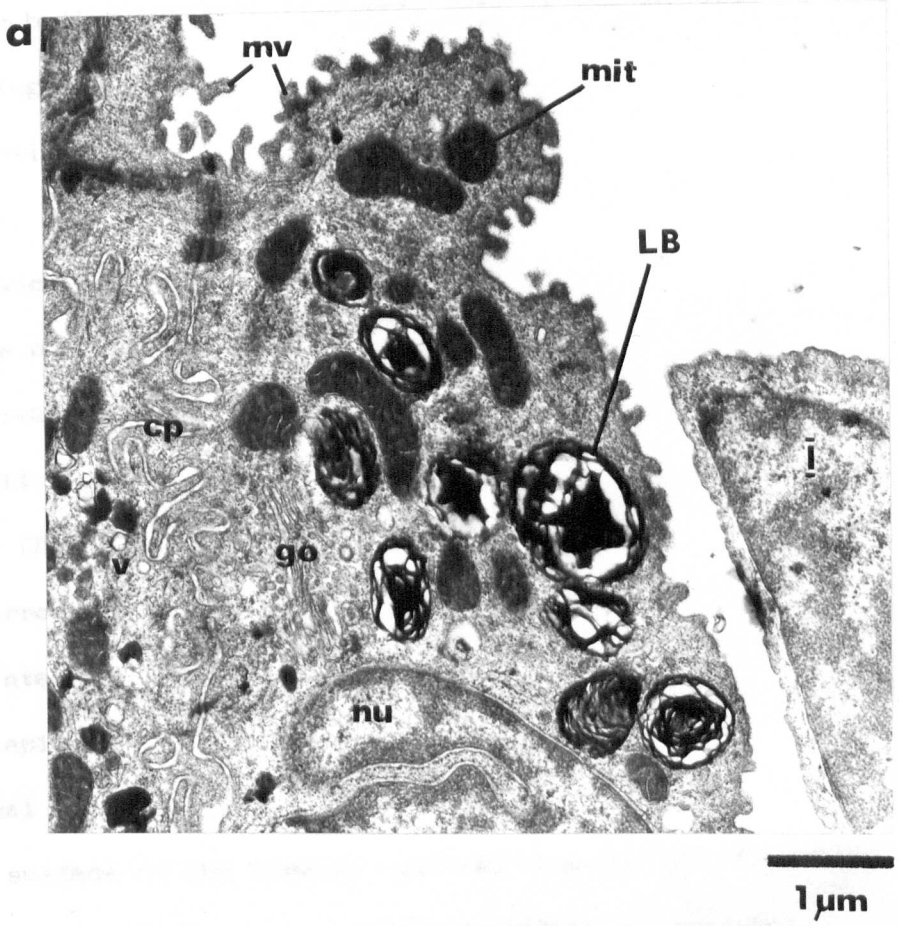
a
mv
mit
LB
cp
v
go
nu
l
1 µm

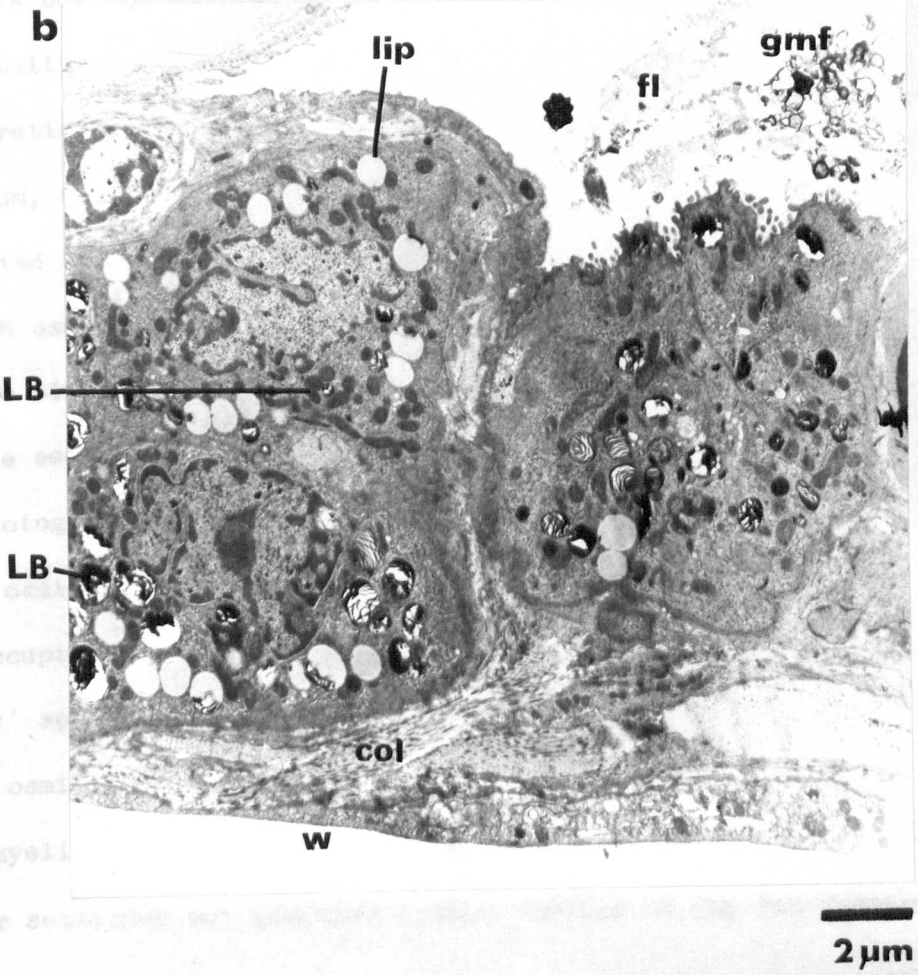
b
lip
gmf
fl
sLB
LB
col
w
2 µm

organelles and similar bodies but with the stain only at the rim (Fig. 4.16c). Only the darkly-staining ones have been found in mammals (Weibel & Palade, 1964), in frogs (Steinsiepe & Weibel, 1970) and in endothelial-type cells of fish gills (Morgan & Tovell, 1973). Sometimes a pericyte accompanies part of the endothelial cell and their basement membranes fuse. Both Type I and endothelial cells have narrow, but not tight, intercellular junctions with terminal bars at intervals.

Large Type II cells are found with their base protruding deep into the interstitium (Fig. 4.15) so that in some planes of section this cell is completely surrounded by its basement membrane and the interstitium with no obvious air interface. The junction of Type II with Type I cells to form a continuous epithelium is by open intercellular junctions usually with extensive terminal bars. The basement membranes of the two are continuous. The air surface of the Type II cell has numerous short microvilli (0.1 μm wide and 0.2 to 0.3 μm in length) which have no internal cytoplasmic filaments but are covered by an extracellular fuzz (Fig. 4.17a). These cells have a multilobed nucleus and cytoplasm rich in organelles; smooth endoplasmic reticulum, a golgi complex, free ribosomes, some rough endoplasmic reticulum, numerous mitochondria, large lipid droplets, large osmiophilic lamellated bodies, small dense osmiophilic bodies and small vesicles coated with osmiophilic material around the periphery (Fig. 4.16a, 4.17). There are no pinocytotic vesicles.

A possible sequence for the formation of the lamellated bodies is suggested by the photographs of Fig. 4.17. Large lipid droplets can accumulate or form osmiophilic material which begins near the rim and extends until it occupies the whole of the droplet, taking a lamellated appearance. 'Empty' spaces then begin to appear amongst the lamellae and some or all of the osmiophilic material is extruded into the air space to form the globular myelin figures of the surfactant (Fig. 4.17b). An actual expulsion was never sectioned but globular myelin figures in the air frequently

bore strong resemblance to the lamellated shapes of the lamellated bodies. Completely empty vacuoles are sometimes found. A second sequence of small vesicles coated with osmiophilic material growing into small dense osmiophilic bodies which enlarge into lamellated bodies is also possible in Fig. 4.17b. The surfactant system of the lung was preserved by airway fixation as flocculent material trapped amongst the microvilli of Type II cells or in small clumps loose in the air space and mixed with globular myelin figures. Tubular myelin figures were never found.

When Type II cells occurred in groups their lateral borders became extended into numerous long slender cytoplasmic processes (0.07 μm wide and 0.3 to 1.3 μm in length) which interdigitated with other cells of the group (Fig. 4.17a). These processes had no cytoplasmic filaments and there was no basement membrane between such neighbouring cells. Sometimes the intercellular junctions greatly enlarged though still filled with many cytoplasmic processes. This is believed to be the process of desquamation of a Type II cell into the air space to form an alveolar macrophage (Fig. 4.18a). Another Type II cell is still left beneath it to maintain the continuity of the alveolar epithelium. Globular myelin figures were often found in the enlarged junctions.

Because of the method of fixation alveolar macrophages were not found free in the air spaces. A mass of entrapped sputum was, however, found (Fig. 4.18b). It contained alveolar macrophages, leucocytes and phagocytosed material. The macrophages had lost the microvilli but still had many cytoplasmic processes. Lipid droplets, lipid with an osmiophilic rim and a few lamellated bodies were also present, but the predominant feature was the numerous large vacuoles containing large densities of globular myelin figures which later became incorporated into the cytoplasm without a limiting membrane.

Occasionally, Type II cells were found with thin, short cytoplasmic extensions that sometimes formed the epithelium of the air to blood barrier

FIG. 4.18 (a) Electron micrograph of Type II cells desquamating. Symbols as in previous figures.

(b) Electron micrograph of sputum. al.m, alveolar macrophage. leuc, leucocyte. lip, lipid droplets. vac, vacuoles. gmf, globular myelin figures in many forms. Note other phagocytosed material.

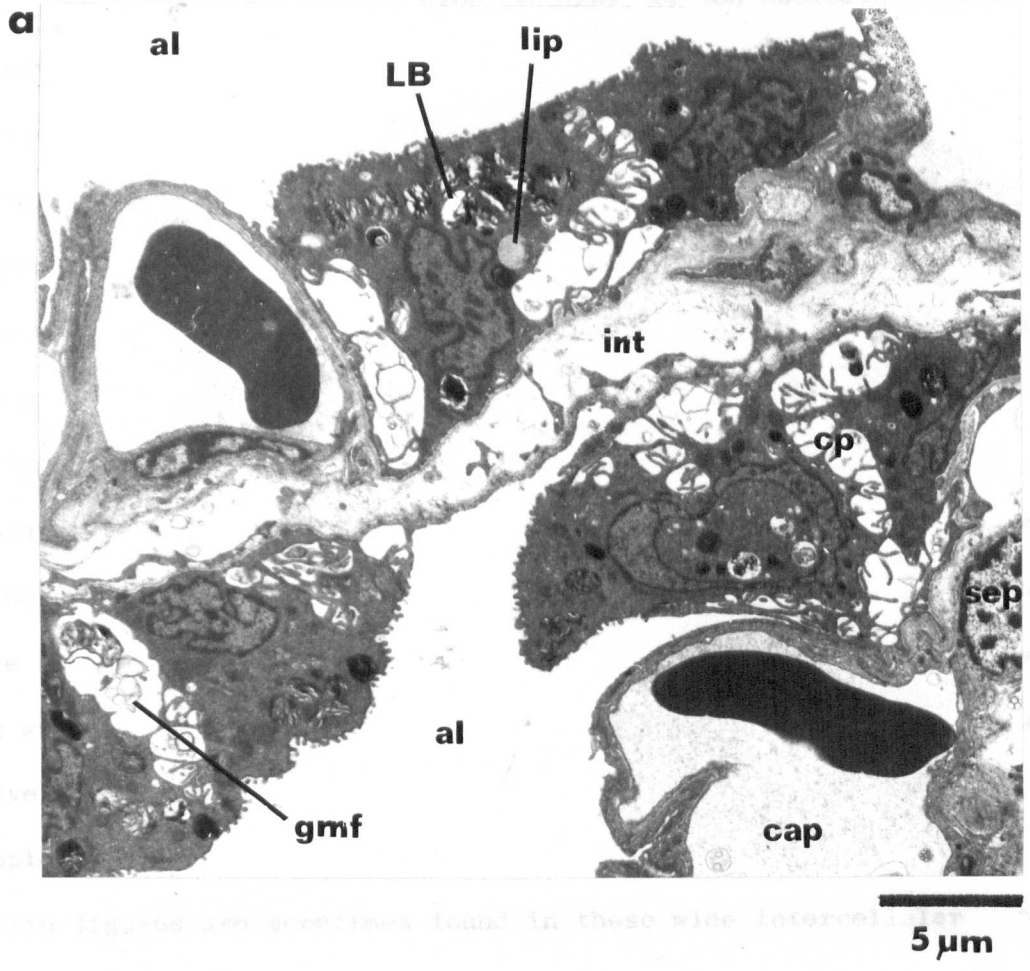
a
al
LB
lip
int
cp
sep
al
gmf
cap
5 µm
b
gmf
lip
al.m
vac.
leuc
gmf
5 µm

(Fig. 4.19a). These extensions could even be found as non-nucleated plates but distinguishable from Type I cells by their microvilli. Although these particular Type II cells have a multilobed nucleus, their cytoplasm is not rich in organelles and there is only the occasional lamellated body. This may represent a Type II cell transforming into a Type I.

The non-ciliated cuboidal epithelium lining regions of the trabecular network have microvilli at the air surface, identical in size and structure to those of Type II cells (Fig. 4.19b). They also possess the occasional lamellated body, lipid droplets (looking like empty vacuoles in this section because of the effect of storage in glutaraldehyde) and an occasional globular myelin figure free in the cytoplasm. The nucleus, however, is not lobulated and its long axis lies orientated parallel to the air surface. Intercellular junctions have narrow regions with terminal bars and wide regions with slender cytoplasmic processes interdigitating with those of neighbours. Globular myelin figures are sometimes found in these wide intercellular regions. It is possible that non-ciliated cuboidal epithelium may represent a stem cell for Type II cells. It may even have phagocytotic properties.

The ciliated cuboidal epithelium of the trabecular network has typical cilia, basal bodies and cross-striated rootlets together with numerous long microvilli (0.1 to 0.13 μm in width and approximately 0.8 μm in length) which are supported internally by cytoplasmic filaments. There is no extracellular fuzz around these microvilli (Fig. 4.20). The nucleus is not lobulated and its long axis is orientated parallel to the air surface. The cytoplasm contains a large number of mitochondria, free ribosomes and lipid vacuoles of varying staining density. Airway brush cells, sensory receptors or Clara cells were not encountered in the trabecular epithelium of Lacerta.

The long rod-shaped, smooth muscle cells of the trabeculae (Fig. 4.20a), arteries (Fig. 4.21b), veins and interstitium of the alveolar septa (Fig. 4.15) are arranged in bundles separated by a network of collagen

FIG. 4.19 (a) Electron micrograph of Type II cell showing a microvillied cytoplasmic extension. A leucocyte, leu, possibly a lymphocyte, is in the capillary lumen.

(b) Electron micrograph of non-ciliated cuboidal epithelium showing microvilli, mv, lamellated bodies, LB, globular myelin figure, gmf, free in the cytoplasm and interdigitating cytoplasmic processes, cp. Note septal cell, sep, in interstitium and smooth muscle cell, sm.

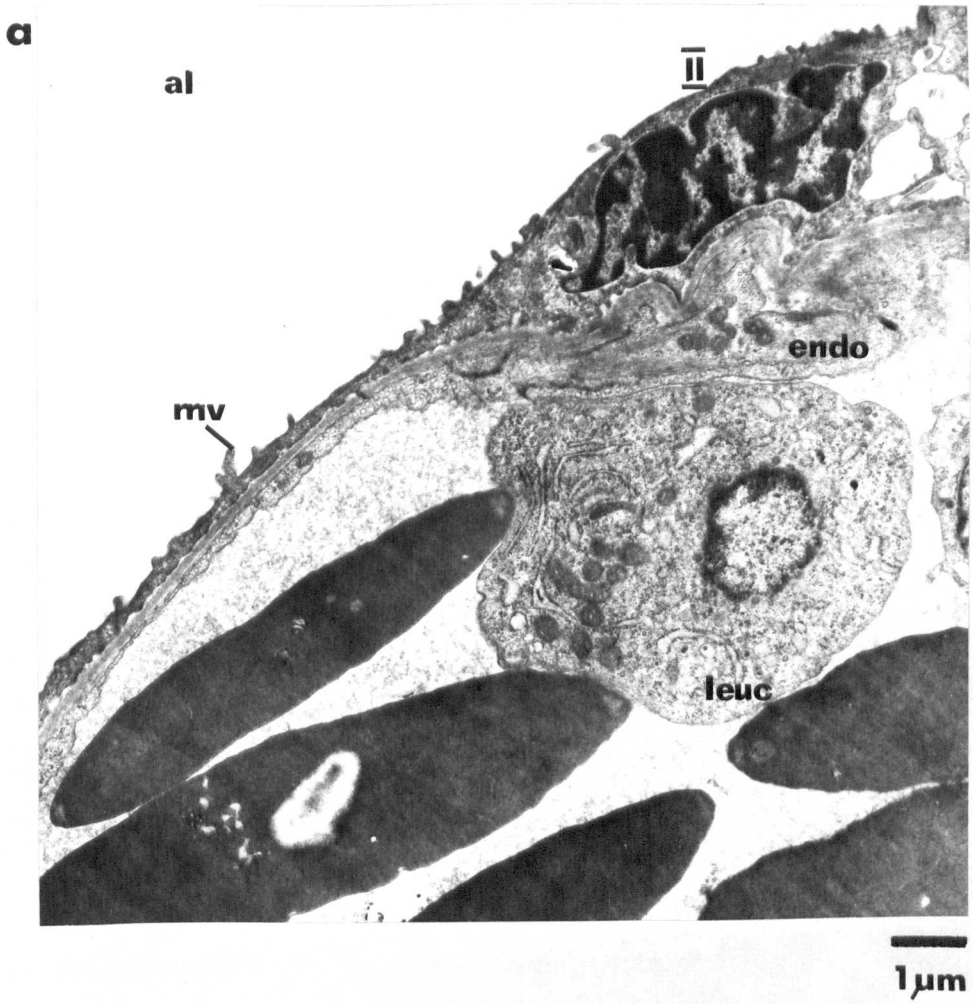
a
al
II
endo
mv
leuc
1 µm

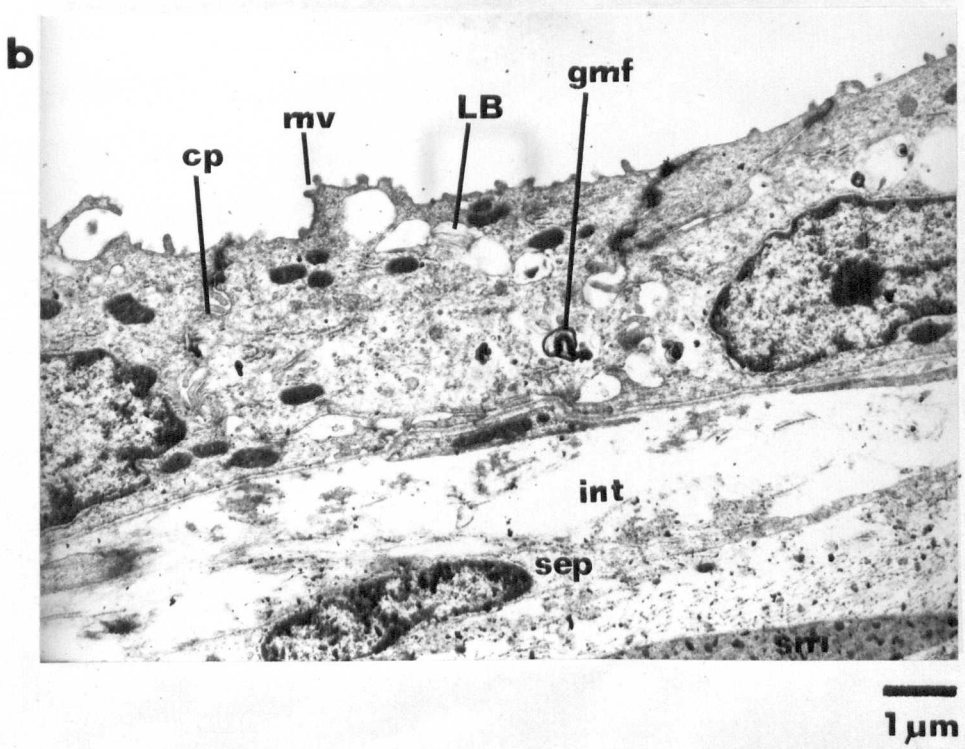
b
gmf
mv
LB
cp
int
sep
1 µm

FIG. 4.20 (a) Electron micrograph of ciliated cuboidal epithelium. Note cilia, cil, microvilli, mi, lipid droplet, lip, septal cells, sep, and smooth muscle cells, sm.

(b) Electron micrograph of ciliated cuboidal epithelium and plasma cells beneath, pl, with greatly enlarged cisternae.

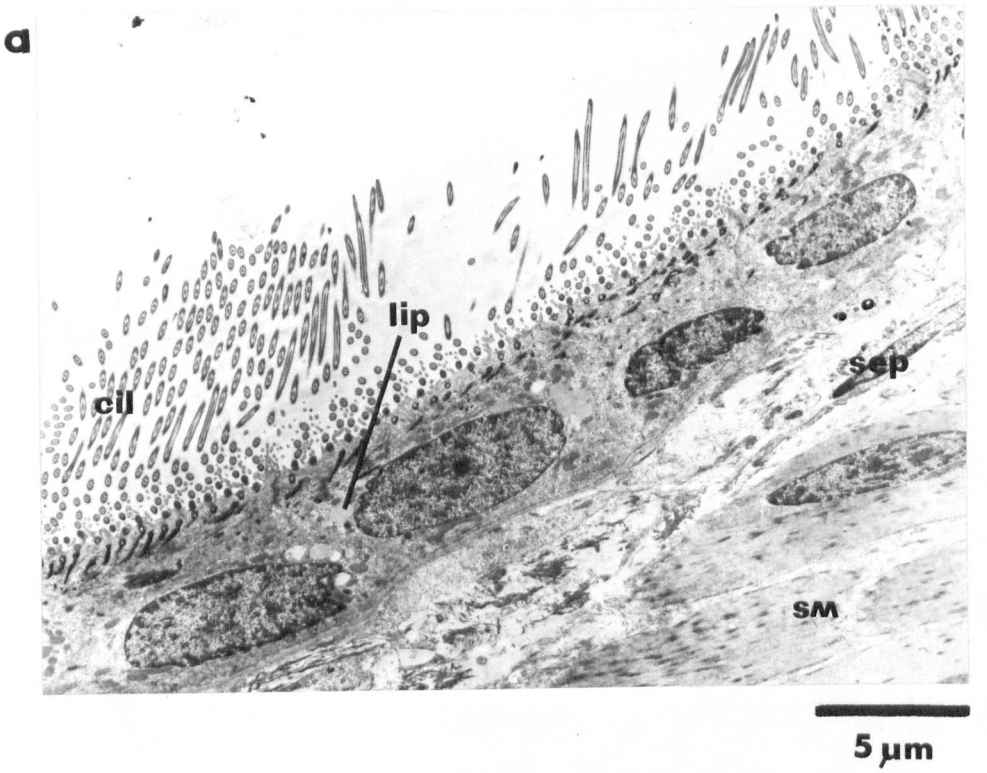
a
lip
cil
sep
SM
5 µm

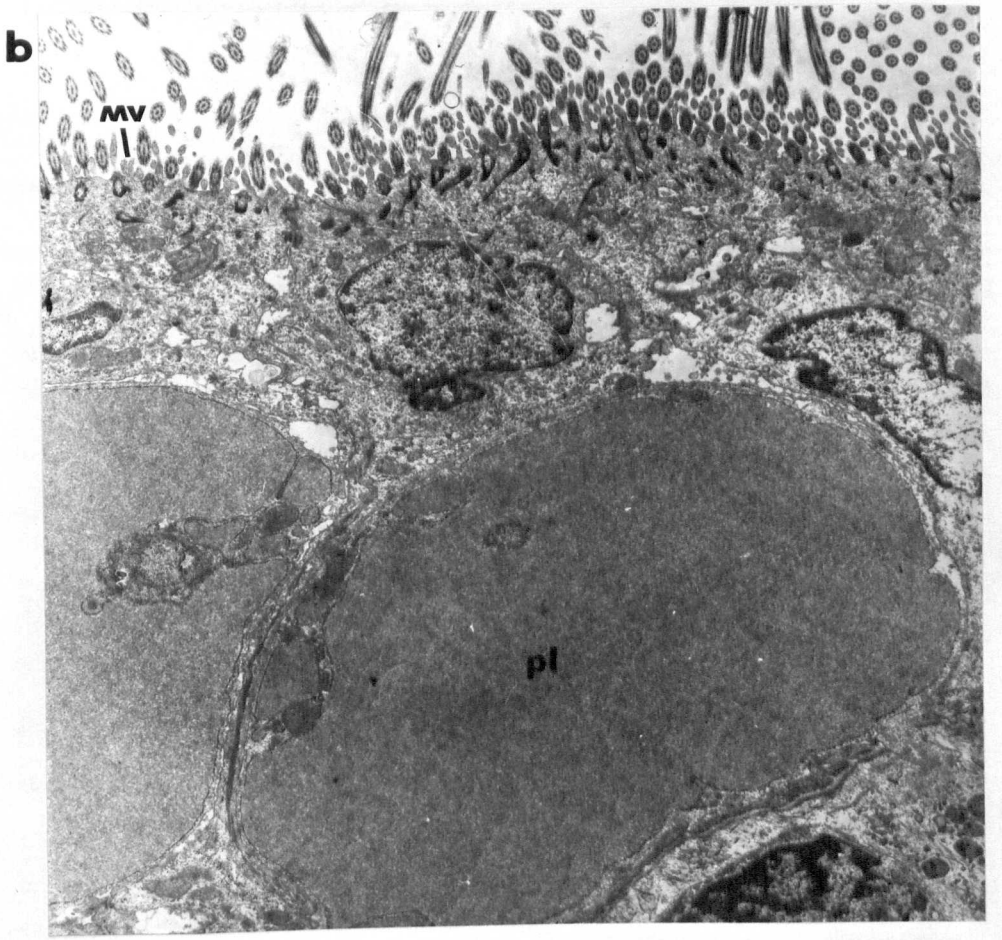
b
MV
pl
2 µm

FIG. 4.21 (a) Electron micrograph of alveolar septum. al, alveolar air space. cap, capillary. nI, nucleus of Type I cell. int, interstitium. sep, septal cells. pl, plasma cells. ls, lymphatic space.

(b) Electron micrograph of large artery, A, and its perivascular lymphatic space, ls. Note R, rod-shaped endothelial bodies arranged in groups, sm, smooth muscle cells in arterial and septal wall, and ly, lymphocyte and gmf, globular myelin figures in the lymphatic space.

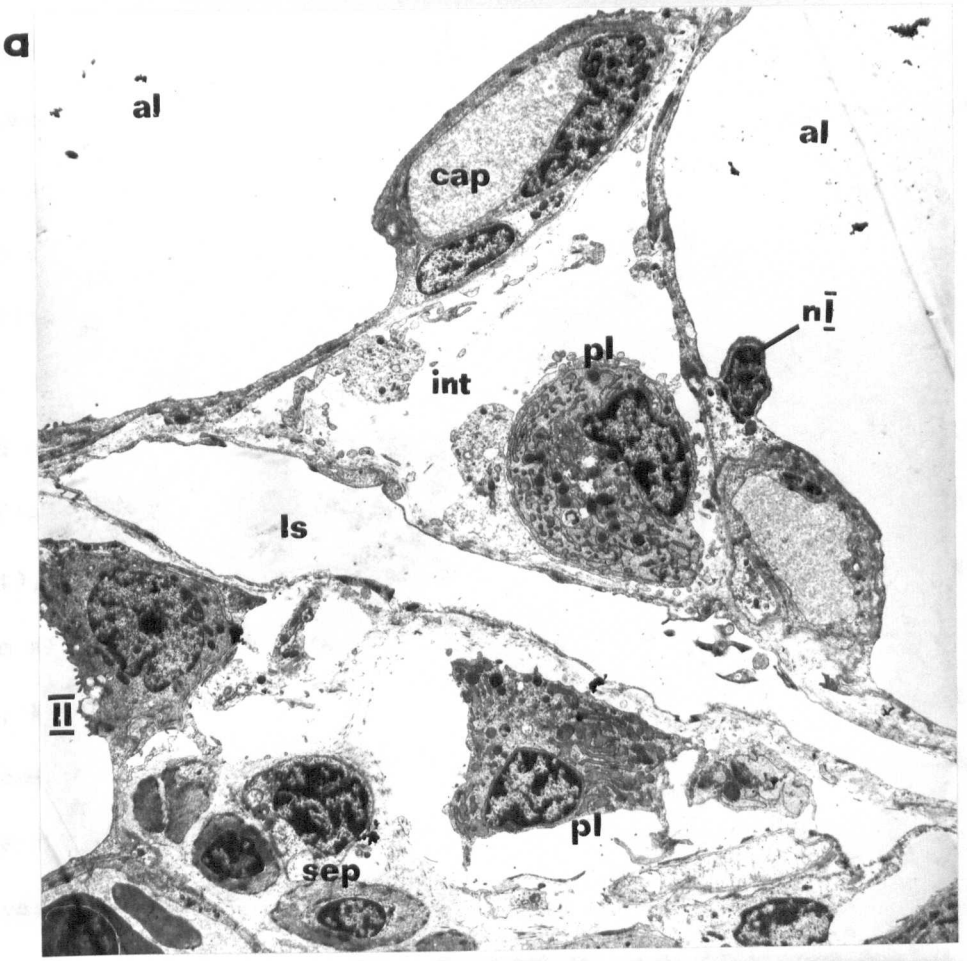
a
al
cap
al
nI
pl
int
ls
II
pl
sep
5 µm

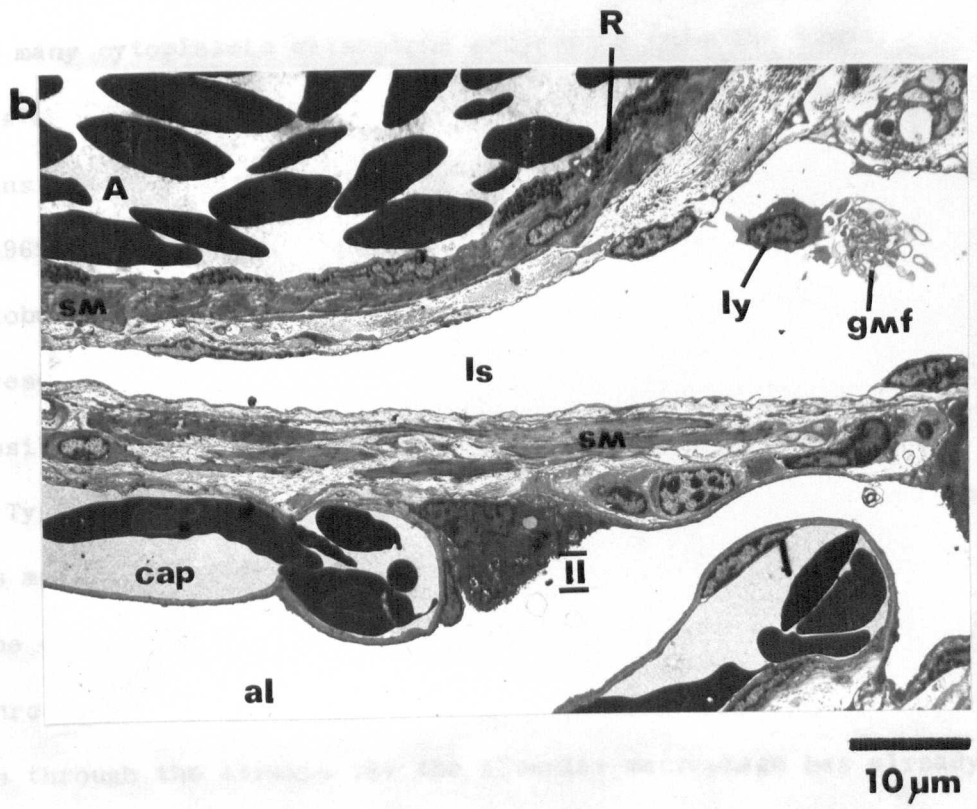
b
R
A
sM
ly
gMf
ls
sM
cap
II
al
10 µm

and elastic fibres and supplied by non-myelinated nerve fibres. Capillaries were never found amongst the smooth muscle cells, not even in the thick trabecular network. Presumably diffusion of nutrients from the respiratory capillaries is adequate.

Some of the components of the lung interstitium are illustrated in Fig. 4.21a. Within its loose amorphous structure there is a network of collagen (Fig. 4.16b) and elastic fibres together with smooth muscle cells, myelinated and non-myelinated nerve bundles and fibres, fibroblasts, small septal cells (less cytoplasm and paler staining nuclei when compared with the fibroblast), lymphocytes, granular leucocytes and plasma cells. This is similar to the mammalian interstitium (Brinkman, 1968, Curry, Simon & Ritchie, 1969, Murata & Spicer, 1974, Rybicka, Daly, Migliore & Norman, 1974). Neither mast cells nor alveolar macrophages were present. Lymphatic channels lie within the interstitium (Fig. 4.21a) and are continuous with that of the arterial perivascular space (Fig. 4.21b). Lymphatic endothelium is very thin (0.1 μm) and wrinkled and is characterised by very flattened nuclei, large pinocytotic vesicles, rod-shaped components of capillary endothelium, large areas of overlapping endothelial cells with many open intercellular junctions and many cytoplasmic extensions projecting into the lumen. This is very similar to the endothelium of intestinal lacteals in the mammal (Dobbins & Emory, 1970) and to mammalian lung lymphatics (Lauweryns & Boussauw, 1969). Within the lymphatic lumen, lymphocytes, a little plasma and globular myelin figures were found but alveolar macrophages were never present.

Possible remnants of globular myelin figures were found in the cytoplasm of Type I cells, the interstitium and in the endothelium and its plasma. This may support Dermer's (1970a) route for surfactant removal. Because of the obvious globular myelin figures in the lymphatic channels, some route through the alveolar septa to these channels must exist. A third route through the airways via the alveolar macrophage has already been described.

Plasma cells found in the interstitium (Fig. 4.21a) of the alveolar septum or beneath the trabecular epithelium had a smooth cell surface with no cytoplasmic projections, many mitochondria, free ribosomes, a golgi complex and large cisternae of rough endoplasmic reticulum. The latter is the distinctive feature of the plasma cell and varies in shape from narrow tubes to a form greatly distended by low electron dense flocculent material (Fig. 4.20b). Dense granules are sometimes present in the cisternae (Fig. 4.21a). These plasma cells are identical to those of mammals (Rhodin, 1963, 1974). A plasma cell was only found once in a capillary during this study. The ultrastructure of the white blood cells (leukocytes, thrombocytes, lymphocytes, monocytes and granulocytes) in reptiles has not been examined here since they have been studied recently by Kelényi & Németh (1969) and Efati, Nir & Yaari (1970).

Lung structure in newborn Lacerta

Newborn Lacerta have lungs with a very small rim of peripheral alveolar tissue which only has one to two layers of very small alveoli and shows little if any antero-posterior gradation in complexity. Alveolar septa show none of the capillary bulging typical of the adult lung (compare Fig. 4.22a with Fig. 4.14b) and in fact appear to be composed of many undifferentiated cells from which it is difficult to distinguish capillaries.

Examination under the electron microscope (Fig. 4.22b) reveals that the interstitium is packed with many cells containing very little cytoplasm. These cells are sometimes found accumulating more cytoplasm and developing an intracellular slit which when larger can contain an erythrocyte. This sequence represents the formation of capillaries in the septum and is similar to the mammalian foetal canalicular stage. Adult-like capillaries are found but they have a semi-collapsed appearance. Much of the alveolar epithelium is thin and squamous, i.e. Type I, but there are also many Type II cells with lamellated bodies. Type II cells with

FIG. 4.22 (a) 1 μm epon section stained with methylene blue of *Lacerta* newborn lung. cart, cartilage. w, outer wall. m, mesentery of pleura. al, alveolar air space. s, septa lacking obvious capillaries and with undifferentiated cells.

(b) Electron micrograph of alveolar septa of *Lacerta* newborn lung.
Note Type I and II cells, the latter with lamellated bodies and sectioned enclosed in interstitium.
cap, capillaries. endo, endothelial cells. p.endo, prospective endothelial cells and sf, components of the surfactant material.

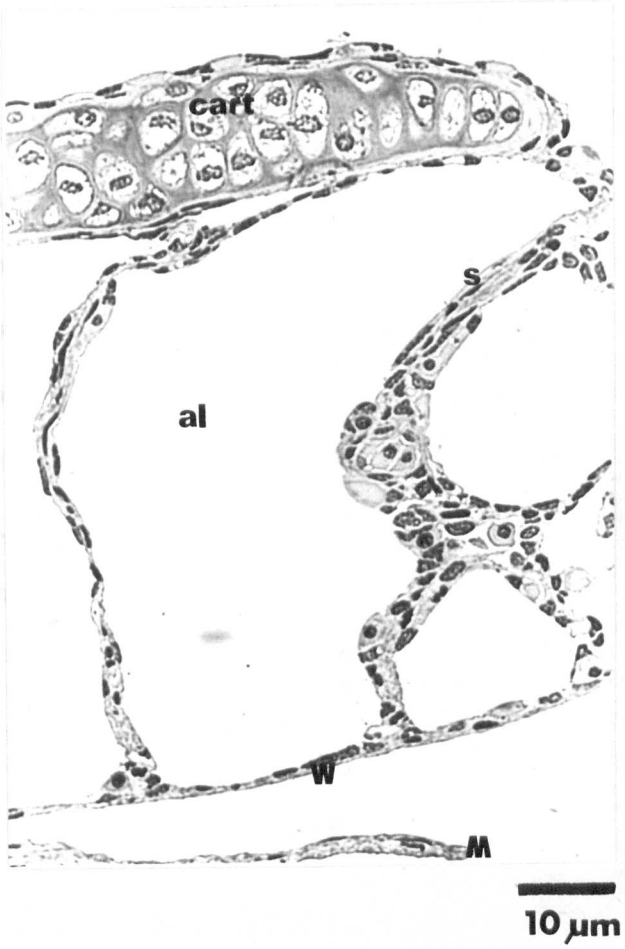
a
cart
s
al
w
M
10 µm

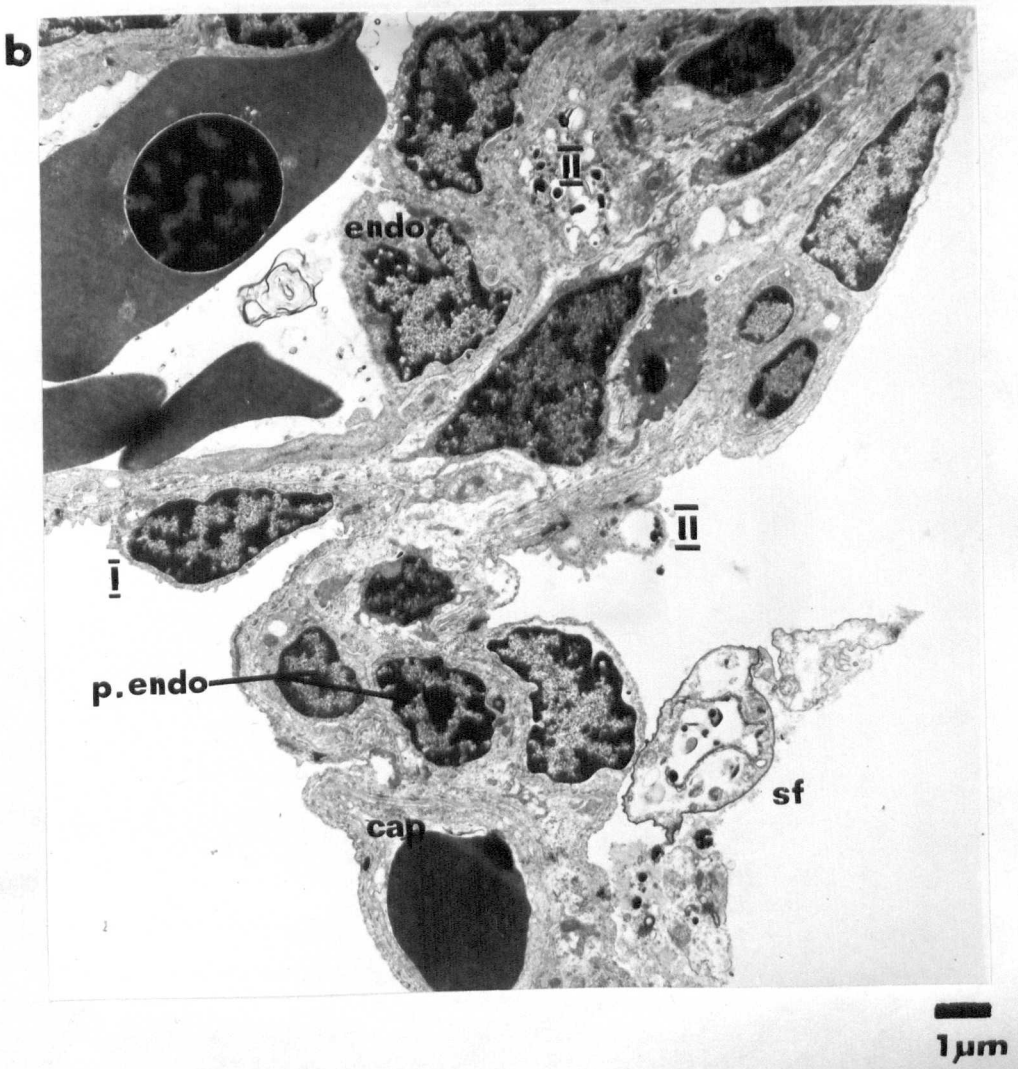
b
II
endo
II
I
p.endo
sf
cap
1 µm

cytoplasmic extensions and fewer lamellated bodies were seen more frequently than in the adult. Non-ciliated, cuboidal epithelial cells similar to those found on the adult trabeculae were often found amongst the Type I and II cells of the septa of the newborn lung.

Because the lungs were fixed initially from the pleural side in the newborn Lacerta (Chapter 5), remnants of the surfactant system were better preserved. They were seen as flocculent material, globular myelin figures and also as a thin, continuous, strongly osmiophilic, surface film similar to that described by Gil & Weibel (1969/70).

DISCUSSION

Differences and similarities between Lacerta lung structure and that of mammals and other vertebrates have already been described and in some cases discussed within the results section. The purpose of this discussion is to consider further (a) the pattern of epithelial and capillary network (double to single) evolution, (b) the formation of surfactant, (c) the manner of lung development and growth in Lacerta as compared with the mammal and finally, (d) how primitive the Lacerta lung might be in terms of its capacity for gas exchange.

Epithelial and capillary evolution and development

There appears to be a progression from Type II cells having cytoplasmic extensions and covering all the respiratory capillaries (in lungfishes, except Polypterus, and amphibians) to a situation where both Type I and II cells form the septal epithelia with the Type II sometimes having cytoplasmic extensions (Testudines), rarely (snakes and lizards) or never (mammal and bird) (Fig. 4.2 and Table 4.1). Some workers (Okada et al, 1962a) are able to distinguish in Amphibia, cells intermediate in structure between Type I and II which they consider to be potential Type I cells although still retaining some microvilli and some lamellated bodies (Table 4.1). It is not known whether there is an evolutionary or physiological significance in the presence of Type I cells in Polypterus or in the fact that Polypterus has only a few Type II cells which lack microvilli.

A similar progression from stem cuboidal cells having the beginnings of Type II characteristics (i.e. some microvilli and some inclusion bodies) and forming the entire epithelium to an epithelium composed of both Type I and II cells, with the former believed to be produced from transformed stem Type II cells, is found during mammalian lung development. During epithelial repair in the adult mammalian lung, Type II

TABLE 4.1

ALVEOLAR EPITHELIAL CELLS OF VERTEBRATE LUNGS

Species	TYPE I			TYPE II				Reference
	Forming air-blood barrier	With Microvilli	With IBs	In Niches	With cytoplasmic extensions forming air-blood barrier	With Microvilli	With IBs	
FISH								
Amia and Lepisosteus (SB)	-	-	-	+	+	-	+ *	Hughes, 1970a.
Polypterus	+	-	-	?	-	-	?p,+*	Kli ka & Lelak, 1967 Kli ka & Janout, 1967
Protopterus	-	-	-	+	+	+	?p,+*	K & L 1967, K & J 1967, DeGroodt, Lagasse & Seybruyns, 1960, Hughes Ryan & Ryan, 1973.
Lepidosiren and Neoceratodus	-	-	-	+	+	+	+ *	Hughes, 1973, Hughes & Weibel, 1976.
AMPHIBIA								
Proteus	-	-	-	+	+	+	+	Hughes, 1970a.
Triturus	+	+	-	+	+	+	-	Okada et al, 1962a.
Rana and Bufo	+	+	(+*)	+	+	+	+ *	Okada et al, 1962a.
Rana	-	-	-	+	+	+	+ *	Kli ka & Lelak, 1967, Weibel, 1972.

TABLE 4.1 (continued)

Species	TYPE I: Forming air-blood barrier	TYPE I: With Microvilli	TYPE I: With IBs	TYPE II: In Niches	TYPE II: With cytoplasmic extensions forming air-blood barrier	TYPE II: With Microvilli	TYPE II: With IBs	Reference
REPTILIA								
Elaphe (snake) Gekko (lizard)	+	-	-	+	-	+	+ *	Okada et al, 1962b.
Lacerta	+	-	-	+	-(+)	+	+ *	This study.
Chrysemys	+	-	-	+	- or +	+	+ *	Perry, 1972.
BIRD								
Chicken (air capillary)	+	-	-	(+)	-	+	+ *	Okada et al, 1965.
(atrium)	-	-	-	+	-	+	+ *	King & Molony, 1971.
MAMMAL	+	-	-	+	-	+	+ *	e.g. Weibel, 1969a,1973.

SYMBOLS:
(SB), swimbladder
+, present
-, absent
?, possibly present
( ), occasionally present
IBs, inclusion bodies
p, pale stain in IBs
*, lamellations in IBs and surfactant present.

cells become cuboidal and may even transform into Type I cells (for references, see Introduction). Kli ka & Lelek (1967) considered that the ciliated epithelium of the Polypterus septa gave rise to Type I cells during growth because they found transitional forms.

In Lacerta, many non-ciliated, cuboidal epithelial cells with microvilli and a few lamellated bodies but without cytoplasmic extensions were found on the newborn lung septa. These cells were only found on the trabeculae of the adult. In the newborn, they may represent Type II stem cells. Since new septa grow from the outer wall and not from the trabeculae, it is thought that in the adult lung these cells act as Type II cells for surfactant production but take no part in forming Type I cells for the septa. Type II cells having only small numbers of lamellated bodies and short, thin cytoplasmic extensions were found frequently in the newborn Lacerta lung but rarely in the adult. It is suggested that, in the light of mammalian evidence and evolutionary trends, these cells represent Type II cells transforming into Type I. Such transitional cells would be expected to be more abundant in the newborn Lacerta lung which has to enter a phase of septal proliferation in order to reach adult complexities. Much careful investigation is required to be sure of the correct direction for the transitional forms.

The physiological importance of the progression from Type II to I cells is in the formation of a progressively thinner air to blood barrier. This epithelial progression is coupled with a transformation from a double to a single capillary network and a reduction in septal interstitial thickness, mainly by the loss of smooth muscle (Fig. 4.2). Thus, if more of the surface area of each capillary can be exposed to air via thinner epithelial (and endothelial) barriers, the greater can be the diffusing capacity of the lung. This could even be accompanied by a reduction in lung weight. The sequence from Amphibia to Testudines to snakes/lizards to mammals/birds is the pathway of these three anatomical progressions and also of an

FIG. 4.23 Very thin septa of Lacerta forming alveolar air spaces, al. 1^{o} septa thickened with smooth muscle to form trabecular network (tb) which is covered with ciliated cuboidal epithelium.

EM sketch of septa showing capillaries, cap, endothelial cells, endo, smooth muscle, sm, septal cells, sep, interstitium, int, Type I and II epithelial cells, the latter having microvilli and lamellated bodies, LB. Note double capillary network but many areas of a single network.

Compare this diagram with amphibian, typical reptilian and mammalian septa of Fig. 4.2.

N.B. Scale incorrect: capillaries and their distance apart in Lacerta are smaller than typical reptile but larger than a mammal.

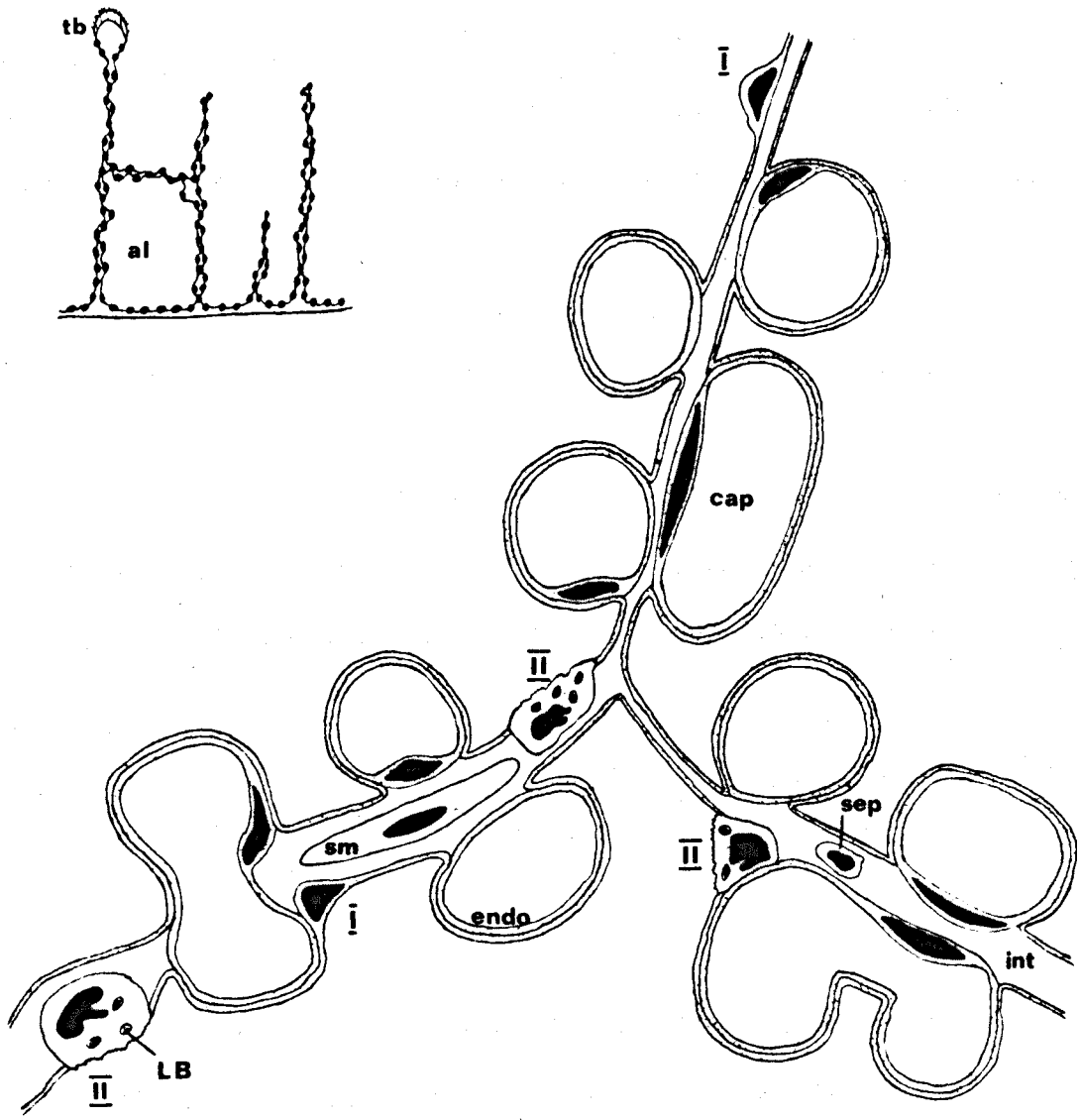
tb
al
I
cap
II
sm
I
endo
II
sep
int
II
LB

increasing capacity for gas exchange (Chapter 1). Lungfish cannot be included in this sequence because they also possess another gas exchanging organ, the gill. Similar progressions are found during mammalian lung development.

Lacerta possess very thin septa, with only a little more smooth muscle than the mammal, together with a mixture of single and double capillary networks. The presence of a single network in lizards (or snakes) has not been documented before, even by Okada et al (1962b). It is thought that these workers must have fixed the lungs in a deflated state because in Lacerta the septa of a deflated lung appear to have only a double capillary network (Fig. 4.13). In Fig. 4.23, the Lacerta septa have been depicted in diagrammatic form and this should be placed in between the typical reptile and the mammal in the evolutionary sequence of Fig. 4.2. In the light of evidence presented here, it is thought that the typical reptilian septum of Fig. 4.2 taken from Okada et al (1962b) more accurately represents that of a tortoise or a terrapin and not that of a snake or lizard. It is not known whether the turtles and Crocodilia have lung septa similar to those of the tortoise or Lacerta.

Surfactant

Surfactant is only present in lungs if the inclusion bodies of the Type II cells possess lamellations (Hughes, 1970a). Both are absent in the newts, Proteus and Triturus (Table 4.1). Similarly, surfactant is only found physiologically in the mammalian foetus when lamellations have begun to form (Reid, 1967). The surfactant found physiologically in Lacerta in Chapter 3 can now also be demonstrated anatomically as lamellated bodies in Type II cells and as flocculent material, globular myelin figures and strongly osmiophilic lines in the air spaces. The function of surfactant has been discussed in Chapter 3. It is of interest to note that lamellated bodies have been found in some fish swimbladders, which have no respiratory role. Hughes (1973) has discussed the needs for a surfactant even in a gas secreting swimbladder.

Tubular myelin figures were not found in Lacerta in agreement with their absence in other non-mammalian lungs (Hughes, Ryan & Ryan, 1973). This may indicate a different type of non-mammalian surfactant. It is of course possible, however, that the method of lung fixation in Lacerta did not allow their preservation.

Lamellated bodies in mammals are believed to be derived from small vesicles of the golgi complex or from small multivesicular bodies which both accumulate dense osmiophilic material and enlarge, finally becoming lamellated (Sorokin, 1966, Kikkawa, Motoyama & Gluck, 1968, Scarpelli, 1968, Dermer, 1969, 1970b, Gil & Reis, 1973, Meyrick & Reid, 1973, Schock, Pattle & Creasey, 1973). From ultrastructural evidence, this is also a possible route for lamellated body formation in Lacerta, although large dense bodies were not found; even the small ones had lamellae. In Lacerta, a second sequence from large lipid droplets accumulating osmiophilic material to lamellated bodies was also indicated. These lipid droplets were seen as empty vacuoles if the lungs were stored for some days in glutaraldehyde. Such a route has not been documented in any other vertebrate lung. It is not known, whether this second route is an artifact of fixation or whether it indicates a different surfactant component.

Lacerta lung development and growth

The Lacerta lung may develop initially as a small sac totally devoid of primary septa or these may always be present as small projecting rudiments. It is not known which pattern occurs. The Lacerta foetal lung does not, therefore, have the glandular stage found in the mammal but the canalicular stage of the two are very similar. Newborn Lacerta alveoli are much smaller than in the adult. In contrast, the newborn mammal has large, primitive alveoli which require the septal proliferation of the alveolar phase in order to form adult alveoli.

Growth in the mammal involves the extension of existing septa without the formation of new ones and hence the alveoli become larger with increasing body weight. In some mammalian species, there may be some new septa formed (for references, see Chapter 5). Growth in Lacerta involves both the extension of existing septa and the formation of new ones, but never to the extent of keeping alveoli at a constant size. The very small, newly forming primary, secondary and tertiary septa can often be seen in Lacerta lung sections.

Lacerta lung, primitive or not?

In architecture, the Lacerta lung is rather primitive (Fig. 4.1 and 4.8) but its septal structure is considered to be very advanced (Fig. 4.23). The latter is the important factor for gas exchange. When compared with the mammal, it appears that some of the Lacerta capillary surface area is wasted because of apposition in the double capillary network, that the capillary density in the septa is slightly lower, that there may be a longer than physiologically necessary capillary length in between arterioles and venules and that alveoli are much larger with a large central air space which maybe a 'dead' space or a reservoir. Despite these differences, Lacerta septa are considered to be a reasonably advanced gas exchanging structure and it is thought that the ten-times lower $\dot{V}o_2$ found in Chapter 1 may be mainly due to a lack of enough surface area in a lung volume which is at least twice as great as a mammal's (Chapter 2 and 3). This possibility is investigated in Chapter 5.

CHAPTER 5

LACERTA LUNG MORPHOMETRY

INTRODUCTION

In previous chapters, it has been established that $\dot{V}o_2$ is proportional to $W^{0.75}$, whether it be standard or maximum rates, and that tidal volume and lung volumes at different inflation pressures are directly proportional to body weight. Since respiratory frequency is independent of body weight, it is found that 'wasted' ventilation, i.e. ventilation requirement, increases with body size. By examination of the morphometrics of the Lacerta lung, an attempt has been made to correlate these physiological scalings with anatomical parameters, viz. alveolar surface area, relative proportions of air in peripheral tissue and central air space. Much information can also be gained by comparing and contrasting various Lacerta lung parameter scalings with those of the mammal and other vertebrates from intra- and interspecific studies.

Of equal importance is the determination of the absolute values for respiratory surface area, alveoli size, number, etc. for Lacerta comparing them, not only with the little available data for reptiles, amphibians and lungfishes, but especially with the highly developed mammalian lung. Since Lacerta $\dot{V}o_2$ is ten times less than a mammal (Chapter 1) and since pulmonary ventilation is not limiting (Chapter 2), is the respiratory surface area of Lacerta also ten times smaller? How does the morphometrically determined pulmonary diffusing capacity of the primitive Lacerta lung compare with that of a mammal? Is it different because of lung or cardiovascular factors or both?

It was found that within lizards of a stated size, large increments in pulmonary ventilation (controlled mainly by tidal volume

changes) were inefficient in terms of O_2 extraction. A preliminary study of the effect of different levels of inflation on lung morphometry was undertaken to see if this inefficiency had any anatomical basis.

From the anatomical study of the Lacerta lung (Chapter 4), it was apparent that there was considerable antero-posterior gradation in decreasing complexity in both the extent of alveolar tissue and the extent to which this tissue was capillarised. In this last chapter, this gradation has been quantified in some detail. A preliminary study has also been made to describe postnatal lung development in terms of morphometry, since L. vivipara (0.2g) lungs were markedly underdeveloped when compared with the adult lung.

The value of lung morphometric studies

Lung morphometry allows anatomical measurements to be made of physiological parameters. Such quantitative analysis of lung structures was not extensively performed until the 1960s. In 1963, Weibel published in a book a detailed study of human lung morphometry and compared his values with the few measurements available in the literature. Using his morphometric techniques, absolute values and relative volume proportions of alveolar air spaces, septal tissue, gross blood vessels and conducting airways can be determined together with alveolar surface area, numbers and dimensions of airways and alveoli plus the dimensions of the capillary network. If the study is extended to the electron microscopic level, epithelial, interstitial, endothelial, capillary lumen and erythrocyte volumes can be estimated. Also, a more accurate surface area estimate and measurements of arithmetic and harmonic mean air-blood barrier distances are possible which allow estimates of morphometric pulmonary diffusing capacity, D_{Lo_2}, to be made (Weibel, 1970/71, 1973) .

Tenney & Remmers, also in 1963, made a comparative morphometric study of mammalian lungs covering 5.5 logarithmic cycles of body weight (shrew to whale) but using only low power light magnifications of thick sections. They were concerned only with total lung volume, alveolar

surface area and alveolar size and their scaling in terms of body weight and oxygen consumption.

With such morphometric techniques, the mammalian lung has now been quantitatively studied during pre- and postnatal development (Emery & Wilcock, 1966, Weibel, 1967, Bartlett, 1970a, Dunnill, 1962) mainly in terms of alveolar development, surface area and D_{Lo_2}. Postnatal growth can be affected by the level of alveolar Po_2 (Bartlett & Remmers, 1971, Burri & Weibel 1971) but not by exercise or excess thyroid activity (Bartlett, 1970a). At high altitudes and low Po_2, there is a compensatory increase in alveolar surface area. The effect of pituitary growth hormones on young and adult rats following pneumonectomy show that regeneration can occur and is achieved by enlargement of structures already present and not by the formation of new alveoli. The level of hormones determine the extent of regeneration but if there is an excess new alveoli will form (Brody & Buhain, 1972, 1973, Buhain & Brody, 1973).

Alveolar size and shape have been studied at various levels of inflation and sometimes during deflation. Initially, it was thought that all volume changes occurred in the alveolar ducts and that the alveoli remained the same size (Macklin, 1950). Through morphometry, it is now known that it is the alveolar air volume that increases linearly throughout lung inflation whereas the alveolar duct volume remains constant. After 40% TLC, the duct volume is responsible for a major part of the inflation and after 90% TLC, duct volume increases considerably (Forrest, 1974). Despite the alveolar size increase, its shape or configuration remains constant throughout the pressure-volume curve (Storey & Staub, 1962, Dunnill, 1967, Klingele & Staub, 1970, Forrest, 1970a,b, 1972, 1974, D'Angelo, 1972, Gil & Weibel, 1972, Weibel et al. 1973). During deflation many alveoli collapse thus considerably reducing the available surface area. On inflation, the alveolar surface unfolds as alveoli open whilst the air-blood barrier becomes thinner. The surface lining material always

smooths out alveolar surface corrugations at all levels of inflation (Forrest, 1970, Weibel et al. 1973). Pulmonary diffusing capacity increases according to the level of inflation (Weibel et al. 1973) as does the physiologically determined value from rest to exercise (Siegwart et al. 1971).

Finally, lung morphometry has been used as a tool to determine the manner in which lung parameters are scaled over intra and interspecific ranges in adults and during postnatal development. In general the mammalian lung volume (Tenney & Remmers, 1963, Weibel, 1972, 1973), and lung weight (Stahl, 1967) are directly proportional to body weight. Alveolar surface area increases linearly with body weight when considered inter or intra-specifically for animals between the shrew and dog in size (Weibel, 1972) but not when heavy sluggish or large aquatic mammals are included. Then the surface area is proportional to the 0.75 power of body weight and is therefore the result of oxygen consumption demands (Tenney & Remmers, 1963). D_{Lo_2} is related to body weight according to the alveolar surface area relationship (Weibel, 1972) and in all Weibel's studies both surface area and D_{Lo_2} are directly proportional to body weight. It is, however, under genetic control since elevated levels of oxygen consumption in waltzing mice as opposed to normal mice cause increased D_{Lo_2} (Geelhaar & Weibel, 1971). The genetically inherited scaling may be modified by the environment but only during postnatal growth (Burri & Weibel, 1971).

Alveolar diameter is proportional to $W^{0.137}$ for non-sluggish mammals (Spells, 1968) but an intraspecific relationship of $W^{0.33}$ has been found for dogs (Siegwart et al. 1971). When heavy sluggish and aquatic mammals are included in the study, alveolar diameter is proportional to $W^{0.185}$ or to $\dot{V}o_2^{-0.71}$, the correlation being considered more exact with metabolic rate than with body weight (Tenney & Remmers, 1963). Alveolar number is only constant if their diameter is proportional to $W^{0.33}$ (Weibel, 1963).

In lower vertebrates, there are only a few morphometric studies of the lung and none are extensive. Krogh in 1904 estimated the alveolar number and size, the alveolar surface area and the capillary density in the septa of the amphibian Rana esculenta. Tenney & Tenney (1970) studied interspecifically a large range of reptiles (4 log. cycles of body weight) and amphibians (3 log. cycles). They found lung weight to be directly related to body weight in both classes but only amphibian lung volumes were directly proportional to body weight, the relationship being $W^{0.75}$ for reptiles. Respiratory surface area was related to $W^{1.0}$ and $W^{0.75}$ for amphibians and reptiles, respectively. The respiratory surface of the skin was also included in the amphibian data and if a respiratory capillary density of $W^{-0.2}$ was taken into account, 'true' respiratory area varied as $W^{0.8}$, virtually the same as in the reptiles. Reptiles were assumed to have a constant capillary density and to have capillaries occupying the whole of the alveolar surface area as is the case in the mammal. Alveolar diameter correlated with $W^{0.2}$ but with a large amount of interspecific variability. Reptiles, generally, have smaller alveoli than the amphibians and after 0.5 kg body weight are said to hold alveoli size constant but again with considerable interspecific variability. The very active Iguana has very small alveoli for its body size indicating an adaptation to metabolic demands. Tenney & Tenney (1970) concluded that body size, metabolic rate and environmental factors would determine lung parameters with the effect varying in different classes (including mammals) but that the invariance of the metabolic rate $\propto W^{0.75}$ and respiratory surface area $\propto W^{0.75}$ ratio would always be achieved (cf. Weibel, 1972).

Perry (1972 and personal communication) has made an intraspecific study of the lungs of the aquatic chelonian Pseudemys and terrestrial Testudo at both the light and electron microscopic level. He was, however, concerned with absolute mean values and not with anatomical scaling.

One small and one large specimen of the garfish Lepisosteus have been used to measure lung volume, alveolar surface area and mean alveolar

diameter (Rahn et al, 1971) using methods of Tenney & Tenney (1970). Lung volume and mean alveolar diameter is similar to amphibians of the same weight, but the surface area is lower due to smaller numbers of alveoli. Hughes et al (1974) find even lower volumes and surface areas for the air sac of the fish Saccobranchus which is more dependent on gill respiration. The respiratory surface area of the air sac is related to $W^{0.662}$ and total respiratory area to $W^{0.69}$. Membrane diffusing capacities of the gill, skin and air sac were also measured. The lungs of 500g Lepidosiren (lungfish) have been examined morphometrically by Hughes & Weibel (1976) and compared with other vertebrate lung data. Fish gill morphometrics have been extensively studied mainly by Hughes (e.g. 1966, 1970b, 1972).

Fixation methods

Various methods are available for fixing the lung; some with more disadvantages than others. These methods are basically:

(i) Instillation of formalin vapour through the trachea into an isolated lung previously inflated with air to the desired degree (Weibel, 1963).

(ii) In situ instillation of glutaraldehyde at a constant pressure (20 to 30 cm H_2O ensuring even inflation of all parts of the lung) until flow ceases by itself. A sternotomy, with wide separation of the chest wall, is performed initially to collapse the lung to its residual volume (Weibel, 1970/71).

(iii) Isolated lungs kept continuously inflated with air at a constant pressure of 20 cm H_2O until dry fixation occurs (Tenney & Remmers, 1963, Bartlett, 1970a,b, Tenney & Tenney, 1970, Rahn et al, 1971).

(iv) Vascular perfusion of fixatives in situ during inflation or deflation of the lungs with air at a constant pressure either by external negative or internal positive pressure in the open thorax condition (Gil & Weibel, 1971, 1972, Weibel et al, 1973, Forrest, 1970a,b, Macklin, 1950 (with intact thorax)).

(v) In situ and with an open thorax, the lungs are inflated with air at a constant pressure or at some point in the ventilation cycle and then fixed by rapid freezing using liquid propane or isopentane (Staub & Storey, 1962, Glazier et al, 1967, D'Angelo 1972, Forrest 1970a,b, 1972, 1974).

Only methods (ii) and (iv) allow electron microscopic evaluation but in the former the surface lining material is lost and in the latter the plasma and the erythrocytes. Dry fixation (method (iii)) causes the extraction of water from the delicate lung tissue without replacement by another fluid, which inevitably results in considerable disproportionate shrinkage and distortion of the structures. Formalin fixation (i)(Weibel, 1963) and rapid freezing (v) (Forrest, 1969) also cause shrinkage often disproportionate and correction factors have to be determined. Glutaraldehyde, on the other hand, does not cause shrinkage (Weibel & Knight, 1964).

Rapid freezing (v) may give a more 'in vivo' picture because fixation is faster than by instillation (ii) or vascular perfusion (iv). For example, capillaries may bulge in fixed as opposed to frozen lung tissue and the erythrocytes may clump giving an abnormally high capillary volume and hematocrit (Staub & Storey, 1962). This criticism is not accepted by Weibel (1970/71). Only the outer margins of large lungs, however, can be 'fixed' by rapid freezing yielding pleural regions only for morphometry.

In situ fixation is superior to isolated lung fixation because the presence of the thorax will give a more natural shape to the lung. This is even more important for primitive sac-like lungs where posterior regions have less tissue and therefore offer least resistance to inflation if not limited by the thorax (Chapter 3). Pressures for isolated lung air inflations and in situ fixative instillations are not comparable (a) because of the higher viscosity of liquid as opposed to air, and (b) because fixation starts as soon as the fixative comes into contact

with the tissue. Both factors would cause lower volumes. Contrary to this, however, Weibel et al (1973) found greater lung volumes under 20 cm H_2O instillation pressure than by vascular perfusion of fixative with the lung held inflated by air at the same pressure. The explanation must lie in the fact that saline pressure-volume curves require lower pressures, though this is not always evident during the first saline inflation (Bachofen et al, 1970).

With these criticisms in mind, it was decided to fix the lungs by <u>in situ</u> tracheal instillation of glutaraldehyde, so that the whole lung could be sampled for both light and electron microscopic evaluation. If the osmolarity of all aqueous solutions are adjusted to be isotonic with lizard blood plasma, dimensional changes due to osmotic swelling or shrinkage will be avoided (Weibel & Knight, 1964). Capillary contents will remain intact permitting the measurement of harmonic mean thickness of the plasma and capillary volume. These measurements are vital for estimating pulmonary diffusing capacity, whereas τ_h of the surface lining layer is not (Weibel, 1970/71).

It is essential to remove as much air as possible before instillation, otherwise, air trapped by liquid under pressure will cause distortion of the lung. In Chapter 3 it has been shown that in <u>Lacerta</u>, sternotomy and wide separation of the chest wall, although causing collapse to the residual volume, afterwards allows unnatural inflation of the lung, especially the posterior region. Deflation to volumes less than residual can be brought about by negative air pressure (but not to the point of vacuum) applied to the tracheal cannula without tearing pleural mesenteries. Also from Chapter 3, a knowledge of the air volumes occurring over the linear part of the P-V curve was obtained. These lung volumes could be obtained by 5, 10 and 15 cm H_2O instillation pressures after initial -20 cm H_2O deflation. The initial sucking pressure during instillation may increase the absolute value of the instillation pressure.

Morphometric analysis

Having fixed the lungs in a suitably inflated state, a statistically acceptable method of sampling must be used. Such methods have been devised for the mammalian lung by Weibel (1963), Weibel & Elias (1967) and Weibel (1967b) and these stereological principles of morphometry extended to many tissues (Weibel, 1969b, Underwood, 1970, De Hoff & Rhines, 1968). Many other workers are now adopting these methods (e.g. Forrest, 1970, Bartlett, 1970a,b).

One has to postulate for all basic stereological principles that orientation is random (or homogeneous) i.e. the structure can be orientated in all dimensions of space. This randomness is essential because morphometry and stereological principles make extensive use of statistical procedures and statistics ask, in most cases, for random conditions of the structure analysed. A tissue structure under investigation can either be randomly distributed within the organ or have stratified regional variations, e.g. alveoli of the mammalian lung are random but the branching airways are not. Even the alveoli are stratified in large mammals with the ventral ones larger (Siegwart et al, 1971). Sampling can thus be either random, systematic or stratified for a random structure, but must only be stratified, i.e. taken at equidistant points, for stratified structures in order to give equal weighting to all areas without excessive random samples being necessary.

For the human lung parenchyma, there are four stages of multiple sampling all of which can be random. Stage 1 is the sampling of the population for each experimental condition. Five animals is statistically considered a large sample number (Weibel, 1969b, personal communication), but a lot of information can be gained from only one animal for each condition, e.g. the five human lungs from a range of body weights used initially by Weibel in 1963. Stage 2 is the random sampling of a number, n, of paraffin sections taken from serial sections or, for electron microscopy,

one perfect section per random tissue cube. Stage 3 is the random sampling of fields, m, from each section which in practice is performed using a systematic grid (the tissue is still randomly distributed with respect to the grid). Stage 4 is the counting, p, of structures again using an effectively random, but systematic grid which is a test system of points and lines. The accuracy of the estimations can be increased by increasing n, m or p with this order indicating the relative increasing importance of the increment. In terms of time efficiency, the minimum statistically acceptable total sample is used.

The Lacerta lung is obviously a stratified tissue since it is more complex anteriorly and therefore the mammalian lung method must be modified. As this is a preliminary study of lizard lung morphometry using modified mammalian methods but with an aim to gain information primarily on body weight relationships, only 6 animals of increasing size were used. Stratified sampling (stage 2) is necessary at equidistant points along the length of the lung giving quantitative information on the trend of the antero-posterior gradation with a final mean value for each structure. Stage 3 and 4 systematic sampling may then be used. In order to determine the total number of points required for suitable accuracy, Weibel (1963) has provided a graph which predicts the probable relative error for a certain total number of points according to the volume density of the structure under investigation. Lacerta lungs were sampled to meet these demands.

Various systematic test systems for counting in stage 4 have been designed by Weibel (1969b), all of which are coherent in the sense that test points and test lines are combined. It is usually considered an advantage to have more test points than test lines at the EM level but with equal values for light microscopic evaluation. A quadratic lattice test system was chosen for the lizard.

The Delesse principle (see Weibel, 1963, 1969b) behind estimating volume and surface area densities is that a two-dimensional picture of the plane of section is extrapolated and calculated in terms of the three-dimensional tissue cube and whole organ under investigation. There are three methods available for measuring volumes (a) planimetry (b) intercept length, and (c) point counting, the latter being the most accurate and efficient (Weibel, 1963). Surface densities can be obtained by counting the number of intersections of the surface with a test line probe at a known magnification, i.e. mean chord length (Tomkeieff, 1945, Campbell & Tomkeieff, 1952, Weibel, 1963). Volume to surface or surface to volume ratios can be determined by a combination of volume and surface density estimations (Chalkley et al, 1949). The former ratio is also a measure of the arithmetic mean thickness $\bar{\tau}$ of a sheet of tissue (Weibel, 1963, Weibel & Knight, 1964). Since the air-blood barrier functions to allow gas diffusion, the mean reciprocal thickness or harmonic mean thickness $\bar{\tau}_h$ of the barrier is a more physiological measurement in terms of diffusion (Weibel, 1963, 1970/71, Weibel & Knight, 1964).

Stereological principles are based on the assumption that tissue sections are true two-dimensional sections with no thickness. Section thickness will cause an overestimation of both surface and volume densities, the so-called Holmes effect, but simple correction formulas have not yet been derived (Weibel, 1969b). Magnussen et al (1974) consider that no correction is necessary for 1 μm araldite or epon sections.

METHODS

All lizards used for any morphometric evaluation were starved for 2 days so that varying amounts of gut filling would not cause unnecessary weight fluctuations. Because of the proximity of the stomach to the medial surface of the lung in the lizard, stomach filling can also reduce the space available for lung expansion. Avery (1973) found that in L. vivipara food never occurred anterior to a point level with the posterior position of the third sternal rib. This position is approximately two-thirds along the length of the expanded lung. The posterior third could therefore be obstructed by feeding.

Nasal cavity volume

'Silcoset' rubber casts of nasal cavities were taken from 15 Lacerta of known body weight. The method of casting has been described in Chapter 4. These casts were weighed and division by the density of 1.18 (ICI, 1972) yielded the volume of each paired nasal cavity, which also included the airspace leading from the internal choanae to the larynx. A $0.5\%^3$ correction for linear shrinkage was not considered necessary.

Tracheal dimensions

Tracheal length was measured whilst in situ to prevent error from tracheal elasticity. Measurement was made from the glottis to the caudal margin of the extrapulmonary bronchi. Since tracheal diameter is constant along its length but slightly oval in section, a mean of the minimum and maximum diameter was taken at any point along the trachea. Tracheal volume was calculated from $2\pi r^2 1$ for 27 lizards. Although the total extrapulmonary bronchial diameter is greater than that of the trachea, a separate estimation of tracheal and bronchial volume only increased the total tracheal volume by 0.5%, as the bronchi are very short. This extra measuring was considered unnecessary.

Lung fixation in situ

Lizards were anaesthetised by intraperitoneal injection of Nembutal (pentobarbitone) with a dose which caused respiration just to cease but with the heart still beating. The trachea was exposed ventrally and a tracheotomy performed below the larynx. A female Luer fitting previously attached to the free end of the tracheal cannula was fitted to the 3-way tap of the inflation/deflation apparatus with the animal lying supine (for details see Chapter 3). The lungs were inflated in approximately 5 half minute steps to a pressure of +3.0 cm H_2O to ensure airtight connections and normal ribcage expansion. Deflation using similar intervals was then performed to a pressure of -20.0 cm H_2O intratracheal pressure. At this point, most of the air was extracted and the ribcage had caved inwards but pleural mesenteries had not been damaged. The trachea was then clamped and the cannula removed and fitted to the glutaraldehyde instillation apparatus (Fig. 5.1b).

The instillation apparatus was made from a graduated 5 ml pipette, the tip of which was shaped into a male Luer fitting. This pipette had a side arm of capillary tubing of 1.0 mm internal diameter. When clamped vertically with the top of the pipette sealed by a rubber bung, liquid can only flow from the Luer tip as air bubbles pass into the pipette via the side arm. Thus the pressure head is constant, being the height from the entrance of the capillary tube into the pipette to the end of the Luer fitting. A negative pressure of -1.6 cm H_2O was caused by the capillary action of the side arm. This could not be avoided since a larger bore released air bubbles which occluded the pipette lumen and restricted the flow of liquid. The negative pressure was accounted for in measuring the true instillation pressure. By this method, a low pressure head but with a large glutaraldehyde reservoir and a rough measurement of the quantity instilled was possible. Three instillation pressures of 5, 10 and 15 cm H_2O were used.

FIG. 5.1 A. Apparatus for fixing the lungs of the 0.2g L. vivipara - for details see text. B. Instillation apparatus for fixing adult lungs. Pressure head is the height of the bar from mid-position of the lungs to the entrance of the capillary bore of the side-arm. Arrow to entrance of capillary bore is the height of the negative pressure caused by the capillary, a constant -1.6 cm H_2O.

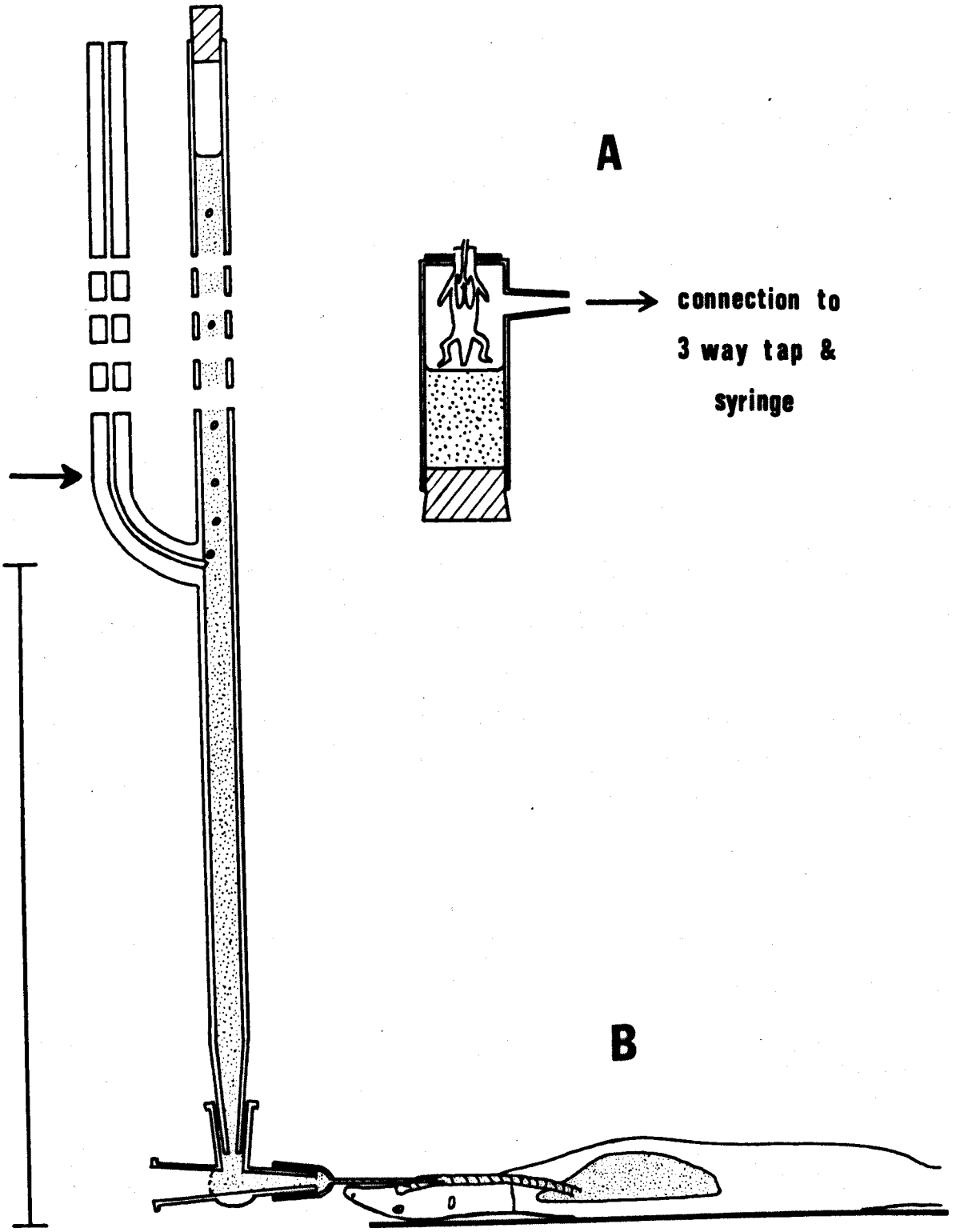
A
connection to
3 way tap &
syringe
B

The tracheal cannula was attached to the Luer of the pipette via a 3-way tap and the whole system was filled with 2% glutaraldehyde in 0.1M cacodylate buffer and checked for air locks. With the tracheal cannula full of glutaraldehyde, it was again inserted into the trachea and securely tied in position. After ensuring there was no tracheal leakage by connecting the pipette's liquid column with the cannula, the tracheal clamp was quickly removed and glutaraldehyde was instilled into the lungs at the chosen pressure. Instillation proceeded rapidly for approximately 15 seconds and then very slowly for several minutes. After 30 minutes the trachea was ligated and the cannula and instillation apparatus removed. By careful dissection, the lungs and trachea were removed from the animal and placed in a bath of glutaraldehyde.

Lung volume by displacement after Scherle (1970) and Weibel (1970/71).

Glutaraldehyde instilled lungs and trachea were held by fine forceps clamped to a micromanipulator. Excess fluid surrounding the lungs was removed before they were lowered and completely submerged in a beaker of glutaraldehyde of known weight on a Mettler 1000 balance. The lung did not touch the walls of the beaker. Assuming a tissue density equal to that of glutaraldehyde, which is 1.012, the volume of the lungs and trachea was thus measured by displacement. Each volume was measured three times and the mean taken, the variation being only 1% of the mean. (Weight measurements were performed quickly to avoid errors due to evaporation). A correction was made for the volume and capillary action of the forceps. The volume (i) thus measured was always a little higher than that measured from the graduated pipette during instillation. Trapped air bubbles and actual tissue volume accounted for this extra volume. (Accuracies of 2 and 4 decimal places respectively were obtained for the pipette and displacement method). From a knowledge of lung tissue weight (see later) and assuming a density of 1.0 it was possible to calculate the volume of trapped air bubbles.

The two bronchi were then ligated as close to the lung as possible and the extraneous tracheal and bronchial tubes removed. Right and left lung volumes (ii) were measured separately by volume displacement. When this bronchial ligature was cut, the lung noticeably decreased slightly in volume though still remaining in its fixed inflated state. Right and left lung volumes (iii) were again measured. When extraneous tracheal and bronchial volume (vol (i) - vol (ii)) is added to this last volume measurement (iii) and trapped air bubbles and actual tissue volume are subtracted, a final total volume is obtained which is close to the volume instilled in the first 15 seconds.

Glutaraldehyde tissue fixation occurs as soon as it comes into contact with the tissue and this must happen within the first 15 seconds, preventing further expansion of the lung. However, a small degree of extensibility when under pressure must remain, since the pressure head continued to force a little more fluid into the lungs in the subsequent few minutes. Once this pressure is released (i.e. when the ligatures are removed), the excess fluid can no longer be retained by the lungs and they return to their initial volume dictated by the 15 seconds fixation. (The accuracy of the graduated pipette was not sufficient to show that tracheal volume must also be slightly greater under a continued pressure head, assuming tracheal tissue behaves like lung tissue. On the other hand, air bubble volume would presumably be reduced.)

By manually depressing the lungs and storing them for a few hours at $4^{\circ}C$, all air bubbles were removed from inside the lung giving right and left lung volumes (iv) slightly greater than volume (iii). Volume (iv) was taken as the final and correct volume for seven lungs fixed at 10 cm H_2O. Several lungs were also fixed at 5 and 15 cm H_2O instillation pressures. The lengths of right and left lungs were also measured, including a separate measurement of the anterior lobe, i.e. lung tissue anterior to the bronchus.

Fixation of the one week old L. vivipara lung

Although cannulation of the trachea was possible, the fine bore capillary cannula which was required proved too resistant to glutaraldehyde flow at 10 cm H_2O pressure head. Instead an alternative method was devised (Fig. 5.1a). The lizard was killed by intraperitoneal injection of Nembutal and decapitated by a transverse cut behind the eyes. This cut passed through the trachea, thus ensuring it was patent since the glottis is often blocked by mucus. A small slit was also made in the abdomen. A latex rubber collar was sealed to the neck of the lizard with neoprene glue and to the open end of a small airtight body chamber. The body of the lizard hung suspended above glutaraldehyde contained at the bottom of the chamber. By means of the latex collar the trachea and lungs were open to the atmosphere whilst the thorax was subjected to pressure within the chamber. As the pressure in the chamber dropped, so air was sucked into the lungs and the ribcage inflated. When a near-maximum inflated appearance was reached, the chamber three-way tap was closed and the apparatus inverted, thus submerging the lizard in glutaraldehyde. After 30 minutes the lizard was removed and the lungs carefully dissected free and placed in a glutaraldehyde bath.

Five out of ten one week old lizards were successfully fixed by this method; failure being due to tracheal blockage or a stiffening of the ribcage at death preventing normal ribcage expansion. Lung fixation was thus from the pleural side and it was not until diffusion of fixative into all the septa had occurred that the air phase within the lung was replaced by liquid using manual manipulation within the glutaraldehyde bath. (By this method, there should be a greater chance of keeping intact any surface lining material.) Lung volume was measured in the same way as in the adult.

Lung tissue weight

Before removal of the lungs from freshly killed lizards, the trachea was ligated to prevent water entering since it was necessary

to keep the outer lung surface moist during the dissection. All pleural mesenteries were cut off close to the lung. Finally with the lungs in a dry dish, the trachea and bronchi were rapidly cut away and the lungs weighed separately. In this time all excess surface moisture on the lungs had evaporated. Unless care is taken, the delicate lung tissue rapidly dehydrates. A moist tissue weight is essential since only this value is a true indication of the functional state of the tissue.

Instillation of fixatives into the lung gives rise to the problem of removing fluid from the alveoli in order to obtain a true moist tissue weight. To determine a suitable method, freshly removed and weighed lungs were submerged in saline so that the internal surfaces were completely wetted. Excess liquid was blotted away and the lung tissue sandwiched in the centre of ten layers of 4 cm^2 of Whatman's No. 1 filter paper placed between two 0.5 cm thick 2 cm x 2 cm squares of plywood. A variety of weights from 0.5 to 4 kg for $\frac{1}{2}$ to 4 minutes were applied to the 'sandwich' to blot the tissue to a consistent dry weight. Three tissue weights were obtained for each lung (the tissue being completely soaked in between blottings). This was also repeated for lungs immersed and fixed in glutaraldehyde instead of saline. To avoid tissue damage, a minimum blotting weight and time was sought which would give a consistent minimum dry tissue weight varying by less than 1% between three readings. A value of 2 kg for one minute answered this criterion. (For 4 cm^2 area a 2 kg weight gives a pressure of 0.5 kg/cm^2.)

It must be emphasised that this tissue press in no way damaged the lungs since there was no evidence of damage or difference when compared with non tissue-pressed lungs at the electron microscopic level. Also, instillation fixed lungs re-filled with glutaraldehyde after tissue pressing to a shape and volume identical to their initial value. The blotted dry tissue weight was consistently 45-50% of the moist tissue weight. By taking a mean value of 47.5%, all blotted tissue weights were converted to normal

weights. A total of 25 tissue weights (fresh and instilled) were obtained.

Lung morphometry

Stage 1 sampling: Six lizard lungs fixed at 10 cm H_2O instillation pressure (0.2g and 3.0g L. vivipara, 5.3g and 9.0g L. sicula and 20.0g and 29.3g L. viridis) together with two lungs (L. vivipara 3.0g) fixed at 5 and 15 cm H_2O were used for microscopic evaluation of lung morphometric parameters.

Light microscopic evaluation of the right lung

(i) Stage 2 sampling. Glutaraldehyde fixed lungs were washed for at least an hour in 0.1M cacodylate buffer and cut transversely into two or three parts or left whole depending on their size. Each piece, approximately 1 cm in length, was placed in a dish of 15% gelatin (in cacodylate buffer) at 37°C for ½ to 1 hour. Initially, all the lungs, especially the whole ones, were depressed many times to flush out the buffer from the lumen and replace it with gelatin. The gelatin-impregnated lungs were then blocked exactly as for paraffin embedding and allowed to set at 4°C. The blocks were orientated for transverse sections and stuck with gelatin to a -20°C chuck head, which was then lowered slowly into a vacuum flask of liquid nitrogen. As the gelatin froze it changed from transparent to opaque finally turning completely white. Rapid freezing of the block by instantaneous immersion caused extensive cracking of the gelatin and lung and hence a more gradual immersion taking approximately 2 minutes was used.

All blocks were sectioned within a few days of being made since storage even in air-tight containers at 4°C led to some dehydration of the gelatin. Hardening and long term storage of gelatin blocks even in 5% formalin (40% suggested by Pearse, 1968) alters the properties of the protein to such an extent that it was found impossible to cut section. Also, the use of glycerol in the proportion of 15% (Pearse, 1968) prevented the gelatin blocks from freezing in liquid nitrogen to a suitable hardness for sectioning.

6 μm serial sections, often in ribbons, were cut on a Cambridge rocking microtome maintained at -20°C in a Slee freezing cabinet. Sections were carefully picked up on standard microscope slides by holding the slide exactly parallel to the face of the knife and then placing it over the section so that even and instantaneous contact was made. The warmth of the slide caused the gelatin to melt and thus adhere to it. With practice, sections could be picked up in this manner without any crinkling or other distortion. A series of sections were thus collected at 90 μm to 360 μm intervals depending on the lung length, so that an average of 80 sections per lung were obtained. If the blocks were correctly orientated before sectioning, loss of interval sections between blocks of the same lung did not occur. The number of sections collected when multiplied by the interval distance always equalled the measured length of that lung. Since there is no shrinkage in gelatin (Campbell & Tomkeieff, 1952) it is, therefore, a fair assumption that the 2 or 3 parts of the same lung separately blocked were sectioned in exactly the same plane.

(ii) Planimetry. Each section was projected and enlarged 4-8 times depending on lung size using a standard photographic enlarger. The outline of the outer lung wall was traced onto thin paper and a line was also drawn following the inner limit of the trabeculae and connecting one to another in a smooth curve without dipping into the alveolar air space. A square of known area was similarly drawn. Each lung section area was cut out and weighed to four places of decimals. Then the area representing the peripheral parenchyma (a) was cut away and the central air space area (b) was weighed. The volumes of (a) and (b) for 90-360 μm wedges taken serially along the length of the lung were calculated from the equation

$$\text{Wedge volume} = \text{Area weight (g)} \times \frac{1}{\text{g wt. of 1 cm}^2 \text{ of paper}} \times (90 \text{ to } 360) \times 10^{-4}$$

By summation of all wedge volumes, total parenchyma (a) and central air space (b) volumes were determined for each lung.

(iii) Volume and surface density determination. Stage 3 and 4 sampling.

Using a Zeis photomicroscope, each section was subjected to stereological counting. An eyepiece square lattice grid of 9 points spaced at 0.45 cm intervals with 12 test lines connecting the points was placed in a x8 eyepiece and used at a total magnification of x320 (Fig. 5.2a). All counts were recorded with a keyboard and an electric counter consisting of 10 counters and 2 totalisers similar to that described by Weibel, Kistler & Scherle (1966) and Weibel (1969b). Seven keys were designated to septal tissue, alveolar air space, gross blood vessels, trabeculae, points not falling within the parenchyma, intersections of the alveolar surface area with the test lines and to test lines not falling within the parenchyma. The first five keys were connected to one of the totalisers.

Initial placement of the test system was over the top left hand corner of the section and after recording the seven parameters, the section was displaced 337.5 μm to the right of the initial position, i.e. the distance of three test lines, using the microscope's slide carriage. By moving in this manner from left to right and right to left across the section, the whole section was systematically sampled (Fig. 5.2b). With practice this could be done accurately taking 10-15 minutes. Fig. 5.2b illustrates how the section was covered by evenly spaced points but with the test lines in groups of 12. In the middle of the lung where the cross-sectional area was at its greatest, 30 to 120 grids for a 3g to 29.3g animal were required to systematically sample one section. Using Weibel's (1963) prediction graph for probable relative error of the volume density estimate for an average of 80 sections per lung, an error of 0.05% was obtained for air of average volume density 0.75, an error of 2% for septa of 0.2 volume density and an error of 10% for both blood vessels and trabeculae of 0.025 volume density each. After each section, the numbers on the counters were transferred to data sheets and the counters reset to zero.

FIG. 5.2 A. Square lattice grid of points and lines used in the eyepiece of compound microscope.

B. Placement of grid over T.S. of lung. In practice section was displaced on microscope stage.

C. T.S. of lung showing alveoli. d = depth of alveolus, di = diameter of alveolus.

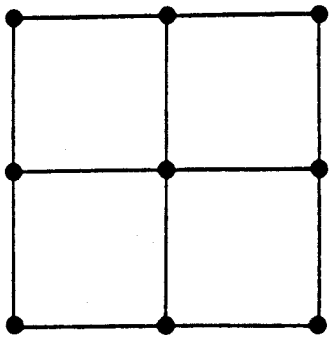

0.45cm actual grid
3.6cm in x8 eyepiece
112.5μm at x320 total magnification

A

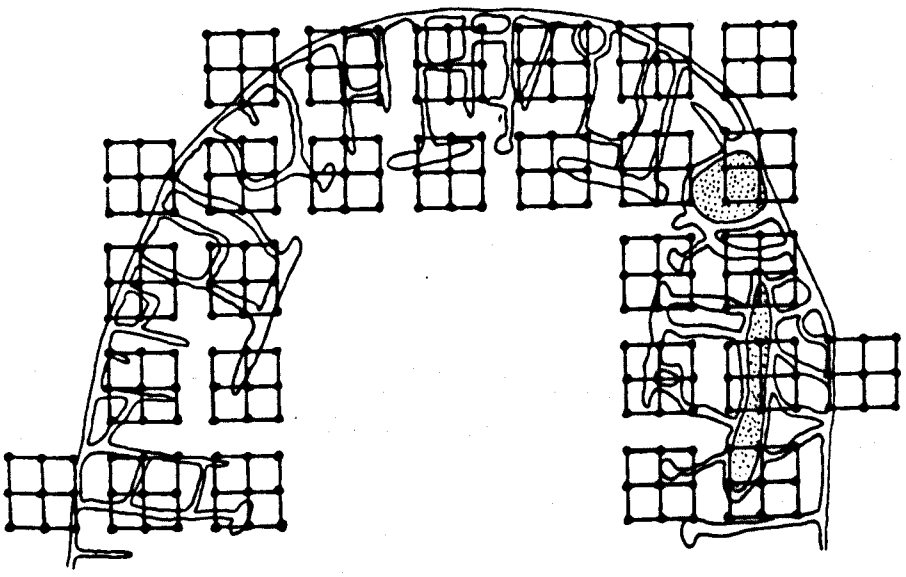

B

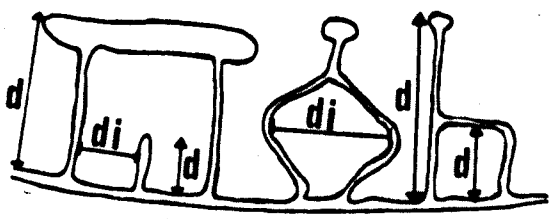

C

The volume densities V_v of septa, alveolar air space, trabeculae and blood vessels were determined for each section as a percentage of the total number of grid points minus those not lying in parenchyma. An average value for each parameter was also obtained for the whole lung and absolute volumes determined from the following equation:-

$$\text{Absolute volume} = V_v \times \text{parenchyma volume}$$

Surface density S_v of alveolar tissue is calculated from the equation $S_v = \frac{2I}{L_T}$ where I is the number of intersections of test lines with the alveolar surface and L_T = possible number of test lines - unused test lines x L where L = test line length. At 320x magnification with an eyepiece of x8, $L = \frac{0.45 \times 8}{320} = 112.5\mu m$.
Surface density was determined for each section and a mean value obtained for the whole lung. The absolute surface area can be calculated from S_v x parenchyma volume.

When point counting, a point may cover two structures but the one touched by the right hand side is the one recorded. Because the mammalian alveolar septa have two active surfaces, it is usual to count one for each intersection of the test line with a septa and only at the end of the counting sequence to multiply by two (Weibel, 1963). This cannot be applied to septa having only one active face, e.g. outer wall. In the lizard about 10-20% of the septa have only one active face, i.e. the outer wall, the walls of large veins and perivascular lymphatic channels surrounding large arteries and on the trabeculae. Hence each active face was counted in the lizard.

(iv) Number and size of alveoli

The alveolus of a lizard lung is either polyhedral or cylindrical. Viewed in transverse sections it must have a minimum of three septal walls before it can be considered to be an alveolus. At a magnification of x100, the number (n) of all alveoli present in each section was counted.

Using a 1 cm graticule in a x8 eyepiece at a total magnification of x160, every 5th, 10th, 15th, etc. alveolus was measured for its diameter and depth (Fig. 5.2c). Measurements of distances between trabeculae and the depths from a trabecula to the first free margin of a septum were also made. Since each section required many measurements, only every 5th, 10th, 15th, etc. section from a series through a lung were used.

Mean depth and diameter were obtained for each section and for the lung as a whole. Since transverse sections never cut alveoli frequently enough to represent their largest cross-section, mean alveolar diameter is always underestimated. Following Weibel (1963) a factor of 1.2 was used to yield 'true' alveolar diameter. This does not apply to the depth measurements.

The density of alveoli per section can be determined from the equation:-

$$\text{Alveolar number/cm}^2 = \frac{n}{\text{area of parenchyma of that section}} \times \frac{1}{\text{Mean corrected alveolar diameter } \bar{di} \text{ for that section}}$$

$$\text{Absolute alveolar number per wedge volume} = \frac{n}{\text{area}} \times \frac{1}{\bar{di}} \times \text{area} \times \text{wedge length.}$$

Densities and absolute numbers of alveoli were thus determined for serial wedge volumes and for the lung as a whole.

Electron microscopic evaluation of the left lung

Stage 2. Glutaraldehyde fixed lungs were cut so that five equidistant rings of tissue, 2 mm wide, were obtained along the length of the lung, but without taking the anterior and posterior tips. Each ring was diced into 2 mm squares and all squares were blocked in epon as described in Chapter 4. Only the lung of L. viridis (20g) was morphometrically analysed. Two blocks per region were randomly selected and sectioned at right angles to the outer wall to obtain one technically perfect section per

block which covered at least 30 copper grid mesh holes (200 mesh size).

At this point sampling deviates from the stage 3 of Weibel's method. From each section an average of 10 micrographs selectively subsampled for capillarised septa were recorded using an AEI 6G electron microscope at a primary magnification of 2,500 times on 8 x 8 cm Kodak sheet film or Ilford EM plates. A total of 80 micrographs from two blocks per region 1-4 were made together with micrographs of a graticule of 1181 line/mm made at the end of each recording period. These micrographs were reduced using a standard photographic enlarger and positive printed onto 35 mm film held, and thus framed, in the projector carriage of the projector unit later used for morphometric analysis. A reduced magnification of 1,125 times thus obtained had a micrograph size of 35 x 30 mm with a subsequent 5 mm loss of the reduced picture. This loss, where possible, was arranged to be in air or non-capillarised septal areas.

For evaluation of the positive film strips, a table projector as described by Weibel (1969b)was used at a final magnification of 11,800 times using a coherent double lattice test system with 576 test prints and 128 test lines of 3.5 cm individual length. Volume densities of air space, capillarised septa and its components (epithelium, interstitium and endothelium), endothelium and interstitium not in the air to blood pathway and capillary lumen and its contents (plasma, erythrocytes and leucocytes) were estimated by point counting. Alveolar, capillary, both within the air to blood pathway and not, and erythrocyte surface area densities were obtained by intersection counting. Average volume and surface densities were obtained from the 80 micrographs. Arithmetic mean thickness was determined for epithelium, interstitium, endothelium and capillary lumen where

$$\bar{\tau} = \frac{V_v}{S_v} \text{ or } \frac{V_v \times L_T}{2I}$$

and harmonic mean thickness of the air-blood barrier and plasma distance was estimated by the method of Weibel & Knight (1964) and Weibel (1970/71) using

the test line probes of the test system above together with a ten class logarithmic scale.

Conversion of volume and surface densities from the selectively subsampled capillarised septa into absolute values for the whole lung is described with the results.

RESULTS

Nasal cavity volume, tracheal dimensions, lung volume, length and weight.

Nasal cavity volume was found to be almost isometric with body weight, NC vol. = $0.0015\ W^{1.05}$ and so also was tracheal volume, Tr. vol. = $0.0022\ W^{0.94}$ (Fig. 5.3). Together, they made extrapulmonary dead space proportional to $W^{1.0}$. For a 30g lizard, nasal cavity volume and tracheal volume were both 0.054 ml giving a total dead space of 0.108 ml. This is considered a fair estimate of extrapulmonary dead space because the nasal cast included the nasopharyngeal ducts which abutt onto the glottis. Although the throat is slightly expanded during inspiration because of gular activity (Chapter 2), its contribution to extrapulmonary dead space is considered negligible but has not been measured. Extrapulmonary dead space is 4.6% of the total respiratory air volume.

Tracheal length of the lizards varied rather more than the cube root of body weight. Tr.L = $0.965\ W^{0.355}$ and tracheal diameter varied rather less, Tr.D = $0.054\ W^{0.29}$ (Fig. 5.4). Lungs fixed at 10 cm H_2O had a mean lung length equal to $0.914\ W^{0.356}$, the left lung being always approximately 5% longer than the right. This condition was reflected in the more posterior margin of the left, black peritoneal lining. For a given size, tracheal and lung lengths were virtually identical.

Total lung volume, as measured by the displacement method, was directly proportional to body weight (Fig. 5.5). Table 5.1 gives the body weight regression analysis data for various lung volumes. The variability of the regression coefficient is due to the small sample size. It is evident that the lung volume of the 0.2g lizard neatly fits the body weight relationship of the adult lungs. Postnatal development has no effect on this parameter.

FIG. 5.3 Logarithmic relationships of nasal cavity volume and tracheal volume to body weight. Correlation coefficient = 0.97 (nasal cavity volume) and 0.98 (tracheal volume).

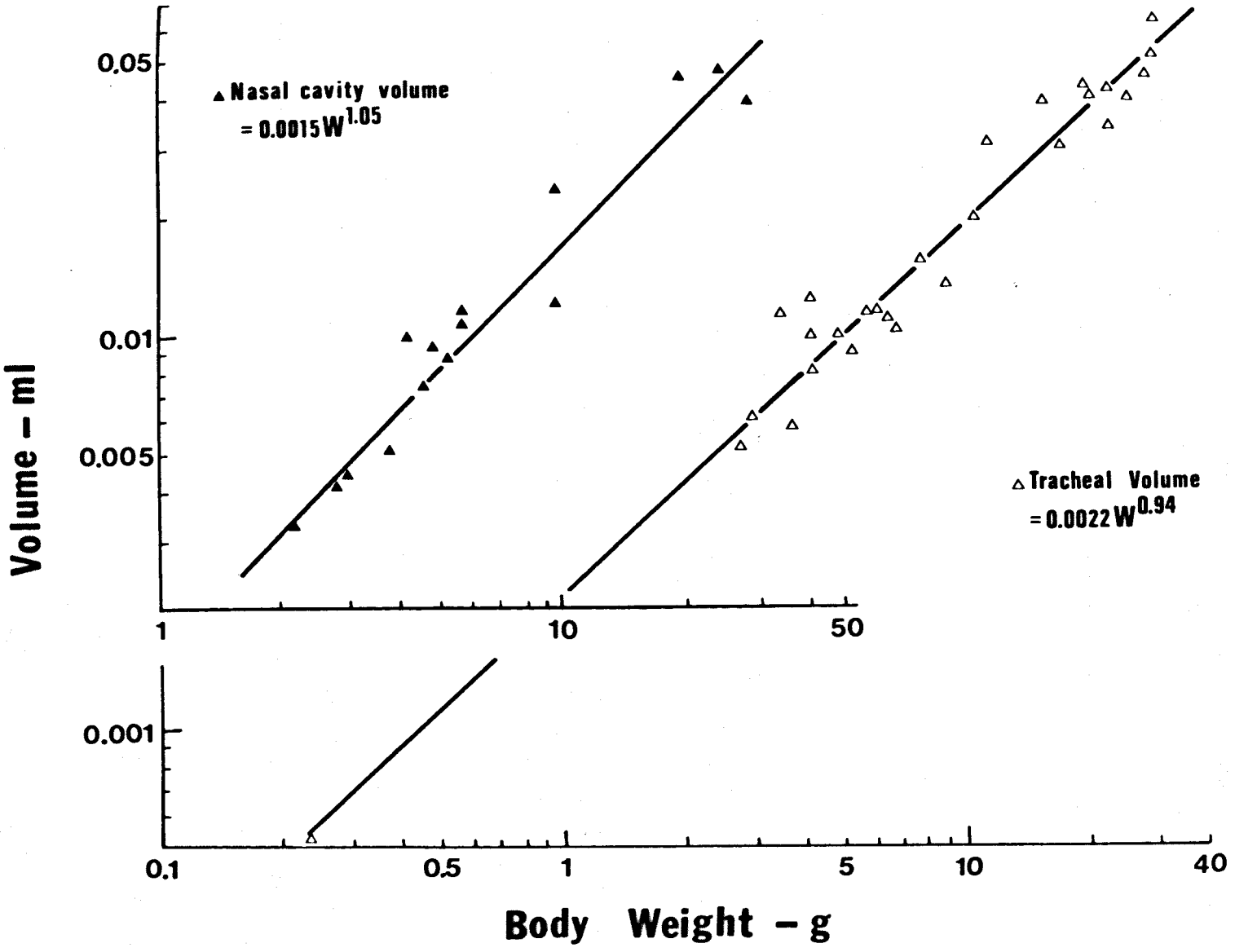
▲ Nasal cavity volume
= 0.0015 W^1.05
△ Tracheal Volume
= 0.0022 W^0.94
0.05
0.01
0.005
0.001
1
10
50
0.1
0.5
1
5
10
40
Volume – ml
Body Weight – g

FIG. 5.4 Logarithmic relationships of tracheal length and diameter to body weight. Correlation coefficient = 0.973 (length) and 0.974 (diameter).

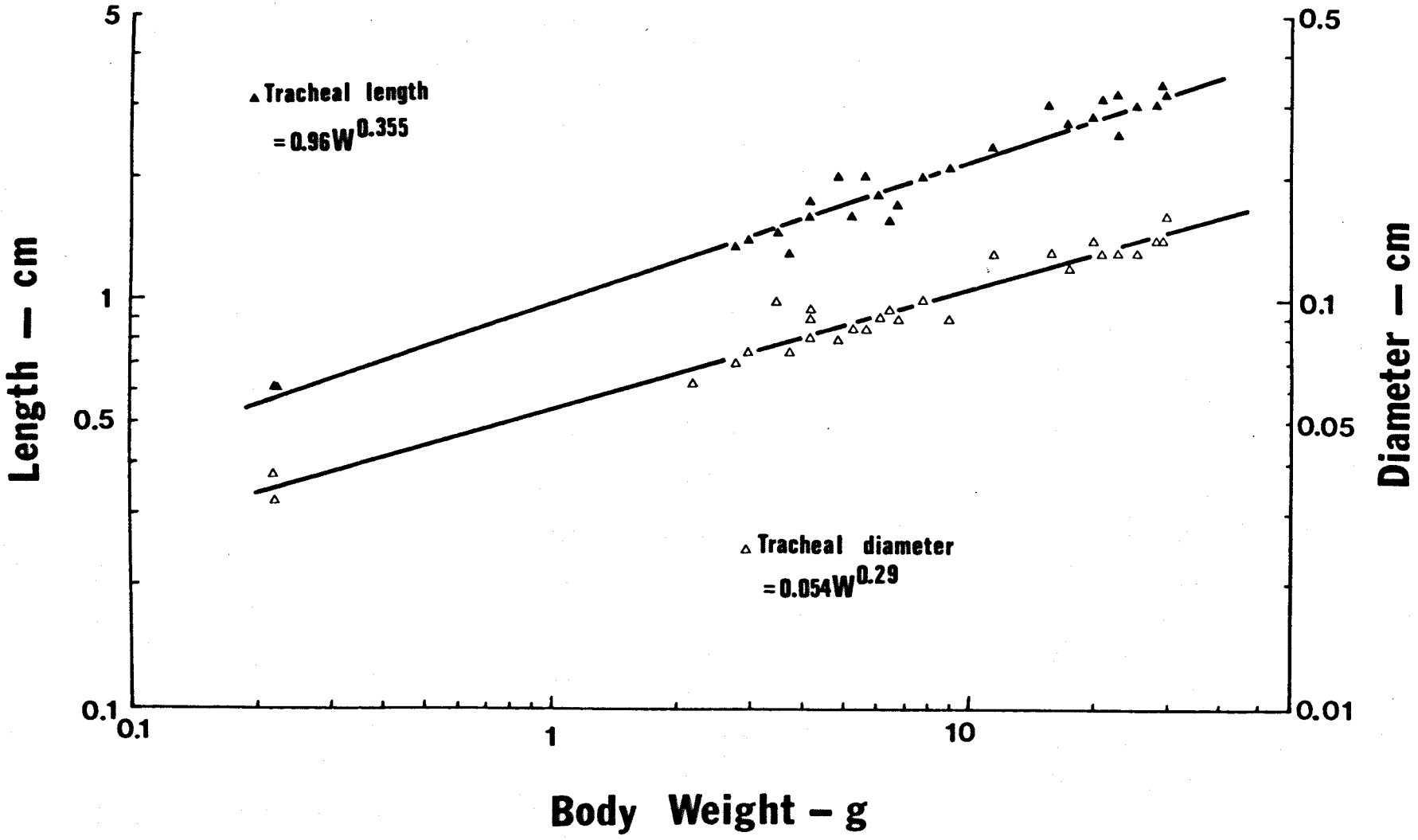
▲ Tracheal length
= 0.96W^0.355
△ Tracheal diameter
= 0.054W^0.29
Length — cm
Diameter — cm
Body Weight — g
5
1
0.5
0.1
0.5
0.1
0.05
0.01
0.1
1
10

FIG. 5.5 Logarithmic relationship between lung volume and body weight. For correlation coefficients and further details see Table 5.1.

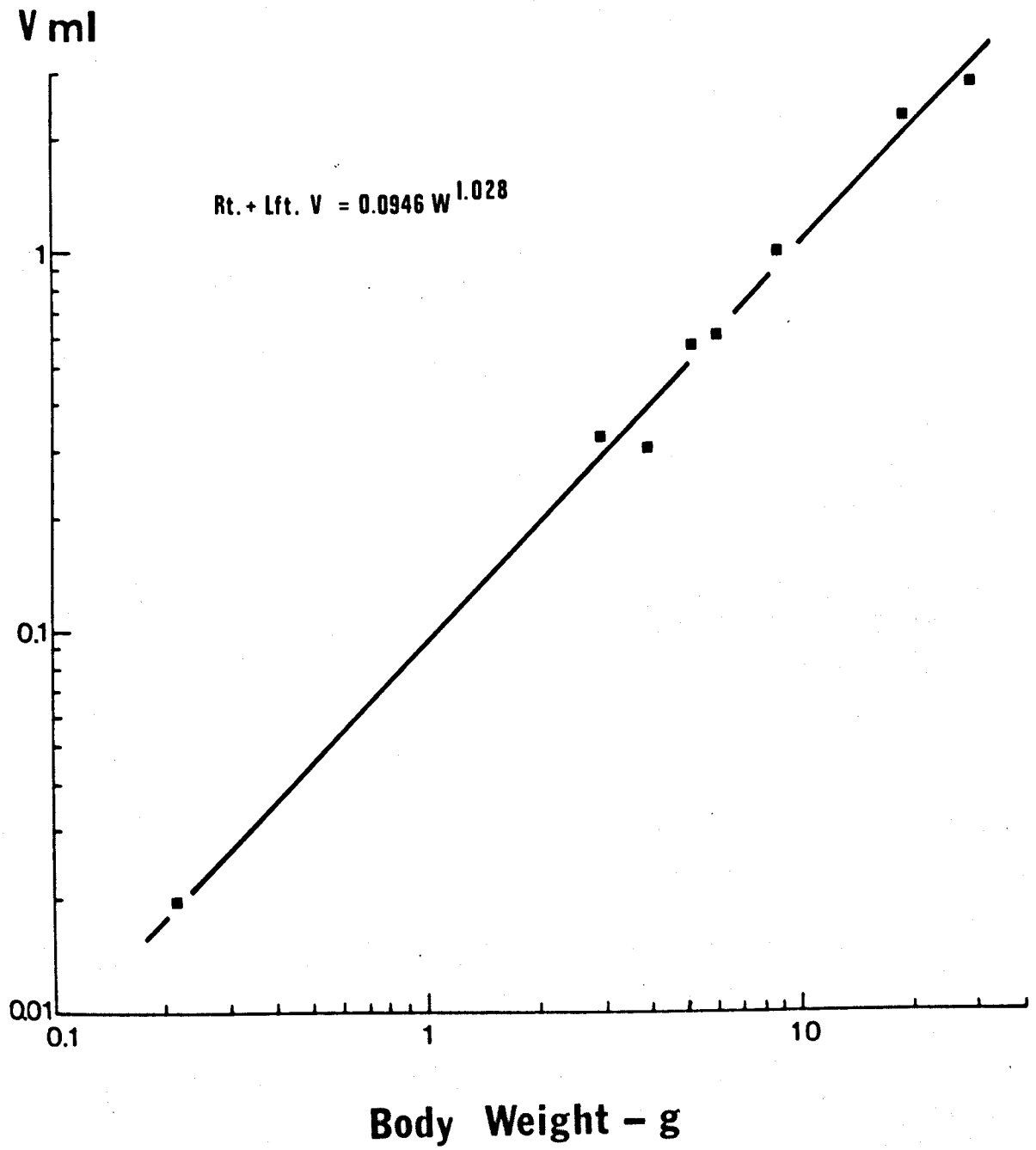
V ml
Rt. + Lft. V = 0.0946 W 1.028
1
0.1
0.01
0.1
1
10
Body Weight – g

FIG. 5.6 Logarithmic relationship between lung weight and body weight. Solid line, adult data, correlation coefficient 0.956. Dashed line, adult + 7 L. vivipara (0.2g), correlation coefficient 0.976. Only the mean point for 0.2g L. vivipara data is plotted but raw data between 0.00045 and 0.0008 used for regression analysis.

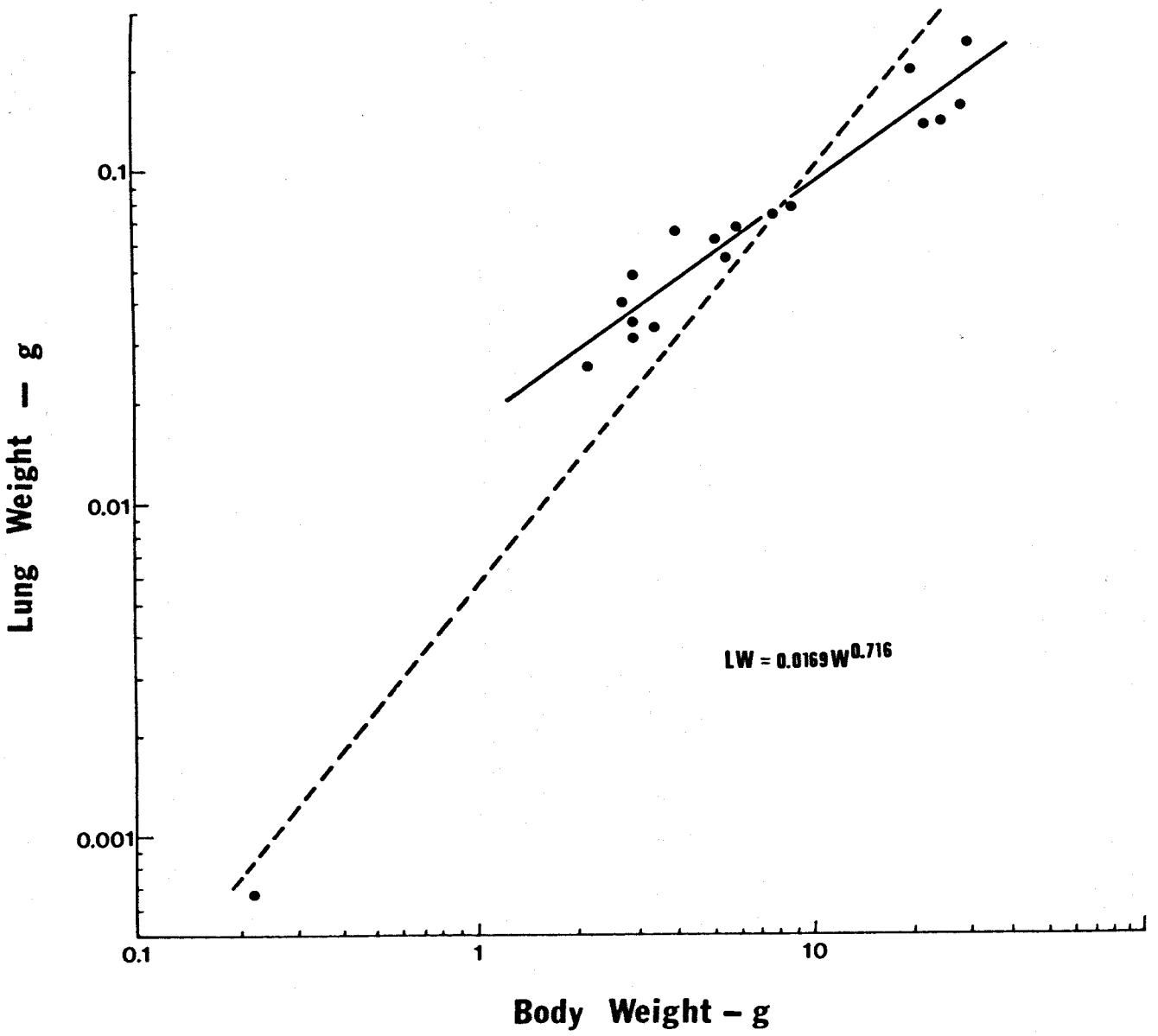
Lung Weight — g
0.1
0.01
0.001
0.1
1
10
Body Weight – g
LW = 0.0169 W^0.716

TABLE 5.1

Relationship of lung volume (ml) to body weight (g) in the equation L. vol. = aW^b, for Lacerta. Number of animals in parenthesis.

Lung	a	b	CC
Right lungs (8)	0.0478	1.0054	0.9956
Left lungs (8)	0.0463	1.0597	0.9968
Right + left lungs (8)	0.0946	1.0285	0.9965
Adult right + left lungs* (5)	0.1158	0.9635	0.9973
Adult right + left lungs* + recently hatched L. vivipara (6)	0.09978	1.0244	0.999
Adult right lung* (5)	0.0626	0.9072	0.996
Adult right lung* + recently hatched L. vivipara (6)	0.0497	1.0013	0.998

* Lungs used for extensive morphometry.

Adult lung weight is not isometric with body weight but is related to $W^{0.716}$ (Fig. 5.6). The lung weight of the 0.2g L. vivipara is well below the expected value determined by extrapolation from the adult regression line, being 0.00082g instead of 0.005g - a sixth less. When included with adult data, a regression slope of 1.2378 is obtained (Table 5.2) which has a high, 0.976, correlation coefficient. This good correlation is due to the 0.2g data extending the body weight range from 1 to 2 log. cycles.

TABLE 5.2

Relationship of lung weight, LW, (g), to body weight, W(g), in Lacerta in the equation LW = aW^b.

	a	b	CC
Adults (18)	0.0169	0.716	0.956
Adults + recently hatched L. vivipara (25)	0.0055	1.2378	0.976
Adults used for extensive morphometry (5)	0.0098	0.711	0.977

For the purpose of comparison with data in the literature, regression analysis was also performed for mean lung length and lung volume when plotted against snout-vent length instead of body weight (Table 5.3). Lung volumes are directly proportional to body weight, whilst lung lengths and snout-vent lengths are cube functions of body weight or lung volume.

TABLE 5.3

Relationship of lung length, LL (cm), or lung volume, L. vol.(ml) to body weight, W (g) or snout-vent length, L.(cm). Number of animals in parenthesis. Lacerta

Equation	a	b	CC
$LL = aW^b$ (16)	0.914	0.356	0.988
$LL = aL^b$ (16)	0.235	1.057	0.99
$L.\ vol. = aW^b$ (8)	0.0946	1.0285	0.9965
$L.\ vol. = aL^b$ (8)	0.0018	3.057	0.989

Planimetry and light microscopic volume evaluation of the right lung at 10 cm H_2O

Sections of gelatin embedded lungs when examined under the microscope showed a 'halo' effect around the lung septa, which was due to gelatin disruption by ice crystal formation. This 'halo' varied from lung to lung and was thus obviously dependent on variations in gelatin impregnation and freezing time. At the level of magnification used the tissue itself appeared undamaged and the resolution without staining or mounting in DPX was good. Thus, all measurements were made on untreated sections with the microscope condensor suitably positioned to make the tissue stand out as green/blue against a whitish gelatin background.

Estimations of lung volume by planimetry were approximately 5% lower than those determined by volume displacement. Because of the many steps and accompanying errors in the planimetry method (i.e. shrinkage when

picking up sections, errors in contour outlines, variations in weight within a sheet of paper and errors in cutting out shapes), it was considered that the volume displacement method was the most accurate. Absolute values for peripheral parenchyma and central air space determined by planimetry were therefore corrected.

Since the 0.2g lizard lung weight does not fit the adult regression slope, regression analysis has only been made on lung parameters from the 5 adult lungs. In the ensuing figures, the 0.2g lizard values have been included for comparison.

Table 5.4 and Fig. 5.7 and 5.8 show that central air space volume increased more with increasing size than did alveolar air. The latter, however, increased (with size) more than lung tissue volume. It is certainly obvious from transverse sections of the lung that there is a greater proportion of parenchyma to central air space in a 3.0g than in a 29.3g lizard. This is shown well in a later figure where wedge volumes in an antero-posterior gradation are depicted for different sized lizards (Fig. 5.13). Unfortunately, the 5 right lungs used for detailed morphometry were not completely isometric in the volume to body weight relationship (Tables 5.1 and 5.4). Thus, regression coefficients of the various lung volume parameters can only indicate relative importances for body weight scaling but cannot give absolute regression slopes.

TABLE 5.4

Relationship between 5 adult Lacerta, right lung volume parameters and body weight (g), $X = aW^b$.

X	a	b	CC
Lung volume (ml)	0.0626	0.907	0.996
Peripheral parenchyma volume (ml)	0.0287	0.807	0.981
Central air space volume (ml)	0.0339	0.970	0.984
Alveolar air volume (ml)	0.0206	0.822	0.978
Total air volume (ml)	0.0546	0.923	0.995
Lung tissue volume (ml or g)	0.0098	0.711	0.976

FIG. 5.7 Logarithmic relationships of total lung volume, central air space and peripheral parenchyma volume to body weight. See Table 5.4.

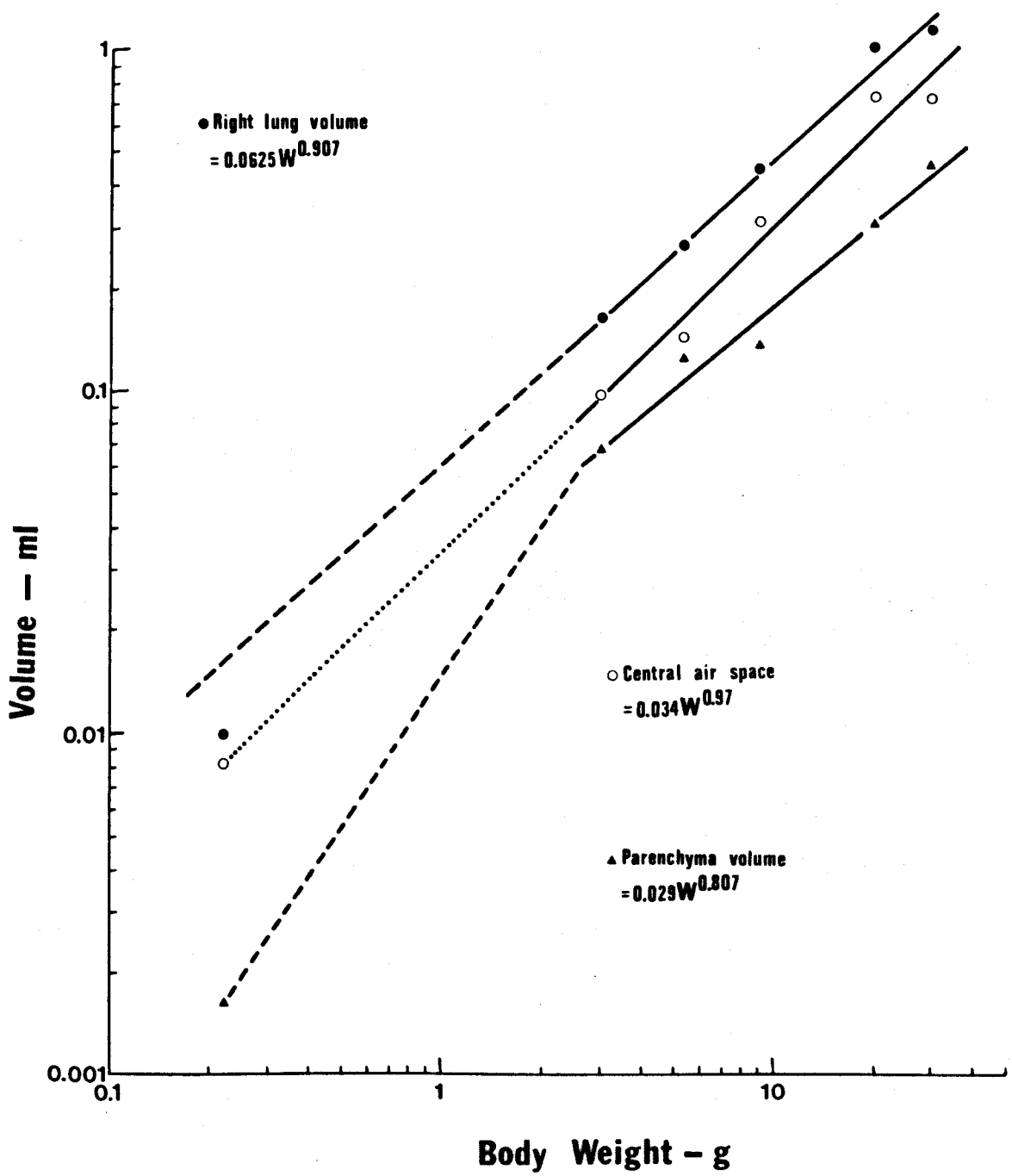
1
0.1
0.01
0.001
0.1
1
10
Volume – ml
Body Weight – g
● Right lung volume
= 0.0625W^0.907
○ Central air space
= 0.034W^0.97
▲ Parenchyma volume
= 0.029W^0.807

FIG. 5.8 Logarithmic relationships of total air volume, alveolar air volume and tissue volume to body weight.

See Table 5.4.

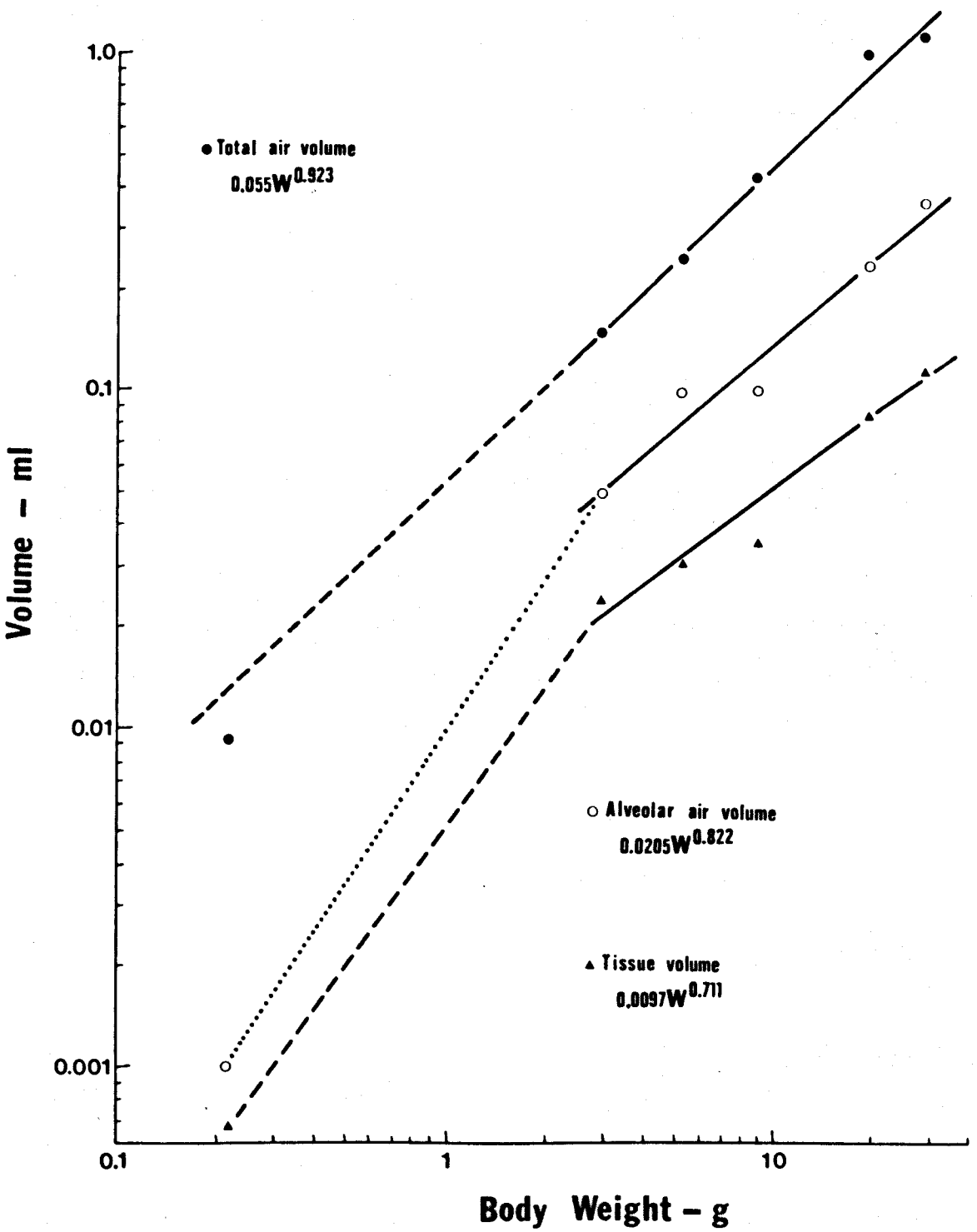
1.0
0.1
0.01
0.001
Volume – ml
● Total air volume
0.055W^0.923
○ Alveolar air volume
0.0205W^0.822
▲ Tissue volume
0.0097W^0.711
0.1
1
10
Body Weight – g

Just as the 0.2g lizard lung volume fitted the adult lung volume relationship to body weight, so also does its central air space and total air volume. Parenchyma and alveolar air volumes, however, do not fit since they are under-developed. This would be expected since lung weight was reduced. In fact, if the peripheral parenchyma volume was predicted from the adult value, it would fill the whole of the lung obliterating the central lumen!

From point counting, the absolute value for total tissue weight was always very similar to the value obtained by weighing, with a maximum difference of only 5%. It is thus a fair assumption that other values, i.e. alveolar air, septa, trabeculae and gross blood vessels, were also accurately determined.

An average of 78% of total tissue weight was occupied by septa, 12.5% by trabeculae and 9.5% by blood vessels (Table 5.5). (It was not possible to determine these three parameters for the 0.2g lizard).
It might be expected that these three tissue weight parameters would increase in the same proportion as each other as size increased. Blood vessel weight, however, has a greater slope than the septa or trabeculae. The explanation lies in the fact that, although capillary size is constant for all body weights, pulmonary vessels will increase in diameter as body weight increases. Thus, the blood vessel volume is bound to be relatively larger in a bigger lizard.

TABLE 5.5

Relationship between tissue weight parameters and body weight in 5 adult right lungs of Lacerta. $X = aW^b$.

X (g)	a	b	CC
Total tissue weight	0.00975	0.711	0.977
Septa weight	0.00759	0.694	0.978
Trabeculae weight	0.00122	0.685	0.970
Gross blood vessel weight	0.001053	0.768	0.932

The 0.2g lizard has very thin trabeculae 35 μm, considerably less than predicted from the adult data (Table 5.6) in which the thickness increases with body weight by a regression coefficient of 0.1. The reason for the thin trabeculae of the 0.2g lizard is probably because of the smaller quantity of tissue that has to be supported and the relative shallowness of the alveoli (Fig. 5.10 and Table 5.6).

Light microscopic alveolar surface area estimations

The mean surface density of the alveoli determined at a magnification of x320 was related to body weight as S_v $cm^2/cm^3 = 352\ W^{-0.122}$ (correlation coefficient = 0.67) and absolute surface area cm^2 was related as $10.0 = W^{0.69}$ (correlation coefficient = 0.959) (Fig. 5.9). It is to be noted that septa weight (Table 5.5) and absolute surface area have the same value for their body weight regression slopes. This is only possible if the septa do not increase in thickness with increasing body weight. No such thickening of the septa was measurable at higher magnifications. Although the periphery of the trabeculae and gross blood vessels increase with body size because of their diameter increase, their relative surface area/unit body weight decreases, i.e. smaller surface to volume ratio. These structures are lined by septa but their relatively reduced surface area had a negligible effect on the absolute surface area to body weight regression slope. This is probably because these lining septa only have one active surface.

Absolute alveolar surface area for the 0.2g lizard is 0.85 cm^2 which is 4 times less than the value, 3.4 cm^2, expected from the adult data. Again, this correlates with the under-developed lung tissue weight; the 6 times less factor for weight becoming 4 for surface area because of the smaller than expected mean alveolar dimension (Fig. 5.10).

Alveolar dimensions

Log. log. plots of mean alveolar depth, diameter and mean size are given in Fig. 5.10. Alveolar depth is usually a little smaller than the diameter. In adults, it was found that alveolar depth changed more with

FIG. 5.9 Logarithmic relationships of absolute surface area and surface density to body weight. Correlation coefficients 0.98 and 0.67, respectively.

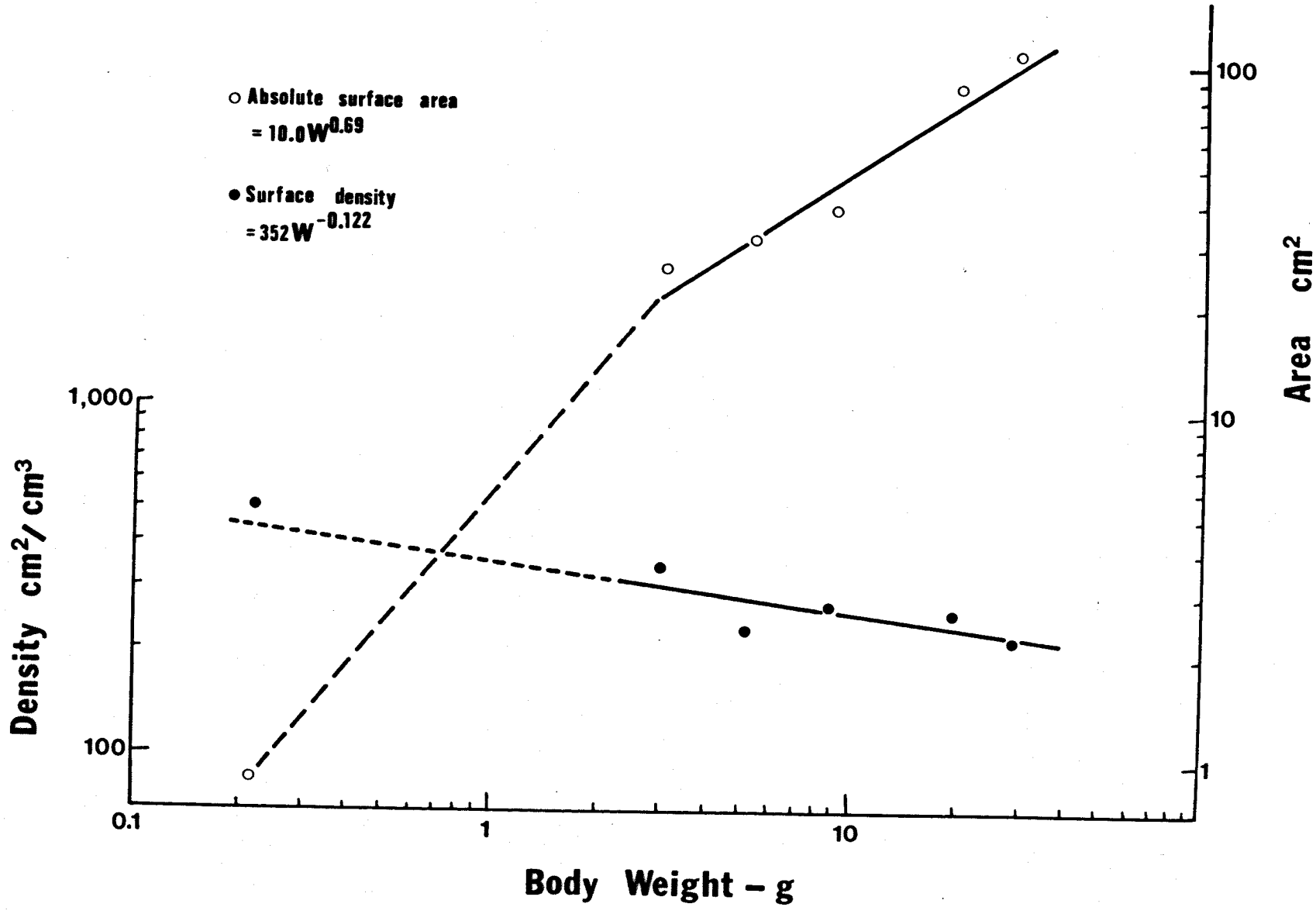
○ Absolute surface area
= 10.0W^0.69
● Surface density
= 352W^-0.122
1,000
100
Density cm²/cm³
0.1
1
10
100
10
1
Area cm²
Body Weight – g

FIG. 5.10 Logarithmic relationships of alveolar depth, diameter and mean dimension and trabecula mesh size to body weight. Correlation coefficients 0.8, 0.93, 0.86 and 0.48, respectively.

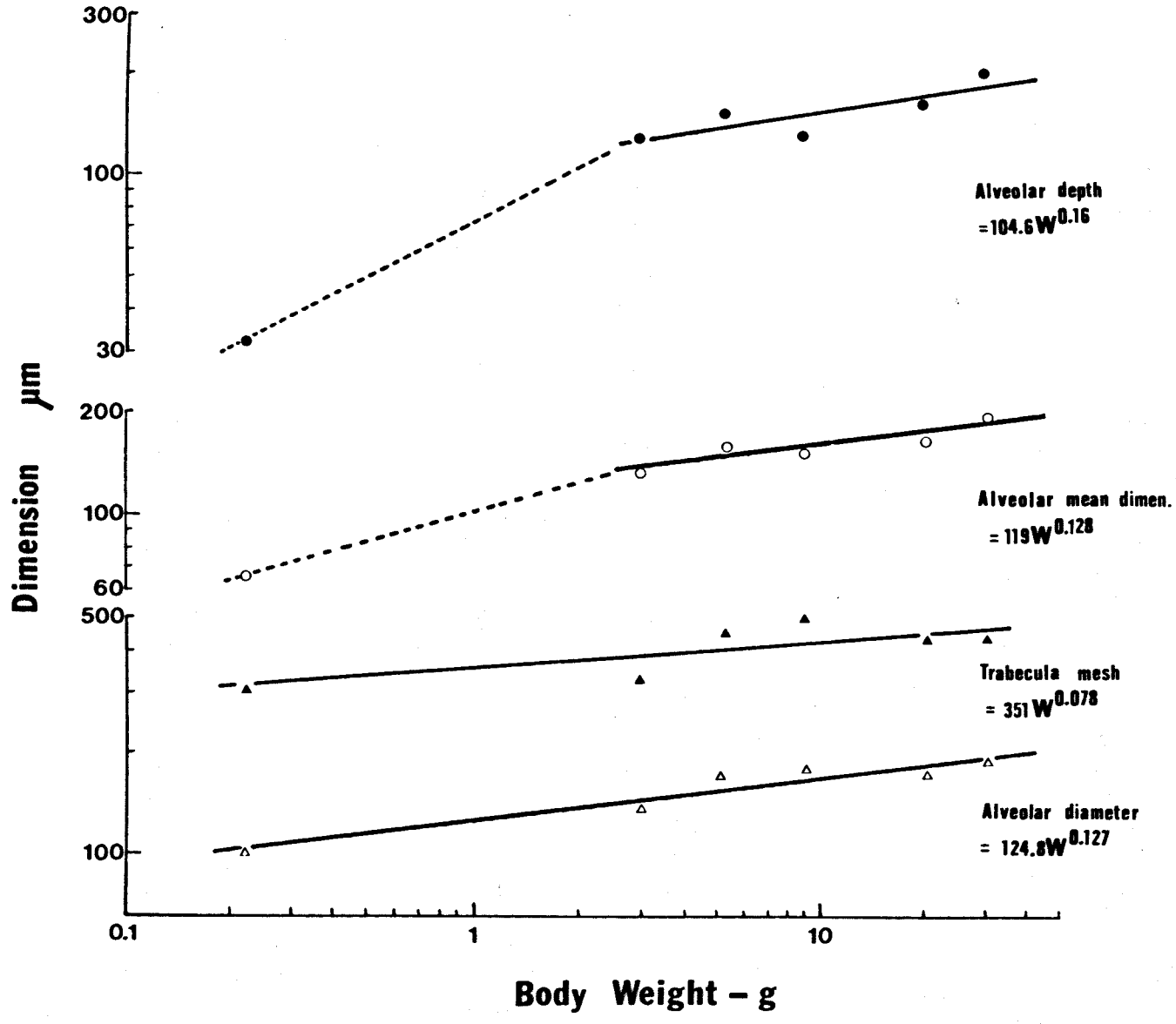
300
100
30
200
100
60
500
100
Dimension µm
Alveolar depth
=104.6W^0.16
Alveolar mean dimen.
= 119W^0.128
Trabecula mesh
= 351W^0.078
Alveolar diameter
= 124.8W^0.127
0.1
1
10
Body Weight – g

FIG. 5.11 Logarithmic relationships of alveolar density and total alveolar number to body weight. Correlation coefficients 0.86 and 0.96, respectively.

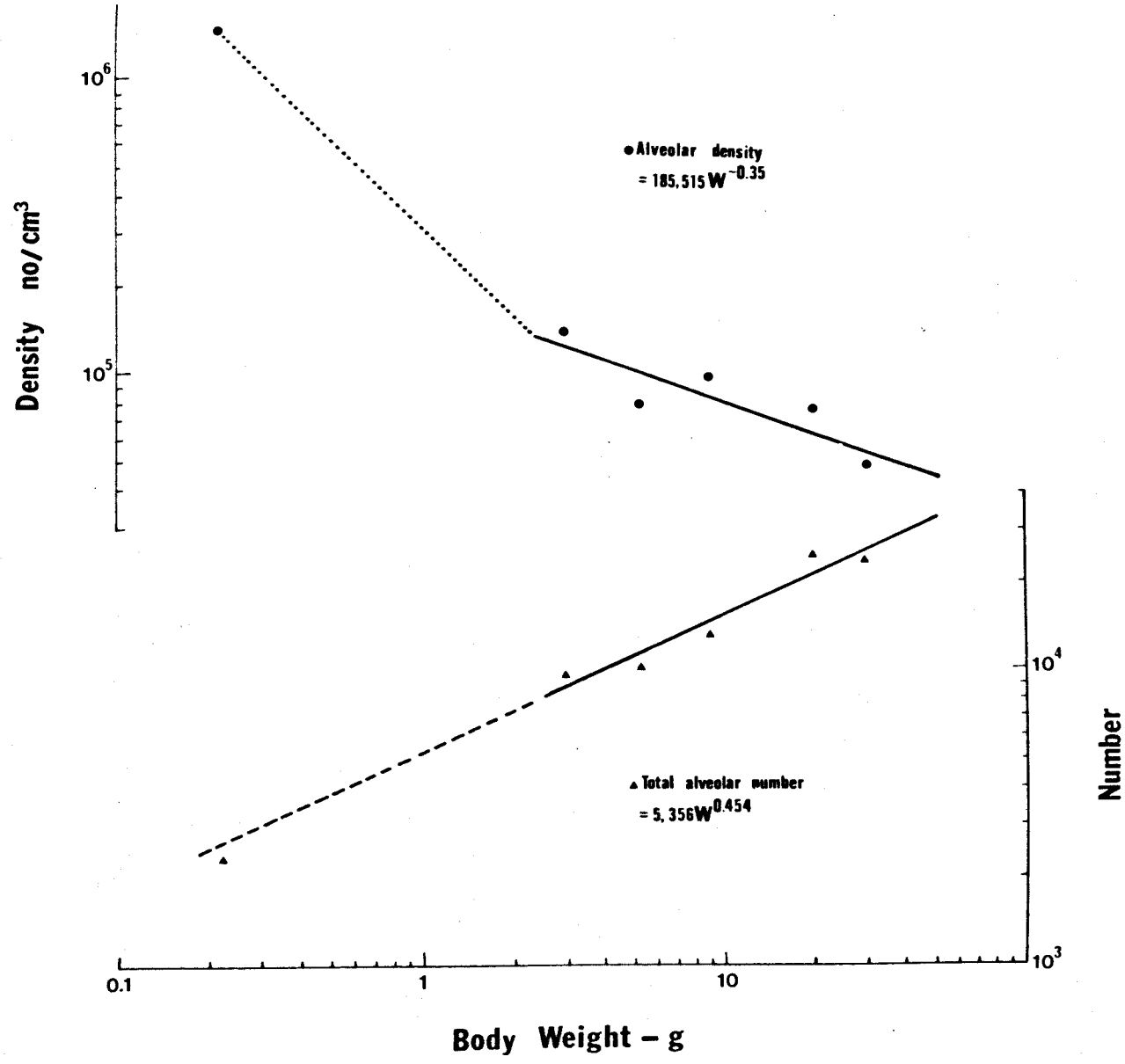
Density no/cm3
10^6
10^5
● Alveolar density
= 185,515 W^-0.35
▲ Total alveolar number
= 5,356W^0.454
10^4
10^3
Number
0.1
1
10
Body Weight – g

TABLE 5.6

Lung parameters for 6 body weights in Lacerta.

Parameter	L. vivipara	L. vivipara	L. sicula	L. sicula	L. viridis	L. viridis
Body weight (g)	0.22	3.0	5.3	9.0	20.0	29.3
Right lung vol. (ml)	0.01	0.17	0.2755	0.46	1.065	1.2248
Central space vol. (ml)	0.00834	0.1	0.146	0.32675	0.744	0.75
Parenchyma vol. (ml)	0.00166	0.07	0.1295	0.13325	0.321	0.474
Alveolar air vol. (ml)	0.00101	0.05	0.09875	0.098	0.238	0.36
Total air vol. (ml)	0.00935	0.15	0.24475	0.42475	0.982	1.11
Lung weight (g)	0.00065	0.0239	0.03075	0.0352	0.083	0.1132
Septa weight (g)	-	0.01845	0.0223	0.0286	0.06525	0.0835
Trabecular weight (g)	-	0.00285	0.0039	0.004825	0.0079	0.0153
Blood vessel weight (g)	-	0.00214	0.0046	-	0.0098	0.0142
Mean S_v (cm^2/cm^3)	512.5	348.0	236.0	278.0	267.0	226.0
Absolute surface area (cm^2)	0.85	24.0	30.06	37.4	85.5	107.0
Alveolar density (no./cm^3)	1,450,000	140,000	79,200	98,000	76,300	49,500
Absolute alveolar number	2,400	9,820	10,250	13,100	24,500	23,450
Mean alveolar diameter (μm)	100	134.92	168	174,38	170	185
Mean alveolar depth (μm)	32	128	149	128	159	200
Mean alveolar dimension (μm)	66	131.5	158.5	151.0	164.5	193
Mean trabecular mesh size (μm)	300	326	446.4	489	428	423.6
Trabecular thickness (μm)	35	120	135	130	150	150

body weight than did diameter. It is to be noted that the mean alveolar dimension has a regression slope very similar to the reciprocal of the slope for surface density, i.e. $W^{+0.131}$ and $W^{-0.122}$, respectively. When measurements are made only in alveolar regions, a surface density measurement is an estimate of mean alveolar dimensions because it is the reciprocal of the mean chord length measurement. (Mammalian mean chord lengths use intercept lengths through alveolar duct regions when estimating S_v and are thus not a measure of alveolar dimension, Weibel, 1963).

In the 0.2g lizard, the alveolar diameter is 100 μm whereas the depth, 32 μm, is considerably less. From the scatter of alveolar diameter data, it is probable that this lizard fits the adult data. This certainly cannot be the case for alveolar depth (Fig. 5.10).

During growth, the number of alveoli increase with a regression coefficient of 0.454 (Fig. 5.11). The alveolar number for the 0.2g lizard also fits this slope very closely whereas its alveolar density is far in excess of that predicted from the adult regression coefficient of -0.35 by a factor of 5. This is a result of the smaller mean alveolar dimension.

Table 5.6 documents all the absolute values obtained for each lung parameter for each of the 5 adult and the 0.2g lizards. All regression analysis data has been given in Table 5.1 to 5.5 and Figs. 5.3 to 5.11.

Surface area and capillarisation

Although surface density measurements were made at x320 magnification which in terms of intercept counts answered the criteria laid down by Weibel (1963), it was found that the surface density estimate increased with increasing magnification until a plateau was reached at x1,000. The reason for this was not that the lower magnifications did not sample enough septa to give an accurate measurement but that the septa had corrugated surfaces due to capillary bulging (Chapter 4). Such corrugations can only be determined accurately at high light microscopic or low electron microscopic magnifications.

To achieve an accurate surface area estimate, 1 μm epon sections stained with methylene blue were taken from the 5 EM antero-posterior regions of the left lung of L. viridis (20g). Surface density measurements were made at x320 and x1,000 on 5 sections per region and the correction factor, Y, determined. Fig. 5.12 illustrates the progressive decrease in this factor from region 1 to 4 with region 5, the most posterior, having a value twice as low as might be expected from previous regions. Y ranged from 1.55 anteriorly to 1.26 posteriorly with a mean value of 1.45 for the whole lung when the proportion of surface area within the different regions is taken into account.

Volume density measurements were also made on these same sections but at x1,600, to determine the % of septal tissue volume that is capillarised, i.e. the part of the septa directly involved in gas exchange. The % of alveolar surface area that is capillarised was also determined (Fig. 5.12). Septal tissue and alveolar surface area were considered uncapillarised if a test line crossing them did not also pass through a capillary. Both %s showed exactly the same antero-posterior relationship as Y with a mean for the whole lung of 78% for volume and 70% for surface area. The explanation of the difference between volume and area %s lies in the fact that the capillary is spherical, having a larger volume to surface ratio, whereas the thin septa in between capillaries have a small volume to surface ratio. The capillaries also appeared larger in diameter and often oval anteriorly but this is most likely to be due to the greater frequency of capillary branching.

The absolute surface area at x320 magnification must, therefore, be corrected by a 1.45 factor to account for capillary bulging (surface corrugations) measurable only at higher magnifications. However, only 70% of this corrected surface area actually contains capillaries and can thus be considered respiratory. It so happens that these two corrections cancel each other out and quite by chance the true respiratory surface area is

FIG. 5.12 Illustrates the decrease in the % tissue volume and % surface containing capillaries as the posterior regions of the lungs are reached. The correction factor, Y, for estimating surface area at low magnifications also decreases similarly (see text). Bar = standard deviation.

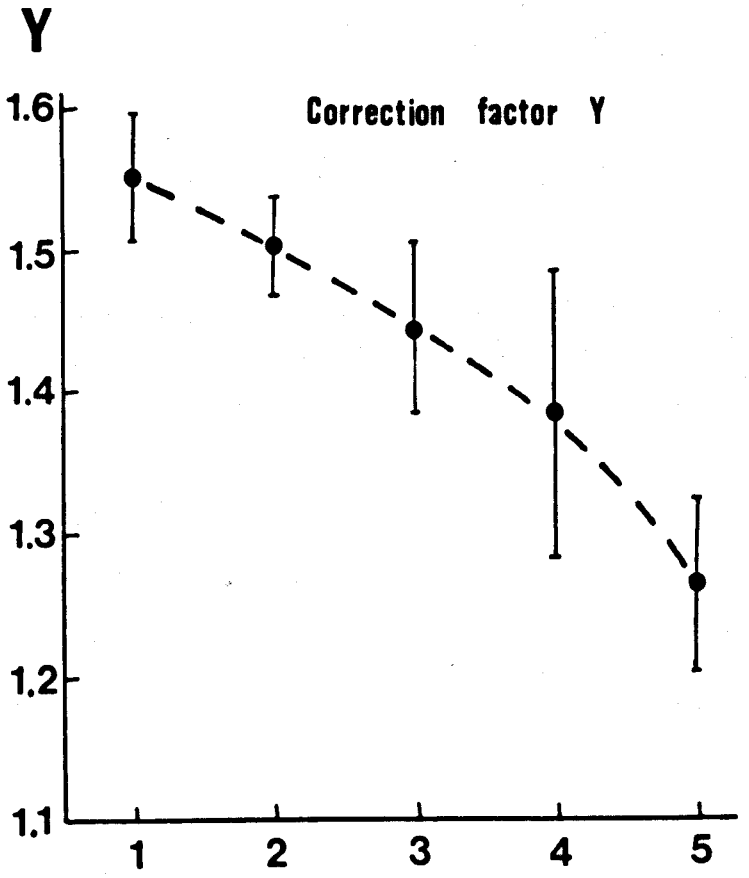
Y
Correction factor Y
1.6
1.5
1.4
1.3
1.2
1.1
1
2
3
4
5

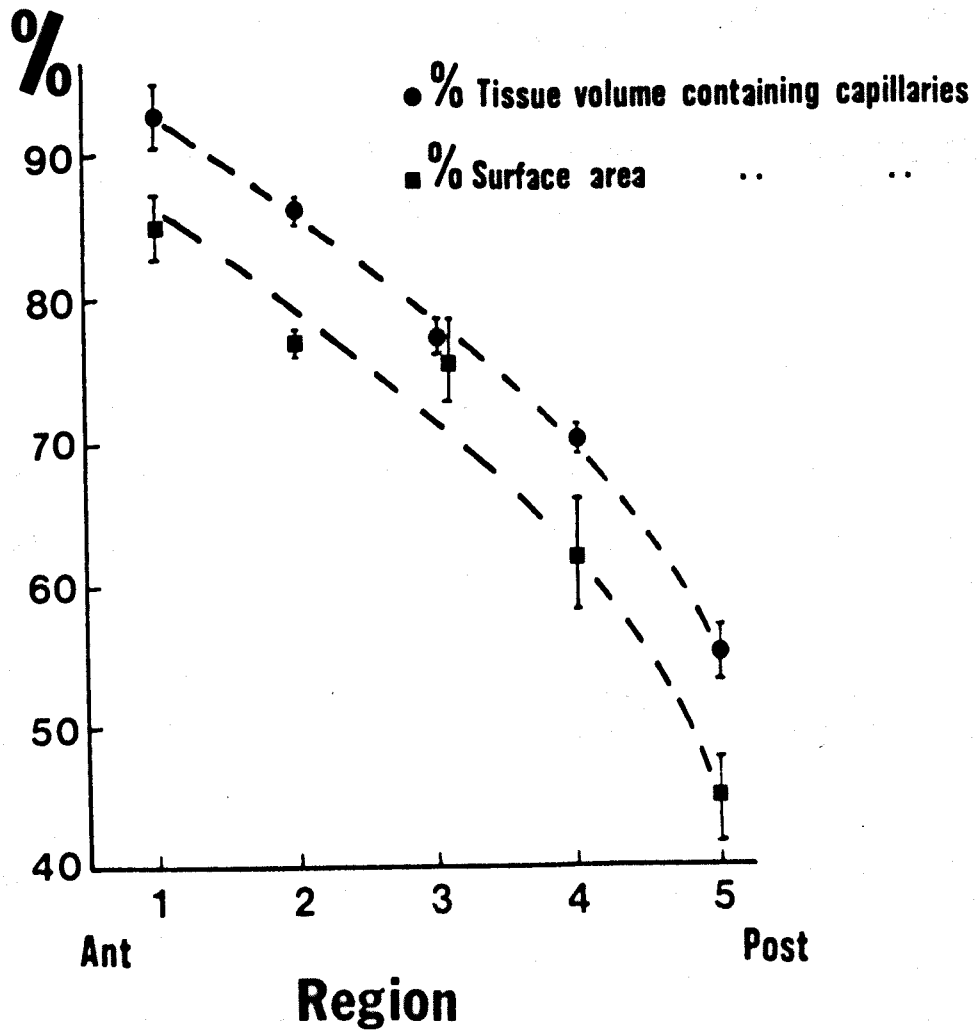
%
% Tissue volume containing capillaries
% Surface area
90
80
70
60
50
40
1
2
3
4
5
Ant
Post
Region

correctly estimated at x320. As far as could be ascertained without detailed morphometric evidence, the degree of corrugation is constant whatever the animal size. Thus the cancelling of correction factors will also apply to the other adult lungs. From the anatomy of the 0.2g L. vivipara lung, there is obviously no capillary bulging (Chapter 4). A true respiratory surface area for this lizard is difficult to ascertain from the preliminary study attempted here.

Antero-posterior gradation

Apart from the gradation in capillarisation, the Lacerta lungs have only been considered in terms of their average parameter values. A lot more information about growth patterns of the lung can be obtained by examining its antero-posterior gradation. Fig. 5.13 illustrates wedge volume profiles of the 5 adult and 0.2g lizard lungs. Total volume profile is virtually symmetrical but with the anterior lobe delaying the initial increase in volume anteriorly. (The photograph of Fig. 4.6 clearly shows this profile). When the individual lungs are compared, it becomes obvious that growth alters the profile in the larger lizards by maintaining the wedge volume of the middle region at a constant volume for a greater linear distance.

In the 29.3g lizard, the peripheral parenchyma profile is shifted anteriorly whilst the central air space profile is shifted posteriorly, i.e. anterior regions have thicker parenchyma walls than posterior regions. In the 3.0g lizard, these shifts, although present, are not very marked. The greater proportion of peripheral parenchyma in small lizards and the corresponding greater proportion of central air space in larger lizards were shown earlier in terms of logarithmic plots against body weight (Fig. 5.7). In the 0.2g lizard, however, peripheral parenchyma thickness is virtually the same in both anterior and posterior regions but it is very thin causing a very large central air space.

Alveolar diameter showed no antero-posterior gradation in the 0.2g lizard, but with increasing lung size, the diameter progressively

FIG. 5.13 Wedge volume profiles in terms of antero-posterior gradation. Solid line total volume, dotted line, central air space volume and dashed line, peripheral parenchyma volume.

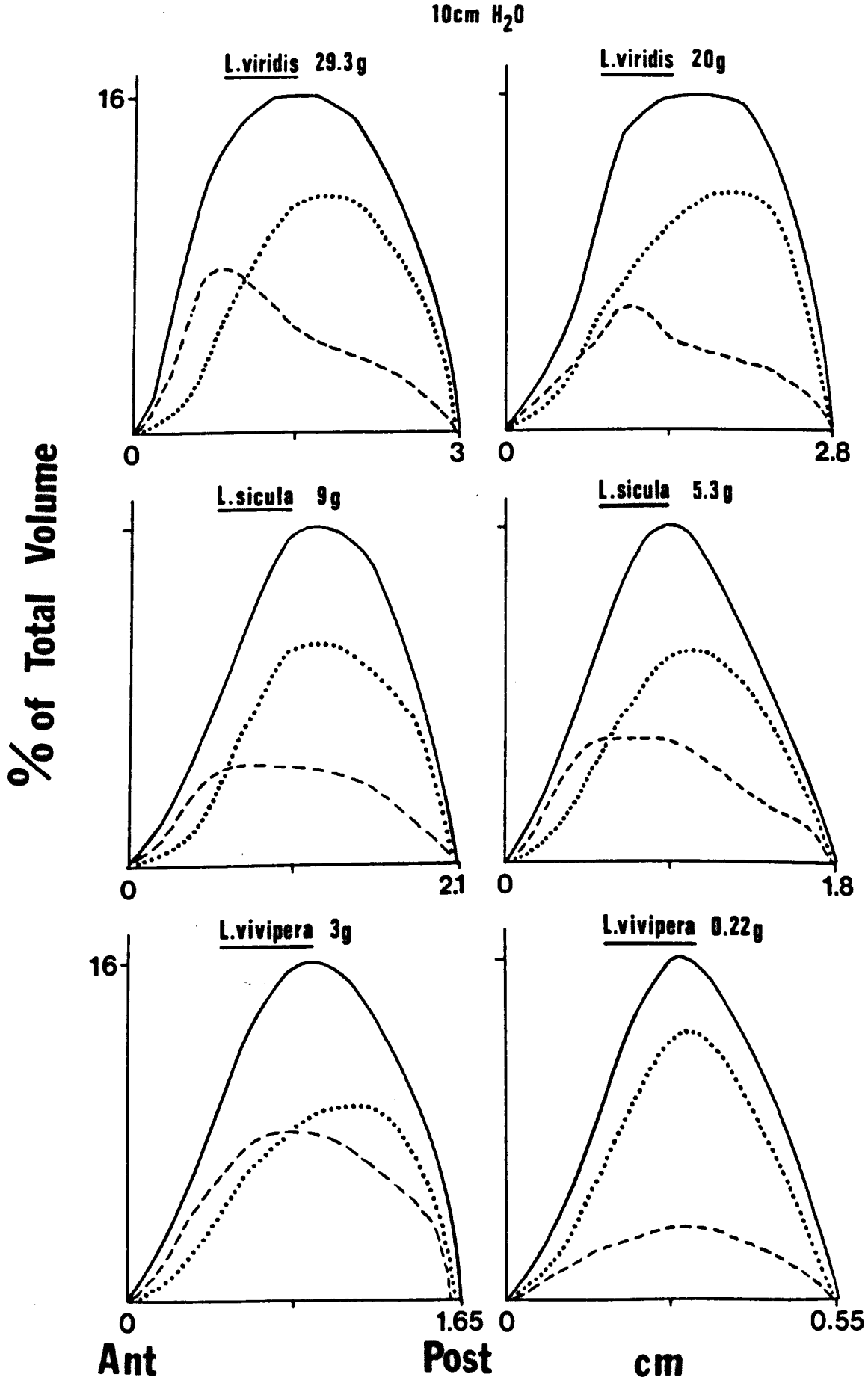
10cm H_2O
L.viridis 29.3g
L.viridis 20g
L.sicula 9g
L.sicula 5.3g
L.vivipera 3g
L.vivipera 0.22g
16
0
3
2.8
2.1
1.8
1.65
0.55
% of Total Volume
Ant
Post
cm

FIG. 5.14 Antero-posterior gradation of alveolar diameter and depth for different body weights.

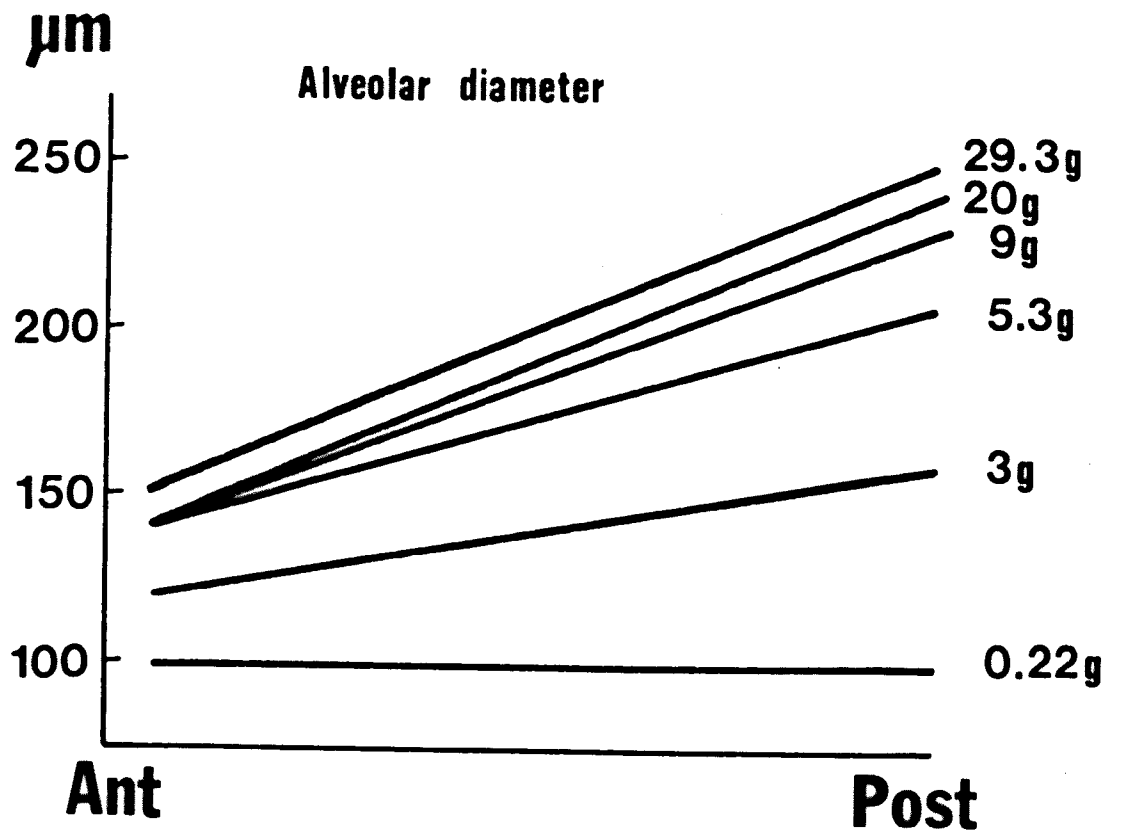
μm
Alveolar diameter
250
200
150
100
29.3g
20g
9g
5.3g
3g
0.22g
Ant
Post

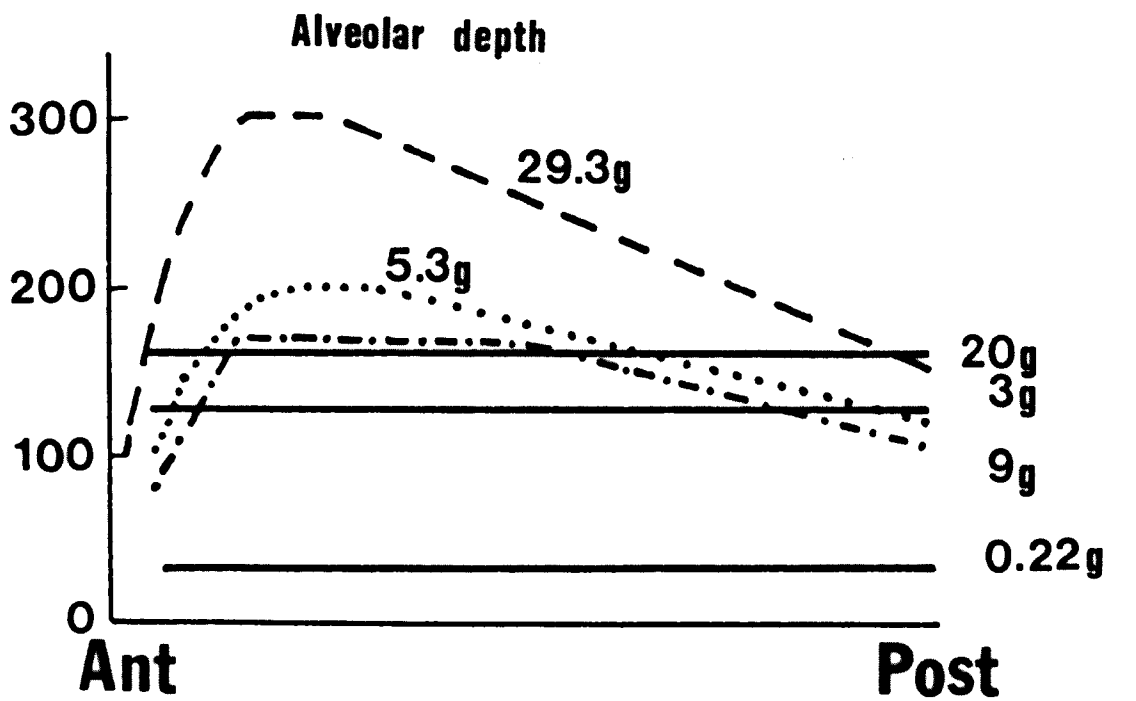
Alveolar depth
300
200
100
0
29.3g
5.3g
20g
3g
9g
0.22g
Ant
Post

FIG. 5.15 Antero-posterior gradation of various lung parameters (volume densities) in L. viridis (29.3g). Antero-posterior gradation of surface and alveolar density in L. sicula (5.3g) solid line and L. viridis (29.3g) dotted line.

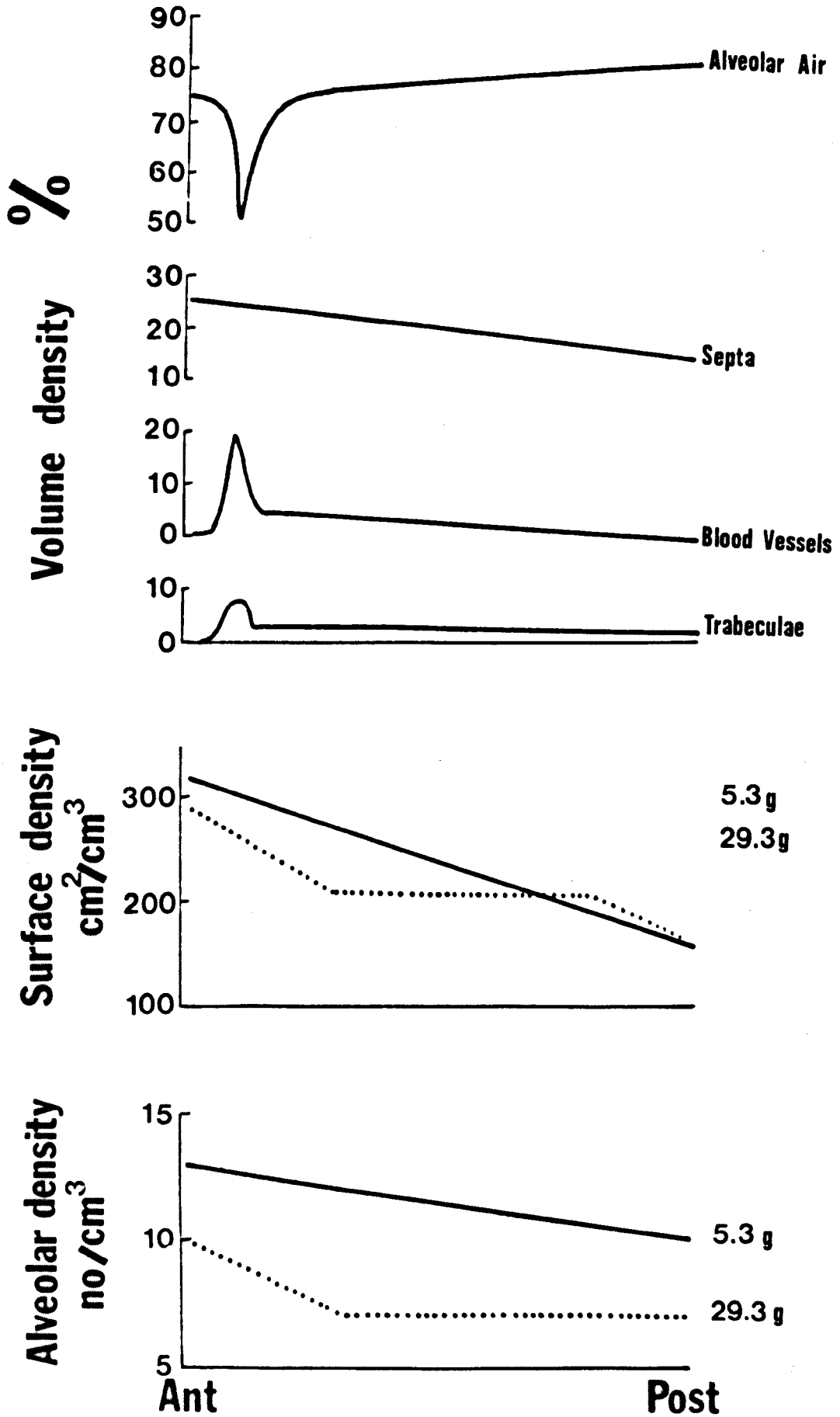
%
90
80
70
60
50
Alveolar Air
Volume density
30
20
10
Septa
20
10
0
Blood Vessels
10
0
Trabeculae
Surface density
cm²/cm³
300
200
100
5.3g
29.3g
Alveolar density
no/cm³
15
10
5
5.3 g
29.3 g
Ant
Post

increased more posteriorly (Fig. 5.14). This suggests that growth in the posterior regions may be mainly due to expansion of existing alveoli rather than to subdivision by septal growth. Outer wall to central lumen stratification causes larger alveoli to be nearer the central lumen (see Chapter 4).

The relationship between alveolar depth and antero-posterior gradation is not so clear (Fig. 5.14). For the 0.2g, 3g and 20g lizards, depth was the same anteriorly as it was posteriorly. For the 5.3g, 9g and 29.3g, however, depth of alveoli increased in the region of greatest parenchyma volume. An explanation for these two patterns cannot be given.

Alveolar air density increases posteriorly whilst septal volume density decreases (Fig. 5.15). Trabecular volume density is initially zero because a major part of the anterior lobe has no central lumen. This is then followed by its highest density when the bronchus (considered to be supporting trabeculae at this point) enters the lung. Trabecular density remained constant for most of the lung length until the most posterior regions were reached. Blood vessel density was also very minimal in the anterior lobe as it is supplied only by fine branches from the major pulmonary artery and vein (Chapter 4). When the pulmonary artery and vein entered the lung around the bronchus, blood vessel density increased tremendously. It then slowly decreased as the posterior tip of the lung was reached because the large supply vessels diminished in diameter from bronchus to posterior regions due to continual branching to and from the capillary beds. The tremendous increase in blood vessel density around the bronchus caused a decrease in alveolar air density but not in septal density. This may imply that, together with the anterior lobe, this bronchal entrance region is the most efficient gas exchanging area of the lung.

Surface area density showed a more distinct antero-posterior gradation than did alveolar density (Fig. 5.15). This is mainly because in posterior regions the alveoli only have 3 walls whereas many alveoli have 4 walls in anterior regions. The difference in antero-posterior relationships

for these two parameters, between the 5.3g and 29.3g reflect the deep alveoli found anteriorly in the latter (Fig. 5.14). This caused a larger reduction initially in alveolar and surface area density. (N.B. Densities were lower in the 29.3g lizard because of its larger alveoli).

Effect of different levels of inflation

Three L. vivipara (3.0g) lungs when fixed at 5, 10 and 15 cm H_2O instillation pressure increased their total lung volume in a linear manner (Fig. 5.16). Thus, these pressures caused volumes found in the linear part of the P-V curves (Chapter 3 and Fig. 3.9). Unfortunately, the left lung volume of the 15 cm H_2O increased its volume disproportionately, thereby reducing the volume of the right lung. Only the right lung was examined in detail morphometrically.

Wedge volume profiles of the right lungs show a slightly greater increase in anterior total volume at 5 cm H_2O and a slightly greater increase in posterior total volume at 10 cm H_2O. Both regions were equally inflated at 15 cm H_2O (Fig. 5.17). It might be expected that the thinner posterior tissue would offer least resistance and therefore posterior regions would show the greatest inflation at 15 cm H_2O. However, the restrictions imposed by pleural mesenteries and the ribcage kept mean lung length (for right and left lungs) the same (1.7 cm) for both 10 and 15 cm H_2O compared with 1.2 cm for 5 cm H_2O. Thus, at 15 cm H_2O, the higher volume has to cause further expansion of anterior regions and circumferential rather than length increases.

Peripheral parenchyma volume was greatest anteriorly at all three pressures, but this was most marked at 5 and 15 cm H_2O. At 5 cm H_2O the greatest total wedge lung volume was in anterior regions and the parenchyma expanded accordingly. At 15 cm H_2O, the excessive inflation caused such great circumferential expansion that parenchyma (outer wall to central lumen) thickness actually decreased causing an extremely large central air space. This compression of the peripheral parenchyma was most noticeably in the

FIG. 5.16 (a) Inflation effects on antero-posterior gradation of alveolar diameter and depth. (b) Effect of lung inflation at 5, 10 and 15 cm H_2O on various lung parameters in *L. vivipara* (3.0g).

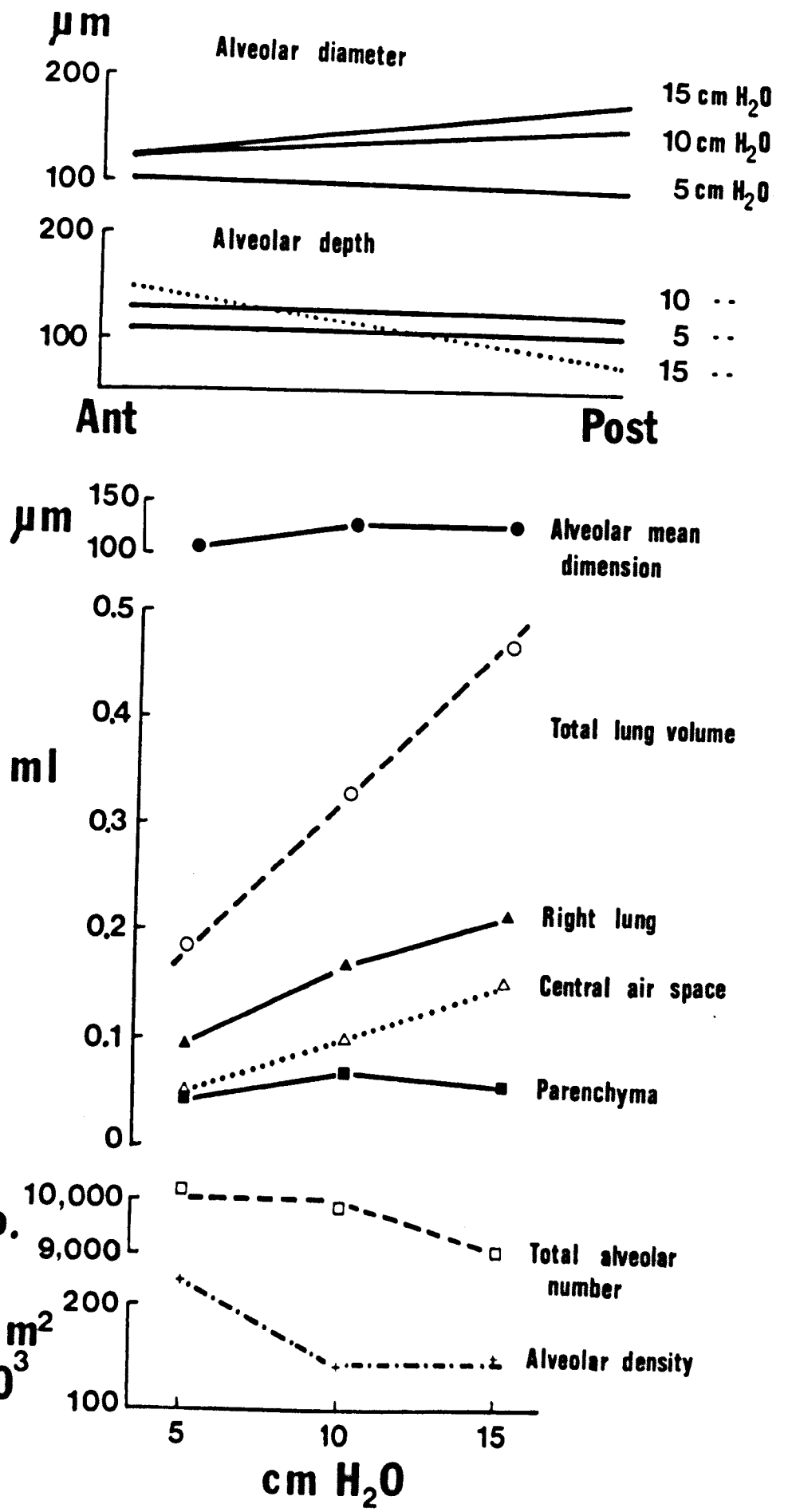
µm
Alveolar diameter
200
100
15 cm H2O
10 cm H2O
5 cm H2O
200
Alveolar depth
100
10 ··
5 ··
15 ··
Ant
Post
µm
150
100
Alveolar mean dimension
0.5
0.4
ml
0.3
0.2
0.1
0
Total lung volume
Right lung
Central air space
Parenchyma
no.
10,000
9,000
Total alveolar number
no/cm2 x 10^3
200
100
Alveolar density
5
10
15
cm H2O

FIG. 5.17 Effect of right lung inflation at 5, 10 and 15 cm H_2O on wedge volume profiles and their antero-posterior gradation in L. vivipara (3.0g).

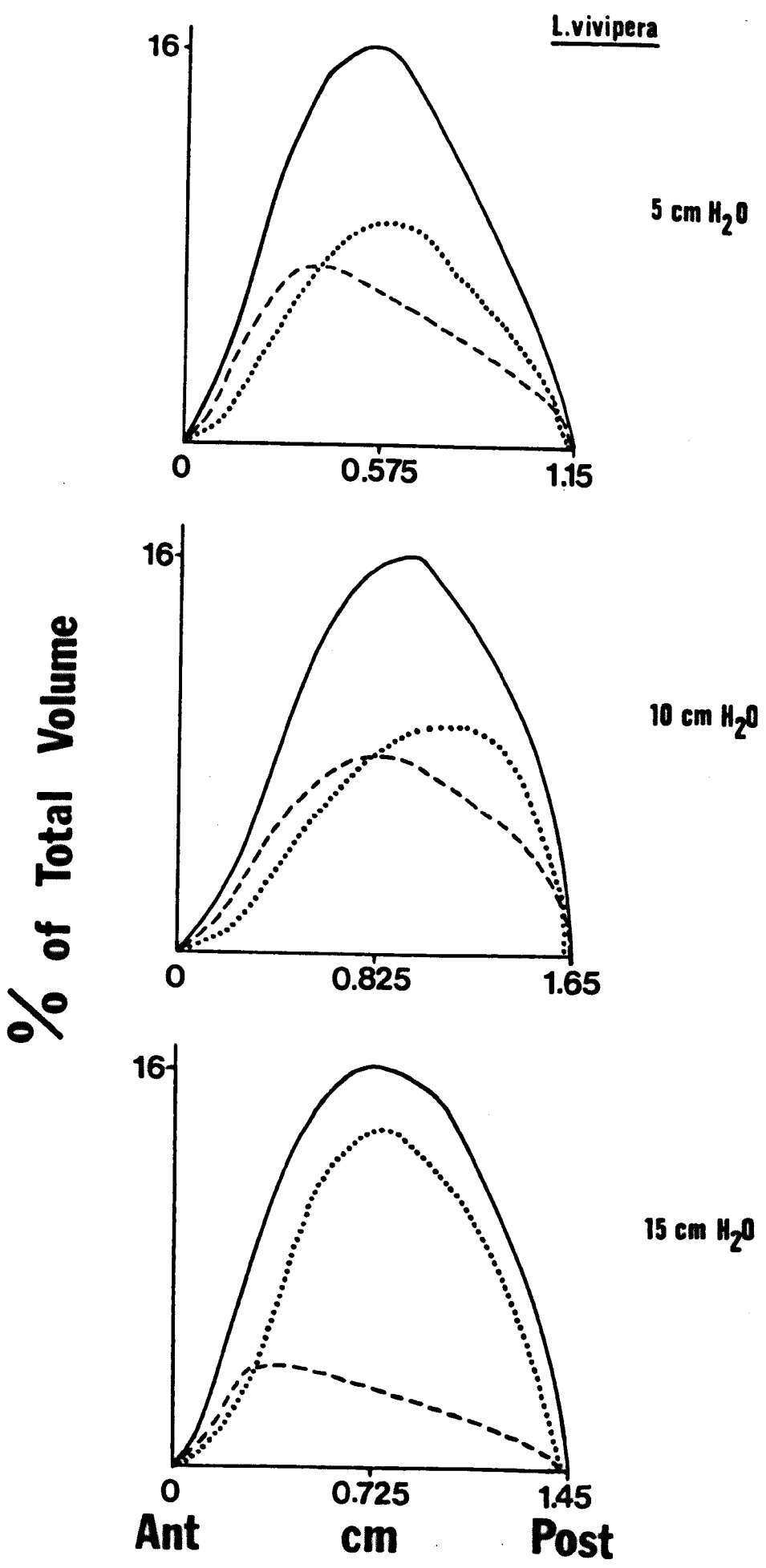
L.vivipera
16
5 cm H_2O
0
0.575
1.15
16
10 cm H_2O
0
0.825
1.65
16
15 cm H_2O
0
0.725
1.45
% of Total Volume
Ant
cm
Post

weaker posterior region. Fig. 5.16 graphs this disproportionate increase at 15 cm H_2O in central air space volume when compared with parenchyma volume. (N.B. Non-linearity of the right total lung volume for the three pressures slightly obscures this).

Antero-posterior gradation plots of alveolar dimensions show that at 5 cm H_2O the diameter is constant (Fig. 5.16). This is probably due to under-inflation of posterior regions. At 10 cm H_2O, alveolar diameter increases posteriorly since posterior regions are becoming more inflated. Gradation is most extensive at 15 cm H_2O due to circumferential overstretching of posterior regions. Mean alveolar diameter increased with lung inflation but was obviously physically restricted at 15 cm H_2O.

Alveolar depth is constant at 5 and 10 cm H_2O during antero-posterior gradation, but is deeper in the latter (Fig. 5.16). At 15 cm H_2O, however, alveolar depth progressively decreases as posterior regions are reached. This is due to parenchyma collapse posteriorly. Although, anteriorly its depth was greater than at the other two pressures, its mean depth was less (Table 5.7). Thus the mean alveolar dimension (diameter + depth) increased from 5 to 10 cm H_2O but then remained constant between 10 and 15 cm H_2O. This was similar to the peripheral parenchyma volume relationship to instillation pressure.

Alveolar number was virtually constant at 5 and 10 cm H_2O but there was some alveolar collapse at 15 cm H_2O. Alveolar density is the reverse image of peripheral parenchyma volume, alveolar number and mean alveolar dimension, as would be expected (Fig. 5.16).

Alveolar surface area, as measured at x320 magnification, increased with lung inflation between 5 and 10 cm H_2O but was then reduced at 15 cm H_2O being 15.5, 24.0 and 16.2 cm^2, respectively. Some reduction in surface area at 15 cm H_2O would be expected from peripheral parenchyma compression and some alveolar collapse, but not to the degree measured. Examination of the septa showed that, whatever the inflation level, they were

TABLE 5.7

Right lung parameters during inflation in 3.0g *L. vivipara*

Parameter	5 cm H_2O	10 cm H_2O	15 cm H_2O
Total lung volume (ml)	0.185	0.33	0.47
Left lung volume (ml)	0.09	0.16	0.255
Right lung volume (ml)	0.095	0.17	0.215
Central air space (ml)	0.05	0.1	0.155
Peripheral volume (ml)	0.045	0.07	0.06
Lung length (cm)	1.15	1.65	1.45
Mean alveolar diameter (μm)	100	135	148
Mean alveolar depth (μm)	110	128	114.5
Mean alveolar dimension (μm)	105	131.5	131.25
Alveolar number	10,150	9,820	9,000
Alveolar density (no./cm^3)	226,000	140,000	150,000
Absolute surface area (cm^2)	15.5	24.0	16.2
Surface density (cm^2/cm^3)	344.4	348	270

of the same thickness. The septa of the outer wall, however, did become thinner at high pressures. Septa at low pressures were folded without causing alveolar collapse but at high pressures they were very straight. At x320 magnification, as has already been shown, surface area estimates fail to measure accurately the surface convolutions due to capillary bulging. Similarly, surfaces closely apposed but not touching, as found in the folded septa of 5 cm H_2O inflation, would also be underestimated. It is considered that some reduction in surface area at 5 cm H_2O compared with 10 cm H_2O should be expected because of complete apposition of some folded regions, but maybe not to the extent measured here. Very straight septa (15 cm H_2O) cross test lines less frequently than the slightly folded ones of 10 cm H_2O, which again at x320 magnification can cause their underestimation. Surface areas must obviously be measured at the electron microscopic level. Neither this nor correction factors were determined for these three lungs.

Electron microscopic evaluation

The left lung of L. viridis (20g) was used for this investigation. Sampling, as described in the methods section, deviated from that of Weibel for Stage 3. This was because (a) the lizard's larger alveoli would require more numerous micrographs to be taken in order to sample a reasonable quantity of tissue, and (b) the lizard has distinct antero-posterior gradation both in alveolar size and capillary density and such inhomogeneity would require rigorous sampling within a region. Thus for lizard homogeneous EM sampling, the lung was selectively subsampled for capillarised regions of the septa. Although region 5 was sectioned, it yielded too small a number of micrographs of capillarised septa. Thus only regions 1 to 4 were evaluated morphometrically.

From light microscopic evaluation, it is known that septal tissue volume for L. viridis (20g) is 0.06525 cm^3 for the left lung. From 1 μm epon sections, it is also known that 78% of this volume is occupied by capillarised septa, i.e. 0.051 cm^3. By volume density measurements at the EM level, 54% of the capillarised tissue contained blood, 9.8% was composed of epithelium, 24.8% of interstitium and 11.4% of endothelium. In absolute terms, capillary blood volume was 54% of 0.051, i.e. 0.0275 cm^3, epithelium was 0.005 cm^3, interstitium 0.01265 cm^3 and endothelium was 0.0058 cm^3. Not all the endothelium and interstitium, even after this selective subsampling, were in the air to blood pathway because they lay between two juxtapposing capillaries. 0.0013 cm^3 of endothelium and 0.00357 cm^3 of interstitium were in such a position. Capillary blood volume had a hematocrit of 35%, i.e. volume density of erythrocytes, and a leucocyte/thrombocyte density of 6.5%. All these volume densities and their absolute values are documented in Table 5.8.

In the air-blood pathway, the epithelium occupied a slightly larger volume than the endothelium, 5.0×10^{-3} cm^3 and 4.5×10^{-3} cm^3, respectively, as might be expected from its more peripheral position.

TABLE 5.8

Septal constituents as a volume % of total septal volume and their absolute values. L. viridis 20g.

	Plasma	Erth.	Leuco.	Total Blood	Epith.	Interst. in Air-Blood Pathway	Endo. in Air-Blood Pathway	Interst. Not	Endo. Not	Total Interst.	Total Endo.	Total Tissue
Volume %	31.5	19	3.5	54	9.8	18.2	9.0	6.6	2.4	24.8	11.4	
Volume % of blood	58.5	35.0	6.5	100	-	-	-	-	-	-	-	
Absolute values $cm^3 \times 10^{-3}$	16.1	9.6	1.79	27.5	5.0	9.08	4.5	3.57	1.3	12.65	5.8	23.45

Total septal tissue volume = 65.25×10^{-3} cm^3 for one lung 20g Lacerta viridis

blood volume = 27.5×10^{-3}

respiratory tissue = 18.58×10^{-3}

Total tissue in respiratory region = 23.45×10^{-3}

Non-capillarised septal tissue volume = 14.25×10^{-3}

The supporting interstitium had twice the volume of either the epithelium or endothelium. If endothelium and interstitium, which are not in the air to blood pathway, are also considered the total endothelial volume is slightly greater than epithelial volume because of apposition of some capillaries in the double capillary network. It is, therefore, very evident that although a double capillary network is present in lizards, two opposing capillaries are shifted slightly with respect to each other to give maximum respiratory surface area. Interstitial support is concentrated away from the air to blood barrier in the region between capillaries. Interstitial volume is 3 times greater than endothelial volume in this region as compared with only being 2 times greater in air to blood pathways (see Table 5.8).

By selective subsampling, the micrograph fields contained 47% septal tissue and 53% air which gave an alveolar surface density of 1,000 cm^2/cm^3. From light microscopic evaluation, true septal volume density was 20.35% giving an alveolar surface density of 267 cm^2/cm^3. To calculate a true absolute surface area, the EM data has to be corrected for biassed sampling. Since true septal volume density was 20.35% of which 78% contained capillaries and since parenchyma volume was 0.321 cm^3, the true alveolar surface area is calculated by the following equation:-

$$\text{Alveolar surface area} = 1{,}000 \times \frac{20.35}{47} \times \frac{78}{100} \times 0.321$$

$$\text{i.e. } S_v(EM) \times \frac{V_v(LM)}{V_v(EM)} \times \begin{matrix}\text{capillarised} \\ \text{volume} \\ \text{correction}\end{matrix} \times \begin{matrix}\text{parenchyma} \\ \text{volume}\end{matrix} = 109 \text{ cm}^2$$

This absolute surface area is, however, derived by assuming that all septal tissue has two active surfaces. The outer wall, trabecular surface and blood vessel septal lining have only one active surface and account for about 10% of septal volume that is capillarised. Micrographs were not taken from these regions. Thus, surface area for the lung should

be 98 cm^2. This is very similar to the 85.5 cm^2 estimated from light microscopy.

Following similar calculations, the capillary surface area in the respiratory pathway, total capillary and erythrocyte surface area have been determined (Table 5.9).

TABLE 5.9

Absolute respiratory surface areas, cm^2, for ½ lung of L. viridis (20g)

Alveolar	Capillary	Total Capillary	Erythrocyte
109	105.5	118.5	130

Arithmetic mean thickness determined from volume to surface ratios of the tissue sheet were calculated using uncorrected volume and surface densities of the septa measured in the micrographs (Table 5.10). The interstitium was approximately twice the thickness of the epithelium or endothelium when in the air to blood pathway, but was considerably thicker in non-respiratory regions. The embedded parts of the endothelium were also thicker than respiratory parts.

TABLE 5.10

Arithmetic mean thickness $\bar{\tau}$ for L. viridis (20g) in μm.

Total Respiratory Tissue	Epithelium	Interstitium	Endothelium	Total Tissue	Total Interst.	Total Endo.
1.77	0.47	0.865	0.435	2.08	1.125	0.475

The harmonic mean thickness, τ_h, of the air to blood pathway was estimated as 0.527 μm and τ_h for plasma, i.e. inner margin of endothelium to erythrocyte surface, was 0.25 μm.

DISCUSSION

Nasal cavity volume and tracheal dimensions

Tracheal length would be expected to vary as the cube of body weight since snout-vent length is proportional to $W^{0.33}$ (Chapter 1). This indeed is the case, $Tr.L \propto W^{0.355}$. The only other data on tracheal morphometry is that of Tenney & Bartlett (1967) for a 10g to 1,000 kg range of mammalian body weight. They state that in mammals $Tr.L \propto W^{0.27}$ but their logarithmic plot would indicate a regression coefficient of 0.37 which is very similar to their 0.39 exponent for tracheal diameter. This would make mammalian tracheal volume proportional to $W^{1.15}$ not $W^{1.05}$. In the lizard, tracheal diameter might also be expected to vary as the cube of body weight but it is proportional to $W^{0.29}$.

TABLE 5.11

Comparison of tracheal dimensions in a 10g lizard and mammal and their relationship to body weight.
Mammalian data is from Tenney & Bartlett (1967).

Dimension	Mammal	Lacerta	L/M ratio
Tr. length, cm	1.0	2.2	2.2
Tr. diam., cm	0.062	0.104	1.68
Tr. vol., ml	0.003	0.0186	6.2
$Tr.L \propto W^b$	$b = 0.37^*$	0.355	
$Tr.D \propto W^b$	$b = 0.39$	0.29	
$Tr.Vol. \propto W^b$	$b = 1.15^*$	0.94	
Tr. Resistance $\propto W^b$	$b = -1.19^*$	-0.85	
Tr. Resistance	$\sim 2{,}750{,}000/r$	$\sim 700{,}000/r$	0.254

* corrected values, see text.

All tracheal parameters, especially the volume, are larger in Lacerta than in the mammal (Table 5.11). This is because the body shape of the lizard demands a long trachea with the diameter accordingly increased. A mammal with a tracheal length of 2.2 cm would have a tracheal diameter of

0.12 cm which is not markedly different from the 0.104 cm diameter of the 2.2 cm long lizard trachea. It would appear, therefore, that both lizards and mammals are subjected to similar design demands for determining relative tracheal length and diameter ratios in the interest of air flow resistance. From Poiseuille's formula:

$$\text{Resistance} = \frac{8\eta l}{\pi r^4}$$ where η = coefficient of air viscosity,

a 10g lizard has a tracheal resistance of approximately $700{,}000\eta l^{-3}$, whereas in a 10g mammal, it is approximately $2{,}750{,}000\eta l^{-3}$. In the design of a trachea, a balance has to be reached between minimizing dead space and the resultant increase in resistance.

During ventilation, the resistance, R, across the trachea is equal to the pressure at one end minus the pressure at the other, ΔP, divided by the air flow, $\dot{V}$.

$$\text{i.e.} \quad R = \frac{\Delta P}{\dot{V}} \quad \text{or} \quad \Delta P = \dot{V} \times R$$

From Chapter 3, it is known that in the lizard ΔP is a constant irrespective of body weight because specific compliance was a constant. If ΔP = constant = $\dot{V} \times R$ and R is proportional to $W^{-0.85}$, it follows that $\dot{V}$ must be proportional to $W^{+0.85}$. This was, in fact, the relationship determined for $\dot{V}$ in Chapter 2. This conclusion assumes that nasal cavity resistance (i.e. upper airway) of the lizard is related to body weight in the same way as tracheal resistance. From its anatomy (Chapter 4), the nasal cavity is obviously a site of high resistance, but no attempt was made to quantify this. Mammalian data is also lacking.

ΔP is also a constant in mammals (Drorbaugh, 1960, Crosfill & Widdicombe, 1961, Stahl, 1967, Schmidt-Nielsen, 1970). R is proportional to $W^{-1.19}$ from tracheal measurements (Tenney & Bartlett, 1967) but total airway (less upper airway) resistance is proportional to $W^{-0.7}$ (Stahl, 1967)

or $W^{-0.86}$ (Spells, 1969/70). Total pulmonary (less upper airway) resistance is $\propto W^{-0.9}$ but total respiratory (less upper airway) resistance is $\propto W^{-0.39}$ (Spells, 1969/70). Spells has discussed possible conclusions from this data but emphasises the need for further extensive data. Flow rate, $\dot{V}$, for the mammal has been given as proportional to $W^{0.7 \text{ to } 0.75}$ (Guyton, 1947) and therefore, total respiratory resistance (less upper airway) might be expected to be related as $W^{-0.7 \text{ to } -0.75}$ not as $W^{-0.39}$. Use of $\Delta P = \dot{V} \times R$ equation for matching respective body weight relationships cannot be made for mammals. Also the mammal/lizard ratio for total respiratory resistance cannot be predicted.

Fixation pressures

It was found to be impossible to use mammal/lizard ratios for ΔP (Chapter 3), $\dot{V}$ (Chapter 2) and R to predict the probable ratio required for fixation. By trial and error, it appeared that 20 cm H_2O for open chest mammals was equivalent to 10 cm H_2O for closed chest lizards. Even if a ratio could be predicted, it is probable that the following anatomical differences would invalidate it. In the mammal, alveolar ducts are 'fixed' first but this does not prevent fixative from continuing to flow to the alveoli. In the lizard, fixative reaches the alveolar septa immediately because there are no ducts. Once 'fixed', although the lizard lungs can be physically forced to expand further, when the pressure is removed, the lungs return to the volume of the immediate fixation (see Methods).

Body weight scaling of lung parameters

Lacerta lung length would be expected to vary as a linear function of body weight, i.e. $\propto W^{0.33}$. Its actual relationship was $W^{0.356}$ and this b and the a exponent were virtually identical with tracheal length. If expressed another way, snout-vent length, L, and lung length, LL, are isometric with $LL \propto L^{1.057}$. Lung volume and body weight are also isometric, $V \propto W^{1.028}$ or, in other words, lung volume is related to the cube of snout-vent length, $V \propto L^{3.057}$. Such measurements have not been made for any other species. In L. vivipara, Avery (1973) also found snout-vent

length to be proportional to $W^{0.33}$ (Chapter 1) and stomach volume and body weight to be isometric. Stomach length, however, and snout-vent length, L, were not isometric, being $L^{0.78}$. Nor was stomach volume, St.V, the cube of snout-vent length, being St.V $\propto L^{2.64}$. There is, therefore, a fundamental difference in linear growth between the lungs and stomach of lizards, although the latter provides the substrate and the former the O_2 for metabolism.

A comparison of lung parameter scaling in mammals, reptiles, amphibians and Lacerta has been made in Table 5.12. Before this is examined, it must be pointed out that intraspecific relationships are likely to be more reliable than interspecific ones, (providing they cover an adequate size range) because variation in lung specialisation and the effects of environment or behaviour between species can secondarily modify lung growth. This is especially true for poikilotherms in which lung complexity is related to the O_2 demands of the animal concerned (Tenney & Tenney, 1970). Even in mammals, postnatal adaptation to $\dot{V}O_2$ increases (Geelhaar & Weibel, 1971) or Po_2 decreases (Burri & Weibel, 1971, Bartlett & Remmers, 1971) cause a decrease in body weight, thereby increasing relative lung volume though not in proportion to the $\dot{V}O_2$ or Po_2 change. A Po_2 increase, on the other hand, causes a true reduction in lung diffusing capacity D_{LO_2}. It is the number of alveoli, not the capillary density, that are modified by functional requirements (Geelhaar & Weibel, 1971).

A further point is that interspecific slopes could be made more meaningful if exactly the same species and number of individuals were used for as many different lung parameters as possible. The importance of small slope differences can then become significant and may show, for example, septal thickening if septa weight has a greater regression coefficient on body weight than does septa surface area. In many studies, alveolar numbers and lung weight parameters are ignored.

Lung weight is more or less directly proportional to body weight (Table 5.12) except in the developing rat lung (Bartlett, 1970a) and in

TABLE 5.12

Interspecific comparison of the relationship between lung parameters and body weight, $X \propto W^b$.

I = intraspecific slope. D = developing lung.

Parameter X		Mammal b	Lacerta b	Reptile b	Amphibian b
Lung weight		0.99 (10)	0.711	1.0 (12)	1.0 (12)
	Rat	0.7* ID (1)			
	Man	1.113-1.137* ID (4)			
	Man	1.04* I (13)			
Lung Volume	Rat	~1.0* ID (1)	1.028	0.75 (12)	1.05 (12)
	Man	1.12-1.286* ID (4)			
		1.02 (11)			
		1.05 (15)			
	Dog	1.0 I (8)			
	Man	~1.0* I (13)			
	Rat	0.85* ID (14)			
	Rat	0.99 ID (16)			
	Rat	0.7 I (16)			
Peripheral Volume		--	0.8 0.875†	?	?
Alveolar Volume	Dog	~1.0 I (8)	0.82 0.9†	?	?
Respiratory Surface area	Rat	1.02 ID (1)	0.69	0.75 (12)	0.8 (12)
	Man	1.028-1.114* ID (4)			
	Rat	0.76 ID (14)			
		0.98 (15)			
	Dog	1.07 I (8)			
		0.74 (11)			
	Man	0.58* I (13)			
		0.95 (15)			
		0.88 (15)			
	Rat	1.6 ID (16)			
		1.0 I (16)			

TABLE 5.12 (continued)

Parameter X		Mammal b	Lacerta b	Reptile b	Amphibian b
D_{Lo_a}	Rat	1.0 ID (14)	0.69′	?	?
		1.18 (10)			
	Dog	1.19 I (8)			
	Dog	1.14 I (8)			
		0.96 (15)			
		0.94 (15)			
		0.84 (15)			
	Rat	1.04 ID (16)			
	Rat	0.73 (16)			
Alveolar dimension		0.2-0.185 (11)	0.13	0.2 (12)	0.2 (12)
		0.137 (9)		After 0.5 kg,	
	Dog	0.33 I (8)		it is constant	
	Man	0.325* I (13)			
	Man	0.248-0.363 ID (4)			
	Rat	0.0 ID (1)			
Alveolar number	Rat	~1.0* ID (1)	0.454	?	?
	Man	1.13-0.93* ID (4)			
	Man	0.0 I (13)			

* Calculated value from published data. ′ Suspected value, see text.

References for Table 5.12 and 5.13

(1) Bartlett, 1970a (2) Burri & Weibel, 1971 (3) Drorbaugh, 1960 (4) Dunnill, 1962
(5) Geelhaar & Weibel, 1971 (6) Perry, 1972 (7) Rahn et al, 1971 (8) Seigwart et al, 1971
(9) Spells, 1968 (10) Stahl, 1967 (11) Tenney & Remmers, 1963 (12) Tenney & Tenney, 1970
(13) Weibel, 1963 (14) Weibel, 1967a (15) Weibel, 1972 (16) Burri, Dbaly & Weibel, 1974.

adult Lacerta, where the relationship is $W^{0.7}$ and $W^{0.711}$, respectively. The relatively heavier lung weights in young rats are mainly due to their initially thicker septa since the respiratory surface area is proportional to $W^{1.02}$. Human lungs are also relatively heavier at birth but development is more advanced than in rats because true alveoli are already formed (Dunnill, 1962, compare with rats, Weibel, 1967a). In contrast to the mammal, Lacerta newborn lungs are very under-developed in lung weight.

Lung volume is also directly proportional to body weight except in interspecific reptile lungs, $W^{0.75}$ (Tenney & Tenney, 1970) and some rat lung studies (see Table 5.12). Many of the discrepancies between rat lung morphometrics may be made clear if attention is paid to the most recent study (Burri, Dbaly & Weibel, 1974). The relative reduction in lung volume of large reptiles in Tenney & Tenney's study (1970) has been shown in Chapter 3 to be a possible artifact caused by using the same fixation pressure for both small and large reptiles, the latter having less compliant lungs. The amphibians they used would, from anatomical evidence, be expected to all have the same compliance. Hence lung volume was directly proportional to body weight for amphibians.

Parenchyma occupied a greater proportion of the lung in heavier mammals (Weibel, 1963, Burri & Weibel, 1971). The peripheral parenchyma also becomes more extensive in larger reptiles (Tenney & Tenney, 1970 and for anatomical papers, see Chapter 4) encroaching on the central air space sometimes to its complete occlusion. Interspecifically in Amphibia, peripheral tissue was a constant fraction of total lung volume (Tenney & Tenney, 1970). The reverse was found intraspecifically in Lacerta, the peripheral tissue becoming less extensive with increasing size.

Respiratory surface area shows considerable variation in its body weight relationship (Table 5.12), depending on the species or even the study. This must indicate its functional dependence. For animals between the shrew and dog in size, the relationship is $W^{0.98}$. This is not

dissimilar from the maximum $\dot{V}o_2$ relationship found over such a size in Pasquis, Lacaisse & Dejours (1970) (see Chapter 1). If these animals are considered as free-living or captive, the $W^{0.98}$ relationship becomes $W^{0.95}$ and $W^{0.88}$, respectively (Weibel, 1972). If heavier mammals are included in the study, $W^{0.98}$ becomes $W^{0.74}$ (Tenney & Remmers, 1963). These larger mammals were aquatic with secondarily thickened septa or were sluggish and would, therefore, be expected to require less surface area. During human lung development the relationship is $W^{1.0}$ (Dunnill, 1962) but after 8 years the relationship becomes $W^{0.58}$. Since lung weight is still proportional to $W^{1.04}$, considerable septal thickening during ageing is indicated. The mammalian value for respiratory surface area relationships to body weight lies between $W^{0.7}$ and $W^{1.0}$. Whether the different values always match $\dot{V}o_2$ relationships to body weight for a particular study has not been investigated, since $\dot{V}o_2$ is rarely measured in parellel with lung morphometric studies. D_{Lo_2}, when measured, has always followed the relationships of surface area to body weight (Weibel, 1972, etc.), being only slightly modified by a harmonic mean thickness which is slightly thicker in larger mammals, $W^{0.05}$.

Respiratory surface area in reptiles was found to be related to $W^{0.75}$ and $W^{0.8}$ for amphibians (Tenney & Tenney, 1970). Although, the amphibians had lung volume, lung weight and total surface area all related to $W^{1.0}$, a correction for a respiratory capillary density relationship of $W^{-0.2}$ caused the $W^{0.8}$ value. In the reptiles, lung weight was proportional to $W^{1.0}$ but volume was related to $W^{0.75}$, hence causing a $W^{0.75}$ relationship for surface area. This 0.75 relationship for reptiles is considered fortuitious and due to the fixation pressure effect on volume. Unless there is considerable thickening of the septa with increasing size, surface area is likely to be nearer a direct proportionality with body weight. Whether capillary density is constant over such a large range of reptiles was not examined. It is certainly known that in the very large reptiles of

Tenney & Tenney's study (1970), there is a greater capacity to increase $\dot{V}o_2$ (Chapter 1). Their reptilian lung morphometry was not treated separately for the different groups: lizards, snakes, tortoises and crocodiles which from the discussion of Chapter 1 would seem desirable. The interspecific relationship of respiratory surface area to body weight must, I think, still remain an open question. In contrast, an 'intraspecific' relationship for the genus Lacerta shows that maximum $\dot{V}o_2$ and respiratory surface area relationships to body weight are very close, being $W^{0.76}$ and $W^{0.69}$, respectively. This similarity is even more striking when one remembers that the lung volumes unfortunately selected for morphometric examination were related to $W^{0.9}$ instead of $W^{1.0}$. Lacerta lung weight was also related to $W^{0.71}$.

Septa become thicker with increasing size from rat to dog (Siegwart et al, 1971) but a respiratory surface area proportionately to $W^{1.07}$ is maintained by the isometric lung weight having 80% parenchyma in the rat but 90% in the dog. There was some septal thickening in the very large reptiles but none in the amphibians (Tenney & Tenney, 1970). In Lacerta, there was also no noticeable septal thickening. Septa thicken with increasing body weight because the larger the alveoli, the more collagen is required to support the septa. Greater centripetal force is required to keep a large alveolus open (Siegwart et al, 1971). There is a positive relationship between alveoli size and septa thickness. The thicker septa of non-mammals may, therefore, be related to alveolar size (see later).

During growth, there are three alternatives for alveolar development of their size and number. Both size and number are modifiable and evolve to match the needs of the species concerned. There can be a constant diameter size but with an increase in alveolar number related to $W^{1.0}$ as in developing rats (Bartlett, 1970a). There can be a constant alveolar number with diameter increasing as $W^{0.33}$ (Weibel, 1963, Siegwart et al, 1971) as in adult man or dogs. Finally, there can be a combination of both number

and diameter increases as found in developing human lungs (Dunnill, 1962) and interspecifically in mammals (Tenney & Remmers, 1963, Spells, 1968). Similarly, in adult guinea pigs, some alveolar size increase occurs but the major change is in number (Forrest, 1970). Lacerta fit the third alternative, alveolar dimension being proportional to $W^{0.13}$ and alveolar number to $W^{0.454}$. The diameter relationship of $W^{0.2}$ for reptiles and amphibians (Tenney & Tenney, 1970) must also indicate the third alternative. In conclusion, the alveolar dimension scaling in Lacerta is similar to that found interspecifically in mammals except that depth alters more than diameter.

From this lung morphometric study of Lacerta, some insight is gained into an anatomical explanation of the greater wastage of ventilation volume found in larger lizards, i.e. $\dot{V}_E/\dot{V}o_2 \propto W^{0.25}$. $\dot{V}_E$ was completely controlled by a $V_T \propto W^{1.0}$ since resting respiratory frequency was constant over the body weight range investigated (Chapter 2). In the lung, $\dot{V}o_2$ scaling was governed by respiratory surface area scaling, both being proportional to $W^{0.7}$ to $W^{0.78}$. Neither $\dot{V}_E$ nor lung volume were adjusted to this scaling, being proportional to $W^{1.0}$. It was found that alveolar air volume, x, was $\propto W^{0.82}$ and that the central air space, y, was $\propto W^{0.97}$ giving y/x ratio $\propto W^{0.15}$. Hence, in the larger lizards, a greater proportion of the inspired air can only reach the alveoli by diffusion from the central air space. This central air space is certainly used as a reservoir of air to allow high O_2 extractions (Chapter 2). It is possible that the discrepancy between an anatomical factor of $W^{0.15}$ proportionality and a physiological one of $W^{0.25}$, can be accounted for by the increased diffusion distances from both alveolar septa to the centre of an alveolus and central air space centre to peripheral parenchyma which occur in larger lizards.

Absolute values for lung parameters

20 and 10 cm H_2O instillation pressures allowed fixation of the mammalian and Lacerta lung, respectively, at $\frac{3}{4}$ total lung capacity. As predicted from tidal volume measurements (Chapter 2) and proven by volume-pressure curve experiments (Chapter 3), lung volume in Lacerta is twice that of a mammal (Table 5.13). For $\frac{3}{4}$ total lung capacity, the volume is one tenth and one twentieth body weight, respectively. Tracheal volume was 1.95% of this volume in Lacerta but only 0.66% in a mammal - this being some indication of the relative extent of extra-pulmonary dead space.

Although lung volume is twice as great in Lacerta, the actual respiratory regions (peripheral parenchyma) occupy the same volumes and contain similar amounts of septa and capillary tissue (Table 5.13). Alveoli are, however, much smaller in the mammal, 5.5 times, than in Lacerta causing 4.4^3 times greater alveolar numbers. By calculation, such alveolar differences should cause 1.65 to 1.75 times greater respiratory surface areas in the mammal. The difference, however, is about three times from morphometric analysis. This can easily be accounted for because only 78% of septal volume in Lacerta contains capillaries or, in other words, only 70% of the surface area is respiratory, and the septa of Lacerta are 1.4 times thicker than the mammal.

Total lung weight, in contrast to septal/capillary weight, is 1.8 times greater in the mammal due to the non-respiratory conducting airways which are not present in Lacerta. When compared at the 1 kg level of body weight, the terrapin Chrysemys has a lung weight 2 times less and a respiratory surface area 4 times less than a mammal (Perry, 1972). This is similar to the findings in Lacerta. Since body weight scaling was not examined in Chrysemys, lung parameters cannot be expressed in absolute terms for a 10g animal as has been done in Table 5.13 for other animals.

TABLE 5.13

Comparison of lung parameters (right + left) for 10g animals.

Parameter	Mammal	Lacerta	Reptile	Amphibian
Total lung volume (TLC) (ml)	0.63 (3) 0.535 (10)	1.27	5.7 (12)	2.4 (12)
$\frac{3}{4}$ TLC (ml)	0.389 (1) 0.32 (5) 0.5 (11) 0.45 (2)	0.95		
Peripheral volume (ml)	-	0.38	?	?
Parenchyma volume (ml)	0.372 (2)	0.36	?	?
Alveolar air volume (ml)	0.295 (2)	0.29	?	?
Central air space (ml)	-	0.57	?	?
Alveolar mean dimension (μm)	36.5 (9)	160	200-600 (12)	400-1,000 (12)
Absolute alveolar number	$\sim 2.5 \times 10^6$ (1)	3.1×10^4	?	?
Lung weight (g)	0.07 (1) 0.162 (2) 0.113 (10)	0.09	0.135 (12)	0.135 (12)
Septa + capillary weight (g)	0.074-0.119 (2)	0.072	?	?
Respiratory surface area (cm^2)	325.2 (1) 300.0 (2)(5)(11) 380 (15)	95.0	70-250 (7)(12) 75 (6)	35-75 (7) (12)

TABLE 5.13 (continued)

Parameter	Mammal	Lacerta	Reptile	Amphibian
Capillary volume (ml)	0.0342 (2) 0.0375 (5)	0.033	?	?
τ_{ht} (μm)	0.3 (5)(15)	0.527	?	?
τ_{hp} (μm)	0.1 (5)	0.27	?	?
$\bar{\tau}$ (μm)	1.25 (5)	1.77	?	?
$\bar{\tau}_{ep}$	0.4 (5)	0.47	?	?
$\bar{\tau}_{int}$	0.54 (5)	0.865	?	?
$\bar{\tau}_{end}$	0.31 (5)	0.435	?	?
Newborn $\bar{\tau}$	4.5 (13)			
Capillary diameter (μm)	7.0-9.0 (13)	8.0-12.0	11.7-16.1 (6)	?
Erythrocyte surface area (cm^2)	480 (8)	113	?	?
Haematocrit (%)	50 (8)	35	?	?
Erythrocyte volume (ml)	0.018 (2)(5)(8)	0.0115	?	?

Mammalian values underlined are those used in text for comparing with Lacerta.

Capillary volume is virtually the same in both Lacerta and the mammal but capillary diameter is 1.25 times greater in the lizard. This diameter increase causes more capillary bulging in the lizard which is augmented by the presence of a double capillary network. A measure of this capillary bulging is given by the surface area correction factor, Y, which is 1.2 in the mammal (Weibel, 1963, Weibel et al, 1973) and 1.45 (mean) in the lizard. Although the presence of the surface lining material may smooth these contours in mammals (Forrest, 1970, Gil-Weibel, 1972), this would be impossible in the lizard because of the greater degree of bulging and the lower capillary density.

Perry (1972) found in the 1 kg reptile, Chrysemys, a mean capillary length approximately twice that of a 70 kg man. Since the capillary density/ cm^2 decreases as size increases in man (Weibel, 1963), the actual weighted difference to Chrysemys must be considerable. In contrast, Lacerta has a mean capillary density only 1.4 times less than a mammal of the same weight. Over the size range studied in Lacerta, capillary density was constant but this was not rigorously tested morphometrically. The terrapin's capillary volume/total lung weight ratio was found to be twice that of a mammal (Perry, 1972) but if factors, such as, the weight of actual respiratory tissue and a mean capillary diameter of 14 μm in the terrapin and 8 μm in the mammal are taken into the consideration, the terrapin has a capillary volume far in excess of the mammal. If one assumes that non-mammalian erythrocytes will travel along capillaries with their pointed ends first, the capillary diameter of the terrapin is much larger than is necessary for the 10 μm 'short' diameter of the erythrocyte (Saint-Girons, 1970), whereas, in Lacerta, it is more closely matched to the 8.3 μm of the erythrocyte.

Only 49% of the capillary surface in Chrysemys is available for gas exchange (i.e. not embedded in the septa) compared with 84% in Lacerta and 98% in mammals (Perry, 1972, Weibel, 1963). This value is 58% in the lungfish Lepidosiren (Hughes & Weibel, 1976). In estimating arithmetic and

harmonic mean thickness, Perry considered that there was a cut off point after which the air to blood barrier would be too thick for gas exchange. Hence, only 74% of the free capillary surface area was considered respiratory. Obviously, with such a cut off point, $\bar{\tau}$ and τ_h will be underestimated in Chrysemys when compared with Lacerta and mammalian data. Chrysemys $\bar{\tau}$ was 0.85 μm and τ_h was 0.46 μm. In Lacerta, $\bar{\tau}$ is 1.77 μm and τ_h is 0.527 μm whilst in the mammal, $\bar{\tau}$ is 1.25 μm and τ_h is 0.3 μm (Table 5.13).

Air to blood barrier thickness, $\bar{\tau}$, is 1.4 times thicker in Lacerta than in the mammal, the greater thickening occurring in the interstitium and endothelium, respectively (Table 5.13). Geelhaar & Weibel (1971) also found that these were the sites of thickening in the normal mouse when compared to the more active waltzing mouse. Since $\bar{\tau}$ is larger in the lizard so also is the harmonic mean thickness of the air to blood barrier thicker. Plasma τ_{hp} was also larger, reflecting the lizard's lower hematocrit and to a lesser extent its greater capillary diameter. Erythrocyte volume was similar in Lacerta and a mammal but because of the 35 and 50% hematocrits, erythrocytic surface area was 4 times greater in the mammal. Newborn $\bar{\tau}$ is thinner in Lacerta than in the mammal and also similar to the adult Lacerta because there is no rapid proliferation of septa or alveoli just after birth in the lizard and because the double capillary network remains double (Chapter 4).

A comparison of Lacerta lung values with those of reptiles and amphibians determined by Tenney & Tenney (1970) can only show that Lacerta fit within the range of reptilian values. A more detailed comparison is impossible because (a) their study is interspecific with its accompanying high degree of variability, especially in a poikilothermic study, (b) the minimum body weight of a reptile was 25g, (c) their study included snakes, tortoises, lizards and crocodiles, (d) the lungs were all considerably over-inflated, and (e) their estimation of surface area did not account for uncapillarised regions and was made at low light magnifications. Further

comparison with Perry's data (1972) is also impossible because his study did not involve body weight scaling.

Estimation of pulmonary diffusing capacity, D_{Lo_2}

Attempts have been made to determine D_{Lo_2} for the Lacerta lung following the morphometric principles given by Weibel (1970/71). Although $\dot{V}o_2$ is ten times greater in the mammal than in Lacerta, the mammalian respiratory surface area is only 3.14 times greater (Table 5.13). How much of this discrepancy is due to barrier thickness differences and therefore to D_{Lo_2}?

The diffusing capacity of the tissue barrier, D_t, is determined by the equation $D_t = K_t \frac{S_a + S_c}{2 \tau_{ht}}$ where K_t is the tissue permeation coefficient, S_a the surface area of the alveoli (respiratory portion), S_c the surface area of the capillaries (respiratory portion) and τ_{ht} the harmonic mean thickness of the tissue barrier, (Weibel, 1970/71). K_t is calculated from the solubility coefficient, α, and the diffusion coefficient, D, for O_2 where $K_t = \alpha D$. These values have been determined for mammalian lung tissue by Grote (1967) and should be applicable to Lacerta. A correction to these coefficients for a Lacerta body temperature of 30°C as compared to the mammalian 37°C was, however, made. It is found that D_t is 5 times greater in the mammal (Table 5.14).

The diffusing capacity of the plasma layer D_p, is determined by the equation $D_p = K_p \frac{S_c + S_e}{2 \tau_{hp}}$ in which K_p is the plasma permeation coefficient, S_e the surface area of the erythrocytes and τ_{hp}, the harmonic mean thickness of the capillary inner wall to erythrocyte. Since S_c and S_e are very similar in value, the equation $D_p = K_p \frac{S_c}{\tau_{hp}}$ is often used (Burri & Weibel, 1971, Geelhaar & Weibel, 1971). Minimum and maximum values of K_p have been used for mammalian D_{po_2} (Weibel, 1970/71) using the data of Dittmer & Grebe (1958), Altman & Dittmer (1971), Yoshida & Ohshima (1966) and Gertz & Loeschcke (1954). These values were also used for Lacerta but again correcting for temperature (Dittmer & Grebe, 1958). It is found that

TABLE 5.14

Comparison of Lacerta and mammalian morphometric Do_2 values at a body weight of 10g. Mammalian data from Geelhaar & Weibel (1971) for the mouse. Do_2 in ml min^{-1} mm Hg^{-1}. K in $cm^2 min^{-1}$ mm Hg^{-1} α in ml ml^{-1} min^{-1} mm Hg^{-1}.

	Do_2	Physical Coefficient	Mammal	Lacerta	M/L Ratio
D_t	(37°C)	3.3×10^{-8}	0.28	0.059	4.75
	(30°C)	3.07×10^{-8}		0.055	5.1
D_p	min.(37°C)	3.2×10^{-8}	0.7	0.1125	6.2
	max.(37°C)	4.3×10^{-8}	0.94	0.1515	6.2
	min.(30°C)	2.975×10^{-8}		0.1045	6.7
	max.(30°C)	4.0×10^{-8}		0.141	6.7
D_m	min.(37°C)		0.198	0.0387	5.1
	max.(37°C)		0.216	0.0425	5.1
	min.(30°C)			0.036	5.5
	max.(30°C)			0.0392	5.5
D_e	min.(37°C)	0.9	0.0278	0.0297	0.935
	max.(37°C)	2.5	0.077	0.0824	0.935
	min.(30°C)	0.78		0.0258	1.075
	max.(30°C)	2.18		0.072	1.075
	min.($\frac{1}{2}\alpha$ 37°C)	0.45		0.0149	1.8
	max.($\frac{1}{2}\alpha$ 37°C)	1.25		0.0412	1.8
	min.($\frac{1}{2}\alpha$ 30°C)	0.39		0.0129	2.15
	max.($\frac{1}{2}\alpha$ 30°C)	1.085		0.03565	2.15
D_L	min.(37°C)		0.031*		
	max.(37°C)		0.064*		
	min.(30°C)			0.024	1.3
	max.(30°C)			0.0495	1.3
	min.($\frac{1}{2}\alpha$ 30°C)			0.0095	3.26
	max.($\frac{1}{2}\alpha$ 30°C)			0.0196	3.26

* These values of Geelhaar & Weibel do not tally with D_m and D_e data. It is suggested that they should be 0.0244 (min.) and 0.057 (max.). This makes the final M/L ratio for D_L equal to 2.5 (min.) or 2.9 (max.).

D_p is 6.7 times greater in the mammal causing a total membrane diffusing capacity, D_m, which is 5.5 times greater in the mammal (Table 5.14). D_m is determined from the equation

$$\frac{1}{D_m} = \frac{1}{D_t} + \frac{1}{D_p}$$

The diffusing capacity of the erythrocytes, D_e, is determined from the equation, $D_e = \theta' Vc$ in which θ' is the rate of association and Vc is the capillary volume or, in other words, the blood volume in the lungs at an instant of time. Vc is also a measure of the blood flow multiplied by the length of time the blood is in the capillaries (Staub, Bishop & Forster, 1962). The faster the flow, the lower the time available for O_2 uptake. Vc was virtually the same in both Lacerta and the mammal but the capillary length may be excessively long in Lacerta (Chapter 4). θ' has been determined by Staub, Bishop & Forster (1962) and by Mochizuki (1966) and is calculated from the following equation:-

$$\theta' = \text{Kc (velocity constant)} \times \frac{O_2}{760 \times 22.4} \times \text{\% saturation of hemoglobin factor} \times O_2 \text{ capacity.}$$

The blood O_2 properties have never been examined in Lacerta and hence data from other lizards must be used in order to determine a lizard θ'. It is known that the O_2 capacity of reptilian blood is only about 10% (Prosser & Brown, 1961, Dawson & Poulson, 1962, Wood & Moberly, 1970, Bennett, 1973b) as opposed to the 20% in mammals. Hence half the mammalian θ' must be used for Lacerta. Although the P_{50} is almost twice that of a mammal, i.e. 42 mm Hg in a 20g mammal and 72 mm Hg in a 20g reptile (Bennett, 1973b), from the data of Staub et al (1962) it would appear that this will not affect Kc markedly. Using a temperature correction to θ' for 30°C, it is found that D_e is 2.15 times greater in the mammal than in Lacerta (Table 5.14). The total diffusing capacity of the lung, D_L, is, therefore,

3.26 (or 2.5 to 2.9, see footnote of Table 5.14) times greater in the mammal, since $\frac{1}{D_L} = \frac{1}{D_m} + \frac{1}{D_e}$.

Thus, although the thicker harmonic mean thicknesses of tissue and plasma of Lacerta converted the respiratory surface area mammal/lizard ratio from 3.16 to a membrane diffusing capacity ratio of 5.5, this was compensated for by a larger lung perfusion, Vc, in Lacerta (i.e. larger relative to respiratory surface area) causing the final pulmonary diffusing capacity ratio to return to 3.26. The question still remains as to why the $\dot{V}o_2$ mammal/lizard ratio is 10 when D_{Lo_2} is 3.26. To expect the two ratios to match requires a similar arterial-venous O_2 difference in Lacerta and mammal, since $D_{Lo_2} \propto \frac{\dot{V}o_2}{\text{A-V diff.}}$. Hence, one could predict that the A-V difference is approximately 3 to 4 times less in Lacerta. Another well known respiratory equation is $\dot{V}o_2$ = cardiac output x A-V difference, again allowing one to predict that cardiac output is 3 to 4 times less in Lacerta.

Examination of the literature for measurements of reptilian A-V difference and cardiac output revealed only data for the iguana. Mammal/lizard ratios for cardiac output of 2 (Tucker, 1966), 4 (Baker & White, 1970) and 3.4 (Dejours, Garey & Rahn, 1970, using Tucker's data) can be obtained. Dejours, Garey & Rahn (1970) have estimated O_2 concentration in arterial blood of the iguana and find that it is a third the concentration in a mammal. This is due partly to the lizard's 10% O_2 capacity as compared to the mammalian 20% O_2 capacity and partly to the left to right cardiac shunt caused by an incomplete ventricular septum which allows bypassing of the lungs. Thus, although blood from the lung is 100% saturated, that reaching the dorsal aorta and hence the rest of the body is only 70% saturated (White, 1968, 1970, Tucker, 1966). Such shunts operate part of the time in iguanas (Tucker, 1966) but are thought to operate all the time in Lacerta (Foxon et al, 1956). Venous O_2 concentrations in iguana were also found to be a third the concentration in the mammalian veins (Dejours, Garey & Rahn, 1970). Thus, A-V differences were approximately 3 times

greater in the mammal than in the lizard. These ratios for the iguana compare well with the predicted mammal/Lacerta ratios. The iguana lung is very similar to Lacerta but may be a little more complex (Chapter 4).

It is of interest to note that the cardiac output/$\dot{V}O_2$ ratio is 40 in the iguana and 15 in the mammal (Dejours, Garey & Rahn, 1970). On the assumption that total body blood volume would be the same in lizards and mammals, cardiac output is relatively high in the lizard. This is necessary to compensate for left to right cardiac shunts and reduced O_2 capacity of the blood. If the lizard could increase its O_2 capacity of the blood to mammalian values, its pulmonary diffusing capacity, D_{LO_2}, would only be 1.3 times less than a mammal's (Table 5.14). Thus the respiratory lung tissue, even with its lower surface area and thicker diffusion pathways, and with its present capillary volume could support mammalian levels of maximum $\dot{V}O_2$. It is the cardiovascular side that is limiting $\dot{V}O_2$, requiring increases in cardiac output and A-V differences to match mammalian values.

Morphometric minimum D_{LO_2} has been shown to be close to but higher than the values determined physiologically for maximum D_{LO_2} whilst under exercise (Siegwart et al, 1971). The physiological measurement, however, is always an underestimating one because of functional inhomogeneities, i.e. unequal distribution of ventilation, perfusion and diffusing capacity, and because the greater the absolute value the more difficult it is to measure accurately (Piiper, 1969, Magnussen et al, 1974). Thus a morphometric value may be more accurate. Weibel et al (1973) have shown, however, that when fixed by vascular perfusion at positive air inflation pressures the maximum D_{LO_2} is only 73% of the value obtained by 20 cm H_2O instillation pressure. Whether this would still occur during negative pressure air inflation is not known. Physiological D_{LO_2} was not measured in Lacerta.

Hughes & Weibel (1976) have compared morphometric D_{Lo_2} and D_{to_2} in Lepidosiren, a terrapin and a tortoise (reptilian data from Perry, unpublished) with those of the rat. The rat D_{Lo_2} was 18 times greater than the value estimated for Lepidosiren and the rat D_{to_2} was 110 times (Lepidosiren), 34 times (terrapin) and 70 times (tortoise). No measurements for maximum $\dot{V}o_2$ are available for these three lower vertebrates.

Lung growth in Lacerta

Although the lung volume of the newborn Lacerta fits the regression lines for the adult data (Fig. 5.5), lung tissue weight and respiratory surface area are underdeveloped by 6 and 4 times the expected value. In contrast, the mammalian newborn has a heavier than expected lung tissue weight but a smaller than expected respiratory surface area because the septa are rather thick (Weibel, 1967). Its lung volume fits regression lines for adult data (Table 5.12). Further newborn differences between Lacerta and mammals have been described in Chapter 4.

The reduction in relative respiratory surface area of the newborn is reflected in their lower than expected minimum and maximum $\dot{V}o_2$ (Mount & Stephens, 1970). Instead of the $\dot{V}o_2$ proportionality to $W^{0.75}$, newborn pigs for 6 days have a $\dot{V}o_2$ proportionality to $W^{1.0}$ or $^{1.03}$ (Mount & Stephens, 1970) which compares well with respiratory surface area proportionality of $W^{1.02}$ in one of the studies on rat lung development (Bartlett, 1970a). A similar developmental change in the $\dot{V}o_2$ v body weight slope which is matched by the change in respiratory surface area v body weight slope has also been found in fishes (Hughes, personal communication).

In Lacerta newborn, however, the reduction in respiratory surface area was not matched by a similar reduction in resting $\dot{V}o_2$, nor even in maximum $\dot{V}o_2$. Whilst accepting the preliminary nature of the investigation into newborn Lacerta lung morphometry and the lack of an EM study, the results are considered reasonably accurate. An explanation for this mismatching cannot be given. Further investigation is obviously required.

Effect of lung inflation in Lacerta

Since only one animal was used morphometrically for each of the three inflation levels, the results obtained can only be indicative of the possible effects of inflation. Further data is obviously necessary. If one can assume that glutaraldehyde instillation causes 'normal' inflation in situ, it is clear that different degrees of inflation are not homogeneously distributed through the lung. Anterior regions of the lung, containing more complexly structured parenchyma, inflate more markedly at low volumes than the posterior regions. This has an obvious advantage in reducing 'wasted' ventilation. Inflation at greater lung volumes causes a greater proportion of posterior expansion and therefore more 'wasted' ventilation. Over-expansion (at 15 cm H_2O) causes equal expansion of both anterior and posterior regions but with a domination of total lung volume by the volume of the central air space. There is also some collapse of parenchyma regions, especially posteriorly. This over-expansion is likely to cause considerable 'wasted' ventilation.

These morphometric findings are in complete agreement with the physiological measurements of ventilation requirement during increasing ventilation volume or tidal volume (Chapter 2), in which $\dot{V}_E/\dot{V}O_2$ increased as $\dot{V}_E$ increased and at maximum $\dot{V}_E$ the 'wastage' of ventilated air became even greater. Inflation causes a disproportionate increase in the central air reservoir relative to the peripheral respiratory parenchyma and therefore also increases diffusion distances from the centre of alveoli to the septa and from the central air space to the septa.

The over-inflation and peripheral collapse of Lacerta lung at 15 cm H_2O in situ instillation serves to illustrate the abnormal effects of air fixing isolated reptilian and amphibian lungs at 20 cm H_2O as in the work of Tenney & Tenney (1970). It is of interest to note that at 90% total lung capacity the alveolar duct volume increases considerably even in the mammal (Forrest, 1974).

Alveoli are cylinders in lizards and truncated spheres in mammals, the configuration of which has been shown to remain constant throughout the pressure-volume curve of the latter (Forrest, 1974). No attempt has been made to calculate configuration dimensions for Lacerta but there are disproportionate changes between depth and diameter which would indicate that the configuration does alter. In mammals, inflation causes alveoli to open with the subsequent unfolding of the respiratory surface together with a reduction in the air-blood barrier distance (Weibel et al, 1973). Since Lacerta alveoli are not positioned at the end of branching airways but lie around the lung periphery, their behaviour during inflation might be expected to be different.

Lacerta septa are highly folded at low levels of inflation and because the alveoli are large there is virtually no alveolar collapse. In contrast, excess surface area is removed by alveolar collapse at low mammalian lung volumes. This 'excess' surface area in the lizard may help to explain its ability for high O_2 extraction at low tidal volumes and frequency. Surface lining material always smooths out the corrugations of the alveolar surface at all levels of mammalian lung inflation (Forrest, 1970a,b, Weibel et al, 1973), so that it is possible that some of the 'excess' surface area may be lost similarly in Lacerta.

GENERAL CONCLUSIONS

It has generally been accepted that the metabolism of all animals is proportional to body weight as $W^{0.75}$ (Kleiber, 1947, Hemmingsen, 1960, Schmidt-Nielsen, 1970). Some workers, however, believe that deviations from a slope of 0.75 can occur in some species or groupings of animals which indicate a specialisation to meet certain metabolic or environmental demands (Stahl, 1967, Bartholomew, 1972). On the other hand, incomplete interspecific data can also give deviations. Intraspecific or intrageneric studies over a sufficient size range are rarely undertaken to examine this possibility of specialisation. In the Lacerta genus (0.2 to 38g) it has been shown that both standard and maximum $\dot{V}O_2$ are proportional to $W^{0.75}$ (range 0.74 to 0.8). This can be interpreted to mean that a $\dot{V}O_2$ proportionality of $W^{0.75}$ is true for all species or that Lacerta do not show a specialisation from the 'average' or 'norm'. Many more detailed intraspecific or intrageneric studies are required to resolve this question.

A procedure giving minimum stress is considered absolutely essential for the measurement of standard $\dot{V}O_2$ scaling particularly if the study is an intrageneric one. For instance, since there were many differences in the diurnal behaviour of the genus Lacerta, $\dot{V}O_2$ measurements in the dark but during the day would have produced deviations from the 0.75 slope. Similarly, minimum stress allowed the standard $\dot{V}O_2$ of Lacerta at 30°C to be a tenth that of a mammal at 37°C which contrasts with the usually accepted fourth to seventh. The greater metabolism in homeotherms is necessary to maintain the body temperature at 37°C using physiological mechanisms; poikilotherms have exploited a low metabolic rate by using behavioural thermoregulation.

Maximum $\dot{V}O_2$, especially with regard to its body weight relationship, is rarely measured which is a serious omission since it is most likely to uncover limitations of the respiratory system. Most estimates of the

respiratory surface area or pulmonary diffusing capacity of an animal are for a maximum surface area and these must be compared with maximum $\dot{V}O_2$, not standard or resting $\dot{V}O_2$. Ultsch (1973) has measured the O_2 exchange capacity ($W^{0.54}$) and resting $\dot{V}O_2$ ($W^{0.65}$) in salamanders and found that the former limits the size of the animal. Weibel (1972) has found that pulmonary diffusing capacity ($W^{0.96}$) is in excess of resting $\dot{V}O_2$ ($W^{0.75}$) but, for the animals selected, data from Pasquis, Lacaisse & Dejours (1970) would indicate that maximum $\dot{V}O_2$ is also proportional to $W^{0.96}$ approximately. A matching of D_{LO_2} and maximum $\dot{V}O_2$ was also found in Lacerta.

Small mammals and Lacerta are capable of increasing their $\dot{V}O_2$ by the same amount (maximum/standard = 7 to 8) but the capacity for activity must be greater in reptiles since they can augment their metabolism by extensive use of anaerobic pathways. The cost of exercise is also a little lower in reptiles, especially Lacerta. Although the Lacerta lung architecture is primitive, the septa themselves are very advanced and closely approximate to the mammal's. The extent of the respiratory surface area, the thickness of the air to blood pathway and the capillary blood volume in Lacerta are considered sufficient to almost support mammalian levels of maximum $\dot{V}O_2$. Such levels are not, however, reached because cardiovascular factors, such as O_2 capacity of the blood and cardiac shunts, limit the system.

Further correlations of physiological and anatomical (using morphometry) parameters were attempted in Lacerta by examining the ventilation volume, O_2 extraction coefficient or ventilation requirement and the distribution of air between alveoli and the central air space of the lung. V_T was proportional to $W^{1.0}$ but since frequency was constant, $\dot{V}_E$ was not adjusted to match the $\dot{V}O_2$ proportionality of $W^{0.75}$. Hence, $\dot{V}_E/\dot{V}O_2$ was proportional to $W^{0.25}$ and larger lizards 'wasted' more of their ventilated volume. This can be correlated with the fact that the proportion

y/x of air in the central air space, y, versus the air in the alveoli, x, is proportional to $W^{0.15}$. In order to inflate the peripheral alveoli sufficiently in larger lizards (septa and lung weight are both proportional to $W^{0.7}$ approximately), the central air space has to over-inflate. Similarly, during standard to maximum $\dot{V}O_2$ the ventilation requirement increases markedly, there being an excessive wastage of ventilated volume. This again is related to anatomical evidence of a y/x ratio increase during V_T increments.

Although mammalian and bird data show that lung volume is proportional to $W^{1.0}$, reptiles have been thought to be proportional to $W^{0.75}$ (Tenney & Tenney, 1970) or to $W^{0.85}$ (Bennett, 1973a). It seems surprising that such a basic parameter as the volume of an organ should be scaled in a manner different to the entire body. Lacerta data for all lung subdivisions, however, continues to support a proportionality of $W^{1.0}$. Compliance differences between reptiles or tidal volume measurements in stressed animals have been suggested in this thesis to explain these anomalies.

It is perhaps consistent that respiratory frequency does not change with either increments in $\dot{V}O_2$ or in body weight. Lacerta certainly have the capacity to alter frequency considerably but this may be controlled by demands other than metabolic. A constant low frequency allows the lungs to remain inflated during the respiratory pause for longer periods and this has been shown to assist in O_2 extraction. When the respiratory frequency is high, O_2 extraction is poor but when frequency is low, O_2 extraction can be higher than a mammal.

REFERENCES

ADAMS, W.E. (1939). The cervical region of the Lacertilia. A critical review of certain aspects of its anatomy. J. Anat. 74, 57-71.

ADAMS, W.E. (1953). The carotid arch in lizards with particular reference to the origin of the internal carotid artery. J. Morph. 92, 115-155.

AGOSTONI, E., THIMM, F.F. & FENN, O.W. (1959). Comparative features of the mechanics of breathing. J. appl. Physiol. 14, 679-683.

AGOSTONI, E. & MEAD, J. (1964). Statics of the Respiratory System. In: Handbook of Physiology. Section 3. Respiration. Vol. I, (ed. W.O. Fenn & H. Rahn). Washington D.C., Am. Physiol. Soc. pp. 387-409.

ALTMAN, P.L. & DITTMER, D.S. (1971). Respiration and Circulation. Biological Handbooks. Federation of American Societies for Experimental Biology.

ANDERSEN, B. & MADSEN, J. (1972). Gas permeability of the alveolo-pleural wall in the mouse lung. Acta physiol. scand. 84, 382-395.

ASMUSSEN, E. (1965). Muscular Exercise. In: Handbook of Physiology. Section 3. Respiration. Vol. II, (ed. W.O. Fenn & H. Rahn). Washington D.C., Am. Physiol. Soc., pp. 939-978.

ASPLUND, K.K. (1970). Metabolic scope and body temperature of whiptail lizards (Cnemidophorus). Herpetologica, 26, 403-411.

ATLAND, P.D. & PARKER, M. (1955). Effects of hypoxia on the box turtle. Amer. J. Physiol. 180, 421-427.

AVERY, M.E. & SAID, S. (1965). Surface phenomena in lungs in health and disease. Medicine, Baltimore, 44, 503-526.

AVERY, R.A. (1971). Estimates of food consumption by the lizard Lacerta vivipara Jacquin. J. Anim. Ecol. 40, 351-365.

AVERY, R.A. (1973). Morphometric and functional studies on the stomach of the lizard, Lacerta vivipara. J. Zool. Lond. 169, 157-167.

AVERY, R.A. & McARDLE, B.H. (1973). The morning emergence of the common lizard Lacerta vivipara Jacquin. Br. J. Herpet. 5, 363-368.

BACHOFEN, H., HILDEBRANDT, J. & BACHOFEN, M. (1970). Pressure-volume curves of air and liquid-filled excised lungs - surface tension in situ. J. appl. Physiol. 29, 422-431.

BACHOFEN, M. & WEIBEL, E.R. (1974). Basic pattern of tissue repair in human lungs following unspecific injury. Chest, 65, 14S-19S.

BAKER, L.A. & WHITE, F.N. (1970). Redistribution of cardiac output in response to heating in Iguana iguana. Comp. Biochem. Physiol. 35, 253-262.

BAKKER, R.T. (1972). Locomotor energetics of lizards and mammals compared. Physiologist, 15.

BALIS, J.U. & CONEN, P.E. (1964). The role of alveolar inclusion bodies in the developing lung. Lab. Invest. 13, 1215-1229.

BARDEN, A. (1942). Activity of the lizard, Cnemidophorus sexlineatus. Ecology, 23, 336-344.

BARGE, J.A.J. (1937). II Kopfdarm. A. Mundhöhle und ihre Organe. 1. Mundhöhlendach und Gaumen. In: Handbuch der Vergleichenden Anatomie der Wirbeltiere. Vol. 3 (ed. L. Bolk, E. Göppert, E. Kallius & W. Lubosch). Berlin, pp.29-48.

BARNES, C.D. & ELTHERINGTON, L.G. (1973). Drug dosage in laboratory animals. A Handbook. University of California Press.

BARTELS, H. (1964). Comparative physiology of oxygen transport in mammals. Lancet, 599-604.

BARTHOLOMEW, G.A. (1972). Energy Metabolism. In: Animal Physiology: Principles and Adaptations, 2nd ed. (ed. M.S. Gordon). New York, Macmillan. pp.63-72.

BARTHOLOMEW, G.A. & TUCKER, V.A. (1963). Control of changes in body temperature, metabolism, and circulation by the agamid lizard, Amphibolurus barbatus. Physiol. Zoöl. 36, 199-218.

BARTHOLOMEW, G.A. & TUCKER, V.A. (1964). Size, body temperature, thermal conductance, O_2 consumption, and heart rate in Australian varanid lizards. Physiol. Zoöl. 37, 341-354.

BARTHOLOMEW, G.A., TUCKER, V.A. & LEE, A.K. (1965). O_2 consumption, thermal conductance and heart rate in the Australian skink Tiliqua scincoides. Copeia, 169-173.

BARTLETT, D. (1970a). Postnatal growth of mammalian lung: influence of exercise and thyroid activity. Respir.Physiol. 9, 50-57.

BARTLETT, D. (1970b). Postnatal growth of mammalian lung: influence of low and high O_2 tensions. Respir.Physiol. 9, 58-64.

BARTLETT, D. & REMMERS, J.E. (1971). Effects of high altitude exposure on the lungs of young rats. Respir. Physiol. 13, 116-125.

BARTLETT, D., REMMERS, J.E. & GAUTIER, H. (1973). Laryngeal regulation of respiratory airflow. Respir. Physiol. 18, 194-204.

BEDDARD, F.E. (1906). Contribution to the anatomy of the Ophidia. Proc. zool. Soc. Lond. 12-44.

BELKIN, D.A. (1961). The running speeds of the lizards Dipsosaurus dorsalis and Callisaurus draconoides. Copeia, 223-224.

BELKIN, D.A. (1968). Aquatic respiration and underwater survival of two freshwater turtle species. Respir. Physiol. 4, 1-14.

BELLAIRS, A. (1969). The Life of Reptiles. Vols. 1 & 2. London, Weidenfield and Nicolson.

BELLAIRS, A. & Boyd, J.D. (1950). The lachrymal apparatus in lizards and snakes. II. The anterior part of the lachrymal duct and its relationship with the palate and with the nasal and vomeronasal organs. Proc. zool. Soc. Lond. 120, 269-310.

BELOFF-CHAIN, A. & ROOKLEDGE, K.A. (1970). A comparative study of the influence of temperature on metabolism of glucose in isolated reptilian and mammalian muscle. Comp. Biochem. Physiol. 37, 67-72.

BENEDICT, F.G. (1932). The Physiology of Large Reptiles. Carnegie Inst. Wash. Publ. No. 425.

BENNETT, A.F. (1972a). The effect of activity on oxygen consumption, oxygen debt, and heart rate in the lizards Varanus gouldii and Sauromalus hispidus. J. comp. Physiol. 79, 259-280.

BENNETT, A.F. (1972b). A comparison of activities of metabolic enzymes in lizards and rats. Comp. Biochem. Physiol. 42B, 637-647.

BENNETT, A.F. (1973a). Ventilation in two species of lizards during rest and activity. Comp. Biochem. Physiol. 46A, 653-671.

BENNETT, A.F. (1973b). Blood physiology and oxygen transport during activity in two lizards, Varanus gouldii and Sauromalus hispidus. Comp. Biochem. Physiol. 46A, 673-690.

BENNETT, A.F. & DAWSON, W.R. (1972). Aerobic and anaerobic metabolism during activity in the lizard Dipsosaurus dorsalis. J. comp. Physiol. 81, 289-299.

BENNETT, A.F. & DAWSON, W.R. (1973). Metabolism. In: Biology of the Reptilia. Physiology A, Vol. 5 (ed. C. Gans). New York, Academic Press. (in press)

BENNETT, A.F. & LICHT, P. (1972). Anaerobic metabolism during activity in lizards. J. comp. Physiol. 81, 277-288.

BERGER, M., HART, J.S. & ROY, O.Z. (1970). Respiration, oxygen consumption and heart rate in some birds during rest and flight. Z. vergl. Physiol. 66, 201-214.

BERTALANFFY, F.D. (1964a). Respiratory tissue: structure, histophysiology, cytodynamics. Part I. Review and basic cytomorphology. Int. Rev. Cytol. 16, 233-328.

BERTALANFFY, F.D. (1964b). Respiratory tissue: structure, histophysiology, cytodynamics. Part II. New approaches and interpretations. Int. Rev. Cytol. 17, 213-299.

BERTALANFFY, F.D. (1968). Dynamics of cellular populations in the lung. In: The Lung. International Academy of Pathology Monographs (ed. A.A. Liebouw & D.E. Smith). Maryland, William & Wickins. pp. 19-30.

BERTALANFFY, L. (1951). Metabolic types and growth types. Am. Nat. 85, 111-117.

BERTALANFFY, L. (1957). Quantitative laws in metabolism and growth. Q. Rev. Biol. 32, 217-231.

BERTIN, L. (1970). Organes de la respiration aérienne. In: Traité de Zoologie. Vol. XIII, Agnathes et Poisons, II (ed. P.P. Grassé), Paris, Masson et Cie., pp.1363-1398.

BETZ, T.W. (1962). Surgical anaesthesia in reptiles, with special reference to the water snake, Natrix rhombifera. Copeia, 284-287.

BOELAERT, R. (1941). Sur la Physiologie de la Respiration de Lacertiens. Archs int. Physiol. 51, 379-436.

BOYDEN, E.A. (1974). The mode of origin of pulmonary acini and respiratory bronchioles in the fetal lung. Am. J. Anat. 141, 317-328.

BOYER, D.R. (1963). Hypoxia: effects on heart rate and respiration in snapping turtle. Science, N.Y. 140, 813-814.

BOYER, D.R. (1966). Comparative effects of hypoxia on respiratory and cardiac function in reptiles. Physiol. Zoöl. 39, 307-316.

BOYER, D.R. (1967). Interaction of temperature and hypoxia on respiratory and cardiac responses in the lizard, Sauromalus obesus. Comp. Biochem. Physiol. 20, 437-447.

BRACKENBURY, J.H. (1971). Airflow dynamics in the avian lung as determined by direct and indirect methods. Respir. Physiol. 13, 319-329.

BRATTSTROM, B.H. (1970). Amphibia. In: Comparative Physiology of Thermoregulation. Vol. 1. Invertebrates and non-mammalian vertebrates. (ed. G.C. Whittow). Academic Press. pp.135-166.

BRAZENOR, C.W. & KAYE, G. (1953). Anaesthesia for reptiles. Copeia, 165-170.

BRETT, J.R. (1965). The relation of size to rate of oxygen consumption and sustained swimming speed of sockeye salmon (Oncorhynchus nerka). J. Fish. Res. Bd Can. 22, 1491-1501.

BRETT, J.R. (1972). The metabolic demand for oxygen in fish, particularly salmonids, and a comparison with other vertebrates. Respir. Physiol. 14, 151-170.

BRETZ, W.L. & SCHMIDT-NIELSEN, K. (1971). Bird respiration: flow patterns in the duck lung. J. exp. Biol. 54, 103-118.

BRINKMAN, G.L. (1968). The mast cell in normal human bronchus and lung. J. Ultrastruct. Res. 23, 115-123.

BRISCOE, W.A. (1965). Lung Volumes. In: Handbook of Physiology. Section 3. Respiration. Vol. II (ed. W.O. Fenn & H. Rahn). Washington D.C., Am. Physiol. Soc. pp. 1345-1379.

BRODY, J.S. & BUHAIN, W.J. (1972). Hormone-induced growth of the adult lung. Am. J. Physiol. 223, 1444-1450.

BRODY, J.S. & BUHAIN, W.J. (1973). Hormonal influence on post-pneumonectomy lung growth in rat. Respir. Physiol. 19, 344-355.

BRUNER, H.L. (1907). On the cephalic veins and sinuses of reptiles, with description of a mechanism for raising the venous blood-pressure in the head. Am. J. Anat. 7, 1-117.

BRUNS, R.R. & PALADE, G.E. (1968). Studies on blood capillaries. I. General organisation of blood capillaries in muscle. J. Cell Biol. 39, 244-276.

BUHAIN, W.J. & BRODY, J.S. (1973). Compensatory growth of the lung following pneumonectomy. J. appl. Physiol. 35, 898-902.

BURNSTOCK, G. & WOOD, M.J. (1967). Innervation of the lungs of the sleepy lizard Trachysaurus rugosus. II. Physiology and Pharmacology. Comp. Biochem. Physiol. 22, 815-831.

BURRI, P.H. (1974). The postnatal growth of the rat lung. Part III: Morphology. Anat. Rec. 180, 77-98.

BURRI, P.H., DBALY, J. & WEIBEL, E.R. (1974). The postnatal growth of the rat lung. Part I: Morphometry. Anat. Rec. 178, 711-730.

BURRI, P.H. & WEIBEL, E.R. (1971). Morphometric estimation of pulmonary diffusion capacity. II. Effect of Po_2 on the growing lung. Adaptation of the growing rat lung to hypoxia and hyperoxia. Respir. Physiol. 11, 247-264.

BUTLER, J. (1957). The adaptation of the relaxed lungs and chest wall to changes in volume. Clin. Sci. 16, 421-433.

BUTLER, J. & SMITH, B.H. (1957). Pressure-volume relationship of the chest in the completely relaxed anaesthetized patient. Clin. Sci. 16, 125-146.

CAMPBELL, H. & TOMKEIEFF, S.I. (1952). Calculation of the internal surface of a lung. Nature, Lond. 170, 117.

CHALKLEY, H.W., CORNFIELD, J. & PARK, H. (1949). A method for estimating volume surface ratios. Science, N.Y. 110, 295-297.

CHASE, W.H. (1959). The surface membrane of pulmonary alveolar walls. Expl Cell Res. 18, 15-28.

CHODROW, R.E. & TAYLOR, C.R. (1973). The cost of limbless locomotion in snakes. Fedn Proc. 32, 422.

CLEMENTS, J.A. (1962). Surface tension in the lungs. Scient. Am. 207, 120-130.

CLEMENTS, J.A. & TIERNEY, D.F. (1965). Alveolar instability associated with altered surface tension. In: Handbook of Physiology. Section 3. Respiration. Vol. II (ed. W.O. Fenn & H. Rahn). Washington D.C., Am. Physiol. Soc. pp. 1565-1583.

CLOUDSLEY-THOMPSON, J.L. (1971). The Temperature and Water Relations of Reptiles. Merrow Publishing Co. Ltd., England.

CRAWFORD, E.C., Jr. & KAMPE, G. (1971). Physiological responses of the lizard Sauromalus obesus to changes in ambient temperature. Am. J. Physiol. 220, 1256-1260.

CROFT, P.G. (1957). Anaesthesia and Euthanasia. In: UFAW Handbook, 2nd edition (ed. A.N. Worden & W. Lane-Patter). pp. 155-165.

CROSFILL, M.C. & WIDDICOMBE, J.G. (1961). Physical characteristics of the chest and lungs and the work of breathing in different mammalian species. J. Physiol. 158, 1-14.

CURRY, R.H., SIMON, G.T. & RITCHIE, A.C. (1969). An electron microscopic study of normal mouse lung and the early diffuse changes following uracil mustard administration. J. Ultrastruct. Res. 28, 335-352.

D'ANGELO, E. (1972). Local alveolar size and transpulmonary pressure in situ and in isolated lungs. Respir. Physiol. 14, 251-266.

D'ANGELO, E. & AGOSTONI, E. (1975). Vertical gradients of pleural and transpulmonary pressure with liquid-filled lungs. Respir. Physiol. 23, 159-173.

DAWSON, W.R. (1960). Physiological responses to temperature in lizard Eumeces obsoletus. Physiol. Zoöl. 33, 87-103.

DAWSON, W.R. (1967). Interspecific variation in physiological responses of lizards to temperature. In: Lizard Ecology: A Symposium. (ed. W.W. Milstead). University of Missouri Press. pp. 230-257.

DAWSON, W.R. & BARTHOLOMEW, G.A. (1956). Relation of O_2 consumption to body weight, temperature and temperature acclimation in lizards, Uta stansburiana and Sceloporus occidentalis. Physiol. Zoöl. 29, 40-51.

DAWSON, W.R. & BARTHOLOMEW, G.A. (1958). Metabolic and cardiac responses to temperature in the lizard Dipsosaurus dorsalis. Physiol. Zoöl. 31, 100-111.

DAWSON, W.R. & POULSON, T.L. (1962). O_2 capacity of lizard bloods. Am. Midl. Nat. 68, 154-164.

DAWSON, W.R. & TEMPLETON, J.R. (1963). Physiological responses to temperature in the lizard Crotaphytus collaris. Physiol. Zoöl. 36, 219-236.

DeGROODT, M., LAGASSE, M. & SEBRUYNS, M. (1960). Elektron-mikroskopische Morphologie der Lungenalveolen des Protopterus und Amblyostoma. International Congress for Electron Microscopy 1958, Proceedings. Berlin, Springer Verlag. pp. 418-421.

De HOFF, K.T. & RHINES, F.N. (1968). Quantitative Microscopy. New York, McGraw-Hill. pp.12-44.

DEJOURS, P. (1964). Control of respiration in muscular exercise. In: Handbook of Physiology. Section 3. Respiration. Vol. I (ed. W.O. Fenn & H. Rahn). Washington D.C., Am. Physiol. Soc. pp. 631-648.

DEJOURS, P., GAREY, W.F. & RAHN, H. (1970). Comparison of ventilatory and circulatory flow rates between animals in various physiological conditions. Respir. Physiol. 9, 108-117.

DENISON, D.M. & KOOYMAN, G.L. (1973). The structure and function of the small airways in pinniped and sea otter lungs. Respir. Physiol. 17, 1-10.

DEPACOS, F. & HART, J.S. (1957). Use of the Pauling O_2 analyzer for measurement of O_2 consumption of animals in open-circuit systems and in a short-lag, closed circuit apparatus. J. appl. Physiol. 10, 388-392.

DERMER, G.B. (1969). The fixation of pulmonary surfactant for electron microscopy. I. The alveolar surface lining layer. J. Ultrastruct. Res. 27, 88-104.

DERMER, G.B. (1970a). The fixation of pulmonary surfactant for electron microscopy. II. Transport of surfactant through the air-blood barrier. J. Ultrastruct. Res. 31, 229-246.

DERMER, G.B. (1970b). The pulmonary surfactant content of the inclusion bodies found within Type II alveolar cells. J. Ultrastruct. Res. 33, 306-317.

DESSAUER, H.C. (1970). Blood chemistry of reptiles: Physiological and evolutionary aspects. In: Biology of the Reptilia. Vol. 3 (ed. Carl Gans & Thomas S. Parsons). London and New York, Academic Press. pp. 1-54.

DIAMOND, L. & LIPSCOMB, W. (1970). Design of small-animal pneumotachograph. J. appl. Physiol. 29, 720-722.

DITTMER, D.S. & GREBE, R.N. (1958). Handbook of Respiration. Philadelphia, London, W.B. Saunders.

DMI'EL, R. (1972). Effect of activity and temperature on metabolism and water loss in snakes. Am. J. Physiol. 223, 510-516.

DMI'EL, R. & BORUT, A. (1972). Thermal behaviour, heat exchange, and metabolism in the desert snake, Spalerosophis cliffordi. Physiol. Zoöl. 45, 78-94.

DOBBINS, W.O. III, & EMORY, L.R. (1970). Intestinal mucosal lymphatic permeability: An electron microscopic study of endothelial vesicles and cell junctions. J. Ultrastruct. Res. 33, 29-59.

DRORBAUGH, J.E. (1960). Pulmonary function in different animals. J. appl. Physiol. 15, 1069-1072.

DRUMMOND, F.H. (1946). Pharyngeo-oesophageal respiration in the lizard Trachysaurus rugosus. Proc. zool. Soc. Lond. 116, 225-228.

DUNKER, H. (1972). Structure of Avian Lungs. Respir. Physiol. 14, 44-63.

DUNNILL, M.S. (1962). Postnatal growth of the lung. Thorax 17, 329-333.

DUNNILL, M.S. (1967). Effect of lung inflation on alveolar surface area in dog. Nature, Lond. 214, 1013-1014.

EFATI, P., NIR, E. & YAARI, A. (1970). Morphological and cytological observations on cells of the hemopoietic system of Agama stellio (Linnaeus). A comparative study. Israel J. med. Sci. 6, 23-31.

EMERY, J.L. & WILCOCK, P.F. (1966). The postnatal development of the lung. Acta anat. 65, 10-29.

ENGEL, S. (1962). Lung Structure. C.C. Thomas, Springfields.

ETHERTON, J.E. & CONNING, D.M. (1971). Early incorporation of labelled palmitate into mouse lung. Experientia 27, 554-555.

EVANS, K.J. (1966). Responses of the locomotor activity rhythms of lizards to simultaneous light and temperature cycles. Comp. Biochem. Physiol. 19, 91-103.

FEDAK, M.A., PINSHOW, B. & SCHMIDT-NIELSEN, K. (1974). Energy cost of bipedal running. Am. J. Physiol. 227, 1038-1044.

FINLEY, T.N., PRATT, S.A., LAOMAN, A.J., BREWEER, L. & McKAY, M.B. (1968). Morphological and lipid analysis of the alveolar lining material in dog lung. J. Lipid Res. 9, 357-365.

FISCHER, K. (1961). Untersuchungen zur Sonnenkompassor ientierung und Laufaktivität von Smaragdeidechsen (Lacerta viridis Laur.) Z. Tierpsychol. 18, 450-470.

FISCHER, K. (1970). Undersuchungen zur Jahresperiodik der Fortpflanzung bei männlichen Ruineneidechsen (Lacerta sicula campestris Betta) III. Spontanos Einsetzen und Ausklingen der Gonadenaktivät; ein Beitrag zur Frage der Circannualen Periodik. Z. vergl. Physiol. 66, 273-293.

FISHER, M.J., WILSON, M.F. & WEBER, K.C. (1970). Determination of alveolar surface area and tension from in situ pressure-volume data. Respir. Physiol. 10, 159-171.

FORREST, J.B. (1969). Measurement of the volume shrinkage of lung tissue due to rapid freezing followed by freeze substitution. J. Physiol. 202, 108-109.

FORREST, J.B. (1970a). The effects of changes in lung volume on the size and shape of alveoli. J. Physiol. 210, 533-548.

FORREST, J.B. (1970b). The effect of hyperventilation on the size and shape of alveoli. Br. J. Anaesth. 42, 810-817.

FORREST, J.B. (1972). The effect of hyperventilation on pulmonary surface activity. Br. J. Anaesth. 44, 313-320.

FORREST, J.B. (1974). Alveolar dimensions following normal and increased ventilation with normocapnia. Respir. Physiol. 20, 51-67.

FOXON, G.E.H., GRIFFITH, J. & PRICE, M. (1956). The mode of action of the heart of the green lizard, Lacerta viridis. Proc. zool. Soc. Lond. 126, 145-157.

FRANCIS, C. & BROOKS, G.R. (1970). Oxygen consumption, rate of heart beat and ventilatory rate in parietalectomized lizards. Comp. Biochem. Physiol. 35, 463-469.

FRASCA, J.M. & PARKS, V.R. (1965). A routine technique for double-staining ultrathin sections using uranyl and lead salts. J. Cell Biol. 25, 157-161.

FRY, F.E.J. (1947). Effect of the environment on animal activity. Ontario Fish Res. Lab. Publ. No. 68, pp.1-62.

FRY, F.E.J. (1957). The Aquatic Respiration of Fish. In: Physiology of Fishes. Vol. 1 (ed. M.E. Brown). London and New York, Academic Press. pp. 1-63.

GALVÃO, P.E., TARASENTCHI, J. & GUERTZENSTEIN, P. (1965). Heat production of tropical snakes in relation to body weight and body surface. Am. J. Physiol. 209, 501-506.

GANS, C. (1970). Strategy and sequence in the evolution of the external gas exchangers of ectothermal vertebrates. Forma et Functio 3, 61-104.

GANS, C. & HUGHES, G.M. (1967). The mechanism of lung ventilation in the tortoise Testudo graeca Linné. J. exp. Biol. 47, 1-20.

GAUNT, A.S. & GANS, C. (1969). Mechanics of respiration in the snapping turtle, Chelydra serpentina (Linné). J. Morph. 128, 195-228.

GAYMER, R. (1971). Comparative studies on the Caecilian amphibian, Hypogeophis rostratus. Ph.D. Thesis, Bristol.

GEELHAAR, A. & WEIBEL, E.R. (1971). Morphometric estimation of pulmonary diffusion capacity. III. The effect of increased oxygen consumption in Japanese waltzing mice. Respir. Physiol. 11, 354-366.

GELINEO, S. & GELINEO, A. (1955). Les échanges respiratoires des lézards noirs de Dalamatie adaptés à différentes temperatures. C.r. Séanc. Soc. Biol. 149, 387-389.

GEORGE, J.C. & SHAH, R.V. (1956). Comparative morphology of the lung in snakes with remarks on the evolution of lung in Reptiles. J. Anim. Morph. Physiol. 3, 1-7.

GEORGE, J.C. & SHAH, R.V. (1965). Evolution of air sacs in Sauropsida. J. Anim. Morph. Physiol. 12, 255-263.

GERTZ, K.H. & LOESCHCKE, H.H. (1954). Bestimmung der Diffusions-Koeffizienten von H_2, O_2, N_2 und He in Wasser und Blutserum bei konstant gehaltener Konvektion. Z. Naturf. 9, 1-9.

GIL, J. (1972). Effect of tricomplex fixation on lung tissue. J. Ultrastruct. Res. 40, 122-131.

GIL, J. & REISS, O.K. (1973). Isolation and characterisation of lamellar bodies and tubular myelin from rat lung homogenates. J. Cell Biol. 58, 152-171.

GIL, J. & WEIBEL, E.R. (1969/70). Improvements in demonstration of lining layer of lung alveoli by electron microscopy. Respir. Physiol. 8, 13-36.

GIL, J. & WEIBEL, E.R. (1971). An improved apparatus for perfusion fixation with automatic pressure control. J. Microsc. 94, 241-244.

GIL, J. & WEIBEL, E.R. (1972). Morphological study of pressure-volume hysteresis in rat lungs fixed by vascular perfusion. Respir. Physiol. 15, 190-213.

GIST, D.H. (1972). The effects of starvation and refeeding on carbohydrate and lipid reserves of Anolis carolinensis. Comp. Biochem. Physiol. 43A, 771-780.

GLAISTER, D.H., SCHROTER, R.C., SUDLOW, M.F. & MILIC-EMILI, J. (1973). Bulk elastic properties of excised lungs and the effect of a transpulmonary pressure gradient. Respir. Physiol. 17, 347-364.

GLASS, N.R. (1967). A technique for fitting nonlinear models to biological data. Ecology, 48, 1010-1013.

GLAZIER, J.B., HUGHES, J.M.B., MALONEY, J.E. & WEST, J.B. (1967). Vertical gradient of alveolar size in lungs of dogs frozen intact. J. appl. Physiol. 23, 694-705.

GOODRICH, E.S. (1958). Studies on the structure and development of vertebrates. Dover Publications Inc. N.Y. Constable & Co. Ltd., London.

GÖPPERT, E. (1937). Atmungssystem (organe der Luftatmung). I. Kehlkopf und Trachea. In: Handbuch der Vergleichenden Anatomie der Wirbeltiere. Vol. 3, (ed. L. Bolk, E. Göppert, E. Kallius, W. Lubusch). Berlin. pp. 797-866.

GRÄPER, L. (1931). Zur vergleichenden Anatomie der Schildkrötenlungen. Gegenbaurs Morph. Jb. 68, 325-374.

GREENWALD, O.E. (1971). The effect of temperature on oxygen consumption and heart rate in the Sonora Gopher snake Pituophis catenifer affinis Hallowell. Copeia, 98-106.

GRIGG, G.C. (1965). Studies on the Queensland Lungfish Neoceratodus forsteri (Kreft). 1. Anatomy, Histology, and Functioning of the Lung. Aust. J. Zool. 13, 243-253.

GROTE, J. (1967). Die Sauerstoffdiffusionskonstanten im Lungengewebe und Wasser und ihre Temperaturabhängigkeit. Pflügers Arch. ges. Physiol. 295, 245-254.

GUIBÉ, J. (1970). L'appareil respiratoire. In: Traité de Zoologie. Vol. XIV. Reptilia, II, (ed. P.P. Grassé). Paris, Masson et Cie. pp. 499-520.

GUYTON, A.C. (1947a). Measurement of the respiratory volumes of laboratory animals. Am. J. Physiol. 150, 70-77.

GUYTON, A.C. (1947b). Analysis of respiratory patterns in laboratory animals. Am. J. Physiol. 150, 78-83.

HEMMINGSEN, A.M. (1960). Energy metabolism as related to body size and respiratory surfaces, and its evolution. Reports of Steno Memorial Hospital and the Nordisk Insulinlaboratorium. Vol. IX. Copenhagen.

HEY, E.N., LLOYD, B.B., CUNNINGHAM, D.J.C., JUKES, M.G.M. & BOLTON, D.P.G. (1966). Effects of various respiratory stimuli on the depth and frequency of breathing in man. Respir. Physiol. 1, 193-205.

HILDEBRANDT, J. (1969). Comparison of mathematical models for cat lung and viscoelastic balloon derived by Laplace transform methods from pressure-volume data. Bull. Math. Biophys. 31, 651-667.

HILLS, B.A. (1971). Geometric irreversibility and compliance hysteresis in the lung. Respir. Physiol. 13, 50-61.

HILLS, B.A. & HUGHES, G.M. (1970). A dimensional analysis of O_2 transfer in the fish gill. Respir. Physiol. 9, 126-140.

HILL, R.W. (1972). Determination of oxygen consumption by use of the paramagnetic oxygen analyser. J. appl. Physiol. 33, 261-263.

HOFFMANN, K. (1955). Aktivitätsregistrierungen bei frisch geschlüpften Eidechsen. Z. vergl. Physiol. 37, 253-262.

HOFFMANN, K. (1959). Die Aktivitätsperiodik von im 18- und 36- Stunden-tag erbrüteten Eidechsen. Z. vergl. Physiol. 42, 422-432.

HOFFMANN, K. (1960). Versuche zur Analyse der Tagesperiodik - I Der Einfluss der Lichtintensität. Z. vergl. Physiol. 43, 544-566.

HOFFMANN, K. (1969). Zum Einfluss der Zeitgeberstärke auf die Phasenlarge der synchronisierten circadianen Periodik. Z. vergl. Physiol. 62, 93-110.

HUDSON, J.W. & BERTRAM, F.W. (1966). Physiological responses to temperature in the ground skink, Lygosoma laterale. Physiol. Zoöl. 39, 21-29.

HUGGINS, S.E., DEAVERS, S., HOFF, H.E. & NAIFEH, K.H. (1970). The role of the vagus in heart and respiratory rates of the alligator. Cardiovascular Research Center Bulletin 8, 148-155.

HUGGINS, S.E., HOFF, H.E. & PEÑA, R.V. (1969). Heart and respiratory rates in crocodilian reptiles under conditions of minimal stimulation. Physiol. Zoöl. 42, 320-333.

HUGGINS, S.E., HOFF, H.E. & VALENTINUZZI, M.E. (1971). O_2 consumption of small caimans under basal conditions. Physiol. Zoöl. 44, 40-47.

HUGGINS, S.E., PARSONS, L.C. & PEÑA, L.V. (1968). Further study of the spontaneous electrical activity of the brain of Caiman sclerops: olfactory lobes. Physiol. Zoöl. 41, 371-383.

HUGGINS, S.E., VALENTINUZZI, M.E. & HOFF, H.E. (1971). Relationship of oxygen consumption to heart rate and respiratory parameters in Caiman sclerops. Physiol. Zoöl. 44, 98-111.

HUGHES, G.M. (1966). The dimensions of fish gills in relation to their function. J. exp. Biol. 45, 177-195.

HUGHES, G.M. (1967). Evolution between air and water. In: Development of the lung. A Ciba Foundation Symposium (ed. A.V. de Reuck & R. Porter). London, Churchill. pp. 64-84.

HUGHES, G.M. (1970a). Ultrastructure of the air-breathing organs of some lower vertebrates. 7th Congrès Internat. de Microscopie Electronique, Grenoble, 3, 599-600.

HUGHES, G.M. (1970b). Morphometric measurements on the gills of fishes in relation to their respiratory function. Folia Morph. 18, 78-95.

HUGHES, G.M. (1972). Morphometrics of fish gills. Respir. Physiol. 14, 1-25.

HUGHES, G.M. (1973). Ultrastructure of the lung of Neoceratodus and Lepidosiren in relation to the lung of other vertebrates. Folia Morph. 21, 151-161.

HUGHES, G.M., GAYMER, R., MOORE, M. & WOAKES, A.J. (1971). Respiratory exchange and body size in the Aldabra giant tortoise. J. exp. Biol. 55, 651-665.

HUGHES, G.M., RYAN, J.W. & RYAN, U. (1973). Freeze-fractured lamellate bodies of Protopterus lung: a comparative study. J. Physiol. 236, 15-16P.

HUGHES, G.M., SINGH, B.R., GUHA, G., DUBE, S.C. & MUNSHI, J.S. (1974). Respiratory surface area of an air-breathing siluroid fish Saccobranchus (= Heternopneustes) fossilis in relation to body size. J. Zool. Lond. 172, 215-232.

HUGHES, G.M. & WEIBEL, E.R. (1976). Morphometry of Fish Lungs. In: Respiration of Amphibious Vertebrates (ed. G.M. Hughes). London and New York, Academic Press.

HUNG, K. HERTWECK, M.S., HARDY, J.D. & LOOSLI, C.G. (1973). Ultrastructure of nerves and associated cells in bronchiolar epithelium of mouse lung. J. Ultrastruct. Res. 43, 426-437.

HUNG, K. & LOOSLI, C.G. (1974). Bronchiolar neuro-epithelial bodies in the neonatal mouse lungs. Am. J. Anat. 140, 191-200.

HUTCHISON, V.H., DOWLING, H.G. & VINEGAR, A. (1966). Thermoregulation in a brooding female Indian python, Python molurus bivittatus. Science, N.Y., 151, 694-696.

HUTCHISON, V.H., WHITFORD, W.G. & KOHL, M.A. (1968). Relation of body size and surface area to gas exchange in anurans. Physiol. Zoöl. 41, 65-85.

HUTTON, K.E., BOYER D.R., WILLIAMS, J.C. & CAMPBELL, P.M. (1960). Effects of temperature and body size upon heart rate and O_2 consumption in turtles. J. cell. comp. Physiol. 55, 87-93.

ICI (1972). Silicones. Two-pack 'Silcoset' R.T.V. rubbers. Technical Information, December 1972.

JACKSON, D.C. (1971). Effect of temperature on ventilation in the turtle, Pseudemys scripta elegans. Respir. Physiol. 12, 131-140.

JACKSON, O.F. (1970). Snake Anaesthesia. Br. J. Herpet. 4, 172-175.

JOHANSEN, K. (1970). Air breathing in Fishes. In: Fish Physiology. Vol. 4 (ed. W.S. Hoar & D.J. Randall). London and New York, Acamedic Press. pp. 361-411.

JOLICOEUR, P. & HEUSNER, A.A. (1971). The allometry equation in the analysis of the standard oxygen consumption and body weight of the white rat. Biometrics 27, 841-855.

KAPANCI, Y., WEIBEL, E.R., KAPLAN, H.P. & ROBINSON, F.R. (1969). Pathogenesis and reversibility of the pulmonary lesions of oxygen toxicity in monkeys. II Ultrastructural and morphometric studies. Lab. Invest. 20, 101-118.

KAPLAN, H.M. (1969). Anesthesia in amphibians and reptiles. Fedn Proc. 28, 1541-1546.

KARLSTROM, E.L. & COOK, S.F. (1955). Notes on snake anesthesia. Copeia 57-58.

KAYSER, C. (1951). La loi des surfaces. Revue Sci. 89, 267-278.

KAYSER, C. & HEUSNER, A. (1964). Étude comparative du métabolisme énergétique dans la série animale. J. Physiol. (Paris) 56, 489-524.

KAYSER, C. & MARX, C. (1951). Le rhythme nycthéméral de l'activité et la mémoire du temps chez le lézard (Lacerta agilis et Lacerta muralis). XX Congr. Int. Phil. Sci. Paris, 1949, 6, Biol. 96-103.

KELÉNYI, G. & NÉMETH, A. (1969). Comparative histochemistry and electron microscopy of the eosinophil leucocytes of vertebrates. I A study of avian, reptilian, amphibian and fish leucocytes. Acta Biol. Acad. Sci. Lung, 20, 405-422.

KIKKAWA, Y., MOTOYAMA, E.K. & GLUCK, L. (1968). Study of the lungs of fetal and newborn rabbits: morphological, biochemical and surface-physical development. Am. J. Path. 52, 177-210.

KILBURN, K.H. (1969). Alveolar clearance of particles. A bullfrog lung model. Archs Environ. Health 18, 556-563.

KING, A.S. & MOLONY, V. (1971). The Anatomy of Respiration. In: Physiology and Biochemistry of the Domestic Fowl. Vol. 1 (ed. D.J. Bell & B.M. Freeman). London and New York, Academic Press. pp. 93-169.

KING, J.R. & FARNER, D.S. (1961). Energy Metabolism, Thermoregulation and Body Temperature. In: Biology and Comparative Physiology of Birds. Vol. 2 (ed. A.J. Marshall). London and New York, Academic Press. pp. 215-288.

KING, T.K.C. (1966). Mechanical properties of the lungs in the rat. J. appl. Physiol. 21, 259-264.

KING, T.K.C. (1966). Measurement of functional residual capacity in the rat. J. appl. Physiol. 21, 233-236.

KIRSCHFIELD, U. (1970). Eine Bauplananalyse der Warenlunge. Zool. Beitr. 16, 401-440.

KLAUFFMAN, S.L., BURRI, P.H. & WEIBEL, E.R. (1974). The postnatal growth of the rat lung. II Autoradiography. Anat. Rec. 180, 63-76.

KLAUS, M., REISS, O.K., TOOLEY, W.H., PIEL, C. & CLEMENTS, J.A. (1962). Alveolar epithelial cell mitochondria as source of the surface-active lung lining. Science, N.Y. 137, 750-751.

KLEIBER, M. (1947). Body size and metabolic rate. Physiol. Rev. 27, 511-541.

KLEIN, F. (1896). Ueber das Verhältnis zwischen Druck und Füllung bei Hohlorganen (Lungen und Herz) und dessen Ableitung aus der Längsdehnung. Z. Biol. 33, 219-263.

KLI KA, E. & JANOUT, V. (1967). The visualization of the lining film of the lung alveolus with the use of Maillet's modification of Champy's method. Folia Morph. 15, 318-329.

KLI KA, E. & LELEK, A. (1967). A contribution to the study of the lungs of Protopterus annecteus and Polypterus senegalesis. Folia Morph. 15, 168-175.

KLINGELE, T.G. & STAUB, N.C. (1970). Alveolar shape changes with volume in isolated, air-filled lobes of cat lung. J. appl. Physiol. 28, 411-414.

KRAHL, V.E. (1964). Anatomy of the Mammalian Lung. In: Handbook of Physiology. Section 3. Respiration. Vol. I (ed. W.O. Fenn & H. Rahn). Washington, D.C., Am. Physiol. Soc. pp. 213-284.

KRAMER, G. (1934). Der Ruheumsatz von Eidechsen und seine quantitative Beziehung zur Individuengrösse. Z. vergl. Physiol. 20, 600-616.

KREHL, L. & SOETBEER, F. (1899). Untersuchungen über die Wärmeokonomie der poikilothermen Wirbelthiere. Pflügers Arch. ges. Physiol. 77, 611-638.

KROGH, A. (1904). On the cutaneous and pulmonary respiration of the frog. Skand. Arch. Physiol. 15, 328-419.

KUHN, C. III & FINKE, E.H. (1972). The topography of the pulmonary alveolus: scanning electron microscopy using different fixations. J. Ultrastruct. Res. 38, 161-173.

LASIEWSKI, R.C. & CALDER, W.A. Jr. (1971). A preliminary allometric analysis of respiratory variables in resting birds. Respir. Physiol. 11, 152-166.

LASIEWSKI, R.C. & DAWSON, W.R. (1967). A re-examination of the relation between standard metabolic rate and body weight in birds. Condor 69, 13-23.

LAUWERYNS, J.M. & BOUSSAUW, L. (1969). The ultrastructure of pulmonary lymphatic capillaries of newborn rabbits and human infants. Lymphology 2, 108-129.

LICHT, P., HOYER, H.E. & OORDT VAN, P.G.W.J. (1969). Influence of photoperiod and temperature on testicular recrudescence and body growth in the lizards, Lacerta sicula and Lacerta muralis. J. Zool. Lond. 157, 469-501.

LIM, T.P.K. & LUFT, U.C. (1959). Alterations in lung compliance and functional residual capacity with posture. J. appl. Physiol. 14, 164-166.

LOOSLI, C.G. & BAKER, R.F. (1962). The human lung: microscopic structure and diffusion. In: Ciba Foundation Symposium. Pulmonary Structure and Function (ed. A.V.S. de Reuck & M. O'Connor). J.A. Churchill Ltd. pp. 194-204.

LUMSDEN, T. (1924). Chelonian respiration (tortoise). J. Physiol. 58, 259-266.

MACKLIN, C.C. (1950). Alveoli of mammalian lung. Anatomical study with clinical correlation. Proc. Inst. Med. Chic. 18, 78-95.

MACKLIN, C.C. (1954). The pulmonary alveolar mucoid film and the pneumocytes. Lancet, 266, 1099-1104.

MAGNUSSEN, H., PERRY, S.F., WILLMER, H. & PIIPER, J. (1974). Transpleural diffusion of inert gases in excised lung lobes of the dog. Respir. Physiol. 20, 1-15.

MARCUS, H. (1927). Lungenstudien. Morph. Jb. 58, 100-121.

MARCUS, H. (1937). Lungen. In: Handbuch der Vergleichenden Anatomie der Wirbeltiere. Vol. 3 (ed. L. Bolk, E. Göppert, E. Kallius & W. Lubosch). Berlin. pp. 909-988.

MARSHALL, R. & WIDDICOMBE, J.G. (1961). Stress relaxation of the human lung. Clin. Sci. 20, 19-31.

McDONALD, H.S. (1959). Respiratory functions of the ophidian air sac. Herpetologica 193-198.

MEAD, J. (1961). Mechanical properties of lungs. Physiol. Rev. 41, 281-330.

MEYRICK, B. & REID, L. (1968). The alveolar brush cell in rat lung - a third pneumocyte. J. Ultrastruct. Res. 23, 71-80.

MEYRICK, B. & REID, L. (1973). Electron microscopic aspects of surfactant secretion. Proc. R. Soc. Med. 66, 386-387.

MILANI, A. (1894). Beiträge zur kenntniss der reptilienlunge. Zool. Jb. (Anat.) 7, 545-592.

MILANI, A. (1897). Beiträge zur kenntniss der reptilienlunge. Zool. Jb. (Anat.) 10, 93-156.

MILLER, D.A. & BONDURANT, S. (1961). Surface characteristics of vertebrate lung extracts. J. appl. Physiol. 16, 1075-1077.

MILLER, W.S. (1893). The structure of the lung. J. Morph. 8, 165-188.

MOBERLY, W.R. (1968a). The metabolic responses of the common iguana, Iguana iguana, to activity under restraint. Comp. Biochem. Physiol. 27, 1-20.

MOBERLY, W.R. (1968b). The metabolic responses of the common iguana, Iguana iguana, to walking and diving. Comp. Biochem. Physiol. 27, 21-32.

MOCHIZUKI, M. (1966). Study on the oxygenation velocity of the human red cell. Jap. J. Physiol. 16, 635-648.

MORGAN, M. & TOVELL, P.W.A. (1973). The structure of the gill of the trout, Salmo gaiodneri (Richardson). Z. Zellforsch. mikrosk. Anat. 142, 147-162.

MOORE, J.A. (1964). Physiology of the Amphibia. Ch. 3. Blood and Respiration. (G.E.U. Foxon). Ch. 4. Physiology of the Amphibian Heart. (A.J. Brady). Academic Press, London and New York.

MOUNT, L.E. & STEPHENS, D.B. (1970). The relation between body size and maximum and minimum metabolic rates in the newborn pig. J. Physiol. 207, 417-427.

MURATA, F. & SPICER, S.S. (1974). Ultrastructural comparison of basophilic leukocytes and mast cells in the guinea pig. Am. J. Anat. 139, 335-352.

MURRISH, D.E. & SCHMIDT-NIELSEN, K. (1970). Exhaled air temperatures and water conservation in lizards. Respir. Physiol. 10, 151-158.

MURRISH, D.E. & VANCE, V.J. (1968). Physiological responses to temperature acclimation in the lizard, Uta mearnsi. Comp. Biochem. Physiol. 27, 329-337.

NAIFEH, K.H., HUGGINS, S.E. & HOFF, H.E. (1970). The nature of the ventilatory period in crocodilian respiration. Respir. Physiol. 10, 338-348.

NAIFEH, K.H., HUGGINS, S.E. & HOFF, H.E. (1971a). The nature of the non-ventilatory period in crocodilian respiration. Respir. Physiol. 11, 178-185.

NAIFEH, K.H., HUGGINS, S.E. & HOFF, H.E. (1971b). Study of the control of crocodilian respiration by anesthetic dissection. Respir. Physiol. 12, 251-260.

NAIFEH, K.H., HUGGINS, S.E. & HOFF, H.E. (1971c). Effects of brain stem section on respiratory patterns of crocodilian reptiles. Respir. Physiol. 13, 186-197.

NAIFEH, K.H., HUGGINS, S.E., HOFF, H.E., HUGG, T.W. & NORTON, R.E. (1970). Respiratory patterns in crocodilian reptiles. Respir. Physiol. 9, 31-42.

NEERGAARD, K. von (1929). Neue Auffassungen über einem Grundbegriff der Atemmechanik. Die Retraktionskraft der Lunge, abhängig von der Oberflächenspannung in den Alveolen. Z. ges. exp. Med. 66, 373-394.

NIDEN, A.H. (1967). Bronchiolar and large alveolar cell in pulmonary phospholipid metabolism. Science, N.Y. 158, 1323-1324.

NIELSEN, B. (1961). On the regulation of respiration in reptiles. I The effect of temperature and CO_2 on the respiration of lizards (Lacerta). J. exp. Biol. 38, 301-314.

NIELSEN, B. (1962). On the regulation of respiration in reptiles. II The effect of hypoxia with and without moderate hypercapnia on the respiration and metabolism of lizards. J. exp. Biol. 39, 107-117.

OELRICH, T.M. (1956). The Anatomy of the Head of Ctenosaura pectinata, (Iguanidae). Museum of Zoology, Univ. of Michigan, No. 94.

OKADA, Y., ISHIKO, S., DAIDO, S., IKEDA, S., GENKA, K. & KITANO, M. (1965). Comparative morphology of the lung with special reference to the alveolar epithelial cells. III Lung of bird. Acta tuberc. Jpn. 14, 35-41.

OKADA, Y., ISHIKO, S., DAIDO, S., KIM, J. & IKEDA, S. (1962a). Comparative morphology of the lung with special reference to the alveolar lining cells. I Lung of Amphibia. Acta tuberc. Jpn. 11, 63-72.

OKADA, Y., ISHIKO, S., DAIDO, S., KIM, J. & IKEDA, S. (1962b). Comparative morphology of the lung with special reference to the alveolar lining cells. II Lung of reptilia. Acta tuberc. Jpn. 12, 1-10.

OTIS, A.B., McKERROW, C.B., BARTLETT, R.A., MEAD, J., McILROY, M.B., SELVERSTONE, N.J. & RADFORD, E.P. Jr. (1956). Mechanical factors in distribution of pulmonary ventilation. J. appl. Physiol. 8, 427-443.

PARSONS, T.S. (1970). The Nose and Jacobson's Organ. (1970). In: Biology of the Reptilia. Vol. 2 (ed. C. Gans & T.S. Parsons). London and New York, Academic Press. pp. 99-191.

PASQUIS, P. & GANOCHAUD, C. (1964). Tapis roulant pour petits animaux (souris) permettant la mesure des échanges gazeux par confinement. J. Physiol. (Paris) 56, 470.

PASQUIS, P., LACAISSE, A. & DEJOURS, P. (1970). Maximal O_2 uptake in 4 species of small mammals. Respir. Physiol. 9, 298-309.

PATT, D.I. & PATT, G.R. (1969). Comparative Vertebrate Histology. New York, Evanston, London. Harper & Row.

PATTLE, R.E. (1958). Properties, function, and origin of the alveolar lining layer. Proc. R. Soc. B. 148, 217-240.

PATTLE, R.E. (1965). Surface lining of lung alveoli. Physiol. Rev. 45, 48-79.

PATTLE, R.E. (1966). Surface Tension and the Lining of the Lung Alveoli. In: Advances in Respiratory Physiology (ed. C.G. Caro). London, Edward Arnold Ltd. pp. 83-105.

PATTLE, R.E. (1969). The Development of the Foetal Lung. In: Ciba Foundation Symposium on Foetal Autonomy (ed. G.E.W. Wolstenholme & M. O'Connor). pp. 132-142.

PATTLE, R.E. (1973). Inter-species differences in surface properties of lungs. Proc. R. Soc. Med. 66, 385-386.

PATTLE, R.E. & HOPKINSON, D.A. (1963). Lung lining in bird, reptile and amphibia. Nature, Lond. 200, 894.

PATTLE, R.E., SCHOCK, C., DIRNHUBER, P. & CREASEY, J.M. (1974). Lung surfactant and organelles after an exposure to dibenzoxazepine (CR). Br. J. exp. Path. 55, 213-220.

PEARSE, A.G.E. (1968). Histochemistry. Theoretical and Applied. Vol. 1, 3rd edition. J.A. Churchill Ltd.

PERRY, S.F. (1971). Alcian blue as an EN BLOC stain for turtle lung goblet cells with and without prior periodate oxidation. Stain Technol. 46, 191-194.

PERRY, S.F. (1972). The lungs of the red-eared turtle, Chrysemys (Pseudemys) scripta elegans as a gas exchange organ: a histological and quantitative morphological study. Ph.D. Thesis Boston University Graduate School.

PERRY, S.F., ALBRIGHT, J.T. & PATT, D.I. (1970). On anatomy and histology of lungs of red-eared turtle. Anat. Rec. 166, 361.

PETRICK, P. & COLLET, A.J. (1970). Fine structure of the secretory activity of the Clara bronchiolar cells in the mouse. 7th Congrès Internat. de Microscopie Electronique, Grenoble, 3, 591-592.

PIIPER, J. (1969). Apparant increase of the O_2 diffusing capacity with increased O_2 uptake in inhomogeneous lungs: theory. Respir. Physiol. 6, 209-218.

POUGH, F.H. (1969). Physiological aspects of the burrowing of sand lizards (Uma, Iguanidae) and other lizards. Comp. Biochem. Physiol. 31, 869-884.

PRATT, C.W. McE. (1948). The morphology of the ethmoidal region of Sphenodon and lizards. Proc. zool. Soc. Lond. 118, 171-201.

PRIETO, A.A. & WHITFORD, W.G. (1971). Physiological response to temperature in the horned lizards, Phyranosoma cornutum and Phyranosoma douglassii. Copeia 498-504.

PROSKE, U. & VAUGHAN, P. (1968). Histological and electrophysiological investigation of lizard skeletal muscle. J. Physiol. 199, 495-509.

PROSSER, C.L. & BROWN, F.A. Jr. (1961). Comparative Animal Physiology. 2nd edition. W.B. Saunders.

RADFORD, E.P. Jr. (1957). Recent studies of mechanical properties of mammalian lungs. In: Tissue Elasticity (ed. J.W. Remmington). pp. 177-190.

RADFORD, E.P. Jr. (1964). Static Mechanical Properties of Mammalian Lungs. In: Handbook of Physiology. Section 3. Respiration. Vol. I (ed. W.O. Fenn & H. Rahn). Washington D.C., Am. Physiol. Soc. pp. 429-449.

RAHN, H., OTIS, A.B., CHADWICK, L.E. & FENN, W.O. (1946). The pressure-volume diagram of the thorax and lung. Am. J. Physiol. 146, 161-178.

RAHN, H., RAHN, K.B., HOWELL, B.J., GANS, G. & TENNEY, S.M. (1971). Air breathing of the Garfish, (Lepisosteus osseus). Respir. Physiol. 11, 285-307.

REICHENBACH-KLINKE, H. & ELKAN, E. (1965). The Principle Diseases of Lower Vertebrates. London and New York, Academic Press.

REID, L. (1967). The Embryology of the Lung. In: Development of the Lung. A Ciba Foundation Symposium, (ed. A.V. de Reuck & R. Porter). London, Churchill. pp. 109-130.

REYNOLDS, E.S. (1963). The use of lead citrate at high pH as an electron-opaque stain in electron microscopy. J. Cell biol. 17, 208-212.

RHODIN, J.A.G. (1963). An Atlas of Ultrastructure. Philadelphia & London, W.B. Saunders.

RHODIN, J.A.G. (1974). Histology. A Text and Atlas. Oxford University Press.

ROBERTS, L.A. (1968). Oxygen consumption in the lizard, Uta stansburiana. Ecology, 49, 809-819.

ROGERS, D.C. (1967). The structure of the carotid bifurcation in the lizards, Tiliqua occipitalis and Trachysaurus rugosus. J. Morph. 122, 115-130.

RUBNER, M. (1883). Ueber den Einfluss der Körpergrösse auf Stoff - und Kraftwechsel. Z. Biol. 19, 535-562.

RYBICKA, K., DALY, B.D.T., MIGLIORE, J.J. & NORMAN, J.C. (1974). Intravascular macrophages in normal calf lung. An electron microscopic study. Am. J. Anat. 139, 353-368.

SAALFIELD, E. von (1934). Die mechanik der atmung bei Uromastix (Lacertilia). Pflügers Arch. ges. Physiol. 233, 431-448.

SAINT-GIRONS, M.C. (1970). Morphology of the Circulating Blood Cells. In: Biology of the Reptilia. Vol. 3 (ed. C. Gans). pp. 73-91.

SALT, G.W. (1943). Lungs and inflation mechanism of Sauromalus obesus. Copeia 193.

SCARPELLI, E.M. (1968). The surfactant system of the lung. Philadelphia, Lea & Febiger.

SCHEID, P. & PIIPER, J. (1972). Cross-current gas exchange in avian lungs: effects of reversed parabronchial air flow in ducks. Respir. Physiol. 16, 304-312.

SCHERLE, W.F. (1970). A simple method for volumetry of organs in quantitative stereology. Mikroskopie 26, 57-60.

SCHULTETUS, R.R. & CRAWFORD, C.C. (1969). Cutaneous gas exchange in Sauromalus obesus and Tupinambis nigropunctatus. Am. Zool. 9, 1099.

SCHMIDT-NIELSEN, K. (1970). Energy metabolism, body size, and problems of scaling. Fedn Proc. 29, 1524-1532.

SCHMIDT-NIELSEN, K. (1972). Locomotion: energetic cost of swimming, flying and running. Science, N.Y. 177, 222-228.

SCHMIDT-NIELSEN, K., HAINSWORTH, F.R. & MURRISH, D.E. (1970). Counter-current heat exchange in the respiratory passage: effect on water and heat balance. Respir. Physiol. 9, 263-276.

SCHMIDT-NIELSEN, K. & LARIMER, J.L. (1958). Oxygen dissociation curve of mammalian blood in relation to body size. Am. J. Physiol. 195, 424-428.

SCHOCK, C., PATTLE, R.E. & CREASEY, J.M. (1973). Methods for electron microscopy of the lamellated osmiophilic bodies of the lung. J. Microsc. 97, 321-330.

SEGREM, N.P. & HART, J.S. (1967). Oxygen supply and performance in Peromyscus: comparison of exercise with cold exposure. Can. J. Physiol. Pharm. 45, 543-549.

SERFATY, A. & PEYRAUD, C. (1960). La mécanique respiratoire chez les reptiles et sa régulation. Bull. Soc. Hist. Nat. Toulouse. 95, 145-170.

SEVERINGHAUS, J.W. (1960). Methods of measurement of blood and gas carbon dioxide during anesthesia. Anesthesiology 22, 429-432.

SIDKY, Y.A. (1967). The carotid sinus in lizards with an anatomical survey of the ventral neck region. J. Morph. 121, 311-321.

SIEGWART, B., GEHR, P., GIL, J. & WEIBEL, E.R. (1971). Morphometric estimation of pulmonary diffusion capacity. IV The normal dog lung. Respir. Physiol. 13, 141-159.

SMITH, M.A. (1964). The British Amphibians and Reptiles. 3rd edition. London, Collins.

SNYDER, G.K. (1971). Adaptive value of a reduced respiratory metabolism in a lizard. A unique case. Respir. Physiol. 13, 90-101.

SOROKIN, S.P. (1967). A morphologic and cytochemical study of the great alveolar cell. J. Histochem. Cytochem. 14, 884-897.

SPELLS, K.E. (1968). Some physical considerations relevant to the dimensions of lung alveoli. Nature, Lond. 219, 64-66.

SPELLS, K.E. (1969/70). Comparative studies in lung mechanics based on a survey of literature data. Respir. Physiol. 8, 37-57.

STAHL, W.R. (1967). Scaling of respiratory variables in mammals. J. appl. Physiol. 22, 453-460.

STANDAERT, T. & JOHANSEN, K. (1974). Cutaneous gas exchange in snakes. J. comp. Physiol. 89, 313-320.

STAUB, N.C., BISHOP, J.M. & FORSTER, R.E. (1962). Importance of diffusion and chemical reaction rates in O_2 uptake in the lung. J. appl. Physiol. 17, 21-27.

STAUB, N.C. & STOREY, W.F. (1962). Relation between morphological and physiological events in lung studied by rapid freezing. J. appl. Physiol. 17, 381-390.

STEBBINS, R.C. (1948). Nasal structure in lizards with reference to olfaction and conditioning of inspired air. Am. J. Anat. 83, 183-222.

STEINSIEPE, K.F. & WEIBEL, E.R. (1970). Elektronenmikroskopische untersuchungen an spezifischen organellen von endothelzellen des frosches (Rana temporaria). Z. Zellforsch. mikrosk. Anat. 108, 105-126.

STORER, T.I., USINGER, R.L., STEBBINS, R.C. & NYBAKKEN, J.W. (1972). General Zoology. 5th edition. McGraw Hill.

STOREY, W. E. & STAUB, N.C.J. (1962). Ventilation of terminal air units. J. appl. Physiol. 17, 391-397.

SUBBA RAO, M.V. & RAJABAI, B.S. (1973). Rhythmic activity in ground dwelling agamid lizard, Sitana ponticeriana. Br. J. Herpet. 4, 328-332.

TAYLOR, C.R. (1973). Energy Cost of Animal Locomotion. In: Comparative Physiology (ed. L. Bolis & K. Schmidt-Nielsen). Amsterdam, North Holland Publishing Co. pp. 23-42.

TAYLOR, C.R., SCHMIDT-NIELSEN, K. & RAAB, J.L. (1970). Scaling of energetic cost of running to body size in mammals. Am. J. Physiol. 219, 1104-1107.

TEMPLETON, J.R. (1964). Cardiovascular responses during buccal and thoracic respiration in the lizard Sauromalus obesus. Comp. Biochem. Physiol. 11, 31-43.

TEMPLETON, J.R. (1970). Reptiles. In: Comparative Physiology of Thermoregulation. Vol. 1. Invertebrates and Non-Mammalian Vertebrates (ed. G.C. Whittow). London and New York, Academic Press. pp. 167-221.

TEMPLETON, J.R. & DAWSON, W.R. (1963). Respiration in the lizard Crotaphytus collaris. Physiol. Zoöl. 36, 104-121.

TENNEY, S.M. & BARTLETT, D. (1967). Comparative quantitative morphology of the mammalian lung: trachea. Respir. Physiol. 3, 130-135.

TENNEY, S.M., BARTLETT, D., FARBER, J.P. & REMMERS, J.E. (1974). Mechanics of the respiratory cycle in the green turtle (Chelonia mydas). Respir. Physiol. 22, 361-368.

TENNEY, S.M. & REMMERS, J.E. (1963). Comparative quantitative morphology of the mammalian lung: diffusing area. Nature, Lond. 197, 54-56.

TENNEY, S.M. & TENNEY, J.B. (1970). Quantitative morphology of cold-blooded lungs: Amphibia and Reptilia. Respir. Physiol. 9, 197-215.

TOMKEIEFF, S.I. (1945). Linear intercepts, areas and volumes. Nature, Lond. 155, 24.

TOYE, S.A. (1972). The locomotory activity of the rainbow lizard Agama agama (L.). Br. J. Herpet. 4, 252-257.

TUCKER, V.A. (1966). O_2 transport by the circulatory system of the green iguana (Iguana iguana) at different body temperatures. J. exp. Biol. 44, 77-92.

TUCKER, V.A. (1968). Respiratory exchange and evaporative water loss in the flying budgerigar. J. exp. Biol. 48, 67-87.

TUCKER, V.A. (1970). Energetic cost of locomotion in animals. Comp. Biochem. Physiol. 34, 841-846.

TURNEY, L.D. & HUTCHISON, V.H. (1974). Metabolic scope, oxygen debt and the diurnal oxygen consumption cycle of the leopard frog, Rana pipiens. Comp. Biochem. Physiol. 49A, 583-601.

UNDERWOOD, E.E. (1970). Quantitative Stereology. Reading. Mass. Addison, Wesley.

UNDERWOOD, G. (1967). A contribution to the classification of snakes. London, Brit. Mus (Nat. Hist.).

UNTERSEE, P., GIL, J. & WEIBEL, E.R. (1971). Visualization of extracellular lining layer of lung alveoli by freeze-etching. Respir. Physiol. 13, 171-185.

VINEGAR, A., HUTCHISON, V.H. & DOWLING, H.G. (1970). Metabolism, energetics and thermoregulation during brooding of snakes of the genus Python (Reptilia, Boidae). Zoologica, N.Y. 55, 19-48.

VOGEL, Zdenek (1963). Reptiles and Amphibians. Their Care and Behaviour. Translated and revised by G. Vevers.

WEIBEL, E.R. (1963). Morphometry of the Human Lung. Berlin, Spring-Verlag.

WEIBEL, E.R. (1967a). Postnatal Growth of the Lung and Pulmonary Gas-Exchange Capacity. In: Development of the Lung. A Ciba Foundation Symposium (ed. A.V. de Reuck & R. Porter). London, Churchill. pp. 139-155.

WEIBEL, E.R. (1967b). Morphometry and Lung Models. In: Quantitative Methods in Morphology (ed. E.R. Weibel & H. Elias). Berlin, Heidelberg, New York, Springer-Verlag. pp. 253-267.

WEIBEL, E.R. (1969a). The Ultrastructure of the Alveolar-Capillary Membrane or Barrier. In: The Pulmonary Circulation and Interstitial Space (ed. A.P. Fishman & H.H. Hecht). University of Chicago Press. pp. 9-27.

WEIBEL, E.R. (1969b). Stereological principles for morphometry in electron microscopic cytology. Int. Rev. Cytol. 26, 235-302.

WEIBEL, E.R. (1970/71). Morphometric estimation of pulmonary diffusion capacity. I Model and method. Respir. Physiol. 11, 54-75.

WEIBEL, E.R. (1971). The mystery of 'non-nucleated plates' of alveolar epithelium explained. Acta anat. 78, 425-443.

WEIBEL, E.R. (1972). Morphometric estimation of pulmonary diffusion capacity. V Comparative morphometry of alveolar lungs. Respir. Physiol. 14, 26-43.

WEIBEL, E.R. (1973). The structural basis of alveolo-capillary gas exchange. Physiol. Rev. 53, 419-495.

WEIBEL, E.R. & ELIAS, H. (1967). Quantitative Methods in Morphology. Berlin, Heidelberg, New York, Springer-Verlag.

WEIBEL, E.R. & GIL, J. (1968). Electron microscopic demonstration of an extracellular duplex lining layer of alveoli. Respir. Physiol. 4, 42-57.

WEIBEL, E.R., KISTLER, G.S. & SCHERLE, W.F. (1966). Practical stereological methods for morphometric cytology. J. Cell Biol. 30, 23-38.

WEIBEL, E.R., KISTLER, G.S. & TÖNDURY, G. (1966). A stereologic electron microscope study of 'tubular myelin figures' in alveolar fluids of rat lungs. Z. Zellforsch. mikrosk. Anat. 69, 418-427.

WEIBEL, E.R. & KNIGHT, B.W. (1964). A morphometric study on the thickness of the pulmonary air-blood barrier. J. Cell Biol. 21, 367-384.

WEIBEL, E.R. & PALADE, G.E. (1964). New cytoplasmic components in arterial endothelia. J. Cell Biol. 23, 101-112.

WEIBEL, E.R., UNTERSEE, P., GIL, J. & ZULAUF, M. (1973). Morphometric estimation of pulmonary diffusion capacity. VI Effect of varying positive pressure inflation of air spaces. Respir. Physiol. 18, 285-308.

WHITE, F.N. (1968). Functional anatomy of the heart of reptiles. Am. Zool. 8, 211-219.

WHITE, F.N. (1970). Central vascular shunts and their control in reptiles. Fedn Proc. 29, 1149-1153.

WHITFORD, W.G. & HUTCHISON, V.H. (1963). Cutaneous and pulmonary gas exchange in the spotted salamander, Ambystoma maculatum. Biol. Bull. mar. biol. Lab., Woods Hole, 124, 344-354.

WHITFORD, W.G. & HUTCHISON, V.H. (1967). Body size and metabolic rate in salamanders. Physiol. Zoöl. 40, 127-133.

WINBERG, G.G. (1956). Rate of metabolism and food requirements of fishes. Fish Res. Bd Can. Trans. Ser. 194, 253.

WILLEM, V. & BERTRAND, M. (1936). Le triphasisme respiratoire chez les lézards. Bull. Acad. r. Med. Belg. 12, 134-155.

WILSON, K.J. (1971). The relationships of activity, energy, metabolism, and body temperature in four species of lizards. Ph.D. Thesis, Monash University.

WOLF, S. (1933). Zur kenntnis von bau und funktion der Reptilienlungen. Zool. Jb. (Anat.) 57, 139-190.

WOOD, S.C. & MOBERLY, W.R. (1970). The influence of temperature on the respiratory properties of iguana blood. Respir. Physiol. 10, 20-29.

WUNDER, B.A. (1970). Energetics of running activity in merriam's chipmunk, Eutanias merriami. Comp. Biochem. Physiol. 33, 821-836.

YOSHIDA, F. & OHSHIMA, N. (1966). Diffusivity of oxygen in blood serum. J. appl. Physiol. 21, 915-919.

YOUNG, S.L., TIERNEY, D.F. & CLEMENTS, J.A. (1970). Mechanism of compliance change in excised rat lungs at low transpulmonary pressure. J. appl. Physiol. 29, 780-785.

YOUSEF, M.K., ROBERTSON, W.D., DILL, D.B. & JOHNSON, H.D. (1970). Energy expenditure of running kangaroo rats Dipodomeys merriami. Comp. Biochem. Physiol. 36, 387-393.

YOUSEF, M.K., ROBERTSON, W.D., DILL, D.B. & JOHNSON, H.D. (1973). Energetic cost of running in the antelope ground squirrel Ammospermophilius leucurus. Physiol. Zoöl. 46, 139-147.

ZAR, J.H. (1968). Calculation and miscalculation of the allometric equation as a model in biological data. Bioscience 18, 1118-1120.

ZEUTHEN, E. (1953). O_2 uptake as related to body size in organisms. Q. Rev. Biol. 28, 1-12.

* ULTSCH, G.R. (1973). A theoretical and experimental investigation of the relationships between metabolic rate, body size and oxygen exchange capacity. Respir. Physiol. 18, 143-160.

APPENDIX I

This appendix extends the description of methods and errors of open and closed circuit respirometry which were presented in Chapter 1 and 2. The small size of the lizards of this study make the examination of errors a very important consideration.

Properties of the analysers

The Beckman CO_2 analyser was calibrated according to the instruction manual for electrical and gas zero. Sensitivities and calibration gases of 0.5, 1.0 and 5.0% were used, linearity only being obtained between 0 and 1.0% CO_2. Calibration curves were constructed for higher CO_2 levels which caused proportionately less deflections. Most experiments were, however, conducted at 0.5 or 1.0% full scale deflection. Although the CO_2 analyser measures the number n of CO_2 molecules, at the levels of CO_2 recorded it was insensitive to pressure and temperature fluctuations. Stability of this analyser was exceptionally good, there being no drift even after 24 hours. The response time at 450 ml min^{-1} was 90% complete in 0.1 sec (Severinghaus, 1960).

The Servomex O_2 analyser also measures the number n of O_2 molecules per ml rather than % O_2, i.e. $n = \frac{PV}{RT}$ (the gas equation) and hence, because of the level of O_2 recorded, it was very pressure sensitive. By recording differentially, variations in barometric pressure and temperature during 24 hours were avoided in open circuits, since they affected reference and sample channels equally. Variations in humidity and flow characteristics of both reference or sample channels altered the O_2 base line. Hence the resistance of dried, calibration gases flowing in the sample circuit had to mimic that operating during lizard gas exchange measurements. The calibration points of Fig. 1.1, 1.3 and 1.7 were therefore critical and short circuits direct to the analyser could not be made.

The instruction manual for the O_2 analyser does not contain details for calibrating it. Its output was recorded at a Rikadenki gain setting of 10 mv for 1% f.s.d. Electrical and 100% N_2 zero were determined independently for both reference and sample channels and made coincident with pen recorder zero. This N_2 zero was performed at the maximum O_2 amplifier gain of 1% f.s.d. Then using an amplifier gain of 25% f.s.d. each channel was independently adjusted using the calibrator screws to read 20.95% on the pen recorder whilst sampling the same dried outside air. Finally switching to differential recording at 1% f.s.d. caused the Servomex output to be coincident with pen zero, i.e. no differential between identical reference and sample gases. It was often necessary to repeat these calibrations in order to obtain a null position on differential. The output of the O_2 analyser was linear being checked occasionally by gas mixtures between 17% and 20.95% O_2.

Stability of the O_2 analyser was very variable over 24 hours, sometimes drifting gradually or in steps. It was often possible to correct for these drifts but if not, the experiment was rejected. The response of the O_2 analyser is only 7 sec for 90% completion at 450 ml min^{-1} for a step O_2 change. It does not follow small % changes as accurately as the CO_2 analyser.

Characteristics of closed respirometry circuits

(a) Constant volume

(i) Closing the system caused a slight pressure build up because of trapped air and hence Po_2 was elevated. The smaller the respirometer, the greater the increase. At the same time, however, there was a drop equivalent to 0.12 to 0.16% O_2 irrespective of respirometer size which was a result of the negative side of the pump being connected to the O_2 analyser (see Fig. 1.1 and 1.2). The reverse would be seen if the opening/closing point of the system was placed between the O_2 analyser and the positive side of the pump. Tests with calibration gases showed that because of O_2 linearity, the new base line still represented 20.95% O_2. (It was technically easier to calibrate the instruments using open circulating systems).

Increasing the reference 'sucking' flow decreased reference Po_2, but caused differential Po_2 to increase. Increasing sample flow caused a greater pressure gradient across the sample channel and hence elevated sample and differential Po_2. Barometric fluctuations did not affect sample closed circuits but by its effect on open reference circuits, differential recordings were altered.

(ii) The temperature cycle every hour of a maximum of 27 to 29°C caused a pressure change of 5 mm Hg in the closed system, but since $n = \frac{PV}{RT}$, differential Po_2 remained constant.

(iii) Lacerta had a mean R of 0.82 causing V to decrease but since it was a constant volume system, n and hence P decreased. Calculation showed that there was a constant overestimation by 4.5% of $\dot{V}o_2$ in 30g lizards and 1.25% in 0.2g lizards, irrespective of the time for which the system remained sealed. Mean 'night' R was therefore recorded as low as 0.765.

(b) Constant pressure

Since it was very difficult to get completely air-tight connections which would not leak under slight pressure gradients, i.e. in the constant volume system, it was decided to have a constant bleed to maintain a constant pressure (Fig. 1.3) rather than have a slow leak through the joints. The position of this bleed on the positive side of the pump prevented unnecessary leakages inwards from suction. It had to be placed after the CO_2 pickup because of the large pressure drop across the micro-catheter cell.

(i) Closing the system trapped air but the slight pressure build up was lost instantly through the bleed. As with the constant volume system, sealing also caused a 0.12 to 0.16% O_2 drop (Fig. 1.1). Increasing the reference flow still increased differential Po_2 but increasing sample flow caused a reduction in sample and hence differential Po_2. This was because the bleed on the positive side of the O_2 analyser maintained it nearer atmospheric and therefore increasing sample flow increased the negative side

of the analyser. (The reverse would occur if the bleed was on the negative side). Barometric fluctuations, with the bleed present, no longer affected sample Po_2.

(ii) During one maximum temperature cycle, 2.3 ml, 3.75 ml and 5.28 ml of fresh air, according to increasing respirometer volume, were sucked in and then pushed out through the bleed. The effect of incoming fresh air was important but the loss of mixed air could be ignored. There was a progressive underestimate of $\dot{V}o_2$ and $\dot{V}co_2$ from a 0.61% in the first hour to a 7.33% error after 12 hours of closure. R was unaffected. The error was irrespective of $\dot{V}o_2$ levels.

(iii) With an R of 0.82, fresh air was always sucked in through the bleed. Calculation showed that there was a progressive underestimation of $\dot{V}o_2$ in the 30g lizard from 0.1% in the first hour to 1.24% after 12 hours and an underestimation of 0.1% to 1.05% for $\dot{V}co_2$. The smaller the $\dot{V}o_2$ the lower the error so that in the 0.2g lizard after 12 hours the error was only 0.065%.

(c) Volume determination of the closed circuit

If v ml of 100% O_2 was injected (at a point before the respirometer, Fig. 1.1) into the system of volume V ml containing 20.95% O_2, an x% elevation of % O_2 occurred and v ml of the new mixture, i.e. 20.95 + x% was lost through the bleed. From the following equations, V can be determined.

$$20.95\ V + 100\ v - (20.95 + x)v = (20.95 + x)V$$

$$\therefore \quad V = \frac{(79.05 - x)v}{x}$$

Similarly v ml injections of 100% CO_2 gave equations for V determination

$$0.03\ V + 100\ v - (0.03 + x)v = (0.03 + x)V$$

$$\therefore \quad V = \frac{(99.7 - x)v}{x}$$

Volume measurements never differed by more than 2% by either method or from estimation to estimation.

Knowing V and using first approximations of x% CO_2 = $\frac{100v}{V}$ and x% O_2 = $\frac{79.05v}{V}$, different injection volumes could be used to calibrate and check for linearity of the analysers.

(d) Mixing in the closed circuit

When a 0.2% step change (approximately) in gas content was made by 100% O_2 or CO_2 injection, 95% mixing was obtained in 5 min for the 7 ml respirometer (Fig. 1.27). In the larger respirometry volumes, mixing was 95% complete in 2 min for the same flow rate of 450 ml min^{-1}. Fig. 1.27 clearly illustrates the pressure sensitivity of the O_2 analyser to closure and injection, whilst the CO_2 analyser is insensitive. Using the CO_2 analyser and a very slow 100% CO_2 injection with a fast Rikadenki paper speed, the time, t, between mixing oscillation peaks can be used to determine V, if flow rate, $\dot{V}$, is accurately known, where $V = t\dot{V}$.

(e) Leakage rates in the closed circuit

In the constant pressure system, 100% O_2 or CO_2 injections were recorded during the fall in the temperature cycle when mixed air is being pushed out through the bleed. Under these conditions, the slope of the plateau obtained after mixing measured the extent of any leakage in terms of x% O_2 or CO_2 hr^{-1} 1% concentration $gradient^{-1}$ (Fig. 1.27). Knowing the volume, V, of the system this was converted to y ml of 100% O_2 or CO_2 hr^{-1} 1% $concentration\ gradient^{-1}$: $\frac{x}{100} V = y$.

Leakage rates of 1.0 ml for 100% CO_2 and 0.0075 ml for 100% O_2 hr^{-1} 1% $concentration\ gradient^{-1}$ were obtained, irrespective of the respirometer size indicating the impermeability of the perspex. These leakages were greater before 80% of the tubing had been replaced by steel. Since the leakage rates for O_2 and CO_2 were different, they were therefore due to Portex tubing permeability and not to joint leakage. The CO_2 molecules were also held for sometime in the walls of the tubing because it required

FIG. 1.27 Trace of % O_2 and % CO_2 during determination of the volume of the closed system, the extent of mixing and the leakage rate. Note the pressure response to opening and closing found only in the O_2 trace.

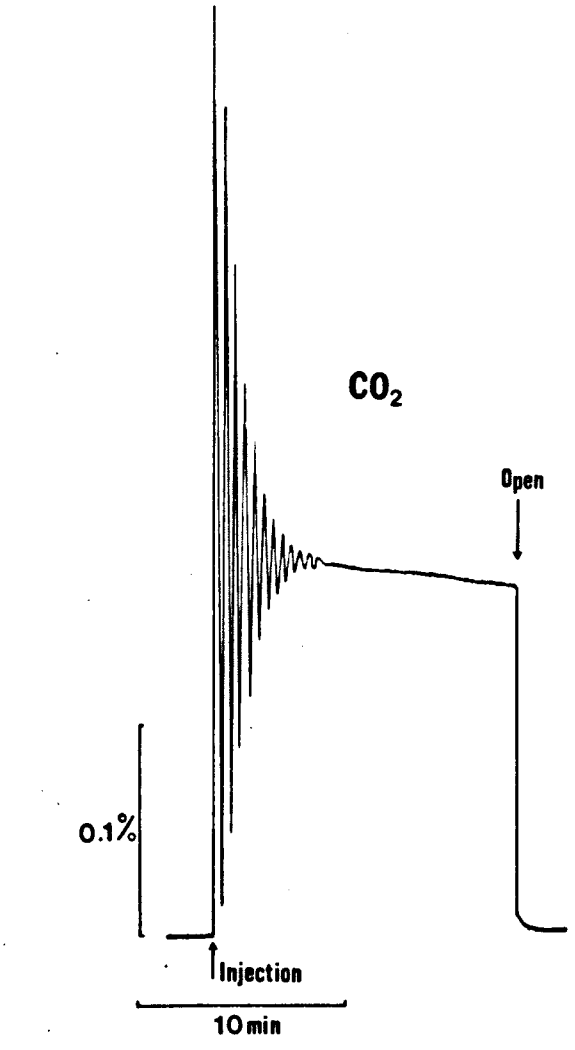
CO_2
Open
0.1%
Injection
10 min

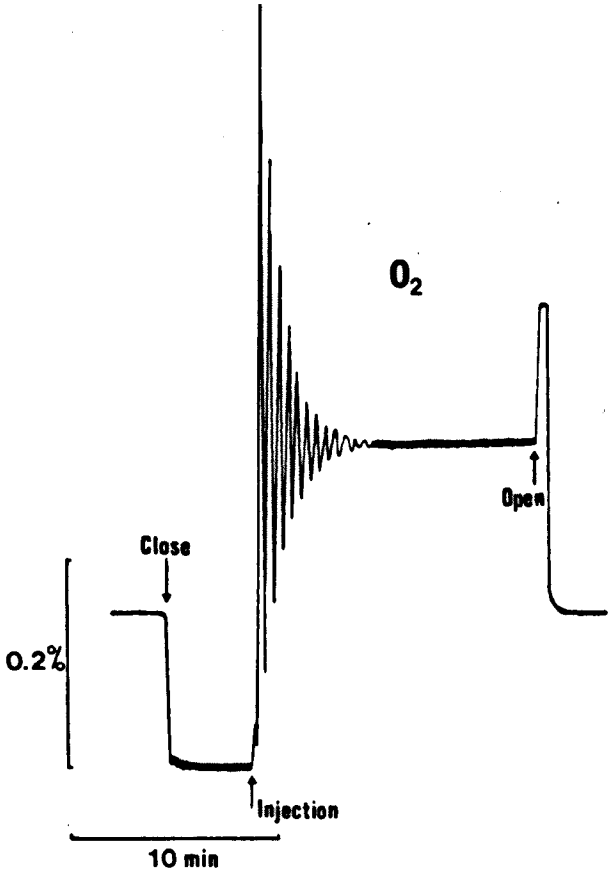
O_2
Open
Close
0.2%
Injection
10 min

an hour's flushing with fresh air before the circuit could be closed without a gradual increase in the level of circulating CO_2. If leakage rates were determined during the rise in temperature, both O_2 and CO_2 rates were elevated by 0.02 to 0.05 ml 100% O_2 or CO_2 hr^{-1} 1% concentration gradient^{-1} for the smallest to largest respirometry volume.

This CO_2 permeability caused a constant underestimation of R from a mean 0.82 to 0.72, 0.7, 0.68 and 0.58 for L. viridis, L. sicula, L. vivipara adult and 0.2g juvenile, respectively for resting $\dot{V}o_2$ measurements. The progressively greater underestimation as the lizard became smaller was due to the ratio of closed respirometry volume to body weight being respectively, 39, 70, 160 and 1,735. (This ratio also caused greater sensitivity and accuracy in the records for larger lizards because the % O_2 or % CO_2 change per hour was obviously greater).

CO_2 permeability of the Portex tubing caused the greatest errors in the closed circuit respirometry. Tygon tubing according to the suppliers (V.A. Howe & Co. Ltd.) would have had a CO_2 permeability of only 0.01 ml 100% CO_2 hr^{-1} 1% concentration gradient^{-1} for a wall thickness of 1 mm and 100 square inches surface area (i.e. that of the existing tubing). This would have caused virtually no underestimation of $\dot{V}co_2$ and R. However, rather than replace the Portex with Tygon tubing, it was decided to convert the system to an open circuit one, having none of the closed circuit errors, especially those for $\dot{V}co_2$.

Derivation of open circuit equations and the errors involved

(a) Steady-state conditions

Basically, $\dot{V}o_2 = \dot{V}_I F_{Io_2} - \dot{V}_E F_{Eo_2}$ or $\dfrac{\dot{V}_I P_{Io_2} - \dot{V}_E P_{Eo_2}}{P_B}$

If R is unity, then $\dot{V}_I$ and $\dot{V}_E$ are of the same value. However if R is greater or less than unity, then $\dot{V}_E$ is greater or less than $\dot{V}_I$, providing outlet CO_2 is not absorbed.

$$\dot{V}_I = \dot{V}_E + \dot{V}o_2 - \dot{V}co_2 \qquad \dot{V}_E = \dot{V}_I - \dot{V}o_2 + \dot{V}co_2$$

and

$$\text{or } \dot{V}_E + \dot{V}o_2 (1 - R) \qquad \text{or } \dot{V}_I - \dot{V}o_2 (1 - R)$$

When metering $\dot{V}_I$,

$$\dot{V}o_2 = \dot{V}_I F_{Io_2} - (\dot{V}_I - \dot{V}o_2 + \dot{V}co_2) F_{Eo_2}$$

$$= \frac{\dot{V}_I (F_{Io_2} - F_{Eo_2}) - \dot{V}co_2 F_{Eo_2}}{1 - F_{Eo_2}}$$

This equation is similar to that of Depocas & Hart (1957, equation 6)

where $$\dot{V}o_2 = \frac{\dot{V}_I P_{Io_2} - (\dot{V}_I + \dot{V}co_2) P_{Eo_2}}{P_B - P_{Eo_2}}$$

If $\dot{V}o_2$ is determined from the approximate equations

$\dot{V}o_2 = \dot{V}_I (F_{Io_2} - F_{Eo_2})$ or $= V_I \frac{(P_{Io_2} - P_{Eo_2})}{P_B}$ without correcting

for deviations from an R of unity, then the % error involved can be calculated from:

$$\dot{V}o_2 = \frac{\dot{V}_I (P_{Io_2} - P_{Eo_2})}{P_B} + \frac{\dot{V}o_2 (1 - R) P_{Eo_2}}{P_B}$$

$$\text{where \% error} = \frac{\frac{\dot{V}o_2 (1 - R) P_{Eo_2}}{P_B}}{\dot{V}o_2 + \frac{\dot{V}_I (1 - R) P_{Eo_2}}{P_B}} \times 100$$

$$= \frac{P_{Eo_2} (1 - R)}{P_{Eo_2} (1 - R) + P_B} \times 100$$

The error is dependent on both R and the level of $\dot{V}o_2$ (i.e. P_{Eo_2}). For example, if R = 0.7, the errors are of underestimation by 5.9%, 5.6% and 3.18% for $\dot{V}o_2$ of 0.1, 1.0 and 10 ml min^{-1}, respectively when $\dot{V}_I$ = 100 ml min^{-1}. The relationship between the error and $\dot{V}o_2$ is exponential with the larger $\dot{V}o_2$ giving the least error. Increasing $\dot{V}_I$ decreases P_{Eo_2} and hence increases the error. If R = 0.9 for a $\dot{V}_I$ of 100 ml min^{-1} then 2.04% and 5.9% errors are obtained for a $\dot{V}o_2$ of 0.1 and 0.016 ml min^{-1} respectively. When R is greater than unity the errors are those of overestimation.

When metering $\dot{V}_E$,

$$\dot{V}o_2 = (\dot{V}_E + \dot{V}o_2 - \dot{V}co_2) F_{Io_2} - \dot{V}_E F_{Eo_2}$$

$$= \frac{\dot{V}_E (F_{Io_2} - F_{Eo_2}) - \dot{V}co_2 F_{Io_2}}{1 - F_{Io_2}}$$

This equation was not derived by Depocas & Hart (1957) but is the one used by Tucker (1968) for birds and has been quoted in some exercising and reptilian $\dot{V}o_2$ measurements.

In terms of partial pressures, this equation can be expressed another way as

$$\dot{V}o_2 = \frac{\left[\dot{V}_E + \dot{V}o_2 (1 - R)\right] P_{Io_2} - \dot{V}_E P_{Eo_2}}{P_B}$$

$$= \frac{\dot{V}_E (P_{Io_2} - P_{Eo_2})}{P_B} + \frac{\dot{V}o_2 (1 - R) P_{Io_2}}{P_B}$$

If $\dot{V}o_2$ is determined from the approximate equation (i.e. the first part of the above equation),

$$\% \text{ error} = \frac{P_{Io_2} (1 - R)}{P_{Io_2} (1 - R) + P_B} \times 100$$

Since P_{Io_2} never changes, the error is a constant value dependent only on R. For example, if R = 0.7 the error is 5.9% but if R = 0.9 then the error is 2.05%, irrespective of $\dot{V}o_2$. An R equal to 0.5 gives an error of 9.1%. When R is less than unity the error is of underestimation but when R is greater than unity it is of overestimation. There is one further error involved with this approximation and that is that $\dot{V}_E$ ought to change as R changes. However, with the lizards, flow differences of 0.15 ml min^{-1} (maximum), due to R and the level of F_{Eo_2} at a $\dot{V}_E$ of 100 ml min^{-1}, are not recordable.

Whether metering $\dot{V}_I$ or $\dot{V}_E$ the error is always of underestimation for an R of less than unity, contrary to Depocas & Hart (1957) who state that $\dot{V}o_2$ is underestimated when $\dot{V}_I$ is metered but overestimated when $\dot{V}_E$ is metered. By using the full equations, these errors are avoided.

Equations for estimating $\dot{V}co_2$ have not previously been derived

Basically, $$\dot{V}co_2 = \dot{V}_E F_{Eco_2} - \dot{V}_I F_{Ico_2}$$

and $$\dot{V}_E = \dot{V}_I - \dot{V}o_2 + \dot{V}co_2 \quad \text{and} \quad \dot{V}_I = \dot{V}_E + \dot{V}o_2 - \dot{V}co_2$$

$$\text{or} \quad \dot{V}_I - \dot{V}co_2 \left(\frac{1 - R}{R}\right) \qquad \text{or} \quad \dot{V}_E + \dot{V}co_2 \left(\frac{1 - R}{R}\right)$$

When metering $\dot{V}_I$,

$$\dot{V}co_2 = \frac{\dot{V}_I (F_{Eco_2} - F_{Ico_2}) - \dot{V}o_2 F_{Eco_2}}{1 - F_{Eco_2}}$$

and when metering $\dot{V}_E$,

$$\dot{V}co_2 = \frac{\dot{V}_E (F_{Eco_2} - F_{Ico_2}) - \dot{V}o_2 F_{Ico_2}}{1 - F_{Ico_2}}$$

If approximate equations of

$$\dot{V}co_2 = \dot{V}_E (F_{Eco_2} - F_{Ico_2}) \quad \text{or} \quad \dot{V}_I (F_{Eco_2} - F_{Ico_2}) \quad \text{are used,}$$

then the errors are, for both instances, due to overestimation if R is less

than unity and vice versa.

$$\text{When metering } \dot{V}_I \text{ the \% error} = \frac{P_{Eco_2}\left(\frac{1-R}{R}\right)}{P_{Eco_2}\left(\frac{1-R}{R}\right) + P_B} \times 100$$

The error is dependent on both R and $\dot{V}co_2$ and for an R of 0.7 the overestimating error is 0.56% and 0.44% for a $\dot{V}co_2$ of 0.1 and 1.0 ml min^{-1} respectively at a $\dot{V}_I$ of 100 ml min^{-1}.

$$\text{When metering } \dot{V}_E \text{ the \% error} = \frac{P_{Ico_2}\left(\frac{1-R}{R}\right)}{P_{Ico_2}\left(\frac{1-R}{R}\right) + P_B} \times 100$$

The error now is dependent only on R since P_{Ico_2} is constant. For example, for R = 0.7 the error is 0.01285% whilst for R = 0.9 the error is 0.0033% of overestimation.

In conclusion, it is obvious that the errors are considerably less for $\dot{V}co_2$ than for $\dot{V}o_2$ and are negligible for $\dot{V}co_2$ when monitoring $\dot{V}_E$. This fact is very important for an accurate estimation of $\dot{V}o_2$ since by the full equation it is dependent on an initial accurate measurement of $\dot{V}co_2$. To ensure maximum accuracy $\dot{V}_E$ was monitored.

Steady-state $\dot{V}o_2$ can also be recorded under conditions where CO_2 is removed from both the inlet and outlet air, so that $F'o_2$ and $\dot{V}_I'$ or $\dot{V}_E'$ are all CO_2-free.

Then $\dot{V}o_2 = \dot{V}_I' F_I'o_2 - \dot{V}_E' F_E'o_2$

and $\dot{V}_I' = \dot{V}_E' + \dot{V}o_2$ and $\dot{V}_E' = \dot{V}_I' - \dot{V}o_2$

Thus by metering $\dot{V}_I'$,

$$\dot{V}o_2 = \dot{V}_I' F_I'o_2 - (\dot{V}_I' - \dot{V}o_2) F_E'o_2$$

$$= \dot{V}_I' \frac{(F_I'o_2 - F_E'o_2)}{1 - F_E'o_2}$$

and by metering $\dot{V}_E'$,

$$\dot{V}o_2 = \dot{V}_E' \frac{(F_I'o_2 - F_E'o_2)}{1 - F_I'o_2}$$

These equations are those initially derived by Depocas & Hart (1957) although in terms of partial pressures. Hill (1972) has recently emphasised that these equations must be used only for totally CO_2-free measurements. He has discussed the errors involved if $\dot{V}_I$ and F_{Io_2} are not CO_2-free whilst $F_E'o_2$ is CO_2-free. In these cases, the greater the $F_E'o_2$ value, the smaller the error. Bennett (1972, 1973) has used these equations, with Hill's modification, in his work on lizards. However, none of these errors pertain to the steady-state equations used in this study for Lacerta where CO_2 is present in both inlet and outlet air.

(b) Dynamic conditions

A form of dynamic equation has been derived by Depocas & Hart (1957) but it is based on a respirometry system of very large volume in which steady states are attained only after a few hours because of very low flow rates. The approximate form of the equation which did not allow for deviations from an R of unity was identical to that of a closed system, where $\dot{V}o_2 = V \frac{dF_{Eo_2}}{dt}$.

If the correction for R is made $\dot{V}o_2 = (\dot{V} - \dot{V}_E) F_{Io_2} - V \frac{dF_{Eo_2}}{dt}$.

Depocas & Hart (1957) take the view that open-circuit systems suffer from the disadvantage of a fairly long equilibration period and are consequently useless when rapid changes in metabolism are to be measured. A more rapid response was found in closed circuits. The opposite was found in this study providing the flow rate was high and the volume small in the dynamic open-circuit conditions. With homogeneous mixing, $V = \tau\dot{V}_E$ where V = volume ml of system, $\dot{V}_E$ = flow rate ml min^{-1} and τ = time constant in min. The smaller τ the more rapid is the response. The determination of τ has

been described in Chapter 1.

Because there is negligible error for $\dot{V}co_2$ when monitoring $\dot{V}_E$,

$$\text{dynamic } \dot{V}co_2 = \dot{V}_E \,(\text{mean } F_{Eco_2} - F_{Ico_2}) \pm \dot{V}_E \tau \frac{\Delta F_{Eco_2}}{\Delta t}$$

The full equation for $\dot{V}o_2$ must be used.

$$\dot{V}o_2 = \frac{\dot{V}_E \,(F_{Io_2} - \text{mean } F_{Eo_2}) - \dot{V}co_2 \, F_{Io_2}}{1 - F_{Io_2}} \pm \dot{V}_E \tau \frac{\Delta F_{Eo_2}}{\Delta t}$$

Any correction that may be applicable to the right hand side of the equation because of small changes in $\dot{V}_E$ when R changes, cannot be estimated.

These dynamic equations have also been extended for use with a face mask, in which V is considerably reduced and hence τ is in sec rather than min. Alteration of $\dot{V}_E$ will affect the absolute value of F_{Eo_2} and F_{Eco_2}, i.e. the sensitivity. Face mask gas exchange measurements have been described in Chapter 2 and they use the dynamic equations described above. There may be some error due to inhomogeneity in the open circuit, i.e. 'effective' volume is less than true volume, but the extent of the error is not measurable.

APPENDIX II

ANAESTHETICS

Introduction

Little data is available in the literature for anaesthesia in reptiles, especially in lizards and crocodiles (see recent review by Kaplan, 1969). Inhalation anaesthesia using ether has been described for snakes, lizards and testudines. Chloroform and halothane have been used in snakes only (Brazenor & Kaye, 1953, Kaplan, 1969, Jackson, 1970). Artificial respiration is often, however, required to ensure recovery. These volatile anaesthetics also affect the lipid components of lung tissue (Croft, 1957) and are therefore unsuitable for this study on Lacerta. Oral anaesthesia by urethane or pentobarbital has been used for testudines and crocodiles (Kaplan, 1969). Intraperitoneal anaesthesia using pentobarbitone (Nembutal) and pentothal sodium (Surital) at a dosage of 15-30 mg/kg has been used successfully in testudines and snakes. Dosages of 2.8 g/kg of urethane for testudines and 200-500 mg/kg of M.S. 222 for snakes are equally successful (Karlstrom & Cook, 1955, Betz, 1962, Kaplan, 1969). Urethane and pentobarbital have also been given intravenously in testudines (Kaplan, 1969). Intraperitoneal dosages of 7 mg/kg for small and 15 mg/kg for large caimans have been used by Naifeh, Huggins & Hoff (1971).

Anaesthesia by ether or general hypothermia are the only methods described for lizards by Kaplan (1969). Examination of the methods used by investigators of lizard respiratory and cardiovascular systems, however, reveal a little more information. General hypothermia is still often used (e.g. Templeton, 1964, and for crocodiles, e.g. Huggins, Deavers, Hoff & Naifeh, 1970). Baker & White (1970) and Huggins et al (1970) have used local anaesthetics, e.g. xylocaine, for the implantation of catheters. Intraperitoneal injections of M.S. 222 at 300-500 mg/kg have been used in

Iguana by Tucker (1966) and Moberly (1968). Pentobarbital has been given intravenously to Iguana by Baker & White (1970) at a dosage of 30 mg/kg or less, administered over a period of 0.5 hr.

Intraperitoneal and intravenous anaesthesia are obviously the more reliable methods, especially the latter. Since the maximum body weight of Lacerta viridis is 35g, intraperitoneal injections are considerably easier than intravenous to administer. The effects of pentobarbitone in three Lacerta species were investigated to determine the correct dosages for light and surgical plane anaesthesia. Nembutal was diluted in lizard Ringer (see Chapter 3) and a volume no greater than 0.01 ml was injected into the abdominal, intraperitoneal cavity, care being taken to avoid all internal organs.

Results

Table 1 lists the progressive effects of Nembutal on each of the Lacerta species. An inability to keep the eyelids open for any length of time is the first sign of anaesthesia. Touching or gentle handling, however, can cause the eyelids to open and weak limb movements to occur for sometime. Picking the lizard up by the tail or turning it on its back causes an arching of the body or a righting reflex until a deeper level of anaesthesia is reached. For surgical plane anaesthesia a further depth has to be attained in which the lizard will not twitch when the tail behind the vent is strongly pinched or the skin under the collar fold is severely scratched. A reflex twitch of the eyelid when it is lightly touched is rarely completely lost. The length of time for which this surgical plane of anaesthesia lasts and the time from injection to full recovery, i.e. co-ordinated limb movement but with the lizard often dopey, have also been determined.

The dosages required for L. viridis and L. sicula are identical but in the smaller lizard the attainment of all levels of anaesthesia and the speed of recovery are quicker. L. sicula were always exceptionally active after injection as they were after any sort of handling.

TABLE 1

Effect of pentobarbitone (Nembutal) anaesthetic on Lacerta at 28°C. Each dosage response is a mean of three individuals.

Dosage mg/kg	Closure of eyes, min.	Loss of touch response, min.	Loss of righting reflex, min.	Loss of collar fold and tail pinching reflex min.	Surgical Plane Period, hr.	Recovery Time hr.
L. Viridis 20-30g						
10	25	-	-	-	-	1 - 3
20	15	30 - 45	60	-	-	7
30	7	10	30	45	6 - 8	10 - 12
40	4 - 7	7	10	30	12	18
50	4	6	10	20	-	-
L. sicula 6-10g						
10	12	-	-	-	-	1
20	6	10	20	60	1 - 3	3 - 5
30	4	6	10	30	2 - 3	3.5 - 5.0
40	5	6	7	25	9	12
50	1 - 3	3 - 6	3 - 6	10 - 20	-	-
L. vivipara 2-4g						
10	30	-	-	-	-	0.5 - 1
20	15	-	-	-	-	2 - 3
30	10	-	-	-	-	2 - 3
40	5	5	6	-	-	6
50	3	3	5	10 - 15	-	-
60	3	3	5	10	-	-

This elevated activity plus the higher standard $\dot{V}o_2\ g^{-1}$ in L. sicula must explain the faster rate of assimilation and degradation of Nembutal.

After injection, L. vivipara were not highly active until the anaesthetic began to take effect when continuous unco-ordinated crawling movement occurred. This often caused the lizard to attempt to crawl up the vertical side of the container and then topple over, slowly right itself and start again. All these spontaneous movements occurred before the eyelids closed and continued for some time afterwards. Testing for reflexes later often initiated these movements for a few minutes. This hyperactivity induced by the anaesthetic must cause the rapid degradation of it, explaining the lack of reflex loss and inability to attain a surgical plane of anaesthesia at a sublethal dose.

Lowering the temperature, i.e. to 20°C, increased the induction and anaesthetic periods by a factor of 3 (only tested in a few) and shifted the effective dosage to 5 mg/kg less than in Table 1.

Nembutal causes a variable amount of mucus secretion in the respiratory passages which often causes the lizard to open its mouth and flick its tongue into the internal and external choanae during the induction period. The external choanae which do not have valves and do not pulsate during respiration, will contract at 5 to 10 sec intervals when partially or completely blocked by mucus. The contraction is in the form of a wave of movement passing around the nares lumen and must be due to blood flow in the cephalic sinuses (Bruner, 1907). During the recovery period, the lizards were often observed to 'sneeze' which may be an attempt to assist in respiratory passage clearance.

Respiratory rate and tidal volume progressively decrease with depth of anaesthesia and lethal doses are due to respiratory apnea. Intercostal pulmonary activity can still persist for some time after reflexes are abolished in these lizards. Reptiles do not have the advantage of a mammalian diaphragm, which continues to function whilst intercostal activity is diminished during surgical plane anaesthesia.

Discussion

Karlstrom & Cook (1955) found that 200-400g snakes at 20°C when given the same anaesthetic dose (mg/kg) as 5-10g individuals, took longer to become anaesthetised but recovered more quickly. Betz (1962) considered that larger snakes required a dosage twice that for a small snake. In contrast, it is known that in general smaller mammals require a greater mg/kg dosage than larger mammals (Barnes & Eltherington, 1973) but there is too much variability in their collected data to suggest a definite $W^{0.75}$ relationship, i.e. the same as standard $\dot{V}o_2$. In Lacerta it is obvious that, although no distinction could be made in actual dosage, the induction period and recovery were quicker in the smaller lizard because of their higher metabolic rate g^{-1}. A possible explanation for the discrepancy between Karlstrom & Cook's data and this study is that their small weight lizards had been starved for many days and would be expected to have a low resistance to anaesthesia, i.e. induced quickly and taking a long time for recovery. Betz (1962) for the same 30 mg/kg dosage found 15 hr elapsed before recovery began in Natrix at 26°C whereas Karlstrom & Cook (1955) found only 5.5 hr for Crotalus of the same weight at 20°C. These data would seem to contradict each other, unless there is a considerable species difference in response.

It is of great interest to note that although a 1 kg mammal would require 30-35 mg/kg of Nembutal, and a 30g mouse requires 50-60 mg/kg, (Barnes & Eltherington, 1973), a 1 kg snake still needs 30 mg/kg and a 30g lizard 30-40 mg/kg. These reptiles consume a tenth of the oxygen needed by a mammal and one might perhaps expect the anaesthetic dosage to be 10 times less. Why this is not the case, is not known.